

Composites based on natural fibres and thermoplastic matrices.

Garkhail, Sanjeev Kumar

The copyright of this thesis rests with the author and no quotation from it or information derived from it may be published without the prior written consent of the author

For additional information about this publication click this link.

<http://qmro.qmul.ac.uk/jspui/handle/123456789/1700>

Information about this research object was correct at the time of download; we occasionally make corrections to records, please therefore check the published record when citing. For more information contact scholarlycommunications@qmul.ac.uk

**COMPOSITES BASED ON NATURAL FIBRES
AND THERMOPLASTIC MATRICES**

Sanjeev Kumar Garkhail

**A thesis submitted for the degree of Doctor of Philosophy at the
University of London**

Supervised by Dr. T. Peijs

Department of Materials
Queen Mary, University of London
Mile End Road, London E1 4NS

January 2002



ABSTRACT

This thesis examines the possibility of reinforcing thermoplastic matrices, notably polypropylene (PP) and polyhydroxyalkanoates (PHAs), by (a vegetable fibre) flax.

An effort is made to enhance/optimize the mechanical properties of flax/PP composites through a micromechanical and macromechanical study. The fibre/matrix interface is modified via chemical modifications as well as modifications in processing parameters (transcrystallinity).

Effects of parameters like fibre length, fibre volume fraction and fibre-matrix interface modification on the mechanical properties of long flax fibre reinforced PP composites (compression moulded) as well as short flax fibre based composites (injection moulded) are studied. In order to get a better insight in the importance of these different parameters for the optimisation of composite performance, the experimental results are compared with model predictions using micromechanical models for random short-fibre-reinforced composites. For the injection moulded composites, different compounding routes are used and compared.

The moisture resistance (pick-up and diffusivity) as well as dimensional stability (swelling) of natural fibre mat reinforced thermoplastics (NMTs), based on different kinds of flax fibres and PPs, are studied. The effects of a novel fibre upgrading method for flax fibres (DuralinTM) on the moisture pick-up and residual tensile properties of NMT composites are explored.

Biodegradable composites based on flax fibre and PHAs are analysed. It is observed that addition of (cheap) flax fibre to polyhydroxybutyrate (PHB) could be advantageous as far as cost-performance of biopolymer composites is concerned, especially for stiffness critical applications. Mechanical properties of 'biocomposites' manufactured through different routes (i.e. injection moulding and compression moulding) are compared. Addition of cheap flax fibres to an expensive and brittle PHA composite leads to enhanced toughness of the composites.

A life cycle assessment (LCA) study on glass-fibre-mat-reinforced-thermoplastic (GMT) and NMT manufactured by a current production method for thermoplastic prepregs followed by compression moulding into an automotive and non-automotive part is carried out.

ACKNOWLEDGEMENTS

I would like to express my sincere gratitude and appreciation to my supervisor Dr. Ton Peijs for his valuable guidance, suggestions, assistance, patience and encouragement throughout this work. Dr. Peijs' fruitful and infectious enthusiasm certainly filled me with positive energy whenever I had discussions with him.

I am obliged to the Technology for Sustainable Development Centre (Technologie voor Duurzame Ontwikkeling (TDO)) at Eindhoven University of Technology (TUE) for initiating this project. I am thankful to TDO for funding the project, providing a friendly working environment and organising presentations, poster sessions and other activities, which showed active involvement of TDO towards the completion of the project. I also acknowledge Dr Gerard Pott, CERES B.V. (Wageningen, The Netherlands) for providing the flax fibres used in this study.

I would like to express my sincere appreciation to the staff and technicians in the Materials Technology (MaTe) Group of the Department of Mechanical Engineering, TUE for helping full-heartedly during the project. I wish to thank Dr Leon Govaert for his guidance and help during experimental work, systems managers Leo Wouters and Patrick Brakel for helping me in solving the problems related to computer and department secretary Marleen Rieken for her concern and help during my stay in Eindhoven. I am also grateful to all the graduate students and colleagues who helped me during the project. Some of them are Rob Heijenrath, Harold van Melick, Erwin Meurs, Pascal Bertens, Bart Wieland, Dr. Jayamol George, Dr. Paul van den Heuvel, Arnim Salbrink, Edwin Klompen and Dr. Frank Swartjes. I would like to thank the workshop staff at the Department of Mechanical Engineering, TUE for helping and designing some of the apparatus used in this study. I am also grateful to my colleagues working at Polymer Technology Group, Department of Chemical Engineering for helping me with some of the experiments and guiding me during my study. I am highly obliged to Dr Sanjay Rastogi for his never-ending encouragement and for his technical discussions.

Words cannot express my gratitude towards my wife Kirti, daughter Prakriti, parents (Mr. B. L. Garkhail and Mrs. Sudesh Garkhail), oma (Mrs. Nell van Amsterdam), brother Gagan, sisters Meenakshi, Pooja, Rita, Lipi, Divya, relatives and friends for their love, moral support and encouragement during this study. I would like to acknowledge all my teachers who taught me directly or indirectly.

Sanjeev Kumar Garkhail

TABLE OF CONTENTS

	Page
ABSTRACT	1
ACKNOWLEDGEMENTS	3
TABLE OF CONTENTS	5
LIST OF FIGURES	11
LIST OF TABLES	23
LIST OF ABBREVIATIONS AND SYMBOLS	26
GLOSSARY	30
CHAPTER 1. INTRODUCTION	32
1.1 Thermoplastic composites.....	34
1.2 Processing of thermoplastic composites.....	36
1.3 Natural fibre reinforced thermoplastic composites: an introduction	40
1.4 Thermoplastic composites based on natural fibres/cellulose: earlier work and present scenario	43
1.4.1 Cellulose ‘filled’ thermoplastic composites.....	44
1.4.2 Natural fibre ‘reinforced’ thermoplastic composites.....	46
1.5 Aim of the thesis	49
1.6 Structure of this thesis	51
CHAPTER 2. NATURAL FIBRES: LITERATURE REVIEW AND CHARACTERISATION	54
2.1 Natural fibres: a literature review	54
2.1.1 Flax fibres	59
2.1.1.1 Flax fibre processing	63
2.1.1.2 Duralin fibres.....	68
2.2 Characterisation of flax fibres- Experimental	71
2.2.1 Materials	72
2.2.2 Methods	72

2.2.2.1	Mechanical properties of flax fibres -----	72
2.2.2.2	Thermal gravimetric analysis (TGA) of flax fibres -----	73
2.2.3	Results and discussions -----	73
2.2.3.1	Mechanical properties of flax fibres -----	73
2.2.3.2	Effect of heat treatment on tensile strength -----	77
2.2.3.3	Thermal gravimetric analysis (TGA) of flax fibres -----	79
2.3	Conclusions-----	83
CHAPTER 3. A STUDY ON FLAX / POLYPROPYLENE INTERFACE:		
CHEMICAL MODIFICATIONS ----- 85		
3.1	Introduction-----	85
3.2	Interface and interphase: theories and characterisation methods -----	86
3.2.1	Theory of adhesion -----	86
3.2.1.1	Fibre surface treatment-----	93
3.2.2	Interface / interphase characterisation methods-----	98
3.2.2.1	Micromechanical tests -----	104
3.3	Experimental -----	108
3.3.1	Materials -----	108
3.3.2	Methods -----	108
3.3.2.1	Surface treatment and analysis-----	108
3.3.2.2	Microcomposites and micro-debonding test-----	109
3.4	Results and discussion -----	
	111	
3.4.1	Influence of flax type -----	113
3.4.2	Influence of fibre modification-----	118
3.4.3	Influence of matrix modification -----	120
3.5	Conclusions-----	124
CHAPTER 4. A STUDY ON FLAX / POLYPROPYLENE INTERFACE:		
TRANSCRYSTALLINITY ----- 125		

4.1	Introduction-----	125
4.2	Theory -----	126
	4.2.1 Transcrystallisation -----	126
	4.2.2 Effects of transcrystallinity on mechanical properties -----	128
4.3	Experimental -----	131
	4.3.1 Materials -----	131
	4.3.2 Methods -----	132
	4.3.2.1 Sample preparation for studying transcrystallinity -----	132
	4.3.2.2 Sample preparation for pull-out testing -----	132
	4.3.2.3 Fibre pull-out test -----	134
	4.3.2.4 Sample preparation for macrocomposites -----	136
	4.3.2.5 Tensile testing of macrocomposites -----	137
4.4	Results and discussions -----	137
	4.4.1 Influence of cooling rate, time and crystallisation temperature on the thickness of transcrystalline layer -----	137
	4.4.2 Influence of fibre type and modifications -----	142
	4.4.3 Influence of matrix modification on the thickness of transcrystalline layer -----	145
	4.4.4 Influence of transcrystallinity on the micromechanical properties of the flax/PP microcomposites -----	146
	4.4.5 Influence of transcrystallinity on the macromechanical properties of the flax/PP macrocomposites -----	149
4.5	Conclusions-----	153
CHAPTER 5. FLAX FIBRE NMT COMPOSITES -----		155
5.1	Introduction-----	155
	5.1.1 Micromechanical models for discontinuous fibre composites	156
	5.1.1.1 Composite stiffness-----	156
	5.1.1.2 Composite strength-----	158
	5.1.1.3 Impact strength-----	160
5.2	Experimental -----	162

5.2.1	Materials -----	162
5.2.2	Test methods-----	164
5.3	Results and Discussions -----	165
5.3.1	Influence of fibre length-----	165
5.3.1.1	Composite stiffness-----	165
5.3.1.2	Composite strength-----	166
5.3.1.3	Impact strength-----	169
5.3.2	Influence of fibre volume fraction-----	172
5.3.2.1	Composite stiffness-----	172
5.3.2.2	Composite strength-----	173
5.3.2.3	Impact strength-----	175
5.3.3	Influence of fibre diameter on composite strength -----	178
5.4	Conclusions-----	181
 CHAPTER 6. FLAX FIBRE INJECTION MOULDED COMPOSITES		183
6.1	Introduction-----	183
6.1.1	Compounding methods for short fibre reinforced composites	184
6.1.2	Compounding methods for long fibre reinforced composites	187
6.1.3	Compounding methods for flax fibre reinforced composites	189
6.2	Experimental -----	189
6.2.1	Materials -----	189
6.2.2	Methods -----	190
6.2.2.1	Compounding -----	190
6.2.2.2	Injection moulding -----	196
6.3	Results and Discussion -----	197
6.3.1	Compounding methods-----	197
6.3.2	Properties of injection moulded composites -----	202
6.3.2.1	Polypropylene based composites -----	202
6.3.2.2	Short fibre composites based on other thermoplastic matrices -----	213
6.4	Conclusions-----	215

CHAPTER 7. ENVIRONMENTAL PROPERTIES OF	
FLAX / POLYPROPYLENE COMPOSITES----- 217	
7.1	Introduction----- 217
7.1.1	Effect of moisture absorption on composites' properties ---- 218
7.1.2	Modelling ----- 219
7.2	Experimental ----- 222
7.2.1	Flax fibre treatment----- 222
7.2.2	Composite manufacturing ----- 222
7.2.3	Moisture absorption of composites and testing----- 223
7.3	Results and Discussions ----- 223
7.4	Conclusions----- 234
CHAPTER 8. BIODEGRADABLE COMPOSITES BASED ON	
FLAX / POLY-HYDROXY-ALKANOATES ----- 235	
8.1	Introduction----- 235
8.1.1	Composites based on biopolymer matrices: a literature review ----- 237
8.1.2	Poly-hydroxy-alkanoates (PHAs)----- 239
8.1.3	Copolymers of poly-hydroxy-alkanoates ----- 241
8.2	Experimental ----- 241
8.2.1	Materials ----- 241
8.2.2	Methods ----- 242
8.2.2.1	Compression moulding ----- 242
8.2.2.2	Injection moulding ----- 243
8.2.2.3	Test methods ----- 243
8.3	Results and discussions ----- 245
8.3.1	NMT ----- 245
8.3.2	Influence of hydroxyvalerate content in the copolymer ----- 248
8.3.3	Influence of cooling temperature ----- 252
8.3.4	Injection moulded composites ----- 253
8.3.5	Biodegradation ----- 256

8.4	Conclusions-----	260
CHAPTER 9. LIFE CYCLE ANALYSIS (LCA) OF		
FLAX / POLYPROPYLENE COMPOSITES----- 261		
9.1	Introduction-----	261
9.2	Materials -----	263
9.3	LCA theory -----	264
	9.3.1 LCA drawbacks -----	275
9.4	Methods-----	276
	9.4.1 Inventory: materials in mining phase -----	277
	9.4.2 Process tree: processing phase -----	279
	9.4.3 Use phase: additional emissions and savings -----	281
	9.4.4 Waste phase-----	283
9.5	Results and discussions-----	284
	9.5.1 Future improvement in environmental impact-----	295
9.6	Conclusions-----	296
CHAPTER 10. CONCLUSIONS AND FUTURE RESEARCH----- 297		
10.1	Conclusions-----	297
10.2	Directions for future research-----	303
REFERENCES ----- 307		
LIST OF PUBLICATIONS ----- 322		
APPENDIX ----- 324		
APPENDIX 2A	Tensile strength plots for different flax fibres -----	324
APPENDIX 2B	Tensile modulus plots for different flax fibres-----	325
APPENDIX 3A	Pull-out force vs. embedded length -----	326
APPENDIX 3B	ESEM pictures of different flax fibres -----	331

LIST OF FIGURES

	Page
CHAPTER 1	
<i>Figure 1.1</i>	Classification of composite materials.----- 33
<i>Figure 1.2</i>	Classification of polymeric materials.----- 33
<i>Figure 1.3</i>	Hot melt impregnation of thermoplastic prepregs. ----- 37
<i>Figure 1.4</i>	The production process for GMT thermoplastic sheets. ----- 37
<i>Figure 1.5</i>	The solution mixing ('paper-making') production process for thermoplastic GMT sheets.----- 38
<i>Figure 1.6</i>	Manually operated compression moulding production line. ----- 39
<i>Figure 1.7</i>	Picture of (a) GMT bumper beam in Freelander car and (b) GMT front end of a car. ----- 40
<i>Figure 1.8</i>	Possibilities of hybrid semi-products for composites.----- 42
<i>Figure 1.9</i>	Some examples of wood filled composites. ----- 46
<i>Figure 1.10</i>	Underbody panelling prototypes for the Mercedes A-class made of flax-fibre-reinforced polypropylene. ----- 47
CHAPTER 2	
<i>Figure 2.1</i>	Schematic structure of cellulose polymer. ----- 55
<i>Figure 2.2</i>	Picture of cellulose crystal unit cell. ----- 56
<i>Figure 2.3</i>	Suggested arrangement of molecules in crystal of (a) cellulose I and (b) cellulose II.----- 56
<i>Figure 2.4</i>	Schematic picture of technical and elementary (fibre cell) flax fibre. ----- 60
<i>Figure 2.5</i>	(a) Picture of the cultivated flax plant (<i>Linum usitatissimum</i>) in bloom and (b) schematic view of the cross-section of the stem of flax plant ----- 62
<i>Figure 2.6</i>	Picture of the cross-section of the stem of flax plant taken through an optical microscope. ----- 62

Figure 2.7	Picture of farmers pulling the flax plant through pulling tractors.	64
Figure 2.8	Picture of (a) an operator taking flax off the scutching turbine and twisting it into tipples, or handful of parallel fibres and (b) the principle of one of the scutching machines. ----	65
Figure 2.9	Flow diagram showing green flax and dew-retted fibre preparation. -----	66
Figure 2.10	Schematic representation of the spiral structure in different layers of flax.-----	67
Figure 2.11	Kink band formation in flax fibres. -----	68
Figure 2.12	Picture of various products manufactured from flax plant.-----	71
Figure 2.13	Typical stress vs. strain curve of a Duralin flax fibre.-----	74
Figure 2.14	Tensile strength of Duralin flax and green flax vs. gauge length and schematic representation of failure mode at different gauge lengths. -----	75
Figure 2.15	SEM pictures of Duralin flax fibres after tensile testing at (a) 3mm gauge length and (b) 100 mm gauge length.-----	76
Figure 2.16	Tensile modulus of Duralin flax vs. gauge length. -----	77
Figure 2.17	Effect of temperature on the tensile strength of flax fibres. (Gauge length = 10 mm, time of exposure = 5 min and testing temperature = Room temperature).-----	78
Figure 2.18	Effect of heat exposure time on the tensile strength of flax fibres. -----	78
Figure 2.19	Effect of heat exposure on weight loss in green flax fibre, measured through TGA (Isothermal exposure).-----	80
Figure 2.20	Effect of heat exposure on weight loss in Duralin flax fibre, measured through TGA (Isothermal exposure).-----	80
Figure 2.21	Effect of heat exposure (at different heating rates) on weight loss in green flax fibre, measured through TGA. -----	82
Figure 2.22	Effect of heat exposure (at different heating rates) on weight loss in Duralin flax fibre, measured through TGA.-----	82

CHAPTER 3

Figure 3.1	Schematic description of various theories of adhesion. (a) adsorption and chemical bonding. (b) diffusion. (c) electrostatic attraction and (d) mechanical interlocking.-----	88
Figure 3.2	Schematic representation of solid-solid and solid-liquid interactions.-----	89
Figure 3.3	Schematic representation of the adhesion process between MA-PP and the flax fibre.-----	96
Figure 3.4	The schematic overview of some of the methods applied to study / measure the interfacial properties. -----	99
Figure 3.5	Schematic representation of different mechanical tests for the measurement of interface related properties.-----	101
Figure 3.6	Schematic representation of Low Energy Ion Spectroscopy (a) principle and (b) set-up. -----	104
Figure 3.7	Typical droplet shape (droplet of PP/MA-PP blend (80:20) on Duralin flax fibre). -----	105
Figure 3.8	Schematic description of the micro-debond test setup. -----	106
Figure 3.9	Typical force traces for the three possible results of a shear test: (a) interface debonding (b) matrix failure and (c) fibre break. -----	106
Figure 3.10	Schematic representation of the pull-out test. -----	107
Figure 3.11	Schematic representation of the set-up used for coating flax fibres. -----	109
Figure 3.12	Procedure for making a thermoplastic microcomposite for microdebonding tests. -----	110
Figure 3.13	Characteristic force/displacement curve of micro-debond test (curve obtained from debonding a droplet of PP/MA-PP blend (90:10) from cleaned Duralin flax). -----	112
Figure 3.14	Characteristic pull-out force vs. embedded length curve (PP-droplet on dew-retted flax).-----	113
Figure 3.15	Interfacial shear strength values of the different flax types. -----	114

Figure 3.16	ESEM pictures of different flax fibres (a) Duralin flax (b) dew-retted flax (c) green flax. -----	116-117
Figure 3.17	Interfacial shear strength values of (normal and hot-cleaned) Duralin flax with varying amounts of MA-PP concentration in the matrix. -----	121
Figure 3.18	Schematic representation of the transformation in the fibre/matrix interface/interphase on increasing the polar groups in the matrix. -----	122
Figure 3.19	ESEM picture of hot-cleaned Duralin flax. -----	123
 CHAPTER 4		
Figure 4.1	Schematic representation of the set-up used for the (flax fibre/PP) microcomposite sample preparation. for fibre pull-out tests. -----	133
Figure 4.2	Schematic representation of a sample prepared for a fibre pull-out test. -----	134
Figure 4.3	A schematic representation of the tensile testing set-up used during the fibre pull-out test.-----	135
Figure 4.4	Picture of disassembled Brabender kneader. -----	136
Figure 4.5	Pictures of Duralin flax in PP (a) quench cooled from 210°C and (b) cooled from 210°C to 130°C at 10°C/min followed by isothermal heating at 130°C for 10 minutes. -----	138
Figure 4.6	Effect of time on transcrystalline thickness in Duralin flax/PP system at a temperature of 138°C. Cooling rate 10°C/min. a) 2 min, b) 6 min c) 10 min, d) 18 min e) 24 min and f) 34 min. -----	140
Figure 4.7	Development of transcrystallinity thickness with time, for different cooling rates and crystallisation temperatures, around Duralin flax, cooled from 210°C to different crystallisation temperatures and with different cooling rates.-----	141

Figure 4.8	Effect of crystallization temperature on transcrystallisation behaviour. (a) 125°C. (b) 130°C (c) 138°C and (d) 140°C. Cooled at 10°C/min from 210°C. Cooling time 10 min. -----	142
Figure 4.9	Effect of fibre type on transcrystallisation behaviour. (a) green flax, (b) dew-retted flax and (c) Duralin flax. at 130°C cooled at 10°C from 210°C. -----	143
Figure 4.10	Development of transcrystallinity thickness with time. for different cooling rates, around alkali treated combed dew-retted flax at 130°C. -----	144
Figure 4.11	Development of transcrystallinity thickness with time. for different cooling rates, around green flax. -----	145
Figure 4.12	Pictures of Duralin flax fibre and (a) PP/MA-PP (95:5 wt/wt) blend and (b) MA-PP matrix. -----	146
Figure 4.13	Picture of a microtomed slice of a pull-out sample, cut perpendicular to a Duralin fibre axis and seen under a polarised light optical microscope, showing the presence of (partial) transcrystallinity around the fibre cell bundle.-----	147
Figure 4.14	Typical curve of a pull-out force measurement.-----	148
Figure 4.15	Maximum pull-out force vs. embedded area for samples cooled from 210°C at 10°C/min followed by the isothermal heating. -----	149
Figure 4.16	Effect of slow cooling on the tensile strength of macrocomposites manufactured by compression moulding of flax/PP compound (Fibre volume content = 20%). -----	150
Figure 4.17	DSC study on flax/PP composite to study the effect of slow cooling on the matrix morphology. -----	151
Figure 4.18	DSC study on flax/PP quench cooled composite. Heating rate of 30°C/min reduced the double peak (Figure 4.17), in quench cooled sample, to single peak. -----	152
Figure 4.19	Fracture surfaces of (a) a quench cooled and (b) a slow cooled flax/PP macrocomposites manufactured by compression moulding of compound. -----	152

CHAPTER 5

Figure 5.1	Schematic representation of paper-making method.-----	163
Figure 5.2	Tensile modulus of the flax /PP composites (○) and the flax/MAPP composites (●) as a function of the flax fibre length. -----	166
Figure 5.3	Tensile strength of the PP/flax composites (○) and the MA-PP/flax composites (●) as a function of the flax fibre length. -----	168
Figure 5.4	Notched Charpy impact strength of the PP/flax composites (○) and the MA-PP/flax (●) as a function of the flax fibre length.-----	171
Figure 5.5	Scanning electron micrograph of fracture surface of PP/flax composite ($V_f=0.2$ and fibre length=25 mm).-----	171
Figure 5.6	Scanning electron micrograph of fracture surface of flax/MA-PP composite ($V_f=0.2$ and fibre length = 25 mm). ----	172
Figure 5.7	Tensile modulus of the PP/flax composites (○) and the MA-PP/flax composites (●) as a function of fibre volume fraction. -----	173
Figure 5.8	Tensile strength of the PP/flax composites (○) and the MA-PP/flax composites (●) as a function of fibre volume fraction. -----	175
Figure 5.9	Notched Charpy impact strength of the PP/flax composites (○) as a function of fibre volume fraction. The solid line represents data for GMT. -----	177
Figure 5.10	Dart impact energy of the PP/flax composites (○) as a function of fibre volume fraction, together with an experimentally obtained data for a commercial GMT-grade. -----	177
Figure 5.11	Fibre diameter distribution of three types of flax fibres: (i) scutched 6 mm long flax, (ii) hackled 6 mm long flax and (iii) scutched 25 mm long flax. -----	180

Figure 5.12	Tensile strength of scutched (dew retted) 6 mm (□) and hackled (warm water retted) 6 mm (■) PP, flax composites as a function of fibre volume fraction. -----	180
 CHAPTER 6		
Figure 6.1	The schematic representation of the pin impregnation process for the production of well-wetted glass/thermoplastic strands. -----	188
Figure 6.2	Amandus Kahl pelletising press (photo courtesy Amandus Kahl GmbH & Co., Hamburg, Germany). -----	192
Figure 6.3	Picture of flax fibre pills made in Amanadus Kahl pelletising press (right) and chopped Duralin flax fibres (left). -----	193
Figure 6.4	Picture of compounding set-up (Werner & Pfleiderer twin screw extruder). -----	194
Figure 6.5	The schematic representation of production of long natural fibre reinforced thermoplastic granules (LFT).-----	195
Figure 6.6	Picture of granules obtained from various operations: (A) kneader, (B) long fibre granules (LFT), (C) Henschel kinetic mixer and (D) twin screw extruder.-----	198
Figure 6.7	Fibre length distribution after various compounding (preparatory) methods. -----	198-200
Figure 6.8	Picture of cross-section of long fibre granule reinforced with natural fibre showing skin-core structure (Fibre content 30wt%, diameter of granule = 5 mm and cutting length = 20 mm).-----	201
Figure 6.9	Tensile modulus of Duralin flax/(MA)PP composites manufactured through compression moulding and injection moulding. -----	203
Figure 6.10	Tensile strength of Duralin flax/(MA)PP composites manufactured through compression moulding and injection moulding. -----	204

Figure 6.11	The picture of fibres left after dissolution of matrix polymer in injection moulded composite. -----	204
Figure 6.12	Fibre length distribution measured after dissolving the matrix in injection moulded composite containing 20 volume% Duralin flax. -----	205
Figure 6.13	Tensile modulus of injection moulded Duralin flax/(MA-)PP composites with varying amount of MA-PP content in the matrix. -----	206
Figure 6.14	Tensile strength of injection moulded Duralin flax/(MA-)PP composites with varying amount of MA-PP content in the matrix. -----	206
Figure 6.15	Fibre length distribution in injection moulded samples. ----	209-210
Figure 6.16	Tensile strength of injection moulded Duralin flax/(MA-)PP composites compounded through various methods. -----	212
Figure 6.17	Stiffness of injection moulded Duralin flax/(MA-)PP composites compounded through various methods. (Extrapolated to fibre content of 30weight% using micromechanical model).-----	213
Figure 6.18	Chemical structure of POM and nylon6. -----	214
 CHAPTER 7		
Figure 7.1	Moisture content as a function of time for a typical Fickian process (Springer, 1981). -----	221
Figure 7.2	Moisture content as a function of time for green flax/PP, Duralin/PP and Duralin/MA-PP composites.-----	224
Figure 7.3	Effect of the relative humidity on the moisture absorption of green and Duralin flax fibres (Stamboulis et al., 2000). -----	226
Figure 7.4	Thickness of composite plates, immersed in water, as a function of time for green flax/PP, Duralin/PP and Duralin/MA-PP composites. -----	227

Figure 7.5	Effect of moisture content on the modulus of green flax/PP, Duralin/PP and Duralin/MA-PP composites. -----	229
Figure 7.6	Effect of moisture content on the tensile strength of green flax/PP, Duralin/PP and Duralin/MA-PP composites.-----	230
Figure 7.7	Effect of relative humidity on the average tensile strength of green- and Duralin flax fibres (8 mm gauge length).-----	231
Figure 7.8	Effect of relative humidity on the average tensile strength of green- and Duralin flax fibres (3.5 mm gauge length). -----	232
Figure 7.9	Time dependence of moisture absorption of green- and Duralin flax fibres at 93% of relative humidity. -----	233

CHAPTER 8

Figure 8.1	Chemical structure of Polyhydroxyalkanoate.-----	240
Figure 8.2	Tensile strength of PHB/flax NMT composites (■), PP/flax (NMT) and PP/glass fibre (GMT) composites as a function of fibre volume fraction.-----	245
Figure 8.3	Initial modulus of PHB/flax NMT composites (■), PP/flax (NMT) and PP/glass fibre (GMT) composites as a function of fibre volume fraction.-----	246
Figure 8.4	Elongation-at-break of PHB/flax NMT composites (■) as a function of fibre volume fraction. -----	247
Figure 8.5	Notched Izod impact resistance of PHB/flax NMT composites (■) as a function of fibre volume fraction. -----	248
Figure 8.6	SEM pictures of impact fracture surface of PHB/flax NMT composites.-----	248
Figure 8.7	Tensile strength of flax/PHB(/HV) composites versus fibre volume fraction and HV content in the copolymer. -----	249
Figure 8.8	Tensile modulus of flax/PHB(/HV) composites versus fibre volume fraction and HV content in the copolymer. -----	249
Figure 8.9	Elongation-at-break of flax/PHB(/HV) composites versus fibre volume fraction and HV content in the copolymer. -----	250

Figure 8.10	Notched Izod impact resistance of flax/PHB(HV) NMT composites versus fibre volume fraction and HV content in the copolymer. -----	251
Figure 8.11	Elongation-at-break (%) of PHB/flax NMT composites as a function of fibre volume fraction and cooling temperature during compression moulding. -----	252
Figure 8.12	Dynamic mechanical characteristics versus temperature for compression moulded PHB samples, which were cooled at (■) 60°C and (▲) 20°C (mould temperature). -----	253
Figure 8.13	Initial modulus of PHB/flax composites as a function of fibre volume fraction and manufacturing method.-----	254
Figure 8.14	Tensile strength of PHB/flax composites as a function of fibre volume fraction and manufacturing method.-----	255
Figure 8.15	Elongation-at-break (%) of PHB/flax composites as a function of fibre volume fraction and manufacturing method.---	255
Figure 8.16	Notched Izod impact resistance of PHB/flax composites as a function of fibre volume fraction and manufacturing method.-----	256
Figure 8.17	Pictures of different stages of biodegradation of PHB/8%HV/flax (20Volume %) composites. -----	258
Figure 8.18	Normalised stiffness and strength of PHB/8%HV/flax composites after burial in soil.-----	259
Figure 8.19	Normalised weight of tensile bars after burial in soil. -----	259
 CHAPTER 9		
Figure 9.1	Flow diagram of life cycle of a product. -----	262
Figure 9.2	Phases of an LCA as described in ISO14040: 1997. -----	268
Figure 9.3	Example of a process tree (Source: SimaPro User manual). -----	270

Figure 9.4	Example of a classification. The highest score is scaled to 100%. The classes are taken from the Eco-indicator 95 method: Greenhouse effect, Ozone layer depletion, Heavy metals, Carcinogen. Winter smog, Summer smog, Pesticides, Energy use Solid waste disposal. -----	272
Figure 9.5	The normalised effect score. The length of the columns is now scaled to a normalised effect score. -----	273
Figure 9.6	Evaluated effect scores. After weighting, the relative importance of the normalised effect scores is added. -----	274
Figure 9.7	The weighted scores can be added for a final judgement. -----	274
Figure 9.8	Graphical representation of the characterisation obtained by scaling the effects due to various combinations of composite use (for non-automotive applications) and disposal. -----	287
Figure 9.9	Graphical representation of the normalised effect score due to various combinations of composite use (for non-automotive applications) and disposal. -----	288
Figure 9.10	Graphical representation of the evaluated effect score due to various combinations of composite use (for non-automotive applications) and disposal. -----	289
Figure 9.11	Graphical representation of the indicator obtained by summarising the evaluated numbers for non-automotive applications. -----	290
Figure 9.12	Graphical representation of the characterisation obtained by scaling the effects due to various combinations of composite use (for automotive applications) and disposal. -----	291
Figure 9.13	Graphical representation of the normalised effect score due to various combinations of composite use (for automotive applications) and disposal. -----	292
Figure 9.14	Graphical representation of the evaluated effect score due to various combinations of composite use (for automotive applications) and disposal. -----	293

Figure 9.15	Graphical representation of the indicator obtained by summarising the evaluated numbers for automotive applications. -----	294
--------------------	--	-----

CHAPTER 10

Figure 10.1	The cross-sectional view of flax fibre showing around 7 fibre cells together forming a technical flax fibre (fibre bundle). -----	304
Figure 10.2	Kelly-Tyson model predictions of the tensile strength of NMT with varying interfacial shear strength and fibre efficiency. -----	305
Figure 10.3	Kelly-Tyson predictions of the tensile strength of NMT with varying fibre strength and fibre efficiency. -----	306

LIST OF TABLES

	Page
CHAPTER 1	
<i>Table 1.1</i> Comparison of properties of GMT and NMT (compression moulded) composites having fibre content of 30wt ⁰ .	43
CHAPTER 2	
<i>Table 2.1</i> Chemical composition of vegetable fibres.	58
<i>Table 2.2</i> Physical characteristics of plant fibres.	58
<i>Table 2.3</i> Morphological characteristics of plant fibres.	59
<i>Table 2.4</i> Mechanical properties of plant fibres.	59
CHAPTER 3	
<i>Table 3.1</i> List of some of the compatibilisers and modifications studied for cellulosic materials and plastic systems.	93
<i>Table 3.2</i> List of some of the cellulose / thermoplastic systems studied.	94
<i>Table 3.3</i> O/C ratios of the different flax types.	114
<i>Table 3.4</i> Interfacial shear strength values of the different flax types with pure PP droplets.	119
<i>Table 3.5</i> O/C ratios of the different flax types.	119
CHAPTER 4	
<i>Table 4.1</i> Conditions used to obtain different transcrystalline thickness for pull-out force testing.	136

Table 4.2	IFSS calculated from the slope of pull-out force vs. embedded area curves (and Equation 3.5) for samples cooled from 210°C at 10°C/minute followed by isothermal heating and quench cooling. -----	149
------------------	--	-----

CHAPTER 6

Table 6.1	Overview of the process parameters used for compounding of PP/flax and (POM) Polyoxymethylene/flax. -----	194
Table 6.2	Parameters for injection moulding process for short flax fibre reinforced polypropylene (112MN40) and flax/POM. -----	197
Table 6.3	Tensile properties of flax /PP composites. (Impact type = notched Charpy Impact test). -----	208
Table 6.4	Effect of injection rate during injection moulding on the tensile properties of flax/PP (112MN40) composite. Fibre loading 20 wt%.-----	209
Table 6.5	Tensile properties of flax /nylon, glass /nylon, flax/POM and glass/POM composites.-----	215

CHAPTER 7

Table 7.1	Maximum moisture content and diffusivity of flax/polypropylene composites. -----	224
Table 7.2	Average maximum moisture content of flax fibres at different levels of Relative Humidity (RH). -----	225

CHAPTER 8

Table 8.1	Properties of Polyesters used.-----	242
------------------	-------------------------------------	-----

CHAPTER 9

Table 9.1	The characterisation step (using weighting factors) produces a number of effect scores. -----	271
Table 9.2	Required properties for an automotive application. -----	277
Table 9.3	The estimated (approximate) fibre volume fraction (V_f) and weight fraction (W_f) of GMT and NMT required (Chapter 5) to obtain the required property for an automotive application. -----	278
Table 9.4	The weight of NMT having the same volume (3.2 times in the case of impact criterion) as 1 kg of GMT. -----	279
Table 9.5	Energy consumption for the production of 1 kg GMT (prepreg) sheet.-----	280
Table 9.6	Data concerning the compression moulding of a GMT product and an NMT product. -----	280
Table 9.7	The extra weight of NMT required due to wastage during processing.-----	281
Table 9.8	Calculation of additional fuel consumption because of added weight (for impact critical applications). -----	282
Table 9.9	Calculation of additional fuel consumption because of added weight, for strength and stiffness criterion. -----	282
Table 9.10	Codes used for various combinations of composite criterion, use and disposal. -----	284

LIST OF ABBREVIATIONS AND SYMBOLS

ABS	Acrylonitrile butadiene styrene
AES	Auger electron spectroscopy
ASA	Alkenyl succinic anhydride
ASTM	American Standards for Testing Methods
BBP	Butyl benzyl phthalate
CFCs	Chlorofluorocarbons
CPE	Chlorinated polyethylene
CTDICC	Cardanol derivative of toluene, 2, 4 di-isocyanate
DMTA	Dynamic mechanical thermal analysis
DSC	Differential Scanning Calorimetry
ECM	Extrusion compression moulding
EPDM rubber	Ethylene propylene diene monomer rubber
ESCA	Electron Spectroscopy for Chemical Analysis
ESEM	Environmental Scanning Electron Microscopy
FTIR	Fourier Transformed Infrared Spectroscopy
GMT	Glass fibre mat reinforced thermoplastic
HB	Hydroxy butyrate
HV	Hydroxy valerate
IFSS	Interfacial shear strength
i-PP	Isotactic polypropylene
IR	Infra red
LCA	Life cycle assessment (or Life Cycle Analysis)
LDPE	Low density polyethylene
LEIS	Low energy ion spectroscopy
LFT	Long fibre reinforced thermoplastic
MAPP	Maleic anhydride grafted polypropylene
MFI	Melt flow index
NMR	Nuclear magnetic resonance
NMT	Natural fibre mat reinforced thermoplastic
PA-6,6	Polyamide-6,6 (Nylon-66)

PBT	Polybutylene terephthalate
PEI	Polyether imide
PEEK	Polyether ether ketone
PEKK	Polyether-ketone-ketone
PES	Polyether sulphone
PET	Polyethylene terephthalate (Polyester)
PHA	Polyhydroxy alkanoate
PHB	Polyhydroxy butyrate
PHB/HV	Polyhydroxy butyrate-co-hydroxyvalerate
PHV	Polyhydroxy valerate
PLA	Polylactic acid
POM	Polyoxy methylene
PP	Polypropylene
PPS	Polyphenylene sulphone
PS	Polystyrene
PVC	Polyvinylchloride
s.d	Standard deviation
SEM	Scanning electron microscopy
SETAC	Society for environmental toxicology and chemistry
SF	Short fibre
SFRP	Short fibre reinforced plastics
SIMS	Secondary-ion mass spectroscopy
SMC	Sheet moulding compound
SPM	Small particulate matter
TGA	Thermogravimetric analysis
UV	Ultra-violet
XPS	X-ray photoelectron spectroscopy

SYMBOLS

<i>C</i>	Specific heat
<i>D</i>	Mass diffusivity

D_c	Mass diffusivity in composite
d_f	Fibre diameter
E_c	Composite stiffness
E_f	Fibre stiffness
E_i	Interface Young's modulus
E_m	Matrix stiffness
γ_1	Surface energy of the adsorbent (for example a fibre)
γ_{12}	Free (interfacial) energy between the components (liquid-solid interface)
γ_2	Surface energy of the adsorbate (for example polymer melt)
γ_c	Critical surface tension of wetting
G_i	Interfacial shear toughness
G_m	Shear modulus of the matrix
γ_{sv}	Surface free energies or surface tensions of the solid-vapour interface
γ_{sl}	Surface free energies or surface tensions of the solid-liquid interface
γ_{lv}	Surface free energies or surface tensions of the liquid-vapour interface
h	Material thickness
k	Fibre efficiency factor
K	Thermal conductivity
χ_i	Fibre geometrical packing factor
L_c	Critical fibre length
L_{em}	Fibre embedded length
L_j	Effective fibre length
M_i	Moisture concentration inside the material
M_m	Maximum moisture content
$M_{m,c}$	Maximum moisture content in composite
$M_{m,f}$	Maximum moisture content in fibre
M_t	Moisture content
μ	Interfacial coefficient of friction
η_{LE}	Fibre length efficiency factor
η_o	Fibre orientation factor
ν	Poisson's ratio

O/C ratio	Oxygen / carbon ratio
ϕ_c	Critical concentration
ϕ_n	Fibre orientation angle
P_o	Matrix shrinkage pressure on fibre
R	Mean spacing of the fibres
ρ	Density
r_f	Fibre radius
σ_f	Tensile stress on the fibre
σ_f	Average fibre strength
$\sigma_{u c}$	Composite tensile strength
σ_m	Matrix tensile strength
$\tan \delta$	Loss factor
τ_i	Interfacial shear (bond) strength
τ_m	Minimum shear stress
T_C	Crystallisation temperature
T_g	Glass-transition temperature
θ	Contact angle
T_{max}	Maximum crystallisation temperature
U_f	Total energy involved in the fracture of the single fibre
U_m	Matrix fracture energy
U_x	Energy factor covering all the fibre-related energy absorption mechanisms
V_f	Fibre volume fraction
γ	Fibre debonding length
W_a	Work of adhesion

GLOSSARY

CO ₂ neutral	Carbon dioxide evolved during disposal is equal to carbon dioxide absorbed during growth.
Cuticle	The protective layer that covers the epidermis in higher plants.
Decortication	Process of breaking the wooden flax stem and removing the woody parts.
Dicotyledonous	A flowering plant with two embryonic seed leaves or cotyledons that usually appear at germination.
Extrusion	The act or process of pushing or thrusting out.
Fibre	A slender and greatly elongated solid substance.
Hackle	A steel flax comb.
Hackling	To comb using a hackle.
Mercerisation	Process of treating fibre (or fabric) with a solution of caustic alkali.
Modulus	The measure of the elastic force on any substance, expressed by the ratio of a stress on a given unit of the substance to the accompanying distortion, or strain.
Non-woven	Form (sheet) made by fibre consolidation through a process not involving weaving e.g. by needle punching.
Pericarp	The wall of a ripened ovary; fruit wall.
Phloem	Tissue in higher plants that conducts synthesised food substances to all parts of the plant.
Plastic	Capable of undergoing continuous deformation without rupture or relaxation (Capable of being formed or shaped)
Plasticiser	Any of various substances added to plastics or other materials to make or keep them soft or pliable.
Plastics	Polymeric materials (usually organic) having large molecular weight, which can be shaped by flow.
Protoplasm	The living contents of a cell.
Retting	A biological process that degrades pectin and lignin, loosening the stem and fibres and allowing them to be separated.

Scutching	Deseeding, breaking by breaker rollers, and beating of fibres.
Shive	A thin piece or fragment; specifically, one of the scales or pieces of the woody part of flax removed by the operation of breaking.
Sliver	A continuous strand of loose fibres e.g. wool, flax, or cotton, ready for drawing and twisting.
Specific property	Specific properties are properties that have been divided by the material density.
Straw	A single dry or ripened stem of an herbaceous plant.
Tex	Unit of linear density of textile materials defined as: Weight in grams per 1000m length of material.

1. INTRODUCTION

In this chapter the subjects of thermoplastic composites and natural fibre composites are introduced. The present scenario, aims of the present thesis and structure of the thesis are presented.

A composite material is defined as a material having two or more chemically distinct phases, which at the microscopic scale are separated by an interface or an interphase. The continuous phase is termed the matrix and other components reinforcements or fillers. Where interface is a two-dimensional separation and interphase is a 3-dimensional separation between the matrix and reinforcement or filler. The term reinforcement is used when improvement in mechanical properties of the composite is achieved, and filler if the result is a cost reduction or some other property modification e.g. toughness. Figure 1.1 shows the classification of composite materials. Ideally, the component added to the matrix would act both as reinforcement and as filler, improving both the mechanical properties and reducing the overall cost. Fibre-reinforced composite materials consist of fibres of high strength and modulus embedded in or bonded to a matrix with distinct interfaces between them. In this form, both fibres and matrix retain their physical and chemical identities, yet they produce a combination of properties that cannot be achieved with either of the constituents acting alone. For some properties, the composite by far exceeds the sum of their constituents. For example, the fracture energy of glass is about 7 J/m, that of a typical plastic about 200 J/m, and a composite of the two about 175,000 J/m (Broutman et al., 1974). In general, fibres are the principal load-carrying members, while the surrounding matrix keeps them together, acting as a load transfer medium between the fibres and protecting them

from environmental damages due to elevated temperatures and humidity (Mallick, 1993).

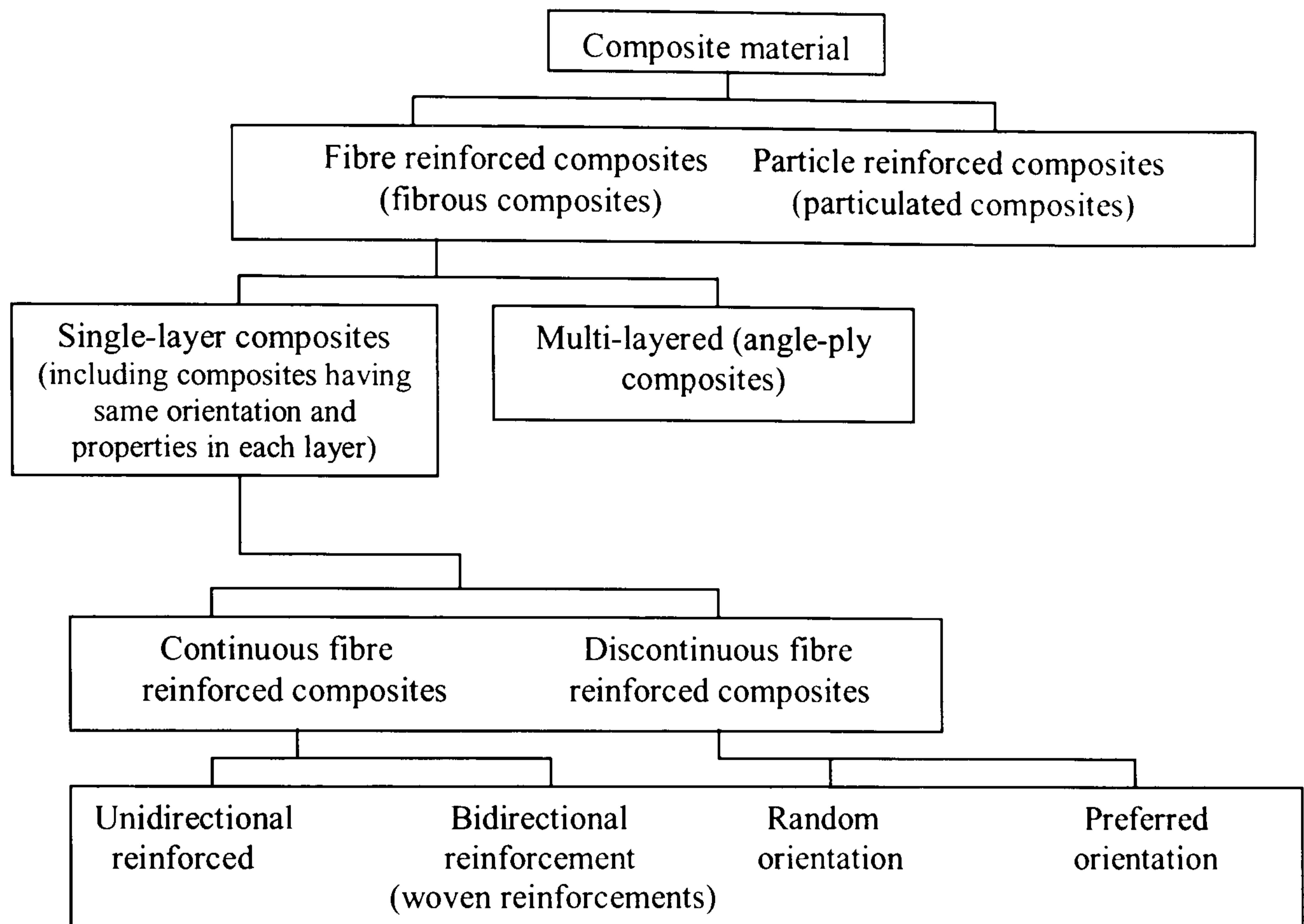


Figure 1.1 Classification of composite materials.

The composite matrix can be a plastic, a metal, a ceramic or some other inorganic material. Plastic (polymer) matrices are of two main types: thermoset or thermoplastic (Figure 1.2).

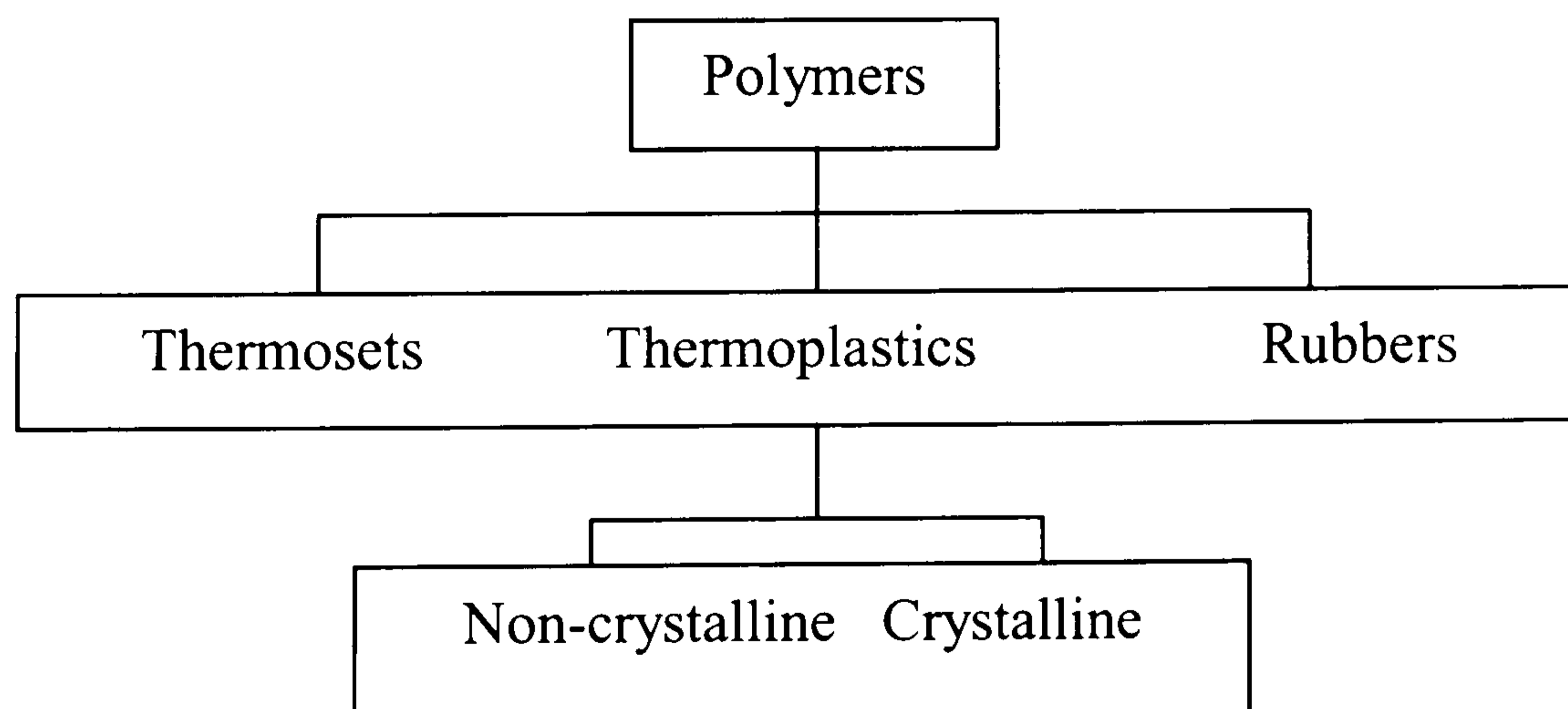


Figure 1.2 Classification of polymeric materials.

Thermoplastics are polymeric materials, which melt or soften when heated but become rigid and hard when cooled. Thus, they can be melted to be reprocessed many times and are therefore recyclable. Thermosets are polymeric materials, which do not melt once they are set or cross-linked. Very high temperatures cause

them to decompose. A large proportion of composites are based on plastic matrices and the choice depends on the properties required for a particular application and the costs involved.

The properties of composites are strongly influenced by factors such as processing conditions, proportions and properties of the matrix and reinforcement, the nature of adhesion between these and the shape, size, orientation and distribution of the reinforcement or filler. The concept of improving the properties of a material through addition of reinforcing material seems to have a long history. The use of straw reinforced clay for making stronger bricks is one of the earliest composites referred in the literature (Prasad, 1992). Steel-rod reinforced concrete is another example of a commonly used composite material. With the development of glass-fibres and other high performance fibres like boron, carbon, aramid (Twaron[®], Kevlar[®]), ultra-high molecular weight polyethylene (Dyneema[®] and Spectra[®]) etc., the fibre-reinforced plastic composites are used in number of areas like sporting goods, marine industry, aerospace industry, bio-medical implants, electrical and electronics industry (e.g. printed-circuit boards), defence etc. Fibre reinforced polymer composites offer a number of potential advantages such as high modulus, specific strength, fracture toughness, excellent durability and design flexibility. Apart from reinforcement/filler, other additives like coupling agent, processing additives or rubber to modify the matrix properties can also be added in the matrix or binding material. These additives are especially chosen to improve some specific property (e.g. polymer viscosity, interfacial adhesion etc.) and are usually added in very small quantities. Depending on the various components present in the composite material as well as the shape, compatibility/bonding between various components of the composites, orientation and quantity of the components, the property of the final material can be engineered.

1.1 Thermoplastic composites

The introduction of thermoplastic resins as matrices for continuous-fibre-reinforced composites has attracted considerable attention since the mid-80s. As matrix materials for composites, thermoplastics offer a wide range of advantages

over thermosets, including high toughness, increased moisture resistance, rapid processing, unlimited shelf-life and better recyclability. Most research activities in this area, however, have been focused on various types of high-temperature polymers such as poly(ether imide) (PEI), poly(phenylene sulphone) (PPS), poly(ether sulphone) (PES) and poly(ether ether ketone) (PEEK). Processing of these high-performance materials generally requires high temperatures and pressures and due to their high price, applications are limited to niche markets, such as aerospace.

Therefore, current research activities have shifted towards the development of 'cost-performance' rather than 'high-performance' thermoplastic composites. Since cost-effectiveness depends also on raw material cost, most composite systems that are considered as an attractive candidate for this 'cost-performance' market are based on E-glass fibres and resins such as polypropylene (PP), polyamide-6,6 (PA-6,6), poly(ethylene terephthalate) (PET) or poly(butylene terephthalate) (PBT). Especially PP offers a number of favourable characteristics as a matrix material for high volume applications of composite materials. It exhibits many beneficial properties such as low price, high toughness, low density, relatively high thermal stability, good (di)electrical properties and chemical resistance. Moreover, PP can easily be processed and recycled and is available in a large number of grades. Especially, upgrading via the use of glass-fillers, focusing on improved stiffness, strength and thermal stability has been very successful in closing the gap between the commodity PP and the engineering thermoplastics. In application terms among the glass-filled thermoplastics, polypropylenes currently have the second highest tonnage use, following Nylon 66 (Gibson, 1995). Glass-mat-reinforced thermoplastic (GMT) materials, being stampable sheet products based on commodity resins such as polypropylene (PP) and moderate loadings of relatively long glass fibres in random array, have proven to be very successful in high-volume markets notably the automotive industry (Berglund and Ericson, 1995). Because of their excellent price-performance ratio, E-glass fibres are by far the most important fibres for these types of composites.

1.2 Processing of thermoplastic composites

Dominant processing routes for the production of glass fibre reinforced thermoplastic include extrusion compounding followed by injection moulding (short fibre composites). The largest tonnage of reinforced polypropylenes is converted into short fibre (SF) reinforced granules by extrusion compounding (Gibson, 1995). Passing the glass reinforcement through an extruder consumes power and causes wear, in addition to producing fibre degradation. Moreover, if only the polymers were passed through the extruder this would reduce the machine capacity needed and possibly avoid the need for using an expensive twin-screw machine. Extrusion compounding method leads to extensive fibre degradation and the maximum fibre length that can be retained appears to be limited to values substantially below 1 mm.

In the last decade, however, there have been two developments, which have extended the range of potential applications (Gibson, 1995). One of these is the strand impregnation technology, which now exists for the production of 'long fibre thermoplastics' (LFTs) injection moulding materials, with considerably enhanced properties. The strand impregnation route for the LFT materials can also be used to manufacture continuous fibre reinforced polypropylenes for stamping, pultrusion and filament winding. Generally the length of the uniaxial strands in LFT compounds is 10 mm for injection moulding or 25 mm for extrusion compression moulding (ECM). Figure 1.3 shows a schematic representation of the hot-melt impregnation of thermoplastic prepregs (Mallick, 1993). Prepregs are intermediate composite products with pre-impregnated fibres. In this process, collimated fibre tows are pulled through a die attached at the end of an extruder, which delivers a fine sheet of hot polymer melt under high pressure to the die. To expose the filaments in the fibre tows to the polymer melt, they are spread by an air jet before the fibre tows enter the die (Figure 1.3). The hot prepreg exiting from the die is rapidly cooled by a cold air jet and wound around a take-up roll.

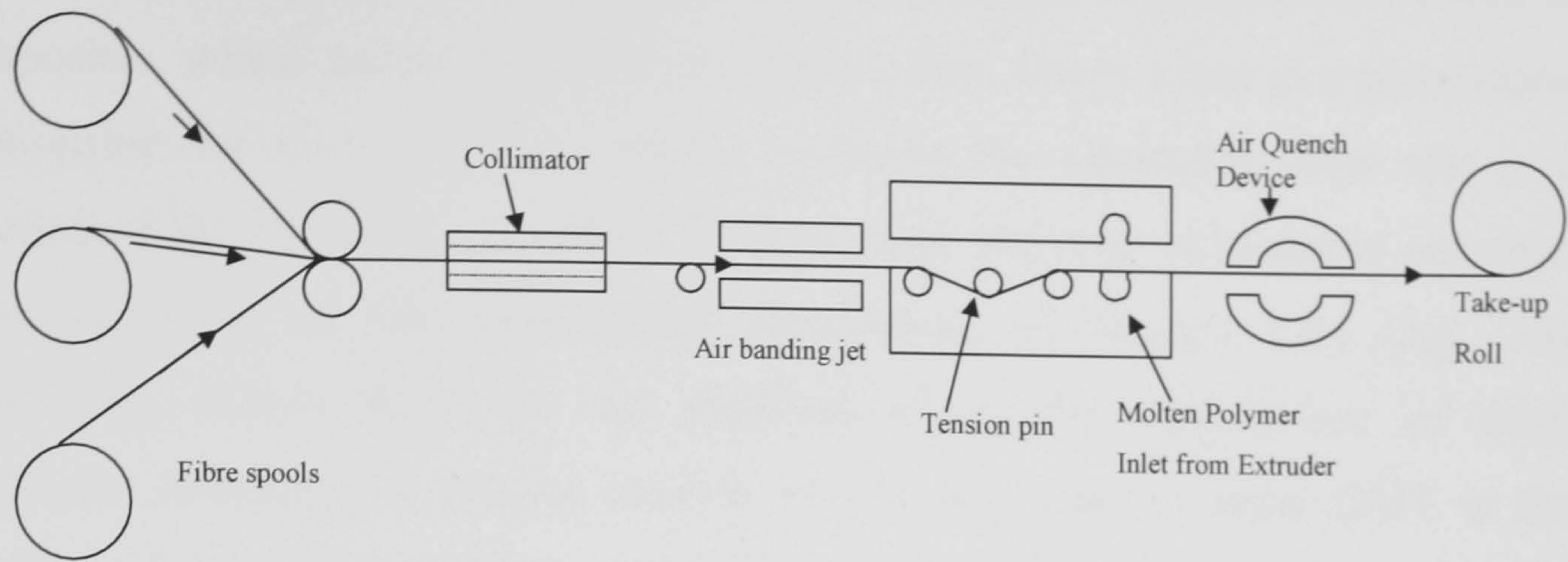


Figure 1.3 Hot melt impregnation of thermoplastic prepregs (Mallick, 1993).

The other significant advance has been the appearance of the glass mat thermoplastics (GMTs). In the late 1980s, following their introduction, GMTs, which are processed by stamping rather than by injection moulding, showed the most rapid growth rate of any type of composite material, achieving a European usage of around 35,000 tonnes per year by 2000 (Brooks, 2000).

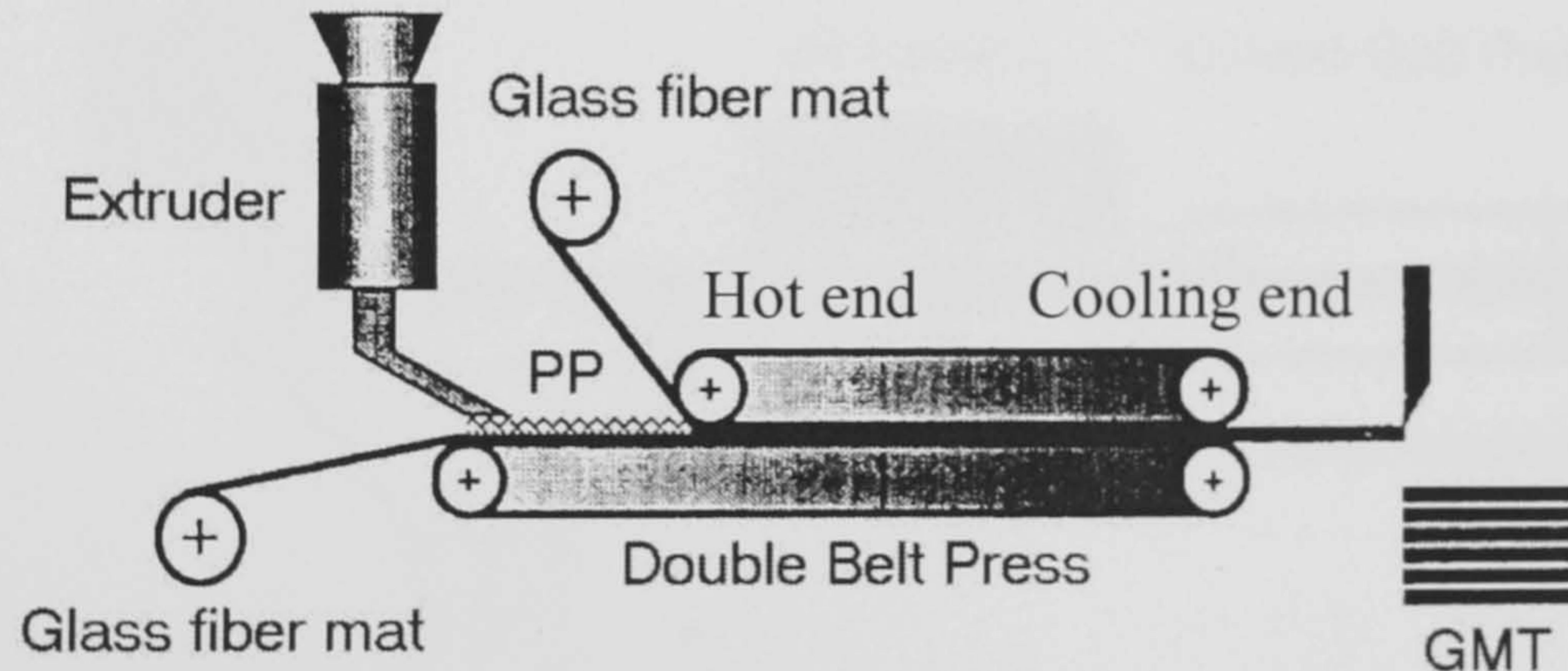


Figure 1.4 The production process for GMT thermoplastic sheets.

Two different methods are available for the manufacture of GMTs. In the melt process (Figure 1.4) polypropylene granulate is heated, in an extruder, until it becomes soft and viscous. The polypropylene paste is transported between two layers of glass fibre mats to a double belt press where the actual impregnation of the fibres take place. The impregnated fibres are cooled to obtain the solidified sheet. The sheets of GMT are cut into more convenient sizes and shipped to the customer. One advantage of this process is that continuous glass fibres can be used.

Due to high viscosity of thermoplastics it is difficult to impregnate the fibres in composites, which can be explained by Darcy's law. Darcy's law is a generalised relationship for flow in porous media. It shows the volumetric flow rate is a function of the flow area, elevation, fluid pressure and a proportionality constant. However, some of the fundamental assumptions of Darcy's Law (e.g. 2-D Newtonian, Stokes flow) are not satisfied during the manufacture of thick composite structures. A second process that is also used to make GMT is the solution mixing process (Figure 1.5). Good mixing is achieved by stirring water, cut glass fibres, polymer powder and a foaming agent vigorously in a large vessel. At the bottom of the vessel the mixture is released on a conveyor belt, where the foam is removed. Next the remaining liquid is dried via infrared heating followed by consolidation in a double belt press. Due to the fact that cut glass fibres are used it is easy to see that only randomly oriented GMT can be made with this process.

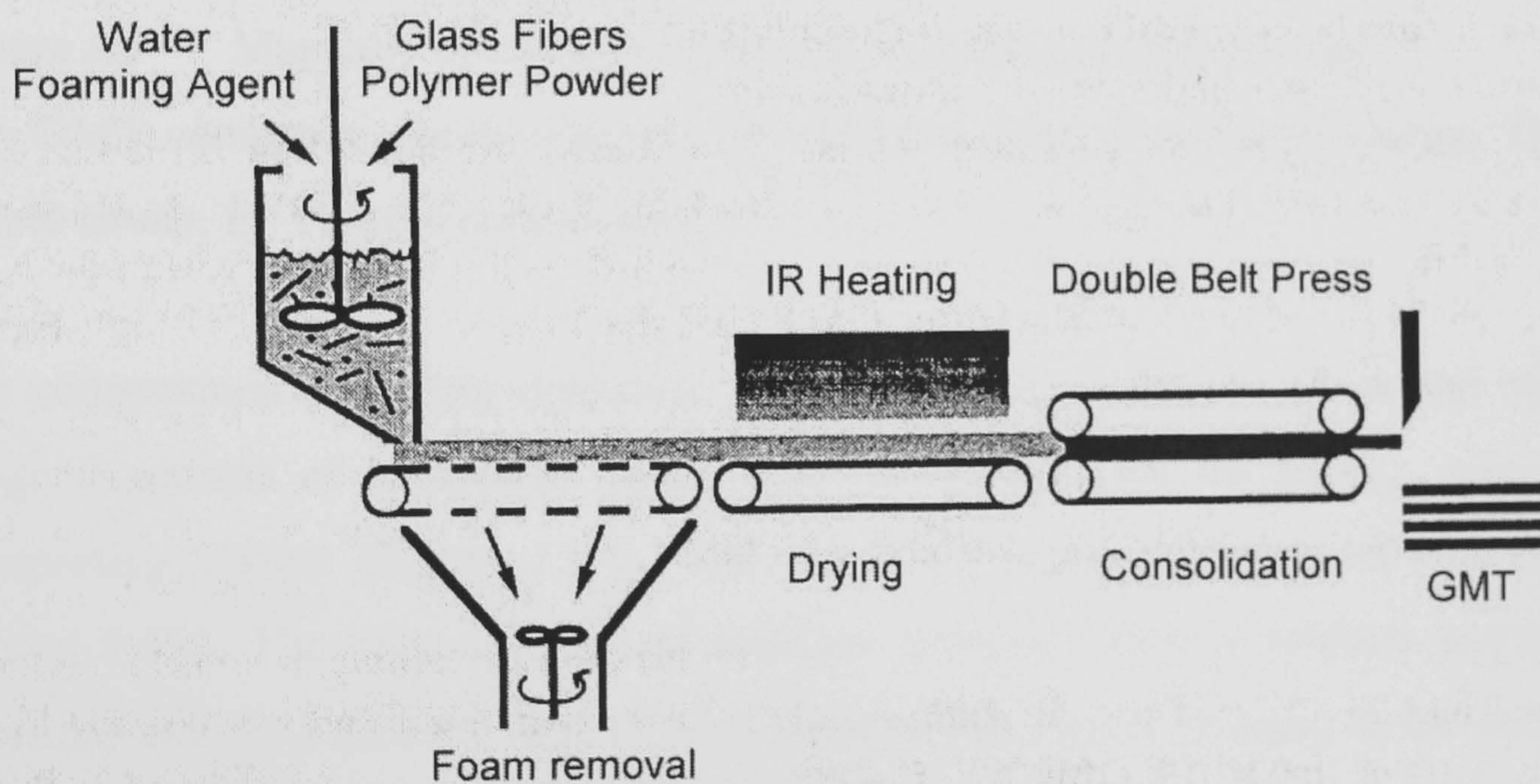


Figure 1.5 The solution mixing ('paper-making') production process of thermoplastic GMT sheets.

Compression moulding (Figure 1.6) is used for transforming sheets, preform mats, etc. into finished products in matched moulds. The principal advantage of compression moulding is its ability to produce parts of complex geometry in short periods of time. Non-uniform thickness, ribs, bosses, flanges, holes and shoulders, for example, can be incorporated during the compression moulding process. Thus, it allows the possibility of eliminating a number of secondary finishing operations such as drilling, forming and welding. In conclusion, the compression moulding

process is suitable for the high-volume production of composite parts and fully automated production lines are also possible. It is considered the primary production method for many structural automotive components.

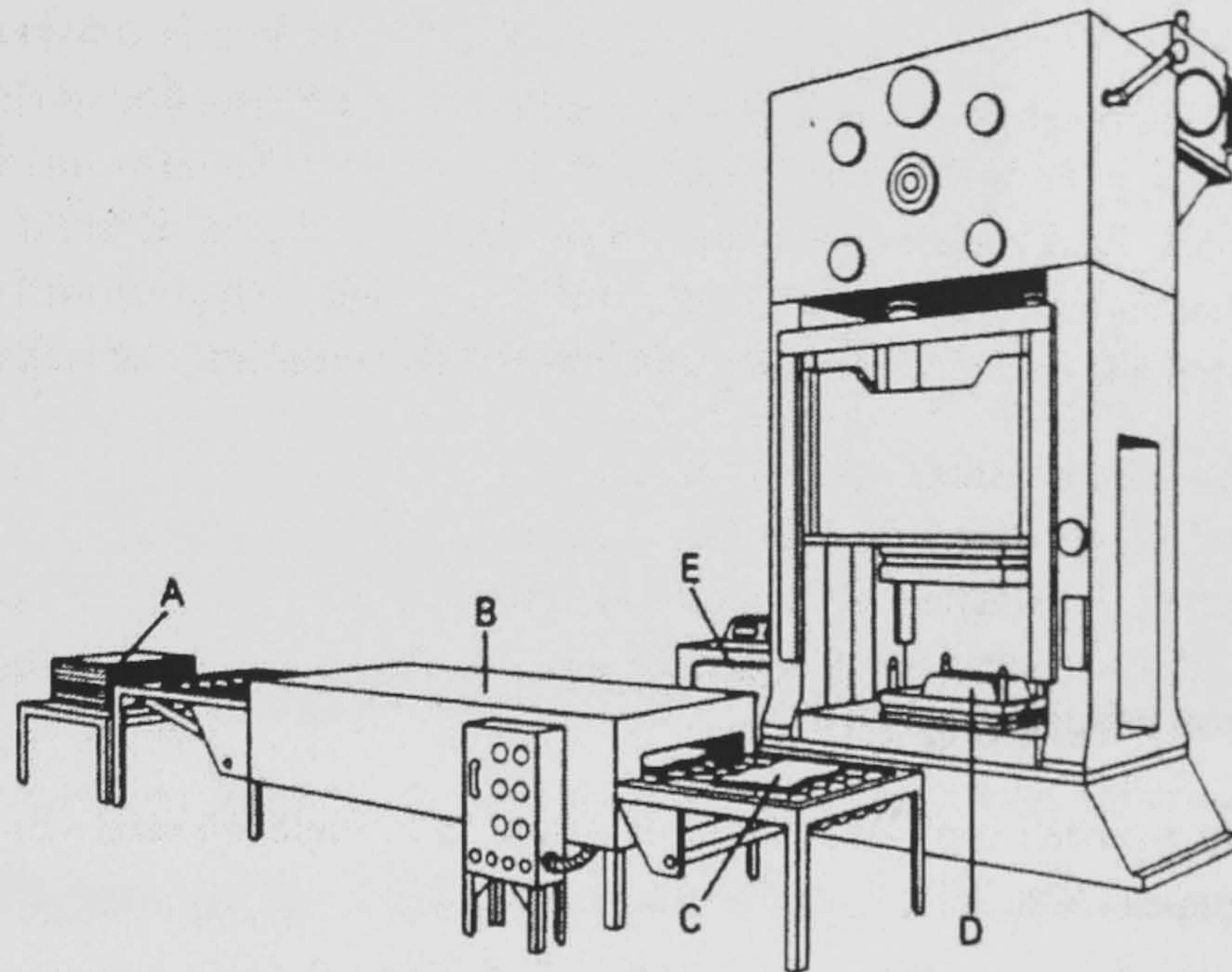
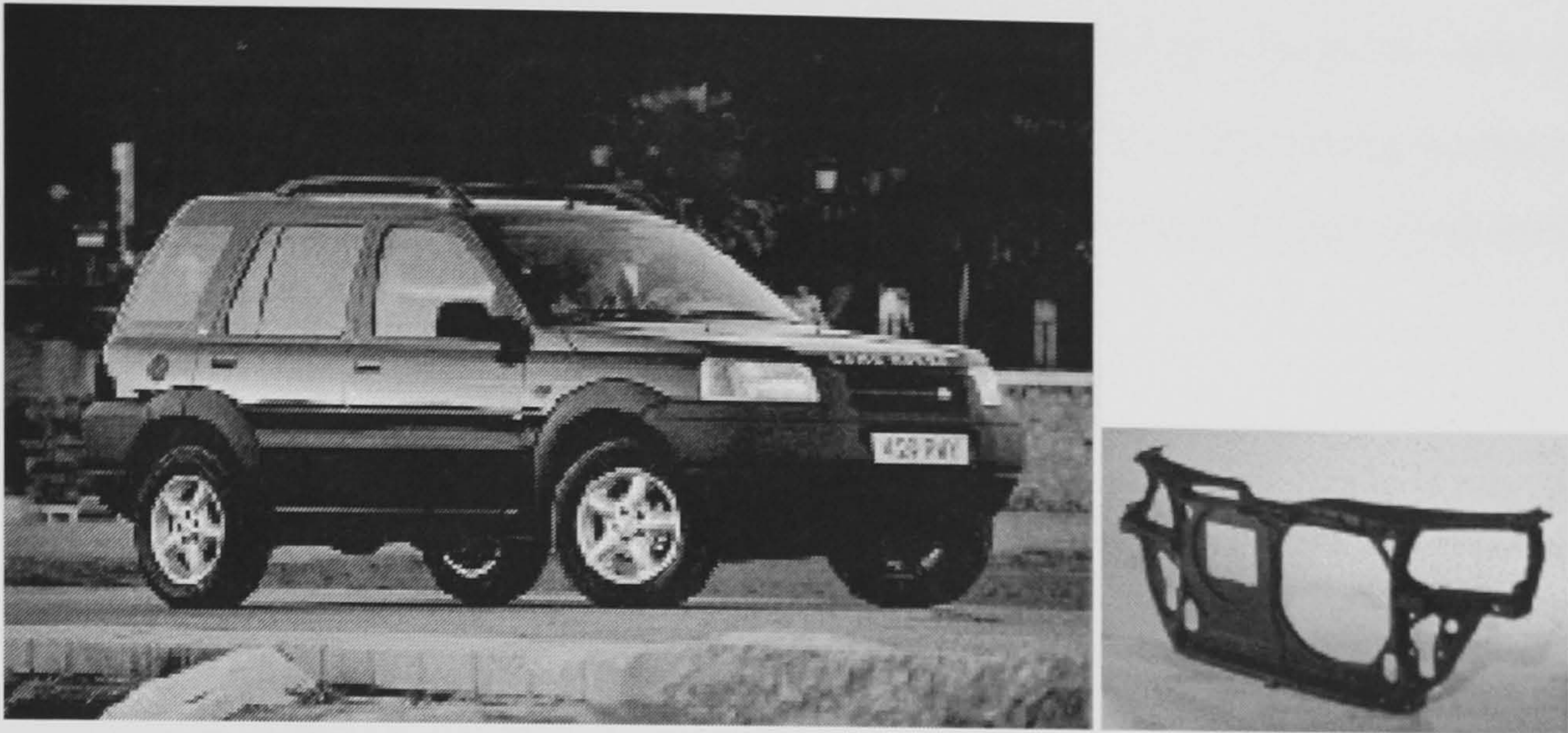


Figure 1.6 Manually operated compression moulding production line.

(A= GMT composite sheets (charge), B= Infrared oven, C= Heated charge, D= Mould cavity, E= Process control unit).

The compression moulding operation begins with the placement of pre-cut and weighed amount of composite sheets such as GMT called the charge, onto a transporting system (Figure 1.6A). The sheets are transported into an IR-oven (Figure 1.6B). The oven consists of multiple sections (with or without hot air insertion) and the residence time of each sheet in one section is equal to the cycle time of the process (0.5 to 1 min). The heated charge (Figure 1.6C, 160-200°C in the case of polypropylene) is placed either manually or automated, onto the bottom half of a pre-heated mould cavity (Figure 1.6D, 50-60°C). The mould is closed quickly after the charge placement. With increasing pressure, the charge in the mould starts to flow and fill the cavity. Flow of the material is needed to expel air entrapped in the mould as well as in the charge. All elements of the process can be controlled from a separate unit (Figure 1.6 E) that takes care of variables such as pressures, cycle and closing time of the mould. Depending on the part complexity, length of flow, fibre content and fibre length, the moulding pressure may vary from 1 to 40 MPa. Usually, high pressures are required for components that contain deep

ribs and bosses. After a reasonable degree of cooling and immobilisation the mould is opened and the part is removed, with or without the help of ejector pins.



(a)

(b)

Figure 1.7 Picture of (a) GMT bumper beam in Freelander car (Source: Website of Landrover) and (b) GMT front end of a car (Courtesy: Dr. Ton Peijs).

1.3 Natural fibre reinforced thermoplastic composites: an introduction

As mentioned before, because of excellent price-performance ratio, E-glass fibres are by far the most important fibres for thermoplastic matrix based composites. However, these fibres do have some disadvantages. Glass fibres are non-renewable and give problems with respect to ultimate disposal at the end of a materials lifetime since they cannot be thermally recycled by incineration and are left behind as a residue that can damage a furnace. They are also very abrasive which leads to an increased wear of processing equipment such as extruders and moulds. Next to some ecological disadvantages, glass fibres can cause problems with respect to health and safety. For example, they give skin irritations during handling of fibre products, processing and cutting of fibre-reinforced parts.

Nowadays, ecological concern has resulted in a renewed interest in natural materials and issues such as recyclability and environmental safety are becoming increasingly important for the introduction of new materials and products. Environmental legislation as well as consumer pressure is increasing the pressure

on manufacturers of materials and end-products to consider the environmental impact of their products at all stages of their life cycle, including ultimate disposal, viz. a 'from cradle to grave' approach. At this moment 'eco-design' is becoming a philosophy that is applied to more and more materials and products. In view of all this an interesting environment friendly reinforcement in engineering composites are natural fibres based on ligno-cellulose such as flax, hemp, kenaf, sisal and jute (Morton and Hearle, 1975). These vegetable fibres are:

- renewable and available in abundance,
- non-abrasive,
- can be incinerated for energy recovery since they possess a good calorific value (18,750 kJ/kg),
- CO₂ neutral when incinerated (however, keeping in mind the CO₂ evolved during fibre growth due to use of machinery, chemicals and other processing equipments the CO₂ saving per part would be reduced),
- give less concern with safety and health during handling of fibre products,
- exhibit excellent mechanical properties, especially when their low price and density (1.4 g/cm³) in comparison to E-glass fibres (2.5 g/cm³) is taken into account,
- flexible, give a safer crash behaviour and have unique acoustic and thermal insulating properties,
- bio-degradable, therefore if added to bio-plastics the degradability property of the matrix would still be maintained along with enhanced mechanical properties.

Although these fibres are abundantly available, especially in developing countries such as Bangladesh and India, most applications are still rather conventional, i.e. ropes, matting, carpet backing and packaging materials. Moreover, in the last few decades the use of natural fibres for these types of applications has been declined due to the introduction of synthetic fibres, such as Nylon and polypropylene. Hence, also in the economic interests of developing countries, there is an urgent need for new application areas for these natural fibres. The combination of interesting mechanical and physical properties together with their environmentally

friendly character has triggered various activities in the area of 'green composites' and many universities and institutes are starting activities in this area through various 'Eco-driven' R&D programmes.

The present project was aimed to study and develop composites based on flax fibre and thermoplastic matrices. Flax fibres were selected for the study because of availability in various forms i.e. long fibres, chopped fibres, non-woven mats and woven fabrics, in Western Europe. Such a study was initiated because of the environmentally sustainable nature of flax fibres along with the economical benefits foreseen from the flax fibres.

The natural fibre reinforced thermoplastic composites can be manufactured through various routes depending on the required properties of the final product (Figure 1.1). Some of the methods include compression moulding of non-woven mat reinforced thermoplastics (NMT) manufactured by the belt-press method, paper-making method and hybrid non-wovens. Another method of manufacturing randomly oriented natural fibre composites is through injection moulding of natural fibre/thermoplastic compound.

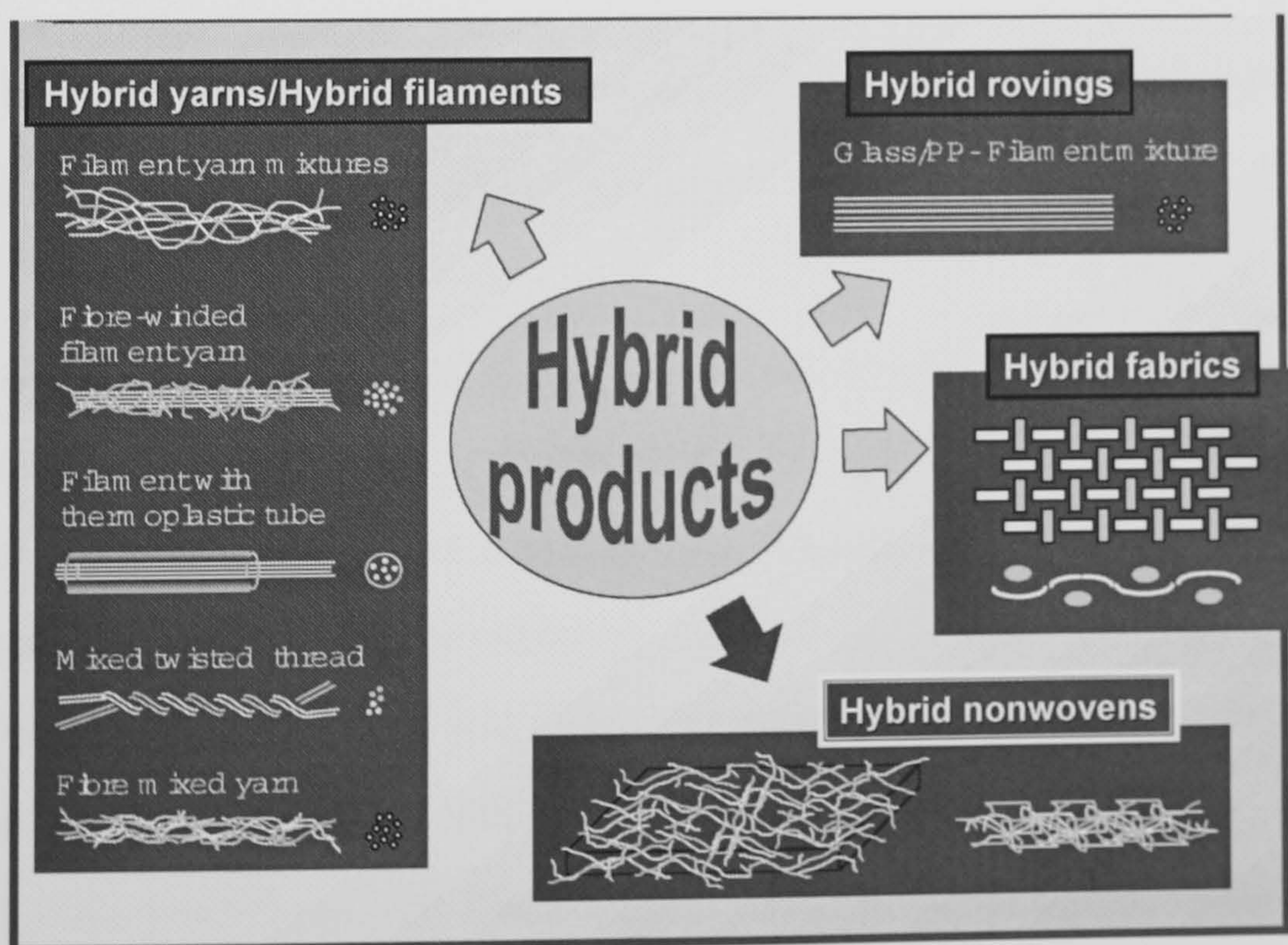


Figure 1.8 Possibilities of hybrid semi-products for composites. (Courtesy: Thüringisches Institut für Textil- und Kunststoff – Forschung, Rudolstadt, Germany).

Figure 1.8 shows the various routes taken to manufacture thermoplastic matrix

based composites from hybrid products of natural and thermoplastic fibres. Since glass fibre reinforced thermoplastics have been successfully used in industry for various applications and because various manufacturing techniques, developed for the production of the same, were tried directly or with some modifications for the development of natural fibre based composites, flax fibre based composites are often compared with the glass fibre based composites. The attempt is to see how far natural fibre based composites can go to replace the glass fibre based composites.

Table 1.1 Comparison of properties of GMT and NMT (compression moulded) composites having fibre content of 30wt%.

<i>Property</i>	<i>Glass/PP</i>	<i>Flax/PP</i>
Strength (MPa)	90	45
Stiffness (GPa)	6	9
Impact strength (notched Charpy, kJ/m ²)	30	7
Moisture absorption	<1%	12%
(Compression moulded, Fibre content=26%w/w)		

1.4 Thermoplastic composites based on natural fibres/cellulose: earlier work and present scenario

As mentioned earlier, the use of straw reinforced clay for making stronger bricks is one of the earliest composites referred in the literature (Prasad, 1992). In the case of plastics matrix, initially the research was focussed on natural-fibre-reinforced composites based on thermoset matrices, such as unsaturated polyester or phenolic resins, together with sisal and jute (Satyanarayana et al., 1981; Chawla and Bastos, 1979). As early as in 1907, when phenolic resins were developed, it was first combined with woodflour and later, paper, as additives before mouldings (Maldas and Salamone, 1996). In the early 1980s up to 60% cellulose loadings were added in polypropylene (PP) extruded sheets and pressure-moulded phenolics, but the cellulose materials were added as fillers with a reduction in price and weight without much improvement in the properties. Cellulosic materials, such as wood in its different forms (i.e., woodflour and woodpulp), cotton, shell flours, ground corn

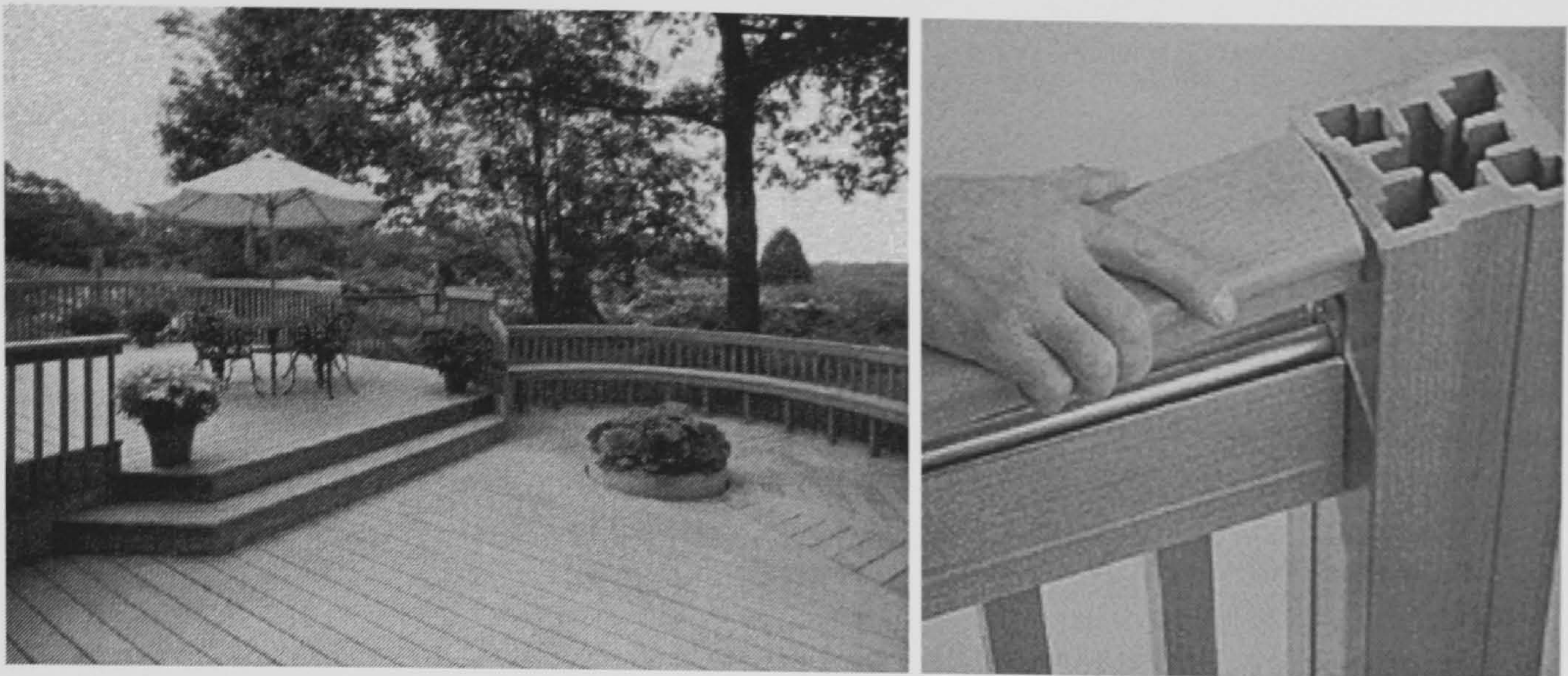
cobs, and other vegetable by-products or agrowastes, are used as the source of cellulosic raw materials for the plastics industry, mainly as cost-cutting fillers (Maldas and Salamone, 1996). More recently, developments shifted to natural fibre reinforced thermoplastic composites (Mieck et al., 1995; Sanadi et al., 1995; Selzer, 1995; Clemons, 1997; Felix, 1997; Herrera-Franco and Aguilar-Vega, 1997; Kuruvila et al., 1997; Oksman, 1997; Park and Balatinecz, 1997). Important advantages of thermoplastics over thermosets are the availability of flexible processing techniques such as extrusion, injection and compression moulding. Moreover, in the case of thermoplastics, known recycling methods based on granulation of used products and subsequent (re)shaping by extrusion or injection moulding are feasible. Also, some of the thermoplastic matrices like Polyhydroxybutyrate (PHB), Starch, Polylactic acid (PLA) etc., offer features like bio-degradability, which could be one of the important features for waste management.

1.4.1 Cellulose 'filled' thermoplastic composites

Cellulose-reinforced thermoplastic composite material have potential applications in the automotive industry, construction materials for low-cost housing, furniture, fencing, road making, packaging materials, grocery bags, garbage cans, flower pots, toys, and many commodity products. One of the first commercial wood-thermoplastic resin composites, called WoodstockTM, was developed by I.C.M.A. of Milan, Italy (Maldas and Salamone, 1996). Woodstock is a blend of polyethylene and PP with up to 50% sawdust. The materials are combined in a high-intensity mixer and then extruded and calendered in sheets. These sheets can be thermoformed into complex shapes, painted, laminated with vinyl or polyurethane foam, or embossed. Alternatively, the composite can be injection moulded with special equipment. American Woodstock, Sheboygan, WI, presently manufactures a woodflour-PP composite for the automotive interior trim market. In 1987, a few new products (e.g., Temple-Eastex and All-Season-WareTM) generically referred to as polymer composite sheets were introduced to the market place. Polymer composite sheet, neither a paperboard nor a plastic, is a synergistic product resulting from a combination of cellulosic fibre and polyolefin resin

(Maldas and Salamone, 1996). Conversion of the sheet is completed through a thermo-pressing operation that heats and densifies the sheets into specific shapes. The thermopressing action yields a moisture-resistant, smooth-surfaced product. The applications of such products are high temperature to frozen food packaging and food service applications. Another manufacturing technology that recycles plastics and paper is being used by Sonoco Products Co., Hartsville, SC, U.S.A., to produce EdgeboardTM, a protective industrial packaging product. Edgeboard has a right-angled edge and is a surface protector made from commingled paper and plastic that are passed through a two-stage extruder. It is the first extruded product of its kind to incorporate high percentages of cellulose (i.e., 50% by weight). This product provides users with moisture resistance and better product surface protection during shipping and distribution (Maldas and Salamone, 1996). Advanced Environmental Recycling Technologies (AERT) and Mobil Chemical Corp. had launched cellulose-polymer composites (Bioplaste and Timbrex, respectively) made of 50% recycled polyolefins and 50% waste woodfour (Maldas and Salamone, 1996). The targets for Bioplaste are the millwood subsurface window sill and door frame markets.

Wood replacement products for building applications such as particleboard and fibreboard materials or 'injection mouldable' wood like Fasal is another area where natural fibres are generating interest. Fasal is a development from the Inter-University Research Institute for Agricultural Biotechnology (IFA), Austria, and contains around 60% of wood fibres, 20% maize, 18% natural resin and 2% natural additives. It is aimed to replace wood in interior or short life products while having the advantage of polymer shaping methods. Due to the high filler content the flow characteristics are however limited.



(a) Wood filled composite terrace

(b) Extruded wood filled composite railing

Figure 1.9 Some examples of wood filled composites.

1.4.2 Natural fibre 'reinforced' thermoplastic composites

Most of the applications listed in the previous section utilise cellulose as a filler mainly for cost reduction purposes. However, natural fibres because of their good mechanical properties may also be utilised for reinforcement of the matrix material. Such applications of natural fibre reinforced thermoplastics are already in the market in the form of NMT sheets (Natural fibre mat thermoplastic) (Hoogen, 1999). The combination of interesting mechanical and physical properties together with their environment friendly character has triggered a number of industrial sectors, notably the automotive industry, to consider these fibres as potential candidates to replace glass fibres in environmentally safe products. In fact, car manufacturers are aiming to make every component recyclable or biodegradable. In a large research programme the Daimler-Chrysler Research Centre in Ulm, Germany has evaluated flax and hemp fibres as potential candidates to replace glass fibres in engineering composites and has developed a number of automotive products based on NMT, being a natural fibre counterpart of glass-mat-reinforced thermoplastics (GMT). Prototype products include underbodies, interior as well as exterior panels. The door panels in the Mercedes (C-class range) have been made from polyurethane reinforced with flax fibres. Very recently Daimler-Chrysler has introduced natural fibres in exterior components. The new Travego travel coach is equipped with a flax-fibre-reinforced engine and transmission cover with improved sound insulation. This innovation is important considering that such exterior

components must be able to withstand extreme environmental conditions such as wetness and chipping. Also Canadian company Cambridge Industries is using flax fibres in a polypropylene matrix to create mouldable material to form the rear-shelf panel of the 2000 Chevrolet Impala (Dellow, 2000). The performance advantages of plant fibres in polymer matrix composites are their chemical properties, high specific stiffness, high specific strength and sound absorption.



Figure 1.10 Underbody panelling prototypes for the Mercedes A-class made of flax-fibre-reinforced polypropylene (photo courtesy Daimler-Chrysler).

Ford's materials engineering department in Cologne, Germany has done considerable development work in the area of injection mouldable flax/PP grades for radiator grills, front ends and engine shields for the new Ford Focus. Parts are around 25-30% lighter than current glass fibre reinforced parts. Also Fiat is active in the area and has developed gaskets, seat parts and handles produced by gas-assisted injection moulding. In the US some programmes are currently initiated to follow the trend set by the European car manufactures. One initiative involves Kafus Environmental Industries, a company that grows kenaf in Texas, and Visteon one of Ford's component subsidiaries. Both companies will collaborate on the development and production of compression moulded parts for use in car

interiors. These parts will be based on nonwoven mats of commingled fibres of kenaf and PP and will be manufactured in a one-step moulding process that is expected to give shorter cycle times than current processes using pre-consolidated sheets.

The growing interest by car manufacturers in natural fibres has triggered at least one major player in the composites industry. Glass fibre manufacturer Owens Corning, although still in a preliminary stage, seems to be exploring the possibilities of participating in the market as a supplier of mat reinforcements for moulding applications and fibres for injection moulding. The involvement of a major player like Owens Corning could be essential in removing one of the main obstacles for future natural fibre use, being the reliability of supply in terms of quality and quantity. Although natural fibres are abundantly available in developing countries like Bangladesh, India and S-E Asia, commercial product developments will only be successful if a constant supply of high quality fibres can be guaranteed!

Some of the interesting developments in natural fibre reinforced composites involve thermoset matrices based on natural resources. For example, in the panel board industry there is a growing interest in non-wood resources like cheap natural fibre residues as well as the use of new formaldehyde free adhesives and binders such as natural resins. Phoenix Biocomposites in the US, for example, is using a soy-based resin in their Environ[®] biocomposite, whereas the BioComposites Centre at the University of Wales, U.K. has developed a resin based on cashew nutshell resin as a formaldehyde free binder for use in fibreboard panels. Cashew nutshell resin is a by-product of the cashew nut industry and a mixture of phenolics extracted from the shells of the cashew nut and a good natural alternative to petro-based phenol. Another interesting development in the area of natural fibre reinforced composites comes from the ACRES (affordable composites from renewable resources) group at the University of Delaware, U.S.A. They have developed natural fibre reinforced soybean oil resin (Khot, 1998; Wool et al., 2000). The Delaware material involves chemically modified soybean oil, a commodity that is 50 percent cheaper than polyester and vinyl ester resins. The use

of soybean oil resin for composite is not a new concept. Henry Ford made car parts like car trunk from soybean oil based plastics in 1930s.

1.5 Aims of the thesis

Some of the hindrances or challenges faced during the successful application of natural-fibre-reinforced thermoplastic composites, for engineering applications, involve:

a) Cellulosic fibres are hydrophilic and therefore the fibre's compatibility with synthetic polymers, which generally are hydrophobic, is limited. This implies very weak interactions and thus a weak interface between the fibre and matrix, leading to materials with inferior performance (Felix and Gatenholm, 1991).

b) Cellulose has a high degree of intermolecular hydrogen bonding. During the mixing of cellulose with plastics especially in injection moulding or extruder mixing, the former tends to agglomerate unless fibres are sufficiently wetted to reduce fibre-fibre bonding (Maldas and Salamone, 1996). Also, during compression moulding of NMT it was observed that natural fibres showed bad flow along with the PP polymer due to fibre-fibre interaction (Vissers, 2000).

c) High moisture absorption by natural fibres can affect the durability of composites in outdoor applications as well as susceptible to poor dimensional stability and rotting (Peijs et al., 1998b). Swelling of fibres can lead to microcracking of the composite and degradation of mechanical properties. The biodegradable nature of natural fibres can be advantageous for some applications where long term and outdoor applications are not very important e.g. packaging.

d) Because of the composite-like structure of natural fibres, in which elementary fibres are bound together by layers of pectin (Bos et al., 1998), the ultimate utilisation of elementary fibres needs extensive cleaning and separation processes without much damage.



e) Since natural fibres start to degrade at the processing temperature of thermoplastics like polypropylene therefore they emanate burning smell, which leads to unhealthy working conditions in the manufacturing plant. A thermogravimetric analysis of flax fibre is given in Chapter 2.

f) One of the advantages attributed to natural fibres include its environment friendly nature i.e. natural fibres are renewable, CO₂ neutral and can be incinerated for energy recovery. However, the methods and materials required to grow natural fibres in fact reduce the eco-performance of natural fibre reinforced composites when compared to the presently used synthetic glass fibres reinforced composites. One of the major reasons for the same includes usage of fertilisers, herbicides, fungicides, pesticides, insecticides, diesel (for heat, pumping etc.) and other chemicals, which have hazardous impact on our bio-sphere. A life cycle analysis of flax fibre based composites is presented in this work (Chapter 9) showing the effects of various stages of fibre and composite processing on environmental impact.

Keeping in mind the above mentioned challenges or shortcomings in the successful application of natural fibre reinforced composites, the following aims of the present work are defined:

- a) Optimise/improve the bonding between flax and thermoplastic (PP) and to study the mechanical properties of the developed composites.
- b) Improve the processing of flax fibre reinforced thermoplastic composites.
- c) Improve the environmental performance of the flax/PP composites.
- d) Develop bio-composites based on bio-plastics (PHB) and flax fibres.
- e) For optimisation of the mechanical properties of flax based composites study the effect of fibre variables like fibre diameter and processing routes.
- f) Conduct the Life Cycle Analysis of flax based thermoplastic composites and compare it with the existing glass based composite.

1.6 Structure of this thesis

The following report is sub-divided in the following way:

Chapter 2: A literature review on natural fibres in general and flax fibres is reported. Also a study on the physical, chemical and mechanical properties of flax fibre is reported and discussed.

Chapter 3: This chapter contains the results of micromechanical study on microcomposites based on various grades of flax fibre and polypropylene matrix. As mentioned earlier the structure and properties of the fibre/matrix interface plays an important role in the mechanical and physical behaviour of composite materials. The interfacial properties of the flax fibre and polypropylene matrix are included in this chapter. The effect of fibre coating and matrix modification with maleic anhydride grafted polypropylene (MAPP) on the fibre-matrix adhesion is studied through mechanical testing i.e. microdebonding test as well as Low Energy Ion Spectroscopy for interface characterisation.

Chapter 4: Apart from the chemical modification of the fibre/matrix interface, the properties of composites also depend on the processing conditions of the composite. One of the factors affected by the processing conditions includes matrix morphology. In this chapter the effect of processing conditions on the matrix morphology (transcrystallinity) as well as mechanical properties of micro- and macro-composites is reported and discussed.

Chapter 5: This chapter deals with the long fibre natural mat reinforced thermoplastic composites (NMT). The results from the optimization of the mechanical properties of (PP/flax) thermoplastic composites manufactured through compression moulding of flax fibre and thermoplastic PP are reported and discussed. The effects of varying fibre length, volume fraction, diameter and fibre-matrix interfacial adhesion on the macromechanical properties of composites, manufactured through compression moulding of flax fibre and thermoplastic PP, are reported and discussed. Simplistic micromechanical models have been used to

get an insight into the mechanical behaviour of the composite as well as to provide a guideline to compare the experimental properties with the theoretical possibilities.

Chapter 6: This chapter deals with the development study on short (natural) fibre reinforced composites manufactured by injection moulding. The effect of various compounding methods on the fibre length distribution as well as mechanical properties of flax fibre reinforced thermoplastic composites is reported and discussed.

Chapter 7: The environmental properties (moisture uptake and dimensional stability) of the developed composite along with the effect of using upgraded flax (Duralin fibres) and interfacial adhesion on these environmental properties are included.

Chapter 8: In this chapter, similar to the PP/flax composite, development of composites based on biodegradable thermoplastics polyhydroxyalkanoates (PHAs) and flax fibres leading to real bio-composites (i.e. obtained from natural resources) is reported. The effect of co-polymer content, fibre volume fraction, composite manufacturing conditions (temperature), annealing treatment, and different composite manufacturing methods (injection moulding and compression moulding) on the mechanical properties of these composites, is included.

Chapter 9: As mentioned earlier, the motivation of the present study was to develop and study composites based on environment sustainable flax fibres and thermoplastic matrices. The reference materials in view were glass-fibre-reinforced-thermoplastics, which are quite successfully used. Chapter 9 involves the comparative study on the effect of flax fibre reinforced and glass fibre reinforced thermoplastics on the environment. A comparative life cycle analysis (LCA) study on different products is reported in this chapter.

Chapter 10: General conclusions of the present study are reported. Also, included are the suggestions for the future research in the area of natural fibre reinforced thermoplastic composites. Micro-mechanical model predictions are used to

highlight the importance of various parameters for improvement in the mechanical properties of NMT composites.

2. NATURAL FIBRES: LITERATURE REVIEW AND CHARACTERISATION

In this chapter the literature review over natural (vegetable) fibres in general and flax fibres, in particular, is included. Also, results from the experimental work, for the characterisation of different kinds of flax fibres, are presented.

2.1 *Natural fibres: a literature review*

In general, natural fibres are classified as vegetable-, animal and mineral fibres. Vegetable fibres are grouped according to their source in plants and are therefore sub-divided into (i) bast or stem fibres (e.g., hemp, jute, ramie, flax), (ii) leaf fibres (e.g., sisal) and (iii) seed-hair fibres (e.g., cotton), although few come from other parts of the plants (e.g., coir from the pericarp of coconut fruits) (Hearle and Peters, 1963). Both bast and leaf fibres provide strength and support to the plant in order to keep it erect. Bast fibres occur in the phloem or bark of certain dicotyledonous plants and are situated next to the outer bark in the bast.

As mentioned earlier (Chapter 1), various natural fibres have been studied and used as reinforcement for composite applications along with thermoplastic as well as thermoset matrices. In our study flax fibres are used as reinforcements, mainly because of their good mechanical properties (Table 2.4) when compared with other natural fibres and also because of their availability in different forms in Western Europe.

Although there are considerable differences in the physical features of the various

vegetable fibres, there is also a great similarity among all the fibres. In general, all plant fibres are based on carbohydrate-based polymers. The most abundant polysaccharide in plants is cellulose, which is composed of glucose units that are joined through hemiacetal linkages in the 1:4 positions. Cellulose can be regarded as a homopolymer containing 2000 or more glucose residues in each molecular chain (Figure 2.1). The configuration of the glucose residues is β and in the crystalline areas these units are organised in *trans* positions:

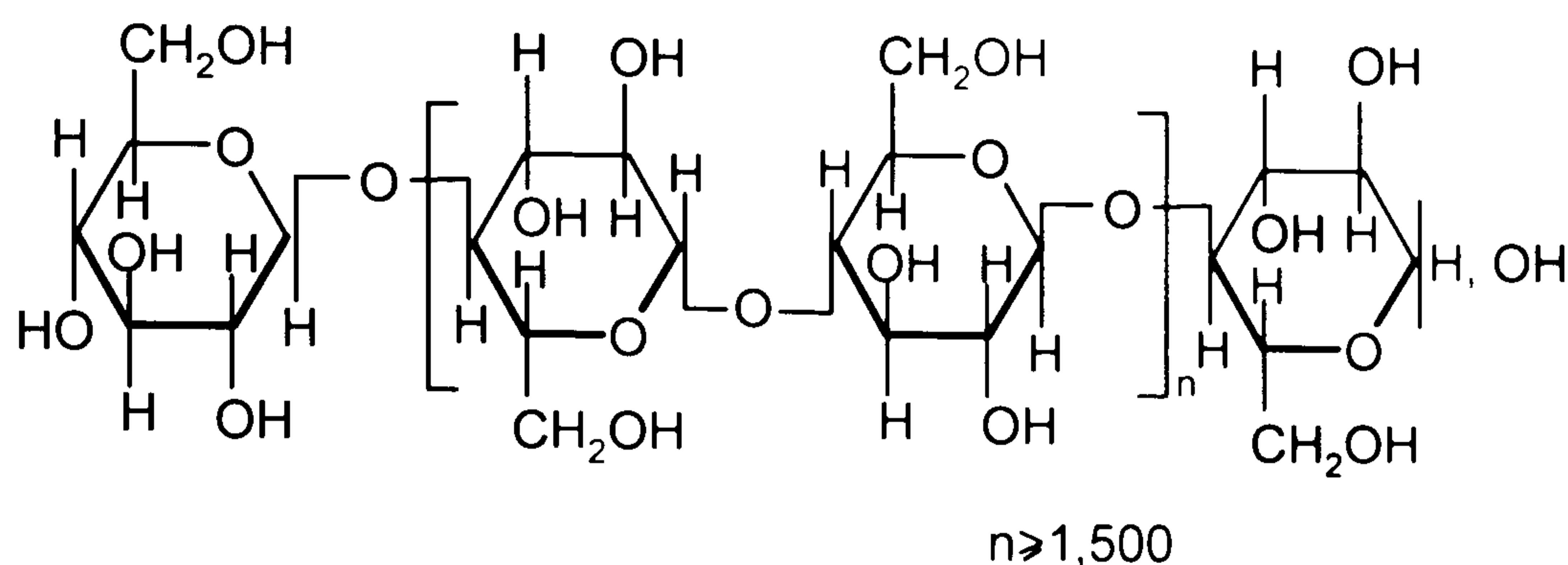


Figure 2.1 Schematic structure of cellulose polymer (Hearle and Peters, 1963).

Such configuration of the glucose residues yields a highly symmetrical and compact molecular chain. Cellulose fibres contain regions in which the chain molecules have a highly ordered (crystalline) arrangement and some in which, there is disorder (amorphous) 'arrangement'. The degree of crystallinity and the close packing in these areas vary depending on the cellulose source and on the chemical treatments to which it has been subjected. Cellulose has been recognised to exist mainly in two crystalline forms designated as Cellulose I and II. The crystal structure of native cellulose is known as Cellulose I, and has a unit cell with the dimensions shown in Figure 2.2. The degree of polymerisation is of the order of 10,000 in native cellulose fibres. The average value of crystallinity is about 66.67%. Cellulose II (Figure 2.3) occurs in regenerated materials (viscose, cellulose sheets) and when native celluloses are treated with strong swelling agents (e.g. sodium hydroxide used in mercerisation) (Hearle and Peters, 1963).

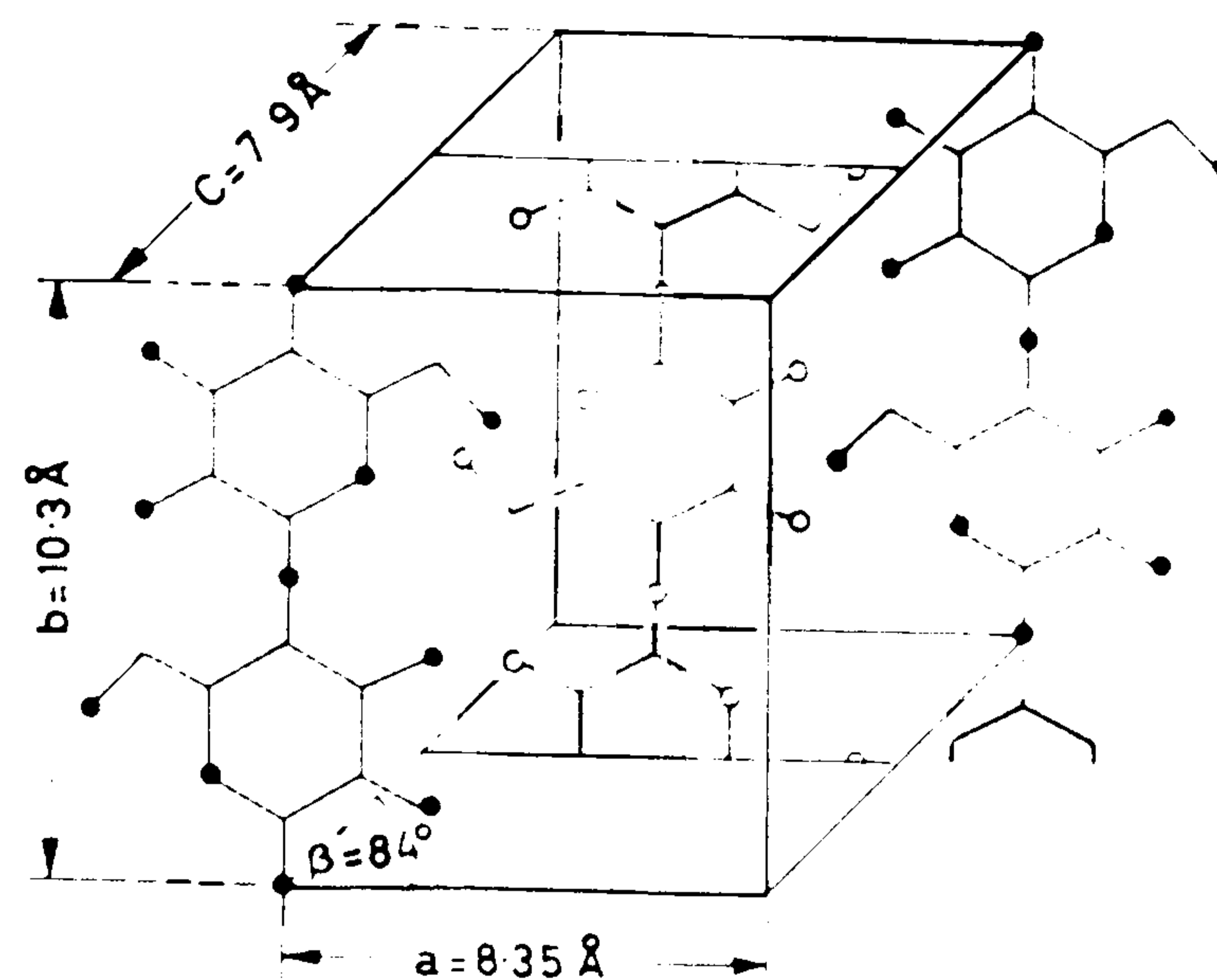


Figure 2.2 Picture of cellulose crystal unit cell (Hearle and Peters, 1963).

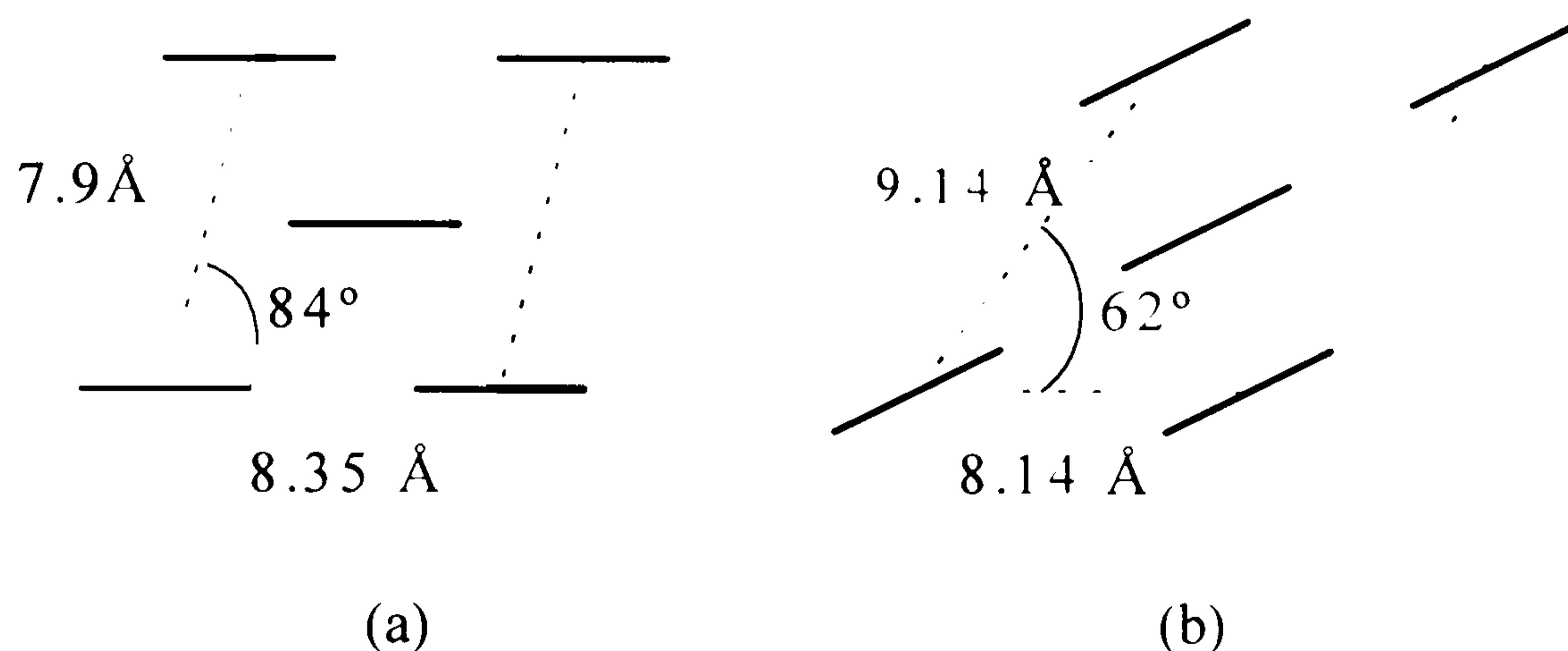


Figure 2.3 Suggested arrangement of molecules in crystal of (a) cellulose I and (b) cellulose II (Morton and Hearle, 1962).

Each glucose residue retains three hydroxyl groups (Figure 2.1 and 2.2), which are responsible for several important characteristics of cellulose fibres:

a) The plurality of hydroxyl groups confers a high degree of intermolecular hydrogen bonding. As a consequence, cellulose fibres possess good mechanical properties and are heat resistant to the extent that they char and decompose before the melting point is reached. Cellulose, when exposed to an ignition source, will decompose and produce, among other things, gaseous products which ignite, propagate the flame, and further decompose the cellulose until only ash remains (Jain et al., 1986; Kaur et al., 1986). Thermal degradation studies of cellulose attribute the drop in weight at 320°C to dehydration and depolymerisation of cellulose followed by evaporation of the volatile products of combustion. This is

followed by oxidation and burning of the high molecular weight charred residues (Jain et al., 1986; Kaur et al., 1986).

b) The hydroxyl groups, at least those in the amorphous regions of the fibre, have a strong affinity for water and other highly polar chemical species. This characteristic of cellulosic fibre is also one of the major drawbacks for the successful use of natural fibres in durable (outdoor) applications because of high moisture absorption and poor dimensional stability (swelling), as well as their susceptibility to rotting.

c) One or more hydroxyl groups per glucose residue can be replaced by a different group following a suitable chemical treatment (Peters, 1963). One of the examples of the treatment is acetylation of cellulose.

The amount of cellulose present varies greatly with the type of plant and is accompanied in nature by a wide variety of other materials notably waxes, lignin, hemi-cellulose (a lower molecular weight, branched polysaccharide), pectic substances etc. (Peters, 1967). Table 2.1, 2.2, 2.3 and 2.4 show the various morphological, mechanical, physical and chemical characteristics of various natural fibres. Chemically, cotton is the purest, containing over 90% cellulose with little or no lignin. The other fibres contain 70-75% cellulose, depending on processing. Boiled and bleached flax and degummed ramie may contain over 95% cellulose. Kenaf and jute contain ligno-cellulose, which contributes to their stiffness. Physical properties of natural fibres are basically influenced by the chemical structure such as cellulose content, degree of polymerisation, orientation of cellulose polymer chains and crystallinity, which are affected by conditions during growth of plants as well as extraction methods used. There is an enormous amount of variability in fibre properties (as shown in Table 2.3 and 2.4) depending upon the part of the plant from which the fibres are taken, the quality of the plant and the location because of the effect of environment on the plant growth (Mukherjee and Radhakrishnan, 1972).

Table 2.1 Chemical composition of vegetable fibres, wt% (McGovern, 1984).

Fibre	Cellulose	Hemi-cellulose	Pectins	Lignin	Water soluble compounds	Fats and Waxes
<i>Seed fibres</i>						
Cotton	91.8	6.4	–	–	1.1	0.7
<i>Bast fibres</i>						
Flax (retted)	71.2	18.6	2.0	2.2	4.3	1.7
Flax (non-retted)	62.8	17.1	4.2	2.8	11.6	1.5
Jute	71.5	13.4	0.2	13.1	1.2	0.6
Ramie	76.2	14.6	2.1	0.7	6.1	0.3
Hemp	74.4	17.9	0.9	3.7	2.3	0.8
<i>Leaf fibres</i>						
Sisal	73.1	13.3	0.9	11.0	1.4	0.3

Table 2.2 Physical characteristics of plant fibres (Heijenrath, 1996).

Fibre	Specific Gravity (g/cm ³)	Moisture Regain (%)	Absorption (%)	Volume swelling (%)
<i>Seed fibres</i>				
Cotton	1.52	7 - 8.5	7 - 8	–
<i>Bast fibres</i>				
Flax	1.40	12	7	30
Jute	1.46	14	12	45
Hemp	1.48	12	8	–
<i>Leaf fibres</i>				
Sisal	1.20 - 1.45	–	11	40

Table 2.3 Morphological characteristics of plant fibres (Heijenrath, 1996).

Fibre	Technical fibre (mm)	Elementary cell (mm)	Cell Diameter (μm)	Fineness (denier)
<i>Seed fibres</i> Cotton	–	15 – 56	12 – 25	–
<i>Bast fibres</i> Flax	300 – 900	13 – 60	12 – 30	1.7 – 18
Jute	1500 – 3600	2 – 5	15 – 25	13 – 27
Hemp	1000 – 3000	5 – 55	16 – 50	3 – 20
<i>Leaf fibres</i> Sisal	600 – 1000	0.8 – 8	15 – 40	9 – 400

Table 2.4 Mechanical properties of plant fibres (Zafeiropoulos, 2001).

Fibre	Strength (MPa)	Ultimate strain at break (%)	Initial modulus (GPa)
Flax	650-2000	2.5	20 – 100
Jute	480-690	1.5	11 – 16
Hemp	900-1080	1.6	10 – 25
Sisal	640	2	15

2.1.1 Flax fibres

Botanically spoken the flax plant is an annual plant *Linum usitatissimum*, a member of family Linaceae, and has been used since ancient times as the fibre for fabric.

The plant grows in moderate temperature and moist climates, and is cultivated in e.g. Belgium, the Netherlands, France, Ireland and Italy. The flax fibre in the stem of the plant forms about 25% by weight although the amount of fibre recovered

after isolation is much smaller than this (up to about 15%) (Peters, 1963).

The term *fibre* is recognised in plant science as referring to a single cell with clearly defined microscopically visible features (Hearle and Peters, 1963). The cell is long compared with its width, and both ends taper to points. The wall is thick and the pits are reduced and usually slit-mouthed. In both stem and leaves, the fibre cells, also called “elementary fibres”, occur in bundles, also called “technical fibres”. In actual practice fibre cells are isolated as bundles (technical fibres). The elementary flax fibres belong to a family of elongated cells found in plants. Individual types of cellulose fibres vary somewhat in their molecular constitution and arrangement (Morton and Hearle, 1962). In all native cellulose (elementary) fibres, the cell-wall consists of long thin threads termed microfibrils. Unlike man-made fibres, natural fibres themselves could be considered as oriented short-fibre composites containing varying volume fractions of cellulosic microfibrils of different lengths. For instance, the 1m long bast fibre bundles consist of elementary fibres, which are approx. 20 to 50mm long, diameters in between 10 and 25 μm and an average aspect ratio of around 1500 (Figure 2.4) (Bos et al., 1997). The elementary fibres overlap over considerable length and are glued together by pectin.

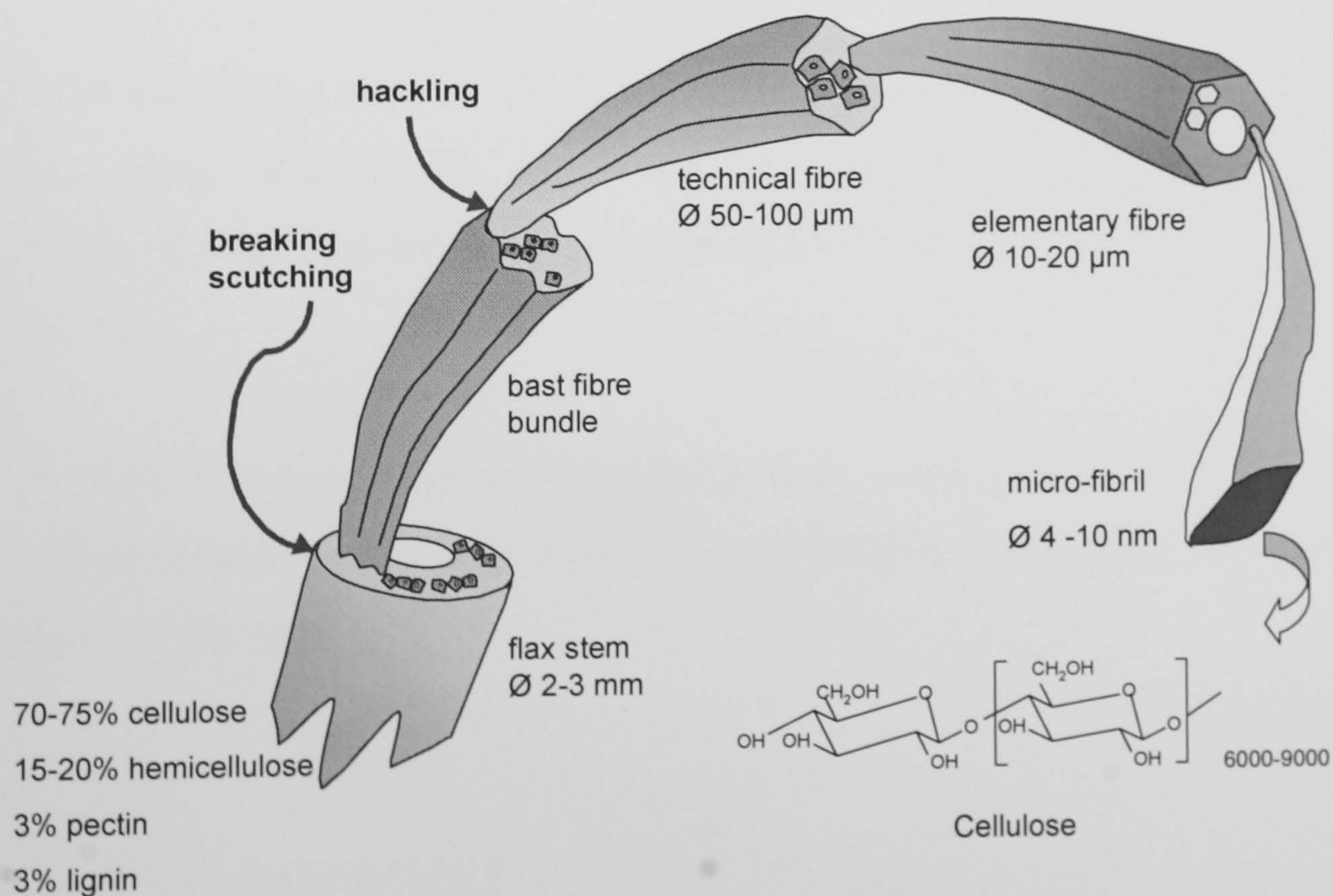


Figure 2.4 Schematic picture of technical and elementary (fibre cell) flax fibre (Bos et al., 1997).

Examination of the cross-section of the stalk (flax plant stem) shows many components (Figure 2.5 and 2.6). There are six annular regions (Peters, 1963; Dijon, 2002):

(i) **Epidermis:** Epidermis forms a protecting layer against mechanical damage, water loss and infection. This consists of a layer of walled cells covered by an external cuticle. There are about 40 openings, known as stomata, per mm². These openings are sufficiently large for retting bacteria to enter.

(ii) **Cortex:** One or two layers of approximately circular parenchyma cells form the cortex. These cells contain colouring matter called chlorophyll and substances known as pectins.

(iii) **Fibre bundles:** The bast fibres are found in this layer, which is the ring of dark cells in Figure 2.5. Each stem contains up to 40 bundles of some 12-40 fibres per bundle. Roughly speaking there are about 1000 flax fibres in each stem. The single fibres are also known as sclerenchyma cell.

(iv) **Cambium:** A ring of thin-walled cells separating the wood from the fibres.

(v) **Wood:** Also called as Xylem, towards the centre of the stem, is a ring of very short, thick, woody cells, which give mechanical support to the plant during growth. Xylem cells act as vessels that conduct water and solutes from the roots to leaves.

(vi) **Pith:** The core of the stem is filled by pith, which consists of thin-walled cells, and encloses the pith cavity, which is an air chamber running for almost the entire length of the stem.

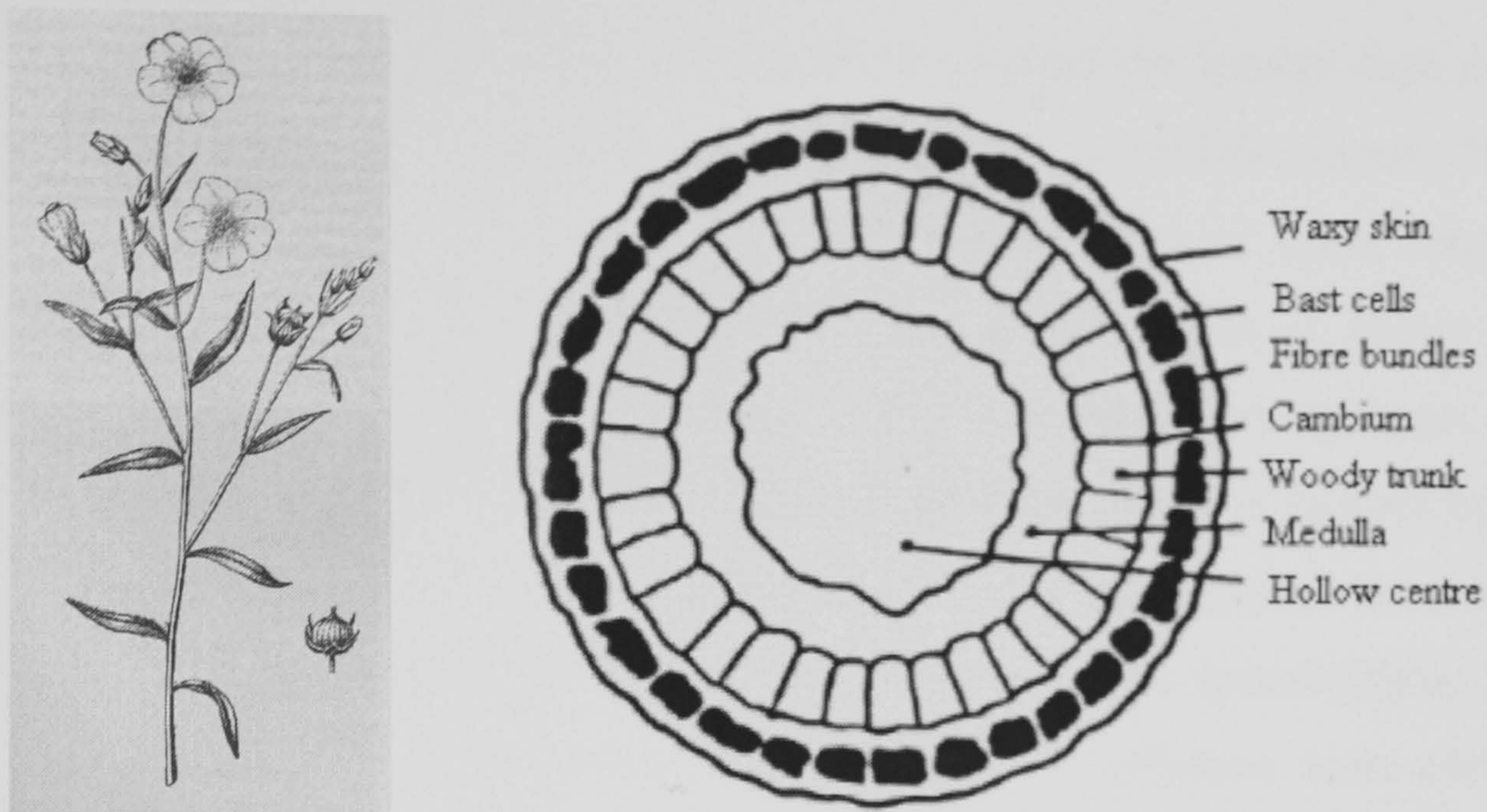


Figure 2.5 (a) Picture of the cultivated flax plant (*Linum usitatissimum*) in bloom (Dewilde, 1987) and (b) schematic view of the cross-section of the stem of flax plant (Peters, 1963).

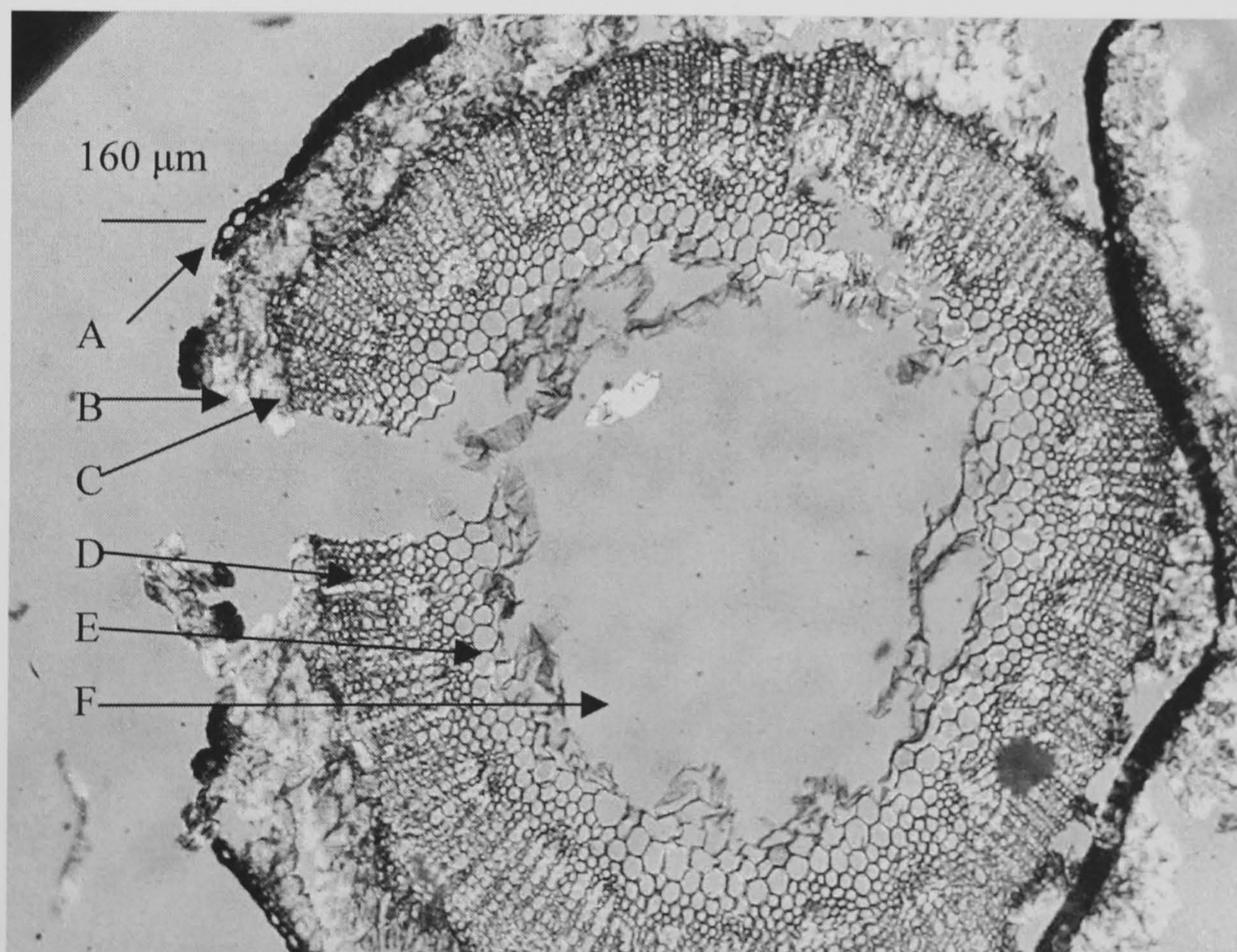


Figure 2.6 Picture of the cross-section (transverse section) of the stem of flax plant taken through an optical microscope (A= Epidermis, B= Fibre bundle in the phloem, C= Cambium, D= Xylem, E= Pith, F= Pith cavity) (Sample source: Dijon, G., Department of Biology, Imperial College of Science, Technology and Medicine, University of London, U.K.)

As shown in Figure 2.5 and 2.6 the flax fibres are organised in bundles, located in

the outer part of the stem of the flax plant, lie around the woody core and are attached to it by pectin. In flax, the fibres originate in the cambium layer. At first, sieve tubes and their companion cells mature in the protophloem. Later, these cells are squashed while the fibres become wider and longer. When all traces of the conducting elements have disappeared, the remaining protophloem is a homogeneous tissue composed of the young single fibre cell. It is distinct from the rest of the phloem. The deposition of a secondary cell wall increases the thickness of the cell wall and at the same time decreases the size of the lumen (Dijon, 2002). The principal chemical constituents of the flax fibre are cellulose, hemi-cellulose, lignin and pectin.

Therefore, the extraction of flax fibres from the stem involves the removal of much extraneous material and separation of the fibres from other parts of the stem to which they are gummed by pectic and hemicellulosic materials.

2.1.1.1 Flax fibre processing

As mentioned earlier, the property of natural fibre vary according to crop variety and weather conditions during growth and harvesting (Pott et al., 2000). The processing of the bast fibres may be divided in the following separate treatments (Peters, 1963):

a) Harvesting and Pre-treatment: The plant is also cultivated for its seed, from which linseed oil is produced. At optimum maturity, the plants are harvested by pulling or mowing (either manually or mechanically). Afterwards they are spread out in the field to dry.



Figure 2.7 Picture of the farmers pulling the flax plant through pulling tractors (Courtesy: Procotex Corporation NV, Gent, Belgium).

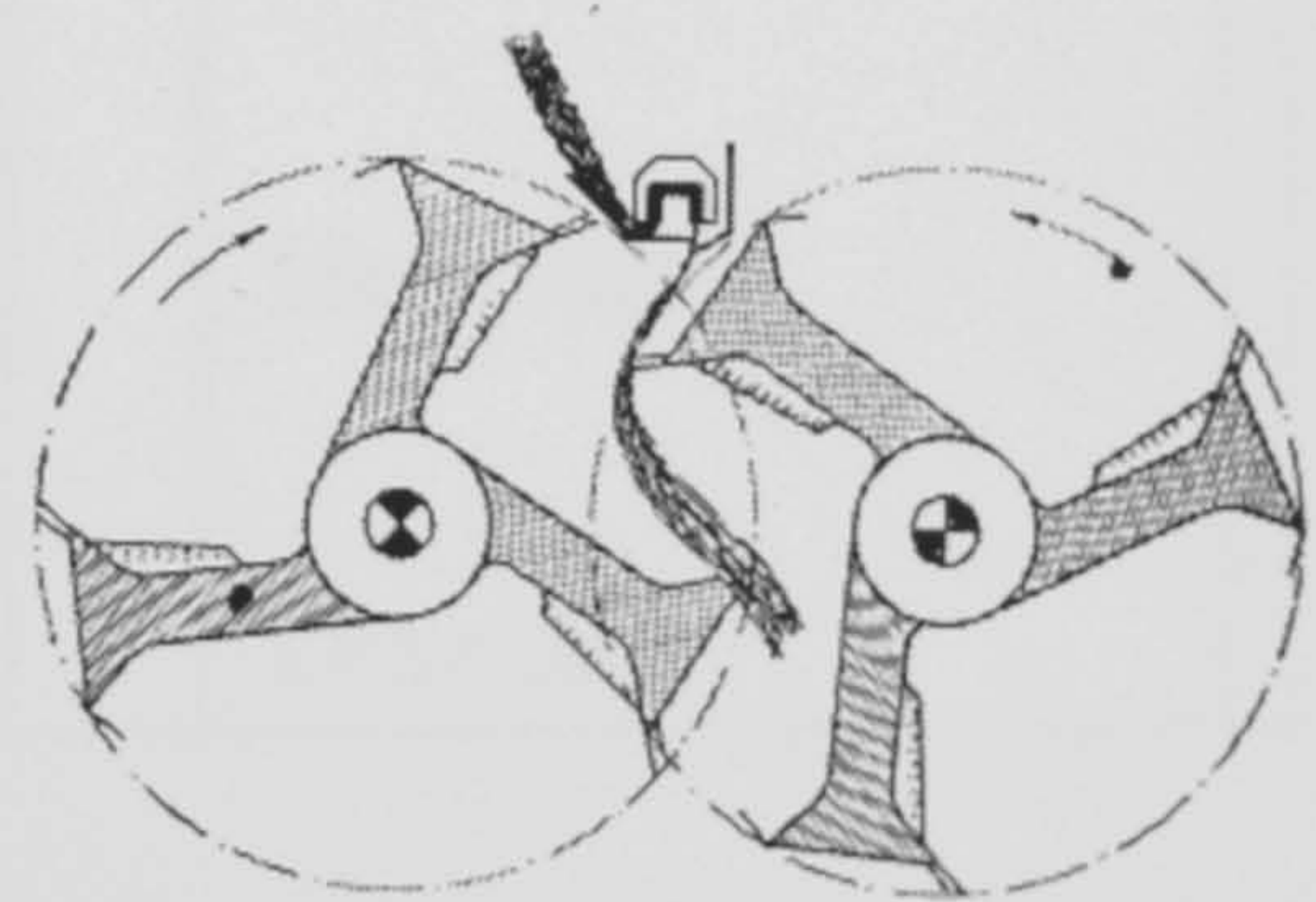
b) Retting: The removal of the bast fibres from bark and woody stem parts is promoted by a biological process called retting (rotting), being an enzymatic or microbial action on the pectinous matter of the stem. Correct retting is of great importance; underretting would mean that the required fibre bundles are not easily separated from the wood and excess retting results in a weakened fibre. Several methods are used for the retting process. *Dew retting* involves the action of dew, sun, and fungi on the plants, spread thinly on the ground, involving the dissolution of the cellular tissue and the larger part of the gummy substances; it requires 4-6 weeks and the action is not uniform. In *water retting* (also called pool and tank retting) bundles of plants are immersed in stagnant pools, rivers, or ditches; the biological effect is achieved through bacterial action. The retting time is 2-4 weeks. Tanks are also used and in these the bundles of straw are placed root downwards. In tanks with warm water the time is reduced to about 4-6 days. Water heated to about 30°C is pumped in to cover the straw and the temperature maintained. During the first 6-8 hours, sometimes termed the “leach”, dirt and colouring matter are dissolved from the fibre. In fermentation processes involved in the bacterial action, acids are formed which may be harmful. They are removed by allowing a slow trickle of water to run in and out of the tank to waste. Water retting gives a uniform product. In *stream retting* the plants are immersed in slow-

moving streams for a longer time; the quality of the product is high. In *chemical retting* the dried plants are placed in a tank and treated with chemicals, such as sodium hydroxide or carbonate or sulphuric acid. The fibres are loosened in a few hours, but control is required to prevent deterioration.

c) Breaking and Scutching: The dried and retted bundles are subsequently passed through fluted rolls to break and reduce the woody portion into small particles throughout its length. The broken pieces of shive are next removed in a “scutching” mill (Figure 2.8) where straw is brought into contact with wide flat blades, made of wood or steel, which scrape or beat off the shive.



(a)



(b)

Figure 2.8 Picture of (a) an operator taking flax off the scutching turbine (Courtesy: Procotex Corporation NV, Gent, Belgium) and twisting it into tipples, or handful of parallel fibres and (b) the principle of one of the scutching machines (Dewilde, 1987).

d) Hackling: The bundles are hackled or combed to separate the short and long fibres, which are then aligned and cleaned.

Although retting tends to separate the bundles of flax fibres into individual fibres, the process is not entirely complete (Hearle and Peters, 1963). A study of the cross-section of a flax fibre shows many fibre cells remaining together in bundles. As mentioned earlier these bundles are also called “technical fibres”. The elementary fibres (cells) are 20 to 50 mm long and one technical fibre contains approximately forty elementary fibres in its cross-section. The fibre separation can also be done by purely mechanical means. Fibres obtained through this method are called ‘green flax’. The processes described above are summarised in Figure 2.9

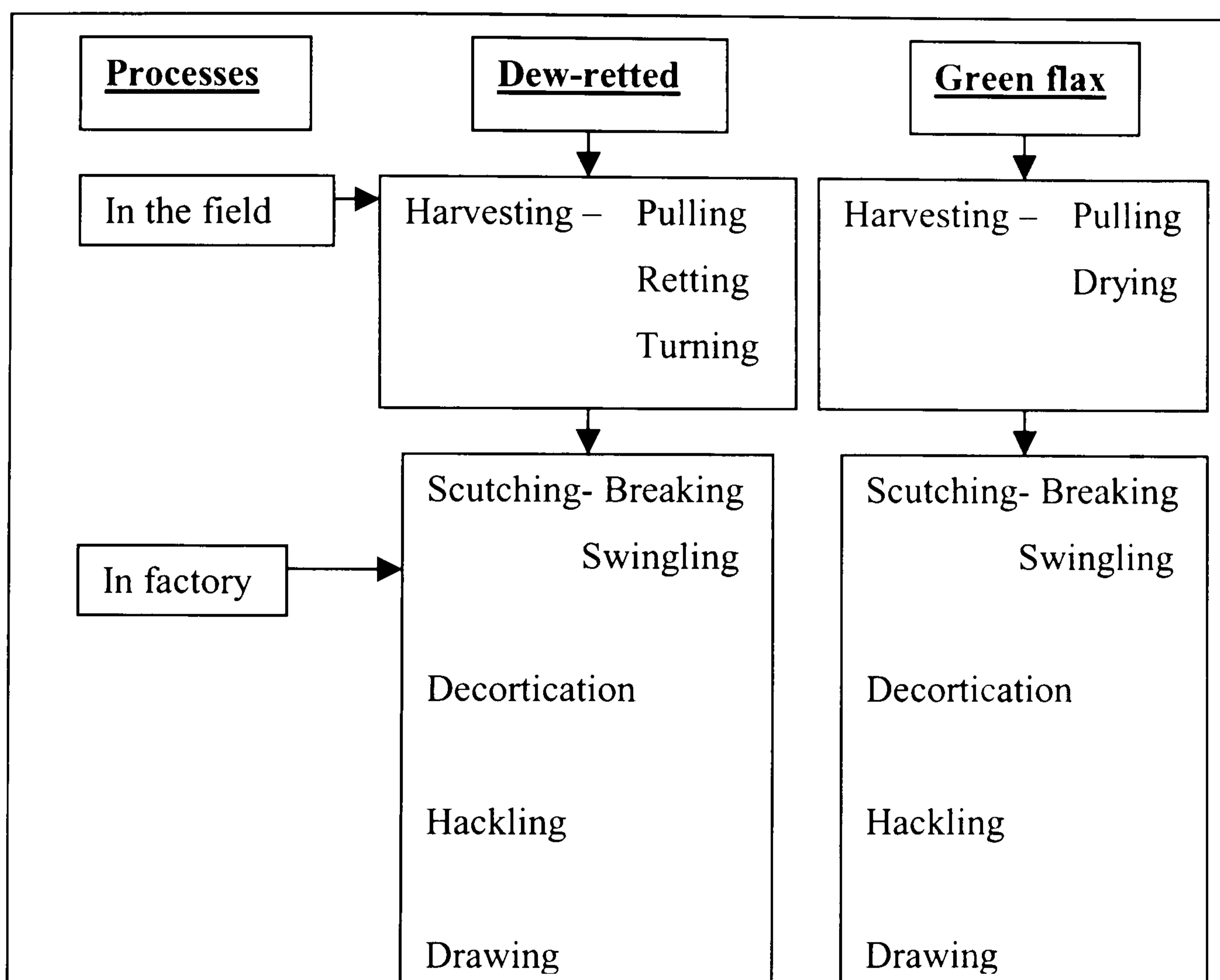


Figure 2.9 Flow diagram showing green flax and dew-retted fibre preparation.

The elementary fibre cells are generally in the form of tubes or hollow cylinders, which normally taper to a point, and in flax they are polygonal when viewed in transverse section. The shape of the fibre varies somewhat from sharply polygonal to oval and irregular, being partly dependent on variety, growth, and maturity. The immature fibres are more oval in shape and possess a large lumen. In the middle of the elementary fibre cells there is a small lumen or hollow canal, which is the empty space that was formerly occupied by the protoplasmic material forming the living part of the cell. The lumen can be as small as 1.5% of the cross-section.

Consequently the elementary fibre cell wall is relatively thick, which accounts for the good mechanical properties of the fibre.

Features that should be especially noted are the presence of cross-markings and fissures (nodes), the small size of the lumen and the thickness of the walls (Hearle and Peters, 1963). The fibre wall is made up of fibrils. The wall structure has three layers (Peters, 1963), the inner and outer of these are thin and have fibrils laid down in a spiral with a Z- twist. The thick middle wall has its fibrils spiralling with an S (Figure 2.9). The microfibrils range between about 80\AA and about 250\AA in width and are held together by amorphous hemi-cellulose, lignin, pectin and other elements like magnesium and calcium (Hearle and Peters, 1963; Bos et al., 1997). These highly crystalline cellulose microfibrils are highly oriented parallel to one another, but they spiral around the fibre, thus reducing the average degree of orientation parallel to the fibre-axis. In flax, ramie, hemp and other bast fibres, the spiral angle is small i.e. less than 6° , so that these fibres are highly oriented and give high strength and low extensibility. In cotton, however, the spiral angle may be as large as 30° and the fibres can extend more easily by stretching the spiral.

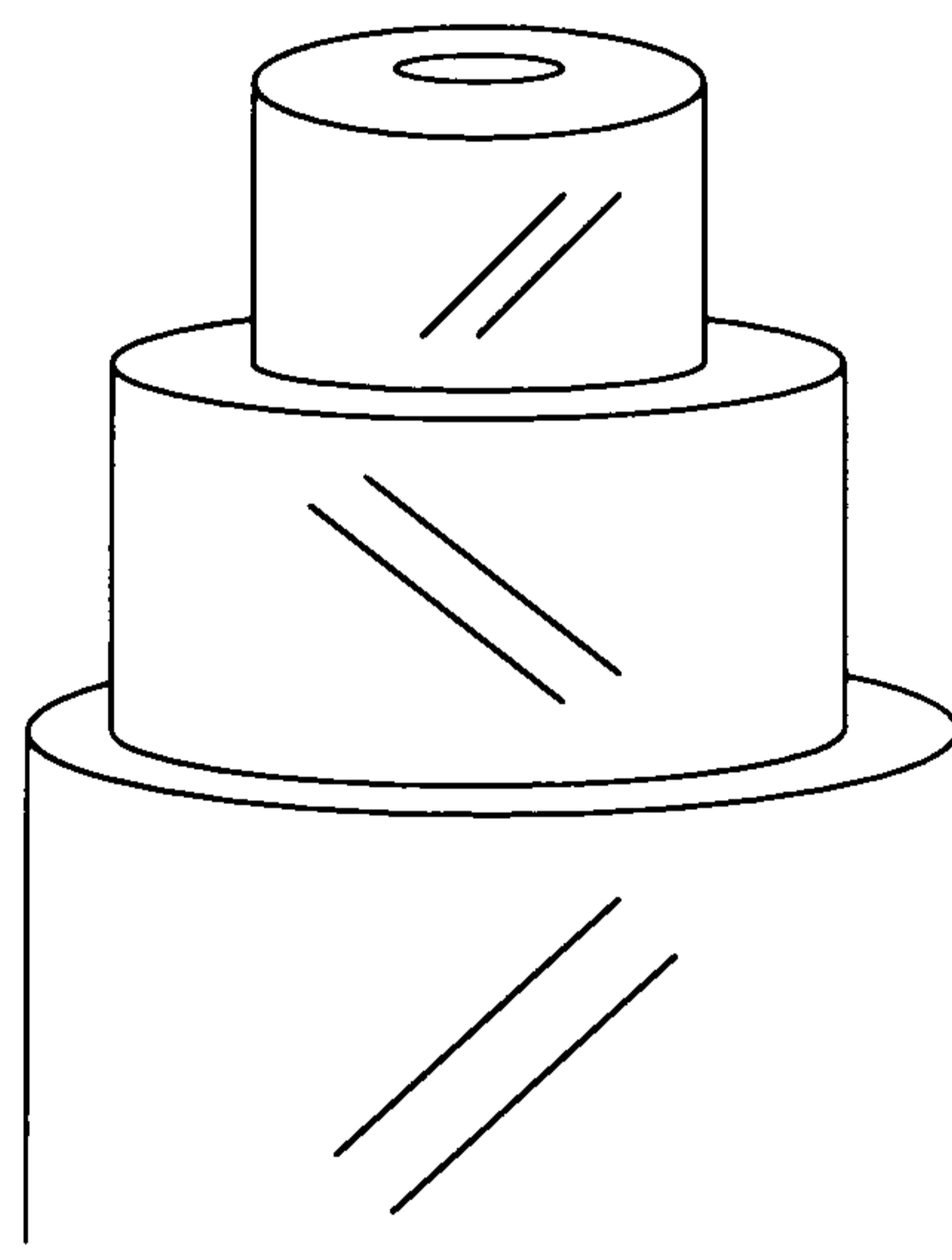


Figure 2.10 Schematic representation of the spiral structure in different layers of flax (Roelofsen, 1951).

The highly oriented crystalline structure, in flax fibres, makes the fibres sensitive to kink band formation (Figure 2.11) under compressive loading, analogous to, for instance, aramid fibres (Bos et al., 1997). The surface structure of fibres has a great influence on their behaviour at every stage of the conversion of raw materials into

final products, and, what may often be more important, on the performance of the products during use (Hearle and Peters, 1963).

The flax fibres have numerous nodes on the surface and there may be as many as 800 in a single fibre. Several explanations have been advanced for cause of the nodes; they may be due to minute fissures or local separation of the fibrils which make up the cell walls or could be points at which the directions of the fibrils is modified. Either of these postulates would explain the fact that on stretching the nodes disappear, since in the former case the fibrils would be pulled together and in the latter allineated. Release of tension brings the fibre back to its original unstretched state and the nodes reappear. Swelling treatments also reduce the intensity of these “dislocations” marks (Peters, 1963).

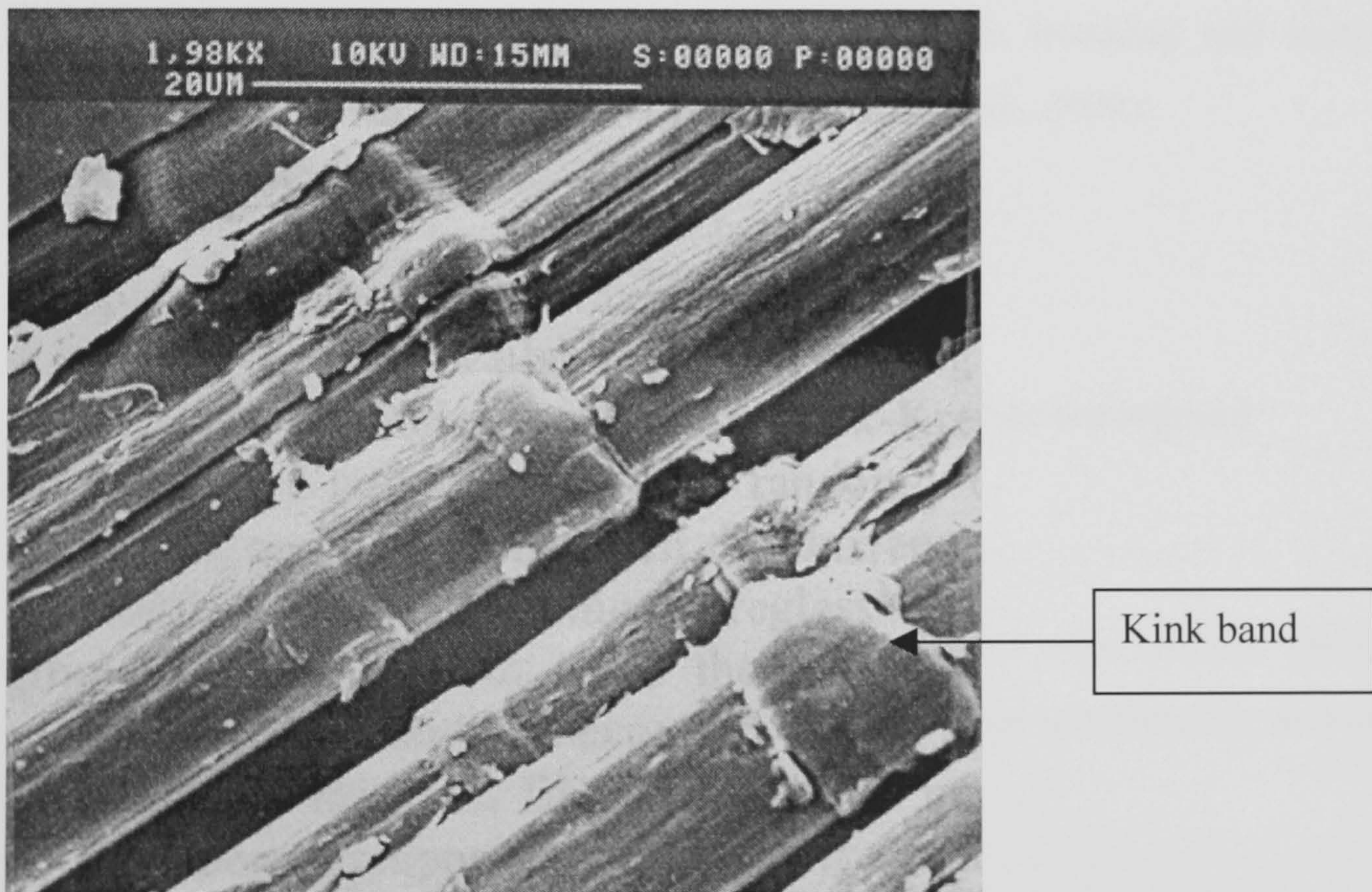


Figure 2.11 Kink band formation in the flax fibres (Heijenrath, 1996).

2.1.1.2 Duralin fibres

As mentioned earlier, the cellulosic fibres have a strong affinity for water and other highly polar, chemical species. This characteristic of cellulosic fibre is also one of the major drawbacks for the successful use of natural fibres in durable (outdoor) applications because of high moisture absorption and poor dimensional stability (swelling), as well as their susceptibility to rotting. To reduce the moisture and rot

sensitivity of flax fibres and to improve their reproducibility as well as quality, a novel flax treatment has been developed (Pott et al., 2000). This flax-treatment process does not use dew-retted flax as feedstock but the full rippled (deseeded) stalk, known as straw flax. The use of straw-flax turned out to be beneficial for both strength and reproducibility (no dew-retting required) of the treated flax. In addition, a valuable by-product, the treated flax-shives, is produced from which e.g. water-resistant chipboards could be made.

The treatment consists of a steaming step of the rippled straw-flax at temperatures above 160°C-180°C for approximately 15 minutes in an autoclave (hydro-thermolysis). This treatment is followed by a drying step and a heating (curing) step above 150°C (up to 180°C) for approximately two hours. After this treatment the fibres easily separate from the stem by a simple breaking and scutching process. The advantages of this process are that (Pott et al., 2000):

- No dew-retting is required
- Fibre yield is increased
- Fibre quality consistency is increased
- Swelling and shrinkage under the influence of moisture are reduced
- Temperature stability is increased
- Resistance to fungus attack is improved
- The mechanical properties of composites reinforced with Duralin fibres are generally better than those of composites containing untreated or dew-retted flax fibres.

The details of the advantages mentioned above are studied and shown in the following Section 2.2 as well as in Chapters 5 and 7 over NMT and Environmental study of Duralin based composites, respectively.

In addition to the benefits mentioned above, the process water generated in Duralin fibre processing can be anaerobically digested to generate methane to fuel about 40% of the energy required for the Duralin process. After this treatment, it is easy to separate the fibres from the stalk (easier than dew-retting) by scutching process

(Pott et al., 2000). The fibres obtained by this procedure are fibre bundles rather than individual fibres.

The weight loss due to extraction of material during hydro-thermolysis is 28% of dry weight for straw without roots and 27% for straw with roots. The bulk of this consists of pectin decomposition products (such as arabinose, galactose and rhamnose), acetic acid and formic acid (Pott et al., 2000). The additional weight loss during curing is less than 0.5%. Since the weight loss during water-retting and dew-retting are approximately 22% and 18% respectively, total weight loss caused by the first step of the Duralin process is approximately 5-10% greater than that caused by retting. On the other hand, because the Duralin process results in a higher fibre yield, the weight loss is concentrated more in the shives than in the fibres. Chemical analysis has shown that during hydro-thermolysis certain compounds move from the shives to the fibres e.g. xylose. Also, it has been found that lignin partially decomposes to form phenol functionalities, while hemicellulose decomposes to form monosaccharides and subsequently to produce aldehydes such as furfural. During curing, furfural can polymerise but can also react on the ortho-site of the phenol ring to form an in situ thermosetting resin, similar to the Bakelite reaction. The process therefore has the effect of converting part of the water and rot-sensitive hemicellulose to less water-sensitive polymers (Pott et al., 2000).

Flax used in industrial applications has to meet different requirements from those in the textile industry. While textile processing requires long, finely separated fibres paralleled into slivers preferably, technical applications primarily need fibres with high strength and a high elastic modulus. Therefore the flax does not necessarily have to be very finely separated and processed in slivers since coarse flax fibres in the 5-10 tex range are suitable for reinforcing plastics. The crucial factor is that mats produced from coarse fibres, because of their structure, have better impregnation properties than fine fibre mats due to high fibre-to-fibre interaction in the case of finely separated flax fibres.

Depending on the fibre preparation route the flax fibre can be processed into different final forms like chopped fibres, non-woven mats and continuous fibres.

Figure 2.12 shows the variety of products, which have been obtained from flax plant. The numbers (total yield weight) in Figure 2.12 only total 800 kg. The difference can be explained by that fact that in water-retting the flax loses 20% of its weight as a result of the dissolved gums. In dew-retting this loss only amounts to 16%, but the amount of seed loss can be higher (Dewilde, 1987).

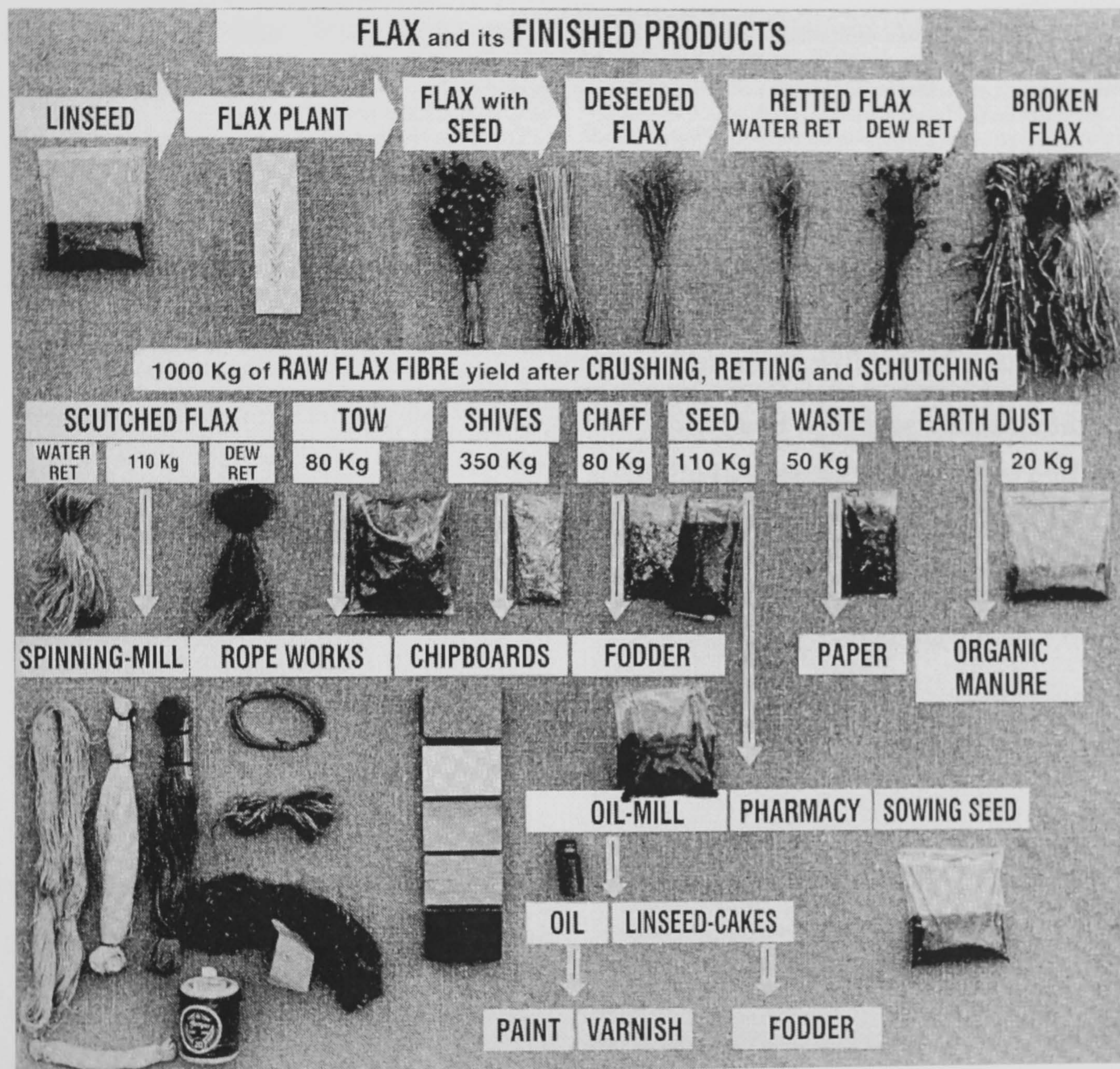


Figure 2.12 Picture of various products manufactured from flax plant (Dewilde, 1987).

2.2 Characterisation of flax fibres- Experimental

An attempt was made to characterise the various kinds of flax fibres. Since the aim was to use these fibres for composite reinforcement applications therefore various factors, which were studied, included fibre mechanical properties and the effect of processing conditions (temperature) on the fibre mechanical properties as well as

fibre degradation. The following sections consist of the details of the above mentioned study.

2.2.1 Materials

In this study three types of flax fibres were used, namely Duralin flax, dew-retted flax, and green flax. The fibres were delivered as continuous or long fibres and chopped fibres with average fibre length of approximately 10 mm by Ceres BV, Wageningen, the Netherlands.

2.2.2 Methods

2.2.2.1 Mechanical properties of flax fibres

A fibre with a relatively small diameter was chosen from the bundle. This was done to ensure that the fibre chosen was closest to the elementary fibre. To facilitate proper handling, the fibres were adhesively bonded on cardboard frames. A typical frame had a rectangular slot with a length equal to the desired gauge length. For each fibre type at least 5 different gauge lengths between 3 mm and 100 mm, were made. After sampling, the fibre diameter was measured for every fibre using an optical microscope. However, these values are only approximate estimations because the fibres are not circular. To minimize these effects an average diameter of about 5 readings per fibre was used for the calculation of the stress values. For each material and gauge length combination 25 fibres were tested. To observe the effect of heat treatment on the mechanical properties, flax fibres were exposed to heat in an oven followed by tensile testing. For the same, samples were heat treated at different temperatures and heat exposure time.

The single fibre tensile tests were performed on a Frank tensile testing machine with a load cell of 50N. For the combination of Duralin flax fibres with a gauge length of 20mm a Frank 81565 tensile testing machine with a load cell of 10N was used. The parts of the cardboard frame parallel to the fibre were cut away after the sample was mounted in the tensile testing machine. The loading speed was 10% of

the initial specimen length per minute. The samples were stored and tested in the laboratory having controlled RH of about 60% and temperature of about 20°C. The fracture surface of flax fibre was observed through Scanning Electron Microscopy (SEM). The observations were made through Cambridge Stereoscan 200. For the same the samples were coated with gold/palladium alloy.

2.2.2.2 Thermal gravimetric analysis (TGA) of flax fibres

TGA of flax fibres was done to study the degradation of flax fibres at elevated temperatures i.e. in the range of the processing temperatures of thermoplastics. The change in weight with respect to the exposure to heat was determined at different temperatures using a thermogravimetric analyser (TGA Perkin Elmer type 131507). The initial weight of the samples was between 5 to 10 mg and the degradation atmosphere was static air. Before conducting the experiment the samples were dried at 80°C for at least 1 week to completely dry the fibres.

2.2.3 Results and discussion

2.2.3.1 Mechanical properties of flax fibres

In general it can be stated that, because of probability of defects, a short fibre is stronger than a long fibre. Moreover, if the span length in a tensile test on a technical fibre exceeds the elementary fibre length, the fibre will preferably fail through the pectin layer (Figure 2.14). However, when the test length is smaller than the elementary fibre length, then the fracture may take place through the elementary fibre (Bos et al., 1997).

Tensile strength

A typical stress versus strain curve of a flax fibre is shown in Figure 2.13. It was observed that there was a fairly linear relation between stress and strain.

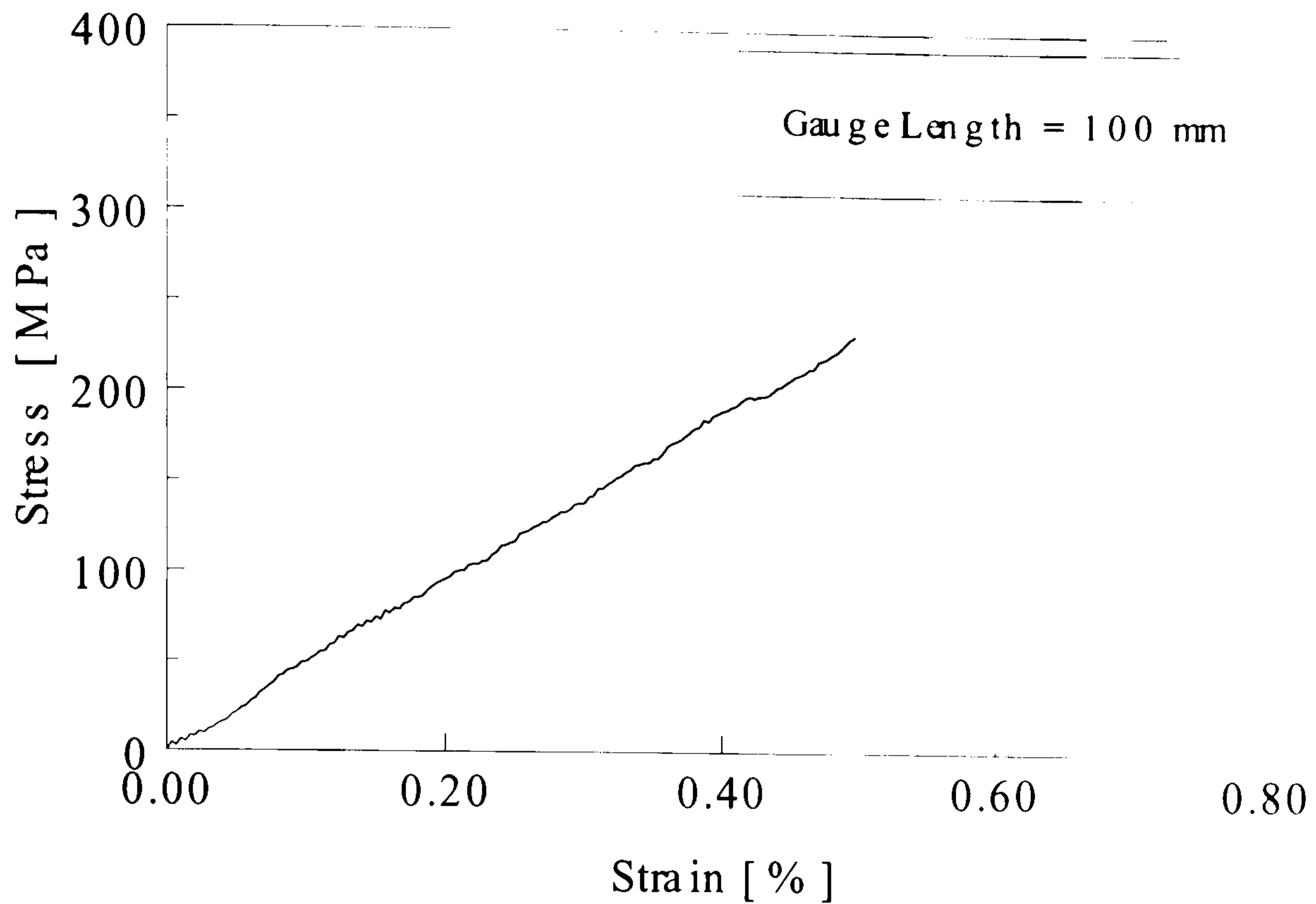


Figure 2.13 Typical stress vs. strain curve of a Duralin flax fibre.

The results of the single fibre tensile test are shown in Figure 2.14 for the Duralin and green flax fibres. The tensile strength versus gauge length curve of the dew-retted flax fibres is about similar to the curves shown in Figure 2.14 and is given in Appendix 2A. As seen from Figure 2.14 the tensile strength of the flax fibres is strongly dependent on the gauge length at which the measurement is performed. The fibre strength is constant, approximately 350 MPa, between a gauge length of about 20mm and 100mm, this is about equal for all three types of flax. Below this gauge length the fibre strength begins to increase towards a value of about 850 MPa, for the Duralin flax fibres, measured at a gauge length of 3mm. The results of the tensile strength of the dew-retted and green flax fibres showed a similar trend as shown in the case of Duralin flax fibres. However, dew-retted and green flax show lower average values for the tensile strength at smaller gauge lengths, e.g. at 3mm gauge length the tensile strength is about 725 MPa for the green flax. The obtained values, for the tensile strength, are comparable with those found in literature (Bos et al., 1997). However, the properties mentioned in Table 2.4 (650-2000 MPa), from literature, are on the higher side showing that the properties were measured at small gauge lengths or at different testing speeds. The flax treatment (to obtain Duralin flax fibres) resulted in a higher average tensile strength compared with the non treated flax fibres and gave less scatter in the tensile

strength results, especially at the smaller gauge lengths, 3 to 25 mm (Figure 2.14, showing average values as well as standard deviations).

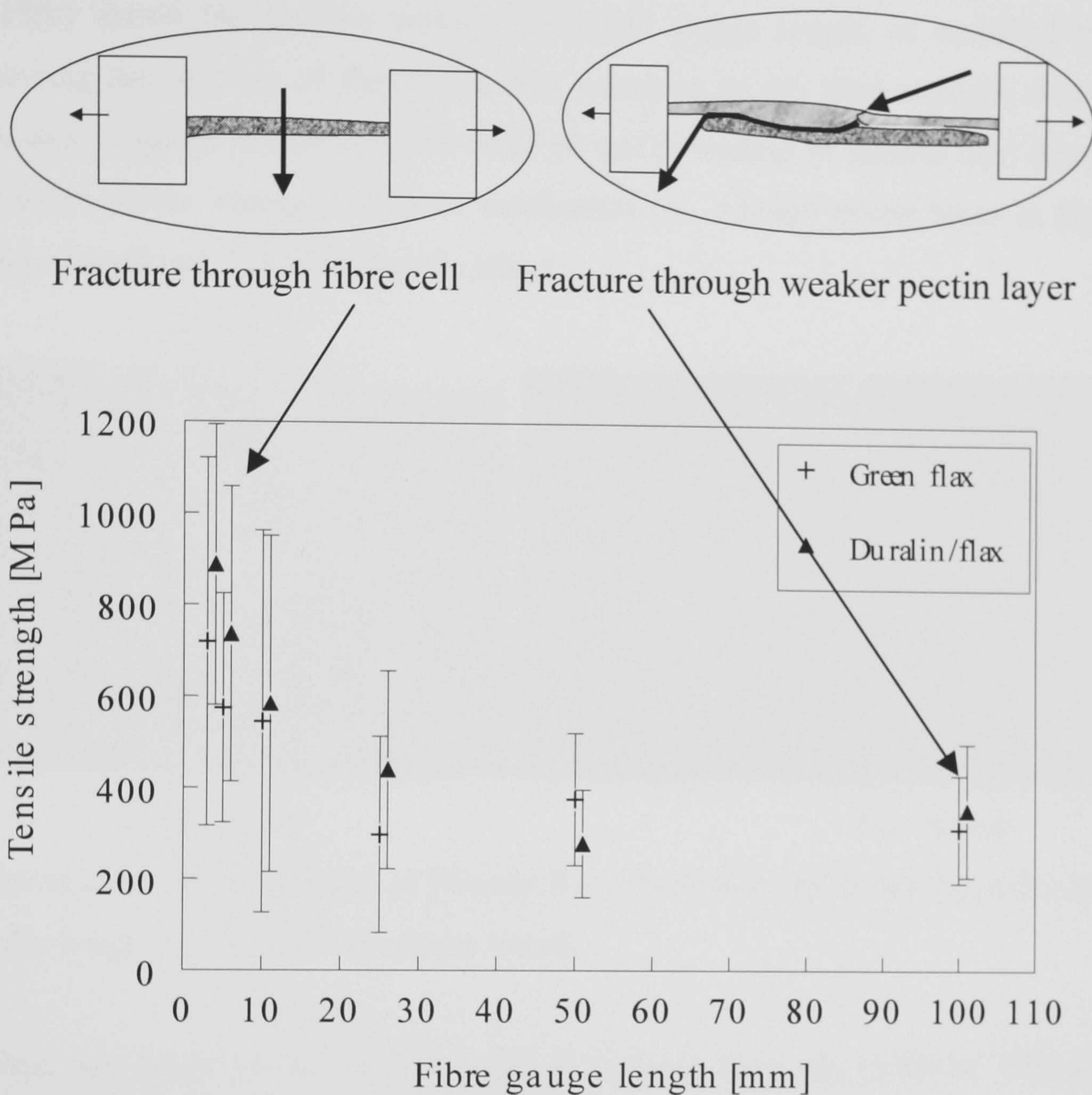
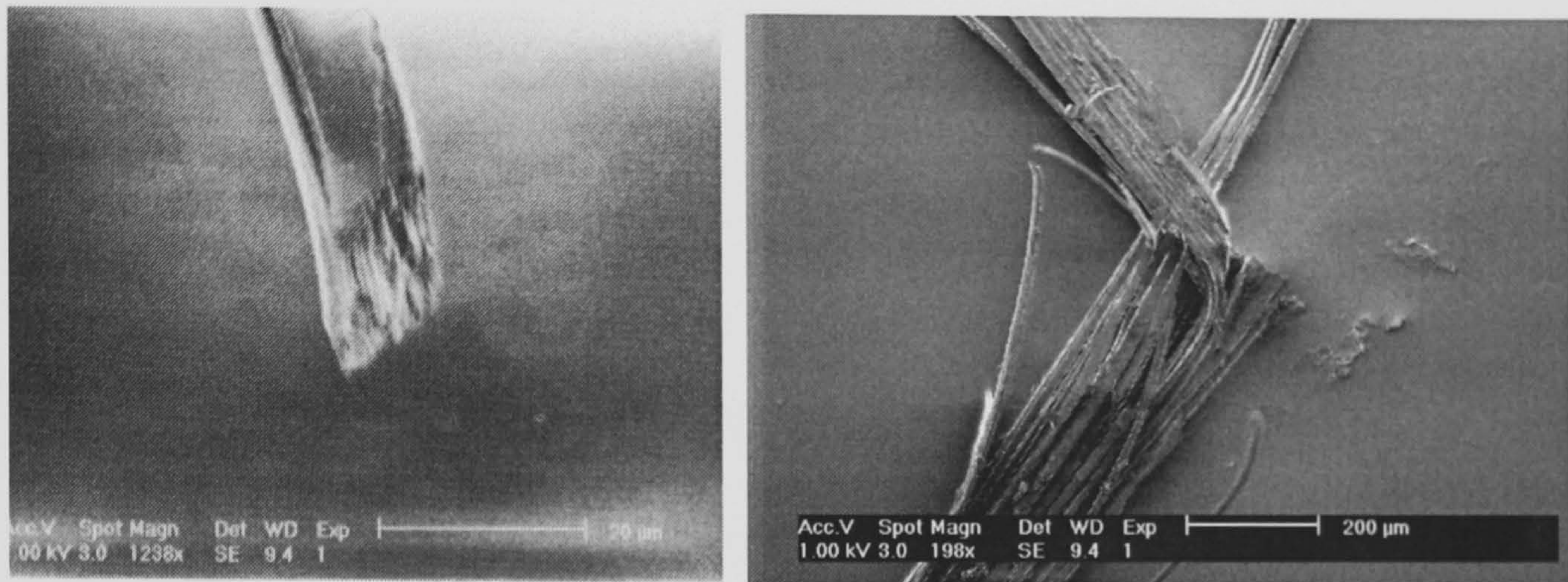


Figure 2.14 Tensile strength of Duralin flax and green flax vs. gauge length and schematic representation of failure mode at different gauge lengths (The error bars show the standard deviation).

As mentioned earlier, at large gauge length fibre failure takes place through the relatively weak pectin layers that bonds the elementary fibres together. The rise in tensile strength at shorter gauge lengths could be caused by a change in failure mechanism (Bos et al., 1997). At gauge lengths below the elementary fibre length (approx. 25mm), failure can no longer take place through the pectin layers, but the stronger cellulosic cell wall of the elementary fibres. This can be seen in Figure 2.15 in which SEM pictures of Duralin flax fibres fracture tips, tested with gauge

lengths of 3 and 100 mm, are given. The change in failure mechanism can be seen clearly from these pictures. In Figure 2.15(a) the fracture surface of single elementary fibre is shown showing fracture through the fibre cell. Whereas, Figure 2.15(b) shows the fracture surface, at higher gauge length, of technical fibre showing the splitting of fibre cells. The reduction in the fibre strength with the increase in gauge length therefore could be due to number of reasons like: increase in weak points, change in failure mechanism i.e. through pectin layer at higher gauge length and due to the bundle effect.



(a) 3 mm

(b) 100 mm

Figure 2.15 SEM pictures of Duralin flax fibres after tensile testing at (a) 3mm gauge length and (b) 100 mm gauge length.

When one single elementary fibre cell is isolated from the technical fibre (cell bundle), strength of approximately 1500 MPa has been reported (Bos et al., 1997). The value measured in this case is far higher than the tensile strength of technical fibres at the same clamp length. The difference, as reported, is most likely due to the bundle effect. Also, with an increase in the gauge length of flax fibres the numbers of weak points increase, leading to a reduction in the tensile strength of the fibre.

Tensile modulus

Figure 2.16 shows the initial modulus of Duralin flax fibres measured for various gauge lengths. As expected, the initial moduli of the different fibres, measured at different gauge lengths, did not vary significantly. The results of the dew-retted

and the green flax fibres are presented in Appendix 2B. The mean modulus of all the fibres measured is about 42 GPa. It was also found that the flax type had no significant influence on the initial modulus.

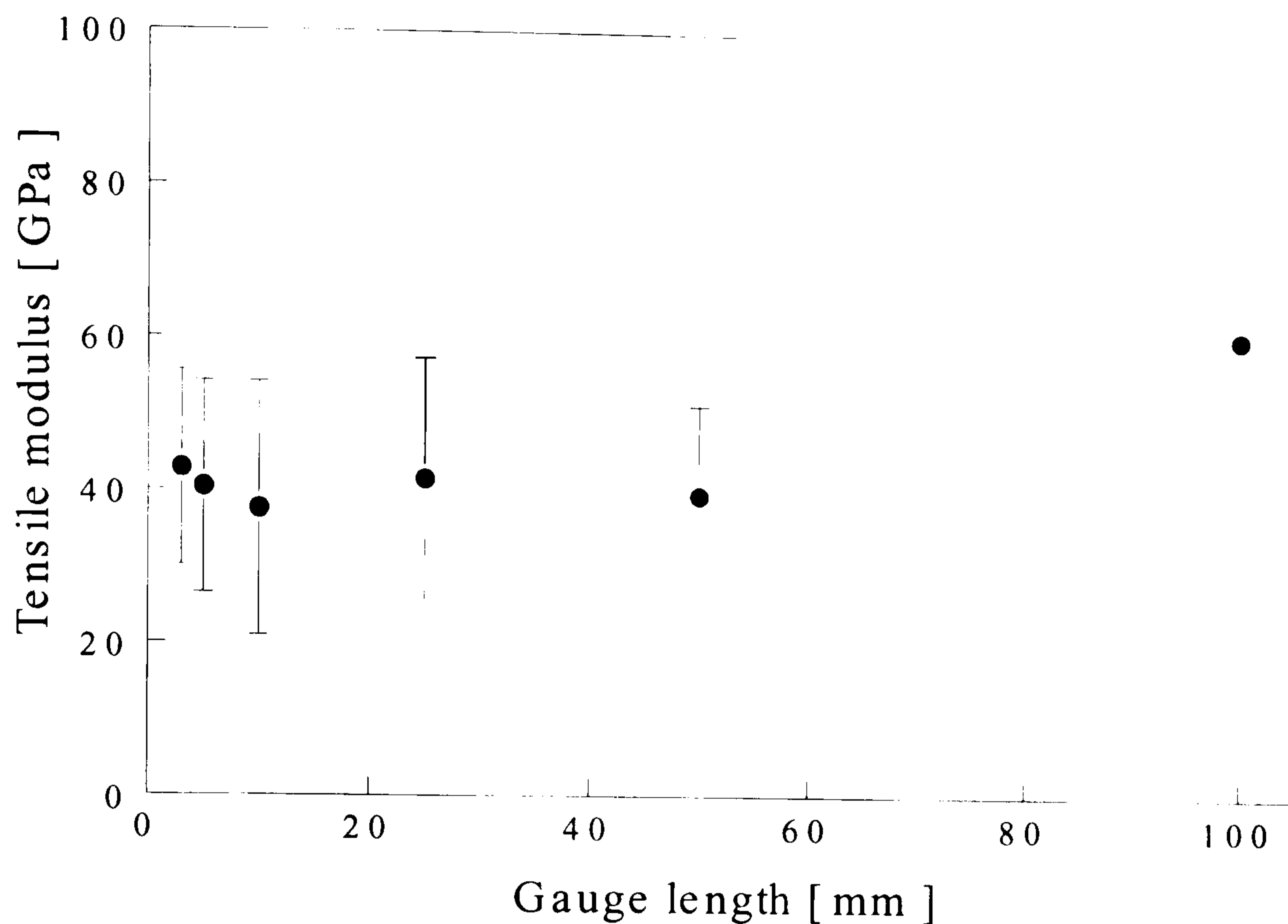


Figure 2.16 Tensile modulus of Duralin flax vs. gauge length (Error bars show the standard deviations).

2.2.3.2 Effect of heat treatment on tensile strength

Figure 2.17 shows the effect of heat treatment on the tensile strength of flax fibre. Also shown is the effect of fibre type on the tensile strength of heat-treated flax fibres. The results showed that fibre treatment (Duralin) not only produces fibres with improved strength but also lead to higher thermal stability when compared with green flax. It was observed that processing the (Duralin) fibres above 220 °C reduces the tensile strength considerably. In the case of green flax the observed reduction in the tensile strength was more prominent.

For processing the fibres at high temperature i.e. around the processing temperature of 220°C and setting the processing timings, it is important to know the effect of exposure to elevated temperatures on the tensile strength of flax

fibres. From Figure 2.18 it can be seen that after 10 minutes of heat treatment at 220°C the tensile strength of Duralin fibre reduces considerably. There is a reduction of 40% in strength when the fibre is kept at a temperature of 220°C for 30 min.

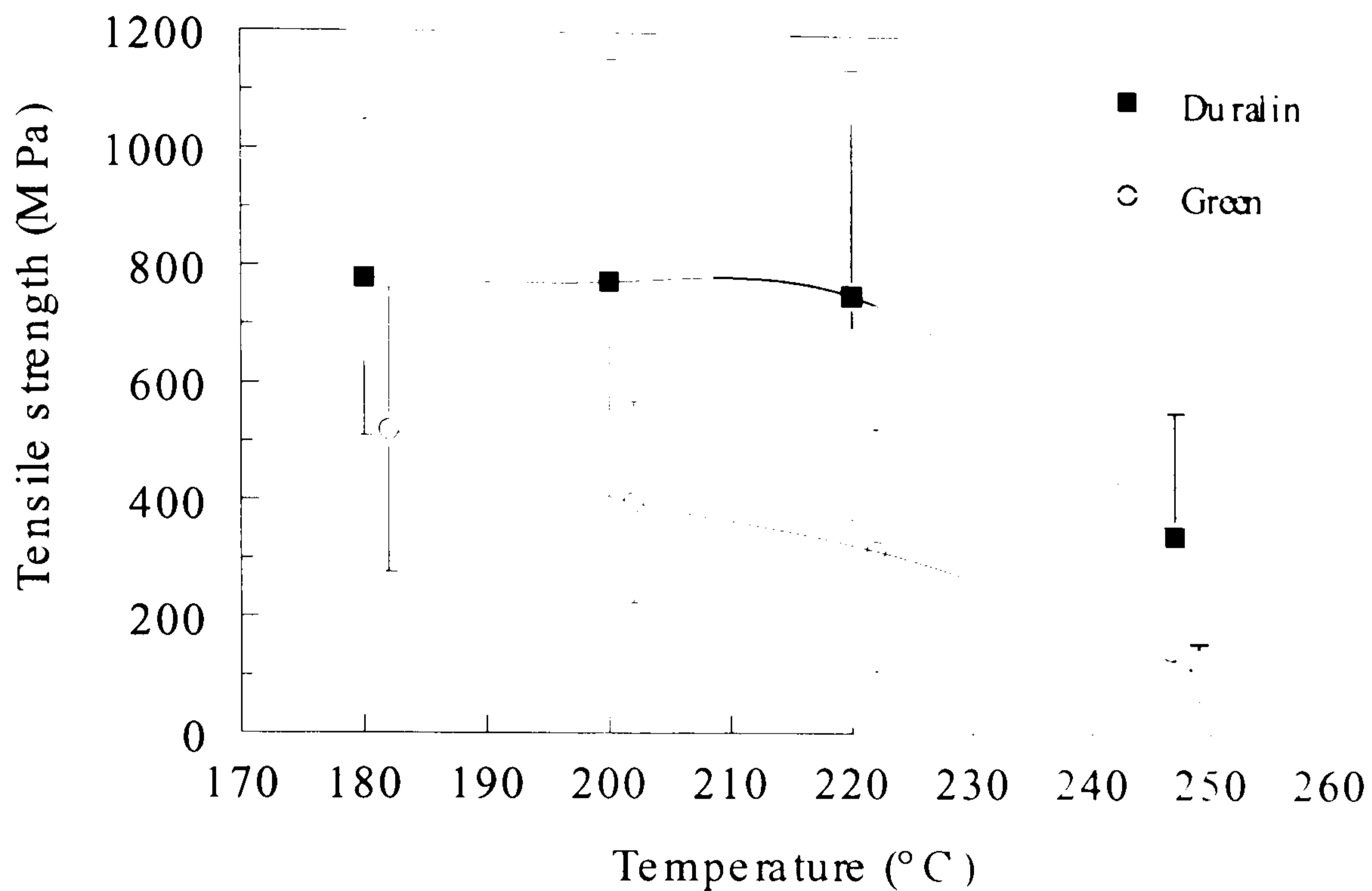


Figure 2.17 Effect of temperature on the tensile strength of flax fibres. (Gauge length = 10 mm, time of exposure = 5 min and testing temperature = Room temperature, error bars in the figure show the standard deviation, Spline curve was fitted using computer program Slide Write).

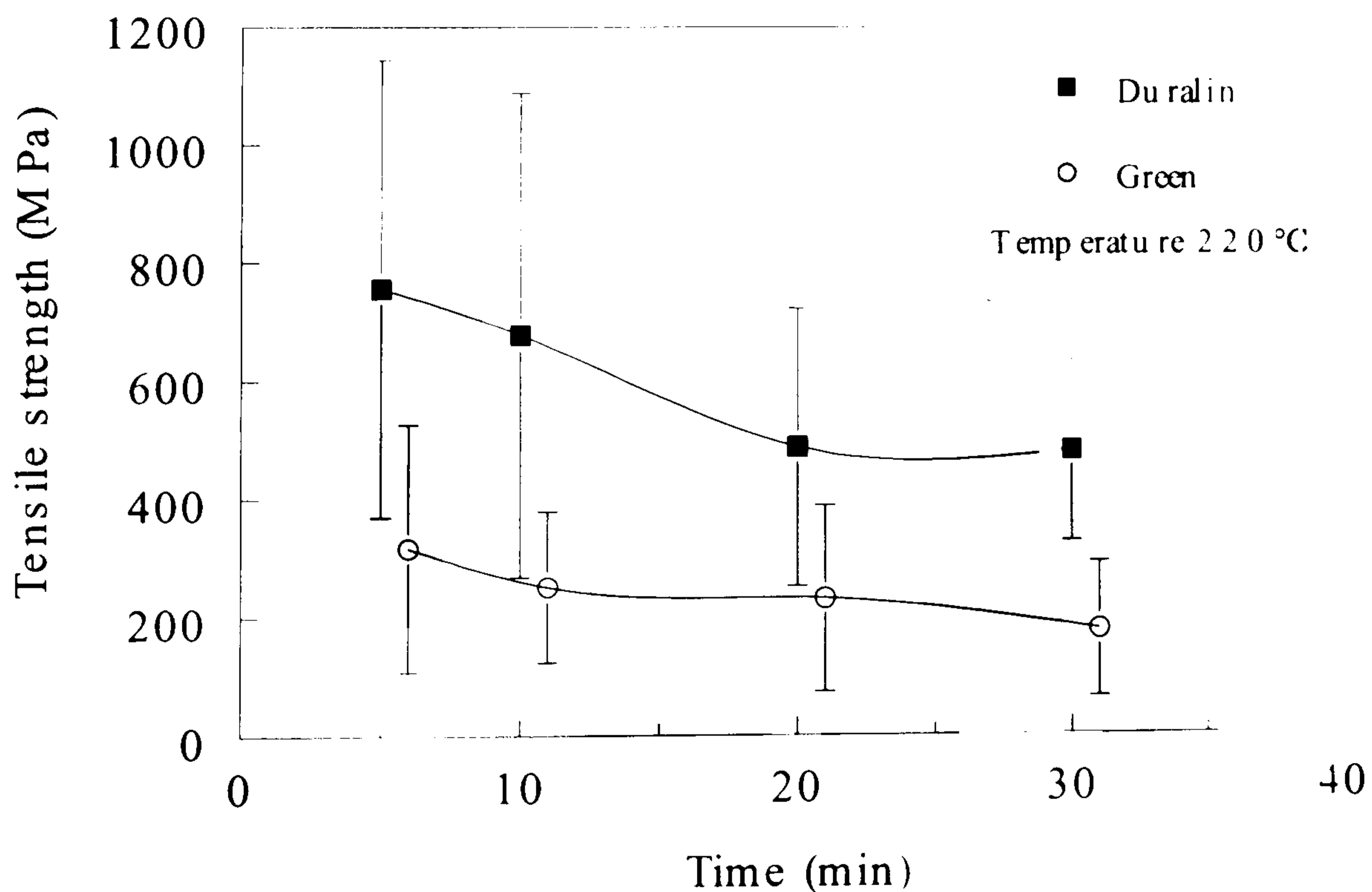


Figure 2.18 Effect of heat exposure time on the tensile strength of flax fibres. (Gauge length = 10 mm, testing temperature = 220°C, Error bars show the standard deviation, Spline curve was fitted using program Slide Write).

2.2.3.3 *Thermal gravimetric analysis (TGA) of flax fibres*

Thermal gravimetric analysis was done on flax fibre to study the effect of heat treatment on flax fibre degradation. Figure 2.19 shows the weight loss, with time, in green flax exposed to temperature between 200°C and 325°C. Similarly, Figure 2.20 shows the weight loss, with time, in Duralin flax exposed to temperature between 200°C to 325°C.

From the Figure 2.19 and 2.20 it can be seen that the weight loss in the case of Duralin fibres is more gradual when compared to green flax exposed at the same temperature for the same duration. A detailed chemical analysis is required to study the chemical differences during thermal degradation of both the fibres, which is beyond the scope of this thesis.

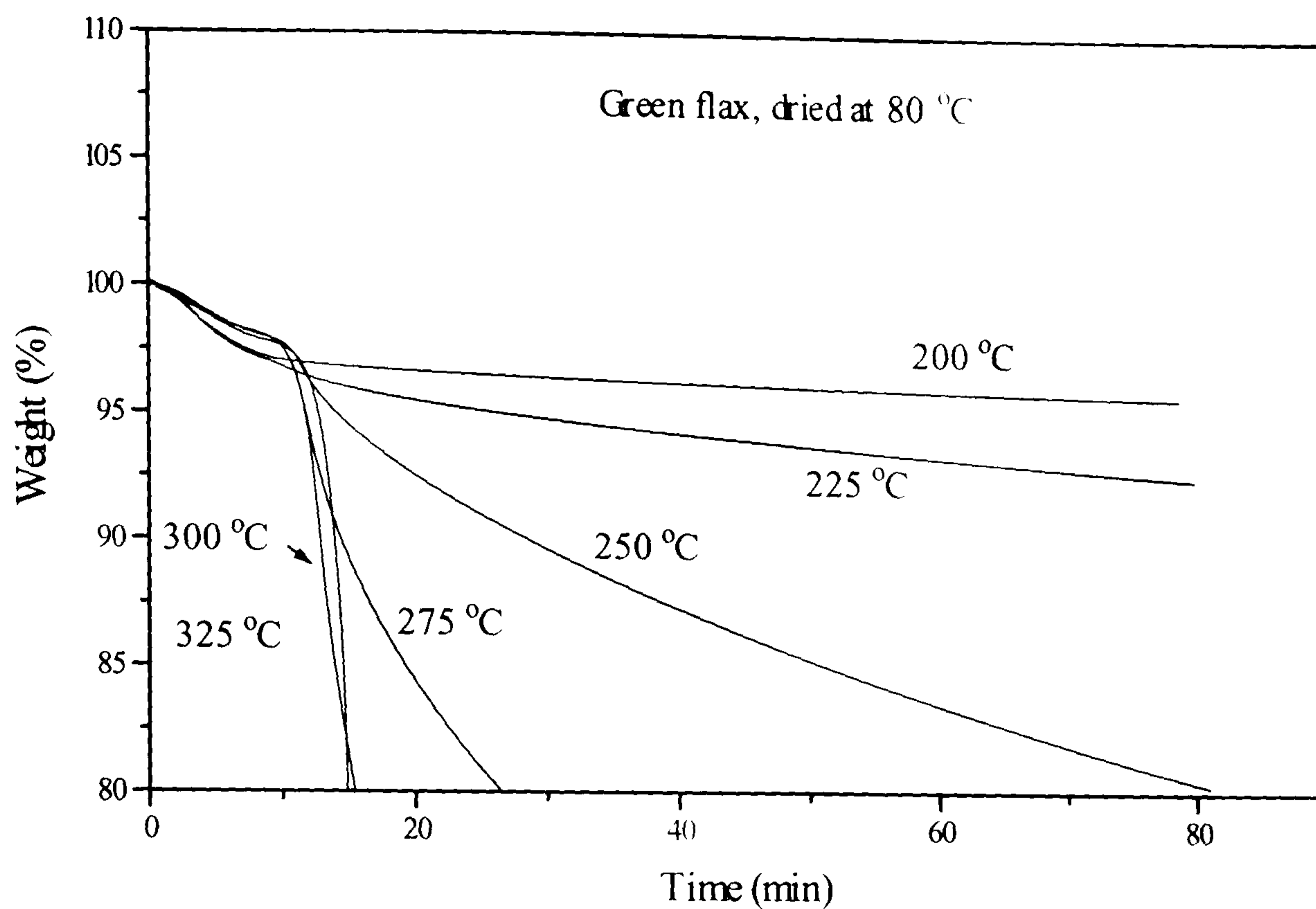


Figure 2.19 Effect of heat exposure on weight loss in green flax fibre (dried at 80°C for one week), measured through TGA (Isothermal exposure).

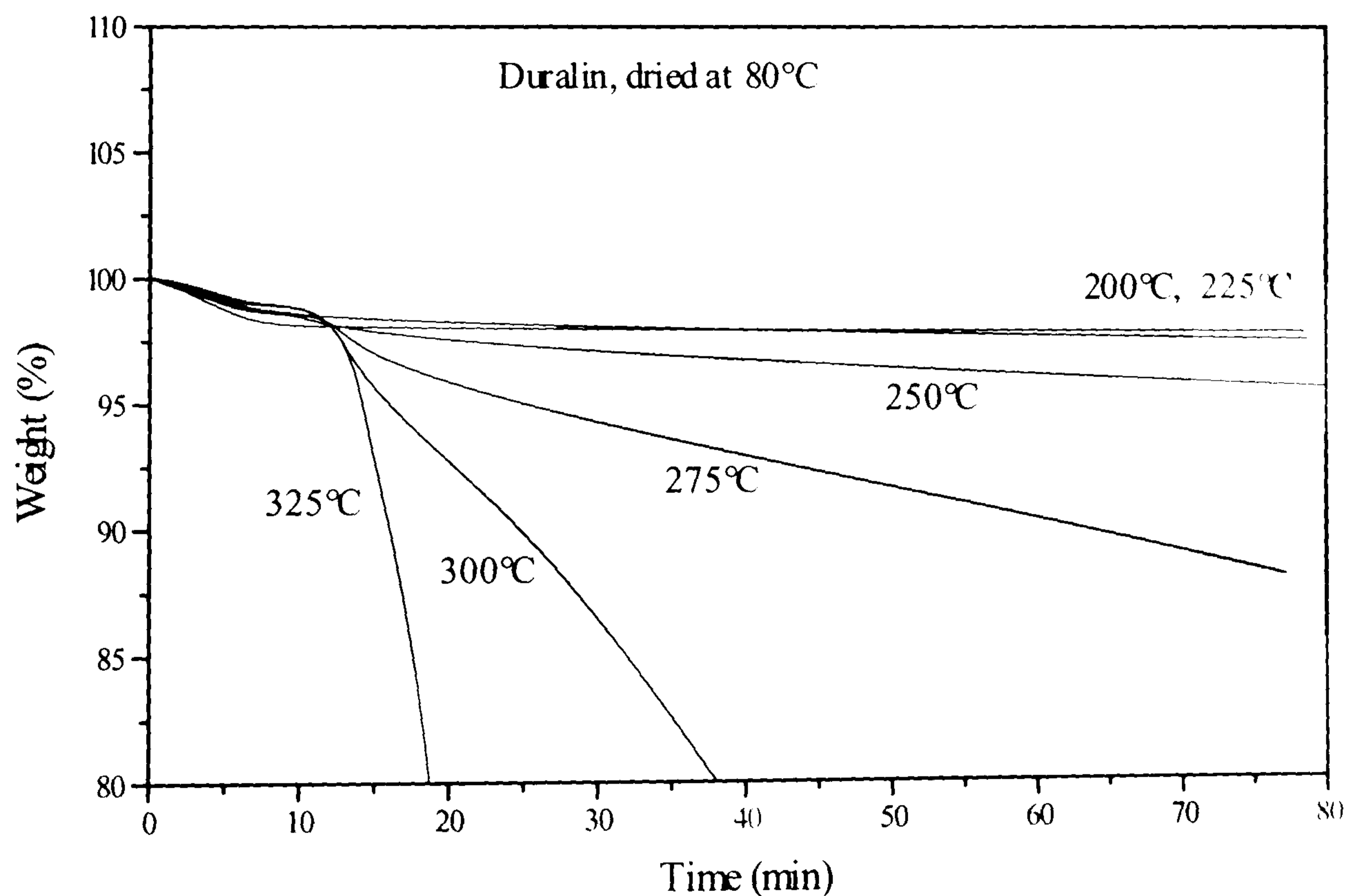


Figure 2.20 Effect of heat exposure on weight loss in Duralin flax fibre (dried at 80°C for one week), measured through TGA (Isothermal exposure).

Figure 2.21 and 2.22 show the effect of heating rate on the weight loss in green flax and Duralin flax, respectively. From the above-mentioned curves it can be concluded that Duralin fibres are thermally more stable than green flax. Also, it can be observed that though weight loss in flax fibres on exposure to temperatures in the range of 200-225°C is around 5% (for exposure time = approx. 30 minutes) but the reduction in the fibre strength is much higher i.e. around 37%. Therefore it is very important to control the processing time as low as possible. For good fibre wetting higher processing time and temperature are required which may be detrimental for fibre tensile properties.

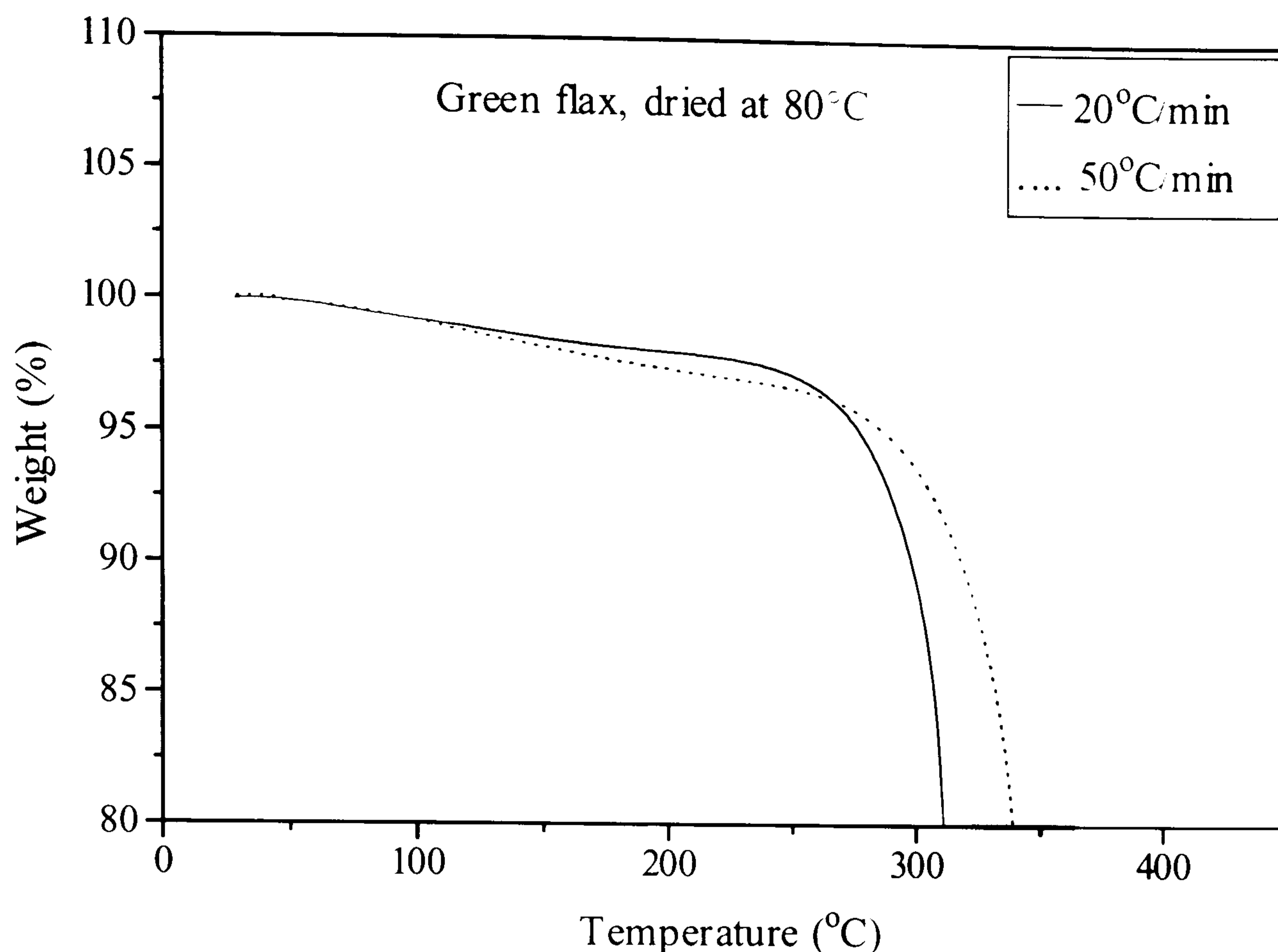


Figure 2.21 Effect of heat exposure (at different heating rates) on weight loss in green flax fibre (dried at 80°C for one week), measured through TGA.

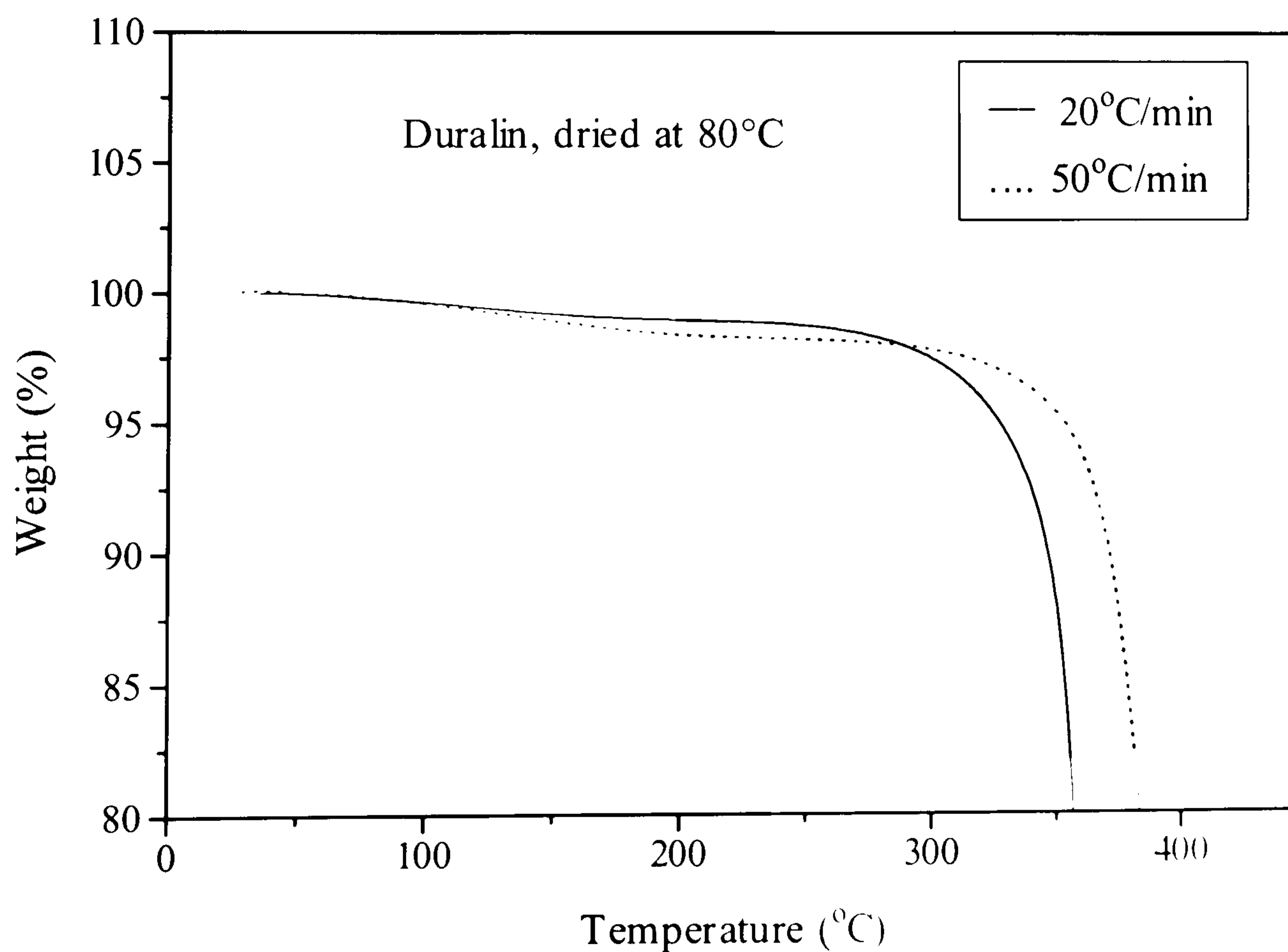


Figure 2.22 Effect of heat exposure (at different heating rates) on weight loss in Duralin flax fibre (dried at 80°C for one week), measured through TGA.

As observed from the thermal study of flax fibre, the processing temperature of flax could be, at most, around 220°C and processing time of 10 to 15 minutes. The longer the exposure to elevated temperatures, the more detrimental it would be for the mechanical properties of flax and hence composite. This limits the number of polymers, which could be used to make composites with flax fibres. Some of the polymers could be polyethylene, polypropylene, biopolymers like polyalkanoate, starch etc. As mentioned in Chapter 1, polypropylene (PP) is one of the most frequently used thermoplastics as a matrix material for composite applications. Some of the advantages offered by PP as a matrix material include:

- a) PP is easy to process and one of the cheapest polymers in the market which is of eminent importance in the 'cost-performance' sector.
- b) PP has a low processing temperature (around 165°C), which is essential because of relatively low thermal stability of natural fibres.
- c) PP has useful stability to protect the hydrophilic natural fibre because of its strong hydrophobic and apolar character.
- d) Finally, PP has been successfully used for composite applications with glass fibres as reinforcement.

Keeping in mind the properties of flax fibre and PP, the latter was selected as the principal matrix material to manufacture flax fibre reinforced composites. However, addition of flax to PP has certain disadvantages i.e. the recyclability of PP would be affected and disposal of composite through incineration would lead to CO₂ emission. Also, disposal of material through landfill has its limitations therefore bio-plastics i.e. polyhydroxyalkanoates (PHAs) were also selected as potential matrix materials.

2.3 Conclusions

From the presented study it can be concluded that flax fibre is a good candidate for

reinforcement of thermoplastics because of its good mechanical properties. The final mechanical property of flax fibre depends on the gauge lengths which could be because of reasons like: reduced number of weak points at smaller gauge lengths and different fracture modes i.e. rupture through fibre cell at low gauge lengths and through 'matrix' material when measured at longer gauge lengths. The ultimate utilisation of fibre mechanical properties seems to need separation of elementary fibres (fibre cells) and removal of impurities. The separation processes can lead to the damage of fibre cells and also add to the cost of these materials.

The final properties of flax fibre depend on the processing and can be engineered through different processing methods. One of the examples of improved performance of flax fibre through processing is Duralin flax, which has lower moisture sensitivity along with improved mechanical properties, when compared to flax fibre obtained through other processing routes like green flax and dew-retted flax. Also, Duralin fibres have improved thermal stability when compared to green flax. Flax fibres in general have low thermal stability and can be processed up to around 200-220°C, which limits the applicability of these fibres. Based on the thermal stability of flax fibres and the advantages offered by PP, the latter was selected as the principal matrix material for further studies.

3. A STUDY ON FLAX / POLYPROPYLENE INTERFACE: CHEMICAL MODIFICATIONS

In this chapter the theory about fibre-matrix interface is presented. Also, results from the micromechanical study, conducted to improve the interfacial bonding between flax and PP via chemical modifications of the matrix as well as flax fibre, are reported and discussed.

3.1 Introduction

The structure and properties of the fibre/matrix interface plays an important role in the mechanical and physical behaviour of composite materials. The fibre/matrix interface in cellulose fibre composites has been modified in different ways i.e. chemical modification (e.g. Felix and Gatenholm, 1991) (fibre coating and matrix modification) and modifications through controlling the processing conditions (transcrystallinity) (e.g. Zafeiropoulos, 2001). In the present chapter the results from a micro-mechanical study on the flax/polypropylene (PP) interface and chemical modification of flax/PP interface are reported and discussed.

As mentioned in the Chapter 1 and 2, for the present study flax fibres are used as reinforcements, mainly because of their good mechanical properties when compared with other natural fibres and also because of their availability in different forms in Western Europe. But since other fibres like hemp, kenaf and sisal are also based on ligno-cellulose, and only differ in the relative amounts of cellulose, hemicellulose and lignin; it is expected that the technology initially developed for flax can be transferred to other vegetable fibres.

PP, as a matrix material, has the perfect stability to protect the hydrophilic natural fibre because of its strong hydrophobic and apolar character. A clear disadvantage of this apolar character for composite applications is its limited wettability as well as poor interfacial bonding with reinforcing fibres. This disadvantage can, however, be overcome by functionalisation of the polymer or fibre, which has proven to be very effective in enhancing fibre/matrix adhesion in composite systems based on polyolefins (Felix and Gatenholm, 1991; Rijsdijk et al., 1993; Bledzki et al., 1996; Joly et al., 1996; Mieck et al., 1995b). One such example is maleic-anhydride grafted PP (MA-PP). Flax fibres contain functional hydroxyl groups that are able to interact chemically or through hydrogen bridges with the MA-PP.

To enhance/optimize the macro-mechanical properties, a micromechanical study was conducted for the flax/PP system. An attempt was made to modify the fibre/matrix interface/interphase via two approaches i.e. fibre treatment and matrix modifications. Effect on the fibre (green, dew-retted and Duralin flax fibres) surface was observed through Scanning Electron Microscopy (SEM) for physical characterisation and Low Energy Ion Spectroscopy (LEIS) for chemical characterisation. Changes in the interfacial adhesion were measured through the micro-debond test (Yue, 1995).

3.2 Interface and interphase: theories and characterisation methods

3.2.1 Theory of adhesion

The properties of composites are strongly influenced by factors such as processing conditions, proportions and properties of the matrix and reinforcement, the nature of adhesion between these, the shape, size, orientation and distribution of the reinforcement or filler and the design of these composites. The interfacial properties of a fibre-reinforced composite significantly affect the overall performance of the material. The interphase may be defined as, "a region

intermediate to two (usually solid) phase in contact, the composition and/or structure and/or properties of which may be variable across the region and which also may differ from the composition and/or structure and/or properties of either of the two contacting phases” (Sharpe and Akovali, 1993). An interphase becomes an interface if its thickness decreases to zero. A strong interface allows effective stress transfer between the matrix and fibres leading to a composite with high strength but low toughness. Conversely, a weak interface would increase the incidence of crack splitting and delamination at the interface during fracture thereby producing a composite with lower strength but high toughness. Therefore, an ideal interface would be a combination of good bonding, in the case where stress transfer is required, along with good energy absorption capability for high toughness e.g. a rubber like interface. Other properties of a composite, such as resistance to creep, fatigue and environmental degradation, are also affected by the characteristics of the interface. In these cases the relationship between properties and interface characteristics are generally complex. Since the nature of bonding between the matrix and the fibre is dependent on the atomic arrangement and chemical properties of the fibre and on the molecular conformations and chemical constitution of the polymer matrix, it follows that the interface is specific to each fibre-matrix system. Many fibres and particulate reinforcing agents are pre-treated before they are used as secondary phases in polymer composites. The most common pre-treatment involves the use of coupling agents to act eventually as a bridge between the filler and the matrix (Richardson, 1997). In many cases even very small additions of suitable coupling agents, e.g. 0.1-0.5 % (by weight) to glass or filler are said to produce significant improvements in engineering properties. The extent of adhesion between a fibre and the plastic matrix may not be directly related to the amount of surface treatment. Often an optimum is observed (Heuvel, 1998). To explain why materials adhere to each other, a large number of adhesion mechanisms have been proposed and recognised (Felix, 1997; Broutman et al., 1974; Voyutskii, 1963; Oksman, 1997; Bascom and Lee, 1990). Figure 3.1 shows a schematic description of various theories of adhesion.

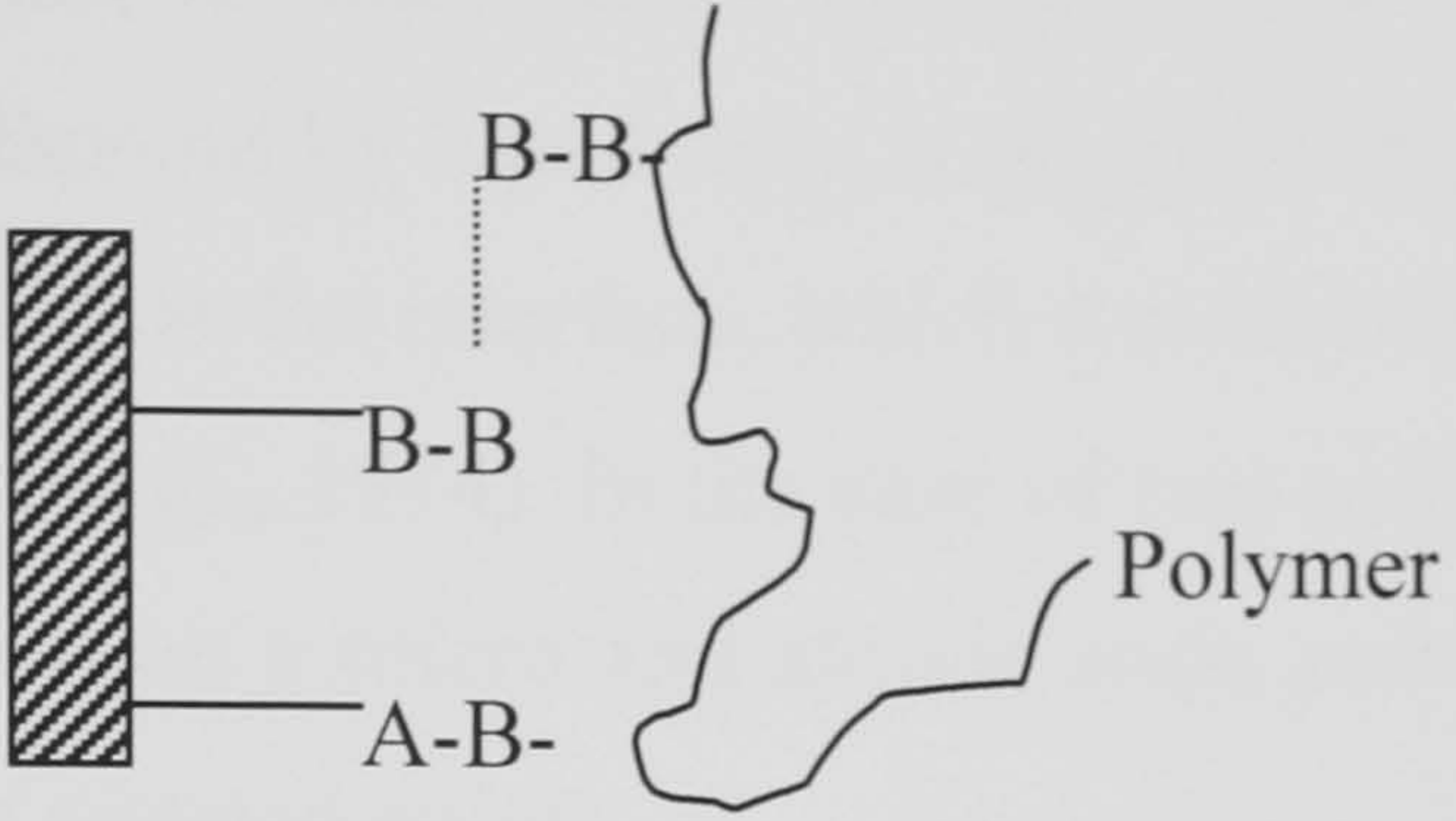
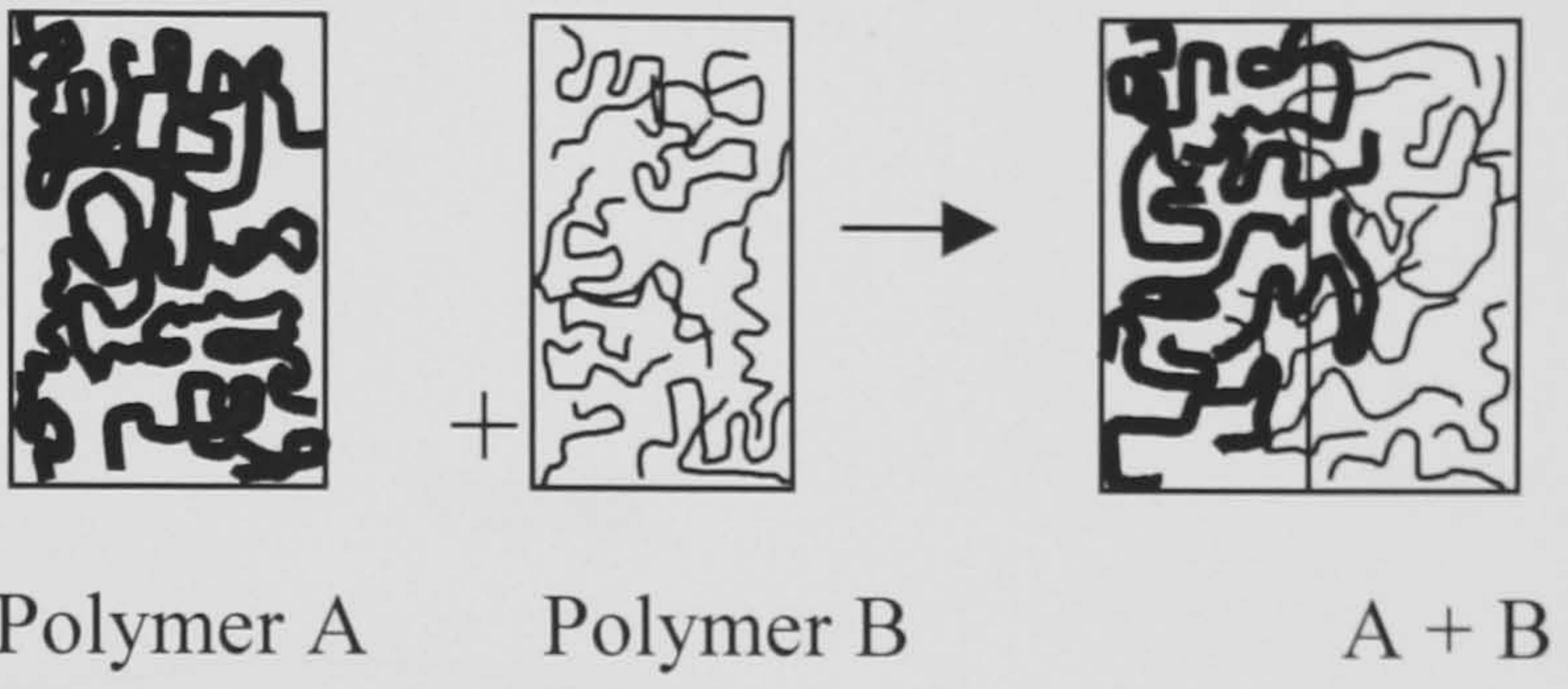
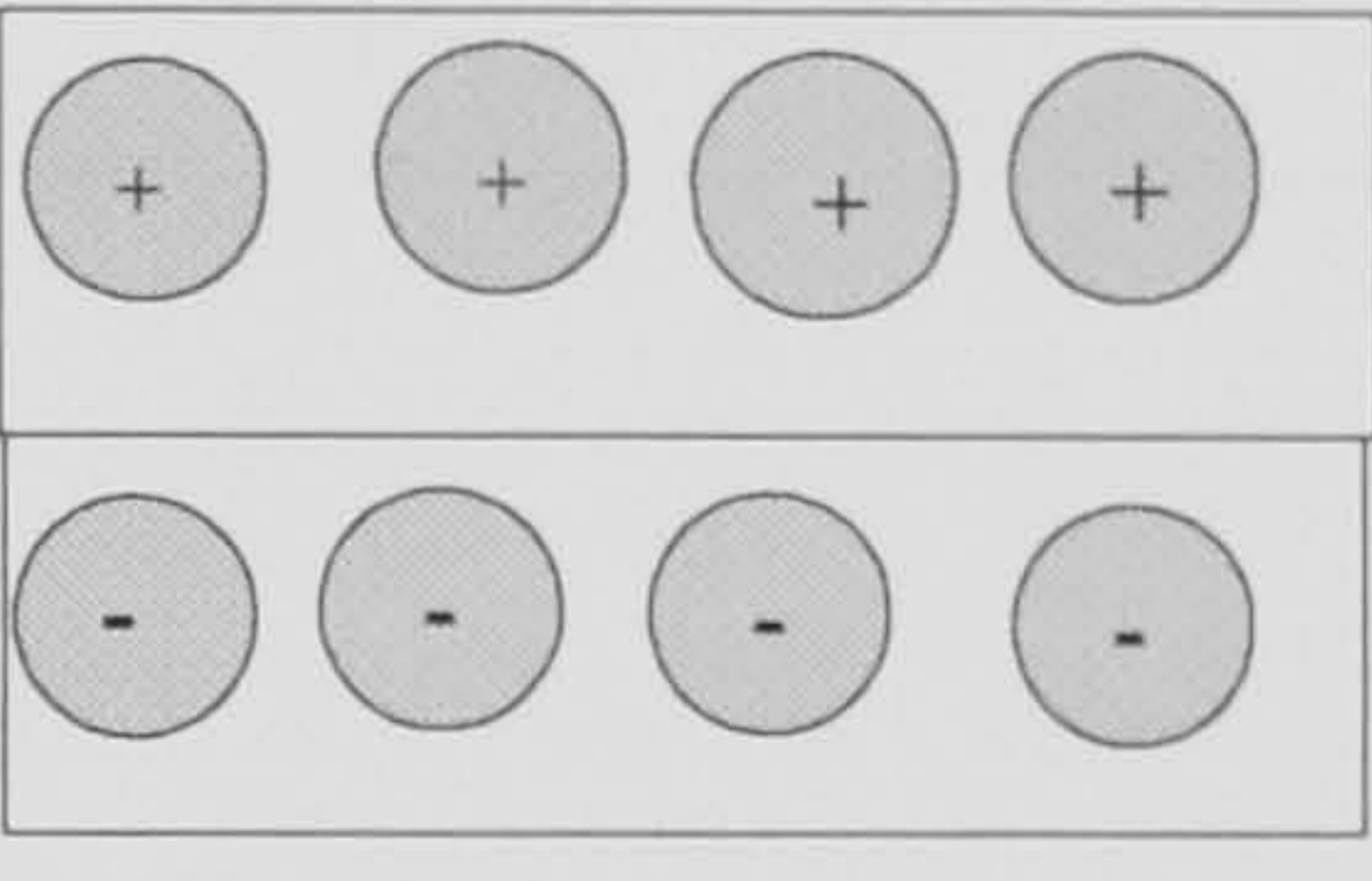
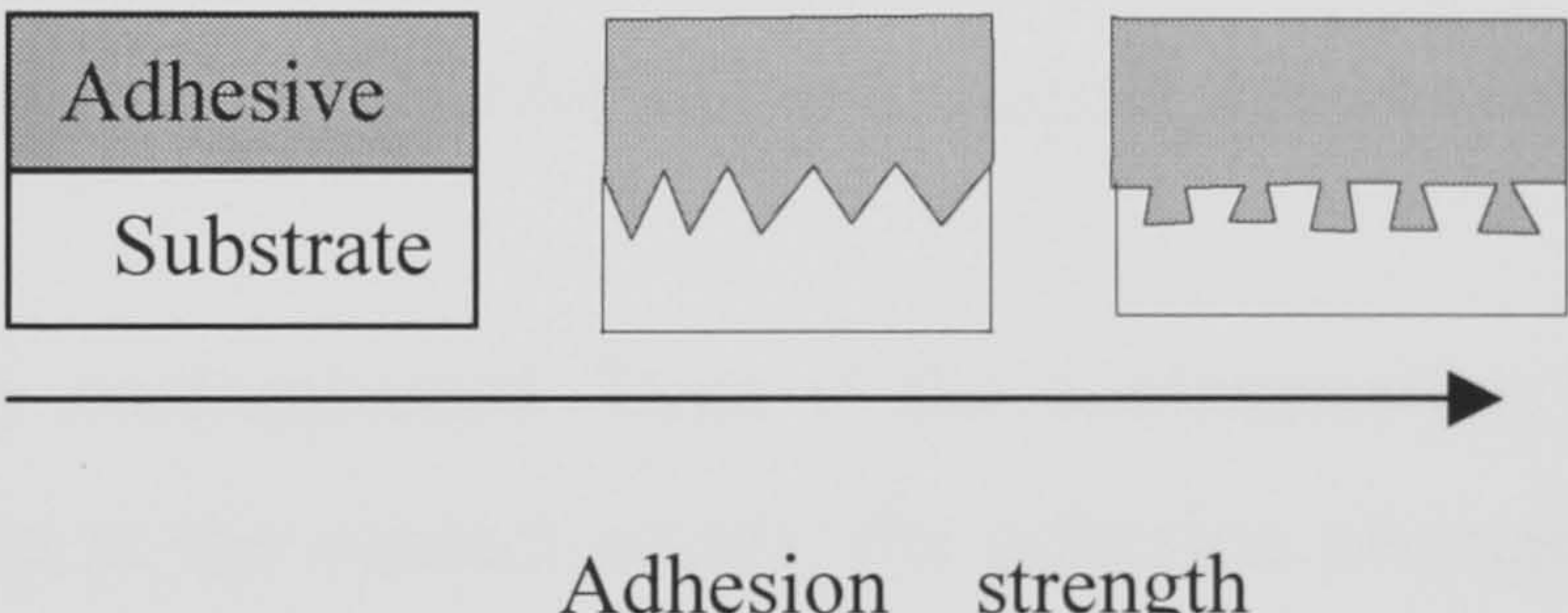
Adhesion mechanism	Schematic description
a) Adsorption and chemical bonding	
b) Diffusion	
c) Electrostatic attraction	
d) Mechanical interlocking	

Figure 3.1 Schematic description of various theories of adhesion, (a) adsorption and chemical bonding, (b) diffusion, (c) electrostatic attraction and (d) mechanical interlocking (Felix, 1997).

A brief description of the adhesion theories is as follows:

a) The wetting, adsorption and chemical bonding theory: When two electrically neutral surfaces are brought sufficiently close together, there is a physical attraction which is best understood by considering the wetting of solid surfaces by liquids. Adsorption is the process whereby a molecule is attracted to a

specific site on a solid surface. The attraction may be the result of Van der Waals forces or stronger specific donor/acceptor interactions (Felix, 1997). Zisman concluded that good wetting of the adherend by liquid resin is of prime importance since poor wetting would produce voids at the interface, which would concentrate stress and initiate cracking (Broutman et al., 1974). In the case of two solids being brought together, the surface roughness on a micro and atomic scale prevents the surfaces coming into contact except at isolated points.

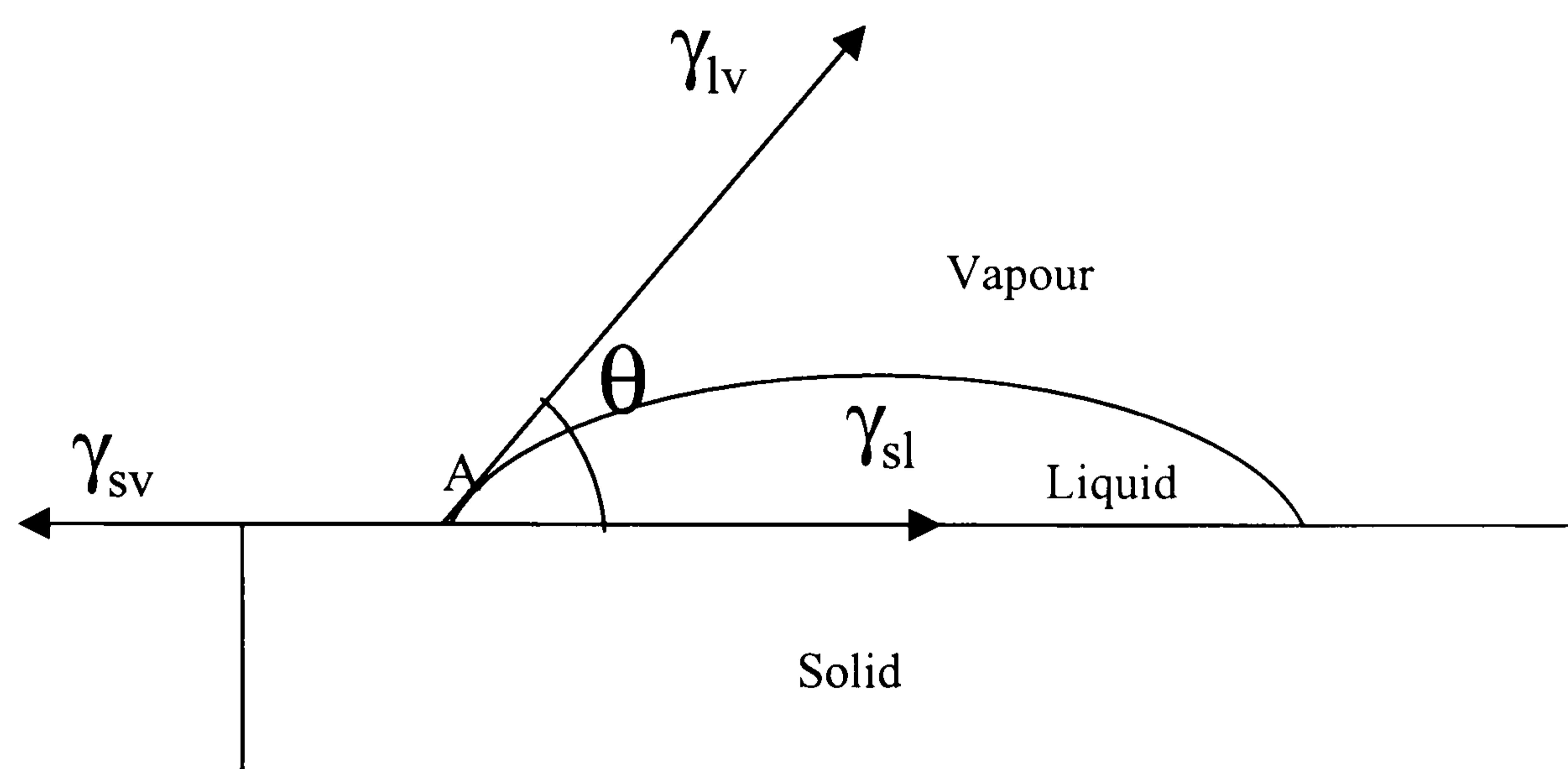


Figure 3.2 Schematic representation of solid-liquid and solid-vapour interactions.

In addition the surfaces are usually contaminated. Even if the contamination is removed, and strong adhesion occurs at the contact points, the adhesion averaged over whole surface will be weak. For effective wetting of a fibre surface, the liquid matrix must cover every hill and valley of the surface to displace all the air.

Physical adsorption of resin on high-energy surfaces would provide adhesive strength far in excess of cohesive strength of organic resins if complete wetting were obtained (Broutman et al., 1974). Lowering the surface energies of the interface between the filler and the matrix is the most common method to improve wetting (Oksman, 1997). This can be achieved by the use of suitable surface treatments or by incorporation of interfacially active additives. Zisman introduced the concept of critical surface tension of wetting (γ_c). In order to obtain complete wetting of a surface, the adhesive must be initially of low viscosity and must have

surface tension lower than the critical surface tension (γ_c) of the reinforcement surface. As mentioned earlier, unwetted areas would produce voids at the interface, which would concentrate stress and initiate cracking (Broutman et al., 1974).

Lotz et al. found that silanes providing the highest critical surface tension (γ_c) also gave the best laminates (Broutman et al., 1974). It is evident, in many cases, that the primary mechanism of adhesion through coupling agents is not by wettability, but after the primary bonding requirements are met further improvements may result by improving wettability, e.g. treated glass by the resin.

The chemical bonding theory was the oldest and still best known of the theories. The coupling agent contains chemical functional groups, which could theoretically react with the reactive groups of the fibres. Adhesion could thus be made to the fibre by covalent bonds. The coupling agent, in addition, might contain one other different functional group, which could theoretically co-react with the matrix. Assuming that this all occurred, the coupling agent acted as a vehicle to bond the glass to the resin with a chain of primary bonds. This should theoretically lead to the strongest interfacial bond (200 – 400 kJ/mole) (Broutman et al., 1974). Coupling agents, e.g. silanes, which are used for adhesion improvement in many multi-component systems, usually function by providing chemical bonds across the interface. The strength of the bond depends on the number and type of bonds and interface fracture must involve bond breakage for optimum strength properties.

b) The electrostatic attraction theory: Forces of attraction occur between two surfaces with different charges. Ionic, hydrogen bonding, acid-base interactions, polar interactions, dipole-dipole interactions and Van der Waals forces across the interface also provide a means to transmit stress. The bond strength of these mechanisms varies considerably; hydrogen, ionic and acid-base bonds give stronger interactions while others are weaker (Oksman, 1997). Fowkes suggested that the work of adhesion could be broken into various parts, corresponding to different types of interactions (Felix, 1997). The detailed description of these

theories and the technique, called inverse gas chromatography, which is used for obtaining estimation of acid/base interaction, is reported by Felix (Felix, 1997).

c) The interdiffusion theory: It is possible to form a bond between two polymer surfaces by diffusion of the polymer molecules from one surface into the molecular network of the other surface at temperatures above their glass transition temperature (Voyutskii, 1963; Felix, 1997; Oksman, 1997), as illustrated in Figure 3.1(b). The bond strength will depend on the amount of molecular entanglement and the number of molecules involved. Interdiffusion may be promoted by the presence of solvents or plasticising agents and the amount of diffusion will depend on the molecular conformation and constituents involved. In a particular study of an interfacial phenomenon the system composed of coated cellulose/Polystyrene (PS) i.e. the butyl benzyl phthalate (BBP) - plasticised polyvinylchloride (PVC) coated cellulose fibres were incorporated into PS matrix (Gatenholm et al., 1993). An interface consisting of a blend of PS and PVC was formed as result of molecular interdiffusion of the two components. In this case plasticiser acted as a cosolvent for PVC and PS at concentrations prevailing in the interface between PS and the plasticised PVC coatings. When incompatible polymers are combined, the diffused layer or interphase is very thin, 0.5 - 10 nm. Systems comprising compatible components, however, may develop interdiffused layers up to 10 microns thick (Felix, 1997).

d) Weak boundary layer theory: Weak boundary layers are cohesively weak, often thin layers at the interface that may be formed from the migration of low molecular weight fractions, lubrications or additives, adsorption of oily contaminants from the environment or the formation of weak oxide layers on metals. In some cases the coupling agents may eliminate weak boundary layers either through chemical reaction or suppression of these layers, therefore leading to enhancement of fibre/matrix adhesion (Felix, 1997; Gassan and Bledzki, 1998).

e) The mechanical interlocking theory: Some bonding may occur purely by the mechanical interlocking of two surfaces as shown in Figure 3.1(d). A resin, which completely wets the fibre surface, follows every detail of that surface. The strength

in shear may be very significant and depends on the degree of roughness. Roughness would increase the work of adhesion because the surface area is increased. Polymer composites are formed when the matrix is in low viscosity so this mechanism may have a significant contribution to the adhesion (Oksman, 1997). The mechanical interlocking differs from the diffusion theory, such that, the latter involves interpenetration of adhesive molecules and substrate molecules at a molecular level, while, in the former case, the adhesive flows into and around pores and projections in the substrate that are much larger than molecules.

f) Effect of morphological features (Adsorption and/or mechanical adhesion): It may be worth mentioning here that in many cases the various adhesion mechanisms mentioned above may work together. A critical issue in the processing of semicrystalline thermoplastic composites is the microstructure or morphology of the matrix material. Morphological features such as degree of crystallinity, spherulite size, lamellae thickness and crystalline orientation have a profound effect on the ultimate properties of the polymer matrix, and thus the composite. These features are, in turn, affected by the variation in the processing conditions. In composites this situation is further complicated by the effect of the reinforcing fibres on the morphology of the matrix. It is well established that incorporation of high modulus fibres in thermoplastics leads to significant improvement of engineering plastics, such as stiffness, tensile strength and heat distortion temperature. It has been proposed that this improvement may result from changes in morphology and crystallinity of the polymer matrix in the interfacial region. Mechanisms responsible for the improvement involve interfacial adsorption yielding an ordered transcrystalline PP interphase having a high density of intermolecular bonds with the fibre surface (Felix and Gatenholm, 1994). The controlled cooling of the matrix might favour the kinetics of approach of matrix molecules on the fibre surface. The stronger and stiffer transcrystalline phase may provide an efficient mechanical interlock on the rough fibre surface.

3.2.1.1 Fibre surface treatment

As mentioned earlier, one of the ways used to enhance adhesion is chemical modification of the fibres or matrix with coupling or compatibilising agents.

Much research work has been done and being presently carried out to overcome the hindrances and therefore enhance the utility of the natural fibres reinforced plastics for applications such as engineering polymeric materials. Some of the various compatibilisers and modifications, used to improve the compatibility in various systems involving natural fibres and thermoplastic matrix materials, are listed in the Table 3.1 along with the references.

Table 3.1 List of some of the compatibilisers and modifications studied for cellulosic materials and plastic systems.

Treatment studied	References
MA-PP	Felix, 1997; Gassan and Bledzki, 1998; Park and Balatinecz, 1997; Bos et al., 1998; Karmaker and Youngquist, 1996; Hornsby et al., 1997; Heijenrath and Peijs, 1996; Mieck et al., 1996.
Silanes	Felix, 1997; Hornsby et al., 1997; Wang and Harrison, 1994; Herrera-Franco and Aguilar-Vega, 1997; Karnani et al., 1997.
Acrylic polymer	Wang and Harrison, 1994.
Plasma treatment	Felix, 1997.
Stearin acid	Hornsby et al., 1997.
Stearic acid	Hornsby et al., 1997.
EPDM rubber	Park and Balatinecz, 1997.
Cardanol derivative of toluene, 2, 4 di-isocyanate (CTDIC)	Kuruvila and Thomas, 1995.
Alkali treatment	Prasad et al., 1983.
Preferential crystallisation studies	Felix, 1997; Felix, J. M., and Gatenholm.

	1994; Wang, G., and Harrison, 1994.
m-phenylene bismaleimide	Sain and Kokta, 1994.
Acetylation	Zafeiropoulos et al., 2000.
Alkenyl succinic anhydride (ASA)	Felix, 1997.

Some of the studied systems, involving cellulosic material and thermoplastic matrices, are given in Table 3.2 along with the references.

Table 3.2 List of some of the cellulose /thermoplastic systems studied.

System studied	References
Flax / polypropylene (PP)	Heijenrath and Peijs, 1996; Mieck et al., 1996; Bos et al., 1998; Peijs et al., 1998.
Cellulose / polystyrene (PS)	Felix, 1997.
Cellulose / PP	Felix, 1997.
Jute / PP	Karmaker and Youngquist, 1996; Gassan and Bledzki, 1998.
Wood fibre / PP	Sain and Kokta, 1994; Wang and Harrison, 1994; Clemons et al., 1997; Park and Balatinecz, 1997.
Cotton / PP	Felix, 1997.
Henequen / low density polyethylene (LDPE)	Herrera-Franco and Aguilar-Vega, 1997.
Kenaf / PP	Karnani et al., 1997.
Sisal / PP	Karnani et al., 1997.
Wheat and flax straw / PP	Hornsby et al., 1997.
Rayon / PP	Felix, 1997.
Paper / PP	Felix, 1997.
Cellulose / Chlorinated Polyethylene (CPE)	Felix, 1997.
Rayon / LDPE	Felix, 1997.

In general it was found that addition of compatibilisers like silanes, iso-cyanate and maleic anhydride-modified-polypropylene (MAPP) lead to improvement in the tensile strength, stiffness and impact properties. Chemical modification methods such as acetylation of the OH-groups have shown to improve the moisture absorption and swelling of natural fibres. However, these improvements were obtained at the expense of the mechanical properties of the fibres, for instance, in the case of dew-retted flax fibres (Zafeiropoulos et al., 2000). In the case of green flax, acetylation is shown to improve the fibre tensile strength (Zafeiropoulos et al., 2000). Also the steam explosion process, in which the hemicellulose, which is responsible for high moisture uptake, is partly removed (Satyanarayana et al., 1981), severely affects the fibre properties.

Generally, to enhance the compatibility between hydrophobic and hydrophilic components of a system, the compatibilising agents have:

- a functional group able to react with the hydroxyl groups of cellulose,
- a more or less long alkyl chain, which decreases the hydrophilicity of the fibre and at the same time, makes its surface more compatible for good adhesion to the matrix.

In previous studies on glass/PP composites (Rijsdijk et al., 1993) and cellulose/PP composites it is shown that an improved fibre/matrix interaction is achieved via blending of the PP with a maleic-anhydride grafted polypropylene copolymer (MA-PP) (Felix and Gatenholm, 1991; Bledzki et al., 1996; Joly et al., 1996; Mieck et al., 1995b). The maleic-anhydride group, present in the MA-PP, not only provides polar interactions but also can covalently link to the hydroxyl groups on the lignocellulosic fibre (Figure 3.3). The formation of ester linkages and hydrogen bonds between the MA- and the -OH of cellulose has been indicated through Fourier Transformed Infrared Spectroscopy (FTIR) and Electron Spectroscopy for Chemical Analysis (ESCA) analysis by Gatenholm et al. (Felix and Gatenholm, 1991). Whereas, the alkyl group molecules chain end promotes adhesion with the bulk polymer matrix through chain entanglements (Gong et al., 1998). Also, the

similarity of the additive and matrix structure can permit the occurrence of segmental crystallisation, which is desirable for cohesive coupling between the copolymer and the PP matrix (Felix and Gatenholm, 1991). After the MA-PP treatment, the surface energy of the fibres is increased to a level much closer to the surface energy of the matrix. Thus, a better wettability and a higher interfacial adhesion are obtained.

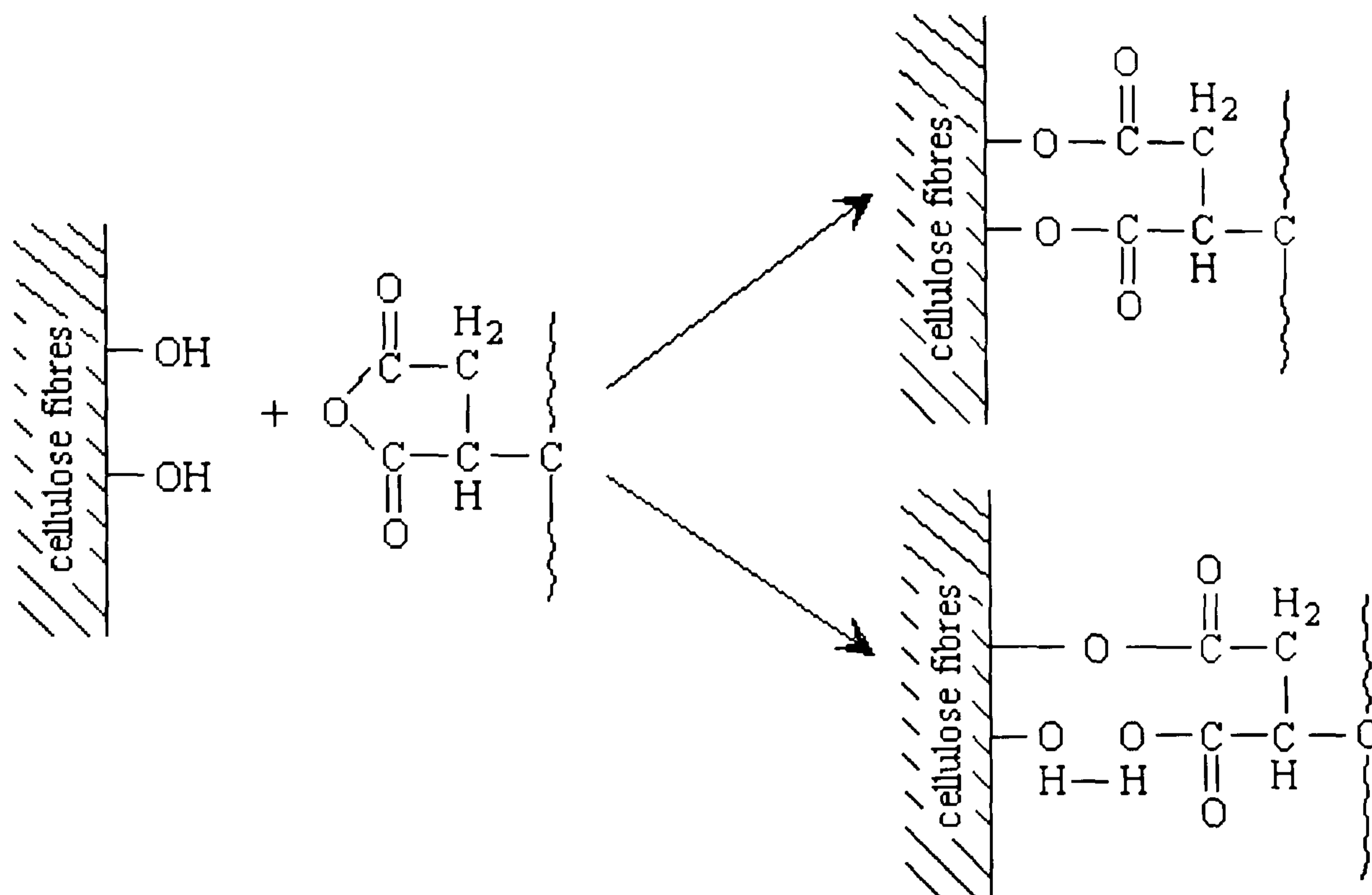


Figure 3.3 Schematic representation of the adhesion process between MA-PP and the flax fibre.

a) Physical state of the fibre surface

The physical state of a fibre surface is a fundamental feature, which plays a role in the adhesion between the fibre and a matrix. The fibre roughness may indeed have a favourable or unfavourable effect on the adhesion. The higher the surface area available, the higher the surface contact with the matrix is possible. However, if the amplitude of the pits (characterising the surface roughness) is too high, a good wetting between the fibre and the matrix may not be reached. In this case unfilled gaps might be the preferential places for the initiation of cracks.

Different experimental techniques are available for characterisation of the physical state of the fibre surface. Each of them has its own domain of application and gives

information concerning the fibre surface at a particular level. The use of Scanning Electron Microscopy (SEM) gives a general view concerning the microscopic fibre surface morphology.

b) Chemical state of the fibre surface

The surface treatment applied to the fibre surface induces changes in the chemical structure of the fibre surface (Felix and Gatenholm, 1991). These changes may also lead to important changes in the reactivity of the fibre surface.

The reactivity of the fibre surface is a crucial factor for understanding the adhesion process between the fibre and the matrix. To understand the adhesion mechanism present at the fibre surface, a thorough physical and chemical characterisation of the fibre surface is needed.

Felix and Gatenholm (Felix and Gatenholm, 1991) had studied the function of coupling agent MA-PP at the molecular level, by using surface analysis techniques such as ESCA and contact angle measurements. Whereas, the nature of adhesion for the system had been investigated using FTIR and titrimetric analyses. In the results of the ESCA measurements they had found that the C-C peak of the treated fibres showed a dramatic increase. Moreover, the O/C ratio and the O/(O-C=O) ratio had decreased by 40 and 50% respectively. However, the gravimetric analyses had shown that the decrease of the O/C ratio of the fibre bulk was only 6%. This indicated that the MA-PP copolymer was concentrated on the surfaces of the treated fibres, thus explaining their hydrophobic properties.

The contact angle measurements had shown that cellulose fibres treated with the copolymer turned totally hydrophobic and according to ESCA this was due to the fact that a considerable amount of copolymer was concentrated on the fibre surfaces. The FTIR and titrimetric analyses had shown that the copolymer was bonded to the fibres by ester linkages and hydrogen bonds.

These results indicate that the important changes take place at the surface of the fibre. A different technique to study the chemical composition of the fibre surface is Low-Energy Ions Scattering (LEIS) (explained in the next section). The difference between this technique (LEIS) and ESCA is the sampling depth. The sampling depth using ESCA is in the range of 10-100 Å, whereas in case of LEIS the sampling depth includes the outer layers of atoms of the sample. So a more detailed image of the outermost layer of the fibre surface chemistry can be detected. The principle of LEIS is shown in Section 3.2.2 (b).

3.2.2 Interface / interphase characterisation methods

Optimisation of interface requires reliable interface strength data and measurement systems. Various methods have been developed to measure and/or characterise the changes in the interface caused by different treatments on the fibre (e.g. chemical treatments) or in the matrix (e.g. addition of functionalised polymer). There are two general approaches to such studies, namely the mechanics approach and the structure approach (Yue, 1995) (Figure 3.4):

a) Mechanics approach: The mechanics approach encompasses development of models to predict the stress distribution in the fibre, matrix and the interface. The interfacial properties of a composite system are characterised by factors such as; the interfacial shear (bond) strength, τ_i , the interfacial toughness, G_i , the interface Young's modulus, E_i , the matrix shrinkage pressure, P_o , on the fibre, and the interfacial coefficient of friction μ . (Yue, 1995; Meurs et al., 1996) It may be noted that the term interface and interphase are replaceable in the above properties. Various mathematical models have been developed based on the properties of the elements constituting the composite e.g. matrix, fibre, filler and additives etc. with assumptions about their interactions, which are useful for prediction of the properties of composite materials. Elasticity theory and finite element analysis have been used to predict E_i and other moduli using more realistic assumptions.

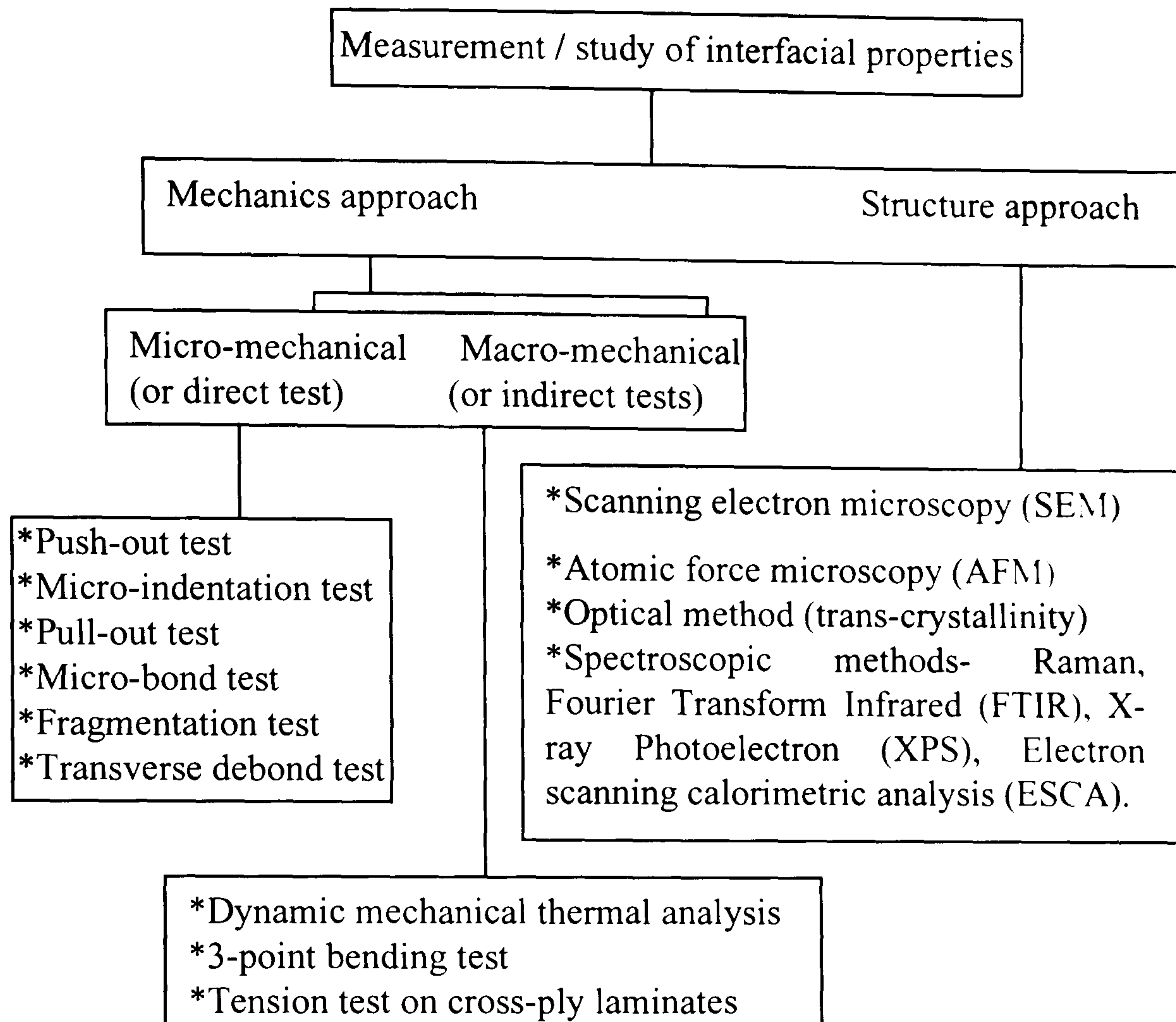


Figure 3.4 The schematic overview of some of the methods applied to study / measure the interfacial properties.

The changes in the interfacial properties are also observed through the changes in the macroscopic mechanical properties of the composites e.g. tensile and impact strength, modulus etc. A macro-mechanical composite property is measured; this is assumed or proved to be related to the interface strength. These techniques give indirect information about the interface properties and never generate pure interface strength. Hence their results cannot be used as absolute interface values (i.e. in micromechanical models); they only have a relative qualitative value (Verpoest and Jones, 1994) (Figure 3.4). To determine the interfacial properties at the micro-scale level various micromechanical test methods are used (Piggott and Dai, 1991; Strong, 1993; Yue, 1995) (Figure 3.4, 3.5) such as:

- i) the pull-out test,
- ii) the micro-debond or microtension test,
- iii) the fragmentation test,

- iv) the microindentation or microcompression test,
- v) short beam shear or three-point bending test,
- vi) Iosipescu test,
- vii) transverse tensile test.

The above mentioned tests are based on the measurement of force required for the failure of the interface. The failure induced during the test may not be adhesive; i.e. the two components may not have separated at the interface. The failure may take place close to the interface but in the reinforcement or in the matrix; also called as cohesive failure (Strong, 1993).

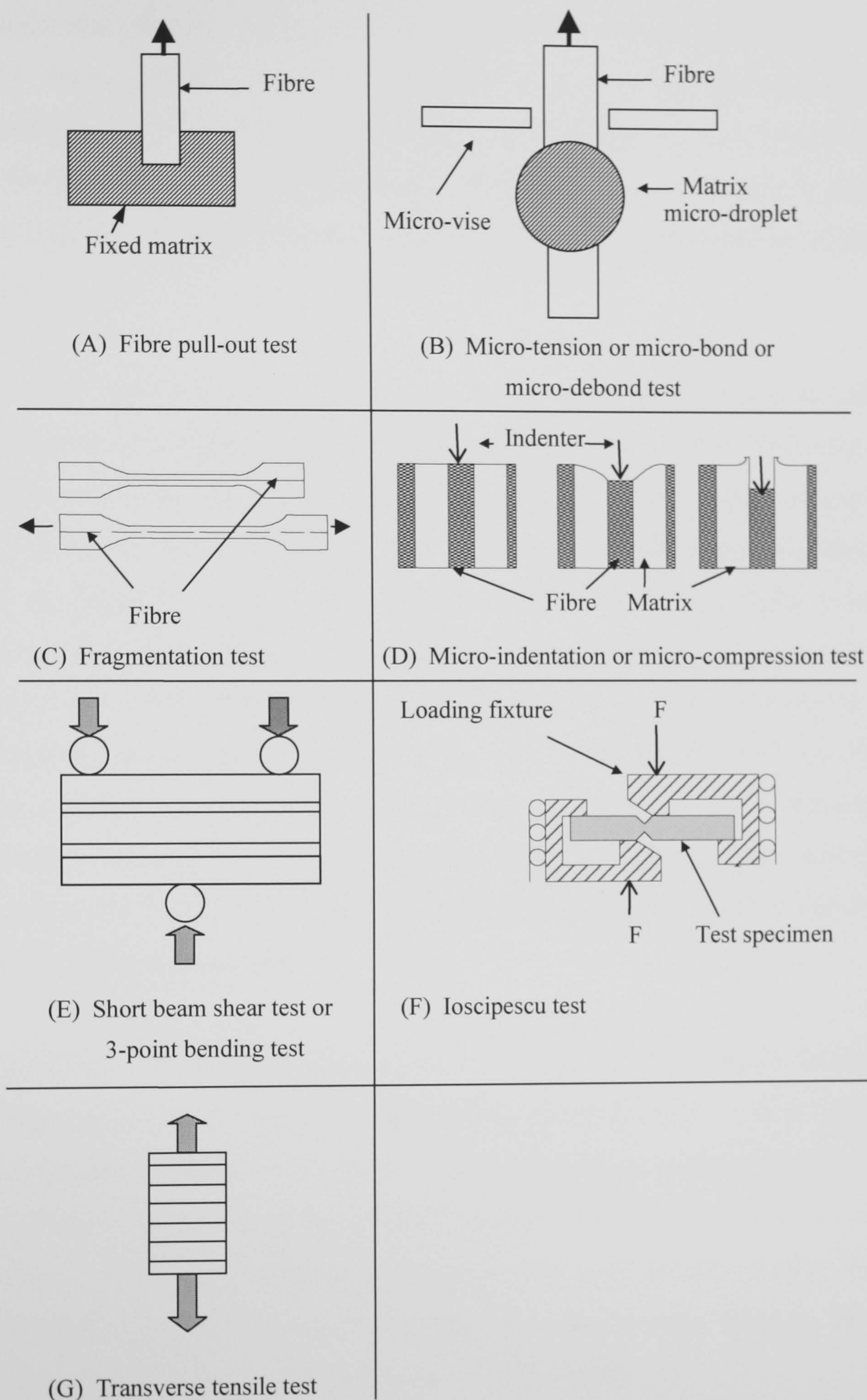


Figure 3.5 Schematic representation of different mechanical tests for the measurement of interface related properties.

b) Structural approach: The structure approach seeks to identify and characterise the physical and chemical nature of the interface and to establish the formation of any new phase (interphase) e.g. transcrystalline layer at the fibre surfaces in reinforced thermoplastics, layers of coupling agents applied to fibre surfaces, new phases formed by matrix-coupling agent interdiffusion etc. The changes in surface structure and composition induced by modifications may be detected by a variety of techniques:

i) Microscopy: Optical microscopy has been used to study the structural changes at the interface i.e. the presence of transcrystallisation at the interface (Misra et al., 1983; Felix and Gatenholm, 1994; Wang and Harrison, 1994). Often a conclusion is drawn from the nature of the fracture surface as to whether there is adhesion between the polymer and the reinforcement surfaces, through scanning electron microscopy (S.E.M) (Gatenholm et al., 1992; Karmaker and Youngquist, 1996; Clemons et al., 1997; Herrera-Franco and Aguilar-Vega, 1997; Hornsby et al., 1997; Karnani et al., 1997; Kuruvila et al., 1997; Gassan and Bledzki, 1998; Oksman and Nilsson, 1998). Such studies provide a qualitative view of the effects of interfacial modification in composites. The locus of failure and the amount of bound matrix after fracture have been studied as a function of controlled interfacial modification (Meurs et al., 1996).

ii) Spectroscopic characterisation methods: have been used to study the chemistry of interfaces in polymer composites (Felix, 1997; Occhiello et al., 1989). Some of the spectroscopic methods used include Fourier Transform Infrared Spectroscopy (FTIR), Electron spectroscopy for chemical analysis (ESCA) also known as X-ray photoelectron spectroscopy (XPS), Low energy ion spectroscopy (LEIS), Auger electron spectroscopy (AES), Secondary-ion mass spectroscopy (SIMS), H^1 and C^{13} nuclear magnetic resonance (NMR) etc. (Strong, 1993).

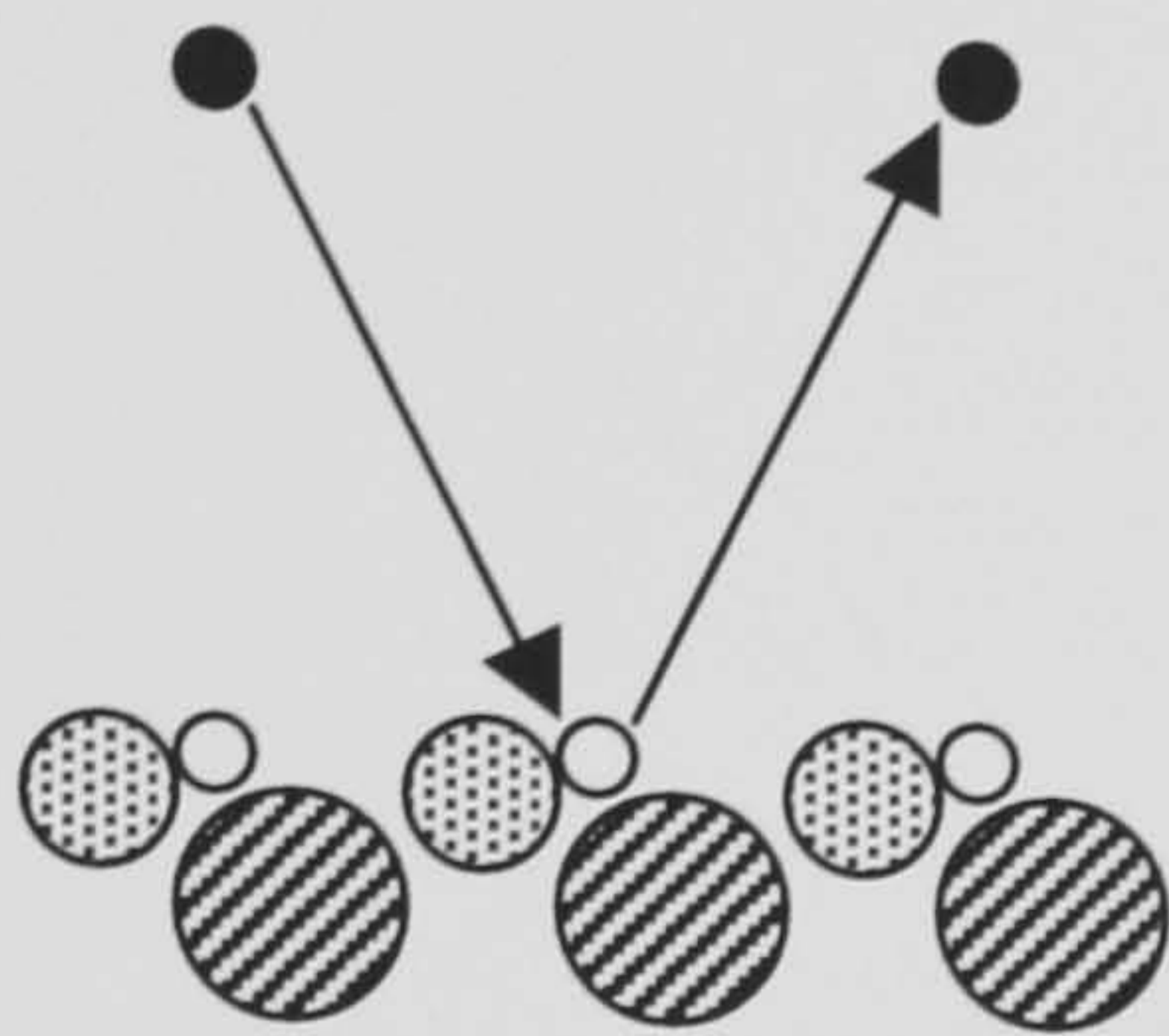
(iii) Material property characterisation methods: The changes in the interphase can be detected by measuring the properties of the material at the interphase e.g. glass-transition temperature (T_g). Methods like Differential Scanning Calorimetry

(DSC) and Dynamic Mechanical Thermal Analysis (DMTA) are used to measure the T_g of the composites.

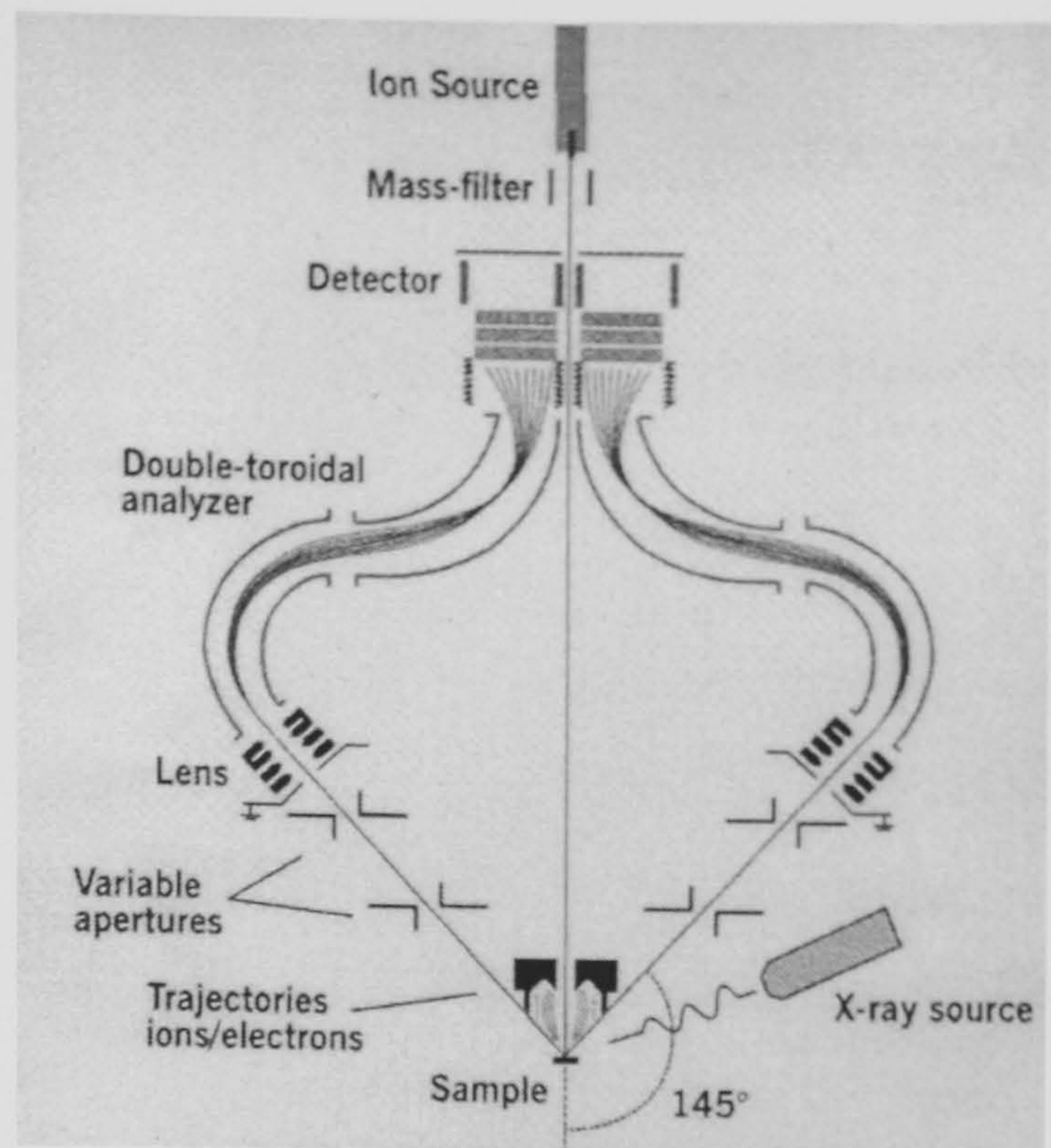
For the present study, we have used LEIS method to study the effect of interface modification on chemical changes on the fibre surface (Structural approach) and effect on the interfacial shear strength between fibre and matrix (Mechanics approach). LEIS method is briefly described as followed:

Low Energy Ion Spectroscopy (LEIS): In LEIS a mono-energetic beam of ions, with energy of 0.1 to 10 keV, strikes the target surface and the energy distribution of ions scattered off at some particular angle is measured (Figure 3.6). According to the laws of conservation of energy and momentum, the energy of the backscattered ions is characteristic of the mass of the target atoms from which they are scattered. The energy spectrum of the scattered noble gas ions shows peaks representing the atomic species present at the outer atomic layers of the surface. The energy spectrum obtained can thus directly be interpreted as a mass spectrum of the surface atoms. The information depth of LEIS is limited to the outer atomic layer(s) because the low-energy noble gas ions have a high neutralisation probability, which is close to unity per collision with a surface atom. This results in a negligible scattered-ion yield from target atoms below the surface layer.

Low energy noble gas ion



(a)



(b)

Figure 3.6 Schematic representation of Low Energy Ion Spectroscopy (a) principle and (b) set-up (Courtesy: Calipso LEIS Expertise Centre, Eindhoven University of Technology, Eindhoven, The Netherlands).

3.2.2.1 Micromechanical tests

As mentioned earlier there are various micromechanical (direct methods through mechanics approach) tests that are used to characterise the composite's interface properties. Among these numerous test methods, the single fibre pull-out test (Chua and Piggott, 1985), micro-debond test (Miller et al., 1987; Wagner et al., 1993; Day and Cauich, 1998), the single fibre fragmentation test (Drzal et al., 1982; Van den Heuvel et al., 1997) and the micro-indentation test (Mandell et al., 1980; Wu and Ferber, 1994) are becoming more popular and are widely used for measuring the interfacial properties in composites. For the present study we have used the micro-debond test for studying the effect of chemical modification on the interface.

The micro-debond test method, which is a modified pull-out test, is developed by Miller et al. (1987). According to the authors, the micro-debond test method is a

revision of the single fibre pull-out test to eliminate the meniscus effect during curing done at elevated temperatures and the potential rupture of the meniscus before debonding. The micro-debond test has been widely used to evaluate the interfacial shear strength for both thermoset and thermoplastic composites (Miller et al., 1987; Wagner et al., 1993; Day and Cauich, 1998).

Microdroplets of resin are deposited on single fibres held horizontally on a mounting plate. To form droplets of thermoplastics, a small piece of polymer film can be placed on the single fibre. Upon melting the thermoplastic film, mounted on the fibre, nearly uniform-sized droplets have been obtained. Their length (also referred as embedded length, L_{em}) can be controlled by the film thickness. A photomicrograph of a typical droplet on a fibre is shown in Figure 3.7.

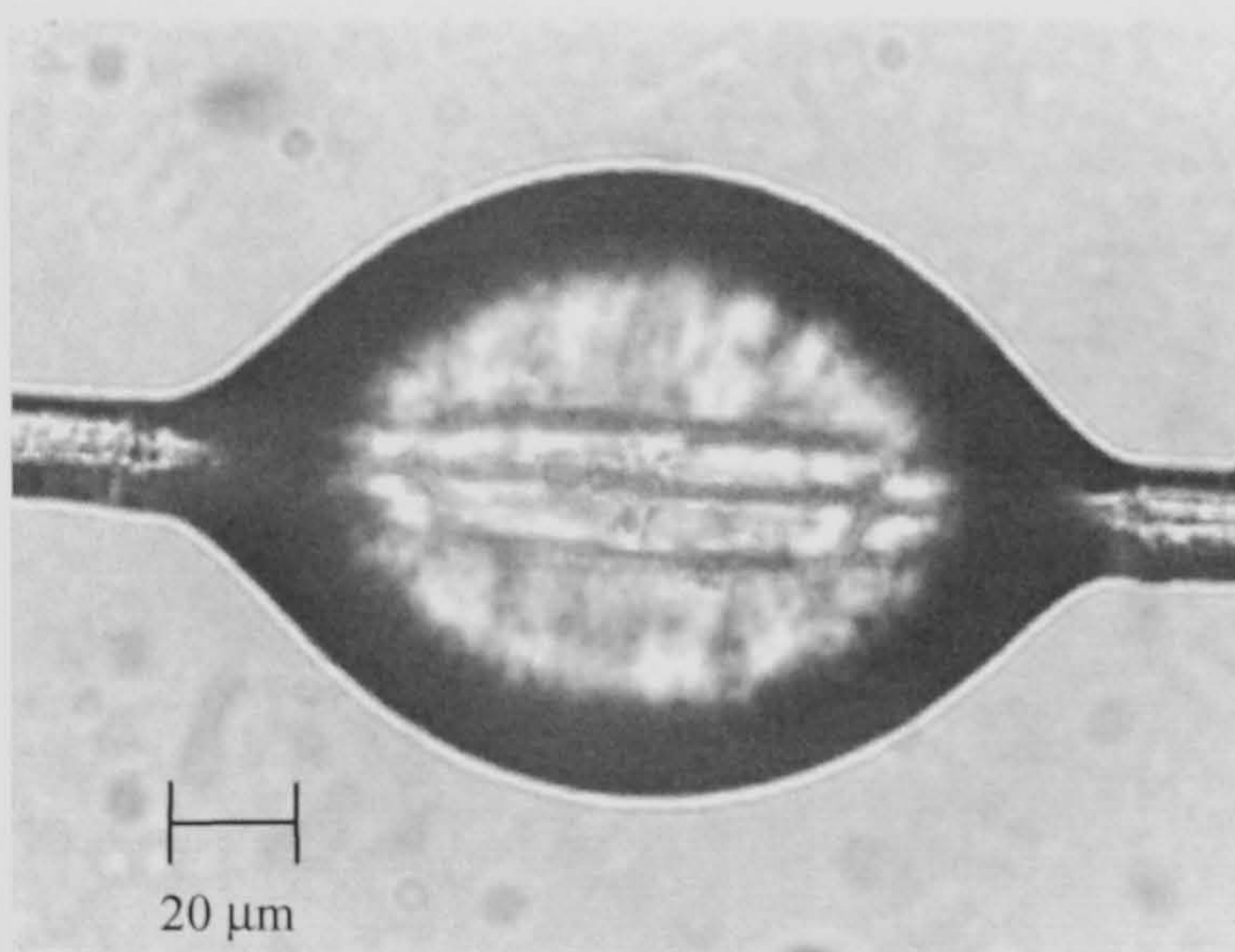


Figure 3.7 Typical droplet shape (droplet of PP/MA-PP blend (80:20) on Duralin flax fibre).

The schematic representation of the micro-debond test set up is shown in Figure 3.8. The fibre specimen is gripped at one end by a jaw in the tensile testing machine, which is pulled upward. Whereas, the movement of the droplet is obstructed by a microvise as shown in Figure 3.8. Due to the obstruction on the polymer droplet movement, the shearing force is transferred to the fibre through the fibre/matrix interface. When the shearing force reaches a critical value, pull-out occurs, and the droplet is displaced downward along the axis of the fibre. Initial tension is subtracted from the recorded force to obtain the pull-out force.

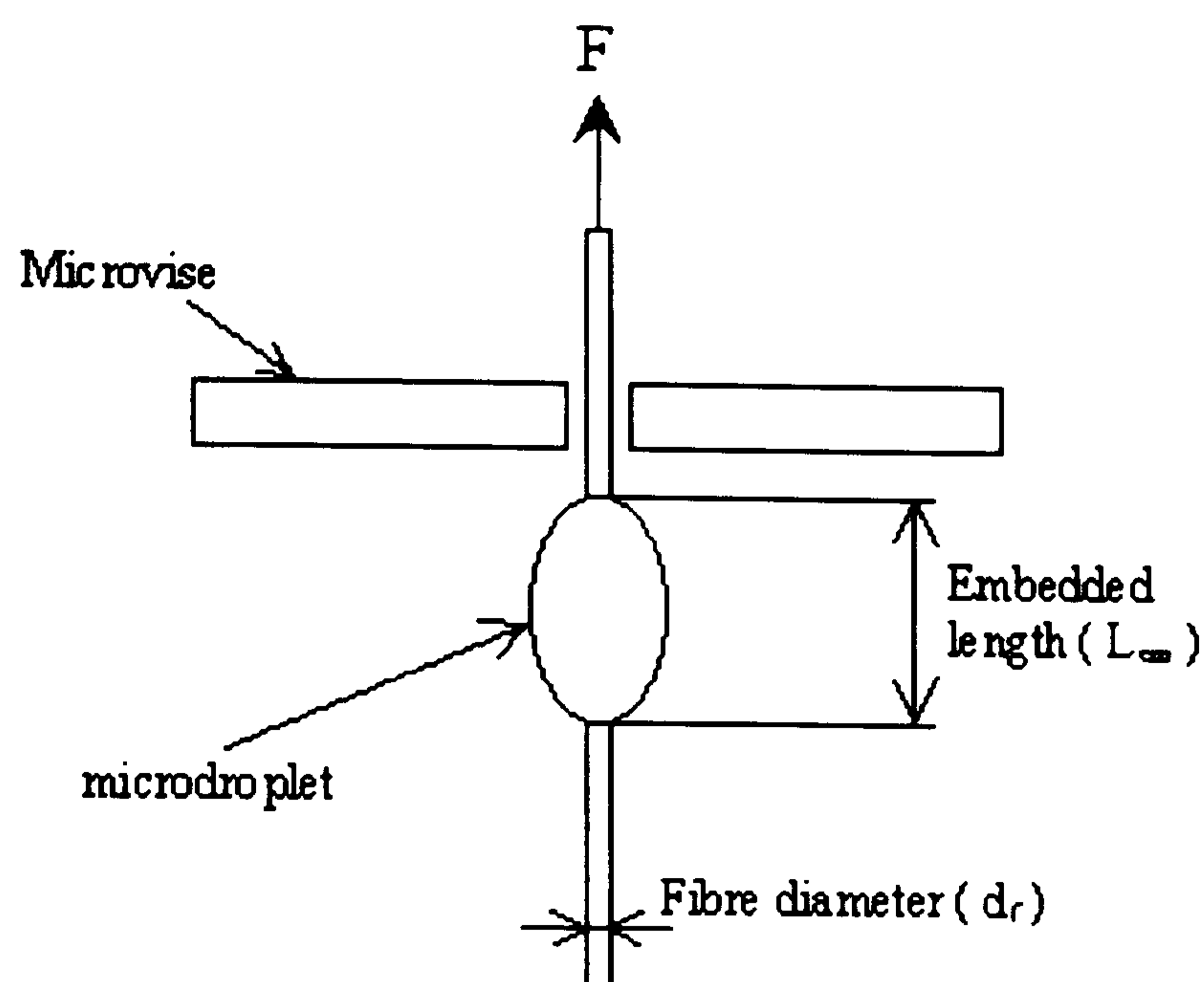


Figure 3.8 Schematic description of the micro-debond test setup.

The problem of detecting and distinguishing interface debonding from matrix failure or fibre breakage is simplified because the recorded force traces are readily distinguishable.

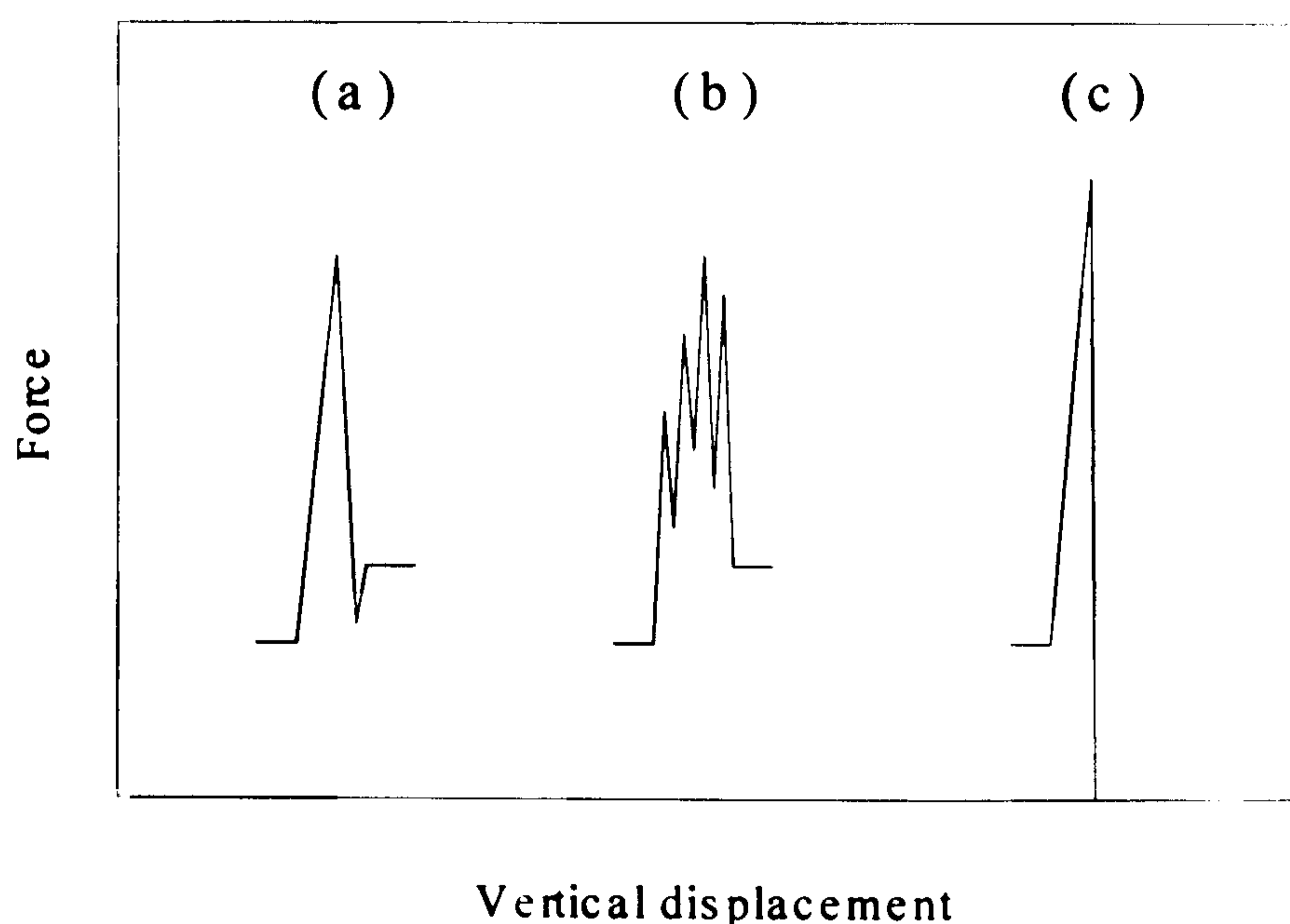


Figure 3.9 Typical force traces for the three possible results of a shear test: (a) interface debonding (b) matrix failure and (c) fibre break.

As illustrated in Figure 3.9, interfacial shear-failure produces a distinctive force peak followed by an almost constant force reading, which represents the frictional resistance between the fibre and the droplet. If the matrix material exhibits a

cohesive failure under the applied force, the recorded force does not show a single peak value. In the case of a fibre rupture, the force drops to zero. Therefore, true bond shearing can be identified through the recorded force curves without examining each specimen after the experiment.

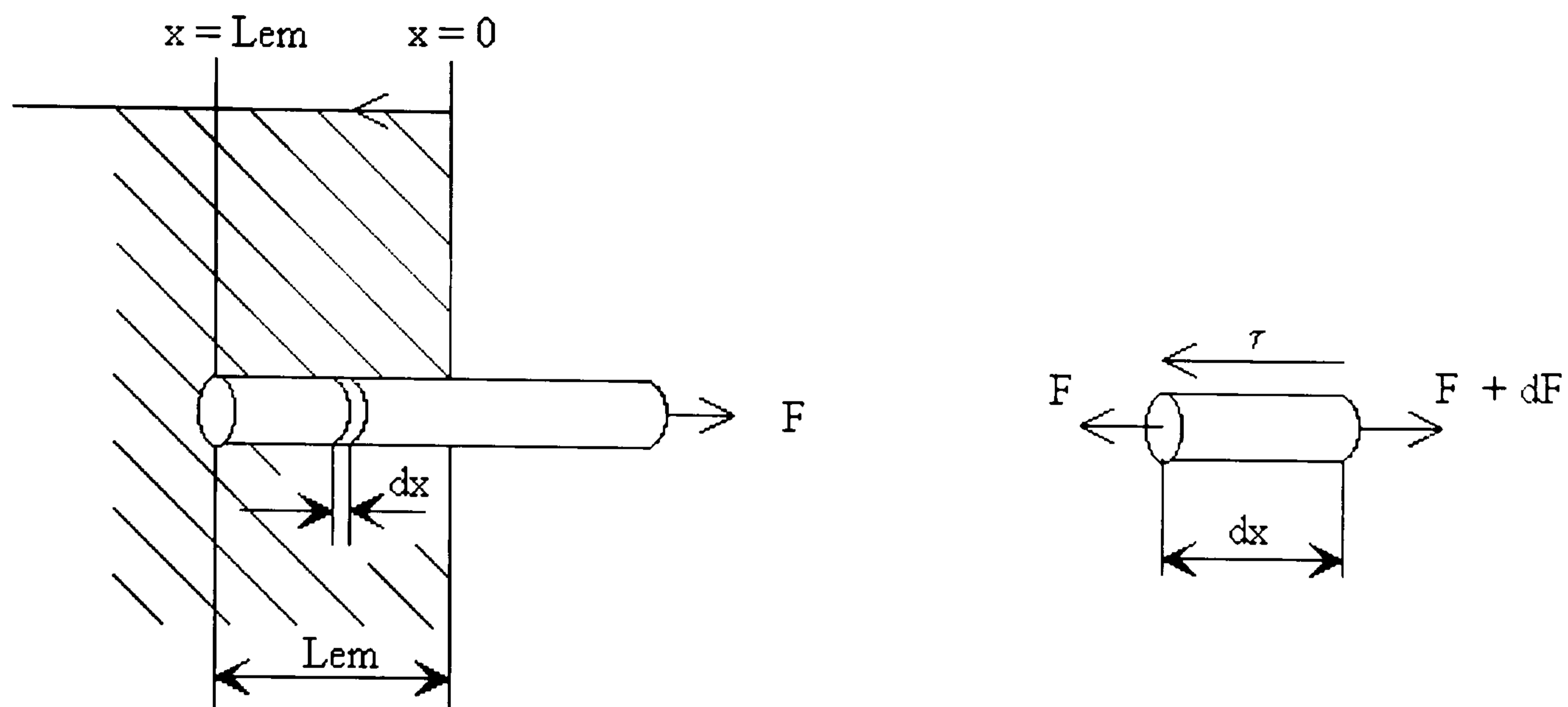


Figure 3.10 Schematic representation of the pull-out test.

In order to calculate the interfacial shear strength as a first approximation, a simple balance of forces can be used (Figure 3.10) assuming that the shear stress at the interface is uniformly distributed along the embedded length L_{em} and no traction on the fibre end. This results in the following relation for the interfacial shear stress.

$$\tau = \frac{r_f \sigma_f}{2 L_{em}} = \frac{F}{\pi d_f L_{em}} \quad (3.1)$$

In Equation 3.1 σ_f is the tensile stress on the fibre, r_f is the fibre radius, d_f is the fibre diameter and L_{em} is the fibre embedded length. According to Equation 3.1 the stress in the specimen is independent of the material properties, and the interfacial strength depends linearly on the embedded length. However, experiments with different embedded lengths show an approximately constant value in the relation between pull-out force and embedded length for larger values of L_{em} , indicating that Equation 3.1 oversimplifies the test (Day and Cauch, 1998; Wagner et al., 1993).

As shown in Figure 3.10, the pull-out test consists of a single fibre embedded in a block of matrix. A monotonically increasing load is applied to the fibre in order to pull it out of the matrix. The analytical equation (Equation 3.1) for the shear stress distribution can be improved by the expression for the stress built up in the fibre, described by Piggott (Meurs, 1998).

3.3 Experimental

3.3.1 Materials

In this study three types of flax fibres were used, namely Duralin flax, dew-retted flax and green flax. The (technical) fibres used were same as described in Chapter 2 (Section 2.2.1). An isotactic-polypropylene (i-PP) matrix (XY6500T Shell) with a melt flow index (MFI) of 35 and a maleic anhydride grafted polypropylene, MA-PP (Polybond® 3002, BP Chemicals Ltd.), were selected as the principal matrix materials for studying the interfacial shear strength. Both the i-PP and the MA-PP were supplied in the form of pellets.

3.3.2 Methods

3.3.2.1 Surface treatment and analysis:

The flax fibres (green flax, dew-retted flax and Duralin flax) were, before treatment, Soxhlet-extracted with toluene for 24 h and dried at 70°C in an oven with circulating air for 24 h. The obtained fibres are mentioned as 'hot-cleaned fibres'. Before the fibre treatment, MA-PP was dissolved in hot toluene (100°C) for 24 h. The fibres were then immersed for 5 min. in the MA-PP/toluene solution (Figure 3.11). The concentration of copolymer in the solution was 5wt% on the fibres. After treatment, the fibres were again Soxhlet-extracted with toluene for 48 h to remove all MA-PP components not covalently bonded to the fibres. Finally, the fibres were dried at 70°C in an oven with circulating air for 24h.

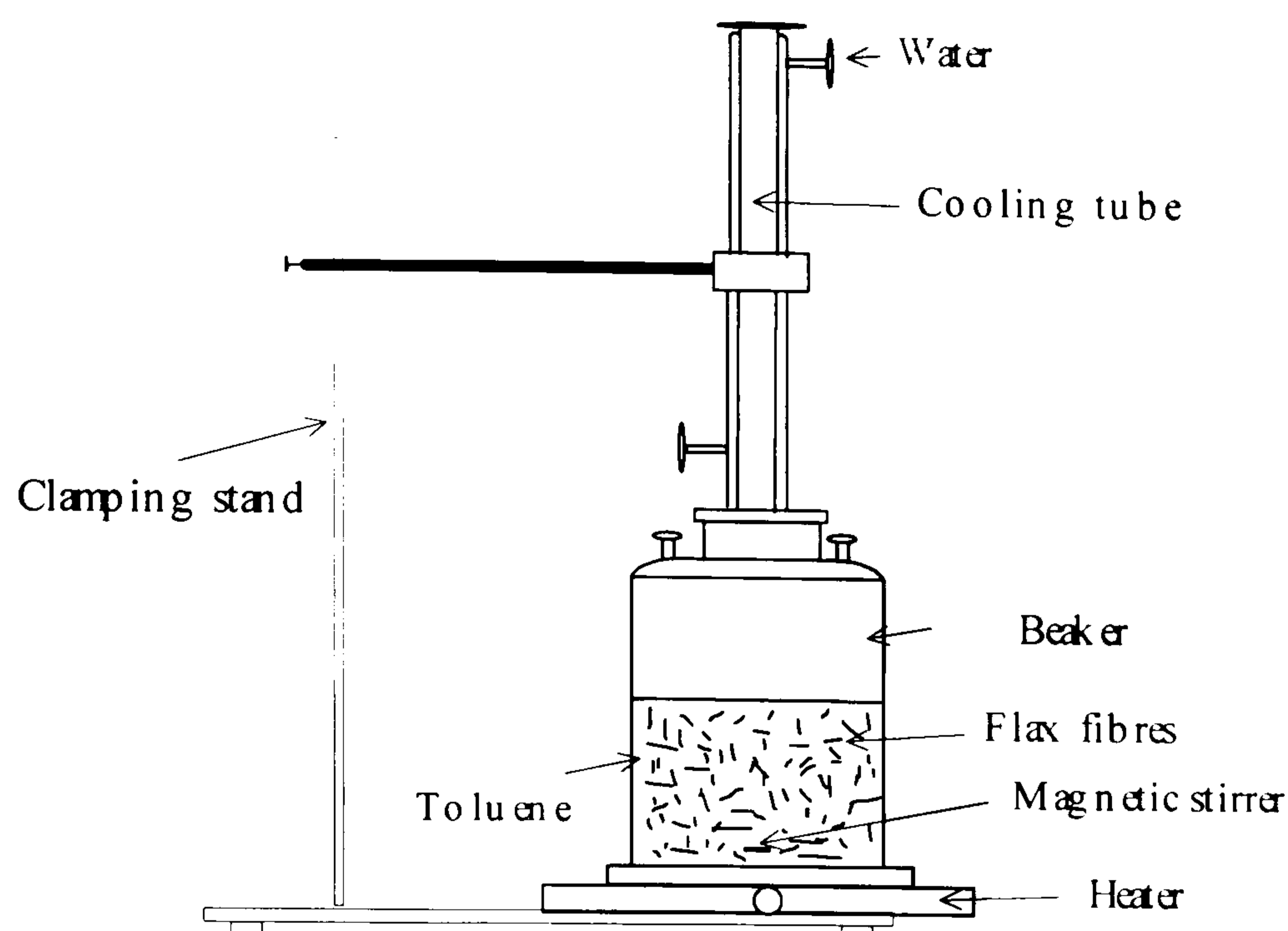


Figure 3.11 Schematic representation of the set-up used for coating flax fibres.

For surface analysis, Low Energy Ion Spectroscopy (LEIS) measurements were done on all the three different flax types. The description of LEIS is given in Section 3.2.2 (b). The first measurements were performed on flax, which had been cleaned for two minutes in cold toluene. This was done to clean the fibre surface. The measurements were also performed on the hot-cleaned fibres. Finally the measurements were performed on the MA-PP treated Duralin flax fibres. For LEIS analysis a surface area of 1mm^2 (fibres) was scanned and an average O/C ratio obtained from 10 spectra is reported. The LEIS results were obtained from lower and outer atomic layers by changing the ion dosage. The effect of modification on the fibre surface morphology was observed through Scanning Electron Microscopy (SEM). The observations were made through Cambridge Stereoscan 200. For the same the samples were coated with gold/palladium alloy. The fibre surface was also observed through Environmental Scanning Electron Microscopy (ESEM). Model: XL30 ESEM-FEG (Philips).

3.3.2.2 Microcomposites and micro-debonding test:

The fibres were taped on a cardboard frame. A typical frame had a rectangular slot with an opening of 10 mm x 20mm. A small piece of polymer film, having

dimensions of 2 mm x 30 mm and thickness of approximately 0.05 mm, was mounted on the single fibre as shown in Figure 3.12. A longitudinal cut was made in the centre of the film almost till the end. The slit film was suspended on the horizontal fibre as illustrated in Figure 3.12.

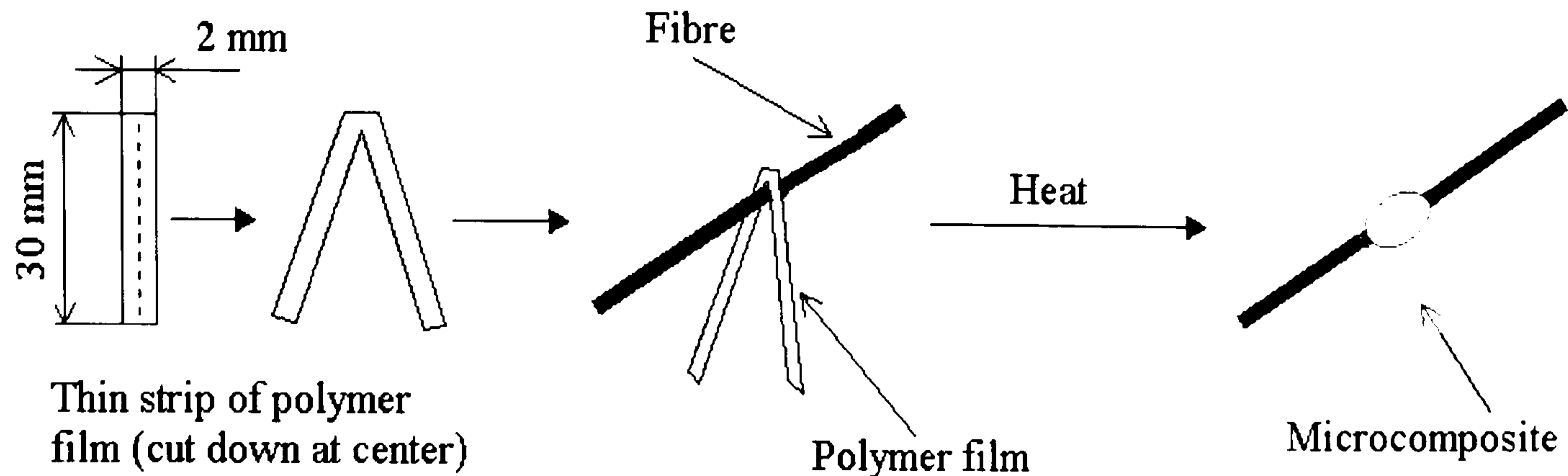


Figure 3.12 Procedure for making a thermoplastic microcomposite for micro-debonding tests.

The fibre and film, mounted on the frame, were then placed in an oven with circulating air for 7.5 min at 205°C. The time and temperature was selected as an optimum for the system, based on a number of trials with different time, temperature and film dimensions.

After manufacturing the microcomposites, the embedded fibre length (L_{cm}), fibre diameter and droplet diameter were measured for every specimen, using an optical microscope.

One end of the frame and the parts of the frame parallel to the fibre were cut away before the sample was mounted in the tensile testing machine (Figure 3.8). The sample was moved upward at a rate of 1 mm/min. The microvise slit width was adjusted to achieve a smallest opening. This was done to obstruct the droplet movement, without touching the fibre surface. Initial tension was subtracted from the recorded force to obtain the pull-out force. At least 17 samples were tested for each flax/matrix combination. The micro-debond tests were performed on a Frank 81565 tensile testing machine with a load cell of 10N. The full load scale was adjusted for every sample. Samples with an embedded length smaller than 500µm

had a full load scale of 1N, whereas samples with an embedded length greater than 500 μ m had a full load scale of 10N.

Different MA-PP concentrations, i.e. 0, 5, 10, 20, and 100wt%, were added (blended) in the droplet matrix. The blends were made in a co-rotating twin-screw extruder.

3.4 Results and discussion

As mentioned before, the fibre/matrix interface was modified through two different routes i.e. matrix modification through blending of MA-PP and fibre modification through fibre coating with MA-PP. This was done to observe the effect of interface modification through different routes.

A characteristic force versus displacement curve of a flax fibre with a matrix-droplet, obtained from the micro-debond test, is shown in Figure 3.13.

In this figure, three processes occurring during the test can be identified. First the fibre is loaded, leading to an elastic stress built up. At the point where the shear strength of the interface is reached, debonding occurs and the onset of debonding frictional resistance to slipping determines the micro-debond process. After that, a stick-slip mechanism may describe the frictional behaviour of the interface.

The interfacial shear strength values were obtained using the assumption that the shear stress at the interface was uniformly distributed along the embedded length, resulting in Equation 3.1. To check if there existed an approximately constant value in the relation between pull-out force and embedded length, this relation was studied for every system.

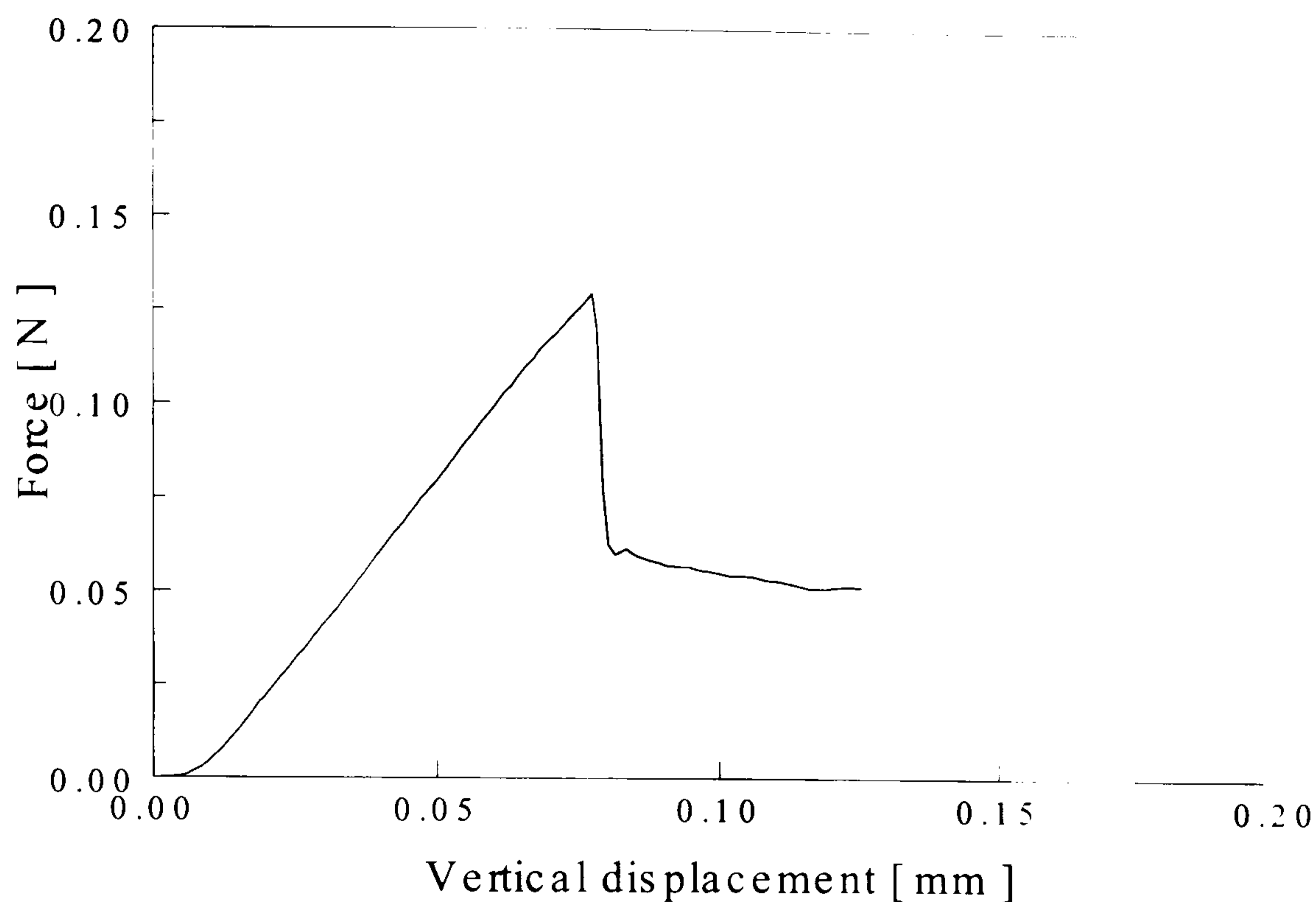


Figure 3.13 Characteristic force/displacement curve of micro-debond test (curve obtained from debonding a droplet of PP/MA-PP blend (90:10) from cleaned Duralin flax).

In Figure 3.14 the relation between pull-out force versus embedded length is plotted for the system PP-droplet on dew-retted flax. The results for all the systems are given in Appendix 3A. From Figure 3.14, and all the other plots in Appendix 3A, it can be seen that there exists a linear relation between the pull-out force and the embedded length. So Equation 3.1 could be used to calculate the interfacial shear strength. The linear plot in Figure 3.14 was made using program Slide Write.

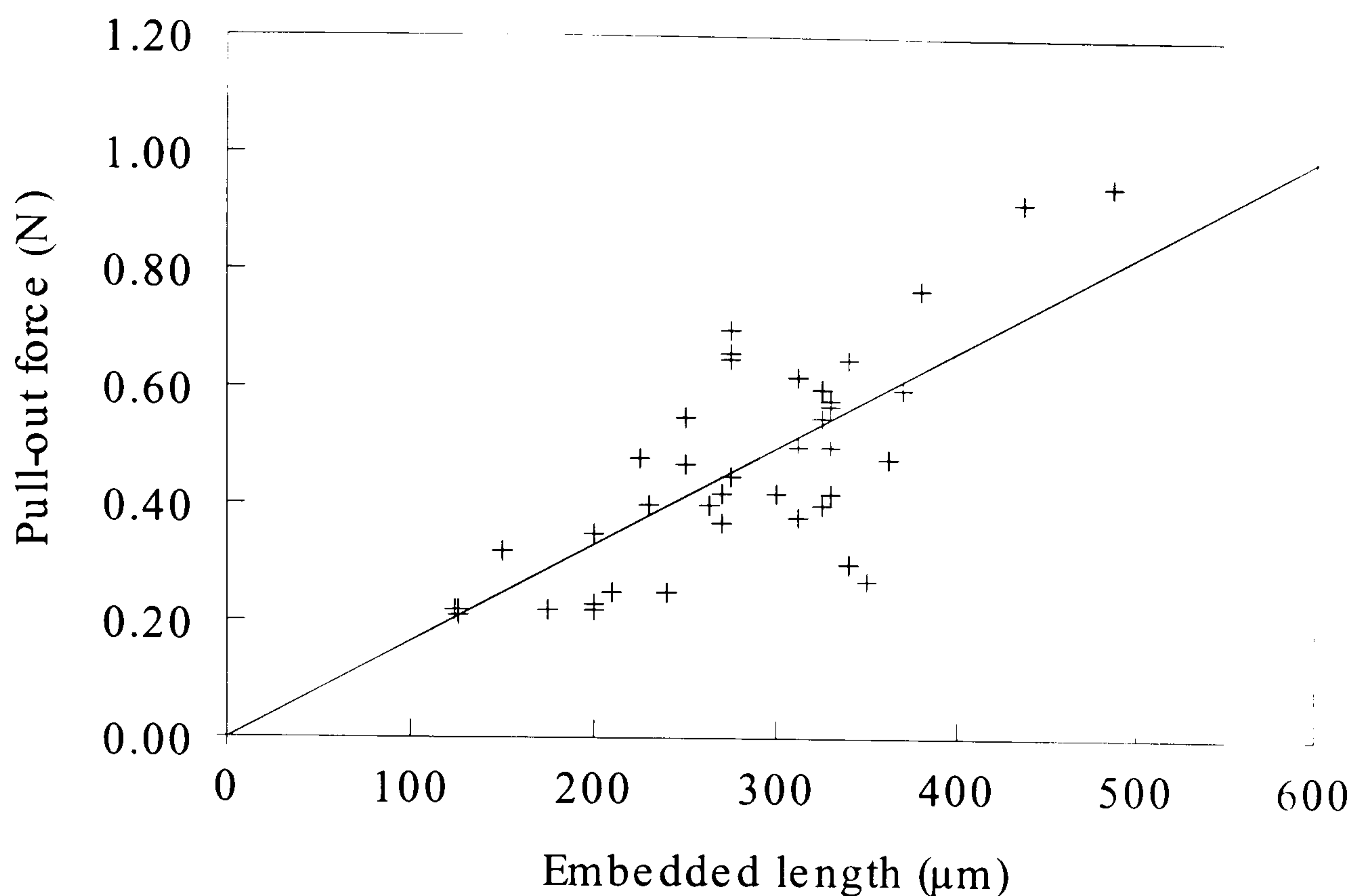


Figure 3.14 Characteristic pull-out force vs. embedded length curve (PP-droplet on dew-retted flax). The linear plot in Figure 3.14 was made using program Slide Write.

3.4.1 Influence of flax type

To study the influence of the flax type on the interfacial shear stress the micro-debond tests were performed using pure PP-droplets on three types of flax (i.e. dew-retted, green and Duralin flax). Also the micro-debond tests were performed using droplets of PP/MA-PP blend (95:5 wt/wt). This was done to investigate the influence of the coupling agent on the interfacial shear strength (IFSS) for the different flax types. IFSS was calculated by measuring pull-out force and substituting the same along with known embedded length (L_{em}) and fibre diameter in Equation 3.1, as explained in Section 3.2.2.1. The results are given in Figure 3.15.

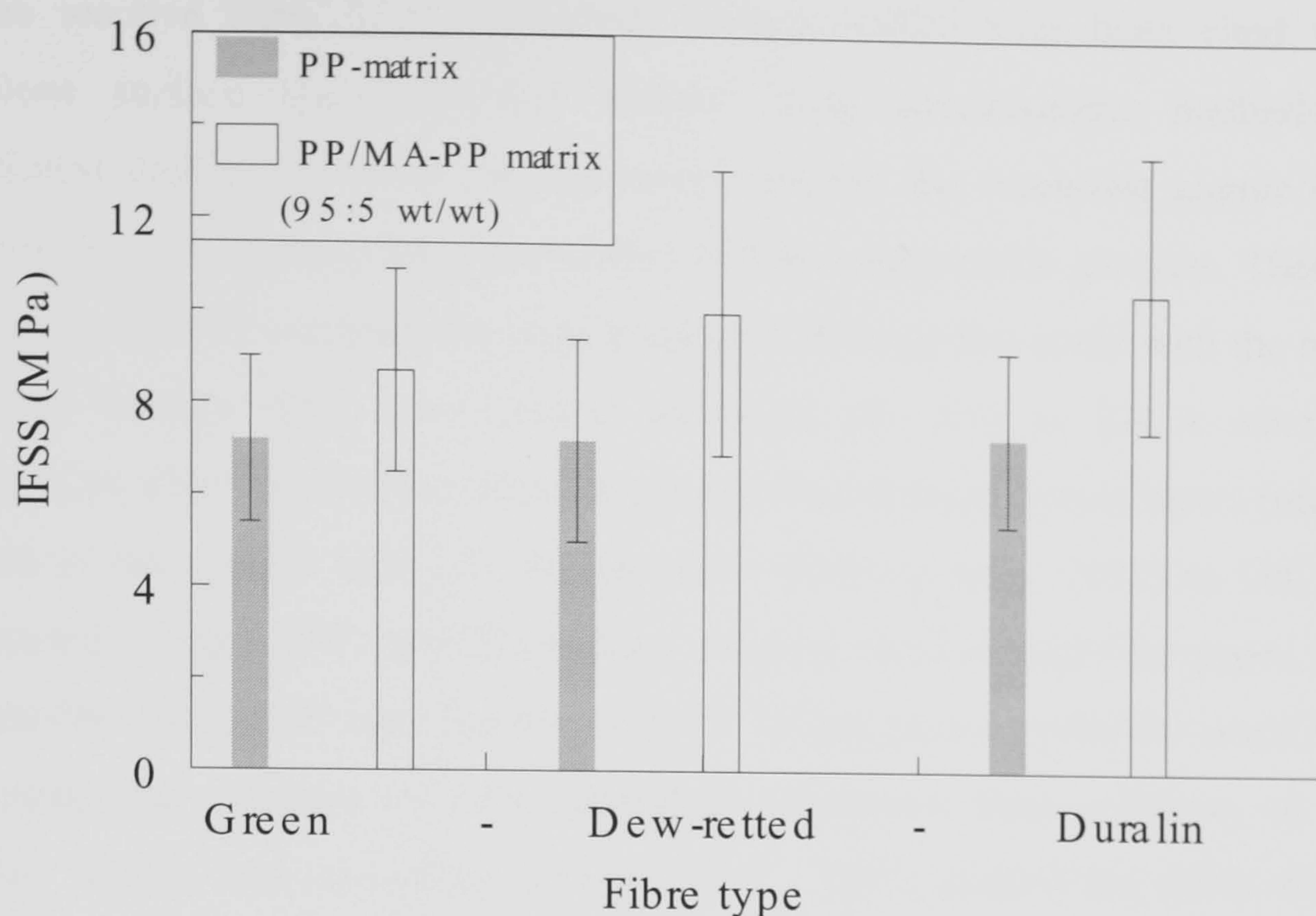


Figure 3.15 Interfacial shear strength values of the different flax types (The error bars plotted in the curve are standard deviations).

The LEIS results of the outer atomic layers obtained from the different flax fibres, which were cleaned in cold toluene for 2 minutes, are given in Table 3.3.

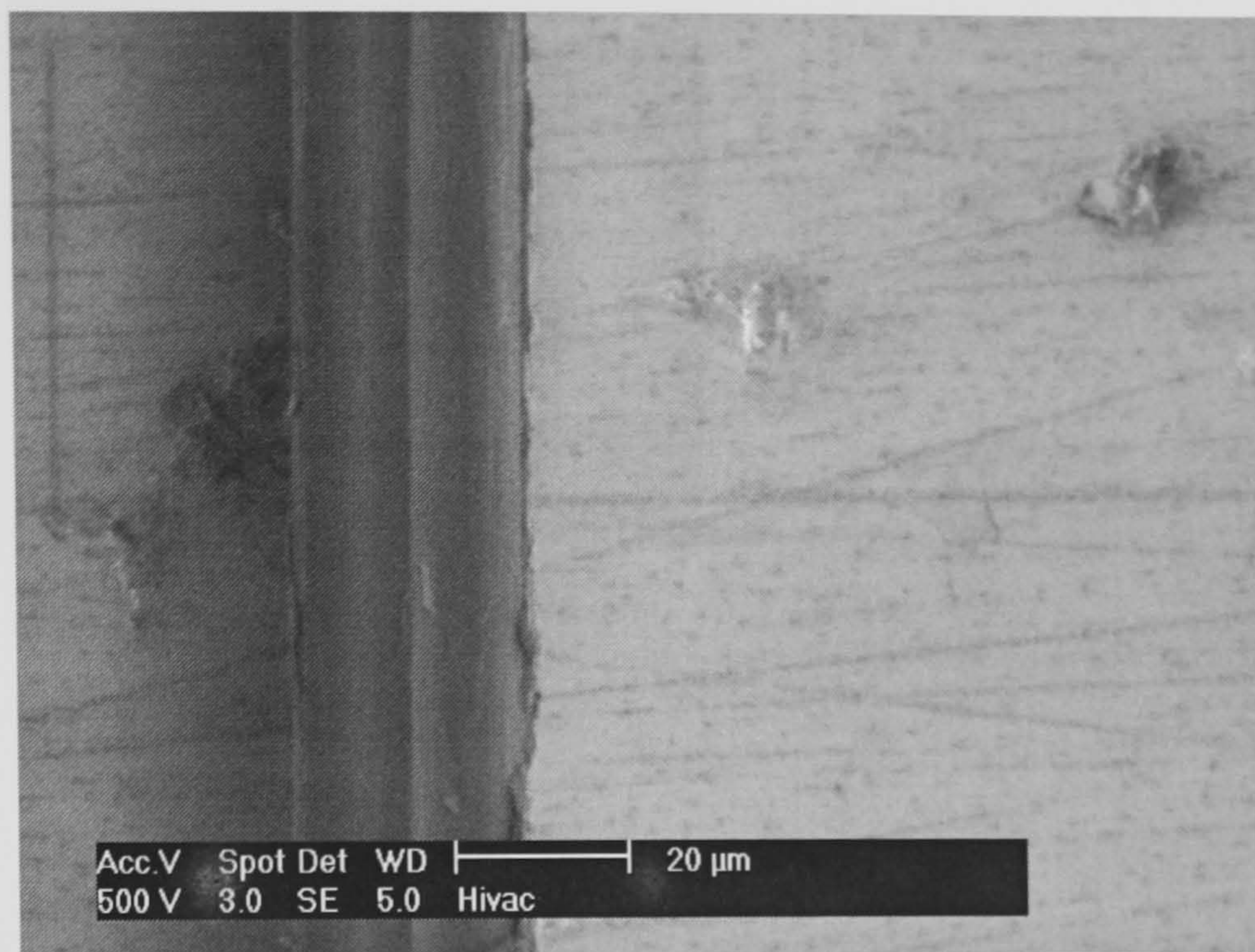
Table 3.3 O/C ratios of the different flax types.

<i>Flax type</i>	<i>O/C ratio</i>
Green	0.10
Dew-rettet	0.21
Duralin	0.45

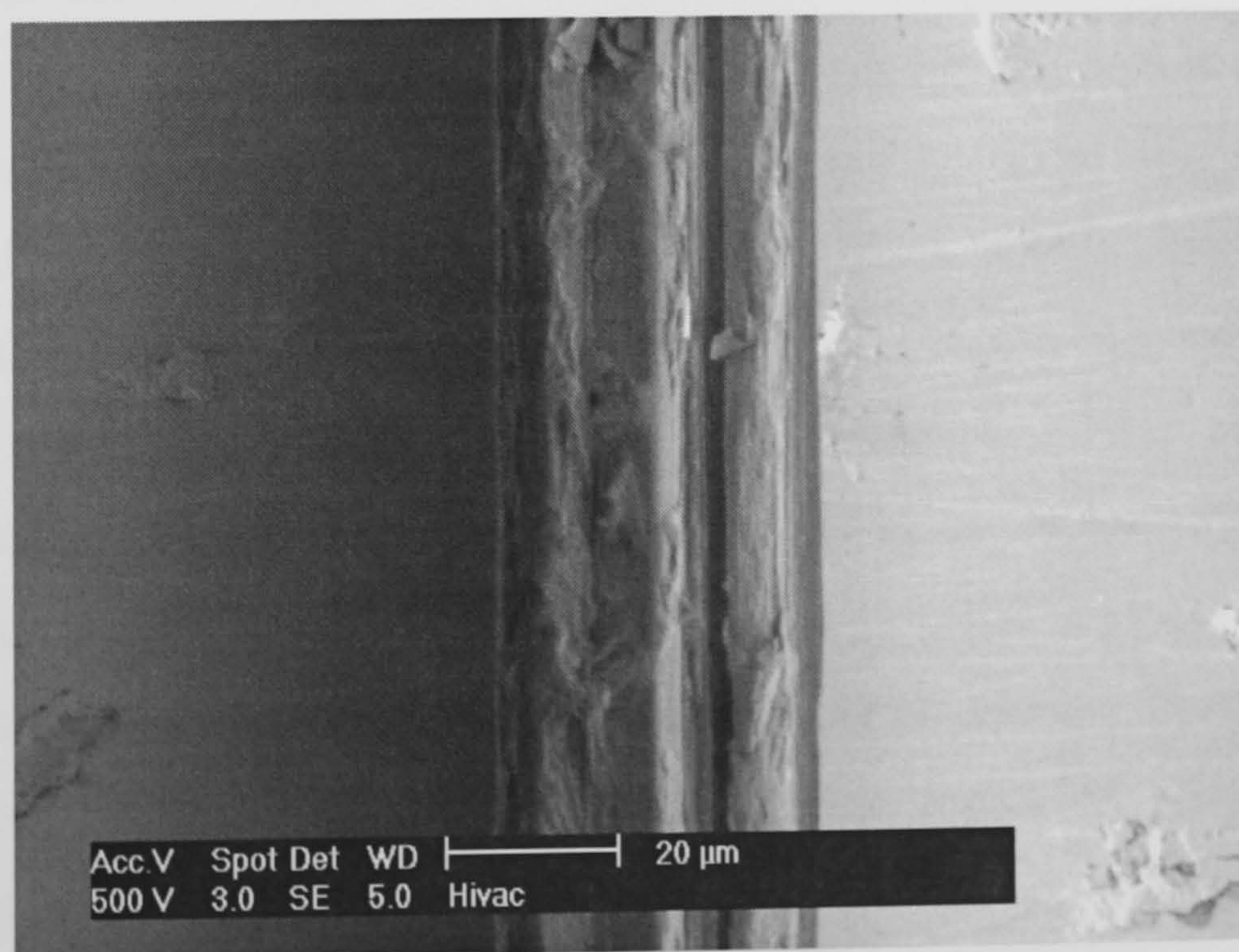
The fibre-matrix interfacial strength is expected to be proportional to the chemical bonds at the interface, which are determined by the surface oxygen concentration. In a separate study (De Kok, 1995), the chemical analyses of carbon fibre revealed that surface treatment yielded an increase of the surface oxygen combined with a significant increase in the transverse strength. A linear relation was found in the interface and transverse strength and the surface oxygen concentration, which

confirmed the assumption of the interface strength being controlled by the number of the reactive sites. In the literature, several studies have been cited where cellulose surface chemistry was studied using spectroscopic methods. As mentioned earlier, the LEIS method mainly studies the outermost atomic layers because of high neutralisation probability of low energy noble gas ions. Therefore we cannot directly compare the results obtained through this study with the results obtained through other spectroscopic technique like XPS or ESCA where the information about the surface chemistry is obtained through deeper layers (outer 2-10 nm of the surface layer). In the literature (Zafeiropoulos, 2001) an O/C ratio (measured through XPS) of 0.83 has been cited for cellulose and filter paper, while a somewhat lower O/C ratio (between 0.62-0.72) has been reported for wood fibres indicating the presence of other chemical substances than cellulose on their surface. Young and co-workers (Young et al., 1995) studied the effect of cold plasma treatments on jute fibres and reported that the untreated jute fibres had an O/C ratio of 0.48, which increased after the treatment to 0.95 reflecting the introduction of oxygen on the surface. Zafeiropoulos (2001) studied the surface chemistry of flax fibres, through XPS, and reported O/C ratio of 0.22 for green flax and 0.25 for dew-retted flax fibres. The O/C ratio in the case of dew-retted fibre measured through XPS is very close to the O/C ratio measured through LEIS i.e. 0.25 and 0.21 respectively. Such a resemblance, ignoring the type of (retting) treatment and the differences due to the sourcing, shows that the O/C ratio of the outer most layer is similar to the information obtained at the deeper layers. However, in the case of green flax the O/C ratio obtained through LEIS is approximately half of that measured through XPS i.e. 0.10 and 0.22 respectively. The reason of differences could lie in the depth of information as well as the sourcing of the fibres. Since the O/C ratio of both the fibres is much less than the O/C ratio of cellulose (0.83) therefore it can be stated that the chemical state of the fibre surface is different than the bulk properties. According to Zafeiropoulos (2001) waxes and fatty substances of a hydrocarbon nature cover the fibre surface, thus rendering such a low O/C ratio.

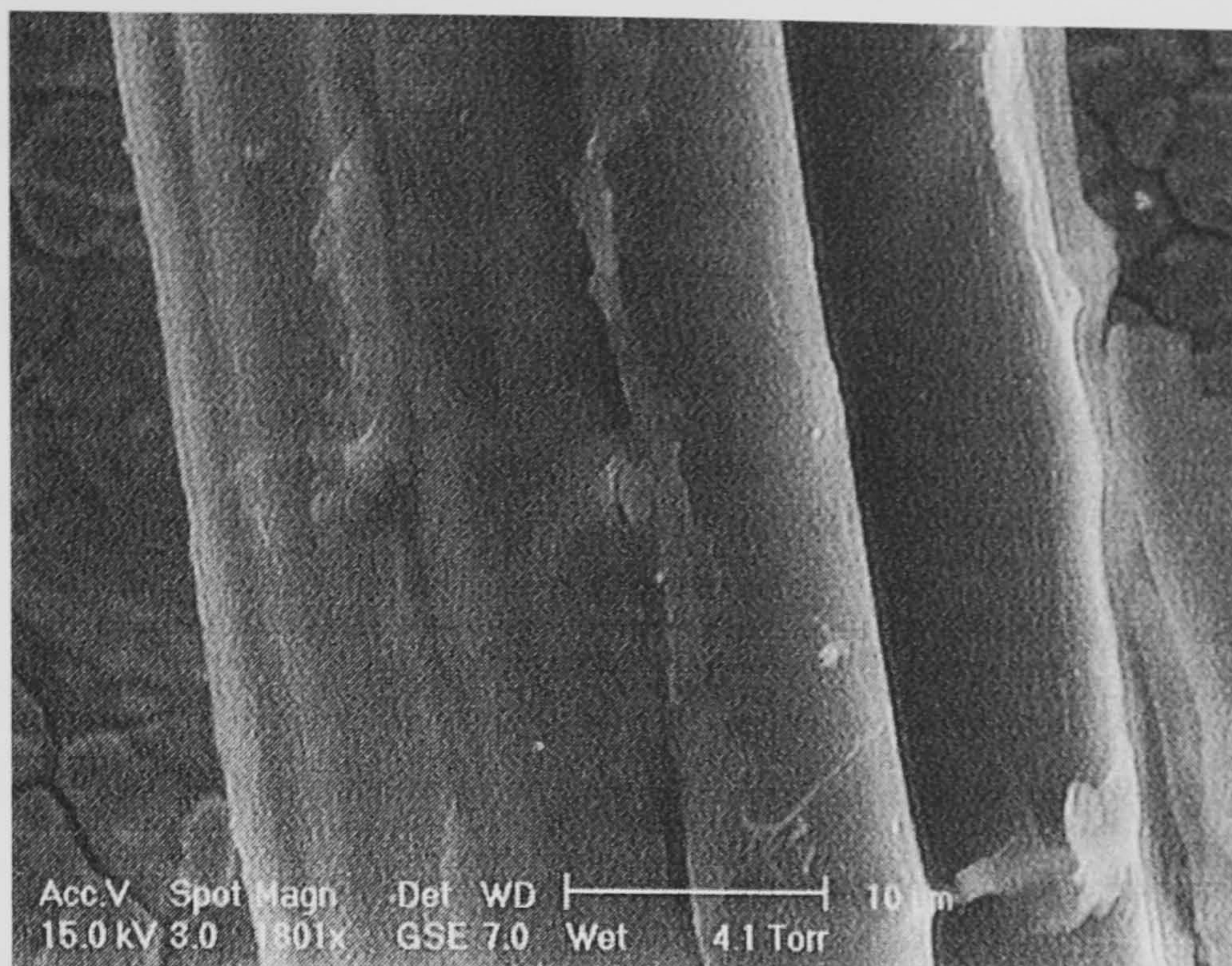
ESEM (Environmental Scanning Electron Microscopy) pictures were examined for the different flax types, to see the differences in the physical state of the fibres.



(a) Duralin flax



(b) dew-retted flax



(c) green flax

Figure 3.16 ESEM pictures of different flax fibres (a) Duralin flax (b) dew-retted flax (c) green flax.

From Figure 3.15 it can be seen that when the pure PP-matrix is used there is not much difference between the interfacial shear strength values of the different flax types. For all the fibre types there is a great scatter in the micro-debond results. This scatter has been reported for different fibre types (carbon and glass fibres) and different matrix materials (epoxy, PC, PBT). The scatter is comparable with those systems and is equal to about 25 - 30% (Miller et al., 1987; Gaur et al., 1989; Wagner et al., 1993).

The LEIS results showed that there was a great difference in the O/C ratio for the different flax types. The green flax and the dew-retted flax showed a lower value of the O/C ratio than Duralin flax. So on Duralin fibres there were relatively more oxygen atoms available for chemical interaction with maleic anhydride groups present in MA-PP.

When a blend of PP/MA-PP (95:5 wt/wt) was used as matrix material it can be seen that there was an increase in the interfacial shear strength values. Both dew-

retted flax and Duralin flax showed an increase (in average values) of about 40% whereas the green flax showed an increase of about 20%.

These results can be explained by two different factors i.e. O/C ratio and surface roughness. Although green fibres seemed to have rougher surface than Duralin fibres, the latter had better adhesion with MAPP, which could be due to higher (4.5 times) O/C ratio compared to green flax. However, dew-retted flax showed similar interfacial shear strength (IFSS) results as Duralin flax inspite of differences in the O/C ratio (2 times higher in Duralin than green flax). This can be the result of differences in surface roughness between Duralin and dew-retted flax, which was also observed through ESEM pictures (Figure 3.16). When compared with Duralin flax, the higher surface roughness of dew-retted flax was probably the cause of the enhanced interfacial adhesion and therefore the resultant IFSS was found equivalent to Duralin flax. The green flax on the contrary showed lower IFSS values, which can be because of 'too low' O/C ratios despite being rougher (Table 3.3).

3.4.2 Influence of fibre modification

The influence of fibre modification was examined by performing the micro-debond test on MA-PP treated green and Duralin flax fibres and hot-cleaned Duralin flax fibres with a pure PP-droplet. These two fibre types were chosen because they represented both extremes, i.e. the lowest O/C ratio and the highest O/C ratio (Table 3.3). The micro-debond results are given in Table 3.4.

Table 3.4 Interfacial shear strength values of the different flax types with pure PP droplets.

Flax	IFSS	
	Mean [MPa]	s.d. [MPa]
Green	7.21	1.83
MA-PP treated green	7.20	2.05
Duralin	7.45	2.13
Hot-cleaned Duralin	6.63	1.29
MA-PP treated Duralin	7.17	2.24

The LEIS results for the outer and lower atomic layers obtained from the different flax fibres (normal fibres, hot-cleaned fibres and MA-PP treated fibres) are given in Table 3.5.

Table 3.5 O/C ratios of the different flax types.

Flax type	O/C ratio	
	Outer layer	lower layer
Green	0.10	0.06
Hot-cleaned green	0.13	0.14
Duralin	0.45	0.35
Hot-cleaned Duralin	0.76	0.86
MA-PP treated Duralin	0.71	0.66

The O/C ratio for the hot-cleaned and normal green flax fibres showed no significant difference and the results for the different atomic layers, obtained by changing the ions dose, were about equal. Whereas the O/C ratio in the case of hot-cleaned Duralin was almost 70% and 150% higher than normal Duralin flax fibres for outer and lower atomic layers, respectively. After the MA-PP treatment there

was a small decrease in the O/C ratio for the outermost atomic layer, whereas, in the lower atomic layer there was a drop in the O/C ratio of 25%. The drop in O/C, measured through ESCA, was also reported by Felix and Gatenholm (1991). They had found in their ESCA experiments on MA-PP treated cellulose filter paper a decrease in the O/C ratio by 40%.

In spite of the above mentioned differences in O/C ratios, it can be seen from the micro-debond results (Table 3.4) that the MA-PP coating treatment had no significant effect on the interfacial shear strength values. The results are almost equal to the untreated fibres. Also, it can be seen that the IFSS in the case of untreated flax and PP/MA-PP (95:5 wt/wt) blend droplet is higher than the coated flax and pure PP-droplet (Table 3.4 and Figure 3.15). This can be because of some changes in the morphology of fibre/matrix interface/interphase or due to improper coating of technical fibre (i.e. fibre cell bundle). ESEM pictures of the normal and MA-PP treated Duralin and green flax fibres are presented in Appendix 3B. The pictures do not show a great difference between the normal and MA-PP treated fibres. Differences in the interfacial shear strength were probably not due to the changes in the fibre surface (physical) structure. To clarify the reason behind the observed differences, further micro-debond experiments were done between Duralin flax and PP/MA-PP droplets with varying amounts of MA-PP content (i.e. 0%, 5%, 10%, 20% and 100%). The results are given in next section.

3.4.3 Influence of matrix modification

The influence of matrix modification was examined by performing the micro-debond test on Duralin flax fibres with droplets containing various amounts of MA-PP and PP. The experiments were also done for hot-cleaned Duralin flax fibres. This was done to see if fibre cleaning had any influence on the interfacial shear strength. The micro-debond results are given in Figure 3.17.

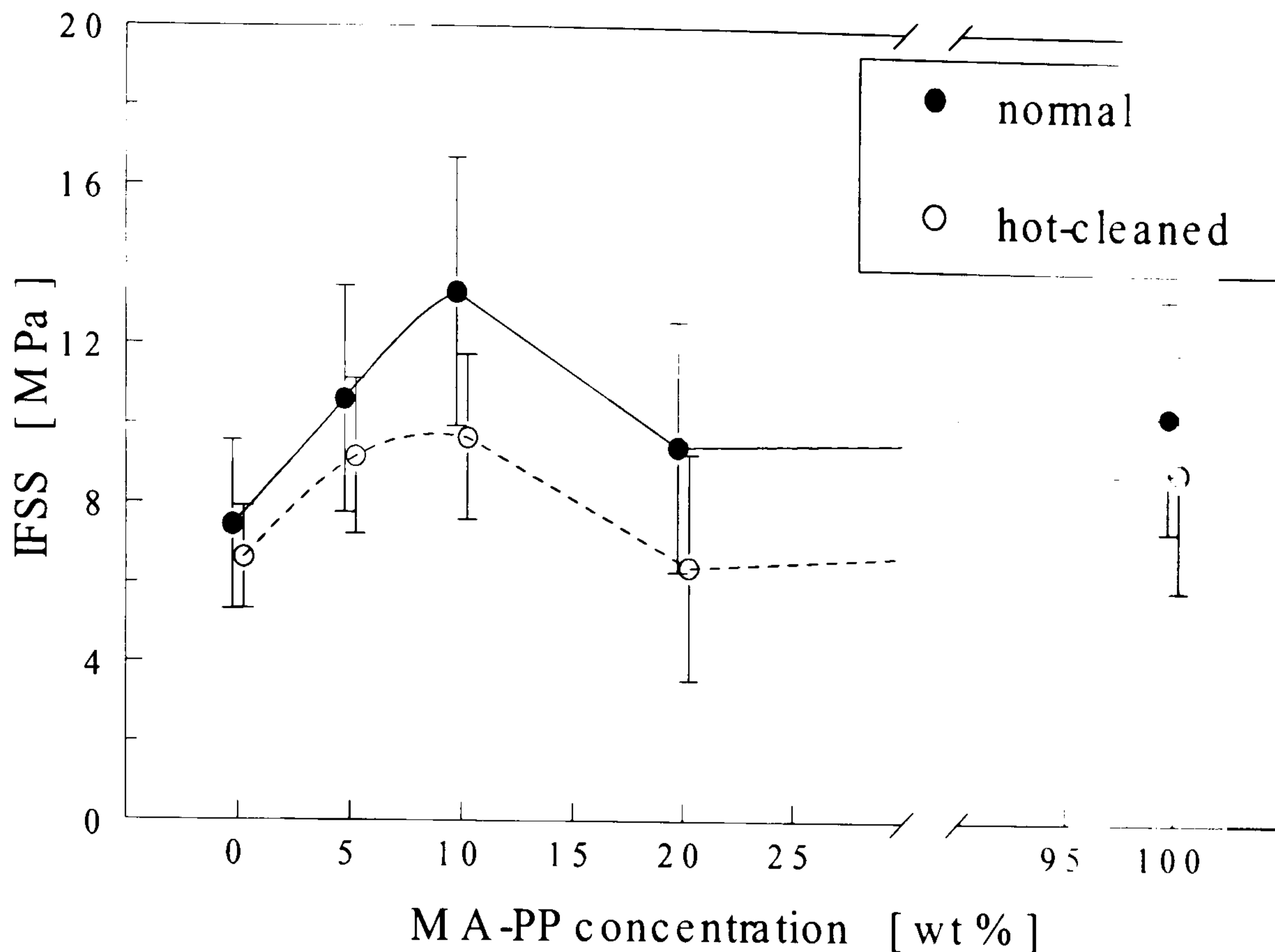


Figure 3.17 Interfacial shear strength values of (normal and hot-cleaned) Duralin flax with varying amounts of MA-PP concentration in the matrix (Spline curves were fitted using program Slide Write; error bars show standard deviations).

The effect of addition of MA-PP on the PP matrix strength is shown in Chapter 6 (Figure 6.14). As seen from Figure 6.14 the tensile strength of PP matrix increases with the 5wt% addition of MA-PP and no significant effect was observed at higher MA-PP loadings. The introduction of 5wt% MA-PP in the matrix resulted in a substantial improvement in the interfacial shear strength (also shown in Section 3.4.1) of the normal fibres. With the amount of MA-PP increasing to 10wt%, the interfacial shear strength reached ~13.4 MPa, which is an increase of almost 80% compared with the matrix without MA-PP and is close to the shear yield stress of the matrix (~16 MPa). However, the interfacial shear strength declined with the further increase in the concentration of MA-PP in the matrix. So the optimal (or critical) MA-PP concentration was 10wt%, for the system used.

In the literature, others also reported a maximum in adhesion, which existed at a specific concentration found through examining the influence of the composition

of copolymers on bonding strength (Schultz et al., 1989; Beck et al., 1996; Gong et al., 1998). Wool (Gong et al., 1998) stated that the critical concentration results from the variation of the secondary structure and molecular connectivity (i.e. the orientation and conformation) of the polymers within the interface. The interfacial shear strength depends on the mode of fracture i.e. adhesive type or cohesive type. When the amount of compatibilising agent is low (less than the critical concentration, ϕ_c), the limiting factor is the adhesive strength. With increasing compatibilising agent concentration, the adhesive strength is improved through an increase in the polar interactions. However, at concentrations greater than ϕ_c , the cohesive strength (i.e. within the matrix) may be reduced due to the dense attachment of the polar molecular chains to the solid substrate and reduction in the chain entanglements of polar molecules with the bulk matrix (Figure 3.18). As a result, the cohesive strength can even be lower than the adhesive strength and the interface may fail cohesively instead of adhesively i.e. through the 'interphase' or bulk matrix, leading to a weaker adhesion.

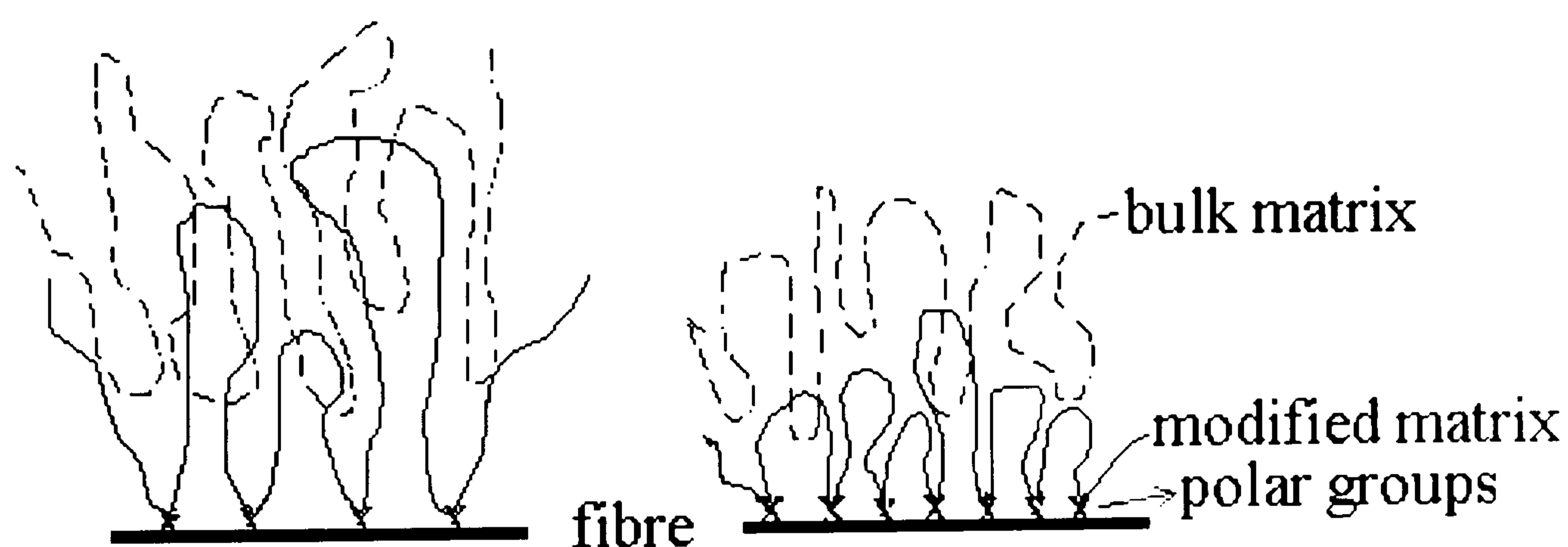


Figure 3.18 Schematic representation of the transformation in the fibre/matrix interface/interphase on increasing the polar groups in the matrix.

The same trend is visible for the hot-cleaned Duralin flax fibres. However, the interfacial shear strength values are lower for all the concentrations of MA-PP used than the corresponding values of the normal Duralin flax fibres (Figure 3.17). In the case of hot-cleaned Duralin fibres and PP/MA-PP blend droplet the optimal concentration is also 10wt%, but the increase in the interfacial shear strength value is 45% instead of 80%. It is rather surprising to find the same optimal

concentration for both systems. The higher O/C ratio had no effect on the optimal concentration. Only the interfacial shear strength value is observed to be affected. ESEM pictures were examined for the normal and hot-cleaned Duralin flax fibres, to see if there was a difference in the physical state of the fibres, which can cause a difference in the interfacial shear strength. The ESEM picture of the hot-cleaned Duralin flax is given in Figure 3.19 and the ESEM picture of normal Duralin flax is already given in Figure 3.16a.

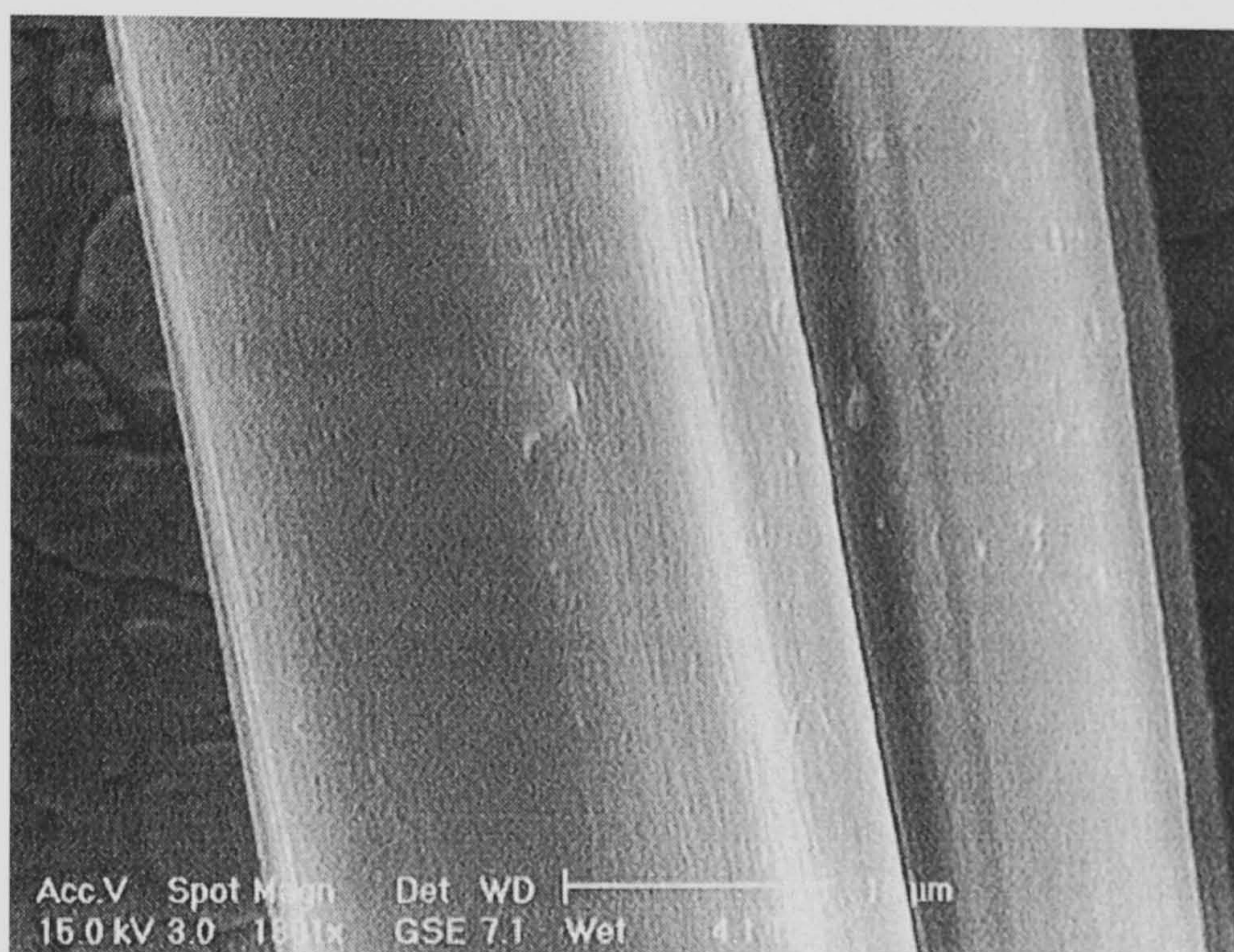


Figure 3.19 ESEM picture of hot-cleaned Duralin flax.

It can be seen that both fibres have a smooth fibre surface and that there is not much difference between the fibres (cleaned and uncleaned). So differences in the interfacial shear strength cannot be attributed to the differences in the physical state (i.e. surface roughness) of the Duralin flax fibres. Increased amount of O/C ratio, probably, enhanced the migration of polar groups in the polymer towards the fibre surface. This also explains the reduction in the IFSS in the case of cleaned Duralin flax and PP/MA-PP blend (Figure 3.17), which is probably because of reduced cohesive strength or chain entanglement within the matrix (Figure 3.18). However, the enhanced O/C ratio of the fibre surface did not shift the optimum concentration of 10wt% MA-PP, which seems to be dependent on matrix. Therefore, there seems to be an optimum amount of O/C ratio on the fibre surface

to obtain maximum IFSS.

3.5 Conclusions

In this study an effort was made to enhance/optimize the mechanical properties of flax/PP composites, mainly, through a micromechanical study. The adhesion between matrix and fibre in microcomposites was studied. An attempt was made to modify the fibre/matrix interface/interphase via chemical modification. Chemical modifications were done by two methods i.e. matrix modification and fibre modification.

The effect on the interface was studied through a micro-debond test. Through this study it can be concluded that flax fibre modification (coating the fibre with MA-PP) has no significant effect on the interfacial shear strength values, for the concentration of MA-PP studied. However, when the PP matrix is modified an optimal MA-PP concentration (in the matrix blend) is observed for the interfacial shear strength values.

Cleaning of Duralin fibre in hot toluene improves the reactivity of flax fibre as observed through the increased amount of O/C ratio on the fibre surface (by LEIS experiments). However, it leads to reduction in the IFSS for all the concentrations of MA-PP. The optimum concentration of MA-PP, in the case of hot-cleaned Duralin fibre is however not affected and shows that the optimum is independent of O/C ratio.

4. A STUDY ON FLAX/POLYPROPYLENE INTERFACE: TRANSCRYSTALLINITY

In this chapter, the theory and experimental results over the occurrence of phenomenon called transcrystallinity in flax/PP composite are reported. Also, the experimental results over the effect of transcrystallinity on (micro- and macro-) mechanical properties of flax/PP composites are reported and discussed.

4.1 Introduction

In the previous chapter a study on the effect of chemical modification on flax/polypropylene interface has been presented. As mentioned earlier, the fibre/matrix interface has been modified in different ways i.e. chemical modification (Felix and Gatenholm, 1991) (fibre coating and matrix modification) but also several attempts have been made to study the effect of matrix morphology around fibre surface, through varying processing conditions, on composite properties (Zafeiropoulos, 2001; Thomason and Van Rooyen, 1992). When a fibre is embedded into a thermoplastic melt it may act as a nucleating site for the growth of spherulites. If there are many nucleation sites along the fibre surface, then the resulting spherulite growth is restricted in the lateral direction, so that a columnar layer, known as transcrystallinity develops and encloses the fibre. The presence of an anisotropic layer such as a transcrystalline interphase may have significant effects on the performance of fibre-reinforced composite materials (Zafeiropoulos, 2001). Although many attempts have been made to study the effect of transcrystallinity, the effects of a transcrystalline interface on the composite's mechanical properties depend on the system studied and are often contradictory. In the present chapter the effect of processing conditions (crystallisation temperature,

cooling rate), fibre type, fibre modification and matrix modification on the crystallisation behaviour of matrix, flax/polypropylene interface and the mechanical properties of the (micro- and macro-) composites is reported and discussed.

The effect of flax fibre reinforcement on crystallisation behaviour of (PP) polypropylene was investigated by using a hot-stage under an optical microscope. For the present study the fibre pull-out method was used to study the effect of processing conditions on the flax/PP interfacial strength. The theory of fibre pull-out method is given in Chapter 3. In the previous chapter (Chapter 3), to study the effect of chemical modification of flax and PP on the flax/PP interface, microdebonding method (instead of pull-out method used in the present chapter) was used. Two different methods were used (i.e. pull-out test in Chapter 4 and microdebonding test in Chapter 3) because of differences in the sample preparation techniques. Since, it was difficult to control precisely the processing conditions in an oven, samples were made on a hot-plate. Hence, a pull-out test was used for the same. On the other hand (in Chapter 3) it was possible to prepare polymer droplets in an oven therefore the microdebond test (a modified form of pull-out test) was used for studying the effect of chemical modifications.

4.2 Theory

4.2.1 Transcrystallisation (Schultz et al., 1989; Thomason, J. L. and Van Rooyen, 1992)

A critical issue in the processing of semicrystalline thermoplastic composites is the microstructure or morphology of the matrix material. Morphological features such as degree of crystallinity, spherulite size, lamella thickness and crystallite orientation have a profound effect on the ultimate properties of the polymer matrix and thus composite. These features are affected by variation in the processing conditions. In composites this situation is further complicated by the effect of the reinforcing fibres on the morphology of the matrix. It is well established that the incorporation of reinforcing fibres in thermoplastics may lead to significant

improvement of mechanical properties such as stiffness, tensile strength and heat distortion temperature. However, within the range of thermoplastic matrices available it has been shown that the improvement in properties gained by adding reinforcement is an order of magnitude greater for semicrystalline polymers than for amorphous polymers (Krautz, 1971; Thomason and Van Rooyen, 1992). It has been proposed that this improvement may result from changes in the morphology and crystallinity of the polymer matrix in the interfacial region.

Crystallization of a polymer from the melt can be divided into a two-stage process, namely nucleation and crystal growth. Two types of nucleation occur, namely heterogeneous and homogeneous nucleation. Heterogeneous nucleation occurs in the presence of foreign surfaces; e.g. particles of impurities, dust or additives present in the sample. Homogeneous nucleation occurs as a result of random fluctuations of order in a super-cooled phase. When heterogeneous nucleation occurs with sufficiently high density along a fibre surface, the resulting crystal growth is restricted to the lateral direction so that a columnar layer develops around the fibre. This phenomenon is known as transcrystallisation.

It is assumed that a crystallising polymer molecule cannot distinguish between a polymer crystal in a spherulite and one in the transcrystalline region. So the crystallisation rates in the interphase and in the matrix should be the same at the same crystallisation temperatures (Thomason and Van Rooyen, 1992). This also causes one of the problems with transcrystallisation because growth of the transcrystalline region is often obstructed by normal spherulites and it is therefore difficult to obtain a relatively large transcrystalline region.

Another method where transcrystallisation occurs is the application of stress between a fibre and a super-cooled polymer melt, independent of fibre type and crystallisation temperature. This is in direct contrast to the results obtained from the quiescent crystallisation, where the occurrence of transcrystallisation does depend on fibre type and crystallisation temperature. Thomason and Van Rooyen (1992-b) showed that transcrystallisation is related to stress-induced nucleation. These stresses are in turn induced during cooling by differences in thermal expansion coefficient between the fibre and the melt. According to Thomason and

Van Rooyen (1992-b) stresses at the interface cannot fully account for the phenomenon of transcrystallisation. It was therefore proposed that the level of interaction between the fibre and the melt also plays a role. A high level of interaction will lead to a greater adsorption of the polymer onto the fibre surface. Some of the suggested factors influencing transcrystallisation include: the axial thermal expansion coefficient of the fibre, the sample cooling rate, the fibre length, the position along the fibre, the polymer molecular weight, temperature gradients along the fibre, the surface energy of the substrate, the chemical composition of the fibre surface, the evolution of volatile products from the nucleant and the crystalline morphology of the nucleating surface (Thomason and Van Rooyen, 1992b). Huang and Petermann (1995) also showed that the formation of a transcrystalline region around a fibre depends on the nucleation density, which has to be very high to induce transcrystallisation. They also did some experiments where instead of a fibre being the origin of nucleation, a scratch that was made into the polymer or in the glass slide, which supports the polymer, formed strain-induced nucleation with a high density and thus formed a transcrystalline region around the scratch. These results reveal that the transcrystalline growth is not solely restricted to the interface areas between a fibre and its matrix but a more general phenomenon. It is also obvious that the stress or strain is one of the factors to influence the nucleation.

4.2.2 Effects of transcrystallinity on mechanical properties

Several studies have been conducted to observe the effect of the transcrystalline region on the mechanical properties. From these studies it became clear that results regarding the effect of a transcrystalline interface on the composite's mechanical properties were quite contradictory. Wood and Marom (1997) proposed, by use of the fragmentation test, that the presence of a transcrystalline layer in a carbon fibre/polycarbonate system lowered the interfacial shear stress. Clark and Kander (1996) on the other hand found that a transcrystalline region in a reinforced Nylon-66 composite was responsible for the increase in interfacial shear strength (IFSS) as measured using a pull-out test. Folkes and Hardwick reported that the generation of a transcrystalline interphase in glass/PP laminated composites causes an

increase in flexural strength and modulus (Folkes and Hardwick, 1987; Folkes and Hardwick, 1990). Transcrystallisation in glass/PP composite is also reported by Pompe and Mader (2000). This study pointed out that when relating transcrystalline effects to mechanical properties of composites one must distinguish between a case where either the whole PP matrix is crystalline and a case where only a transcrystalline interphase is formed. Depending on these conditions either an improvement or reduction in composite properties can be obtained. The influence of transcrystallinity on the stress transfer capability in poly-caprolactone (PCL)/Kevlar 149 model composite was investigated by pull-out test by Gati and Wagner (1997). It was found that the presence of transcrystallinity produces little effect on the interfacial stress transfer capacity between PCL and Kevlar 149. Surface induced transcrystallisation by fibres has been reported in polymers such as poly(ether-ketone-ketone) (PEKK), poly(ether-ether-ketone) (PEEK) and poly (phenylene-sulphide) (PPS) by Chen and Hsiao (1992). Four types of fibres were used for transcrystallisation study. Transcrystallinity was shown to have a positive effect on the interfacial bond strength as measured by the microdebond test.

Felix and Gatenholm studied the effect of transcrystalline morphology on the interfacial adhesion in cotton/PP composites by using a single fibre fragmentation test (Felix and Gatenholm, 1994). The results showed that the transcrystalline morphology at the fibre/matrix interface improved interfacial shear strength considerably when a tensile load was applied in the fibre direction. The results showed an increase from 6MPa (in the control sample) to 12MPa in the interfacial shear strength after an isothermal crystallization for 5 min. The enhancement in composite mechanical properties owing to transcrystalline interphase has been explained in many different ways in literature (Felix, 1997). It has been suggested that transcrystalline interphase, owing to its intermediate modulus, may lower the stress concentration around the fibres. It has also been suggested that the transcrystalline layer may provide a protective sheet around the fibres, which prevents them from necking during tensile loading. For the cotton/PP system, Felix (1997) proposed two mechanisms responsible for the increase in IFSS when a transcrystalline layer is present. First, relatively slow crystallisation, which is required for a distinct transcrystalline layer to form, allows the PP molecules to

approach and adsorb on the cellulose surface in an energetically favourable manner. The adsorption configuration is proposed to involve the interaction of α -carbon/methyl moieties of PP and the oxygens in the glucosidic linkages in cellulose. There is regularity in the position of both moieties, and thus equilibrium adsorption would facilitate the formation of a high degree of interactions between the cellulose and the PP. The second mechanism involves a more powerful mechanical interlock created when the pores of the rough cotton surface are filled with the transcrystalline phase, which is stronger and stiffer in the direction of shear than a fine spherulitic or a disordered layer. The increase in IFSS with thickness of the transcrystalline layer may be caused by changes in the shear deformation mechanism of the lamellae. Gray studied the nucleation ability of wood pulps containing large quantities of lignin and hemicellulose in addition to cellulose with cotton fibre (Gray, 1974). It was found that wood fibres showed few or no spherulites on their surface whereas the cotton fibres were completely covered with transcrystalline material. Zafeiropoulos, Baillie and Matthews found, by use of the single fibre fragmentation test, that the interfacial adhesion in a dew-retted flax/iPP system was improved by the presence of a transcrystalline layer when compared to a system without a transcrystalline layer (Zafeiropoulos, 2001). However they did not observe any difference in systems containing a transcrystalline layer with respect to transcrystalline thickness or crystallisation temperature.

Pull-out testing: The theory on the pull-out testing is described in Chapter 3 (Section 3.2.2). One of the difficulties one has to face with flax fibres (and other fibres in general) is related to the fineness of the fibre and the corresponding small embedded depth in the matrix that is required to pull the fibre out, instead of breaking it. A major disadvantage of the pull-out test is that a broad distribution is found in the results, which can be explained by the fact that almost all fibre/resin combinations have non-uniformity in their surface. Also Equation 3.5 suggests that the cross-section of the fibre is perfectly circular, which is not the case for vegetable fibres.

Furthermore, Marotzke found, using finite element analysis, that the existence of a meniscus decreased and shifted the maximum stresses into the meniscus, i.e. the

interface is unloaded. The neglect of this geometrical parameter in the evaluation of the test data hence would result in an inaccurate estimation of interfacial shear strength (IFSS) (Meurs, 1998). The effect of the microvoid gap may also affect the obtained results. Gaur et al. (1989) examined the effects of the location of load application in microdebond pull-out experiments by varying the gap width between the microvoid plates. Their conclusion was that the measured IFSS values tend to increase as the gap begins to widen, leveling off at higher gap widths. On analysing the stress distribution and force balance, they concluded that the increase in the IFSS represents an overestimation of the intrinsic value, which is best evaluated with the gap width as small as practicable. Assuming that the interface fails when the stress applied at a point on the interface exceeds a critical stress, a droplet loaded at points close to the fibre would debond at a lower applied force than the same droplet under load at points away from the fibre. This is because the stress is more concentrated near the top of the droplet for the former case; the calculated bond strength would therefore also be lower (Gaur et al., 1989; Beck et al., 1996).

Chua and Piggot (1985) studied the effect of the free fibre length on the pull-out test for a glass/PP composite. The free fibre length is the distance between the place where the fibre is gripped and the surface of a polymer. They found that the pull-out test is an extremely complex process. For the most simple system, i.e. straight fibres with constant cross-sections and clean interface failure (no polymer left adhering to the fibre), it is governed by at least five different variables, namely interfacial pressure, interfacial friction coefficient, work of fracture of the interface, fibre embedded length and free fibre length.

4.3 Experimental

4.3.1 Materials

In this study three types of flax fibres were used, namely Duralin flax, dew-retted flax and green flax. The (technical) fibres used were same as described in Chapter 2 (Section 2.2.1). The details of i-PP matrix and MA-PP matrix materials, used for

studying the interfacial shear strength as well as for manufacturing macrocomposites, are given in Chapter 3 (Section 3.3.1).

4.3.2 Methods

4.3.2.1 Sample preparation for studying transcrystallinity:

To follow the crystallisation kinetics, cooling rate and crystallisation temperatures were varied. The transcrystalline layer thickness was measured under different conditions, i.e. crystallisation temperature, time and cooling rate. These experiments were carried out on a hot-stage and observed through a polarised light microscope. A small piece of matrix film was placed on a microscope slide, which was kept on a hot stage held at 210°C. A fibre was placed on the molten polymer and covered by another piece of matrix film. The system was left for 5 minutes to ensure complete melting of the polymer, after which the sample was cooled at controlled cooling rate to the desired crystallisation temperature. The investigations were done for different matrices i.e. PP, MA-PP and a blend of PP/MA-PP (95:5 wt/wt). The hot-stage used was Linkham Scientific LTS 350 and the temperature controller unit was Linkham TP 93. The matrix morphology was observed through a Zeiss polarising microscope.

The effect of fibre treatment on the transcrystallinity behaviour of (treated) flax/PP microcomposites was observed. A hydrolysed silane solution was prepared by adding 3 ml 3-amino-propyl-tri (ethoxy)-silane to a solution of acetone and acidified water (95:5 v/v). Fibres were dipped in this solution for 1.5 hours. Afterwards they were dried in an air-circulated oven at 80°C.

4.3.2.2 Sample preparation for pull-out testing:

The preparation of samples used for testing the micromechanical properties of the transcrystalline layer in a Duralin flax/PP system is explained as follows. A single flax fibre was chosen from a bundle of flax fibres. Care was taken about the selection of fibre diameter because the fibre had to be drawn through a capillary

serving as a ‘holding frame’ and the inside diameter of the capillary used was 215 μm . Precaution was taken not to select split or bent fibres as these could cause a fibre break. Following the fibre selection, a single fibre was pulled through the capillary, which had a funnel shaped entrance. The funnel shape was to ease the entrance of the fibre into the capillary.

As shown in Figure 4.1, two capillaries were fixed in a capillary holder on a temperature and heating rate controllable hot stage. The fibres were inserted into holes, which were punched in the polymer film by a needle. The hole was made to ensure that the fibre remained straight and to facilitate the complete fibre insertion till the surface of the heating plate. In order to get a range of embedded lengths, PP films with thickness between 0.2 and 1.3 mm were used. The reason of punching a hole in PP film instead of direct fibre insertion into the molten PP was that molten PP is very viscous and pushing a fibre in it generally resulted in a fibre break or fibre bending.

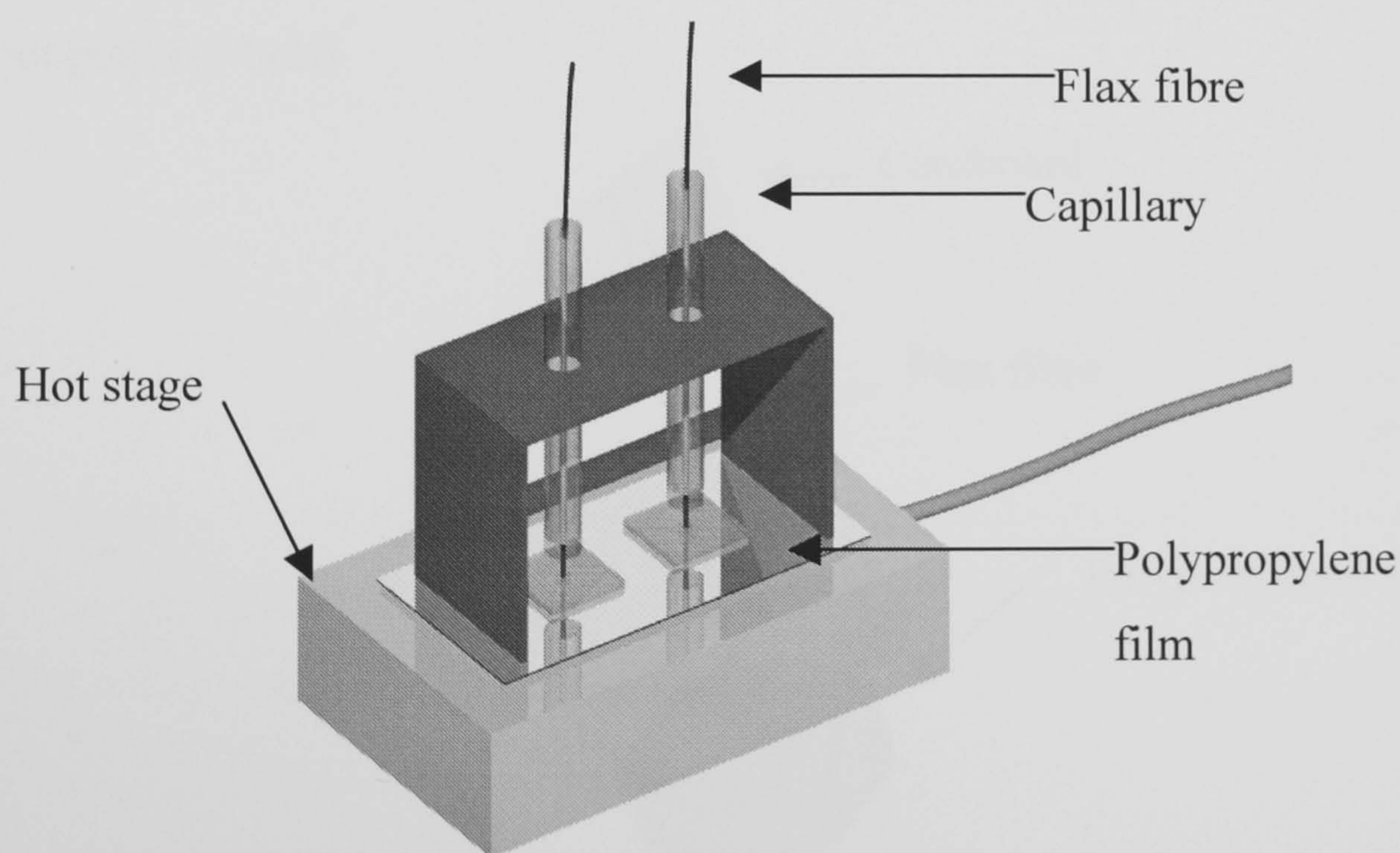


Figure 4.1 Schematic representation of the set-up used for the (flax fibre/PP) microcomposite sample preparation, for fibre pull-out tests.

When the fibre was pulled through the capillary and lowered into the PP film the hot-stage was turned on and the heating started. First the plate was heated to 210°C and kept for 10 minutes, to melt all of the PP film around the fibre and to ensure

that no residual stresses were left in the PP. This was followed by controlled cooling at 10°C/min to the crystallisation temperature i.e. 130°C or 138°C. When the crystallisation temperature (130/138°C) was reached it was kept steady for 5 to 10 min. After keeping the temperature steady for 5 to 10 min at 130 to 138°C the sample was cooled to room temperature. Around 15 samples were tested for each testing condition.

After preparation of the samples, the effect of transcrystallinity on the interfacial shear strength of the flax/PP system was tested using a tensile testing machine.

4.3.2.3 *Fibre pull-out test:*

A schematic representation of a pull-out sample is shown in Figure 4.2. As shown in the picture, to prevent fibre slippage and to facilitate fixation of the fibre in the tensile testing clamp a piece of cardboard paper was glued to the fibre by an adhesive. The pull-out samples were marked with ink on the fibre at the tip of the pull-out polymer bead.

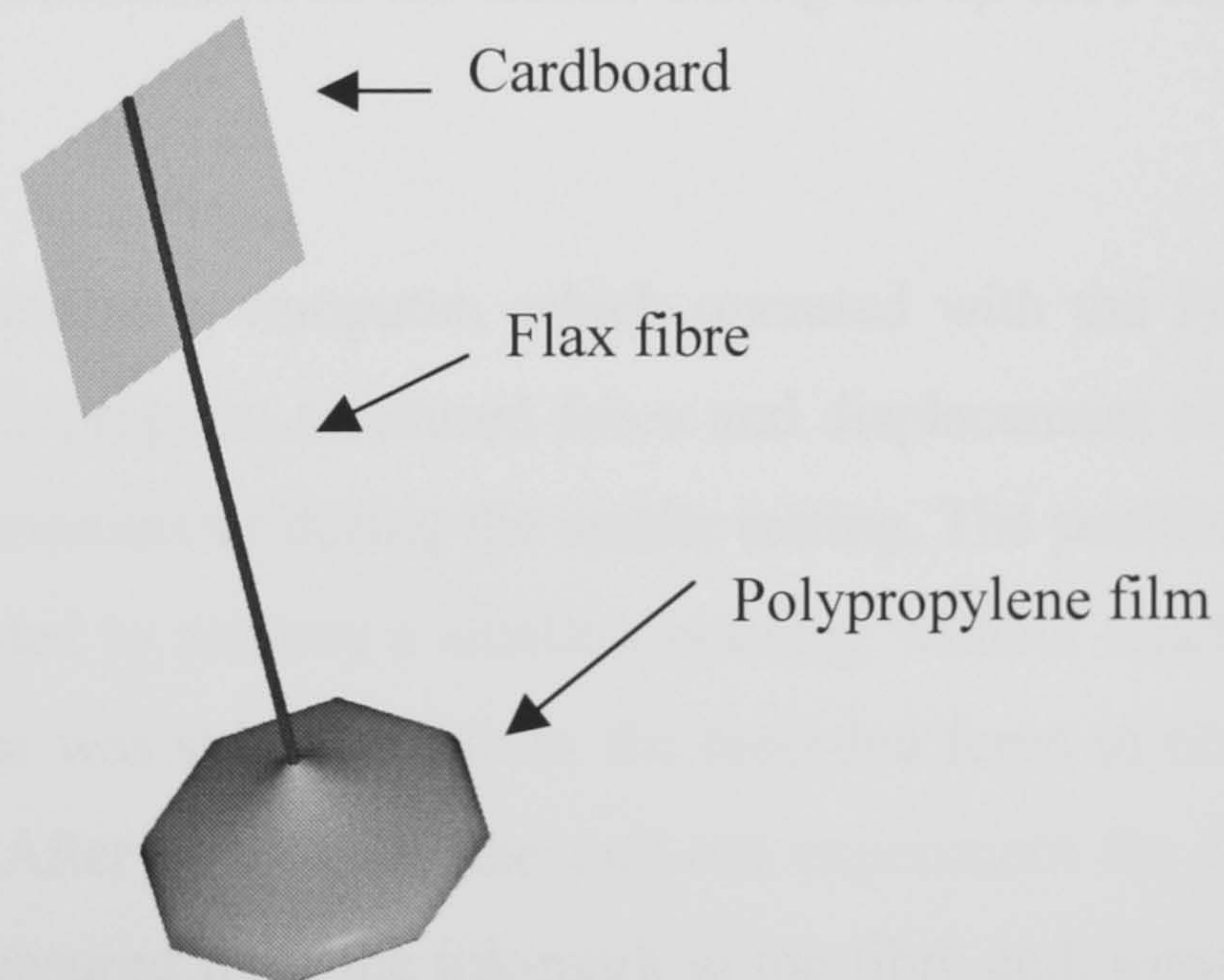


Figure 4.2 Schematic representation of a sample prepared for a fibre pull-out test.

To test the interfacial shear strength a tensile tester (Frank type 81565) with a load cell of 10 N was used. The set up of the test is partially shown in Figure 4.3. As shown in Figure 4.3, the sample was fixed in the upper clamp of the tensile testing

machine, which was moved upward at a rate of 1 mm/min. The micrometer with sharp edged clamps, which was designed to obstruct the polymer drop from upward movement leading to fibre debonding or pull-out, was fixed in the lower clamp of the tensile testing machine.

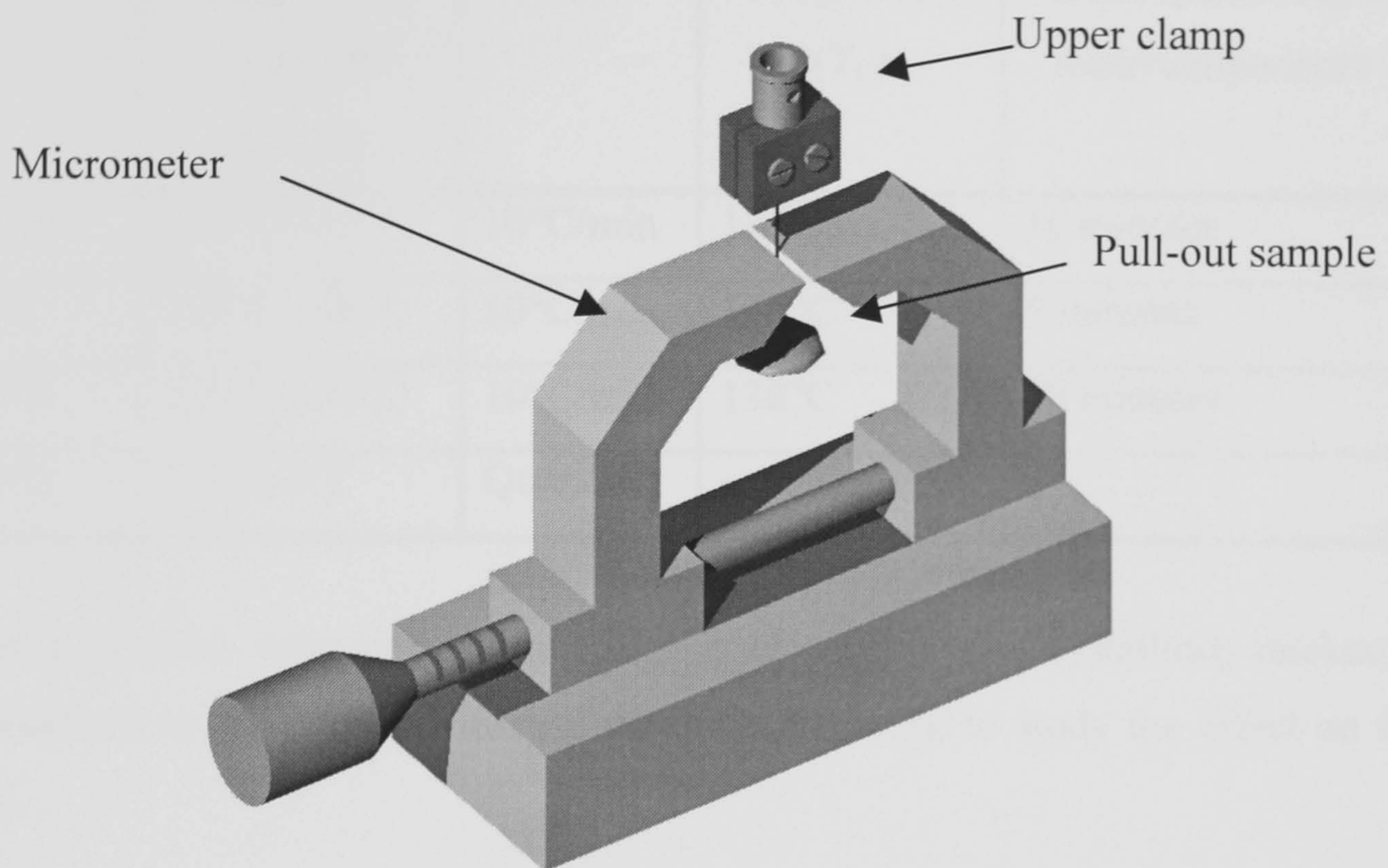


Figure 4.3 A schematic representation of the tensile testing set-up used during the fibre pull-out test.

The tensile tester was connected to a computer, which operated with the Frank Data Acquisition program. This program measured force and displacement of the upper clamp compared to the micrometer during the tensile testing. The position of microvise slit width was adjusted to achieve a smallest opening without touching the fibre surface. Initial tension was subtracted from the recorded force to obtain the maximum pull-out force. After conducting the pull-out experiment the fibre embedded length (L_{em}) was measured from the ink-mark to the fibre end, using an optical microscope. The fibre diameter was also measured for every specimen. With the measured value of the maximum pull-out force the interfacial shear strength was calculated by using Equation 3.1, where the assumption was made that the shear stress was uniformly distributed along the embedded length. The sample preparation was carried out with four different conditions, which are shown in Table 4.1. Around 15 samples were tested for each condition.

Table 4.1 Conditions used to obtain different transcrystalline thickness for pull-out force testing.

Sample	Temperature range with controlled cooling	Cooling rate	Crystallisation Temperature (T_c)	Time at T_c before further quenching to room temperature
A/D/H	210°C-130°C	10°C/min	130°C	10 minutes
B/G	210°C-138°C	10°C/min	138°C	5 minutes
C/F/J	210°C-138°C	10°C/min	138°C	10 minutes
E/I/Q	210°C-RT	Quench	-	-

These conditions were selected on the basis of varying transcrystallinity thickness, as observed in the transcrystallinity study (Figure 4.7), to study the effect on the IFSS.

4.3.2.4 Sample preparation for macrocomposites:

To study the effect of transcrystallinity on the mechanical properties of macrocomposites, samples were made by compression moulding of Duralin flax/PP compound. The compound, consisting of Duralin short chopped fibres with approximately 10 mm length and (MA)PP, was prepared in a kneader (HBI System 90). Figure 4.4 shows a disassembled twin-screw kneader.

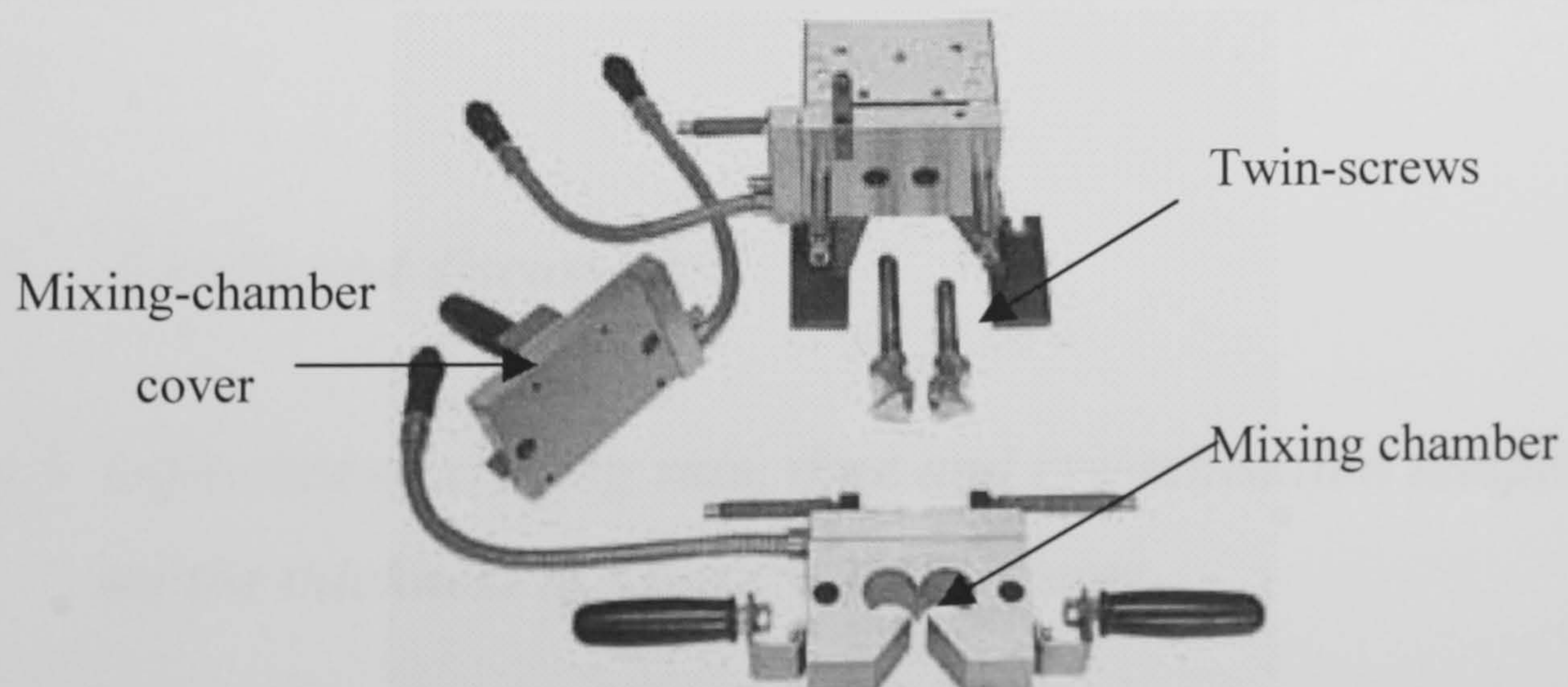


Figure 4.4 Picture of disassembled Brabender kneader (Courtesy: Brabender OHG, www.brabender.com).

The kneading was done for 30 minutes at 210°C and 30 rpm. The mixed compound contained 0%, 20% and 100% w/w MA-PP content. During compression moulding, the mixed compound was heated to 205°C, maintained for 15 minutes, followed by quench cooling. Another set of samples was made by slow cooling from 205°C to 130°C, maintained for 10 minutes (138°C for 30 minutes in the case of 0% MA-PP), followed by quench cooling. This was done to observe the effect of slow cooling on the morphology of matrix and on the mechanical properties of the macrocomposites. Due to the limitations of the compression moulding set-up used, the cooling rate was not controlled. The matrix morphology was observed through a polarised optical microscope. For the same the sample was obtained by microtoming the macrocomposites. The effect of slow cooling on the crystallinity and matrix morphology was studied through differential scanning calorimetric (DSC) studies. The study was done on Perkin Elmer (Pyris 1) differential scanning calorimeter.

4.3.2.5 Tensile testing of macrocomposites:

Uniaxial tensile tests on randomly oriented flax fibre reinforced (MA)PP composites were performed on a Frank tensile testing machine, type 81565, according to ASTM standard (D638M). The tests were performed with a gauge length of 52 mm and a test speed of 5 mm/min. An extensometer was used to monitor the elongation of the tested specimen. At least 10 samples were tested for each condition. The fracture surface of the macrocomposites was observed using Environmental Scanning Electron Microscope (ESEM), Philips: XL30 ESEM-FEG.

4.4 Results and discussions

4.4.1 Influence of cooling rate, time and crystallisation temperature on the thickness of transcrystalline layer

The experiments were carried out to investigate the formation of a transcrystalline zone or interphase in a PP matrix. It was observed that the flax fibre surface was a

good nucleating agent for polypropylene matrix leading to development of a well-defined transcrystalline interphase around it. Figure 4.5 (b) shows the pictures, taken from a polarised optical microscope, of the transcrystallinity around a Duralin flax fibre in PP matrix cooled from 210°C to 130°C at a rate of 10°C/min and kept isothermally (130°C) for 10 minutes. Also shown is the picture (Figure 4.5a) of flax in PP, quench cooled from 210°C.

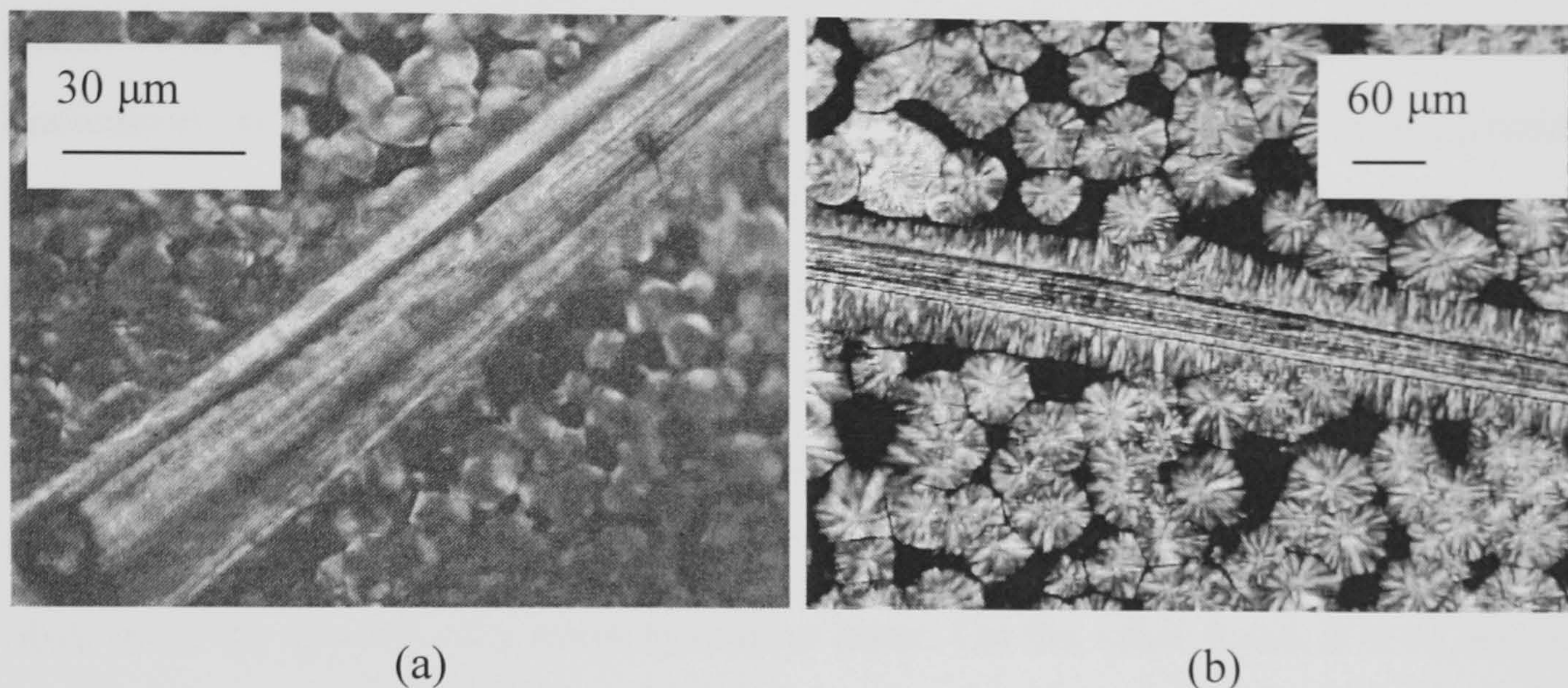


Figure 4.5 Pictures of Duralin flax in PP (a) quench cooled from 210°C and (b) cooled from 210°C to 130°C at 10°C/min followed by isothermal heating at 130°C for 10 minutes.

As shown in the Figure 4.5(b), the transcrystalline region is seen as a white band of densely packed radially oriented crystalline lamellae on both sides of the fibre. As the matrix was cooled from melting temperature to the crystallisation temperature, it was observed that nucleation of PP took place at the surface sites of fibres. The stable nuclei grew radially if there was no nucleus adjacent to them. In this stage growth of individual spherulites was observed. After the fibre was filled with nuclei, a layer of transcrystallinity formed and the growth of crystals was restricted to the direction normal to the fibres. Growth of the transcrystalline layer was finally hindered by spherulites nucleated in the bulk matrix. Figure 4.6 shows the transcrystalline formation around Duralin flax in a PP matrix at a constant temperature of 138°C. From the figure it is clear that the thickness of the transcrystalline layer increased with time, when the sample was kept at a constant temperature, and reached a maximum value after a certain time. The transcrystalline thickness formation around Duralin flax in PP matrix with time for different cooling rates and crystallisation temperature (T_c) is given in Figure 4.7.

The maximum thickness seems to be affected by the cooling rate as well as crystallisation temperature. Higher transcrystalline layer thicknesses were obtained at higher T_c , which was because of the space available in the bulk matrix as the spherulite growth in the bulk matrix was reduced. Also, it took more time to develop the transcrystalline thickness fully. The higher T_c probably reduced the spherulite growth in the bulk matrix because of the higher energy in the bulk matrix leading to enhanced mobility of polymer and therefore reduced amount of nucleation in the bulk matrix. Figure 4.8 shows the effect of crystallization temperature on the transcrystallisation behaviour. It was observed that the growth rate of transcrystalline and spherulites region was same upto 138°C. It is therefore assumed that the crystallisation rate at the interface and matrix is same for all temperatures up to 138°C. When the crystallization took place at a temperature below 130°C, the nucleation density in the bulk matrix was too high, which obstructed the growth of a transcrystalline layer. On the other hand, it is of interest to note that there existed a maximum crystallisation temperature (T_{max}) for development of transcrystalline layer, within the time span studied and at a cooling rate of 10°C/min. T_{max} in Duralin flax/PP system was observed at 140°C. For T_c higher than T_{max} , no transcrystalline layer was observed. However, the crystal growth was observed in the bulk matrix at temperature higher than T_{max} . The idea that transcrystallisation is caused by stress-induced nucleation due to mismatch in thermal expansion coefficients would explain the existence of a temperature boundary for transcrystallisation (Thomason and Van Rooyen, 1992b). It has been shown that at a particular level of undercooling there is a minimum shear stress τ_m necessary to produce stress-induced crystallisation. It has also been shown that, as the crystallisation temperature is reduced, τ_m is also reduced. It can therefore be suggested that the product of the applied cooling rate and a difference in thermal expansion will lead to a certain level of strain rate at the fibre-melt interface, inducing some level of interfacial stress τ_i . As the temperature is reduced, τ_m is reduced but τ_i will probably increase due to increasing relaxation times at lower temperatures. Thus τ_i will eventually increase above τ_m , giving rise to stress-induced nucleation at the interface, and leading to the subsequent growth of a transcrystalline interface. However, if crystallisation occurs in the bulk matrix

before τ_i increases above τ_m , then no stress-induced nucleation will occur at the interface and only heterogeneous nucleation of spherulites will be observed.

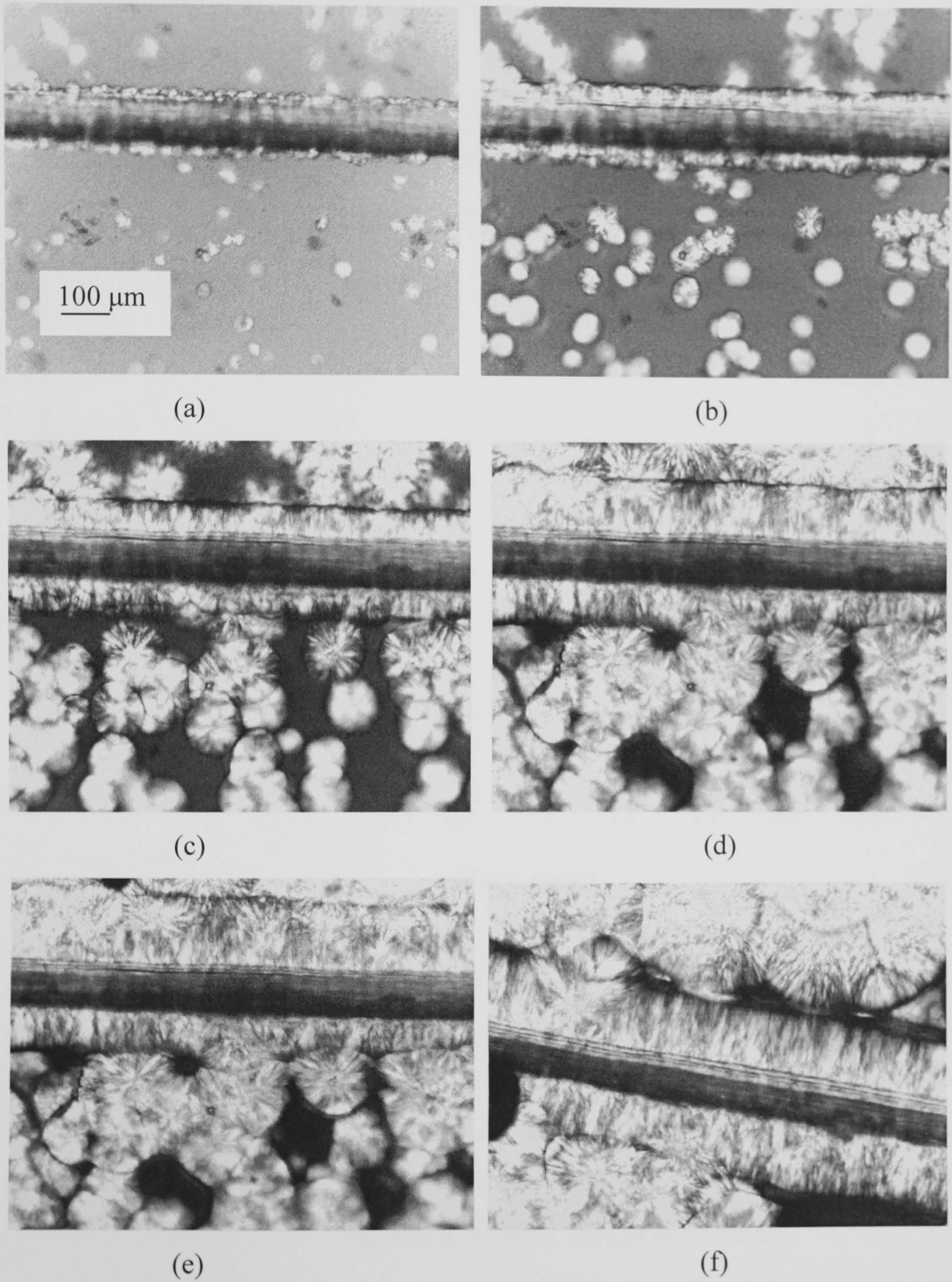


Figure 4.6 Effect of crystallisation time on transcrystalline thickness in Duralin flax/PP system at a temperature of 138°C. Cooling rate 10°C/min. a) 2 min, b) 6 min c) 10 min, d) 18 min e) 24 min and f) 34 min.

Transcrystalline growth was also observed to be influenced by the cooling rate (Figure 4.7). In the case of Duralin flax/PP system it was observed that the transcrystalline layer thickness reduced with an increase in the cooling rate when the sample was cooled from 210°C to 130°C. An optimum of 5°C/min was observed in the case of above mentioned sample and conditions. However, the effect of cooling rate, on the transcrystalline layer thickness, is observed to be contradictory for different systems studied.

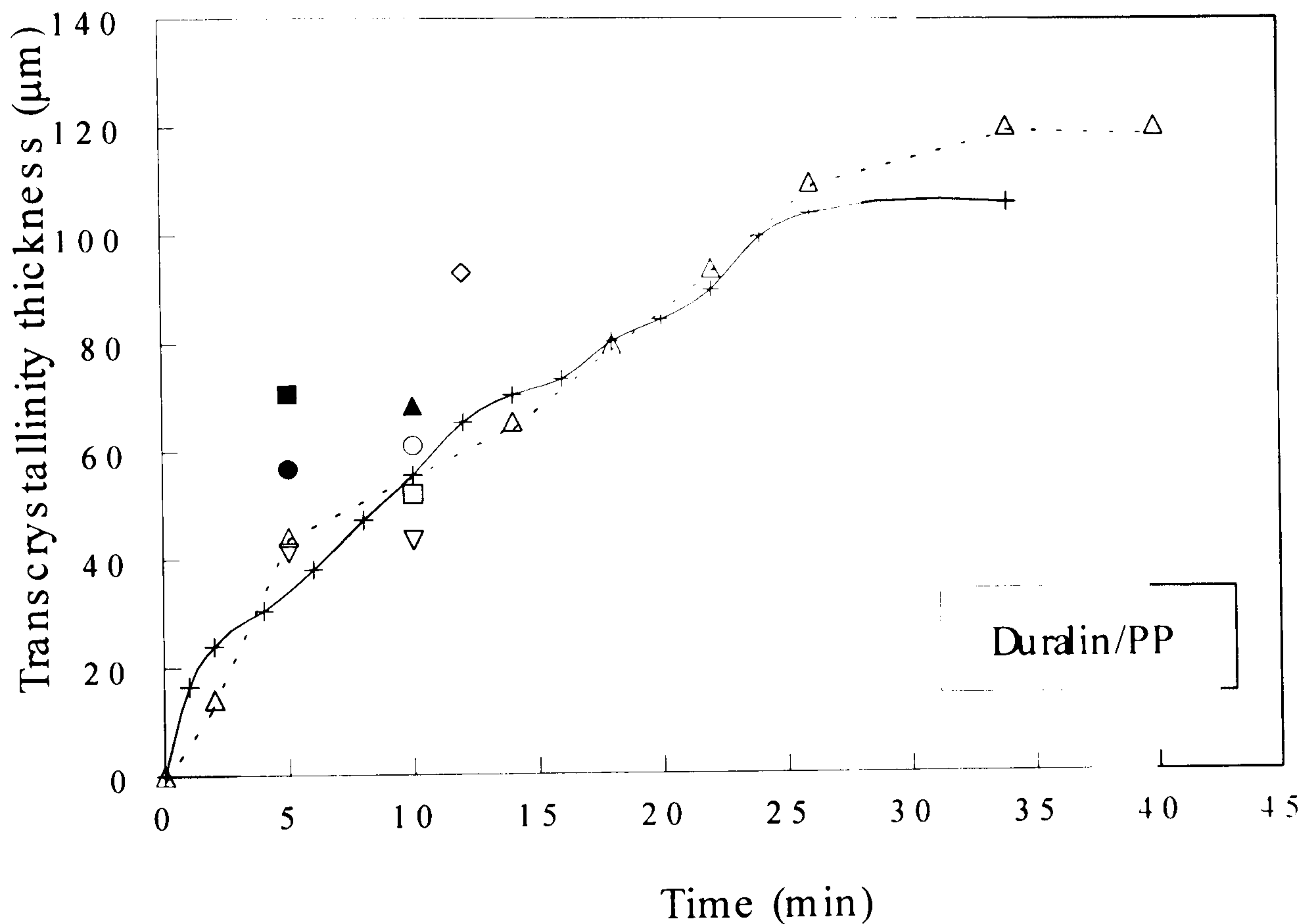


Figure 4.7 Development of transcrystallinity thickness with time, for different cooling rates and crystallisation temperatures, around Duralin flax, cooled from 210°C to different crystallisation temperatures and with different cooling rates. □ = 125°C at 10°C/min, ○ = 130°C at 1°C/min, ■ = 130°C at 5°C/min, ▲ = 130°C at 10°C/min, ● = 130°C at 20°C/min, ▽ = 130°C at 30°C/min, ◇ = 135°C at 10°C/min, + = 138°C at 10°C/min and △ = 140°C cooled at 10°C/min.

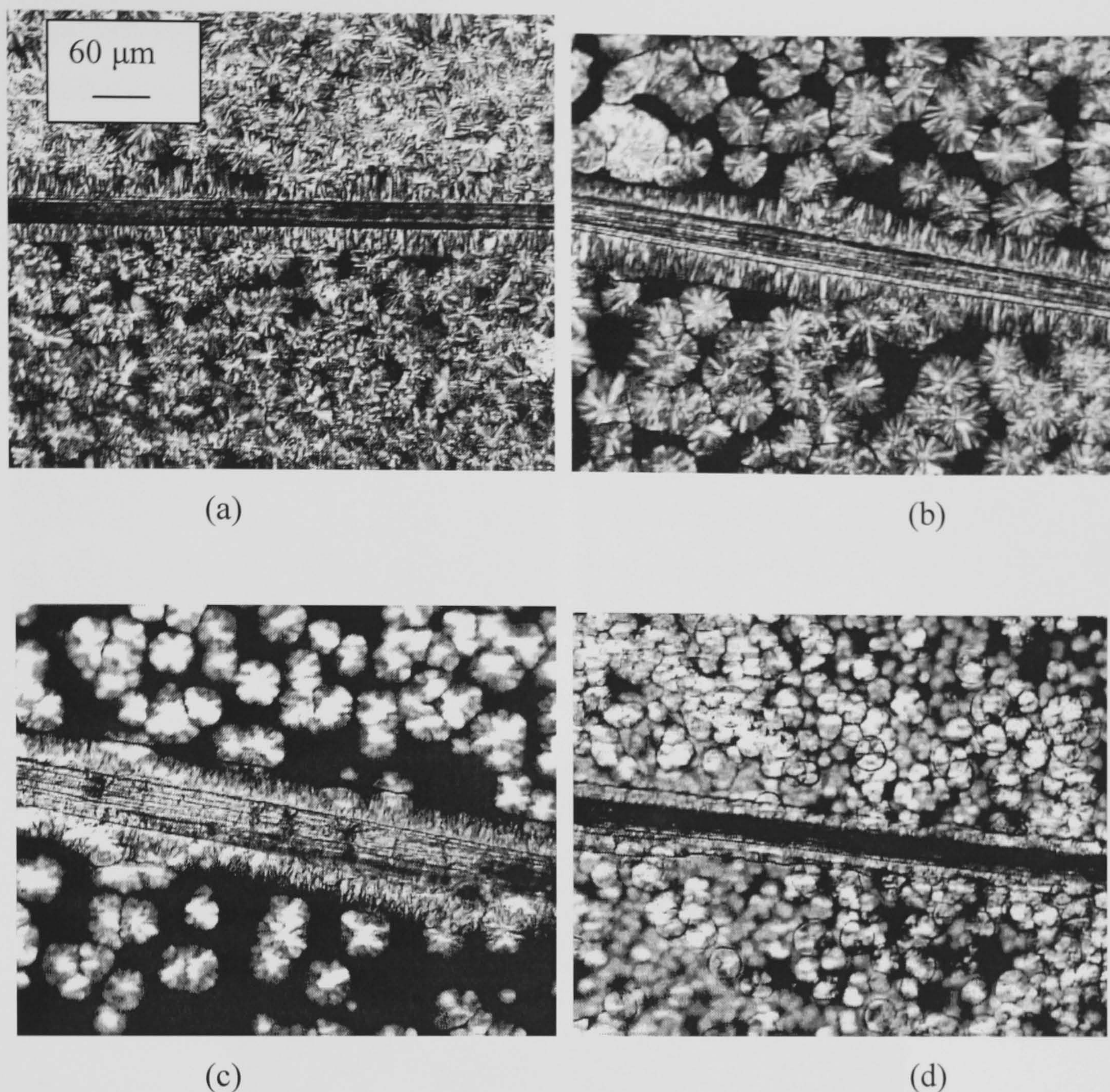


Figure 4.8 Effect of crystallization temperature on transcrystallisation behaviour in (technical) Duralin flax/PP system. (a) 125°C, (b) 130°C, (c) 138°C and (d) 140°C. Cooled at 10°C/min from 210°C. Cooling time 10 min. (All 4 pictures had same magnification).

4.4.2 Influence of fibre type and modifications

The formation of transcrystallinity around different types of flax fibres i.e. Duralin, green and dew-retted flax in PP matrix is shown in Figure 4.9. A uniform layer of transcrystallisation was observed in Duralin fibre. In the case of Duralin fibre, the fibre surface was smooth and uniform and as a result transcrystalline formation was more uniform compared to green and dew-retted flax. It has been reported that surface topography rather than surface chemistry dominates the nucleation process

(Gray, 1974b). Figure 4.10 and 4.11 show the transcrystalline thickness in alkali treated and silane treated fibres respectively.

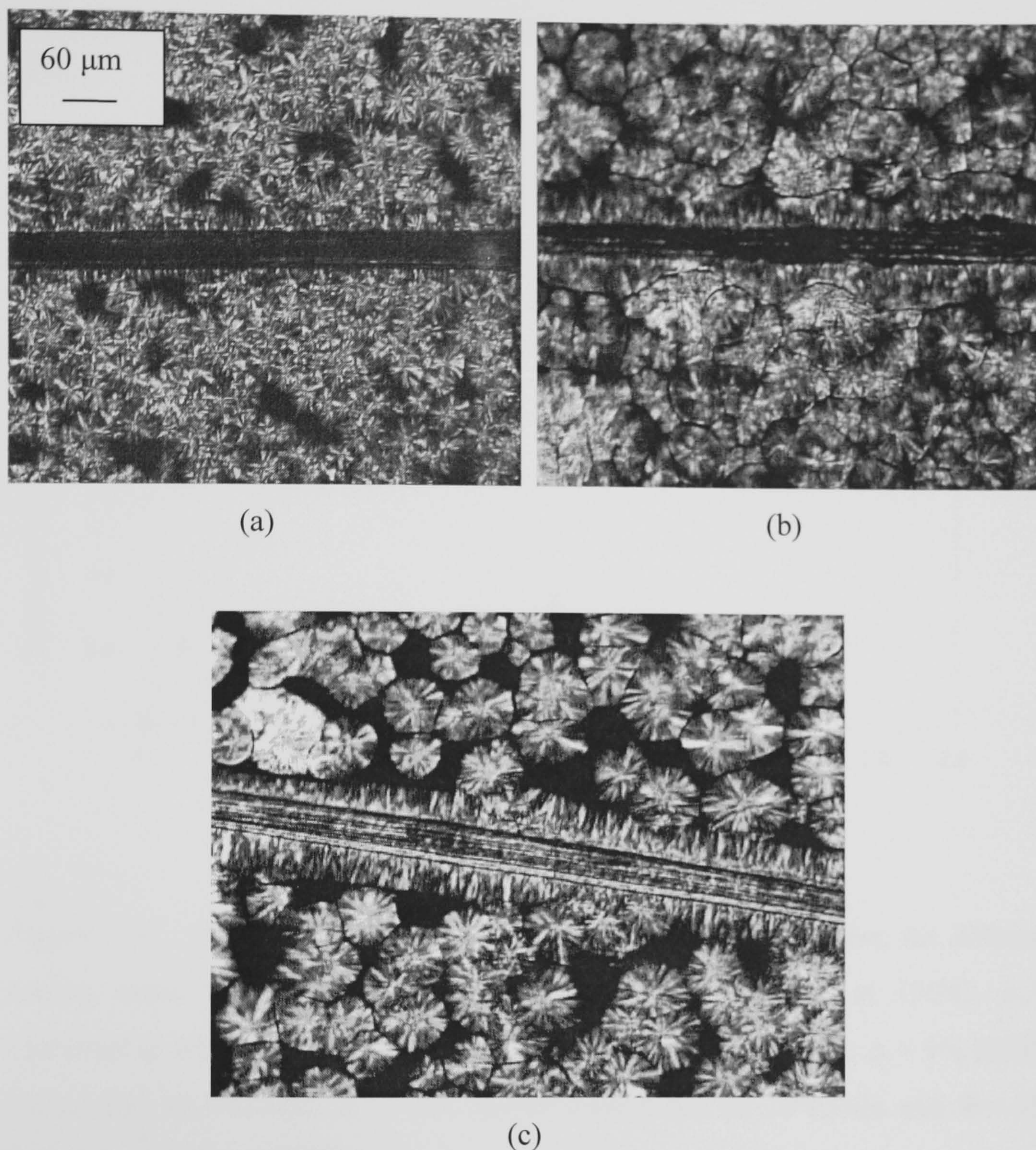


Figure 4.9 Effect of fibre type on transcrystallisation behaviour, (a) green flax, (b) dew-retted flax and (c) Duralin flax, at 130°C cooled at 10°C from 210°C (All three figures had same magnification as (a)).

The effect of cooling rate was contradictory for different systems studied i.e. the transcrystallinity thickness reduced with an increase in the cooling rate (crystallisation temperature of 130°C) in the case of Duralin flax/PP system whereas it increased with increasing cooling rate in the case of silane treated green flax fibres. In the case of Duralin/PP and alkali treated combed dew-retted/PP

system a maximum transcrystalline layer thickness was observed when the samples were cooled at $5^{\circ}\text{C}/\text{min}$ (from 210°C to 130°C). No such maximum (at $5^{\circ}\text{C}/\text{min}$) was observed in the case of silane treated sample (when cooled to 130°C from 210°C).

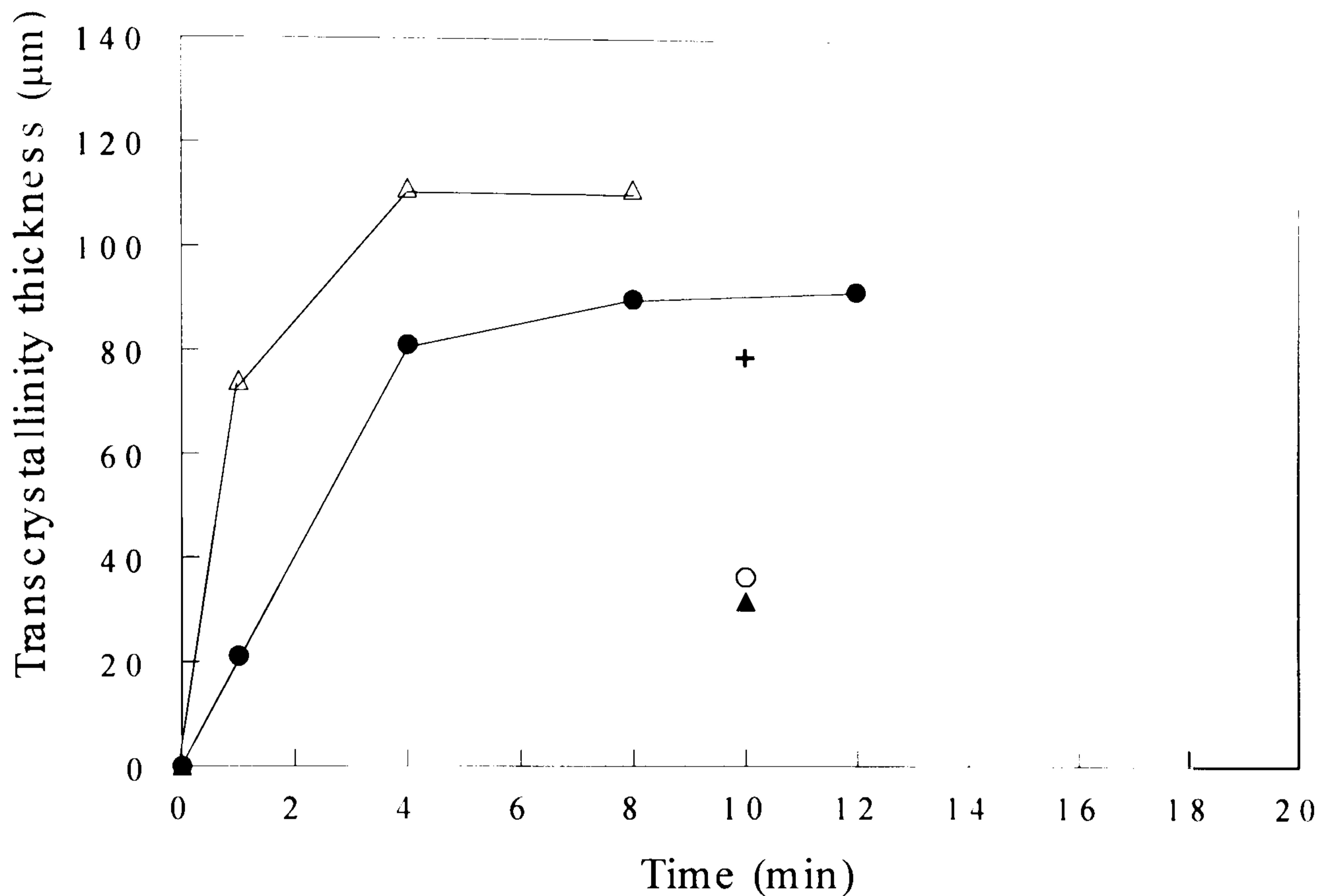


Figure 4.10 Development of transcrystallinity thickness with time, for different cooling rates, around alkali treated combed dew-retted flax at 130°C . + = Untreated at $10^{\circ}\text{C}/\text{min}$, O = 0.5% NaOH treated flax at $10^{\circ}\text{C}/\text{min}$, Δ = 5% NaOH treated flax at $5^{\circ}\text{C}/\text{min}$, \blacktriangle = 5% NaOH treated flax at $10^{\circ}\text{C}/\text{min}$ and \bullet = 5% NaOH treated flax at $20^{\circ}\text{C}/\text{min}$.

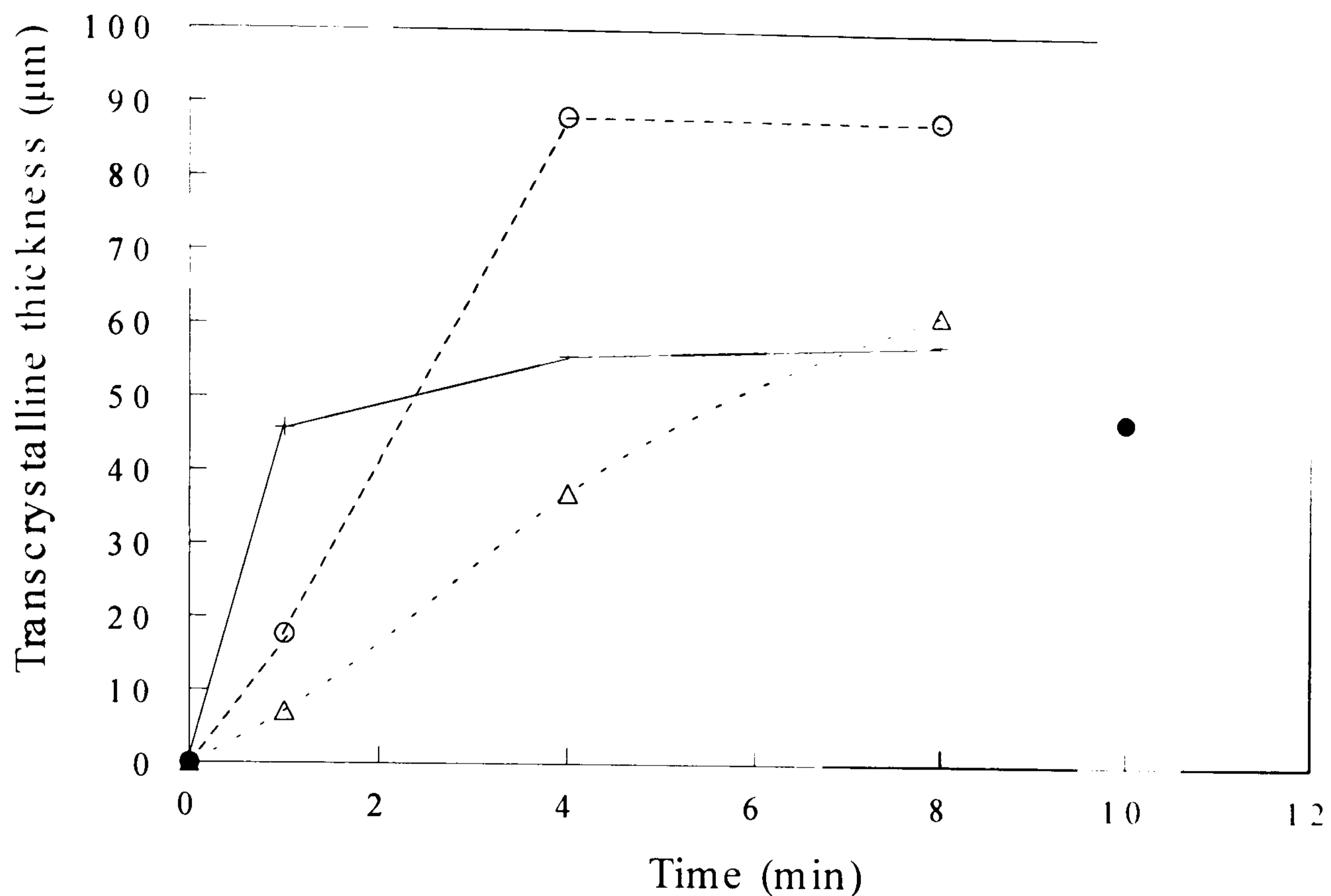


Figure 4.11 Development of transcrystallinity thickness with time, for different cooling rates, around green flax. + = Silane treated fibre at 130°C cooled at 5°C/min, Δ = Silane treated fibre at 130°C cooled at 10°C/min, O = Silane treated fibre at 130°C cooled at 20°C/min, and ● = Untreated flax at 135°C cooled at 10°C/min.

From the results (Figure 4.10), the effect of alkali treatment (of combed dew-retted flax) on the transcrystalline layer thickness of PP matrix is not clear. However, higher transcrystalline layer thickness was observed in the case of silane treated green flax/PP when compared to untreated green flax/PP system (Figure 4.11). This could be due to the improved interaction between alkyl-silane pendants and PP macromolecules.

4.4.3 Influence of matrix modification on the thickness of transcrystalline layer

In Figure 4.12(a) a picture of a Duralin flax fibre and a PP/MA-PP (95:5 wt/wt) blend matrix is shown. In this figure it can be clearly seen that the addition of 5 wt% MA-PP in the matrix caused a change in the crystallisation behaviour when

compared with the PP matrix. No transcrystalline region was observed. However, large number of small spherulites were observed in the bulk matrix. In Figure 4.12(b) a picture of a Duralin flax and MA-PP matrix is shown. The presence of spherulites can be seen on the fibre surface and in the bulk matrix.

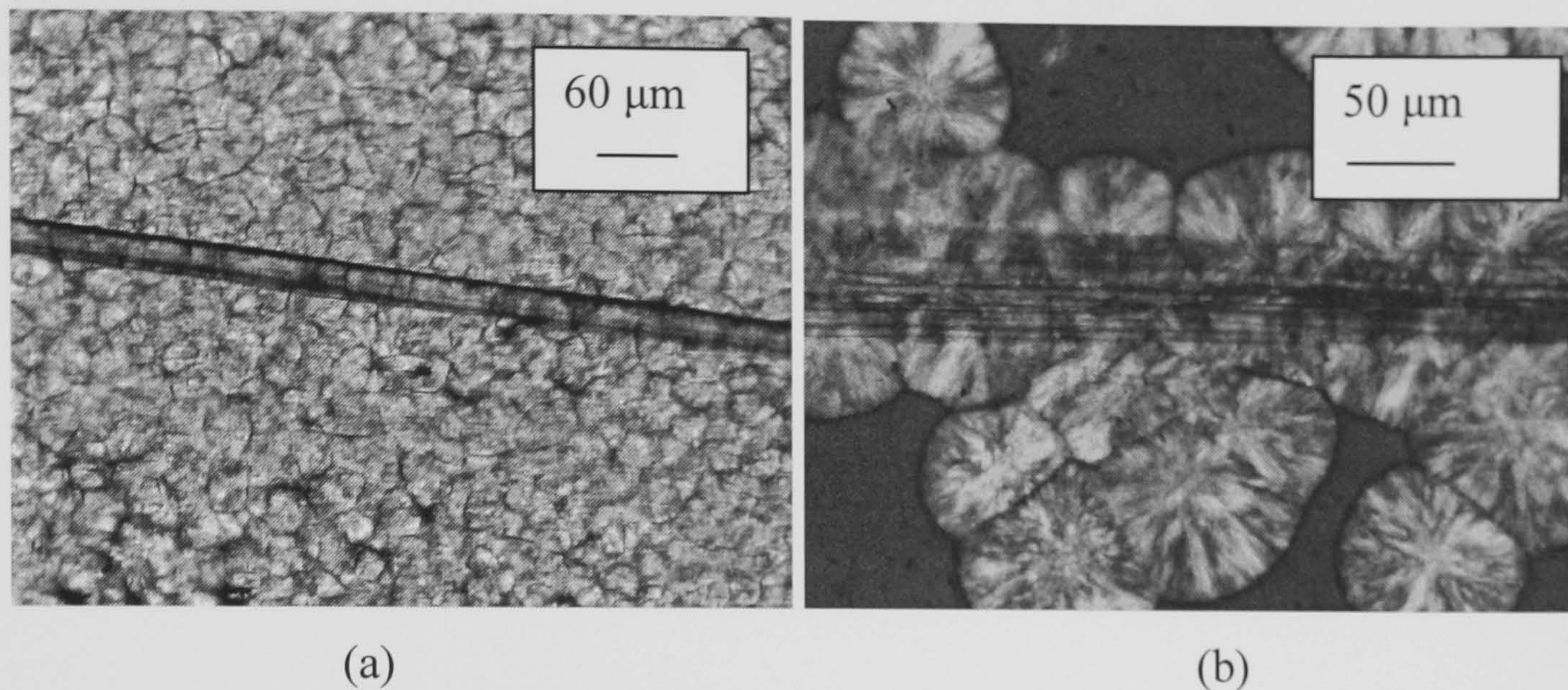


Figure 4.12 Pictures of Duralin flax fibre and (a) PP/MA-PP (95:5 wt/wt) blend and (b) MA-PP matrix.

The observed effect of addition of MA-PP on the matrix morphology as well as transcrystalline layer (when compared with unmodified PP matrix) could be due to the interaction within MA-PP grafted macromolecules as well as interaction with cellulose fibres.

4.4.4 Influence of transcrystallinity on the micromechanical properties of the flax/PP microcomposites

For studying the effect of the transcrystalline layer on the mechanical properties only Duralin fibre was used, because Duralin fibre showed a uniform layer of transcrystallinity. Figure 4.13 shows a picture of a microtomed slice of the pull-out sample, cut perpendicular to the fibre axis and observed under an optical polarised light microscope. The picture shows the presence of a transcrystalline layer around Duralin fibre indicated by the white arrow. However, the transcrystallinity is only partial, which could be due to incomplete wetting. The white spots in the middle of the picture are different elementary fibre cells.

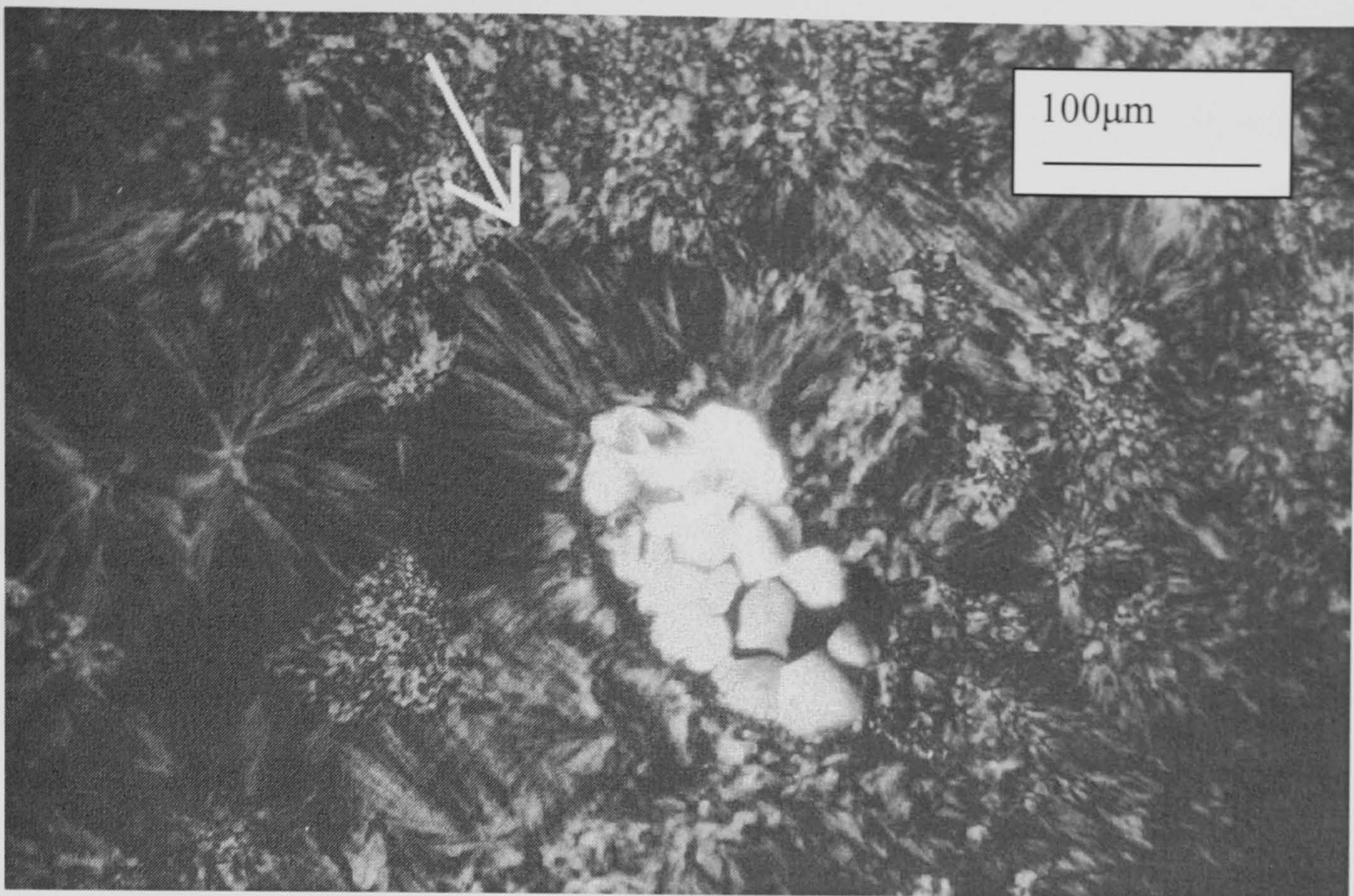


Figure 4.13 Picture of a microtomed slice of a pull-out sample, cut perpendicular to a Duralin fibre axis and seen under a polarised light optical microscope, showing the presence of (partial) transcrystallinity around the fibre cell bundle.

As mentioned earlier (Section 4.1), the microdebond test was used to study the effect of chemical modification (fibre as well as matrix) on the interfacial shear strength (IFSS). Due to the limitations of the set-up used to study the transcrystallinity, the fibre pull-out test (instead of microdebond tests) was used for studying the effect of transcrystallinity. The samples were made as described in Section 4.3.2.2. Similar to the curve obtained with microdebond test (Figure 3.13), a typical pull-out curve, which was measured by the tensile testing machine, looks like Figure 4.14. From the figure it can be seen that three events occurred during the pull-out test. First the fibre was loaded, leading to an elastic stress build up to the point where the shear strength of the interface was reached, then the fibre came loose from the matrix and debonding occurred. This was observed by a sudden drop in the pull-out force. After this friction at the fibre-matrix interface may describe the behaviour of the pull-out force, which decreased because of the decrease in the interface area.

Determination of IFSS: The maximum pull-out forces recorded for the samples are given in Figure 4.15 as a function of the embedded area. Four different test conditions were used to estimate the effect of transcrystallinity on the fibre pull-out force and the IFSS, as shown in Table 4.1. As shown in Figure 4.15, the pull-out curves do not differ much from each other. The IFSS, calculated through Equation 3.1 and also estimated as the slope of each graph, seems to decrease with the increase in the transcrystallinity thickness (Table 4.2). However, since the differences were very marginal and also because of large scatter it is difficult to give conclusive results. This could be because of incomplete wetting.

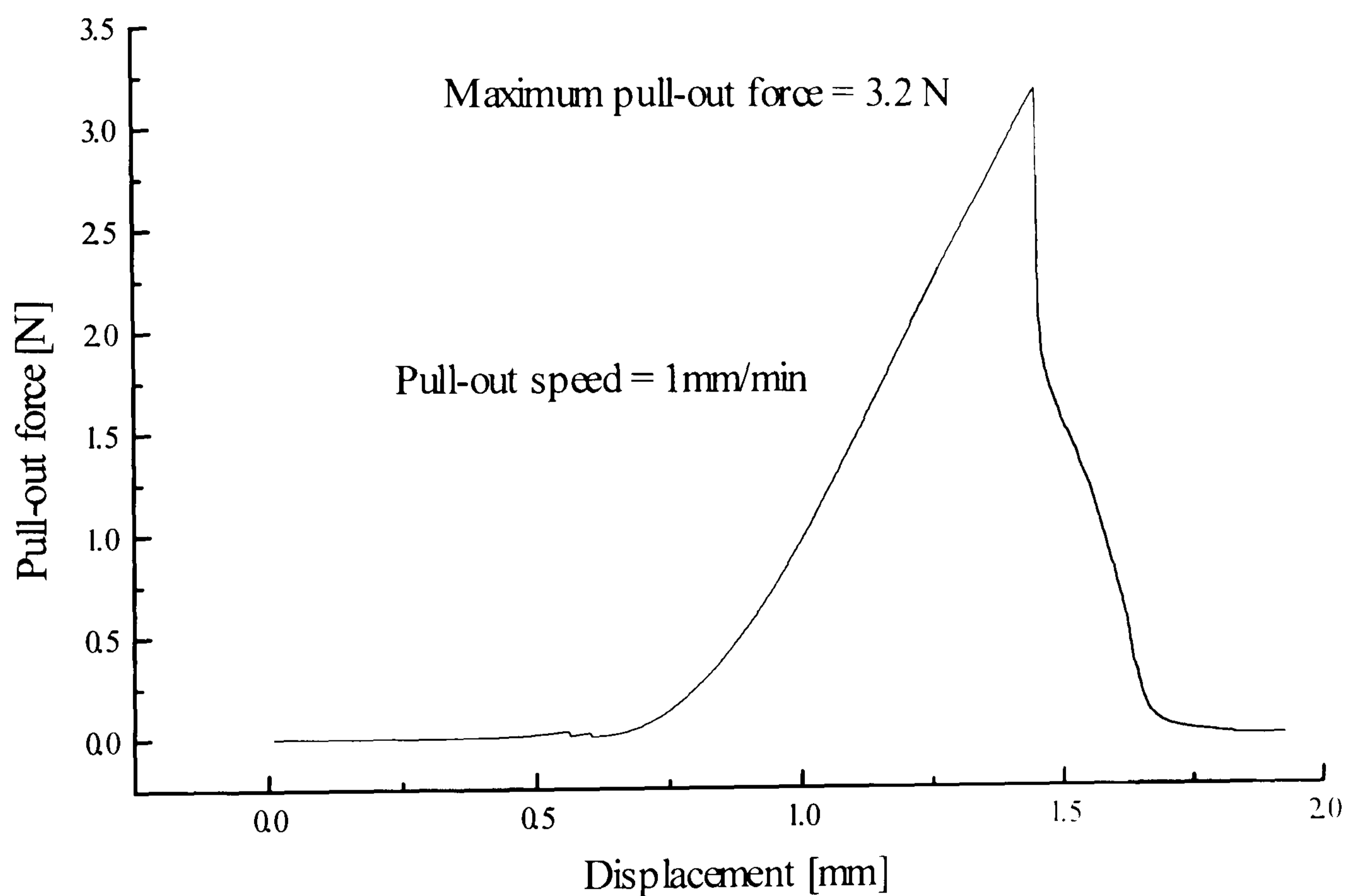


Figure 4.14 Typical curve of a pull-out force measurement.

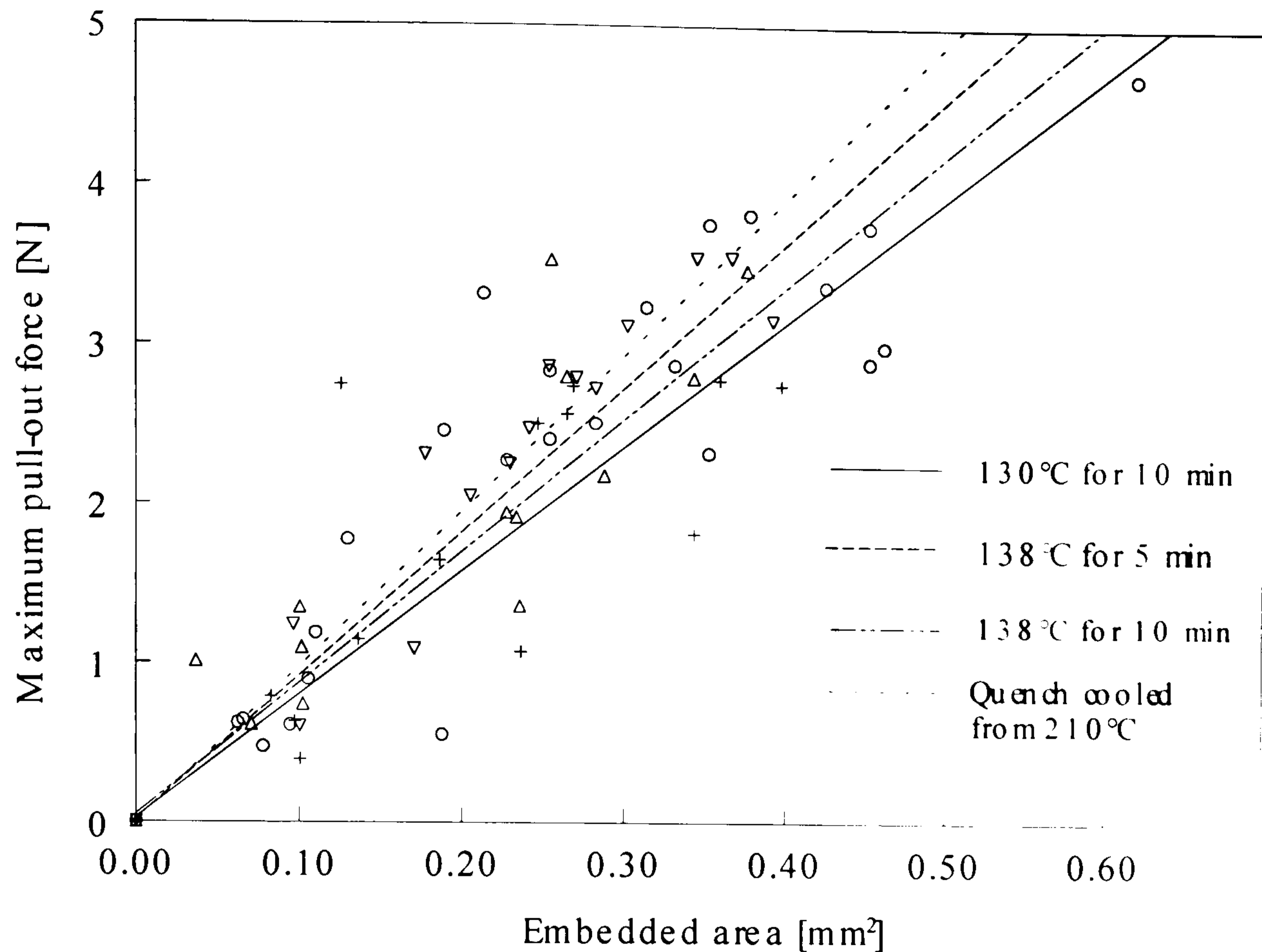


Figure 4.15 Maximum pull-out force vs. embedded area for samples cooled from 210°C at 10°C/min followed by the isothermal heating at: (a) + - 130°C for 10 min, Δ - 138°C for 5 min, O- 138°C for 10 min and ∇ - Quench cooled from 210°C. Isothermal heating is followed by quench cooling to room temperature.

Table 4.2 IFSS calculated from the slope of pull-out force vs. embedded area curves (and Equation 3.5) for samples cooled from 210°C at 10°C/minute followed by isothermal heating and quench cooling.

	<i>130°C for 10 min</i>	<i>138°C for 5 min</i>	<i>138°C for 10 min</i>	<i>Quench cooled</i>
<i>IFSS (MPa)</i>	7.8	9.0	8.3	9.8

4.4.5 Influence of transcrystallinity on the macromechanical properties of the flax/PP macrocomposites

The effect of cooling conditions on the tensile strength of PP/Duralin macrocomposites is shown in Figure 4.16.

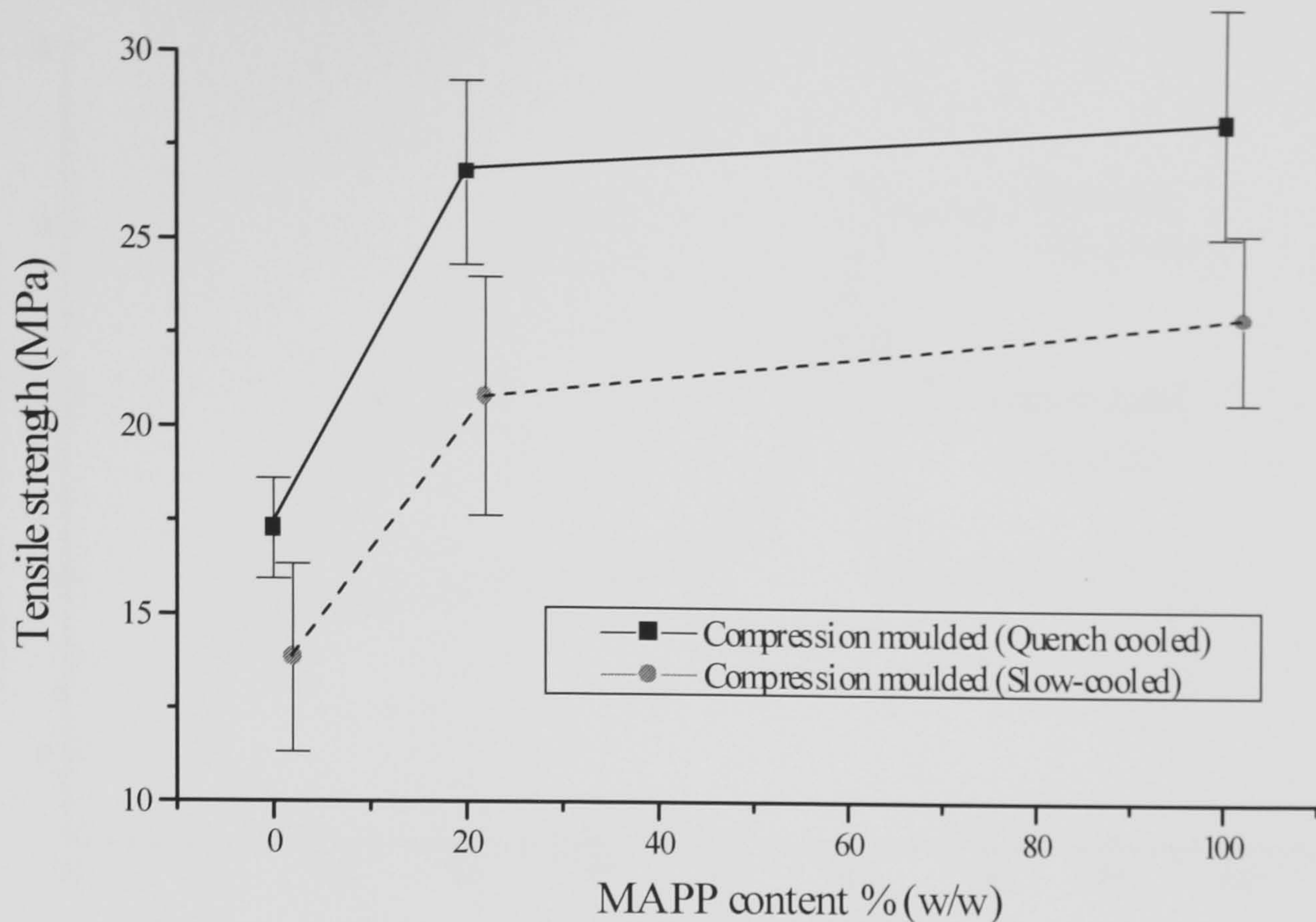


Figure 4.16 Effect of slow cooling on the tensile strength of macrocomposites manufactured by compression moulding of flax/PP compound (Fibre volume content = 20%; error bars show the standard deviations).

From the Figure 4.16 it is clear that quench cooled samples exhibited higher strength than slow cooled samples for all concentrations of MA-PP. As mentioned in Chapter 2, the tensile strength of flax fibre decreased when exposed to heat for longer times. Since the sample was cooled slowly (around 1°C/min), it was therefore longer exposed to a temperature of around 210°C. This might have led to a decrease in the tensile strength of flax thus resulting in a drop in composite strength. The reduction in tensile strength could also be attributed to the brittle nature of the crystalline sample. Due to slow cooling, more perfect crystals were formed as shown by differential scanning calorimetry (Figure 4.17).

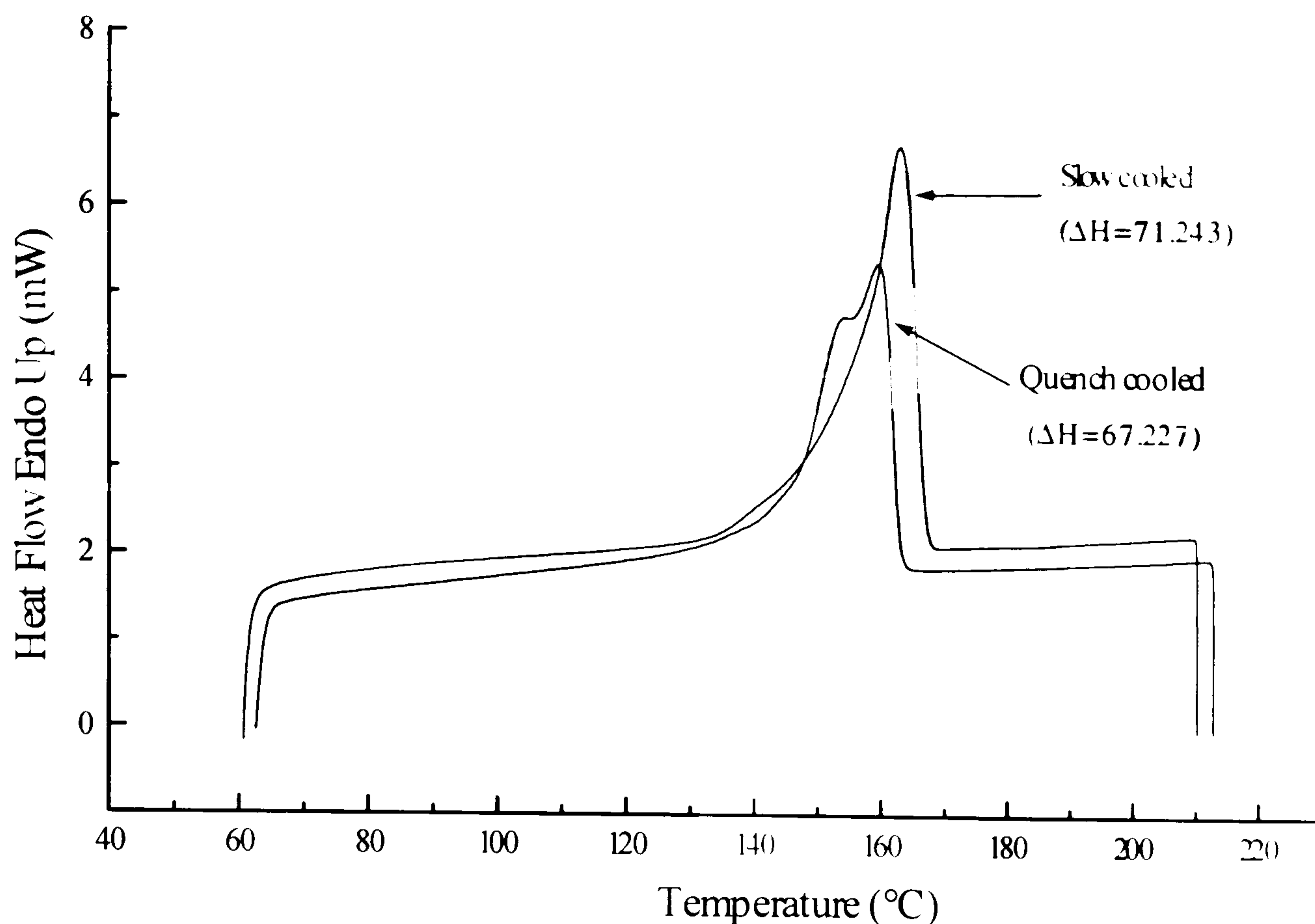


Figure 4.17 DSC study on flax/PP composite to study the effect of slow cooling on the matrix morphology. Heating program: Hold for 5 min. at 60°C, followed by heating from 60°C to 210°C at 10°C/min.

As seen in Figure 4.17, slow cooled samples exhibited single peak during the melting cycle and a double peak was given by quench cooled samples. The double peak was because of recrystallisation of crystals into more perfect crystals. This was confirmed when the sample was heated at 30°C/min instead of 10°C/min (Figure 4.18). The double peak, which was observed in the case of quench cooled sample, disappeared when the sample was heated at 30°C/min. This could be due to the reason that the sample did not get enough time to recrystallise hence showing a single melting peak. The difference in the fracture of slow cooled and quench cooled samples was also observed through the fracture surface as observed by ESEM (Figure 4.19). It can be seen that the slowly cooled sample exhibited a granular fracture surface, which could be due to the crystalline nature of the matrix morphology, leading to brittle fracture. On the other side quench cooled samples with more amorphous PP matrix had a higher strength because of more molecular entanglements hence leading to improved stress transfer and also exhibiting smoother fracture surfaces.

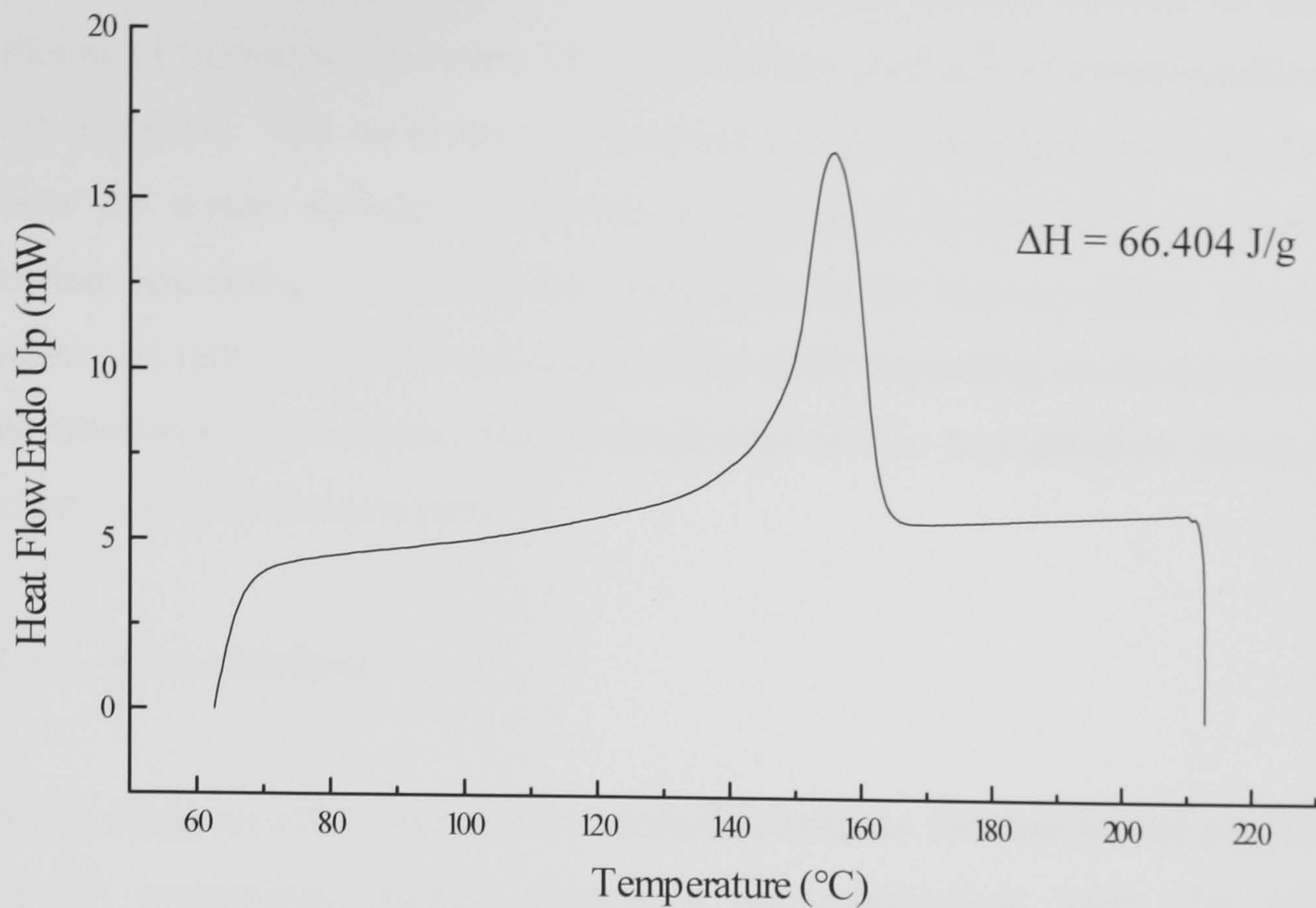
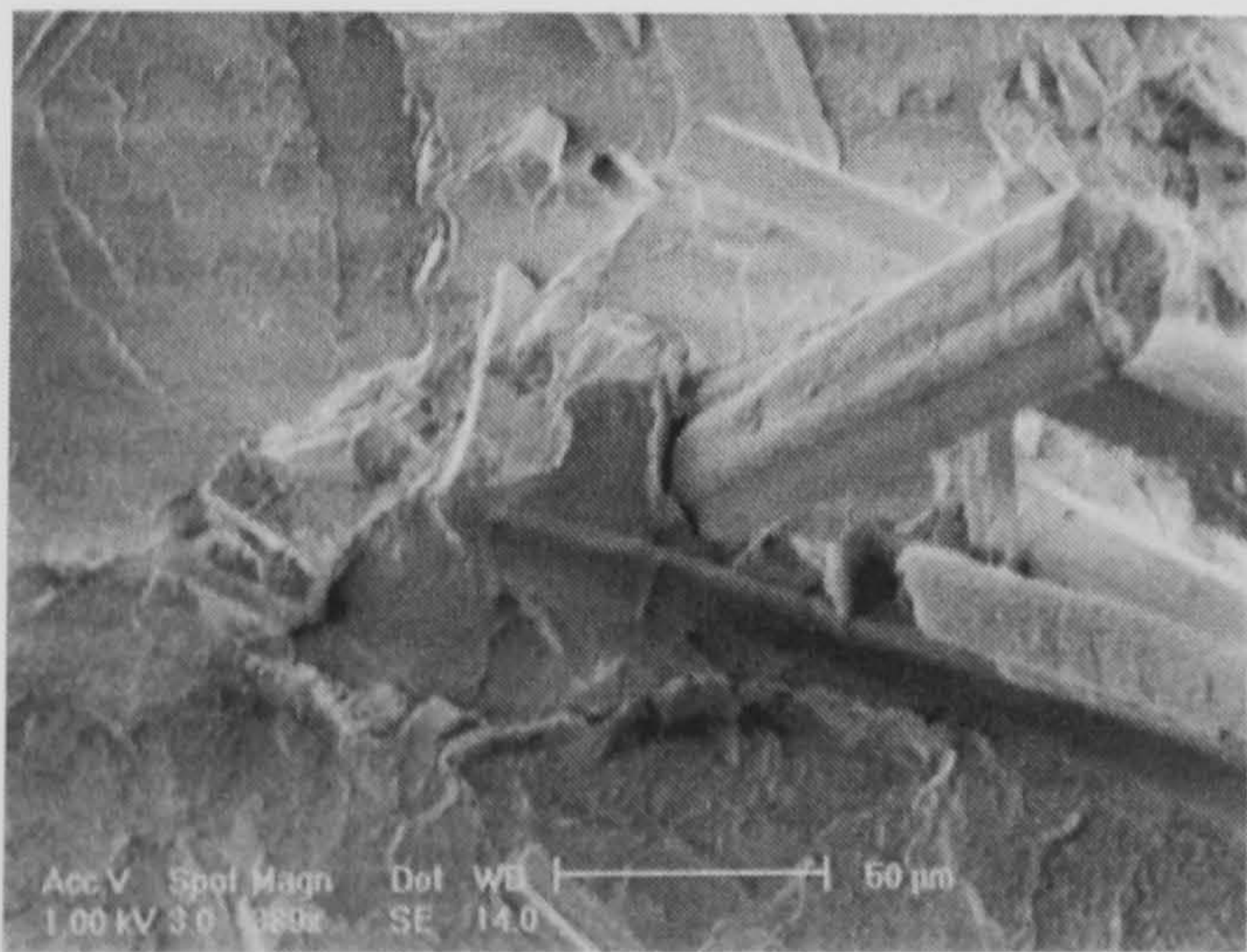
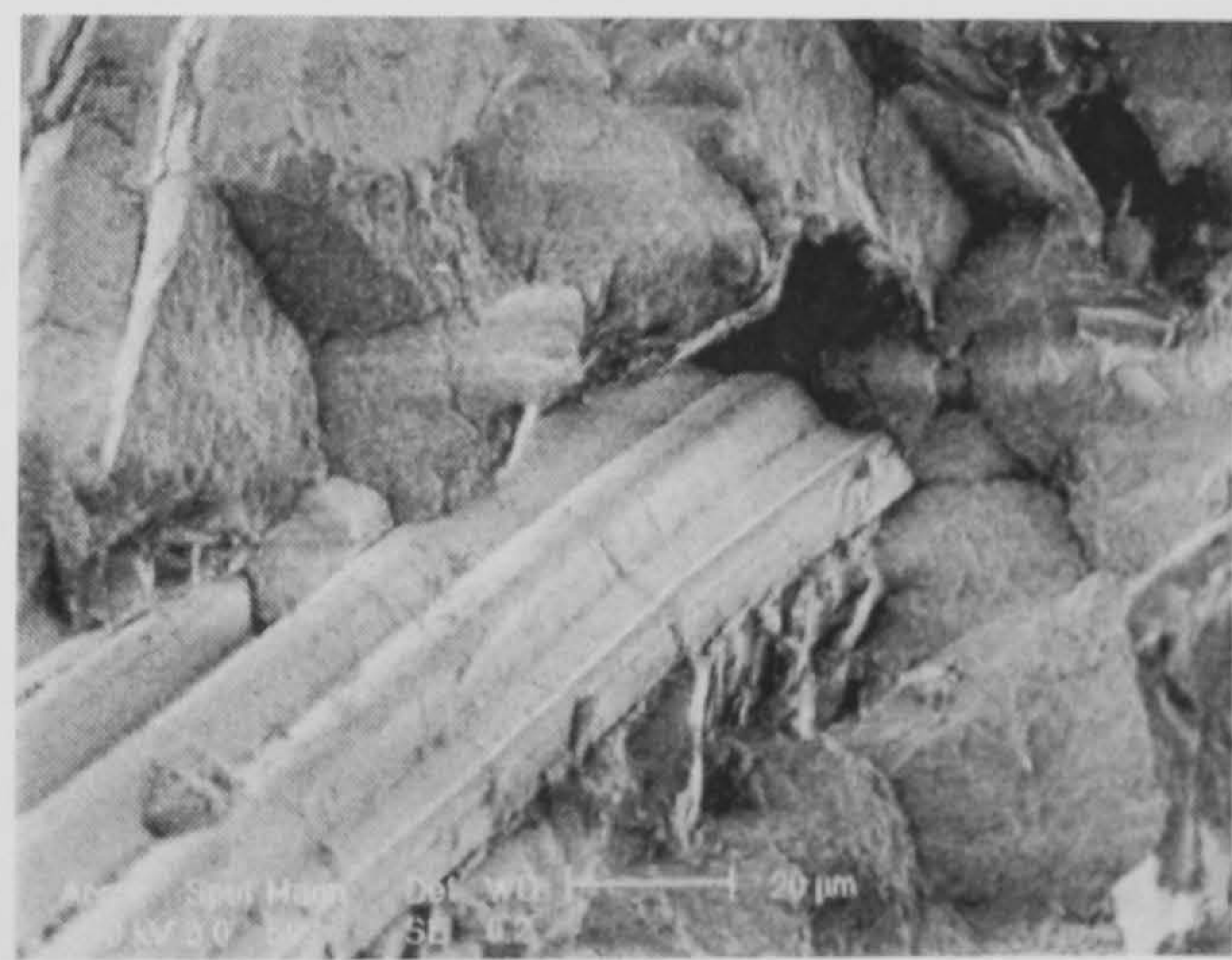


Figure 4.18 DSC study on flax/PP quench cooled composite. A heating rate of 30°C/min reduced the double peak (Figure 4.17), in the quench cooled sample, to a single peak. Heating program: Hold for 5 min. at 60°C, followed by heating from 60°C to 210°C at 30°C/min.



(a)



(b)

Figure 4.19 Fracture surfaces of (a) a quench cooled and (b) a slow cooled flax/PP macrocomposites manufactured by compression moulding of compound.

Another important factor affecting the influence of transcrystallinity on mechanical properties is the fibre content. Chen and Hsiao (1992) reported that as the fibre content increases the transcrystallinity decreases. At higher fibre content the matrix spacing between the fibres is smaller, limiting the growth of the transcrystalline

interface. In the case of the flax/PP system also, mainly because of the large amount of impurities, no clear indication of the presence of transcrystalline layer was observed. The occurrence of a transcrystalline interphase has been found to allow for a new damage mechanism to take place in composite samples under tension consisting of interlaminar separation in the transcrystalline region. The extent and nature of this damage generation differ depending on the crystal form in the transcrystalline region. The impingement of two crystallisation fronts would result in a weak fracture path.

4.5 Conclusions

In this study an effort was made to enhance/optimize the mechanical properties of flax/PP composites, mainly, through a micromechanical study. The adhesion between matrix and fibre in microcomposites was studied. An attempt was made to modify the fibre/matrix interface/interphase via modifications in the processing parameters like cooling rate, crystallinity temperature and cooling time. The influence of matrix modification on the crystallisation behaviour was also studied.

The results of modifications in processing parameters showed that flax fibres are good nucleating agents in polypropylene matrix leading to a uniform transcrystalline layer around the fibre surface.

The transcrystallisation layer formation around Duralin flax in PP matrix was studied in detail. The crystallisation temperature, cooling rate and time influences the thickness of a transcrystalline layer. In general an increase in the thickness of transcrystalline layer is observed at higher crystallisation temperature (T_c). Complete development of transcrystalline layer takes longer time at higher T_c . However, as T_c is increased beyond certain value (for a cooling rate of $10^\circ\text{C}/\text{min}$) no transcrystallisation layer is formed. This maximum T_c of 140°C can be explained by the effect of stress-induced crystallisation.

The effect of cooling rate is contradictory with different systems studied.

Silane treatment of green flax leads to enhancement in the transcrystalline layer thickness.

The decrease in the interfacial shear strength with increasing transcrystalline thickness, in the case of Duralin flax/PP microcomposites, was observed through fibre pull-out tests. However, the differences observed were very small and experimental scatter was very high therefore no major conclusion involving the effect of transcrystallinity on IFSS can be made. A typical value for the IFSS, with a transcrystalline layer as an interface, obtained in the present study through the fibre pull-out test was ~ 8 MPa.

The effect of slow cooling on the tensile strength of macrocomposites, manufactured by compression moulding of flax/PP compound, was also studied. Slow cooling of Duralin flax/PP compound resulted into a reduction in tensile strength of the macrocomposites, which could be because of a drop in the tensile strength of the flax fibre (Chapter 2). The decrease in the tensile strength could also be because of a reduction in matrix molecular entanglements as slow cooled samples exhibited higher crystallinity and hence showed brittle fracture, which was observed through the differential scanning calorimetric study and fracture surface morphology study, respectively.

5. FLAX FIBRE NMT COMPOSITES

In this chapter, the theory about the mechanical models for short fibre reinforced composites is included. Also, the experimental results over the effects of fibre-matrix parameters on the macro-mechanical properties of randomly oriented short fibre (compression-moulded) flax/PP composites are included and discussed.

5.1 Introduction

In continuation from Chapter 3 and 4, where study of the interface between flax and PP has been reported and discussed, Chapter 5 deals with the development of natural-fibre-mat-reinforced thermoplastics (NMTs) being GMT-like materials based on natural fibres (manufactured through compression moulding). The macro-mechanical properties of the developed flax/PP composites are reported and discussed.

Similar to the work presented in Chapter 3 and 4, (PP) polypropylene was used as the matrix material and (MA-PP) maleic-anhydride grafted PP was used to enhance the adhesion between PP and flax fibres. As discussed in Chapter 1, for the present study, glass fibre reinforced composites are taken as reference materials. In order to be able to obtain properties similar to glass-fibre-reinforced composites it was expected that both flax content and the flax fibre length should be as high as possible. However, high fibre loading and high fibre lengths would also affect the rheology and limit the processability of such composites, and therefore, a balance between mechanical performance and processability should be found.

In this research the influence of fibre length and fibre volume fraction was investigated on random, flax-mat-reinforced PP composites. The composites were manufactured using a film-stacking method and a suspension impregnation or so-called ‘paper-making’ method, followed by compression moulding, respectively. The paper-making method allows for a systematic variation of the fibre length, since no fibre break-up occurs during processing. The use of conventional melt-processing methods for the production of short-fibre-reinforced compounds such as extruders would degrade the fibre length and are therefore not suitable for such a systematic study. In addition, the influence of maleic-anhydride grafted PP (MA-PP) on the mechanical performance of PP/flax composites was studied.

As discussed in Chapter 1, 2 and 3, flax fibre contains functional hydroxyl groups that are able to interact chemically with the MA-PP. From this improved interfacial bond strength between the flax fibre and the modified PP was expected. In order to get a better insight in the importance of all these different parameters the experimental results were compared with model predictions using relatively simplistic micro-mechanical models for random short-fibre-reinforced composites (Cox, 1952; Krenchel, 1964; Kelly and Tyson, 1965; Folkes, 1985; Kelly and Macmillan, 1986).

The results on the influence of fibre processing on the mechanical performance of flax-fibre-reinforced composites are also reported and discussed.

5.1.1 Micromechanical models for discontinuous fibre composites

5.1.1.1 Composite stiffness

For the modelling of the stiffness of a short-fibre-reinforced composite, Cox introduced a fibre length efficiency factor into the ‘rule-of-mixtures’ equation for the composite stiffness E_c (Cox, 1952). In this way the ‘ineffective’ loading of fibres over their stress transfer length can be taken into account. Since the fibre is only partly utilised in the case of a short fibre composite, these effects have to be

taken into account when modelling the mechanical performance of such composites. The expression used by Cox yields:

$$E_c = \eta_{LE} V_f E_f + (1 - V_f) E_m \quad (5.1)$$

In the case of stiffness related problems, Cox's 'shear lag' model is used for the calculation of the fibre length efficiency factor η_{LE} under the assumption of elastic fibres in an elastic matrix, leading to (Ericson and Berglund, 1992; Rosenthal, 1992; Ericson and Berglund, 1993; Pan, 1993; Thomason and Vlug, 1996; Thomason et al., 1996):

$$\eta_{LE} = \left[1 - \frac{\tanh(\beta L / 2)}{\beta L / 2} \right] \quad (5.2)$$

where

$$\beta = \frac{2}{D} \left[\frac{2G_m}{E_f \ln(R / r)} \right]^{1/2} \quad (5.3)$$

The R/r factor can be related to the fibre volume fraction V_f by:

$$\ln(R / r) = \ln(\sqrt{\pi / \chi_i V_f}) \quad (5.4)$$

so that Equation 5.3 can be rewritten as

$$\beta = \frac{2}{D} \left[\frac{2G_m}{E_f \ln(\sqrt{\pi / \chi_i V_f})} \right]^{1/2} \quad (5.5)$$

where G_m is the shear modulus of the matrix, χ_i depends on the geometrical packing arrangement of the fibres, r is the fibre radius and R is related to the mean spacing of the fibres. In this study a square packed fibre arrangement is assumed, following Thomason et al., where similar equations were used for the modelling of glass/PP composites (Thomason and Vlug, 1996). The inter-fibre spacing in the composite is $2R$ and χ_i equals 4. Besides ineffective fibre length, fibres are also only partially utilised due to fibre (mis)orientation. In order to take this into

account, the theory of Cox was extended by Krenchel (1964), who took fibre orientation into account by adding a fibre orientation factor η_o into the 'rule-of-mixtures' equation.

$$E_c = \eta_o \eta_{LE} V_f E_f + (1 - V_f) E_m \quad (5.6)$$

The Krenchel orientation factor η_o allows for the introduction of a fibre orientation distribution. If transverse deformations are neglected, η_o is given by:

$$\eta_o = \sum_n a_n \cos^4 \phi_n \quad (5.7)$$

where a_n is the fraction of fibres with orientation angle ϕ_n with respect to the loading axis. For a two-dimensional (in-plane) random orientation of the fibres it can be shown that $\eta_o = 3/8$. In a three-dimensional random fibre orientation the fibre orientation factor yields the value of 1/5. For thin section laminates with fibre lengths greater than the thickness of the sample, fibres are expected to be oriented mainly in two directions, although deviations may occur due to out-of-plane oriented fibres or bend fibres. Especially in the case of fairly flexible fibres like flax this bending action is likely to occur.

5.1.1.2 Composite strength

For the modelling of the strength of discontinuous fibre composites, Kelly and Tyson (1965) extended the 'rule-of-mixtures' equation for composite strength in a way similar to Cox's 'rule-of-mixtures' for composite stiffness:

$$\sigma_{uc} = \eta_o \eta_{LS} V_f \sigma_f + (1 - V_f) \sigma_m \quad (5.8)$$

where η_{LS} is the fibre length efficiency factor and η_o is the fibre orientation factor, similar to the Cox-Krenchel model, to take off-axis fibre orientation into account. For the fibre length efficiency factor Kelly and Tyson (1965) used:

$$\eta_{LS} = \frac{1}{V_f} \left(\sum_i \left[\frac{L_i V_i}{2L_c} \right] + \sum_j \left[V_j \left(1 - \frac{L_c}{2L_j} \right) \right] \right) \quad (5.9)$$

The first summation term in Equation 5.9 accounts for the contribution of all fibres of sub-critical lengths ($L < L_c$). The second summation term incorporates the strength contribution from fibres whose lengths are super-critical ($L > L_c$). A combination of Equation 5.8 and 5.9 results in the Kelly-Tyson model for the prediction of the strength (σ_{uc}) of a polymer composite reinforced with short off-axis fibres (Kelly and Tyson, 1965; Kelly and Macmillan, 1986):

$$\sigma_{uc} = \eta_o \left(\sum_i \left[\frac{\tau L_i V_i}{D} \right] + \sum_j \left[\sigma_j V_j \left(1 - \frac{L_c}{2L_j} \right) \right] \right) + (1 - V_f) \sigma_m \quad (5.10)$$

In the case of stiffness, the related Cox-Krenchel model, including a theoretical orientation parameter for in-plane random fibre orientations ($\eta_o = 3/8$), can be used quite effectively for the prediction of the stiffness of random fibre composites (Thomason et al., 1996). However, previous studies have shown that the Kelly-Tyson model yields far too high values for strength of random fibre composites. Shao-Yun et al. have modified the model further by considering the distribution function for the fibre length and the fibre orientation in the fibre efficiency factor for the strength of the composites ($\eta_o^* \eta_{LS}$) (Fu Shao-Yun and Lauke Bernd, 1996). Therefore an additional (in)efficiency factor (k), which basically becomes a fitting parameter, can be included in Equation 5.10 to account for the fibre length, strength and orientation distribution in the random short-fibre composites:

$$\sigma_{uc} = k \eta_o \left(\sum_i \left[\frac{\tau L_i V_i}{D} \right] + \sum_j \left[\sigma_j V_j \left(1 - \frac{L_c}{2L_j} \right) \right] \right) + (1 - V_f) \sigma_m \quad (5.11)$$

Thomason et al. used a value of 0.2 for η_o in the Kelly-Tyson model for predicting the tensile strength of GMT materials, which was obtained by fitting this η_o factor to the experimental data (Thomason et al., 1996). In this case the orientation parameter η_o has however no longer any physical meaning and becomes a fitting

parameter. If we, however, translate their fitting parameter $\eta_o = 0.2$ into a case using the more realistic orientation parameter of $\eta_o = 3/8$, in combination with an additional (fitted) efficiency factor k this yields an efficiency factor for glass/polypropylene composites of $k=0.53$. Although these simplistic micromechanical models are to a certain extent based on fitting, they do provide insight into the mechanical behaviour of the composite. For example, comparing the k -values of composites manufactured by different processing methods and/or containing different types of reinforcements gives some insight into the efficiency of those processing methods and reinforcements.

5.1.1.3 Impact strength

Various energy dissipation mechanisms may operate when a discontinuous fibre-reinforced composite fractures from an existing notch, viz. matrix fracture and deformation, fibre-matrix debonding, fibre pull-out and fibre fracture (Thomason and Vlug, 1997; Wells and Beaumont, 1985; Wells and Beaumont, 1985b; Wells and Beaumont, 1988). Based on these mechanisms various models have been proposed to predict the impact strength of a composite. According to Wells and Beaumont a composite containing randomly dispersed and aligned short fibres of uniform strength will always exhibit fibre pull-out preceding fast fracture (Wells and Beaumont, 1988). Thomason et al. showed that for randomly oriented short-glass-fibre/PP composites fibre fracture is a dominant energy dissipation mechanism (Thomason and Vlug, 1997). The problem of identifying the dominant mechanism of fracture can be tackled in two complimentary ways: either the dominance of more easily recognisable mechanisms like fibre pull-out are determined by optical or electron microscopy, or a correlation is made between these mechanism and theoretical models (Wells and Beaumont, 1988). Cottrell (1964) developed a model for unidirectional reinforcement, which includes all the above mentioned energy-dissipation mechanisms i.e. matrix fracture, fibre fracture, debonding and pull-out. As for the model predictions, it follows that the impact energy is expected to increase with increasing fibre length, up to fibre lengths equal to the critical fibre length. At fibre lengths above the critical length the impact energy is expected to decrease again (Cottrell, 1964). This occurrence of a

maximum in impact strength can be attributed to the predicted change in failure mode from fibre pull-out at short (subcritical) fibre lengths to fibre breakage at high (supercritical) fibre lengths. According to the model, the toughness of the composite can be equated to the fracture energy of the matrix, or some fraction of it, in the absence of pull-out or any other toughening mechanism (Wells and Beaumont, 1988). This means the work of fibre pull-out tends to zero as the length, ' l ', of a fibre with uniform strength increases to infinity. Therefore this theory seems only applicable for systems where pull-out is the major fracture mechanism. Cooper has shown, that the Cottrell model holds good for an epoxy / phosphor-bronze model system with uniform, discontinuous and unidirectional reinforcements with the controlled amount and size of the flaws (Cooper, 1970). However, in thermoplastic composites generally no maximum in toughness is observed but a plateau value is reached with increasing fibre length (Thomason and Vlug, 1997; Wells and Beaumont, 1985; Wells and Beaumont, 1988; Bijsterbosch, 1992; Gupta et al., 1989). Wells and Beaumont have shown that in the case of the brittle reinforcements with the distribution of flaws and their size along the fibre length, the average pull-out length increases to a constant value with increasing fibre lengths (Wells and Beaumont, 1988). Also in the case of fibres with uniform strength they have shown a peak in the average pull-out length. Thomason et al. found a direct relationship between tensile strength and Charpy impact strength of random in-plane glass fibre-reinforced PP laminates (Thomason and Vlug, 1997). Based on their observations they developed a fibre strain energy model, similar to the rule-of-mixture equation for strength and modulus of the composites:

$$U_c = U_x V_f + (1 - V_f) U_m \quad (5.12)$$

where U_x is the energy factor covering all the fibre-related energy absorption mechanisms. Through experimental data and assuming the fibre fracture as a dominant energy absorption mechanism they found that:

$$U_x = U_f [L / (L + L_c)] \quad (5.13)$$

where U_f is the total energy involved in the fracture of the single fibres and is given by:

$$U_f = \sigma_f^2 y / 2 E_f \quad (5.14)$$

where 'y' is the length of the fibre debonding prior to fibre fracture in a composite containing continuous fibres. Therefore Equation 5.12 can be modified, by substituting Equation 5.13 and 5.14 as:

$$U_c = V_f (\sigma_f^2 y / 2 E_f) [L / (L + L_c)] + (1 - V_f) U_m \quad (5.15)$$

However, the equation above was developed for unidirectional continuous-fibre-reinforced composites and the effect of fibre orientation is not taken into account. Again, also here the model was fitted on the experimental data, in this case using debond length y as a fitting parameter. For the PP/glass composites studied, a value of 12 mm for debond length was found to give good agreement between the above mentioned fibre strain energy model and experimental data. However, because of this fitting procedure the debond length lost its physical meaning. In fact for some composites the fitted debond length y was higher than the actual fibre length, meaning that also here we have to interpret the results only in a fairly qualitative manner.

5.2 *Experimental*

5.2.1 *Materials*

In this study random non-woven flax fibre mats in combination with an isotactic-polypropylene (i-PP) matrix of Shell (XY6500T) with a melt flow index of 35 were used. The Young's modulus of the neat PP matrix was approximately 1.6 GPa and the yield stress about 32 MPa. Dew-retted flax fibres were used to manufacture the composites. The fibres were converted into a non-woven mat (725 g/m²) by Eco Fibre Products BV (The Netherlands) via a conventional punch-needling process. In order to study the effect of improved fibre matrix adhesion on composite performance, 5 wt.% of a maleic-anhydride-grafted polypropylene (MA-PP) (Polybond® 3002, BP Chemicals Ltd.) was added to the PP homopolymer. This blend composition with a PP/Polybond® 3002 ratio of 95/5

will simply be designated as MA-PP. Compounding of this blend was carried out in a co-rotating twin-screw extruder (Werner and Pfleiderer ZSK 25), with standard screw geometry, at 200 °C. Extruded strands were palletised to be used for film blowing subsequently. NMT composite plates with different fibre contents were manufactured using the film-stacking method. In this film-stacking method, pre-dried (24 hrs. at 80°C) non-woven flax mats in combination with PP or MA-PP films were stacked alternately. PP films as well as the MA-PP films based on the PP/Polybond® blend were made using film-blowing equipment (Collin 30-25D/400). Impregnation of the non-woven mats was achieved by applying heat (200 °C) and pressure (25 bar) in a hot-press for 15 min. The obtained composite plates were cut into dog-bone shaped tensile specimens according to ASTM D638-91 specifications.

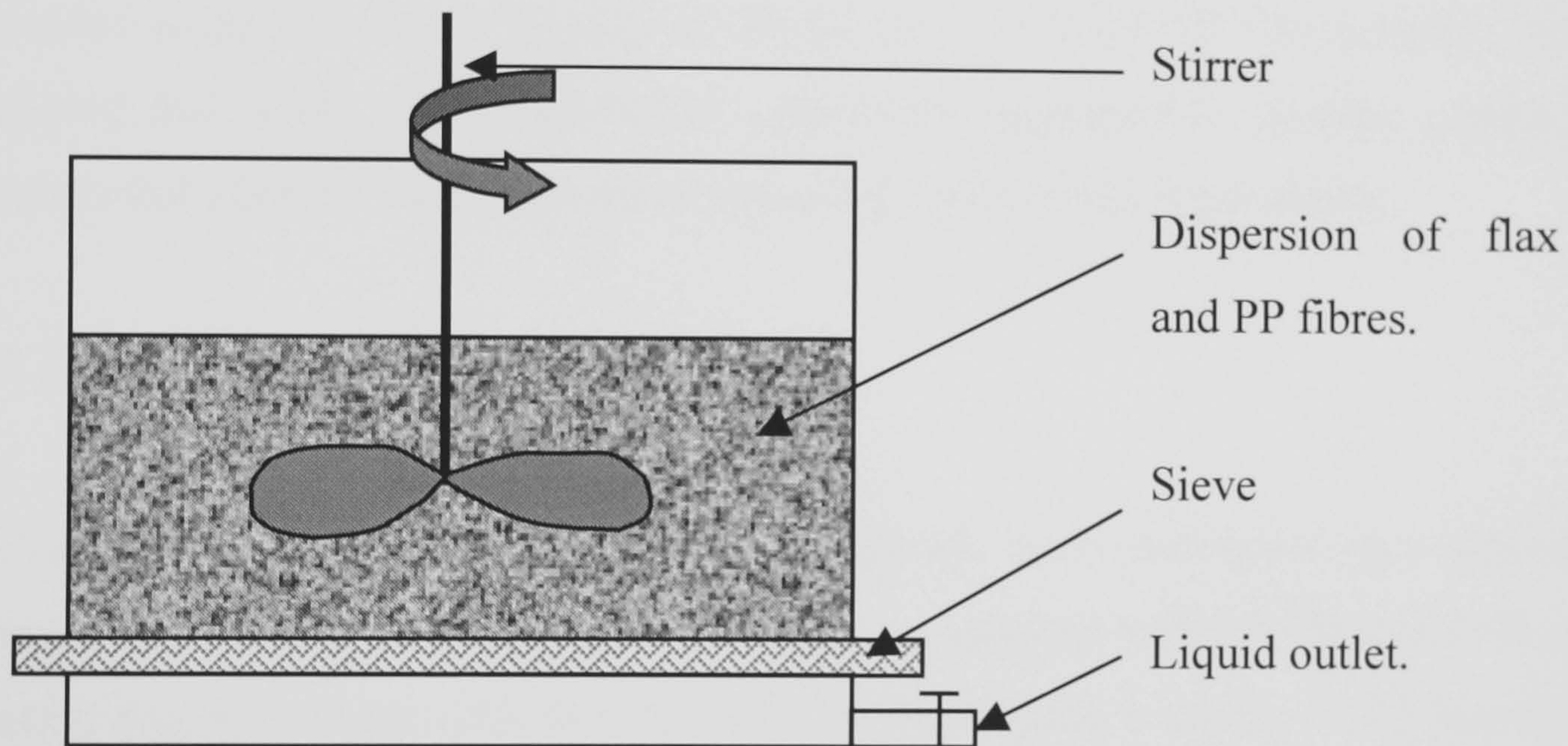


Figure 5.1 Schematic representation of paper-making method used to study the effect of fibre length on the composite properties.

As shown in Figure 5.1, in the suspension impregnation or paper-making process a dispersion of flax fibres and i-PP fibres (Young's modulus = 1.6 GPa and yield stress = 29 MPa) was made in an ethanol/water (1:1) mixture. In separate production runs, three different flax fibre lengths were used (3, 6 and 25 mm). After mixing the fibres, the liquid (ethanol/water mixture) was removed through the outlet while obtaining the mixture of fibres on the sieve. After drying the materials at room temperature for 24 hours and at 60°C for one hour, the lofted mixture of flax fibres and PP fibres was consolidated in a hot-press. In the case of the paper-making process interface modification through the use of MA-PP was

done in a different way than in the case of film-stacked composites. In the case of the suspension impregnation route the fibres were pre-treated (coated) with pure MA-PP (Hostaprime® HC5, Hoechst). Degreasing of the flax fibres was executed via extraction of the flax fibres with an ethanol/toluene (2:1) mixture, refluxed for three hours. The extraction fluid was replaced by a new fresh fluid, which was refluxed for another hour. The fibres were subsequently washed for approximately 30 minutes with cold ethanol, followed by 6 litres of cold water over a Büchner-funnel. The extracted fibres were dried at 60°C in an oven with circulating air for 24 hours. Afterwards they were immersed in a solution of MA-PP copolymer in hot toluene (100°C) for 10 minutes. The concentration of copolymer in solution was approximately 2 wt.% on the fibres. After treatment, the fibres were extracted with toluene for one hour and a half to remove all components not chemically bonded to the flax fibres. Finally, the fibres were dried at 60°C for 24 hours. These treated flax fibres were used in the suspension impregnation process, yielding a composite plate by the compression moulding method described above.

5.2.2 Test methods

Uniaxial tensile tests on random flax composites were performed on a universal tensile testing machine. Specimens were in accordance with ASTM D638-91 and had a dog-bone shape with an overall length of 200 mm, a width of 12.5 mm and a thickness of 2 mm. An extensometer was used to monitor the elongation of the tested specimen. At least 10 specimens were tested for each condition.

High-speed dart and notched Charpy impact testing were performed on a Zwick Rel servo-hydraulic testing machine. Charpy impact tests were carried out on notched samples with a width of 12.7 mm and a thickness of 4 mm. The samples were loaded over a span of 44 mm at a speed of 3.5 m/s using the servo-hydraulic testing machine equipped with a Charpy impact test fixture. The impact energy was calculated by dividing the total absorbed energy by the cross-sectional area of the sample behind the notch. It may be worth mentioning here that the impact energy measured is only for relative comparison and does not give the accurate toughness of the material. For accurate measurement of toughness, various

correction factors like geometrical and kinetic energy correction factors are to be considered (Plati and Williams, 1975). Next to Charpy impact tests, high-speed dart impact tests were performed for the determination of the penetration resistance of the composite plates. Full-penetrating dart impacts were conducted utilising the servo-hydraulic testing instrument equipped with a dart impact test fixture. Impacts were performed using a hemispherical dart of 10 mm at a test speed of 4 m/s. The laminates, having dimensions of 70 mm x 70 mm x 4 mm, were clamped between two plates with a cylindrical opening in the centre with a diameter of 20 mm. Load values during penetration were recorded using a piezo electrical transducer and impact energies were calculated from the recorded load-time curves. At least 10 specimens were tested for each condition (fibre length and fibre volume fraction) in a controlled testing condition of 60% RH and temperature of about 20°C.

5.3 Results and Discussion

5.3.1 Influence of fibre length

5.3.1.1 Composite stiffness:

The results of the tensile tests on the flax-fibre-reinforced PP composites, with varying fibre lengths as manufactured using the paper-making process, are given in Figure 5.2 and 5.3. Figure 5.2 shows the Young's modulus for the systems based on PP and MA-PP together with the Cox-Krenchel model predictions. In the model a modulus of 45 GPa for the flax fibre and a modulus of 1.6 GPa for the PP matrix is used, both values were obtained from tensile tests on the single fibres and the bulk matrix. The matrix shear modulus (G_m) of 615 MPa is used which was calculated by using relation $G=E/2(1+\nu)$ where E is the tensile modulus and ν is the Poisson's ratio. Poisson's ratio of 0.3 is used for the calculations. The volume fraction of flax fibre was 0.2 for all the fibre lengths. The fibre orientation efficiency factor (η_o) of 3/8 and an average fibre diameter of 50 μm is used for the model. A rather good agreement is found between the model predictions and experimental data. No effect of improved adhesion on the modulus of PP/flax composites is observed indicating good wetting of the fibres. Only the data for a

fibre length of 3 mm shows a somewhat increased composite stiffness with the use of MA-PP. Presumably, the higher interfacial bond strength in case of MA-PP flax leads to a slight decrease of the critical fibre length and consequently a small improvement in composite stiffness might occur for this type of composite. At fibre lengths of 6 and 25 mm this improvement is not observed since in both cases the fibre length is well above the critical fibre length, which is around 2.5 mm for the PP/flax system used. No fibre length dependence is observed for the developed MA-PP/flax, as the fibre lengths are higher than critical lengths thus showing a plateau zone in the curve.

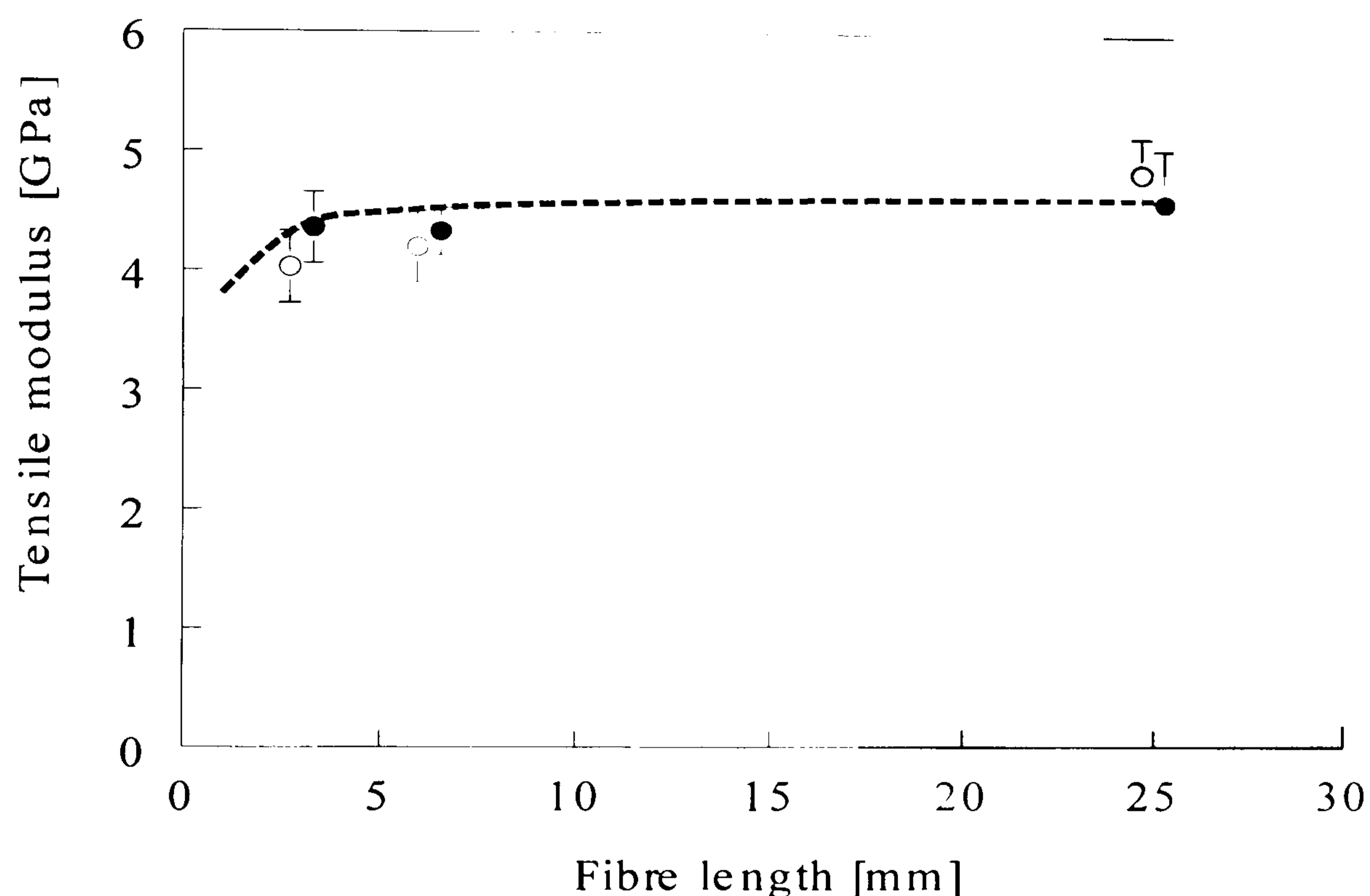


Figure 5.2 Tensile modulus of the flax /PP composites (○) and the flax/MAPP composites (●) as a function of the flax fibre length. The dashed line represents the Cox-Krenchel prediction for both the PP/flax and MA-PP/flax composite systems (Error bars show standard deviation).

5.3.1.2 Composite strength:

For the model predictions using the Kelly-Tyson equation a fibre strength of 710 MPa, as obtained from the single fibre tensile test, is used together with an interfacial bond strength (τ) of 7 MPa for PP/flax (Chapter 3) and 16 MPa for MA-PP flax. The interfacial shear strength value of 16 MPa for the MA-PP/flax system is taken similar to the shear yield stress of the pure PP matrix as calculated from

the Von Mises yield criterion ($29/\sqrt{3}$ MPa). This means that for this composite system perfect adhesion, i.e. a matrix dominated rather than an interface dominated shear failure mode is assumed. Hence, this will give some insight into the importance of interface modifications for maximising composite strength. As matrix strength a value of 29 MPa is used. The critical fibre length of 2.5 mm for PP/flax and 1.1 mm for MAPP/flax is used, which was calculated by using the relation $L_c = \sigma_f * D / 2\tau$ where σ_f is the fibre strength, D is average fibre diameter and τ is the interfacial shear strength. The volume fraction of flax fibre in the composites was about 0.2 for all the fibre lengths.

In Figure 5.3 both the results of the tensile strength measurements as well as the model predictions for PP/flax and MA-PP/flax as a function of the fibre length are plotted using the fibre orientation factor η_o of 3/8 and a fitted efficiency parameter k of 0.24. It is worth mentioning here that the efficiency parameter k is not a constant parameter for a system but depends on the parameters like uniformity, fibre length, fibre diameter (which is related to fibre length in the case of natural fibres), presence of woody particles etc. A fibre diameter of 50 μm is used for the model, which may also be different for different fibres. Comparing now this efficiency parameter ($k = 0.24$) with that for a PP/glass system ($k = 0.53$) as recalculated from the data reported by Thomason et al. (1996), it becomes clear that the reinforcing efficiency of flax fibre is less than those of glass fibres. One reason for this could be the fairly large scatter in the strength values of natural fibres, which are not taken into account in the current model. In the case of a fairly brittle failure mode weak fibres may trigger catastrophic fracture of the composite material, leading to an overall low value for strength. Another, probably more important and most likely related effect is the poor lateral strength of the natural fibres as they are used today. Unlike isotropic glass fibres, natural fibres exhibit like most biological materials a hierarchical composite-like structure. They consist of cellulose microfibrils with diameters in the order of a couple of nanometers, which form together so-called elementary fibres (fibre cells) of 10-20 μm in diameter. The fibre cells are bond together by pectin, forming the next hierarchical microstructure; a fibre cell bundle with a diameter of around 50-100 μm . These fibre cell bundles are subsequently arranged in the form of bundles in the stem of

the plant and are bond together by a weak pectin and lignin matrix. Depending on the effectiveness of the fibre opening process one can go down in microstructure, hence removing weak spots in the composite-like structure and obtaining reinforcing elements of higher strength. Unfortunately, however, despite attempts like steam explosion where one tries to separate the elementary fibres from the technical fibres, most of today's fibres used in composite application are fibre bundles and/or technical fibres. They are produced using mechanical fibre opening processes like breaking of the flax stem and scutching and have a fairly poor strength (600-800 MPa) compared to glass fibres. Elementary fibres, however, have much higher strengths (1200-1500 MPa) and could on a weight basis compete with glass fibres (2400 MPa) (Bos et al., 1998). Even higher strengths are foreseen when microfibrils could be used as reinforcing elements in nanocomposites. Clearly, future developments in this area should therefore focus on further optimisation of the fibre opening process.

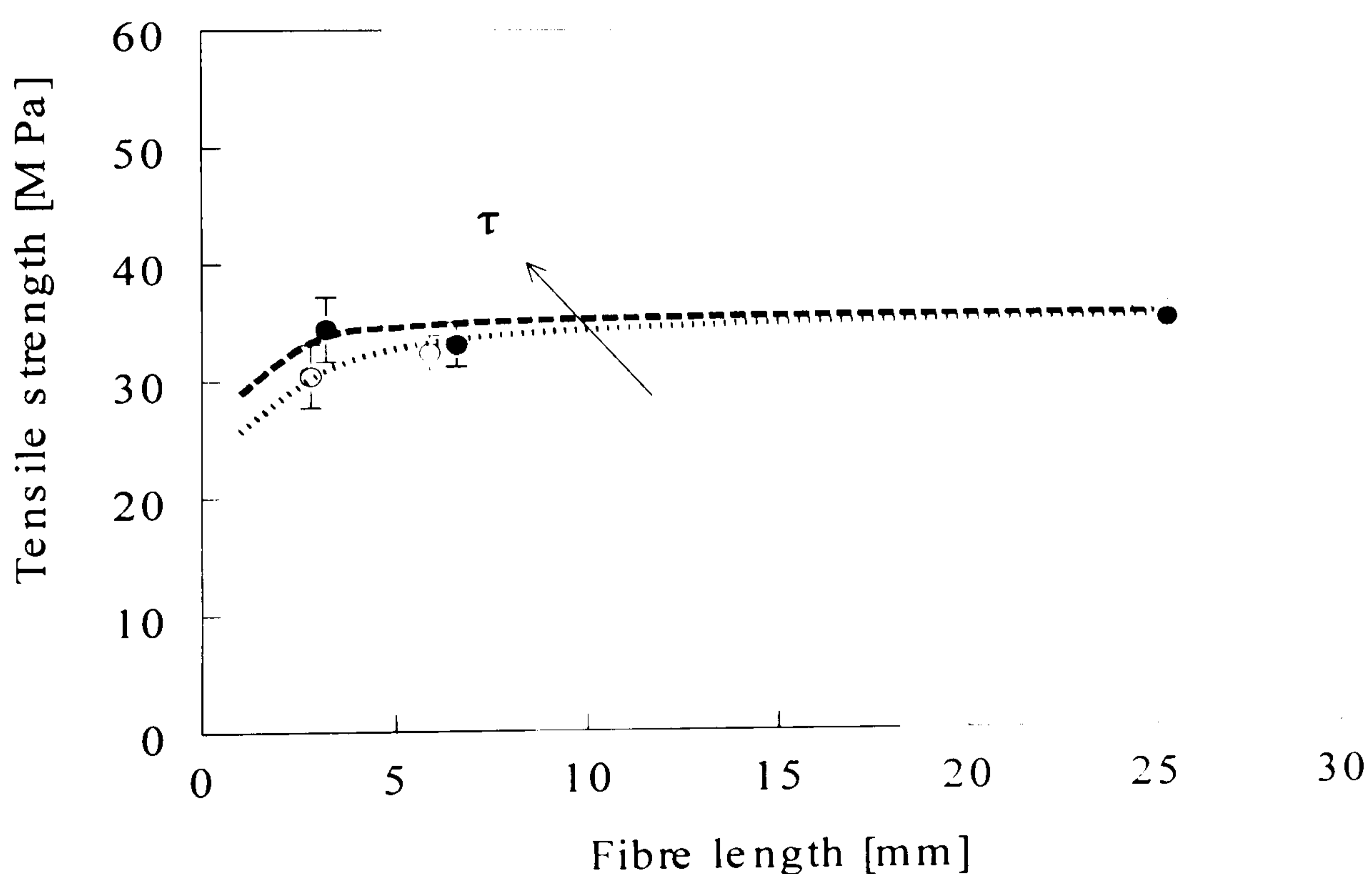


Figure 5.3 Tensile strength of the PP/flax composites (○) and the MA-PP/flax composites (●) as a function of the flax fibre length. The dotted line and the dashed line represent the Kelly-Tyson prediction for the PP/flax and the MA-PP/flax composites, respectively (Error bars show standard deviation).

With respect to the effect of enhanced interfacial bonding as a route to improvement in composite strength it becomes clear from the model predictions that, at least compared to routes that focus on the optimisation of fibre strength, no

major effects can be envisaged. Only in the case of relatively short fibres interface modification may have a significant effect on composite strength. Still, interface optimisation is a topic of concern and will definitely affect the durability of the composite in a positive way (Van den Oever and Peijs, 1998). However, for strength optimisation its effect will be too small to bridge the gap with glass fibre systems. Regarding the effect of fibre length, similar to the stiffness there appears to be no significant influence on the measured composite strength. Due to the easier way of mixing and consequently better impregnation, the composite with 3 mm long fibres may have a higher quality than the 6 and 25 mm ones. Moreover, during the chopping of the fibres into the desired length the weak internal interactions between the fibre cells result in extensive fibrillation or splitting of these short fibres and a decrease of the flax fibre diameter and consequently, an increase in fibre aspect ratio. As a result, the stress transfer becomes more effective which may yield a composite with relatively better properties.

5.3.1.3 Impact strength:

The results from the notched Charpy impact tests are plotted in Figure 5.4 as a function of fibre length. It can be seen that in the case of PP/flax the impact energy increases with increasing fibre length until a plateau level is reached, whereas in the case of MA-PP/flax the impact energy increases and then drops of at the highest fibre length. At relatively low fibre lengths the impact strength for MA-PP composites is higher than that of PP composites, whereas at fibre lengths of 25 mm the impact energy decreases in the case of MA-PP and is lower than that of PP /flax. This behaviour can be explained by the decrease in critical fibre length with the addition of MA-PP, thus leading to additional energy contributions by fibre fracture for the shorter fibre system. Whereas at higher fibre lengths ($L \gg L_c$) the improved adhesion leads to a decrease in energy dissipation because of limited fibre debonding and pull-out mechanisms. This was also observed through scanning electron microscopy (SEM) as shown in Figure 5.5 and 5.6, where the PP/flax composites show longer fibre pull-out lengths as compared to the MA-PP/flax composites with fibre lengths of 25 mm. In case of PP flax composites the trend in impact strength versus fibre length is similar to the experimental trend

observed by various workers in the area of thermoplastic based composites (Thomason and Vlug, 1997; Wells and Beaumont, 1985; Wells and Beaumont, 1988; Bijsterbosch, 1992; Gupta et al., 1989) and is in agreement with the strain energy model predictions (Equation 5.15) for PP/glass systems. The model, using 'debond length' (y) as a fitting parameter, is plotted with the experimental data in Figure 5.3. In the case of PP/flax system we found a fitted 'debond length' of 8 mm, which is lower than the value reported by Thomason et. al. ($y = 12$) for a PP/glass system (Thomason and Vlug, 1997). As mentioned earlier the effect of fibre orientation is not taken into account in the strain energy model and the 'debond length' may not be considered as a real measure for actual debonding. However, from this analysis it can be concluded that to improve the impact strength of PP/flax composites the fibre strength is to be further improved to obtain debonding and pull-out at higher fibre lengths and higher fibre strain energies at shorter fibre lengths. For the model predictions (Equation 5.15) the fibre strength (σ_f) of 710 MPa, fibre modulus (E_f) of 45 GPa, fibre volume fraction (V_f) of 0.2, matrix fracture energy (U_m) of 6.34 kJ/m² which was calculated by Charpy impact testing, critical fibre length (L_c) of 2.5 mm and debond length parameter (y) of 8 mm is used. The critical fibre length was calculated by using the relation $L_c = \sigma_f D / 2 \tau$. Where, σ_f is the average fibre strength, D is the average fibre diameter and τ is the average interfacial shear strength. An average fibre diameter of 50 μ m and an interfacial bond strength (τ) of 7 MPa for PP/flax were used to calculate critical fibre length. The trend in impact strength as observed for the MA-PP based system seems to be in agreement with the Cottrell model, which also shows an optimum in the impact energy versus fibre length curve. In the Cottrell model this optimum is calculated, for aligned short fibre composite systems with fibres of uniform strength, at a fibre length equal to the critical fibre length, being 2.5 mm for PP/flax and 1.1 mm for MAPP/flax composite systems used. Clearly, in a system based on randomly oriented flax fibres with a high variation in strength, length and diameter such model can only be used in a qualitative manner. Still, the trend observed indicates that for the modified PP/flax composite energy absorption is to some extent governed by pull-out and debonding. Although the optimum in impact energy as a function of fibre length can be explained on the bases of fibre pull-out mechanisms as the principal mechanism of energy absorption, this trend is

rarely observed in real composites. As mentioned earlier, most thermoplastic composites show a maximum plateau value for impact energy rather than a drop at high fibre length. Although the drop observed here is only minor it is still an indication for the importance of fibre pull-out as an energy absorption mechanism in this composite system.

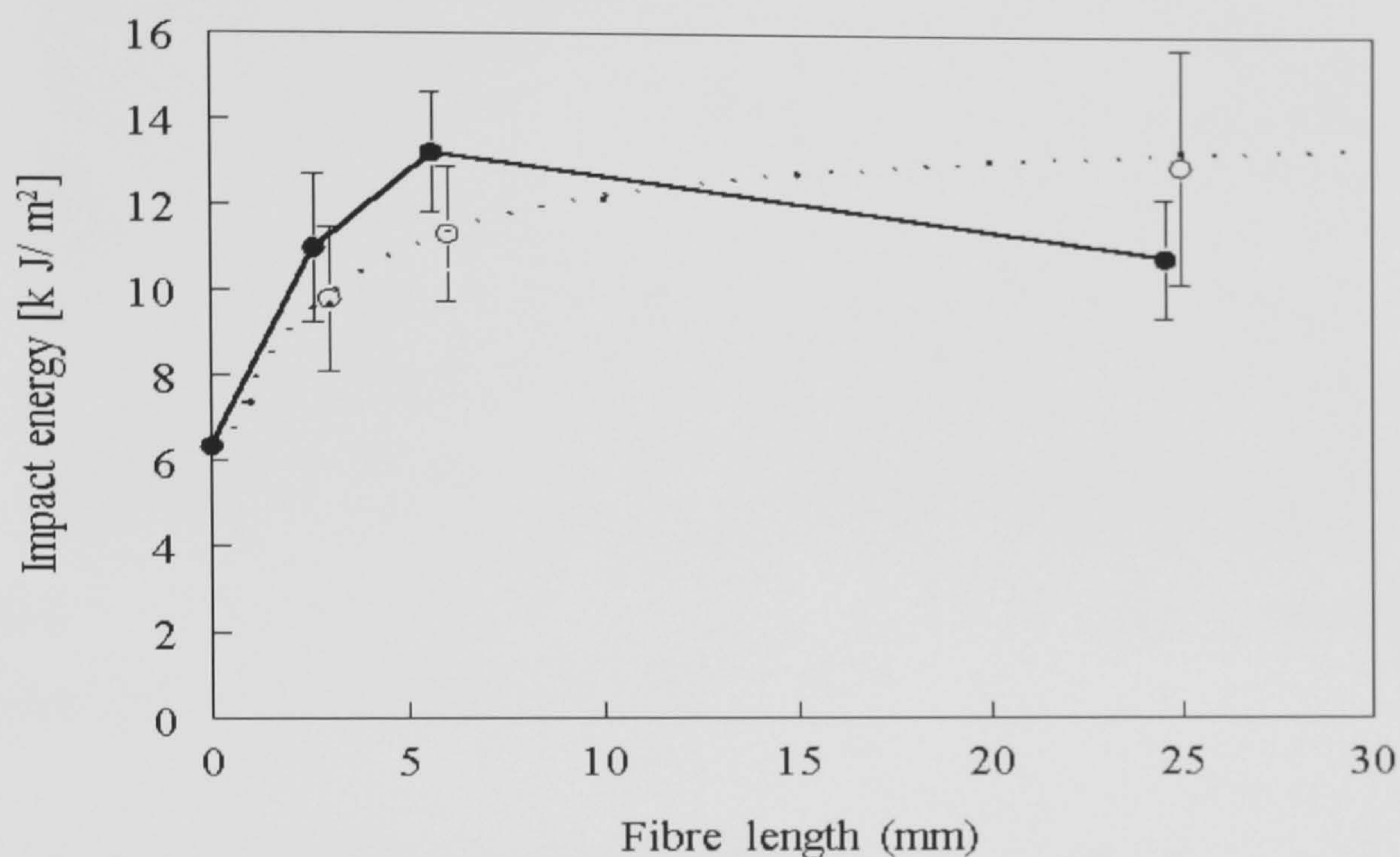


Figure 5.4 Notched Charpy impact strength of the PP/flax composites (○) and the MA-PP/flax (●) as a function of the flax fibre length. The dotted line represents the fibre strain energy model predictions for PP/flax (Error bars show standard deviations).



Figure 5.5 Scanning electron micrograph of fracture surface of PP/flax composite ($V_f=0.2$ and fibre length=25 mm).



Figure 5.6 Scanning electron micrograph of fracture surface of flax/MA-PP composite ($V_f=0.2$ and fibre length = 25 mm).

5.3.2 Influence of fibre volume fraction

5.3.2.1 Composite stiffness:

The influence of fibre volume fraction was investigated on composites based on non-woven fibre mats, which were manufactured using the film-stacking technique. Figure 5.7 shows the tensile modulus of the (MA-)PP/flax composites together with the Cox-Krenchel prediction and data of commercially available glass-mat-reinforced thermoplastic (GMT) materials, as a function of fibre volume fraction (Berglund and Ericson, 1995). Based on the data obtained, it can be concluded that the stiffness of flax-fibre-reinforced PP is comparable to E-glass-fibre-reinforced PP composites. Especially, when the relatively low density of the flax fibre (1.4 g/cm^3 for flax compared to 2.5 g/cm^3 for E-glass) is taken into account, the stiffness per unit weight can even surpass that of GMT materials. Moreover, as a result of the price competitiveness of flax fibres compared to E-glass fibres these materials are particularly of interest from a cost-performance point of view. A rather good agreement is found between the experimental data and the predictions using the Cox-Krenchel model (Equation 5.6). However,

because of large scatter in the properties of flax fibres a large scatter in the composite properties can be observed. Again, in the model a modulus of 45 GPa for the flax fibre and a modulus of 1.6 GPa for the PP matrix is used, together with an effective fibre length of 25 mm for the random flax mat material and the orientation factor η_o of 3/8. As mentioned before, the matrix shear modulus (G_m) of 615 MPa and an average fibre diameter of 50 μm is used.

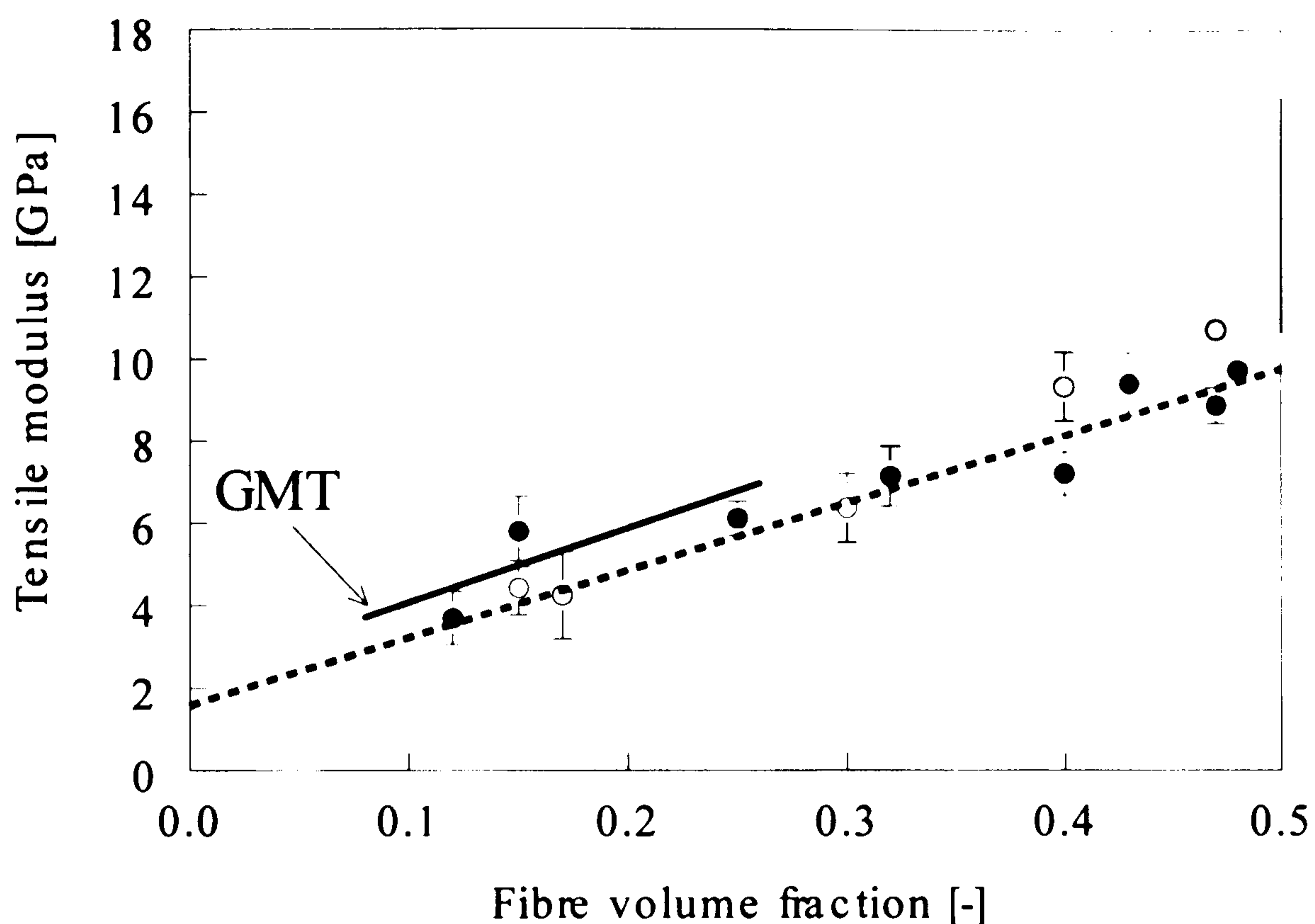


Figure 5.7 Tensile modulus of the PP/flax composites (○) and the MA-PP/flax composites (●) as a function of fibre volume fraction. The dashed line represents the Cox-Krenchel prediction for both PP/flax and MA-PP/flax. The solid line represents the data for commercially available GMT (Error bars show standard deviations).

5.3.2.2 Composite strength:

Figure 5.8 shows the tensile strength of the manufactured PP/flax and MA-PP/flax composites, together with the Kelly-Tyson predictions for PP/flax and MA-PP/flax as well as data of commercial glass fibre based GMT materials (Berglund and Ericson, 1995). In the model the same material parameters are used as in the Cox-Krenchel model for the prediction of composite stiffness as a function of the fibre volume fraction. Again, fibre strength (σ_f) of 710 MPa, effective fibre length (L_j)

of 25 mm and fibre diameter of 50 μm is used. The orientation factor η_o of $3/8$, interfacial shear strength of 7 MPa for PP/flax and 18 MPa for MAPP/flax system is used for the model calculations. The interfacial shear strength value of 18 MPa for the MA-PP/flax system is taken similar to the shear yield stress of the pure PP matrix as calculated from the Von Mises yield criterion ($32/\sqrt{3}$ MPa). This means that for this composite system perfect adhesion, i.e. a matrix dominated rather than an interface dominated shear failure mode is assumed. Hence, this will give some insight into the importance of interface modifications for maximising composite strength. The critical fibre length of 2.5 mm for PP/flax and 0.986 mm for MAPP/flax is used, which was calculated by using the relation $L_c = \sigma_f * D / 2\tau$ where σ_f is the fibre strength, D is average fibre diameter and τ is the interfacial shear strength. As matrix strength a value of 32 MPa is used. Based on the linear fitting of the experimental data the efficiency parameters of 0.15 and 0.24 were found for the PP/flax and MAPP/flax composites, respectively. The k value for PP/flax system ($k=0.15$) is lower than that found in paper-making method ($k=0.24$ as mentioned in the Section 5.3.1.2, 'Influence of fibre length on composite strength') which shows that paper-making method has improved the fibre efficiency. However, addition of MAPP seems to have increased the fibre efficiency (from 0.15 to 0.24), which could be because of improvement of fibre matrix adhesion. No such improvement was found in the case of paper-making method as both PP/flax and MAPP/flax systems exhibited an efficiency k of 0.24. This observation is also similar to the observations mentioned in Chapter 3 where addition of MAPP in the matrix was found effective when MAPP was added in matrix instead of fibre coating. Overall, these micromechanical calculations also clearly indicate that differences in interfacial shear strength of the order of 5-15 MPa, as can be expected for PP based composites have no significant influence on the predicted composite strength in the case of these long fibre composite systems (Figure 5.8). Clearly, GMT materials show superior strengths compared to the manufactured NMTs for all volume fractions. With respect to the effect of improved interfacial bonding in the case of MA-PP/flax composites, similar to the model predictions, no significant effects on tensile strength was found. Moreover, based on micromechanical calculations no major further improvements can be envisaged in the case of NMTs based on relatively long fibres, since already an 'upper adhesion

limit of matrix dominated shear failure is used for the calculation of the theoretical strength of MA-PP/flax. Obviously, the strength of the flax fibre composites is intrinsically limited by the relatively weak technical flax fibres. These results indicate that, for the development of a strength competitive NMT, future research should focus on the optimisation of fibre strength rather than interface strength. The key area for the improvement of the tensile strength of the PP/flax composites lies clearly not only in the interface modifications for improved adhesion but mainly in modifications in the fibre opening process leading to improved fibre strength.

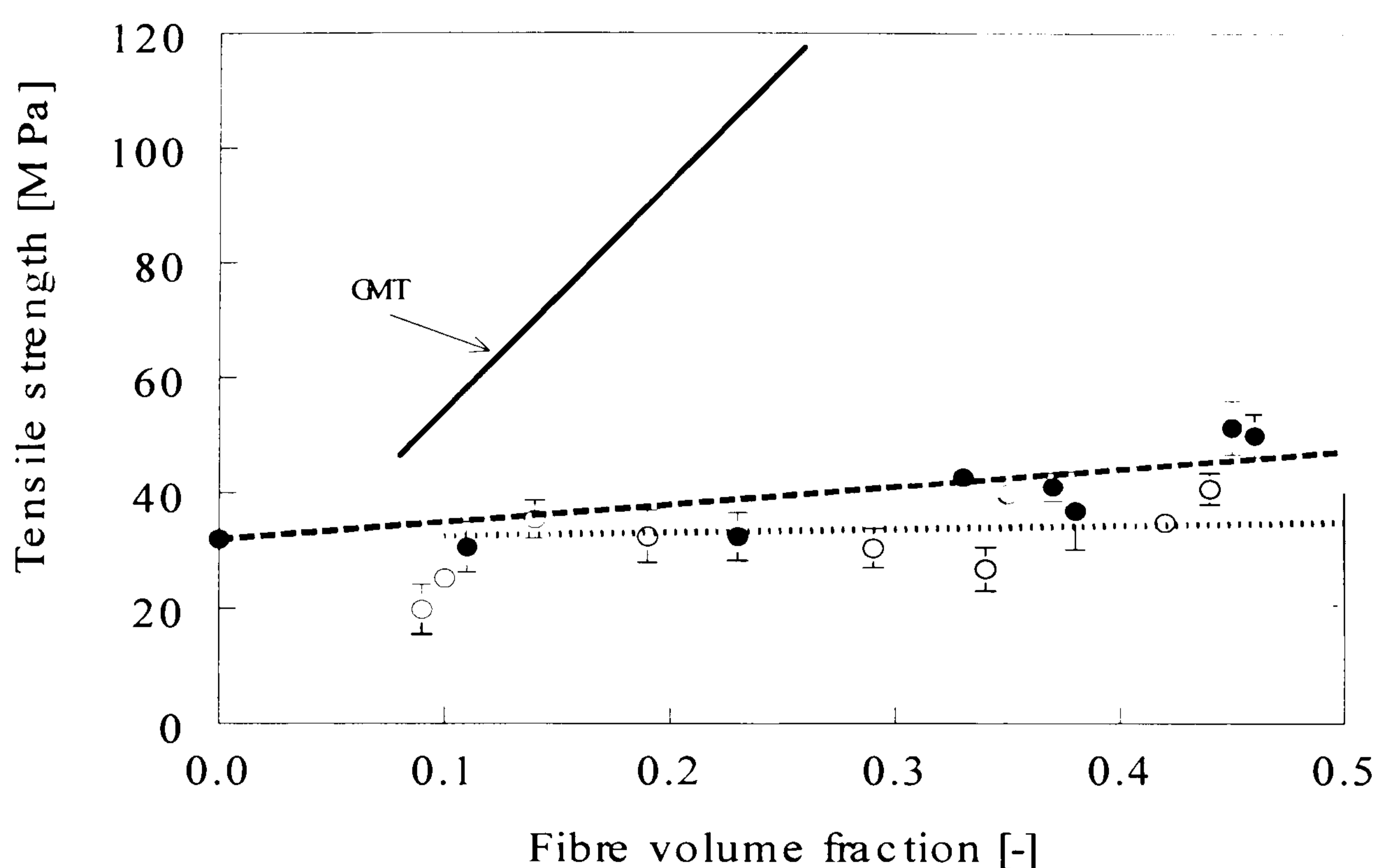


Figure 5.8 Tensile strength of the PP/flax composites (○) and the MA-PP/flax composites (●) as a function of fibre volume fraction. The dotted and dashed lines represent the Kelly-Tyson predictions for PP/flax and MA-PP/flax composites, respectively. The solid line represents the data for commercially available GMT (Error bars show standard deviations).

5.3.2.3 Impact strength:

Figure 5.9 shows the influence of fibre content on the notched Charpy impact energy of PP/flax composites. The absorbed impact energy increases with increasing flax fibre content up to 25% volume fraction beyond which no further improvement in impact energy was measured. At high fibre lengths the impact

energy absorbed by natural fibre composites can be mainly attributed to fibre fracture. The fairly good wet-out of the fibres in combination with the relatively low strength of flax fibres yields composites that fail in fairly brittle manner. Due to the relatively low fibre strength the contribution in energy dissipation by fibre debonding and pull-out mechanisms is expected to be relatively low. It is expected that this brittle failure mode, which increases with increasing fibre volume fraction, lead to the plateau zone at higher fibre volume fractions. For comparison again data for a commercial GMT is plotted. Clearly NMT is inferior to GMT when it comes down to impact strength. Compared to PP/glass, PP/flax composites absorb less energy by mechanisms like fibre pull-out as well as fibre strain energy. Since PP/flax composites exhibit comparable interfacial properties to PP/glass composites but much lower fibre strengths these composites are likely to fail in a rather brittle failure mode with fibre fracture at relatively low strain levels likely to be favoured over fibre pull-out. However, in the case of glass fibres the fibre strength over interface strength ratio is much higher, which means that in these composites more pull-out will take place in combination with fibre fracture at much higher strain (energy) levels. Figure 5.10 shows the results obtained from the high-speed dart impact testing of the same PP/flax composite system. Clearly the trend is quite similar to that of the Charpy impact testing. Further improvement of the impact performance of NMT is key for a successful large scale introduction in applications where currently GMT materials are used since many of today's applications where GMT has replaced sheet moulding compounds (SMCs) are driven by the excellent impact performance of GMT.

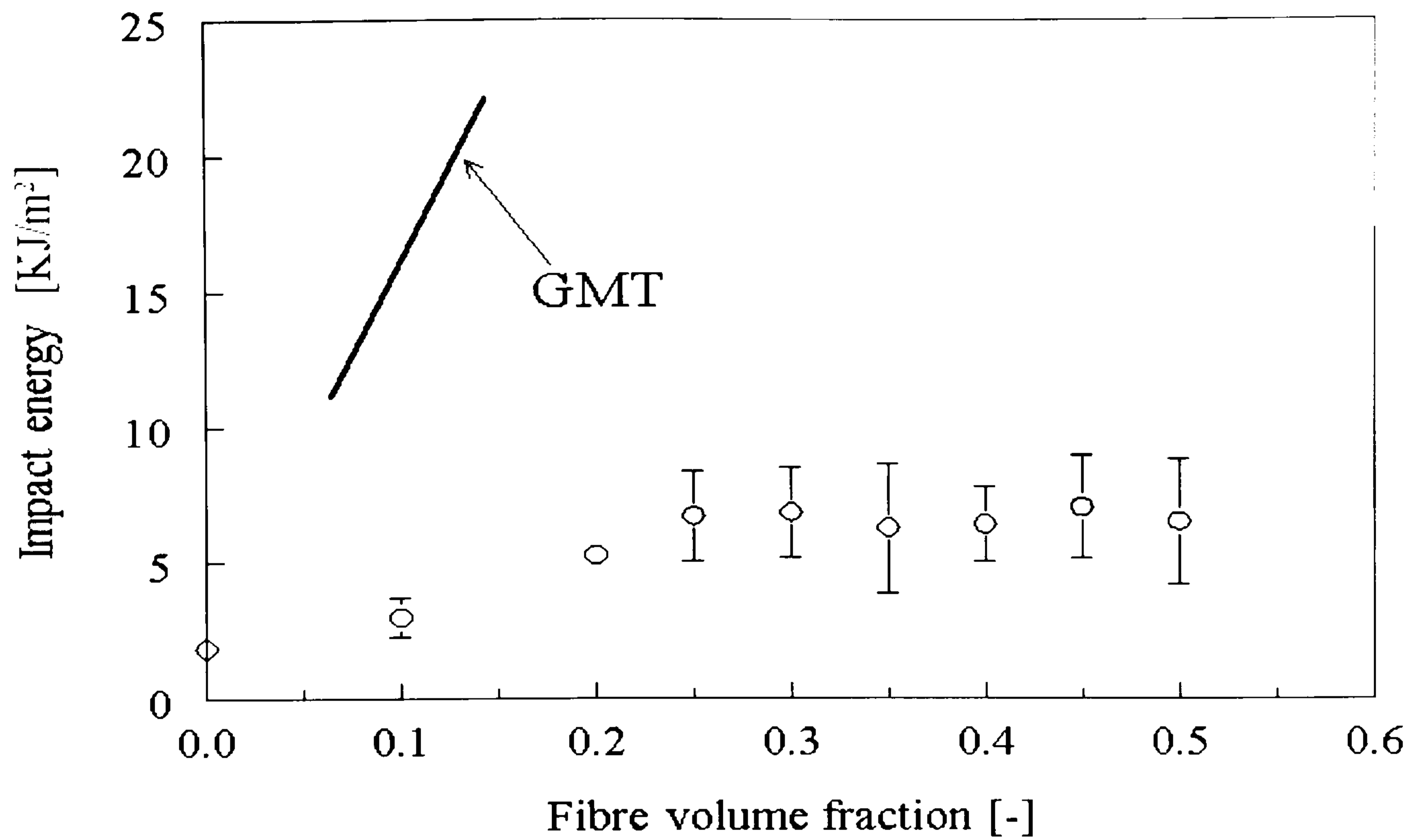


Figure 5.9 Notched Charpy impact strength of the PP/flax composites (O) as a function of fibre volume fraction. The solid line represents data for GMT (Error bars show standard deviations).

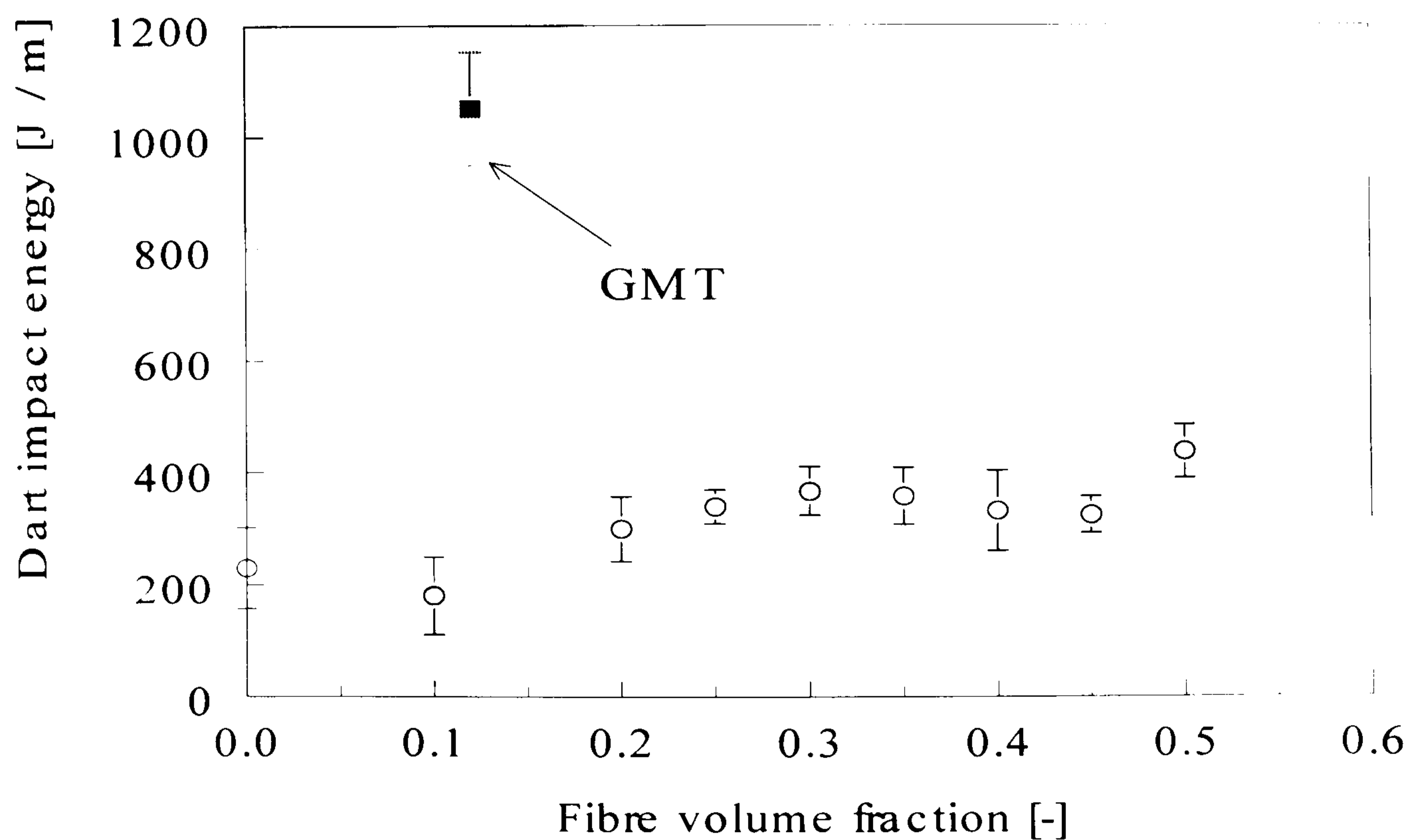


Figure 5.10 Dart impact energy of the PP/flax composites (O) as a function of fibre volume fraction, together with an experimentally obtained data for a commercial GMT-grade (Error bars show standard deviations).

5.3.3 Influence of fibre diameter on composite strength

As mentioned earlier, future developments towards improved strength and impact properties of NMT should focus on further optimisation of fibre processing. Depending on the effectiveness of the fibre opening process one can go further down in microstructure, hence obtaining reinforcing elements of higher strength. Most of today's fibres used for composite application are either fibre bundles and/or technical fibres. They are produced using mechanical fibre opening processes like breaking of the flax stem and scutching and have a fairly poor strength. A preliminary study was therefore carried out to see if an additional hackling operation, where the fibre tows are combed to remove impurities like woody parts and to obtain a larger quantity of thinner technical fibres rather than coarse fibre bundles, may lead to fibres of higher strength. Two types of flax fibres, both of equal length (6 mm), however, processed in different ways, were used: (i) scutched flax fibres and (ii) hackled flax fibres, where the fibre bundles are combed to separate the fibre bundles into individual technical fibres. Next to effects directly related to fibre processing, another reason for these additional experiments using hackled fibres is related to the influence of a decrease in fibre diameter on the improvement of fibre strength. As discussed earlier, a small improvement in tensile strength with interface modification was observed only for composites based on flax fibre lengths of 3 mm. For the composite systems based on 3 mm flax fibres the experimental data (Figure 5.3) is also in better agreement with the model predictions than in the case of high fibre lengths. It was argued that these relatively high strength values in the case of 3 mm fibres were due to a decrease in fibre diameter as a result of fibre splitting of the technical flax fibre when cut into 3 mm fibre lengths. In order to justify this reasoning, additional experiments using hackled fibres were performed to investigate the effect of different fibre diameters on the tensile strength values of the composites. The fibre diameter distribution of these fibres is plotted in Figure 5.11. Next to these 6 mm fibres also the fibre diameter distribution of a 25 mm scutched fibre was measured to show the effect of fibre length on the average fibre diameter. Clearly, the 25 mm long scutched flax fibre exhibits the highest mean fibre diameter since less splitting occurs during cutting of these long fibres. In order to take these differences in fibre

diameter into account, the flax fibre diameter distribution of Figure 5.11 was incorporated in the Kelly-Tyson model. For experimental validation, composites based on the two types of 6 mm long flax fibres and an unmodified PP matrix were prepared using the suspension impregnation process. Figure 5.12 shows the tensile strength of both types of composites for two fibre volume fractions. For dew-retted scutched flax fibres (6 mm) the fibre strength of 710 MPa is used for the model calculations. Whereas, for warm water retted hackled flax (also 6 mm), fibre strength of 810 MPa is used. Based on linear fitting of the experimental data an efficiency parameter k of 0.39 was used in the model calculations for scutched (dew-retted) as well as hackled (warm water retted) flax. To obtain an approximate idea about the uppermost strength possibilities with randomly oriented flax/PP composites, the Kelly-Tyson predictions for elementary flax fibre/PP composite is also plotted. For the model calculations, fibre strength of 1500 MPa (Bos et al., 1998), fibre diameter of 20 μm and fibre length of 6 mm is used. As mentioned earlier, it was found that the efficiency parameter k is not a constant for a system but depends on parameters like uniformity, presence of impurities etc. therefore it may be expected that the fibre efficiency parameter k would also be higher in the case of elementary fibres. Similar to the glass/PP system, (a probably too high) efficiency parameter k of 0.53 is used for the model calculations. Also the other applied material parameters in the model are the same as before, viz. an interfacial bond strength of 7 MPa for PP/flax composites and the orientation factor η_o of 3/8. The critical fibre length of 2.5 mm for dew-retted scutched flax/PP and 2.8 mm for warm water retted hackled flax/ PP is used. Critical fibre length was calculated by using the relation $L_c = \sigma_f * D / 2\tau$ where σ_f is the fibre strength, D is average fibre diameter and τ is the interfacial shear strength. As matrix strength a value of 29 MPa is used. From the strength data it can be seen that the scutched fibre composite shows inferior properties compared to the hackled (combed) flax fibre composites. The improvement obtained using an additional hackling step is not that dramatic. However, more significant improvements are foreseen if further optimisations in the area of fibre opening could lead to the use of elementary fibres or even microfibrils.

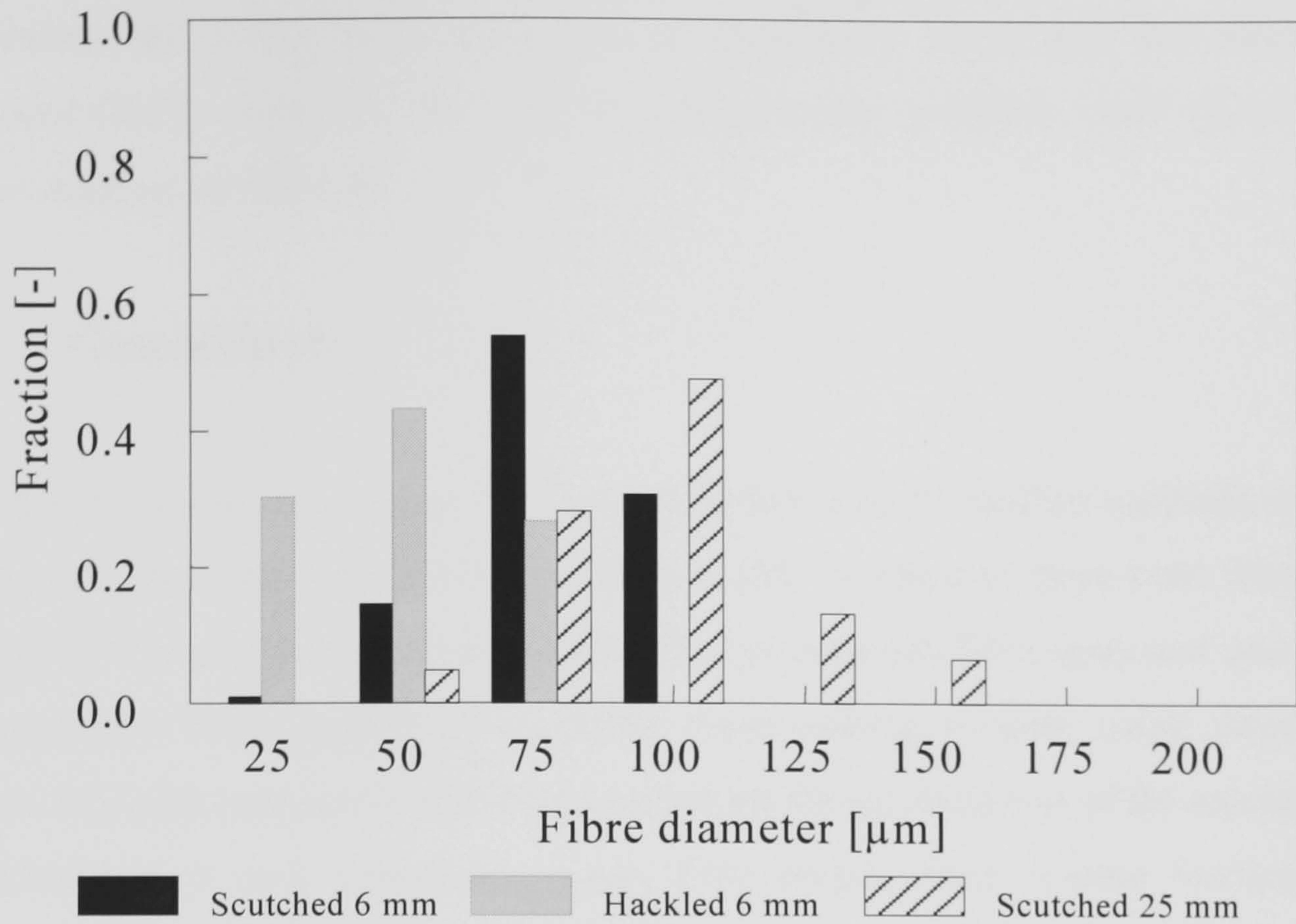


Figure 5.11 Fibre diameter distribution of three types of flax fibres: (i) scutched 6 mm long flax, (ii) hackled 6 mm long flax and (iii) scutched 25 mm long flax.

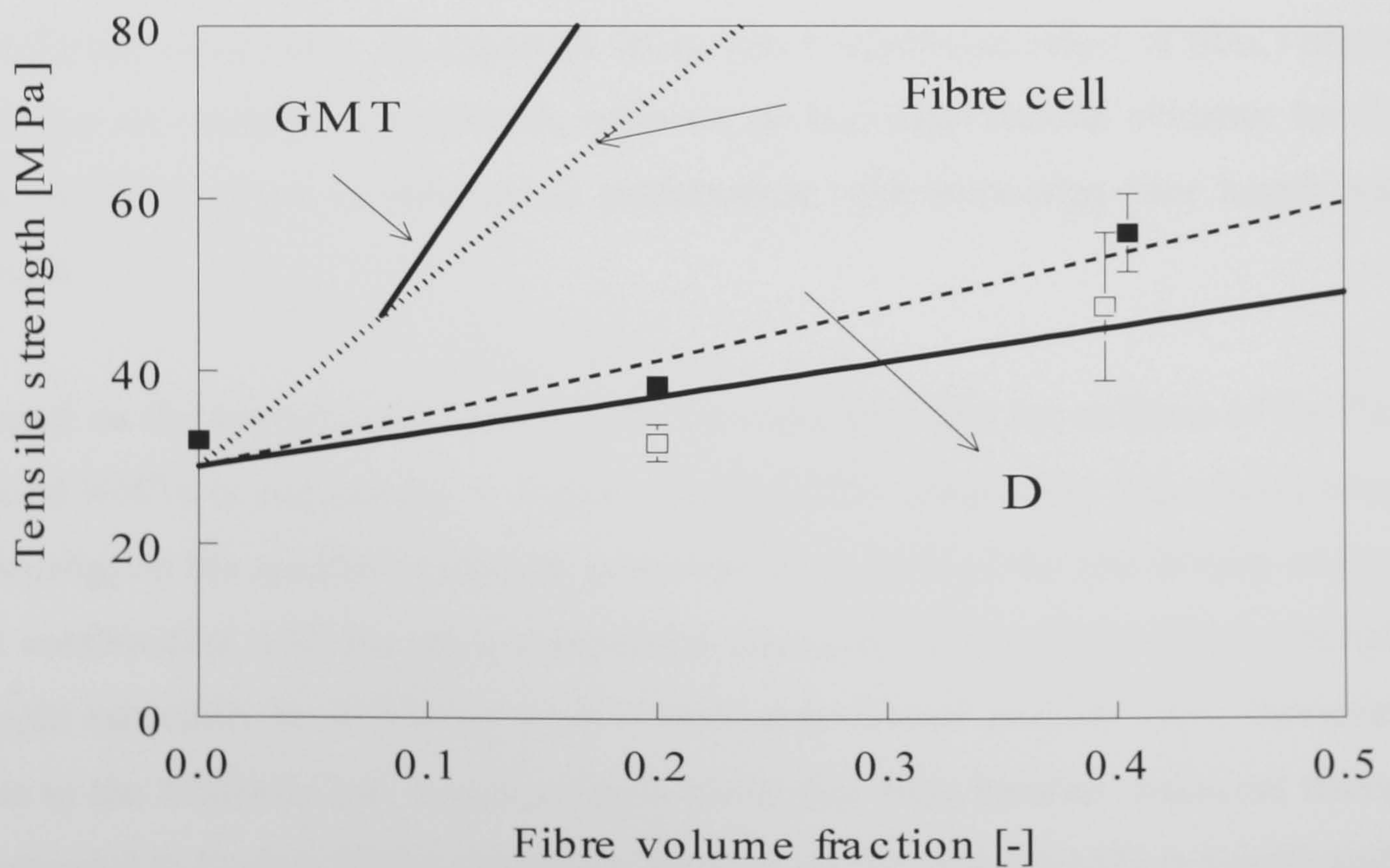


Figure 5.12 Tensile strength of scutched (dew retted) 6 mm (□) and hackled (warm water retted) 6 mm (■) PP/flax composites as a function of fibre volume fraction. The dashed line and the solid line represent Kelly-Tyson predictions for the PP/flax composites using warm water retted hackled (small fibre diameter) and

the dew retted (large fibre diameter) flax fibres, respectively. The dotted line represents the Kelly-Tyson prediction of elementary fibres and the solid line (marked GMT) represents the data for commercially available GMT (Error bars show standard deviations).

5.4 Conclusions

For the production of random PP/flax composites two production methods similar to the commercially known methods for glass/PP composites were used. First, the so-called film-stacking method based on flax non-woven fibre mats and secondly, a suspension impregnation or so-called paper-making process using short flax fibres. Material parameters that were studied for the optimisation of the mechanical performance of such composites were: fibre length, fibre volume fraction and interface modification through the use of a maleic-anhydride grafted PP grade. In order to get a better insight in the importance of these different parameters for the optimisation of composite performance, the experimental results were compared with model predictions using micromechanical models for random short-fibre-reinforced composites. As expected, there was a significant effect of fibre volume fraction on mechanical properties, whereas, no real experimental evidence for the anticipated increase in mechanical performance with increasing fibre length was found.

Based on the experimental results it can be concluded that the stiffness of the flax based NMTs is comparable to E-glass based GMTs composites. Especially, when focusing on the specific composite properties as a result of the low density of flax. In combination with the price-competitive character of flax fibres these materials might especially be of interest from a 'cost-performance' point of view. However, due to the relatively low tensile strength of the flax fibre bundles (technical fibres) compared to E-glass fibres, the tensile strength of flax based NMTs is significantly lower than that of their glass fibre counterparts. In short, it can be concluded that NMTs based on a PP matrix and flax fibres can compete with E-glass based GMT materials in stiffness critical structures, whereas for strength and impact critical applications these materials still need to be optimised further. To close the gap

with GMT these optimisations should mainly focus on fibre strength through new developments in the fibre opening process, rather than on the optimisation of the interfacial bond strength.

6. FLAX FIBRE INJECTION MOULDED COMPOSITES

In this chapter, the various fibre/matrix compounding routes, preceding injection moulding process, are introduced. Novel compounding routes for flax based composites are described. The effects of processing and fibre/matrix parameters on the macro-mechanical properties of flax fibre reinforced thermoplastic (injection-moulded) composites are included and discussed.

6.1 Introduction

In the previous chapter the study on long flax fibre (non-woven flax fibre mat) reinforced thermoplastics, manufactured by compression moulding, was reported and discussed. The present chapter focuses on short flax fibre as well as long flax fibre reinforced thermoplastics manufactured by injection moulding method. The properties of natural-fibre-mat-reinforced thermoplastic (NMT), in the previous chapter, were compared with glass mat reinforced thermoplastic (GMT). GMT competes with sheet metals, thermoset sheet moulding compounds (SMC) and injection moulded thermoplastics for components where surface finish is not critical (Berglund and Ericson, 1995). Compared with GMT, large injection moulded structures are often more expensive, with lower stiffness and impact strength. Most composite parts are large parts produced in small quantities, the major exception being injection moulded short fibre reinforced composite parts. More complicated articles need compression flow moulding or injection moulding technologies. Also, the short fabrication times and reduced finishing operations needed during injection moulding lead to considerable cost reduction. Injection moulding offers the advantage of rapid processing into complex shapes but at the

expense of fibre length retention. This technique requires high capital investment for equipment and tooling so that only large-scale mass production is economic. Composite materials for injection moulding must be capable of flow under pressure and are therefore usually filled or short fibre-reinforced thermoplastics with relatively low filler fraction (typically <50wt.% or 30vol.%), though thermosets can also be produced by the process. Parts are therefore not fully structural, but with careful design are being used in load bearing and other demanding applications. Injection moulded composites account for a substantial part (>50%) of the overall composites market and have shown a growth rate of 6-8% in recent years, a trend which is predicted to continue. Transport, consumer products, electrical and electronic, building and construction applications are the main sectors in which growth is taking place (Brooks, 2000). Glass fibre is by far the most widely used reinforcement, with practically all injection moulding thermoplastic resins available as glass-reinforced grades and usually supplied as ready-to-mould granular compounds in 25kg bags or as bulk material. Glass-reinforced polypropylene, polystyrene, acrylonitrile butadiene styrene (ABS), and Nylon (polyamide) are sold in the largest volumes and a great deal of experience exists for the processing of these materials. Most major resin producers supply their resins as glass-reinforced grades with a range of glass contents from 20 to 40wt.%. The best performance for cost is obtained within the range 20-40%. Too low a fraction does not give significant property improvements while too high a fraction makes the material difficult to process and compromises properties such as impact performance (Brooks, 2000).

6.1.1 Compounding methods for short fibre reinforced composites

Injection moulding and extrusion compression moulding (ECM) of fibre-reinforced composite articles require a compounding step in which the fibre is brought into intimate contact with the molten polymer. For manufacturing short fibre composites, in the case of glass/polypropylene, compounding is accomplished mainly with an extruder producing a mixture for ECM or granules as feedstock for injection moulding. As mentioned in Chapter 1 (Section: Processing of Thermoplastics) the largest tonnage of reinforced polypropylenes is converted into

short fibre reinforced plastics (SFRP) by extrusion compounding. The route of manufacturing SFRP in the case of glass/PP systems mainly involves the use of one of mainly three different possible types of compounder (Jakopin, 1984):

1. Single screw extruder
2. Twin screw extruder
3. Co-kneaders.

Single screw extruders are widely used and, with a properly designed screw profile, can produce compound with an acceptably low level of fibre degradation. They have the lowest capital cost of the three different types of compounder but are not very versatile if required to work with a variety of different types of compound.

Twin screw extruders are more expensive but are frequently built in a modular format, which allows different geometries of mixing and compounding regions to be used for different materials. Twin screw machines may be either intermeshing or non-intermeshing and either co-rotating or contra-rotating. Modern compounding twin screw machines tend to be of the inter-meshing type. The co-rotating design is generally preferred over the counter-rotating one, as the latter configuration produces a 'nip' between the screws where high pressures can be generated, along with screw wear and fibre breakage. With either single or twin screw machines it has been demonstrated that fibre breakage can be reduced to a worthwhile extent by melting the resin prior to attempting to incorporate the glass. In the preferred version of the process, the thermoplastic granules are melted, along with other ingredients such as coupling additives, pigment, stabilisers and processing aids in the first stage of the barrel of the extruder, before adding the reinforcement downstream. The reinforcement to be added can be either in the form of chopped strands or continuous rovings, in which case the rotation of the screws is relied upon to chop the glass. Sufficient work is applied to the material in the extruder to wet out and disperse the reinforcement, after which the compound is passed through a die face cutter and chopped into granules.

In addition to rotation of the screw, co-kneader machines employ a reciprocating motion of the screw within the barrel to mix the material. Both the screw and the barrel wall have protruding pins, which assist in breaking up and redistributing the flow of the material. There have been many refinements to the process of compounding extrusion over the years, resulting in considerable improvements in the reproducibility and especially in the fibre length retention in the materials produced by this route. Significant future improvements in fibre length retention, however, seem unlikely, as the maximum length that can be retained appears to be limited to values substantially below 1 mm (Gibson, 1995). Fibre lengths before compounding are usually in the range 3-6mm, but the compounding process and subsequent injection moulding degrades the fibres to average lengths in the range 0.3-1mm. Although short, these lengths still have aspect ratios up to 100 and impart significant reinforcement to the base resin (Brooks, 2000).

In the case of extrusion compounded polypropylenes the greater part of the fibre breakage usually takes place at the compounding stage: additional breakage during injection moulding is fairly small, provided the process is operated under reasonable conditions, so the fibre length distribution can be regarded as effectively stabilised by the compounding process (Gibson, 1995).

Moriwaki (1996) studied the effect of direct injection moulding, in which preliminary melt compounding method is eliminated, on the mechanical properties of nylon 6 alloy and glass fibre composites. Glass fibre strength in moulded parts, made by the direct injection moulding process was 20% higher than the strength of glass fibres in parts made by a two-step process. The enhanced tensile strength of the composites moulded by the direct injection process was attributed to the longer glass fibres remaining in the parts and reduced fibre deterioration. Since melt mixing occurs only once, the breakage of glass fibres in direct injection moulded parts was smaller and the weighted average glass fibre length exceeded 300 μ m. Also, direct injection moulded parts are characterised by having a distribution that extends to longer fibre lengths, the latter having greater reinforcing efficiency. Apart from the advantages mentioned above there are also reduced production costs. Dry blends of chopped glass fibres and nylon chips, before feeding to the injection moulding machine, were made in a drum blender (Moriwaki, 1996). Such

a blending did not pose any problems since the size of the chopped glass fibre strands was very close to that of the plastic pellets and the blends were easy flowing. The dry blend could be fed to the injection moulding machine through an auger feeder.

6.1.2 Compounding methods for long fibre reinforced composites

There has been substantial interest in the possibility of alternative processes to compounding extrusion for the production of reinforced injection moulding materials. As mentioned before, passing the glass reinforcement through an extruder consumes power and causes machine wear, in addition to producing fibre degradation. Therefore to avoid above mentioned problems and to improve the properties of the composites through reduced fibre (length) degradation, other methods have been developed like continuous strand impregnation process or pultrusion process. These compounds enable 'long' fibres to be present in components after injection moulding and high volume fractions of fibres can be efficiently impregnated. The melt pultrusion technique first commercialised by ICI for the production of 'Vertron' moulding materials produces chopped unidirectional strands. The above mentioned pultrusion process (Figure 6.1) relies on two effects to produce good impregnation of the strands. First, the fibre tow is spread out and flattened as much as possible, to reduce the distance, which the resin must flow into the fibres to achieve impregnation. Secondly, the action of the fibre tow passing over the pin generates a pressure in the wedge of molten polymer approaching the pin in a similar manner to the action of the oil in a lubricated bearing. This pressure forces the resin to flow laterally into the reinforcement.

Generally the length of the uniaxial strands in long fibre thermoplastic (LFT) compounds is 10 mm for injection moulding or 25 mm for extrusion compression moulding (ECM). Although composites with acceptable properties could be achieved with shorter strand lengths than this, the length is currently determined by the capabilities of the chopping stage of the process, which must be able to cope with strand speeds of up to 30m/min.

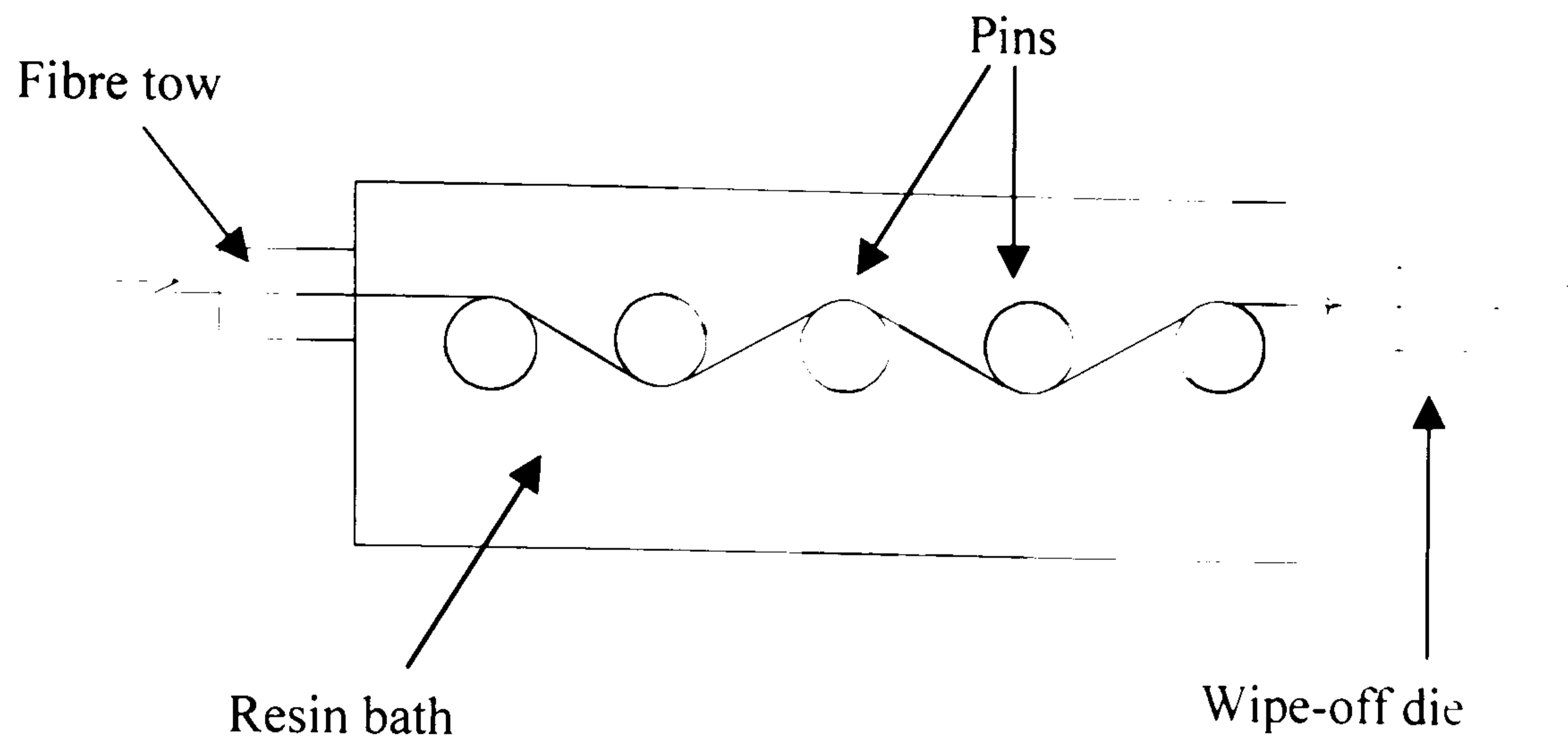


Figure 6.1 The schematic representation of the pin impregnation process for the production of well-wetted glass/thermoplastic strands.

Shorter strand lengths could also eliminate some of the feed problems, which are sometimes a feature of the processing of LFTs – because of their increased aspect ratio compared to conventional granules. However, it should be pointed out that fibre lengths are again degraded during the injection moulding process but can retain average lengths in excess of 2mm. Verton materials, although giving an improvement in reinforcement performance, are more difficult to process, in that they have higher viscosities for the same glass content and fibres can agglomerate in the flow channels. To achieve good impregnation in a high speed pultrusion process, and to minimise fibre breakage during subsequent moulding it is necessary to operate with a low viscosity resin. Nylon 66, which has a lower melt viscosity than many thermoplastics, was found to be particularly suitable for strand impregnation processes. In the case of long fibre (LF) polypropylene it is often necessary to use special grades of resin with lower viscosity than the normally used grades in conventional processing operations. Because of the improved reinforcing efficiency obtainable in LF systems, the threshold level of molecular weight needed to achieve acceptable engineering properties is lower than with short fibre (SF) compounds or with unfilled moulding resins. As a further aid to impregnation the glass fibre filaments used in the strand pultrusion process often have a larger diameter, sometimes up to 20 μm , compared with conventional glass fibres which are normally about 10 μm in diameter (Gibson, 1995).

6.1.3 Compounding methods for flax fibre reinforced composites

The methods used for the easily free flowing glass fibres, to manufacture SF composites, do not work for the fluffy flax fibres and new methods have to be developed. In the case of flax fibres, feeding through a hopper leads to fibre agglomeration and the feeding is not properly controlled. Since flax fibres are not free flowing therefore when fed with polymer chips they form bundles leading to blocking of the barrel.

As mentioned before, the property of a composite may depend on the processing route taken to manufacture the composite. For example, in the case of injection moulded composites, the method of addition of fibre to the polymer matrix (compounding) can influence the morphology and hence the final properties of the composite. The present study includes optimisation of compounding method, for flax fibre and thermoplastic matrices, followed by injection moulding.

6.2 Experimental

6.2.1 Materials

An isotactic-polypropylene (i-PP) matrix of Shell (XY6500T) with a melt flow index of 35 was used. The Young's modulus of the neat PP matrix was approximately 1.6 GPa and the yield stress about 32 MPa. Duralin flax fibres were used to manufacture the composites. The properties of various other polymers used are:

PP NED: 6.7 dtex, 60mm length, produced by STEEN (Schwarzenbeck), Germany.

MFI (230°C / 2.16 kg) = 40 g /10 min

MFI (190°C / 5.00 kg) = 65 g /10 min, Density of 0.9 g/cm³.

PP Stamylan 112MN40: manufactured by the DSM Company. Density = 0.905 g/cm³.

MFI (230°C / 2.16 kg) = 47 g /10min.

MFI (230°C / 5 kg) = 158 g /10min,

Charpy impact strength (notched, at 23°C) = 2.0 kJ/m².

Tensile strength at yield = 35 MPa, tensile strength at break = 22 MPa.

Maleic anhydride grafted PP (Polybond 3150): Manufactured by Uniroyal chemical, MFI (230°C / 2.16 kg) = 50 g /10 min, Density at 23°C = 0.91 g/cc, Melting point = 157°C.

Nylon 6 (Akulon F223-D): Manufactured by DSM Company, Density = 1.13 g/cc, Charpy impact strength (notched, at 23°C) = 35 kJ/m².

Tensile strength (yield stress at 50 mm/min) = 60 MPa, yield strain = 20 %.

Tensile modulus (at 1 mm/min) = 1.7 GPa.

(POM) Polyoxymethylene: Hostaform C 9021, Density = 1.41, MFI (190°C /2.16 kg) = 9.5 g /10 min. Melting point = 166°C.

6.2.2 Methods

6.2.2.1 Compounding

As mentioned before, the several previously stated compounding methods used for (free flowing) glass fibre/thermoplastic based (injection moulded) composites can not be used as such for the flax fibres based composites. Therefore different methods were tried for compounding of flax with polypropylene:

Kneading: To study the effect of composite manufacturing method (i.e. compression moulding and injection moulding) and maleic-anhydride grafted polypropylene (MA-PP) content on the mechanical properties of composites, samples were made through injection moulding of Duralin short chopped fibres of approximately 10 mm length. Prior to moulding the polymer (blend) / flax fibre combination were blended for 30 min at 210°C in a kneader (HBI System 90) at 30 rpm. A figure of the kneader is shown in Chapter 4 (Section 4.3.2.4: Sample

preparation for macrocomposites). The mixed compound was granulated and injection moulded using an Arburg 220D injection-moulding machine. Processing specifications were: temperature zone 1 up to 4: 200/210/215/220°C, injection pressure: 750 bar, mould temperature: 40°C and cooling time: 18 s. The dumbbell-shaped samples having dimensions according to standard ASTM D638M (150x10x3.5 mm) were stored for at least 24 hours before testing. In the case of Nylon 6 compounding was done at 225°C at rotor speed of 10 RPM.

Henschel kinetic mixer: In this method fibres and polymer powder or polymer granules are simply introduced into the mixer together with possible additives, such as coupling agents. The rapid stirring generates heat that causes the polymer to soften and almost melt, at which point the fibres and polymer combine. The hot fibre/polymer mixture is then dumped into a cold mixer in which the material is broken down to small granules. These granules are suitable for use as a feedstock for injection moulding. Where there is too much difference in the shape and size of the granules, it is necessary to sieve out the bigger granules. For the present study, Henschel FM 200, coupled to a cool mixer KM 350 was used. The rotor speed up to 166°C was 1320 rpm; from 166°C to 171°C it was 660 rpm.

Pelletising press followed by extruder mixing: The most commonly used compound method is twin-screw extrusion, where a fast output of the material can be obtained with excellent fibre dispersion. However, this method does not work efficiently in the case of fluffy flax fibres, which have a tendency to entangle. Another method tested, for feeding the flax fibres to the extruder, was the use of compressed pellets of flax fibres. The compressed pellets were made in an Amandus Kahl pelletising press (Figure 6.2) usually used to prepare cattle food. The advantage of the compressed pellet method is the possibility of using an extruder in the compounding step. The granules made in an extruder are more regularly shaped than those made in a Henschel mixer or Kneader and therefore cause fewer problems in transport through pipes. Not only that, the pelletising process would be cheaper, more simplified and can be applied for large-scale production.

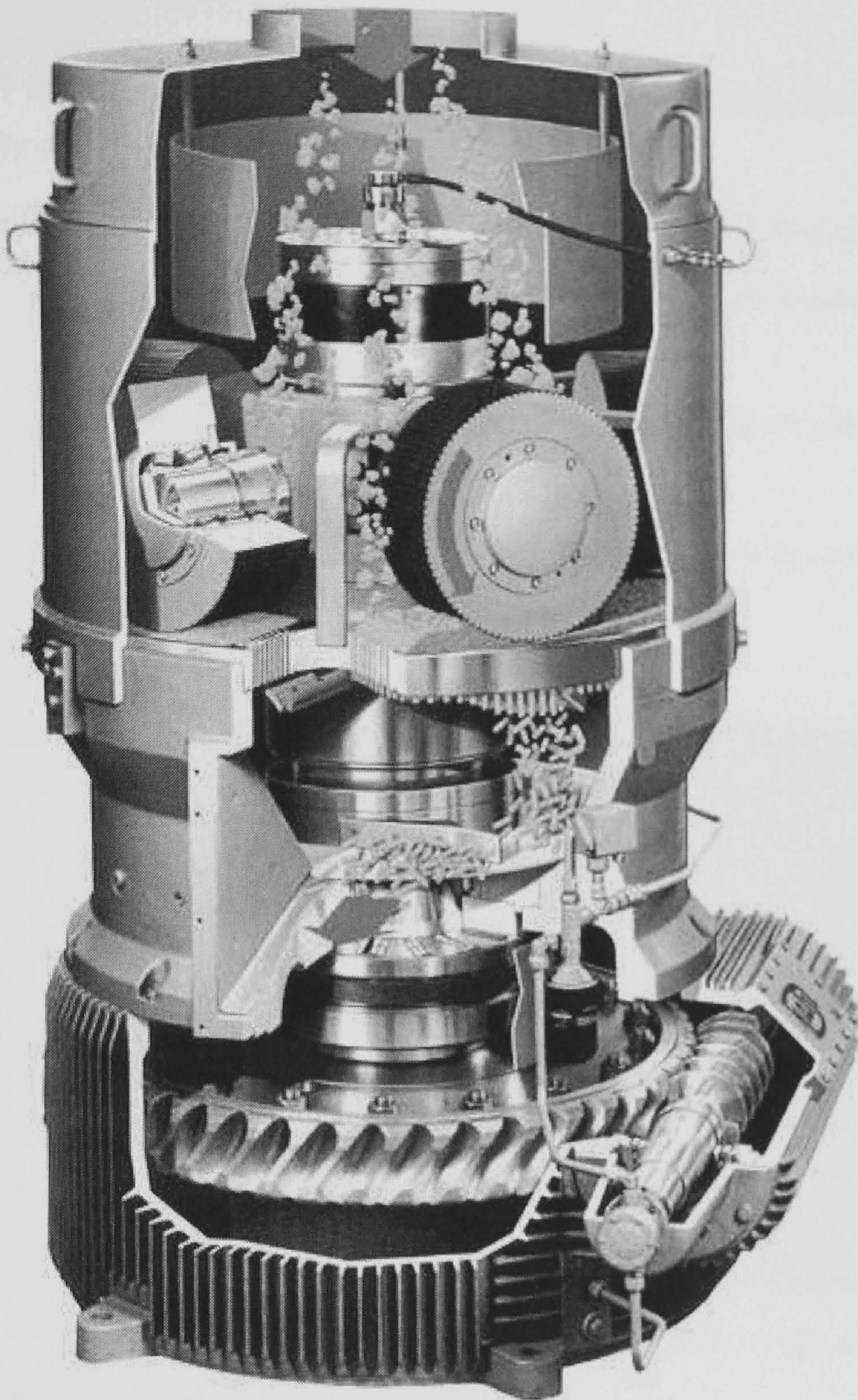


Figure 6.2 Amandus Kahl pelletising press (photo courtesy Amandus Kahl GmbH & Co., Hamburg, Germany. (www.amandus-kahl-group.de)).

The various features of the pelletising presses are:

1. The product is fed by gravity into the large pelletising chamber and thus avoids blocking.
2. The speed of the pan grinder rollers is approximately 2.5 m/s; therefore the product is effectively deaerated.
3. The thick product layer between the pan grinder rollers and the large die surface result in a high throughput, even in the case of products, which are difficult

to pelletise.

4. The pan grinder roller to die gap can be adjusted during operation, thus the pellet quality can be controlled.
5. Permanently lubricated pan grinder roller bearings with special seals prevent the product being pelletised from contamination by lubricating grease and grease losses.
6. Quick die changing increases the availability of the complete plant.
7. Liquid variations in the product are permissible.
8. Mixtures with high levels of fat and molasses (up to 50%) can be effectively pelletised.

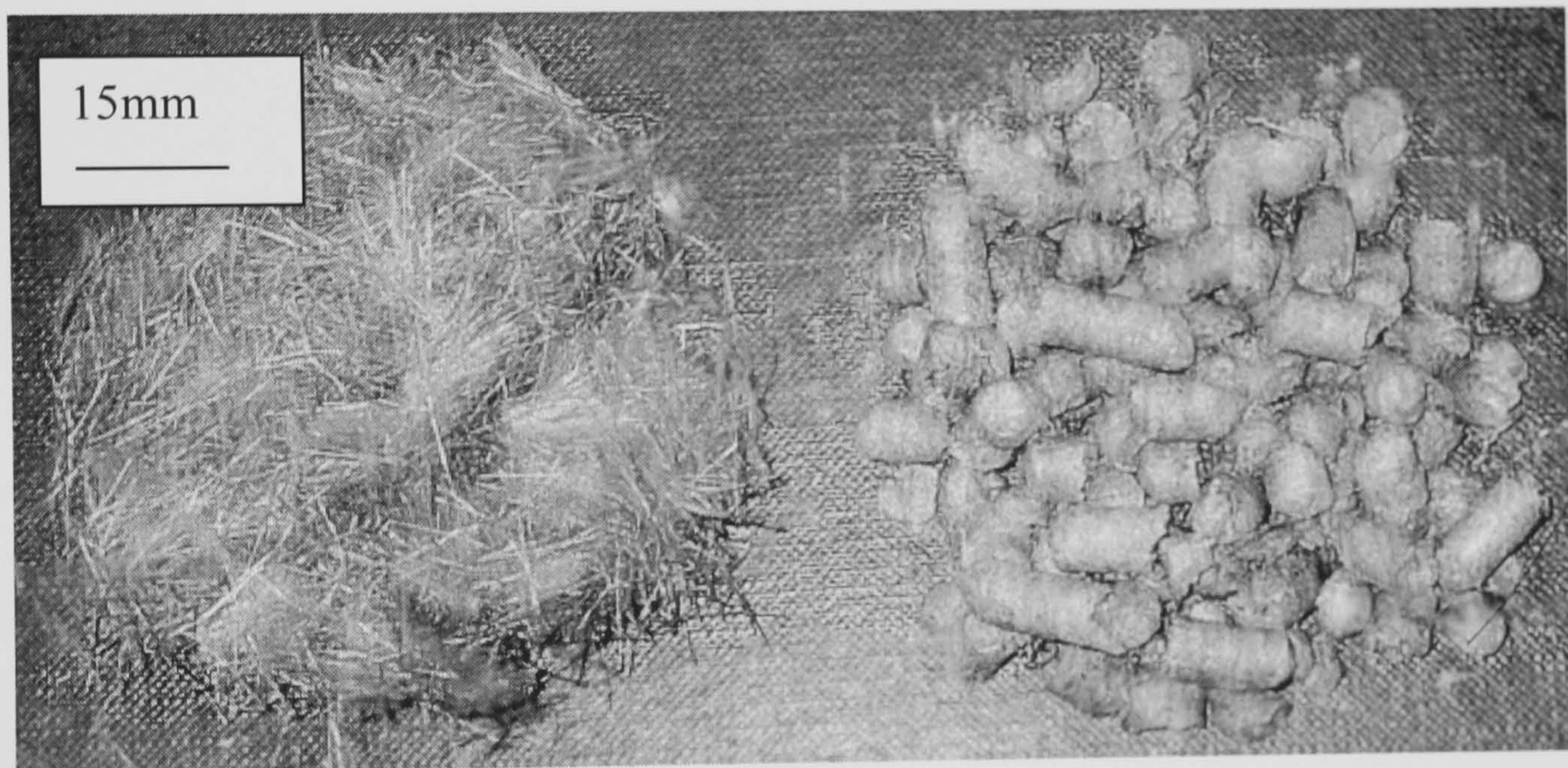


Figure 6.3 Picture of flax fibre pills made in Amanadus Kahl pelletising press (right) and chopped Duralin flax fibres (left).

The fibre pills obtained through the pelletising press were compounded on a Werner and Pfleiderer co-rotating twin-screw extruder (ZSK 25) (Figure 6.4). The screw had a diameter of 25 mm and a length of 1060 mm ($l/d = 42$) and were configured as follows: ts, 5*t, 3*kt1, tneg, 3*t, 3*kt2, tneg, 4*t, kt1, kt2, tneg, 3*t, 2*tt, 2*t, where ts= small transport element 25mm, t= transport element 36mm, tt= transport element with teeth 20mm, tneg= negative transport element, kt1= kneading element 36mm, kt2= kneading element 24mm.

At the end of the extruder the melt went through a die plate with two holes (diameter: 4mm), into a waterbath, finally followed by a cutter. The matrix

material was fed into the extruder in zone 0 using a K-Tron gravimetric feeder at a rate of 100 g/min. As no suitable gravimetric feeding system was available for dosing of the flax pills a volumetric feeding screw was used. This screw fed the pills at a rate of 35-50 g/min to a Werner & Pfleiderer twin screw side feeder (ZSB) connected to the first feeding hole (third element), which transported the pills into the extruder. No degassing was used and, after cutting, the pellets were dried and sieved to 7mm.

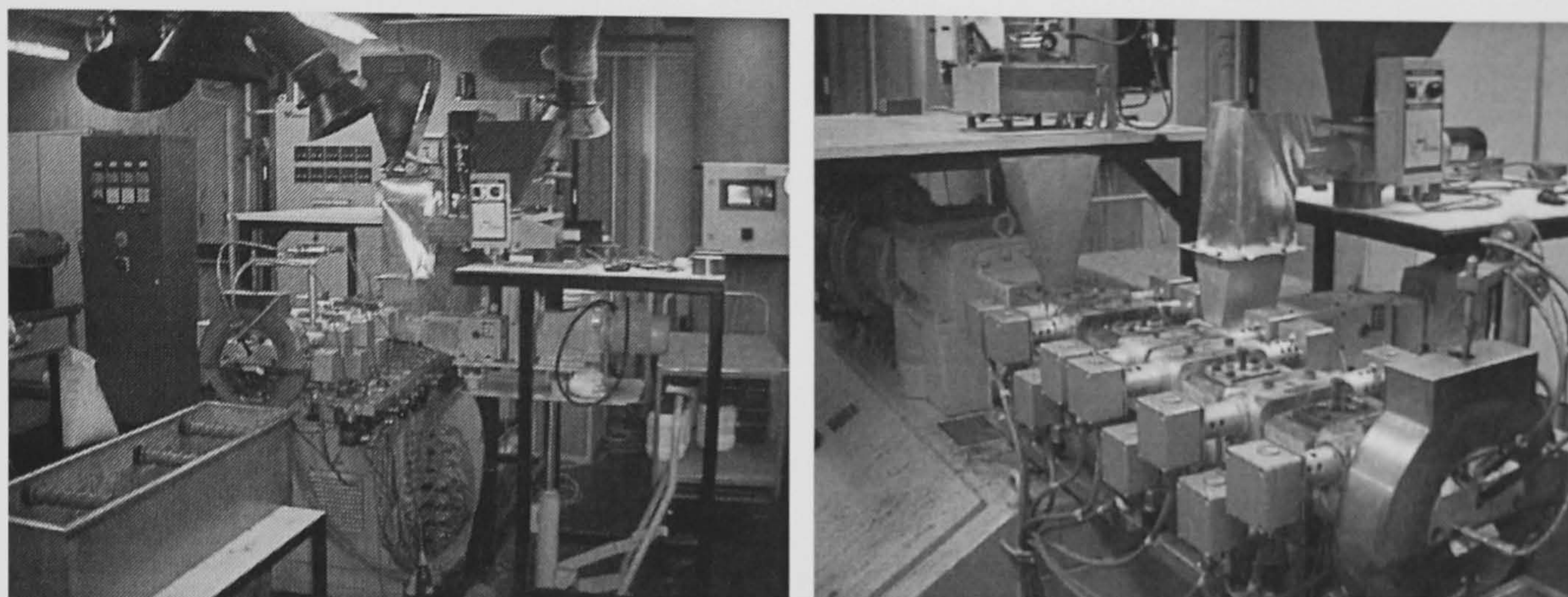


Figure 6.4 Picture of compounding set-up (Werner & Pfleiderer twin screw extruder).

Table 6.1 Overview of the process parameters used for compounding of PP/flax and (POM) Polyoxymethylene/flax.

	Temperature of different zones in the barrel (°C)										Die (°C)	r.p.m.	Torque
	T1	T2	T3	T4	T5	T6	T7	T8	T9	T10			
PP	195	200	200	200	200	200	200	200	210	220	100	60%	
POM	175	180	190	200	200	200	200	200	210	220	100	80%	

Production of long fibre granules: Thüringisches Institut für Textil- und Kunststoff-Forschung (TITK), Rudolstadt-Schwarza, Germany, developed a procedure that produces long fibre granules from fibre slivers manufactured through textile preparatory method. The principle (Figure 6.5) of the process involves fibre slivers that consist of a mixture of natural fibres and synthetic thermoplastic fibres. The blended sliver is heated in a preheating zone, pulled through a jet and then twisted. The natural fibres are impregnated with the melting

matrix polymer fibres by twisting. A compact material rope is formed that can be drawn off continuously. After the twisting, the rope is cooled in the cooling zone. Finally the rope is cut to make pellets (granules). For the needle-punching process the cellulosic natural fibres as flax should have a minimum fibre length of 20 mm. The manufacturing of a sliver for long fibre granules requires a minimum fibre length of more than 40 mm. The long fibre granules can be used for injection moulding processes. The granule material can be adapted to the specific processing requirements regarding fibre content, fibre length and material composition.

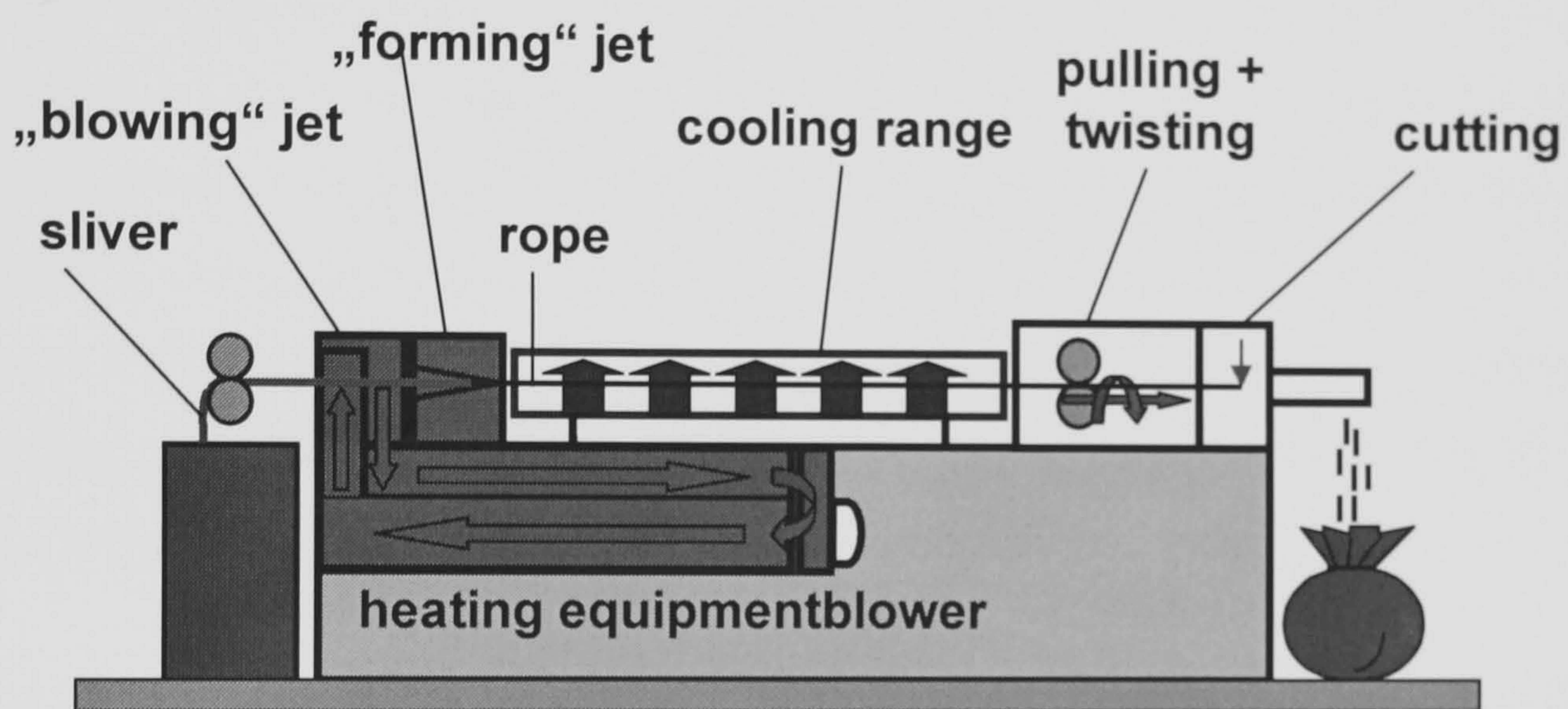


Figure 6.5 The schematic representation of production of long natural fibre reinforced thermoplastic granules (LFT) (Courtesy: Nechwatal and Reussmann, Thüringisches Institut für Textil-und Kunststoff – Forschung, Rudolstadt, Germany).

The compounding stage can lead to significant fibre breakage, which can have an appreciable effect on the mechanical properties of the final composite. It is therefore important to assess the effect of processing variables on the extent of fibre degradation and fibre length distribution in the moulded material. Fibres were extracted from the compounded material and fibre length was measured. For the same the PP matrix was dissolved in hot Xylene. After dissolution of the matrix flax fibres were isolated by means of filtration. Pictures of these fibres were taken through a Zeiss M35F light microscope. The fibre length distribution was measured by putting the pictures on a CRP pin board and pointing out the fibre

dimensions. IMAN, a computer program developed at Eindhoven Polymer Laboratories, was used to process the data for 150 fibres.

6.2.2.2 *Injection moulding*

The mechanical and physical properties of moulded parts, particularly of those made of thermoplastics, do not only depend on the chemical constitution of the material and its corresponding properties. The processing conditions exercise a considerable influence on properties of moulded parts. The properties such as strength, toughness, hardness, heat distortion etc. vary depending on the processing technique. The most important structural characteristics of thermoplastics dependent on processing condition are: molecular orientation, residual stresses, crystalline structure, degree of crystallinity and orientation of fillers. For the present study, tensile pieces were made in ARBURG 250-75 A 220 D injection moulding machine. Parameters used for the injection moulding of flax/PP are given in Tables 6.2.

Tensile tests were performed on a Frank 81565 tensile testing machine at a crosshead speed of 5 mm/min according to ASTM D 638 method. Tensile property evaluations were carried out at temperatures below and above ambient temperature using a temperature cabinet and controller. Samples were conditioned at the test temperature, for 10 minutes, prior to testing. Charpy (notched) impact tests were also conducted on injection moulded samples. For each condition ten different samples were tested. The samples were tested in the laboratory having controlled RH of about 60% and temperature of about 20°C.

Table 6.2 Parameters for the injection moulding process for short flax fibre reinforced polypropylene (112MN40) and flax/POM.

Parameter	Flax/PP	Flax/POM
Temperature zone 1	195°C	195°C
Temperature zone 2	200°C	200°C
Temperature zone 3	205°C	205°C
Temperature zone 4	210°C	210°C
Dosing volume	20 cc	20 cc
Circulating rate of screw	11.04 m/min	13.8 m/min
Injection pressure	700 bar	1000 bar
Injection rate	17.6 cc/s	22 cc/s
Holding pressure	525/490/420 bar	800/800/800 bar
Holding pressure time	2.5/5.0/3.0 s	5.0/5.0/5.0 s
Cooling time	25 s	20 s
Cycle time	42.2 s	41.7 s
Temperature of the mould	40°C	90°C

6.3 Results and Discussion

6.3.1 Compounding methods

The picture of granules obtained from various compounding methods is given in Figure 6.6.

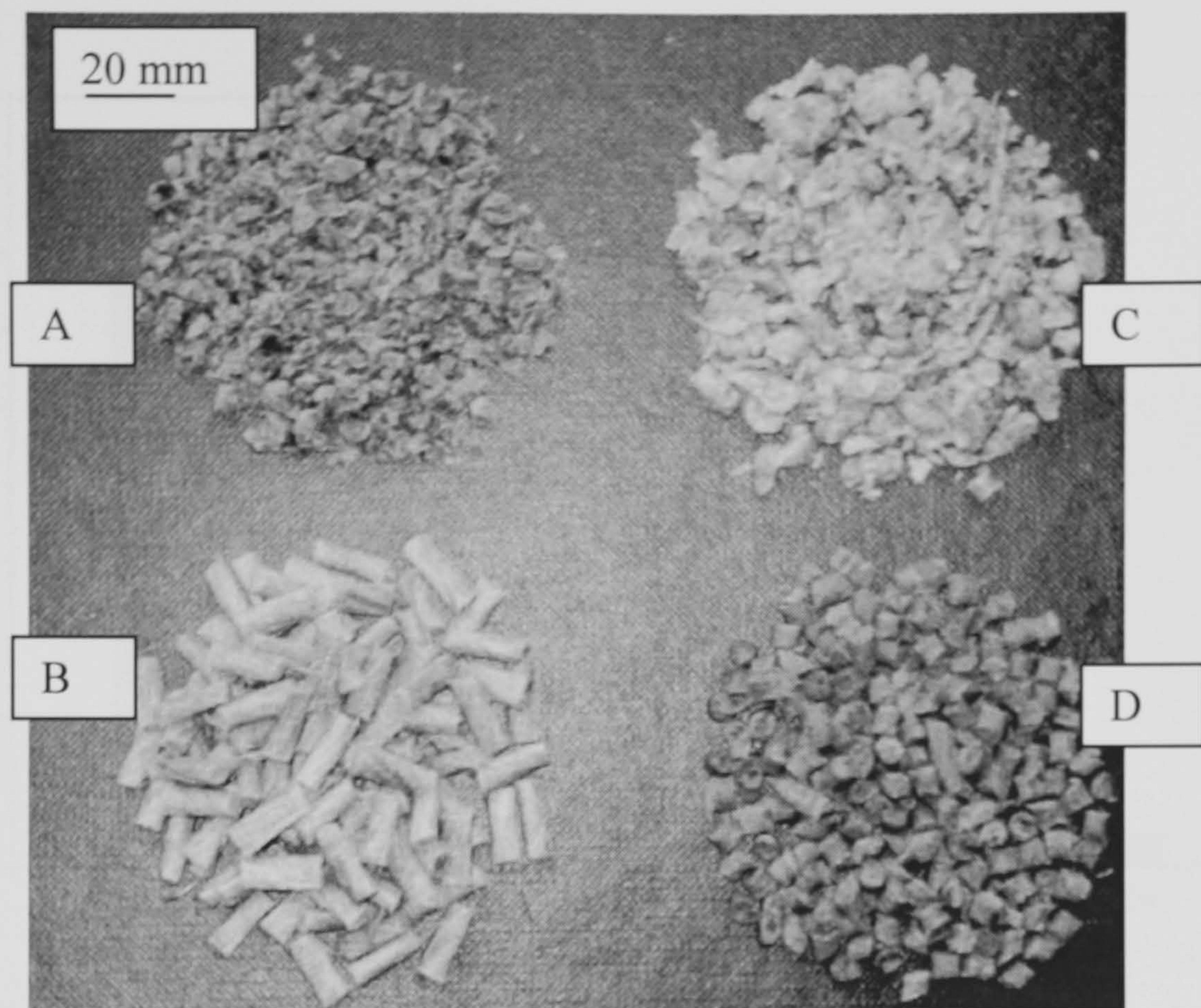
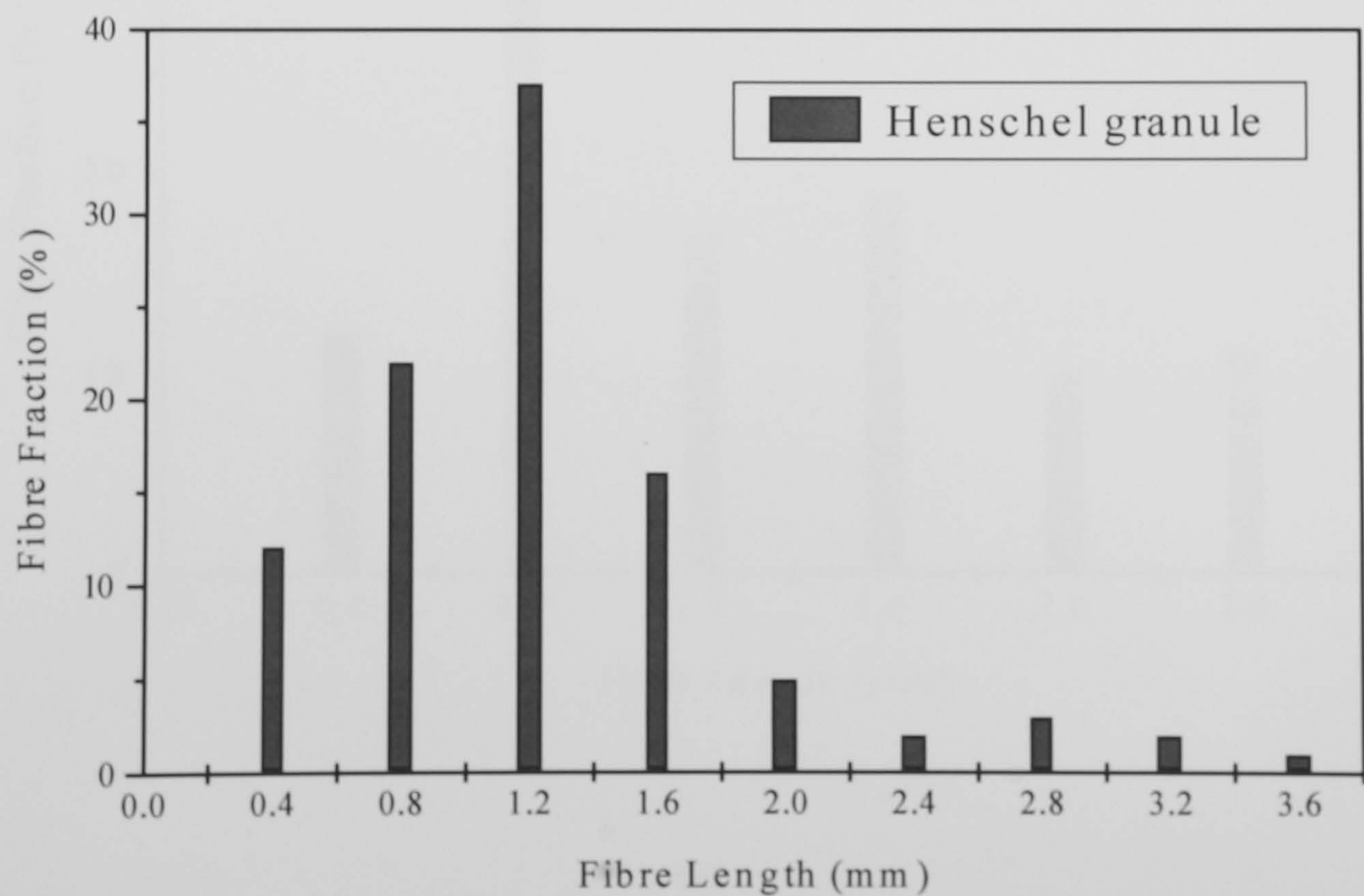
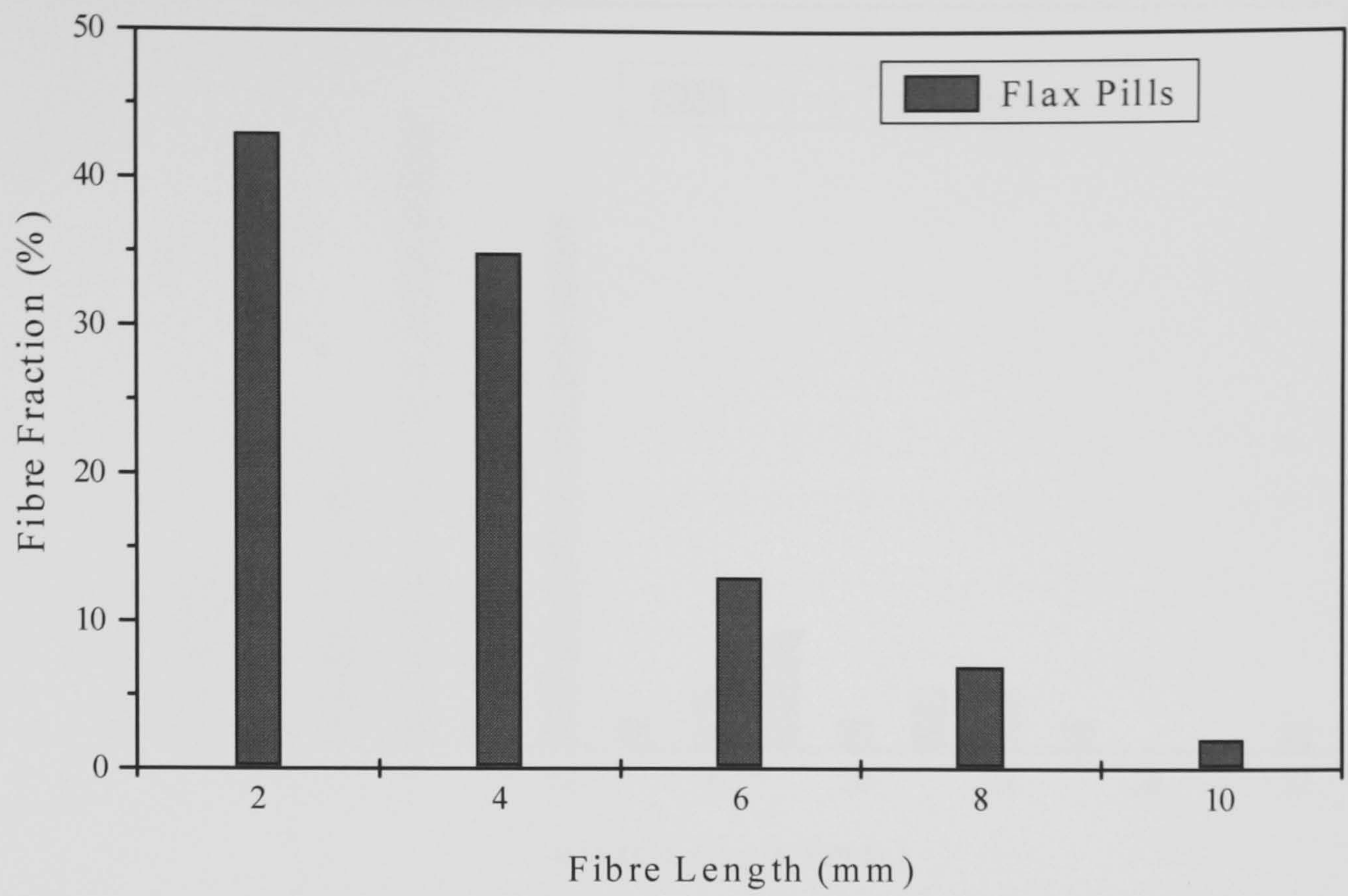


Figure 6.6 Picture of granules obtained from various operations: (A) kneader, (B) long fibre granules (LFT), (C) Henschel kinetic mixer and (D) twin screw extruder.

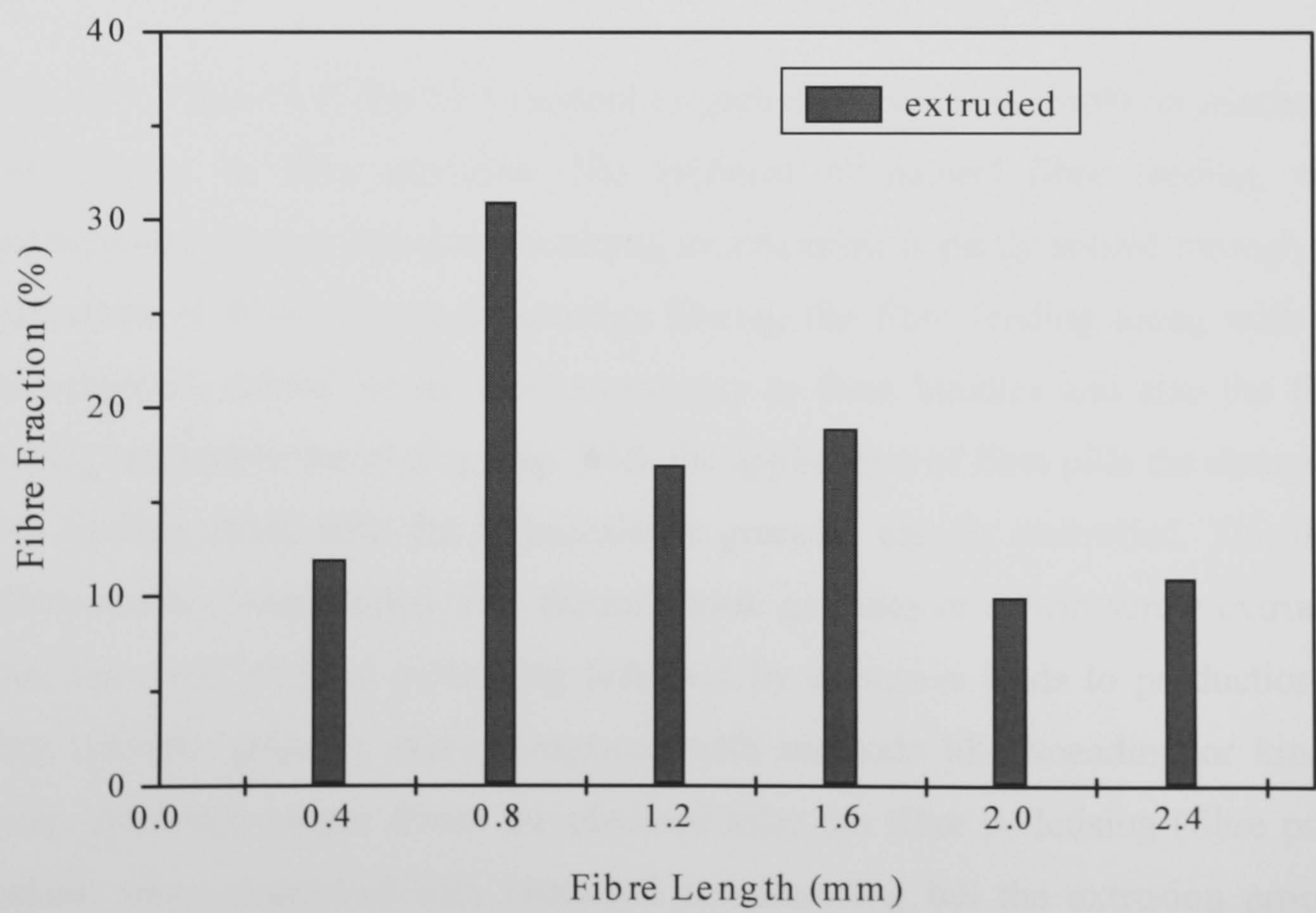
The fibre length distribution in flax fibre pills as well as compounded granules are given in Figure 6.7.



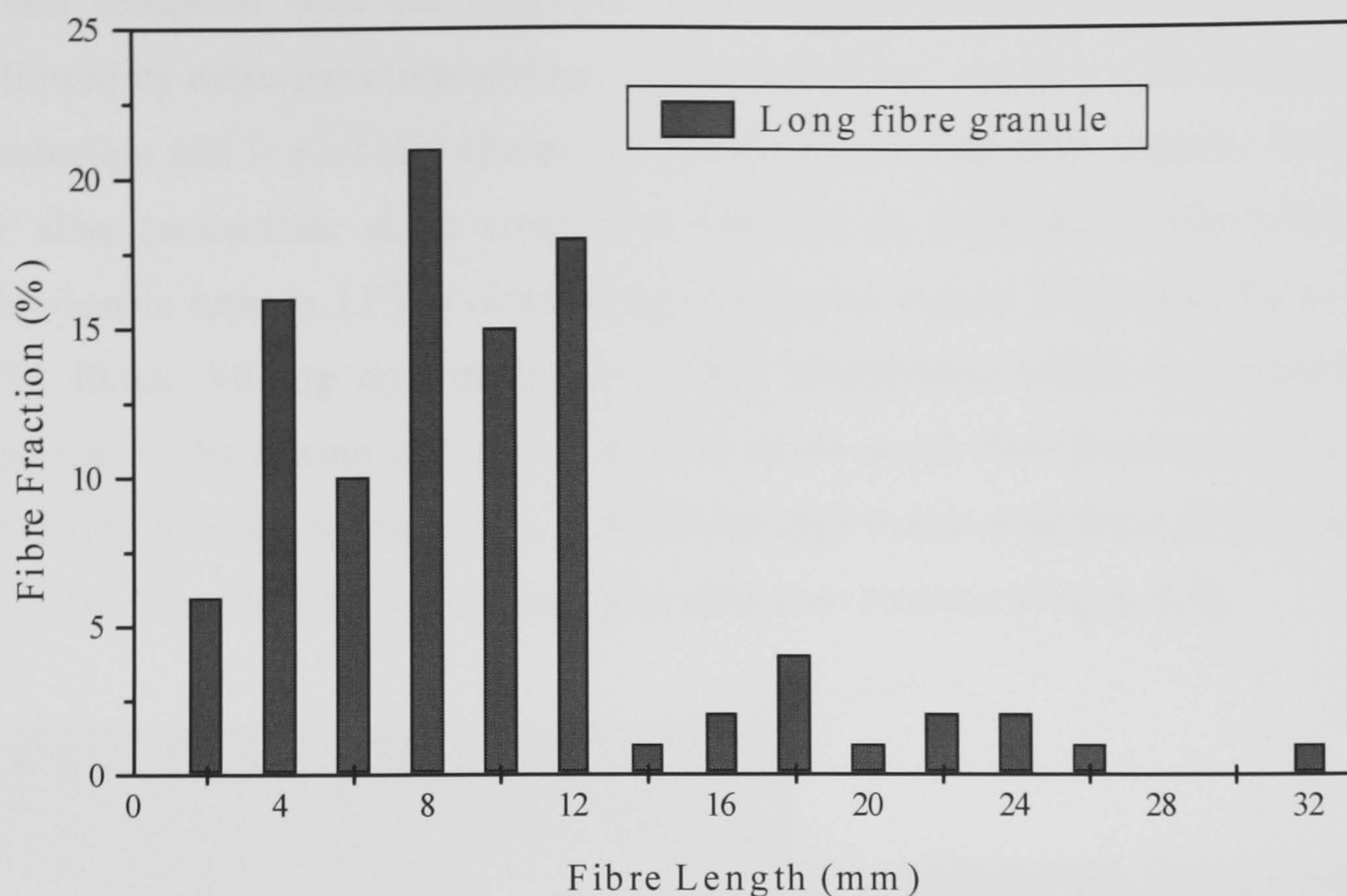
(a)



(b)



(c)



(d)

Figure 6.7 Fibre length distribution after various compounding (preparatory) methods.

As seen in Figure 6.7, the LFT method of granule production results in maximum fibre lengths in fibre granules. The problem of natural fibre feeding, with thermoplastic, during injection moulding or extrusion is partly solved through the application of fibre pill manufacturing. During the fibre feeding along with the thermoplastic, natural fibres have a tendency to form bundles and also the fibre feeding can lead to barrel clogging. With the application of fibre pills the dosage of fibre feeding along with the thermoplastic granules can be controlled. The fibre pellets can be compounded with thermoplastic granules in a twin screw extruder. Also, the route of fibre pelletising followed by extrusion leads to production of more uniform granules when compared with methods like kneading or kinetic mixer. Although longer fibres are obtained after the fibre pelletising (fibre pills) method, when compared with Henschel compounding but the extrusion process which follows fibre pelletising method leads to fibre length degradation. Therefore, overall, the Henschel (kinetic mixer) compounding method seems to be better than pelletising method followed by twin-screw extrusion, considering fibre length degradation. However, the pelletiser route is preferable for the large-scale production of composites.

When compared with the long fibre granules the method of fibre pelletising followed by extrusion compounding is more simplified, can be used for large scale production and is probably cheaper as production of long fibre granules involves PP fibre production, sliver production followed by granulation. The particular fibre/matrix ratio in LFT is obtained by mixing the natural fibres with the matrix (PP) fibres. Mixing ensures an even fibre distribution within the composite. Because of the mixing step and as a result of the good fibre distribution it is not needed to melt the whole matrix material but only in the outer layer of the granule cylinder. Thus the LFT granule has got a skin-core structure (Figure 6.8).

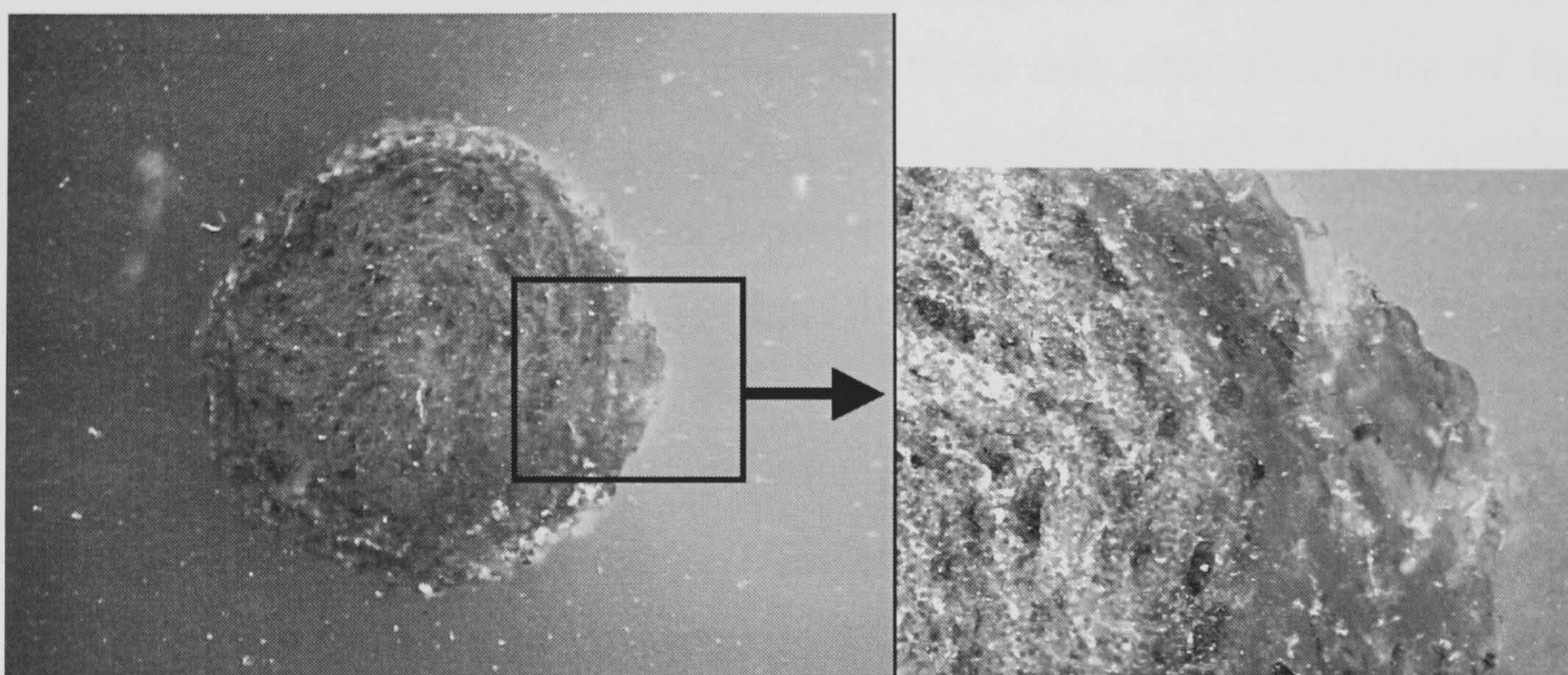


Figure 6.8 Picture of cross-section of long fibre granule reinforced with natural fibre showing skin-core structure (Fibre content 30wt%, diameter of granule = 5 mm and cutting length = 20 mm) (Courtesy: Nechwatal and Reussmann, (TITK) Thüringisches Institut für Textil-und Kunststoff – Forschung, Rudolstadt, Germany).

As only a small part of the matrix fibres melt, bonding the outer natural fibres, the thermal strain is much lower than in usual compounding processes. Also, because of the twisting during the manufacturing of LFT the fibres are arranged helically in the granule. Because of the twisting during granule production some single natural fibres are longer than the granule and the length of fibres can be set dependent on the twisting state.

6.3.2 Properties of injection moulded composites

6.3.2.1 Polypropylene based composites

Figure 6.9 and 6.10 show the stiffness and strength of compression moulded (NMT) and injection moulded (compounding done via a kneader) Duralin flax/(MAPP/PP = 5:95 wt/wt) composites. It was found that kneader compounding followed by injection moulding reduced the fibre length from 10 mm to around 1 mm (Figure 6.11 and 6.12). Figure 6.11 shows the picture of fibres left after dissolution of the matrix in injection moulded composites. Figure 6.12 shows the fibre length distribution measured from the fibres left after dissolution of the matrix polymer. In spite of such a reduction in the fibre length during injection moulding, from Figure 6.9 and 6.10, it can be seen that injection moulded samples showed tensile properties similar to that of long fibre (fibre length ~ 25 mm) compression moulded composites. This could be because of: (a) improved fibre efficiency because of dimensional changes and (b) changes in fibre orientation along the matrix flow, in the case of injection moulded composites. Dimensional changes can play an important role since the flax fibre itself is a composite containing fibre cells bound together by pectin (discussed in Chapter 2). Also, it is shown that the fibre tensile strength is strongly dependent on the fibre length therefore reduction in fibre length could have led to separation of fibre bundles to fibre cells or splitting hence leading to improved fibre efficiency through enhanced fibre tensile properties (of fibre cells).

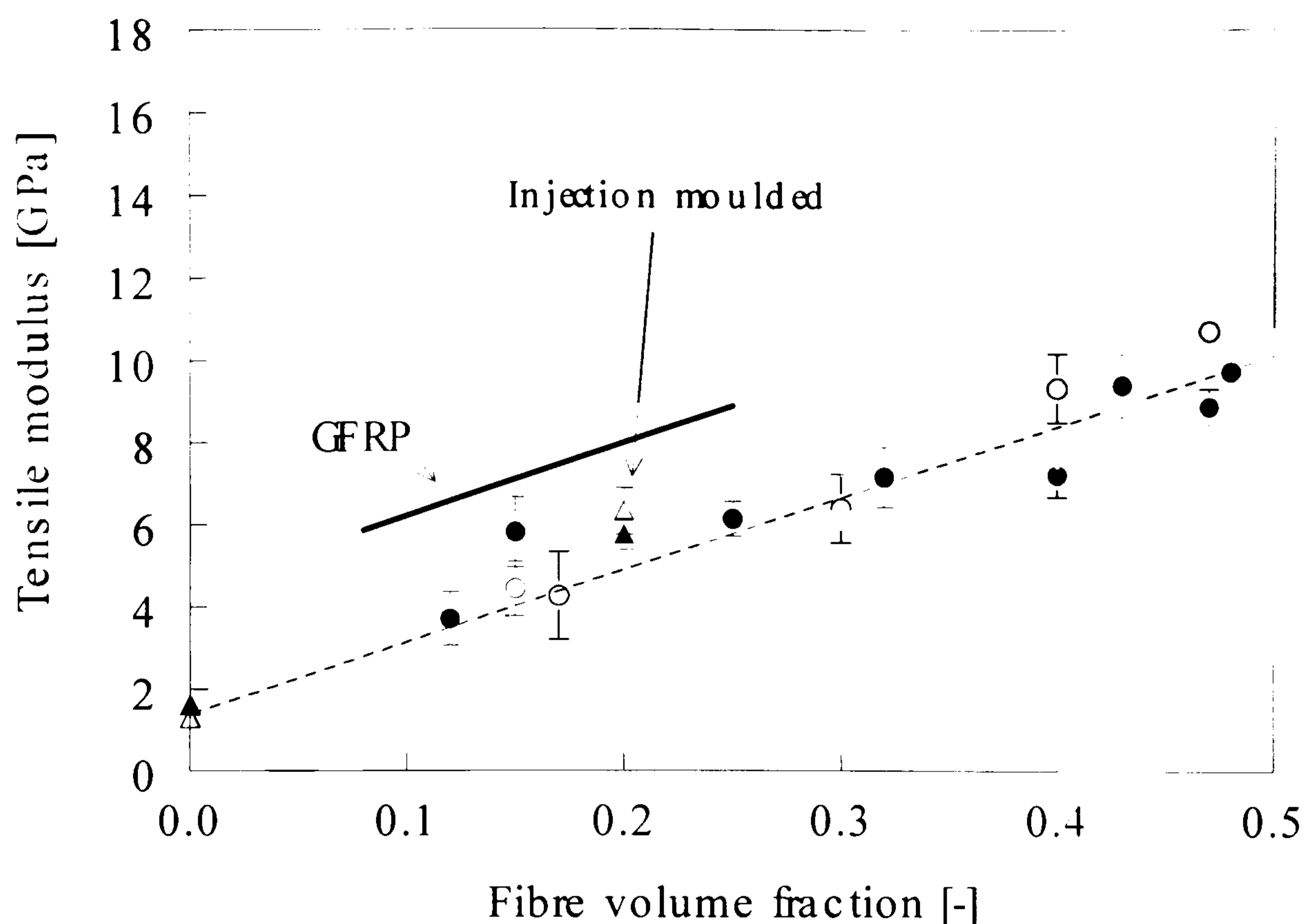


Figure 6.9 Tensile modulus of Duralin flax/(MA)PP composites manufactured through compression moulding and injection moulding. (○) Compression moulded PP/flax, (●) compression moulded MA-PP/flax, (Δ) injection moulded PP/flax and (▲) injection moulded MA-PP/flax composites. Also shown are data for injection moulded short glass fibre/MA-PP composites (GRPP) (Source: Fu et al., 2000). (The dotted line is a linear fit of compression moulded PP/flax composites, plotted by Slide Write program, with an R^2 value of 0.96 and the error bars show standard deviations).

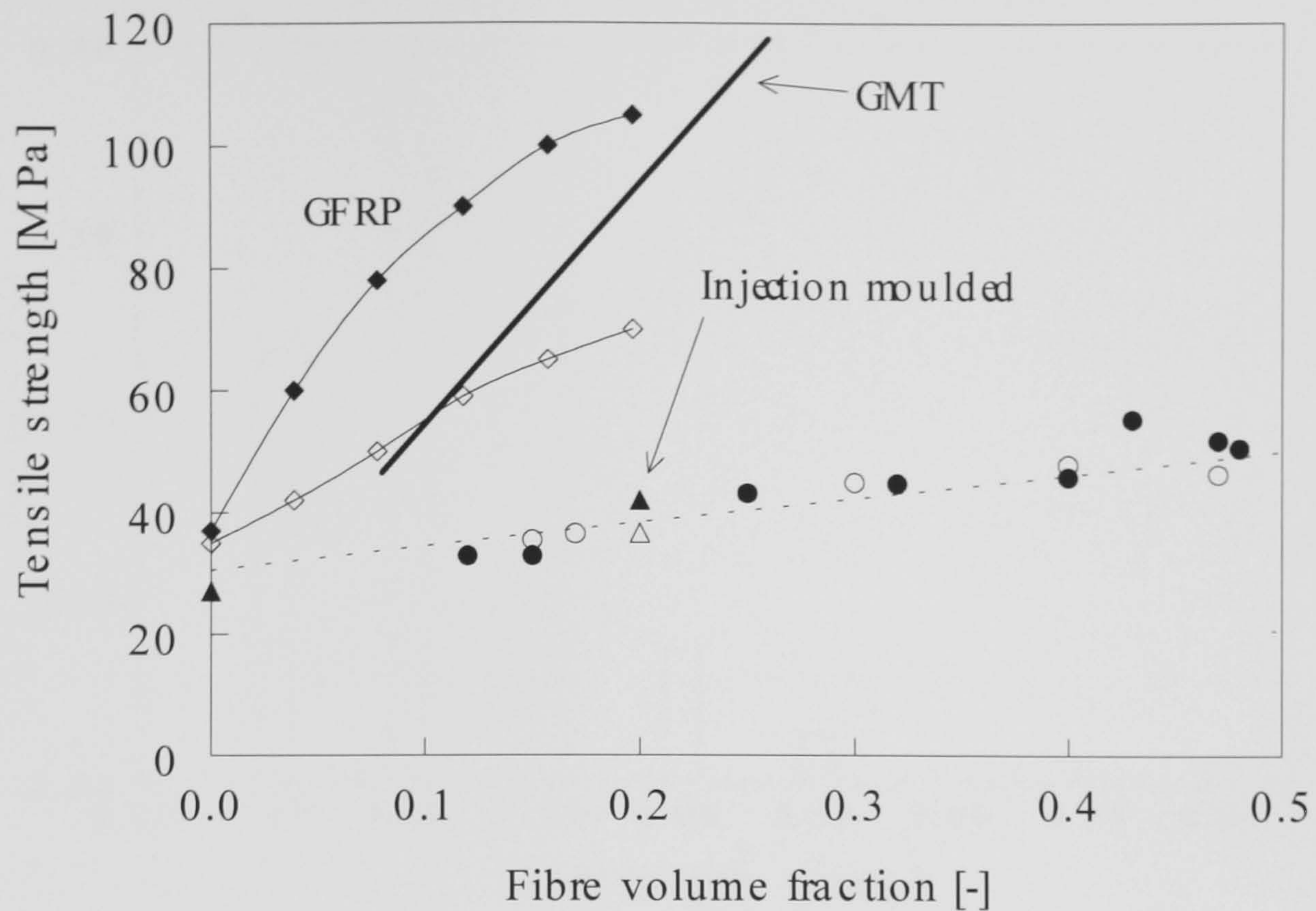


Figure 6.10 Tensile strength of Duralin flax/(MA)PP composites manufactured through compression moulding and injection moulding. (○) Compression moulded PP/flax, (●) MA-PP/flax, (△) injection moulded PP/flax and (▲) injection moulded MA-PP/flax composites. Also, shown are the data (Gibson, 1995) for injection moulded (sized) glass fibre reinforced PP (GFRP) with (◆) and without (◇) compatibiliser MA-PP. The dotted line is a linear fit (obtained by Slide Write program) of strength data of compression moulded PP/flax composites with an R^2 value of 0.91. The data of GFRP is fitted by Spline curves using Slide Write program.

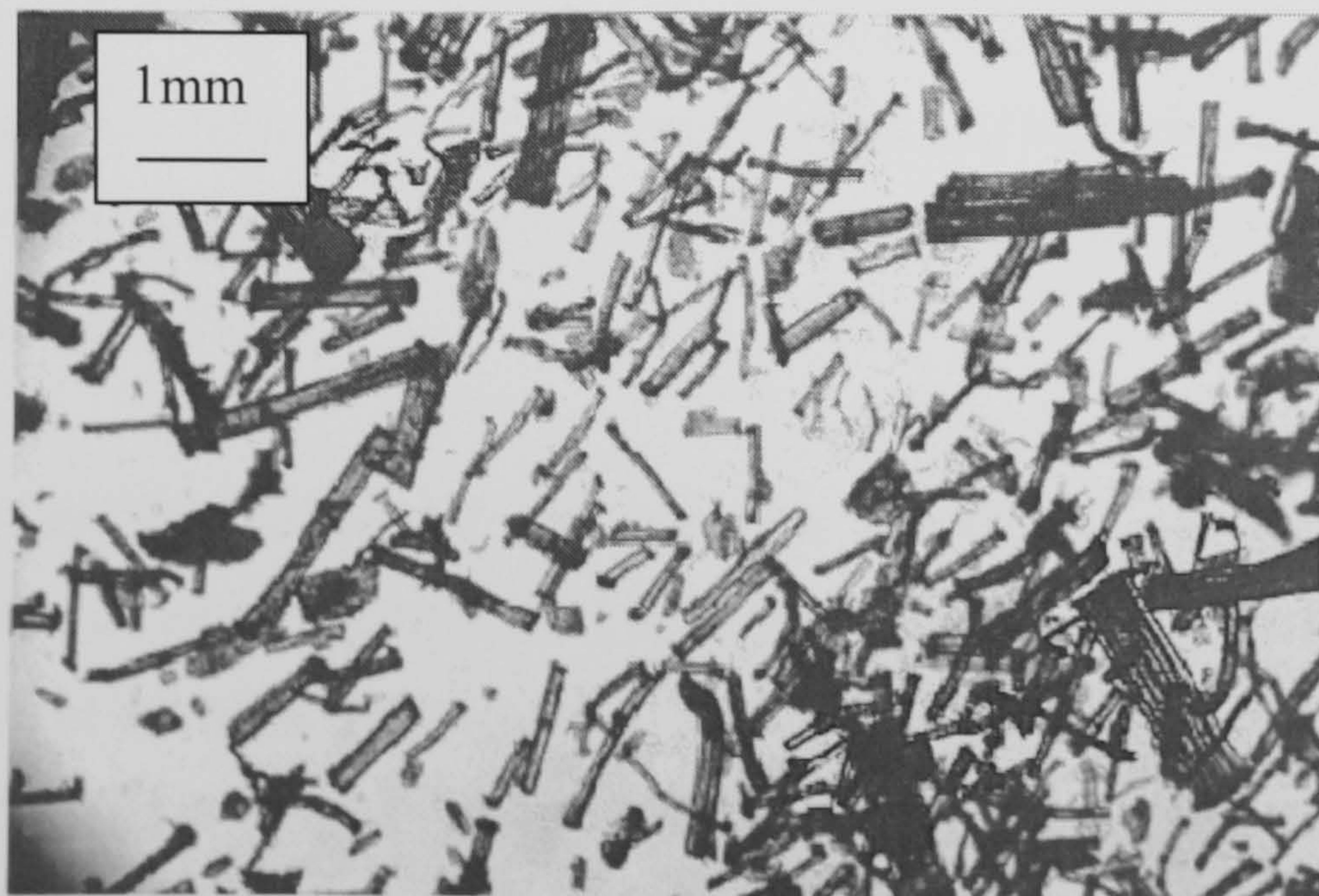


Figure 6.11 The picture of Duralin flax fibres left after dissolution of (MA)PP matrix polymer in injection moulded composite.

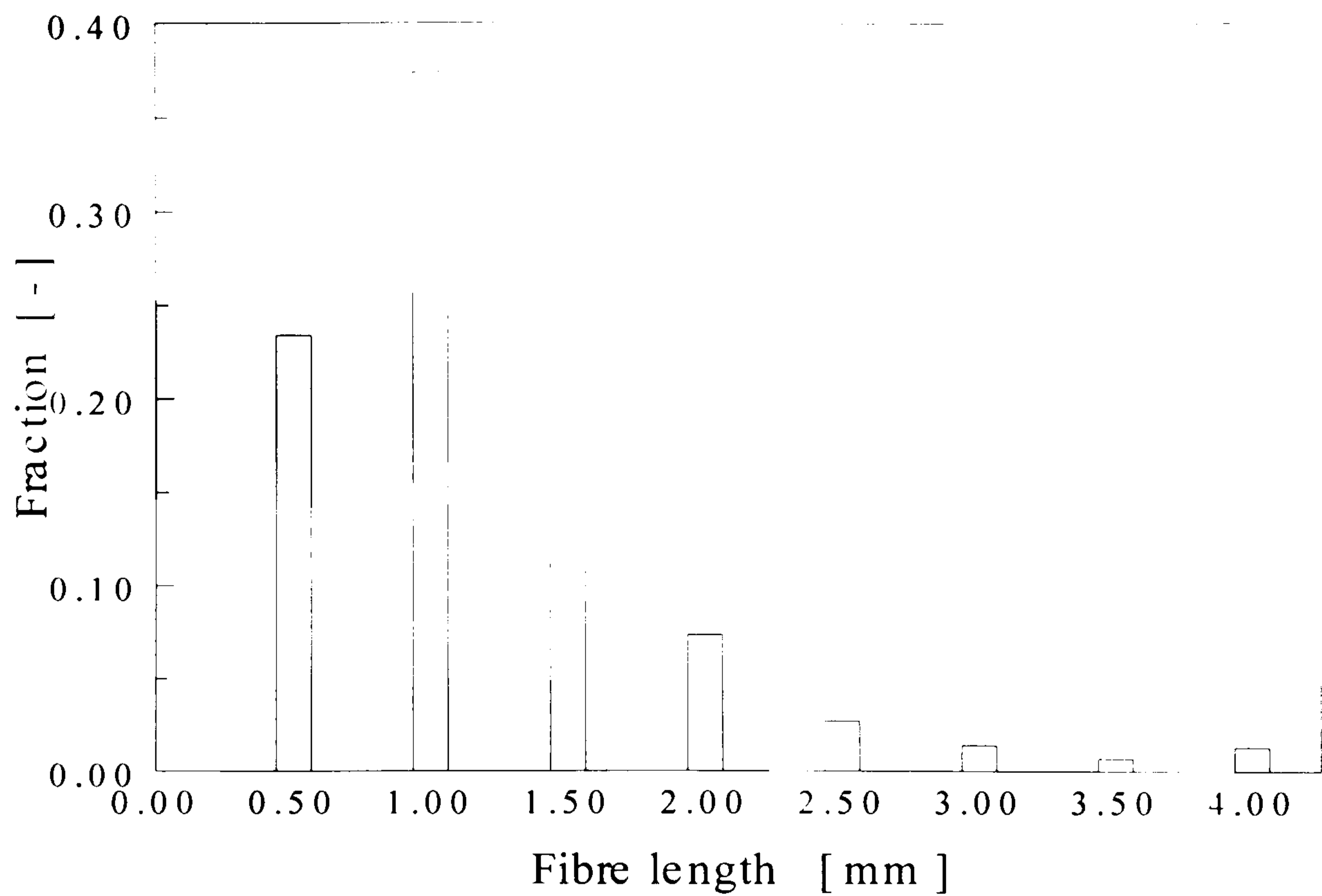


Figure 6.12 Fibre length distribution measured after dissolving the matrix (in hot xylene) in injection moulded composite containing 20 volume% Duralin flax.

The influence of MA-PP concentration on composites, which were manufactured through injection moulding (compounding via a kneader), was investigated. The materials investigated consisted of composites with 20 vol. % of short flax fibres. As reference a pure PP matrix was used. The tensile modulus of the injection moulded Duralin flax/(MA-)PP composites is given in Figure 6.13. From Figure 6.13 it can be seen that the modulus results show an approximately constant value of 6.2 GPa and 1.7 GPa for the 20 volume% series and the reference PP material, respectively. As expected no influence of fibre/matrix adhesion on composite stiffness was observed.

The tensile strength values of the injection moulded Duralin flax/(MA-)PP composites are given in Figure 6.14. The matrix tensile strength shows a constant value of around 30 MPa. On increasing the amount of MA-PP in flax/(MA-)PP composite (20% fibre volume content) a maximum tensile strength was observed at 20 wt% MA-PP.

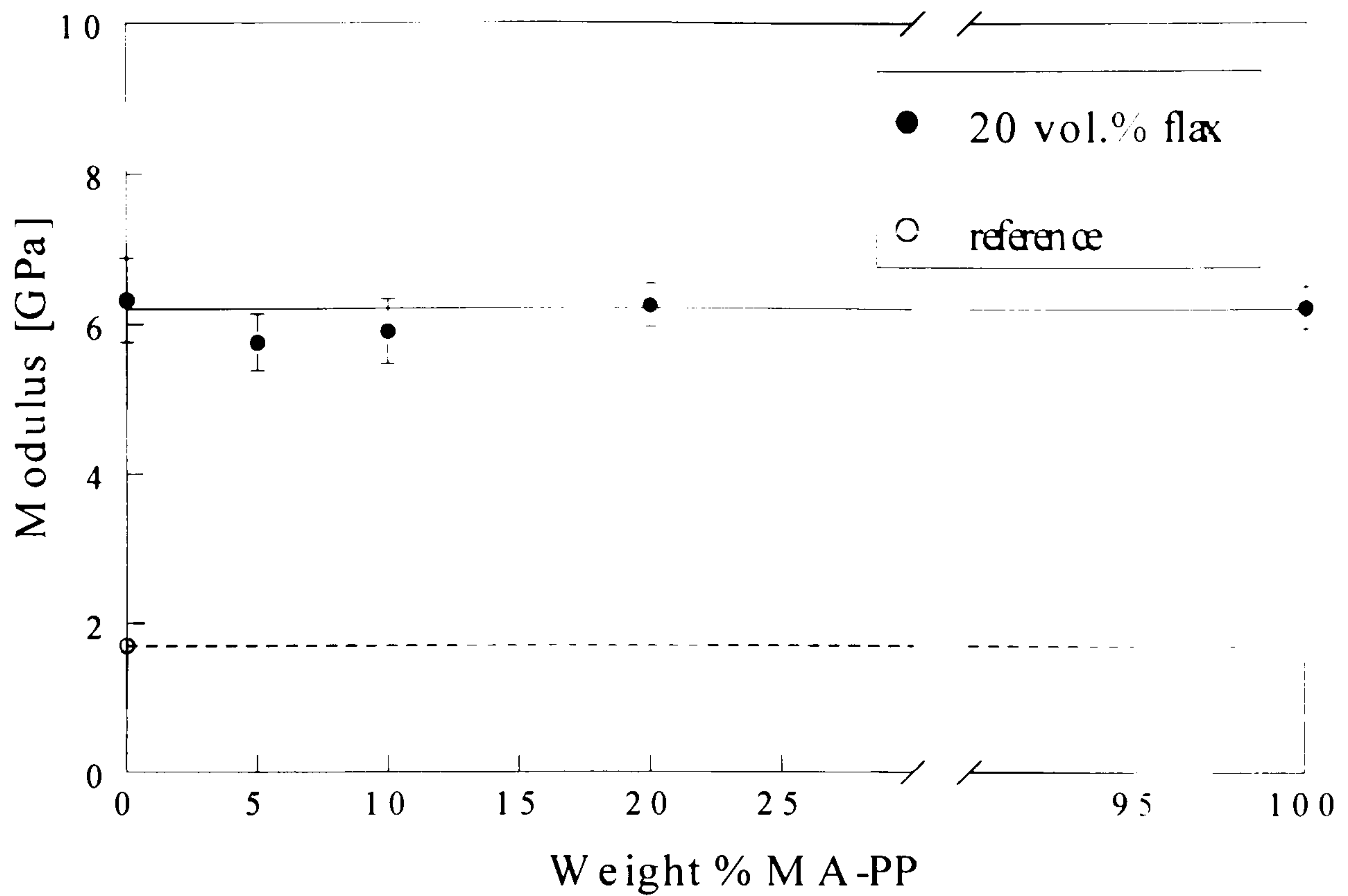


Figure 6.13 Tensile modulus of injection moulded Duralin flax/(MA-)PP composites with varying amount of MA-PP content in the matrix (Error bars shown in the figure are standard deviations and the solid and dotted lines are horizontal reference lines).

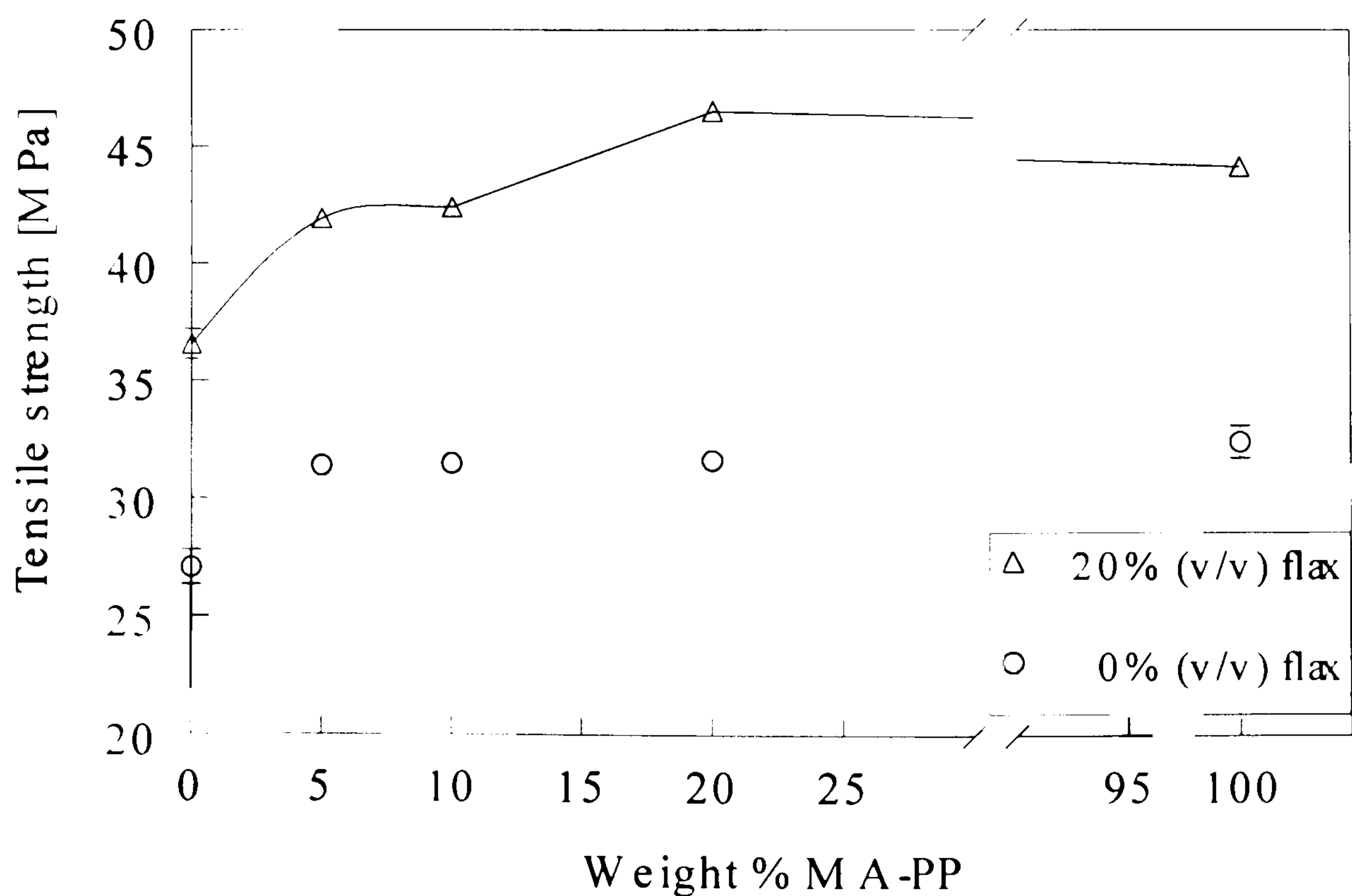


Figure 6.14 Tensile strength of injection moulded Duralin flax/(MA-)PP composites with varying amount of MA-PP content in the matrix. The data for flax/(MA)PP composites are fitted by Spline curve using Slide Write program.

However, optimum interfacial shear strength was observed at 10wt% MA-PP content, in micro-composites, measured through micro-debond tests (Chapter 3). The observed optimum in micro-debond results is not directly reflected in the macro-composites properties, which can be because of effect of fibre volume fraction (single fibre versus real composite).

The tensile properties of flax/PP composites, compounded through various methods followed by injection moulding, are given in Table 6.3. From the Table 6.3 it can be concluded that an increase of testing temperature led to a drop in tensile properties. Addition of higher fibre contents, in the case of the fibre pelletising method followed by double screw extruder did not lead to improvement in the tensile properties. Such behaviour could be because of the reduction in fibre length as well as fibre degradation but addition of 3wt% MA-PP led to enhancement in the tensile properties. The composite tensile properties were even less than the tensile properties of pure PP, which was compensated by addition of coupling agent MA-PP.

Table 6.3 Tensile properties of flax /PP composites. (Impact type = notched Charpy Impact test).

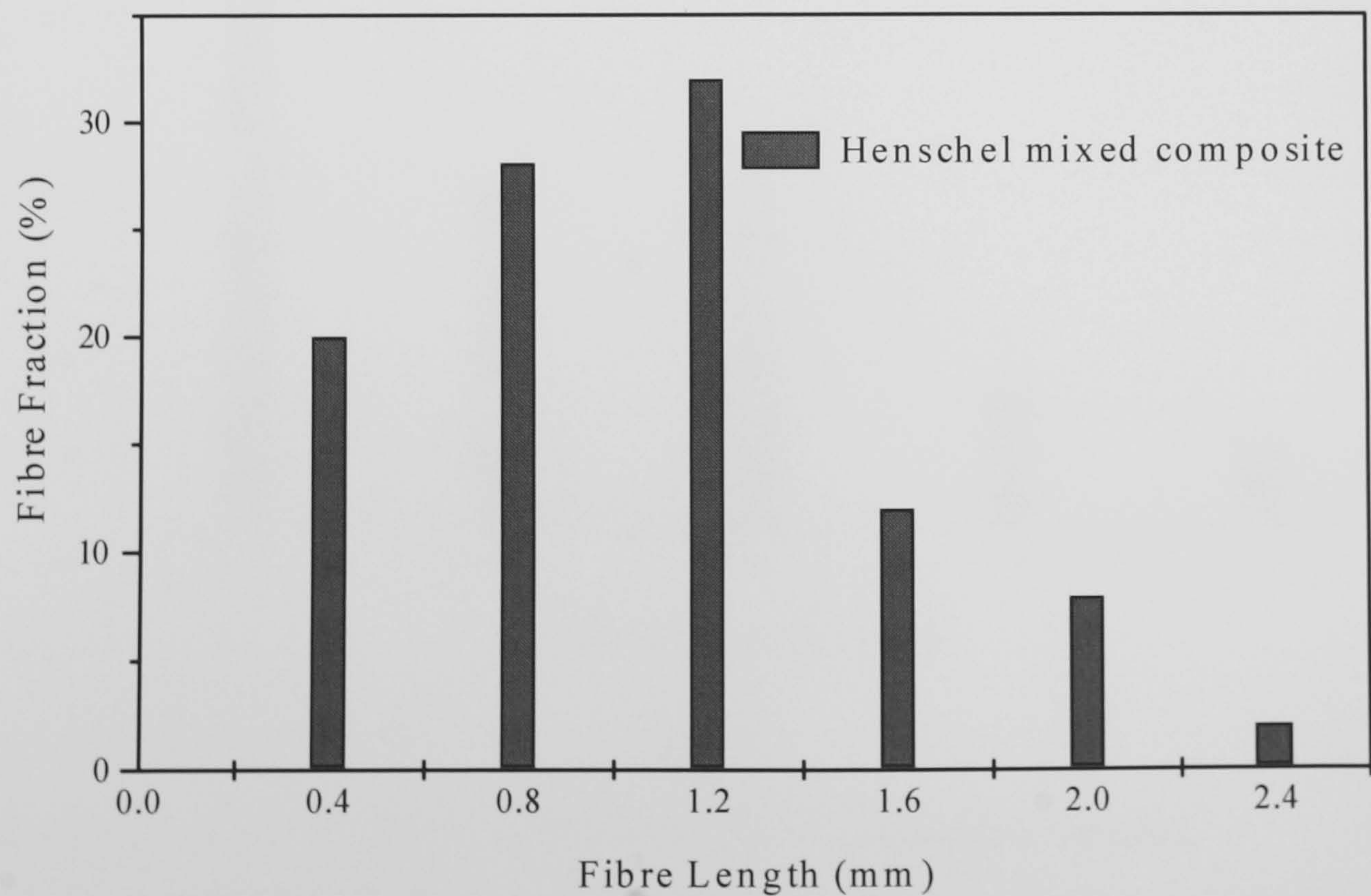
Method	Polymer Type PP	Reinforcement Wt%	Testing Condition °C	Tensile Strength MPa	Young's Modulus GPa	Impact Strength kJ/m ²	
Double screw Extruder	PP	0	RT	32 ± 1	2.0 ± 0.16	1.81 ± 0.35	
	PP /MA-PP (3wt%)	0 (MA-PP = Polybond)	RT	34.5 ± 1	2.0 ± 0.15	2.03 ± 0.14	
	PP	10% Duralin fibre pills	-25	49 ± 0.21	4.2 ± 0.13	1.83 ± 0.28	
			RT	29.3 ± 0.36	2.1 ± 0.19		
			+80	13.2 ± 0.07	0.58 ± 0.1		
	PP	20% Duralin fibre pills	-25	45.7 ± 0.93	5.3 ± 0.13	1.88 ± 0.13	
			RT	28.8 ± 0.94	2.6 ± 0.16		
			+80	13.3 ± 0.06	0.7 ± 0.15		
	PP	25% Duralin fibre pills + 3% Polybond 3150	RT	35.2 ± 0.27	4.2 ± 0.26	3.4 ± 0.14	
			+80	19.9 ± 0.79	1.6 ± 0.13		
	Kneader	PP	28% Duralin + 5% Polybond	RT	42 ± 0.35	6.2 ± 0.4	–
	Henschel Mixer	PP	27.5 % Duralin fibre + 2.5% MAPP	-25	39.92 ± 1.4	4.5 ± 0.16	–
RT				32.0 ± 0.8	3.8 ± 0.45		
+80				25.35 ± 1.8	2.5 ± 0.37		
Long fibre granules	PP	30%Dew-retted fibre	-25	41.1 ± 0.64	6.0 ± 0.21	5.3 ± 0.23	
			RT	32.1 ± 1.25	4.8 ± 0.5		
			+80	24.3 ± 2.32	4.1 ± 0.59		
		30% Duralin fibre	RT	35 ± 0.8	5.0 ± 1.19	7.23 ± 0.87	

Table 6.4 shows the effect of injection rate, during injection moulding, on the tensile strength of flax/PP(112MN40) composite. As observed the increase in the injection pressure led to minor improvement in the tensile properties. Such improvement in the tensile properties could be due to the improved fibre orientation along the polymer flow and hence along the tensile bars.

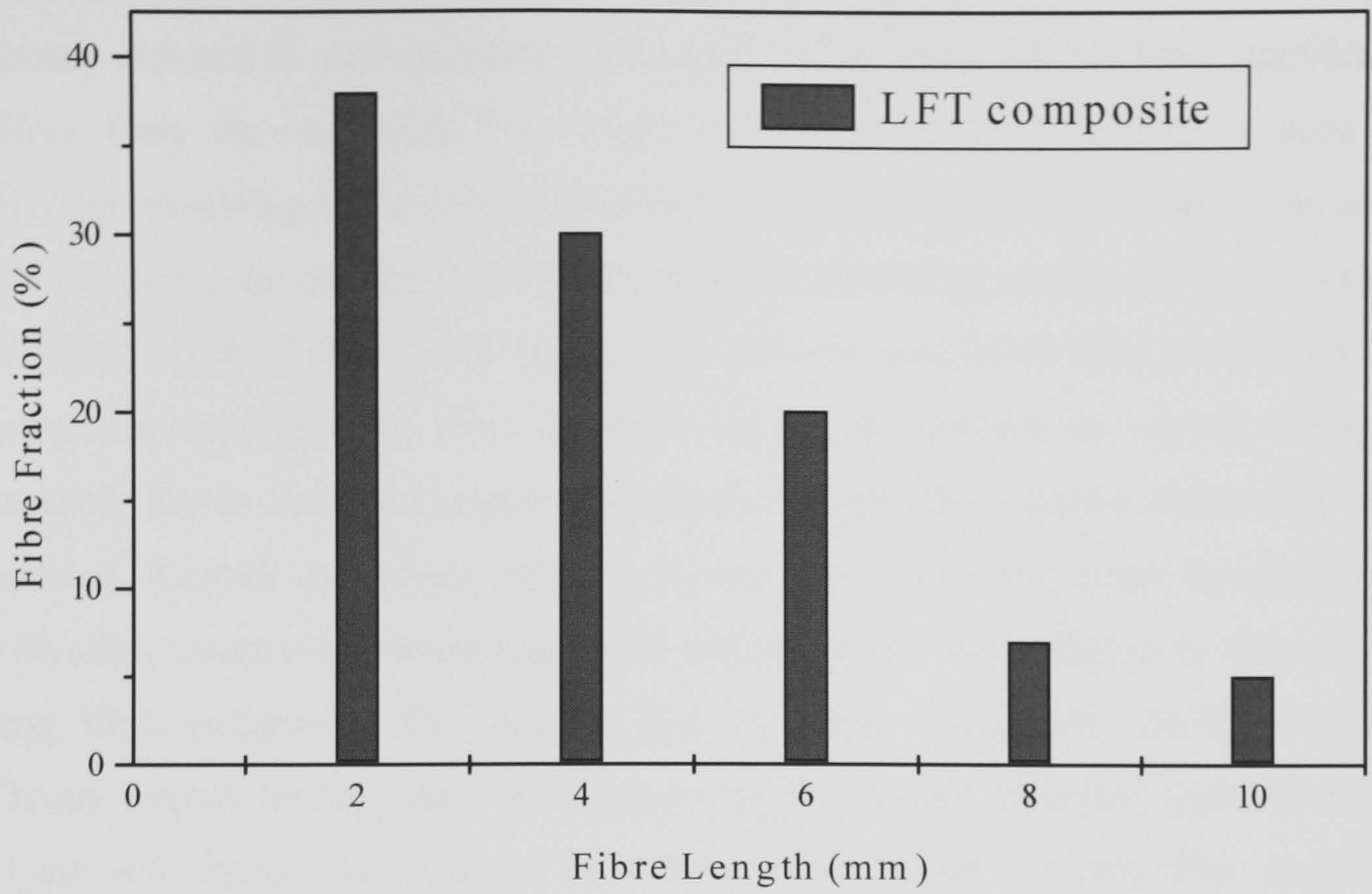
Table 6.4 Effect of injection rate during injection moulding on the tensile properties of flax/PP (112MN40) composite. Fibre loading 20 wt%.

Injection Speed (cc/s)	Tensile Strength (MPa)	Young's Modulus (GPa)
11	28.74 ± 0.23	2.34 ± 0.8
17.6	28.97 ± 0.14	2.47 ± 0.23
26.40	28.77 ± 0.09	2.63 ± 0.16
35.20	29.5 ± 0.11	2.8 ± 0.28
44	29.71 ± 0.60	2.8 ± 0.32

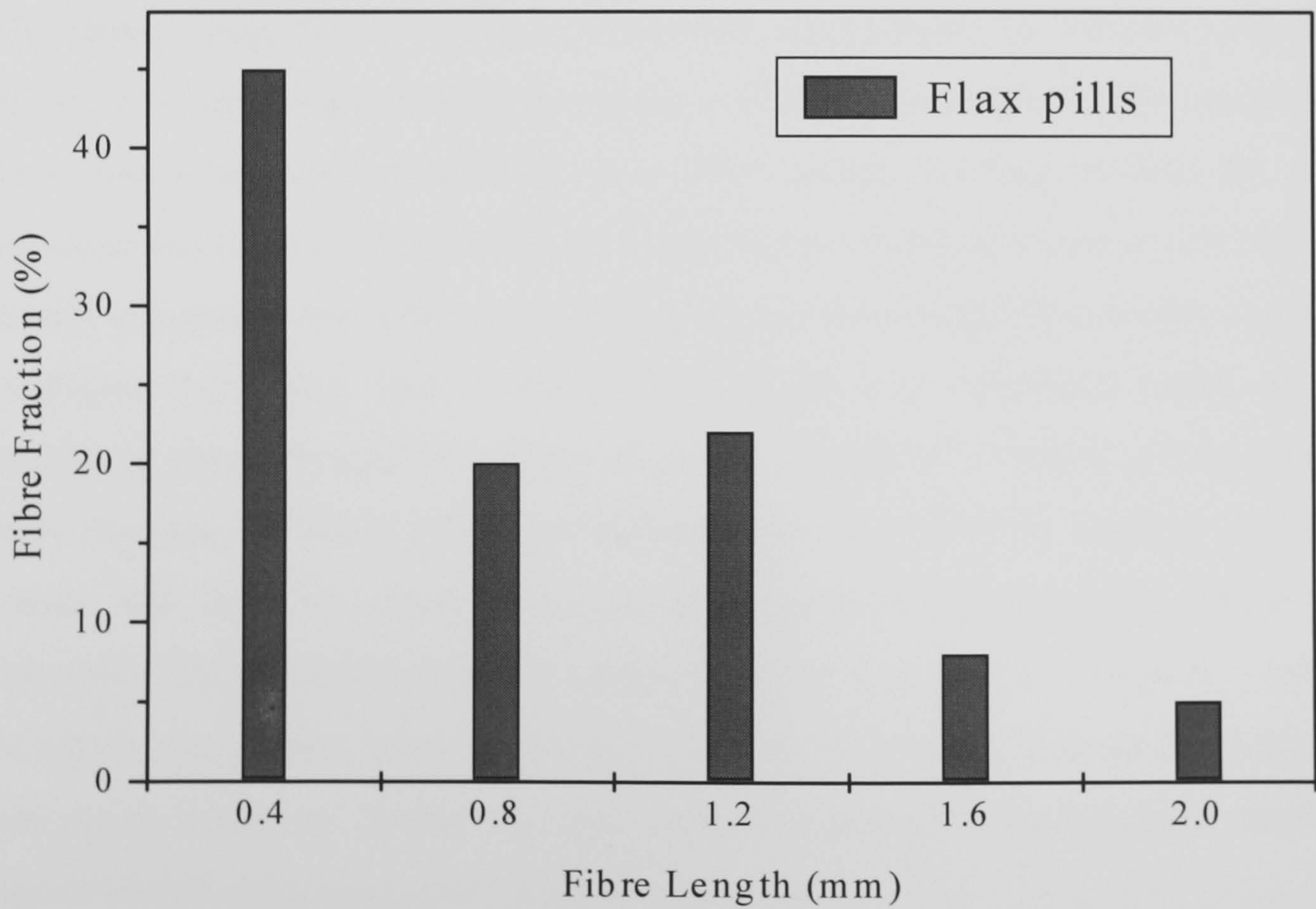
In order to find out the fibre length distribution, fibres were extracted from the moulded parts and fibre length was measured. The fibre length distribution in injection moulded samples is given in Figure 6.15.



(a)



(b)



(c)

Figure 6.15 Fibre length distribution in injection moulded samples.

On comparing Figure 6.15 with the fibre length distribution in Figure 6.7 it can be stated that injection moulding led to fibre length reduction in the case of long fibre

granules. In the case of Henschel compounded granules the fibre length was already reduced to such an extent that injection moulding did not have significant effect. Only the maximum fibre length reduced from 3.6 to 2.4mm because of injection moulding in the case of Henschel compounded granules. Also, in the case of extrusion compounded flax/PP, the injection moulding process led to reduction in fibre length. From Table 6.3 it can also be concluded that production of composite through long fibre granules led to an increase in impact strength probably due to increased energy absorption through fibre fracture, debonding and pull-out. As such the impact strength of long fibre composite cannot be compared with other composites, as the composite fracture mode was different. In the case of long fibre composites the samples did not break completely, during notched Charpy impact testing, and the presence of a skin-core structure was observed. Figure 6.8 shows the presence of a skin-core structure in long fibre granules reinforced with natural fibres (30wt%).

The tensile properties of various composites compounded by various techniques followed by injection moulding are given in Figure 6.16 and 6.17. For comparison these properties were normalised to a fibre weight fraction of 30% by using micromechanical models (Chapter 5). Kelly-Tyson model was used to calculate the tensile strength of the composites. For the same, the average fibre length as shown in Figure 6.15 was used. Critical fibre length was calculated based on the interfacial shear strength of 10MPa, the fibre strength of 750MPa and an average fibre diameter of 30 μ m. Fibre orientation factor (η_o) of 0.571 (instead of 0.375, which was used for compression moulded composites) was used, which was calculated via fitting the stiffness values of injection moulded composite with the Cox-Krenchel model. Fibre efficiency parameter (k) of 0.312 was used, which was calculated based on fitting the experimental values of the injection moulded flax/(MA)PP composites with the theoretical values.

Cox-Krenchel model was used to calculate the stiffness of the composites. For the same, as mentioned above, the fibre orientation factor (η_o) of 0.571 was used. Fibre stiffness of 42GPa was used for the calculations.

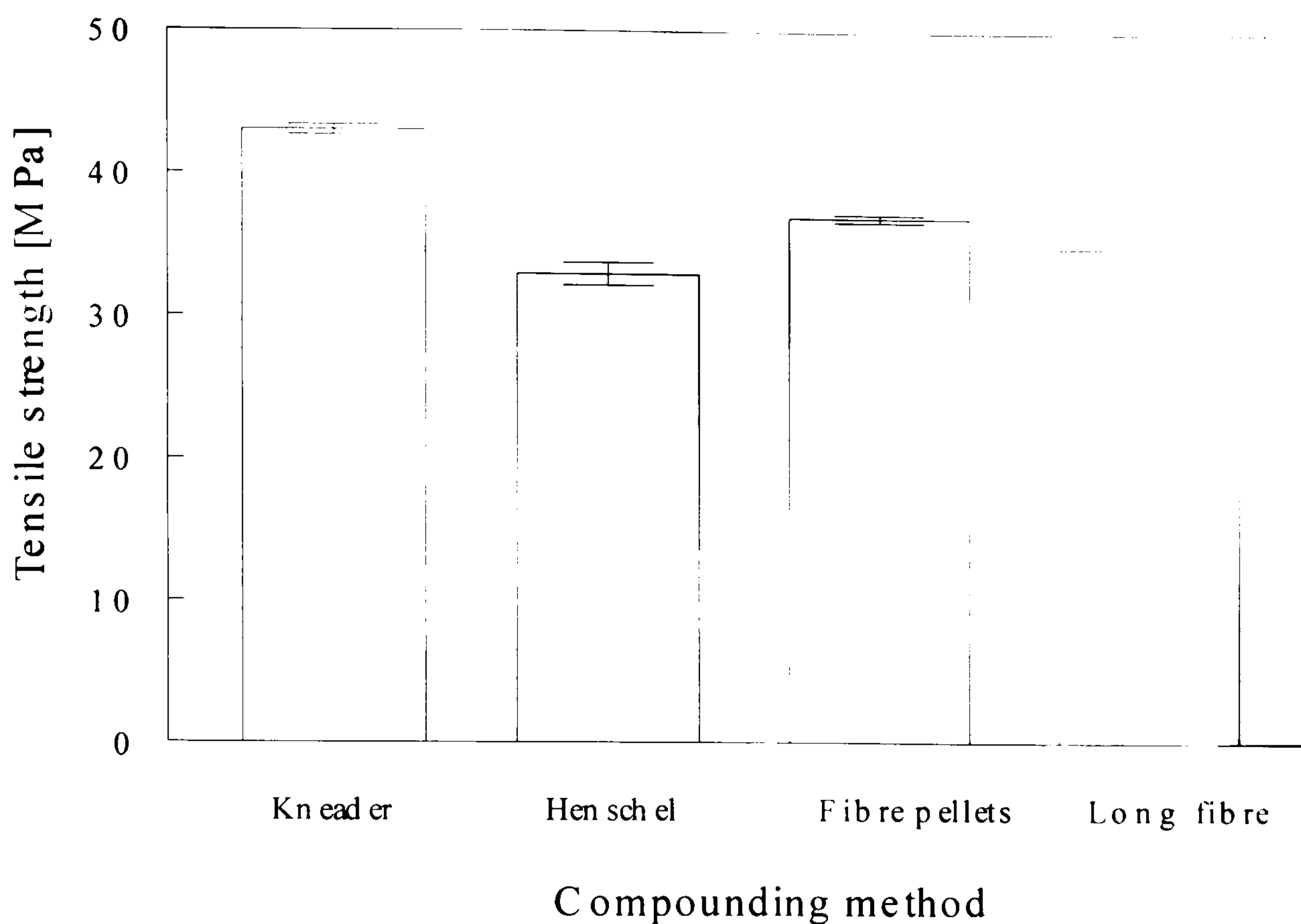


Figure 6.16 Tensile strength of injection moulded Duralin flax/(MA-)PP composites compounded through various methods (Fibre weight fraction = 30%; error bars show standard deviations).

As seen from Figure 6.16, compounding through kneader led to highest tensile strength. However it is worth mentioning here that long fibre composites did not contain any coupling agent and addition of the same is expected to enhance the tensile properties of the composites. The tensile strength of kneader compounded composite was better than Henschel compounded as well as twin screw extrusion (fibre pellets) compounded composites, which was probably because of longer fibre lengths in the kneader compounded composite as seen from the fibre length distribution in the composites. Batches with small quantities were made in the lab scale kneader and hence this method is not appropriate for large scale production. Production trials in the large scale kneaders have to be done to see the effect of scale on the properties of the composite. Though fibres were longer in the case of LFT still tensile strength was lower than composites made via kneader compounding. Such a difference could be because of effect of coupling agent, which was not used in the case of LFT.

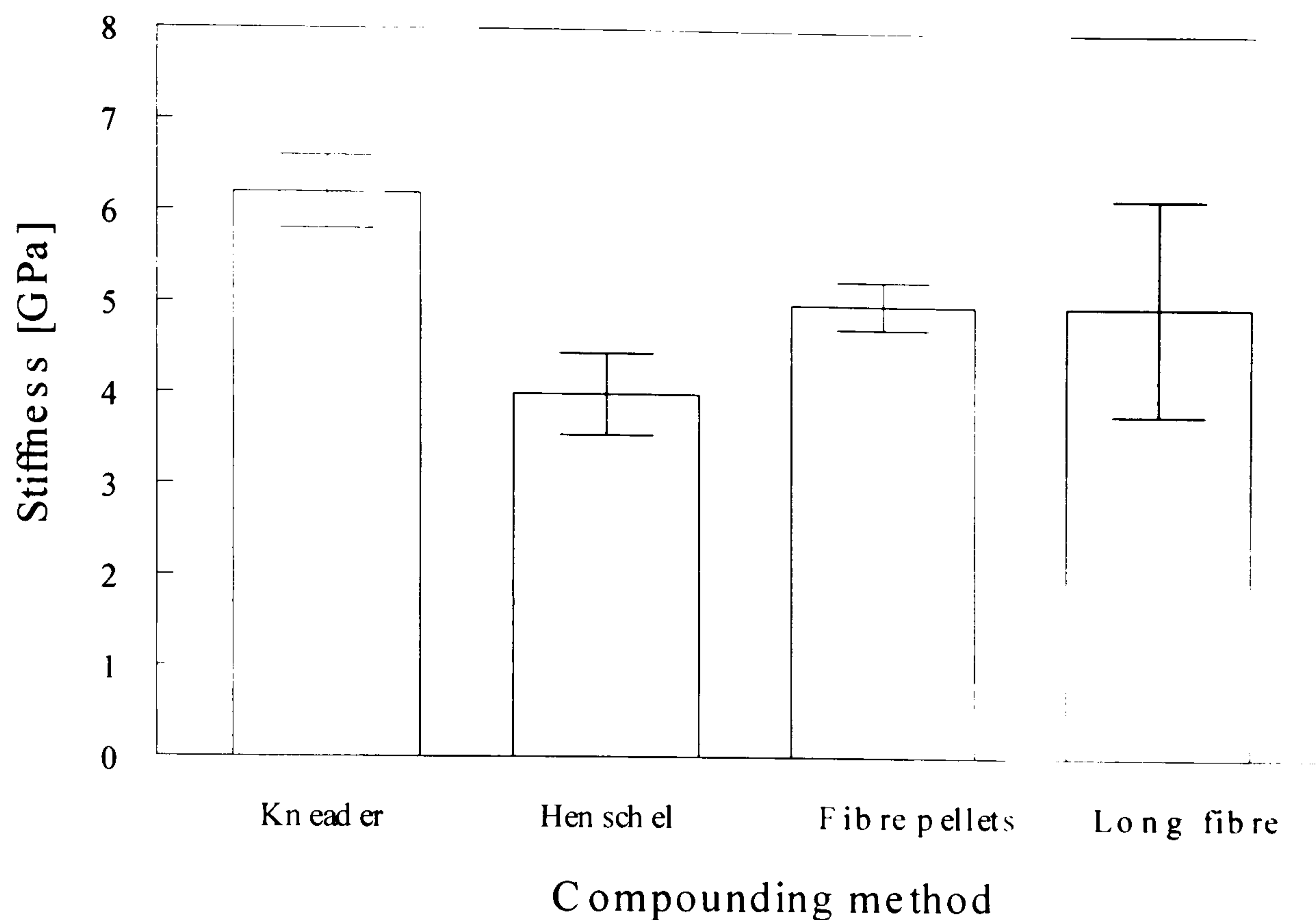


Figure 6.17 Stiffness of injection moulded Duralin flax/(MA-)PP composites compounded through various methods. (Extrapolated to fibre content of 30weight% using Cox-Krenchel micromechanical model; error bars show standard deviations).

Similar to tensile strength the stiffness of ‘kneader compounded’ composite was found to be highest among composites manufactured through various compounding methods. However such a difference in stiffness cannot be attributed to longer fibre length retention as well as adhesion enhancement through addition of coupling agent, as in the case of composite strength. The difference could be related to the fibre dispersion in the matrix.

6.3.2.2 Short fibre composites based on other thermoplastic matrices

Although several thermoplastics are used as a matrix material for composites, polyamides (Nylons) are one of the most used matrix materials for composites based on glass fibres, especially for less demanding (low-performance) products. The performance as well as thermal stability of natural fibres limits its application

to few thermoplastics. In Western-Europe polyamides account for more than half of the market share (Bijsterbosch, 1992). Considering the thermal stability of natural fibres, the processing temperature of Nylon6 (225°C) is almost at the edge of the processability of natural fibres. Another engineering polymer is polyoxymethylene (POM), which can be processed at comparatively lower temperature of around 170°C. Some of the applications involving POM polymer include rollers, bearings, gearwheels, housing parts etc and the mechanical as well as thermal performance of the polymer is improved by addition of glass fibres.

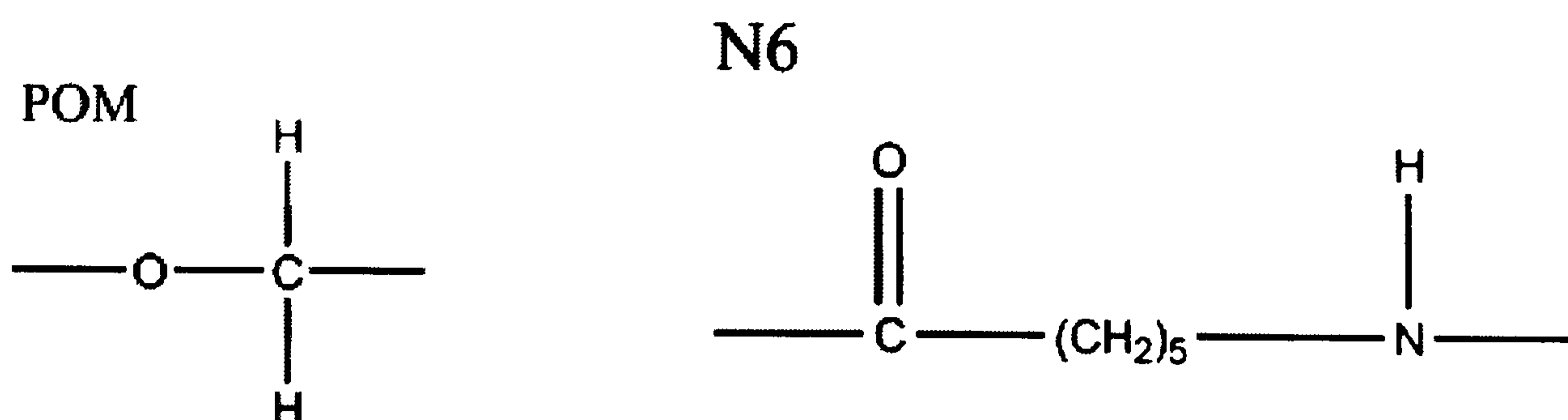


Figure 6.18 Chemical structure of POM and Nylon6.

Table 6.5 shows the effect of addition of Duralin flax fibre in Nylon6 and POM matrices. Addition of 30wt% flax led to 23% increase in the tensile strength of Nylon6. This improvement in strength was similar to the improvement in PP/flax composite (31% improvement) compounded by kneader. Nylon6/flax composites were also compounded by kneader. No significant improvement was observed in the case of POM thermoplastic, which was compounded with flax by a twin-screw extruder. The dependence of difference in the improvement in tensile properties of Nylon6 and POM on the differences in compounding methods needs to be ascertained by further study.

Table 6.5 Tensile properties of flax /Nylon, glass /Nylon, flax/POM and glass/POM composites.

Composite	Tensile Strength MPa	Tensile Modulus GPa
PA	67 ± 2.28	2.7
Flax /Nylon (31 fibre wt %)	90.8 ± 1	8.5
Glass/Nylon (32 fibre wt%)	200	9.4
POM	61 ± 1	2.6
Flax/POM (30 fibre wt%)	62 ± 1	5.7 ± 0.5
Glass/POM (30 fibre wt%)	125	9.3

6.4 Conclusions

Based on the comparative study between compression moulded and injection moulded Duralin flax/PP composites, it can be concluded that the reduction in fibre length associated with injection moulding did not affect the tensile properties significantly. The reduction in the fibre length may be counterbalanced by improvement in the fibre orientation along the polymer flow and fibre efficiency through dimensional changes. The addition of MA-PP led to improvement in the tensile strength of injection moulded composite. The optimum at 20wt% MA-PP content observed for injection moulded composite was different when compared with the micro-mechanical study where an optimum was observed at 10wt% MA-PP. The difference could be because of effect of fibre volume fraction (single fibre specimen versus real composite).

Compounding of flax with PP was carried out by four different methods: kneader, Henschel kinetic mixer, production of LFT granules through pultrusion and extrusion compounding. The problem of fibre feeding, in the case of fluffy flax

fibres during mixing with polymer via extruder, can be solved through the application of the Amandus Kahl pelletising method. The pelletising method is cheaper than the long fibre granulation method, also more uniform granules are obtained when compared with mixing by kneading. From the analysis of fibre length distribution in compressed fibre pills as well as compounded material, it was found that considerable fibre breakage occurs in the compounding stage itself in the case of kinetic mixing and extrusion.

The fibre addition through fibre pills followed by extruder led to reductions in tensile strength when compared to pure PP. However the addition of the coupling agent MA-PP led to improvement in the tensile properties. Due to higher fibre length through the LFT method, increased composite toughness was observed. Kneader compounded composites showed maximum tensile strength as well as stiffness when compared with other compounding methods. This could be because of higher fibre length retention, as observed by fibre length distribution, as well as higher fibre matrix adhesion in the system studied. However, further improvement in tensile properties, on addition of coupling agent, in the case of LFT composites is expected. The effect of fibre addition on the tensile properties was more pronounced in the case of Nylon6 when compared with POM. The difference could also be due to the differences in compounding methods. Further study, which could involve compounding Nylon6 and POM by different methods, is required to find the reason behind the above mentioned difference.

7. ENVIRONMENTAL PROPERTIES OF FLAX/POLYPROPYLENE COMPOSITES

In this chapter, the literature and theory of moisture absorption by composites are introduced. The results showing the effects of aqueous exposure of flax-PP NMT composites on the moisture pick-up, dimensional stability and the mechanical properties are reported and discussed.

7.1 Introduction

A major restriction in the successful use of natural fibres in durable composite applications is their high moisture absorption and poor dimensional stability (swelling) as well as their susceptibility to rotting. Swelling of fibres can lead to micro-cracking of the composite and degradation of mechanical properties. Moisture absorption of composites based on natural fibres depends on the physical structure as well as the chemical structure of the fibres and their interaction with the matrix material. Giridhar et al. (1986) have shown that the moisture absorption of natural fibre reinforced thermoset resins depends on the level of resin absorption into the fibre prior to curing, the cellulose content of the fibre and the resin-fibre interface. They have shown that sisal fibre (a natural fibre) absorbed less moisture content than jute fibre (also a natural fibre) mainly because of its compact structure but the former absorbed higher moisture content after impregnation (and curing) with an epoxy resin. This striking disparity between jute and sisal composites were attributed on one hand to the basic compactness of sisal fibres (and hence low moisture absorption of virgin sisal fibres as compared to that of virgin jute fibres), and on the other hand to the high cellulose content of sisal fibres (and hence the

lower reduction in the moisture absorption level of virgin sisal as compared to jute upon impregnation with the resin). Thus, according to Giridhar et al. (1986), the basic compactness in the physical structure of the fibre accounts for the absorption level in an unimpregnated (virgin) fibre, the chemical nature (cellulose content) appears to govern largely the absorption behaviour of an impregnated fibre (the composite). Also, the higher moisture absorption in sisal /epoxy composite could be due to the poor interfacial adhesion (or reduced resin absorption). In the case of jute/epoxy composites it has been shown that the velocity of moisture absorption and the moisture content at equilibrium distinctly increase with increasing fibre content. This increasing moisture absorption is attributed to the higher hydrophilic nature of the jute fibre compared to the matrix and the higher amount of interfacial areas (capillary effect) in the fibre and composites. Lowered moisture at equilibrium on application of chemically treated cellulose fibres (e.g. silanized or polyvinylacetate treatment), because of reduced amount of hydroxyl groups free to bind moisture, has been reported (Gassan and Bledzki, 1999).

7.1.1 Effect of moisture absorption on composites' properties

The absorbed moisture affects the fibre/matrix interface and hence the mechanical and physical properties of the composites. The fibre modification has shown to reduce the effect of moisture absorption on some of the mechanical properties of composites. The reduced effect of moisture absorption on the mechanical properties has been attributed to the improved fibre/matrix bonding which reduce the moisture-caused fibre-matrix debonding. For instance, the drop in the normalised tensile strength (ratio of tensile strength after cyclic moisture treatment to that before treatment) in the case of treated jute fibre/epoxy composites was same as that of untreated composites. However, the effect of cyclic moisture treatment on the normalised stiffness was found to be more prominent in the case of untreated jute/epoxy composites than treated jute/epoxy composites. On the other hand impact energy is shown to increase with increasing number of moisture treatment cycles, in the case of treated jute/epoxy composites, because of enhanced energy absorption due to increase in fibre/matrix debonding (Gassan and Bledzki,

1999). Unlike cyclic moisture treatment, which involves repeated cycles of wetting followed by drying, storage of modified jute/epoxy composite in distilled water was reported to have no significant effect on the tensile strength of composites (Gassan and Bledzki, 1997). Also, the effect of moisture on the stiffness of composites was distinctly weaker when the coupling agent was used. Karmaker et al. (1994) have shown that moisture absorption by jute fibres leads to swelling which fills the gap between the fibre and (PP) matrix, caused by thermal shrinkage of polymer melt. The increased tensile strength of jute fibres on wetting as well as because of swelling of jute fibres, causing a radial pressure on polymer matrix, results in higher values of shear strength.

7.1.2 Modelling

Different models have been developed in order to describe the moisture absorption of materials (Springer, 1981). A problem, in which the temperature and the moisture distribution inside the material are to be determined, is often referred to as the 'moisture problem'. Such problems can be solved analytically and the moisture absorption can be called 'Fickian' when the following assumptions can be made:

1. Heat transfer is by conduction only and can be described by Fourier's law.
2. A concentration dependent form of Fick's law can describe moisture diffusion
3. The temperature inside the material approaches the equilibrium much faster than the concentration gradient, hence the energy (Fourier) and the mass transfer (Fick) equations are decoupled
4. The thermal conductivity and the mass diffusivity depend only on the temperature and are independent of moisture concentration or of the stress levels inside the material

Calculations can be made requiring knowledge of the following parameters:

1. Geometry (material thickness h in case of a 1-dimensional problem).

2. Boundary conditions: ambient temperature and relative humidity (100% in case of immersion).
3. Initial conditions: temperature and moisture concentration M_i inside the material.
4. Material properties: density ρ , specific heat C , thermal conductivity K , mass diffusivity D , maximum moisture content M_m and a relationship between the maximum moisture content and the ambient conditions.

Mass diffusion coefficient (D) characterises the speed at which moisture is transported through the material. The value of D depends on the material, on the fluid surrounding the material, on the moisture concentration in the material, on the stress level inside the material and on the temperature. In calculating the moisture content inside the material D is assumed to depend only on temperature. In many practical problems this is an adequate approximation (Springer, 1981).

Rao et al. (1983) reported the validity of the Fickian diffusion model for carefully fabricated jute-epoxy composites, the fibres being permeable both to moisture and the matrix resin.

Whether moisture transported through a composite is by Fickian or by anomalous diffusion depends on the material and on the environmental conditions. Thus, whether or not Fick's law is applicable in a given situation cannot be guessed 'a priori' but must be determined by tests.

The moisture content M_t as a function of the square root of time for a typical Fickian process is schematically given in Figure 7.1. For a one dimensional diffusion process through either side of a solid of finite thickness (h), the relative moisture absorption can be described by the following equation (Springer, 1981):

$$\frac{M_t}{M_m} = 1 - \frac{8}{\pi^2} \sum_{j=0}^{\infty} \frac{1}{(2j+1)^2} e^{-\frac{D(2j+1)^2 \pi^2 t}{h^2}} \quad (7.1)$$

This equation has been used to calculate the diffusivity D and the maximum moisture content M_m of the materials (Springer, 1981).

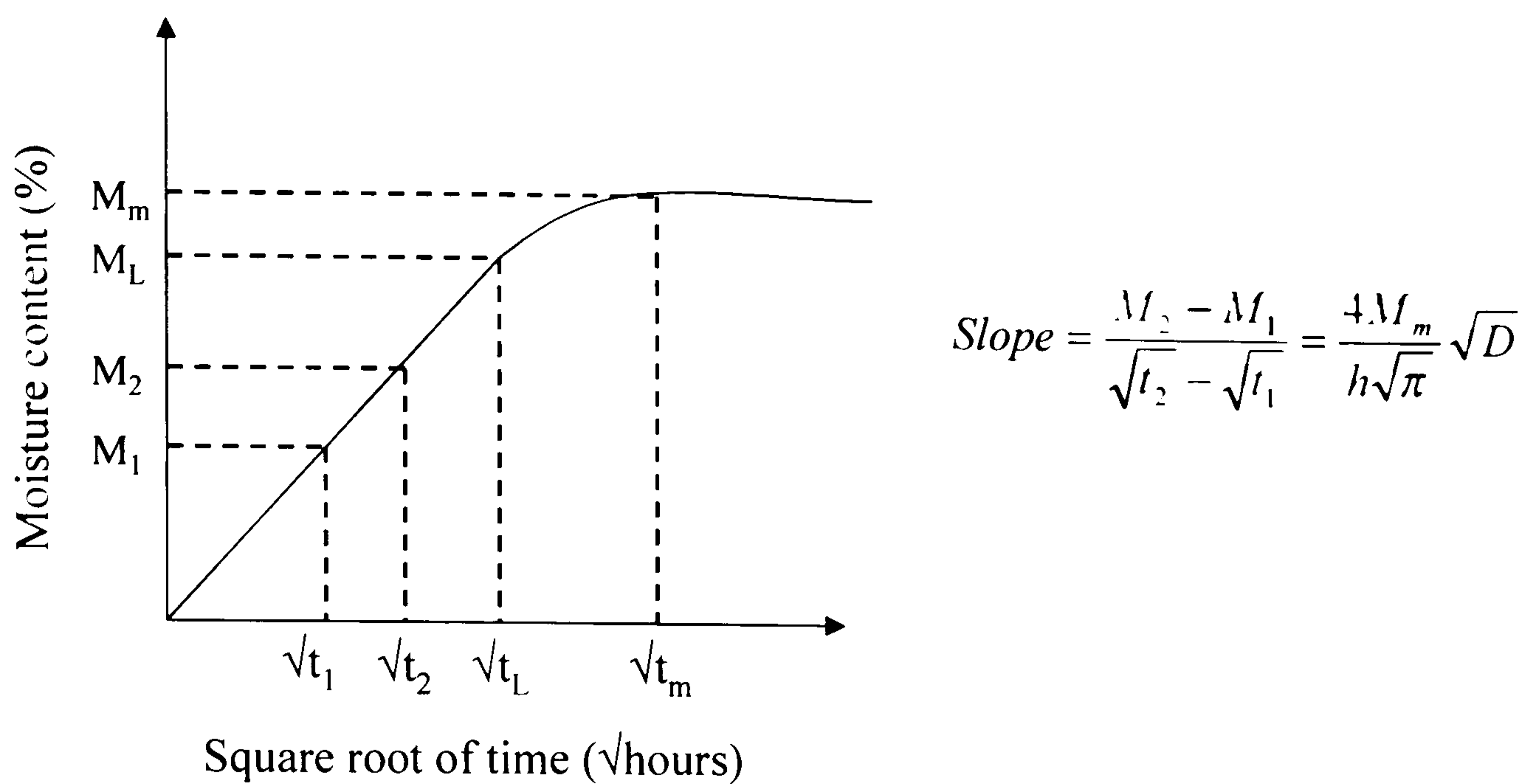


Figure 7.1 Moisture content as a function of time for a typical Fickian process (Springer, 1981).

As discussed in Chapter 2, recently a novel upgrading process for ligno-cellulosic materials has been developed to improve the poor environmental- and dimensional stability of these materials (Ruyter and Hortulanus, 1993). This upgrading process, which was initially developed for wood, has also proven its applicability to natural fibres and has led to the development of upgraded flax, the so-called Duralin flax (Pott et al., 1997). The process is currently commercialised by Ceres B.V. (Wageningen, The Netherlands) and the availability of an upgrading process for natural fibres could remove one of the main restrictions for the successful application of natural fibres in high-quality engineering composites.

In the present chapter a study on the environmental behaviour of natural-fibre-mat-reinforced thermoplastics (NMTs), being glass-mat-reinforced thermoplastic (GMT) -like materials (Berglund and Ericson, 1995) based on flax fibres and a polypropylene (PP) matrix (Heijenrath and Peijs, 1996; Mieck et al., 1996; Mieck et al., 1997; Peijs et al., 1998; Garkhail et al., 2000), is reported and discussed. The effect of the upgrading treatment is evaluated by comparing the moisture absorption, swelling and residual mechanical properties of NMTs based on Duralin- and green-flax-fibre mats. Furthermore, the influence of the fibre/matrix interface on these properties is investigated by using maleic-anhydride grafted PP

(MA-PP) as an adhesion promoter (Felix and Gatenholm, 1991; Mieck et al., 1995b; Bledzki and Gassan, 1997; Peijs et al., 1998; Garkhail et al., 2000).

7.2 Experimental

7.2.1 Flax fibre treatment

The procedure for flax fibre treatment, to develop Duralin flax fibre, is described in Chapter 2. The fibres were supplied by Ceres, Wageningen, the Netherlands. These treated flax fibre bundles were subsequently converted into a non-woven mat by Eco Fibre Products B.V., the Netherlands, via a conventional punch-needling process.

7.2.2 Composite manufacturing

In this study randomly oriented non-woven needled flax fibre mats in combination with an isotactic-polypropylene (PP) matrix of Montell (XS6500S) with a melt flow index of 38 were used. As an adhesion promoter maleic-anhydride modified polypropylene (MA-PP) was used (Felix and Gatenholm, 1991; Mieck et al., 1995b). The blending of PP with a commercially available MA-PP (Polybond 3002, BP Chemical Ltd.) was performed on a Werner and Pfleiderer ZSK 25 co-rotating twin-screw extruder. In this study 5 wt.% of MA-PP was added to the i-PP. For convenience, this blend will simply be designated as MA-PP. Next, the PP and MA-PP pellets were compression moulded into 0.1 mm thick sheets using a hot-press. NMT composites were made using the film stacking method. First, flax fibre mats (250x250 mm, 725 g/m²) were cut and dried in an oven at 60°C for 2 hours. Alternating layers of non-woven flax mats and PP-sheets were stacked and impregnation was achieved by applying heat (200°C) and pressure for about 15 minutes. The composites obtained after cooling had a thickness of approximately 3mm and a fibre volume fraction of about 38%. As a reference, similar composite plates based on non-woven 'green flax' mats were made.

7.2.3 Moisture absorption of composites and testing

The obtained composite plates were pre-dried in an oven at 60°C for one day to reach the initial moisture level. Next, these plates were cut into specimens of 200x200 mm, which were immersed into a tank filled with tap water. Three different types of NMTs were evaluated: (i) treated Duralin flax/PP, (ii) treated Duralin flax/MA-PP and (iii) untreated green flax/PP as a reference.

In order to measure the water absorption of the composites, all samples were immersed in water for about 60 days at room temperature. The weight and the thickness of the NMT plates were measured at different time intervals and the moisture content as well as swell% versus time was plotted. The maximum moisture content $M_{m,c}$ was found from the intercept at the saturation point and the diffusivity D_c was calculated from the slope (Figure 7.1) by fitting Equation 7.2 (Springer, 1981) to the experimental data.

$$Slope = \frac{M_2 - M_1}{\sqrt{t_2} - \sqrt{t_1}} = \frac{4M_m}{h\sqrt{\pi}} \sqrt{D} \quad (7.2)$$

At certain moisture levels tensile tests were performed on test specimens cut from these plates to investigate the effect of moisture on residual strength and stiffness. For each condition ten different samples were tested. The samples were tested in the laboratory having controlled RH of about 60% and temperature of about 20°C.

7.3 Results and Discussion

Figure 7.2 shows the moisture absorption of flax/PP NMT plates as a function of time. By fitting Equation 7.2 to the experimental data, the maximum moisture content in the composite ($M_{m,c}$) and the diffusivity (D_c) of the different types of composites were determined (Table 7.1). Green flax fibre based composites are clearly more sensitive to moisture than the other two types of composites based on upgraded Duralin flax. The maximum moisture content in Duralin flax fibre composites is reduced by around 30% compared to green flax fibre composites. Also, the diffusivity of Duralin flax fibre composites (Table 7.1), as calculated

from the initial slope of the moisture uptake curves, is much lower than that for NMTs based on green flax fibre mats.

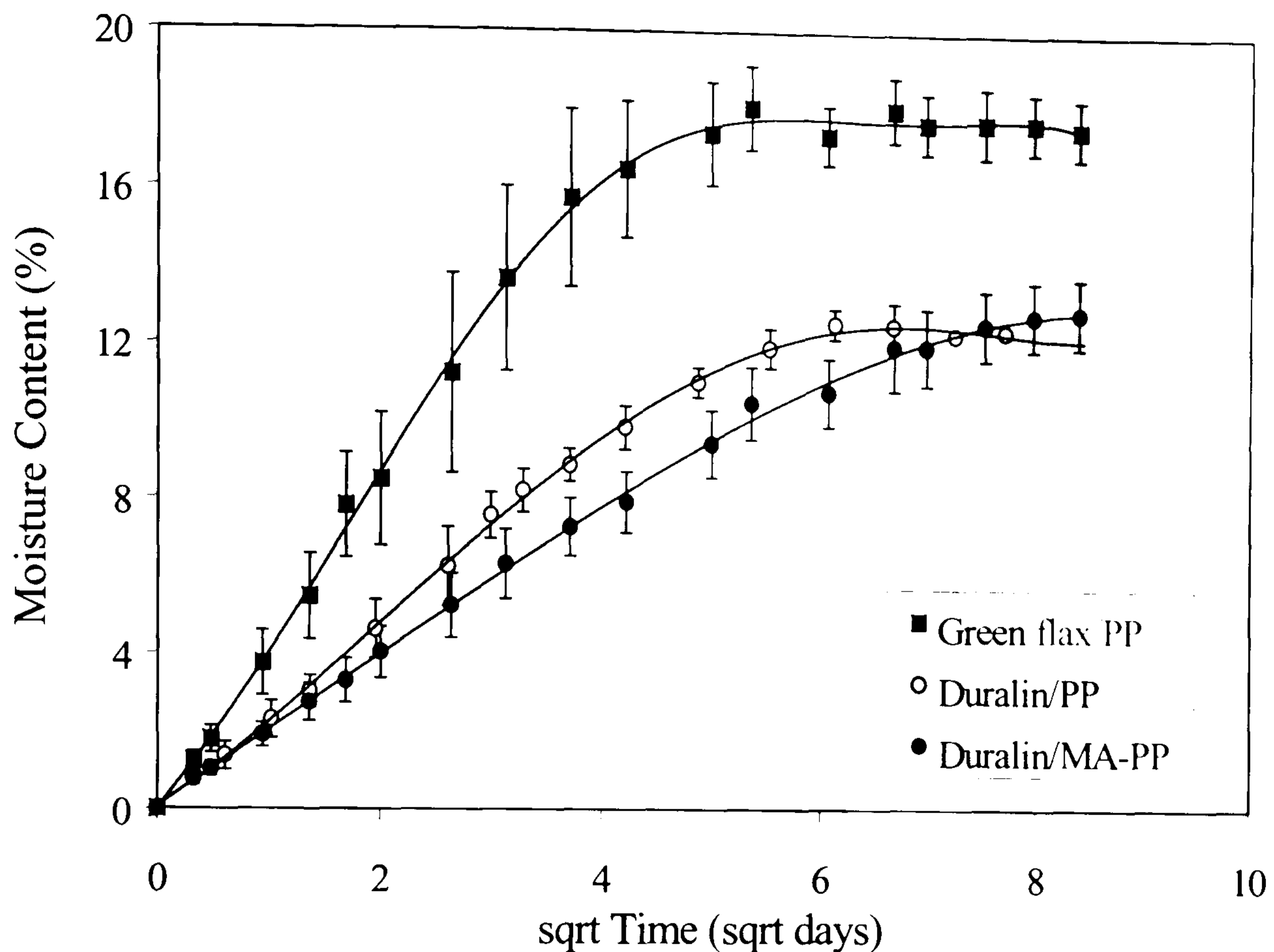


Figure 7.2 Moisture content as a function of time for green flax/PP, Duralin/PP and Duralin/MA-PP composites. (Moisture content in GMT was below 1%). The data are fitted by Spline curves using Slide Write program and the error bars show standard deviations.

Table 7.1 Maximum moisture content and diffusivity of flax/polypropylene composites.

Composite	Max. Moisture Content $M_{m,c}$ (%)	Diffusivity D_c (cm^2/s)
Green flax/PP	18.0	1.3×10^{-2}
Duralin flax/PP	12.8	7.8×10^{-3}
Duralin flax/MA-PP	13.5	5.0×10^{-3}

It is interesting to note that the use of MA-PP as a compatibiliser lowers the diffusivity even further. Clearly, the initial moisture uptake in this composite system is taking place at a lower rate than for the PP system without

compatibiliser. The maximum moisture content level is, however, similar for both PP and MA-PP based treated flax systems. The higher diffusivity for the PP system without compatibiliser, indicates that initially a fair amount of moisture uptake takes place along the fibre/matrix interface. For Duralin flax PP, as well as for green flax/PP, a plateau value for moisture uptake is reached after about one month immersion in water. Compared to the moisture absorption data of single fibres (Stamboulis et al., 2000) (Table 7.2, Figure 7.3), the moisture absorption of the composites is quite high.

Table 7.2 Average maximum moisture content of flax fibres at different levels of Relative Humidity (RH) (Stamboulis et al., 2000).

Flax Fibre	Maximum Moisture Content			
	$M_{m,f}$ (%)			
	20% RH	66% RH	93% RH	100% RH
Green	3.61	15.03	24.0	-
Duralin	2.70	10.76	9.0	14.33

NOTE: The desired relative humidity in the case of flax fibre treatment were obtained by selecting different salts in the dessicators e.g. dessicators having solutions of potassium acetate, sodium nitrate, ammonium monophosphate and distilled water had a relative humidity of 20, 66, 93 and 100% respectively (Stamboulis et al., 2000).

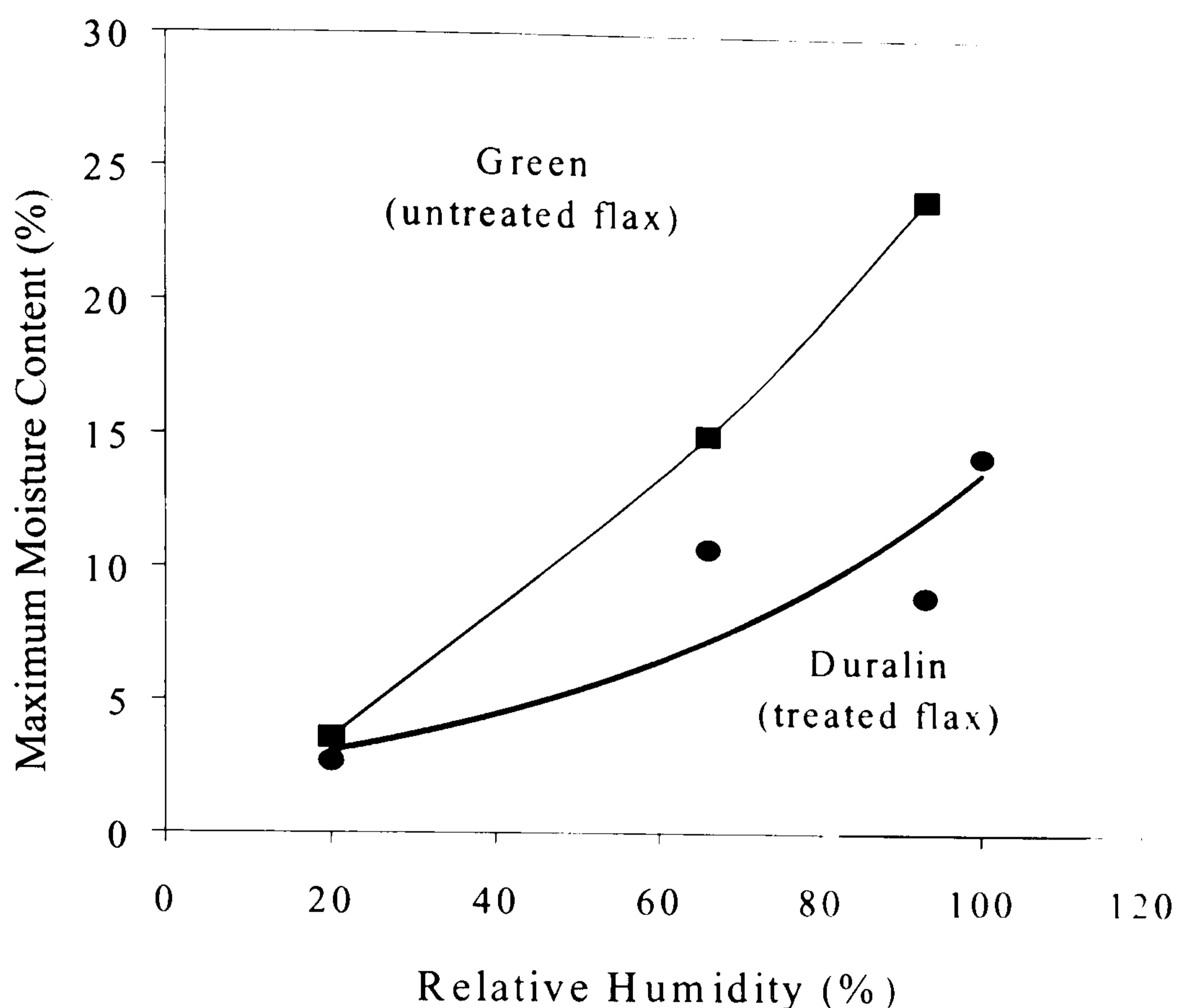


Figure 7.3 Effect of the relative humidity on the moisture absorption of green and Duralin flax fibres (Stamboulis et al., 2000).

Based on a fibre volume fraction of 0.38 and assuming that only the fibre is responsible for moisture uptake in the composites the moisture absorption should be much lower and in the order of 6% for Duralin based composites and 12% for green flax fibre composites. However, in reality these composites absorb up to 12% and 18%, respectively. The difference in moisture content between a fibre in air and a fibre in a composite is similar for both Duralin- and green flax and around 6%. This difference in moisture absorption by fibre in air and composites is probably the result of voids, which are often present in natural fibre composites.

It can be expected that the absorption of moisture affects the dimensional stability of the composite plates. Figure 7.4 shows the thickness-swell of the samples immersed in water for 60 days at room temperature. The performance of the Duralin composites is much better than that of the green flax based composites. The thickness of the green flax composite increases by about 13%, whereas the Duralin flax composite swells about 9%.

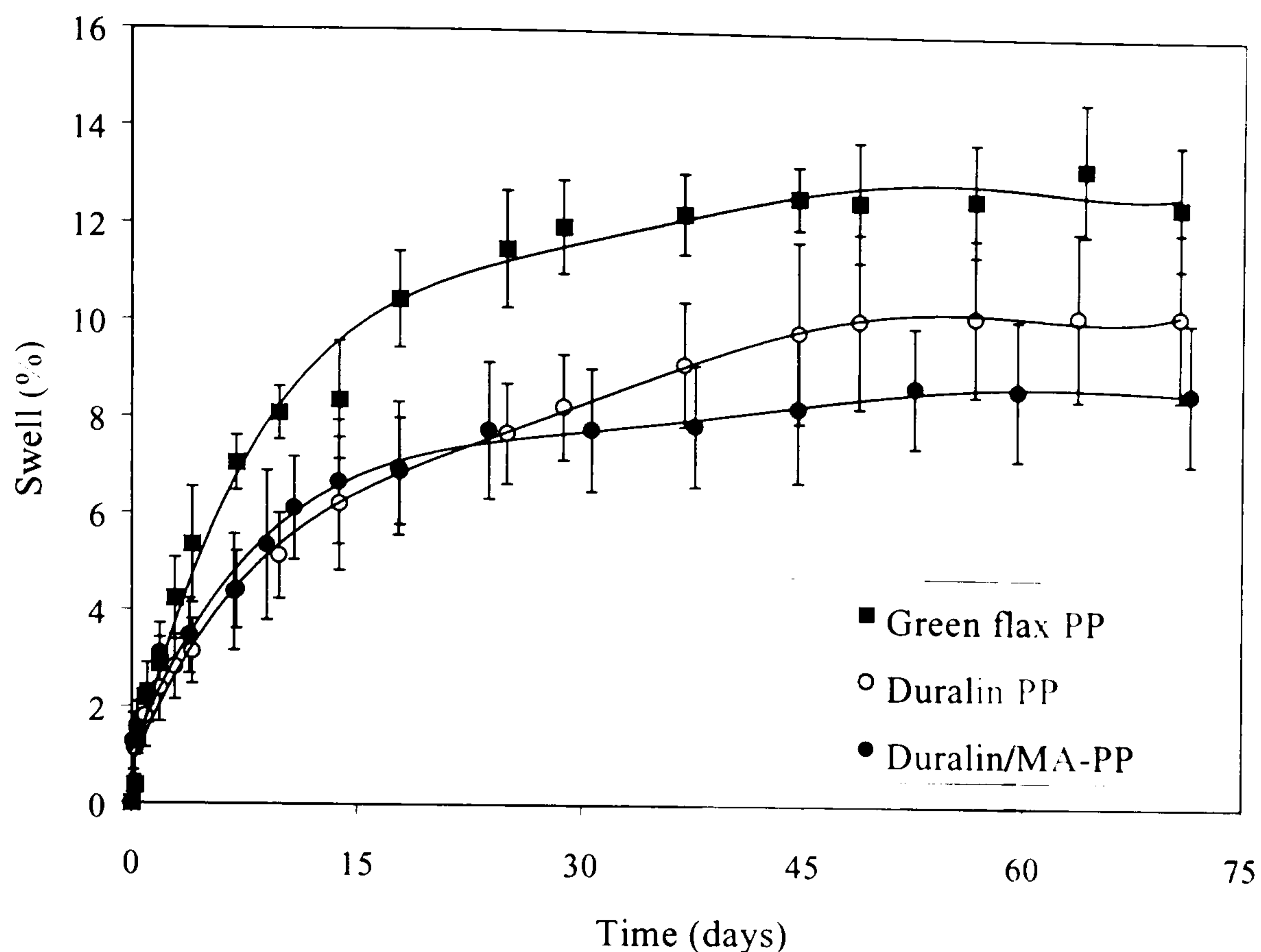


Figure 7.4 Thickness of composite plates, immersed in water, as a function of time for green flax/PP, Duralin/PP and Duralin/MA-PP composites. The data are fitted by Spline curves using Slide Write program and the error bars show standard deviations.

With respect to the durability of natural fibre composites, the most serious effect of moisture absorption is the degradation of mechanical properties. Therefore, the residual stiffness and strength of NMTs based on green- and Duralin flax was measured as a function of moisture content. The initial stiffness and strength values for these type of natural-fibre-reinforced composites is about 8 GPa and 50 MPa, respectively. In Figure 7.5 the normalised (control sample value is taken as 100%) stiffness is plotted as a function of moisture content. In the case of Duralin composites an initial increase in stiffness is followed by a drop in composite stiffness, whereas for green flax fibre based composites no significant increase in stiffness is observed and the drop in stiffness is more obvious. For green flax composites the drop in the modulus of the saturated samples is quite significant and is about 40% lower than that of dry samples. As mentioned in Chapter 2, flax fibre is an aggregate of thousands of layers of crystalline fibrils having an angle of 5° inclination to the fibre axis (Sharma et al., 1995). The effect of moisture on

these micro-fibrils would also depend on the tension subjected to these fibres during the treatment. In general, cellulosic fibres tend to retain liquids in the interfibrillar space, which leads to swelling and therefore an increase in the interfibrillar distance (Aguilar-Vega and Cruz-Ramos, 1995). Since, the cellulose chains are laterally held together by hydrogen bonds across adjacent hydroxyl groups, water cannot penetrate into the crystalline regions, but penetration into the more accessible amorphous regions results in the formation of hydrogen bonds between the water molecules and the cellulose hydroxyl groups (Cockett and Hilton, 1961). There is a strong interaction of the initial portion of water molecules with hydroxyl groups of cellulose leading to the formation of solid solution within the amorphous region. It has been speculated that water molecules release stress introduced into the amorphous region during drying and, thus, allow better alignment of cellulosic chains, which would result in densification of the cellulosic part. Such a hypothesis explains the phenomenon of increase in the density of cellulose at lower moisture content (Alinec, 1989). It was observed that the total volume of moist fibres was less than the sum of the dry sample and water, and this was interpreted as a contraction of the whole system rather than one of the components i.e. absorption of moisture led to the better alignment of cellulosic chains leading to an increase in density and hence contraction of the system. The above mentioned hypothesis also explains the initial increase in the stiffness and the tensile strength of dry cellulosic fibres upon sorption of a small amount of water. In other words, on the absorption of small amount of moisture, the stresses in the cellulose are relaxed along with an improved alignment of molecular chains leading to an improvement in the tensile properties along the fibre axis. Similar to the fibre stiffness and hence composite stiffness seems to improve at mild levels of moisture uptake. As mentioned before, at a higher moisture content, water diffuses into the interfibrillar space leading to swelling. In this way water acts as a plasticiser and it permits the cellulose molecules to move free. Consequently the mass of cellulose is softened and can change shape more easily with an application of force (Stamboulis et al., 2000). Therefore at higher moisture content the stiffness of fibre as well as composite decreases. In the case of green flax based composites (Figure 7.5) the initial increase in stiffness, at low moisture content, is lower and

drop (in stiffness) is higher at higher moisture content when compared to Duralin flax. These observed differences between the two fibres (Duralin and green) could be related to the differences of chemical constituents as well as physical structure of the two fibres. Since Duralin fibres are heat-treated therefore initial absorption of moisture has a higher effect on the internal stresses, developed during the treatment, the stiffness of the fibre as well as composites. On the other hand, due to curing of lignin and hemi-cellulose content in Duralin flax (as explained in Chapter 2) these fibres are more compact, hence the plasticising effect is reduced when compared to green flax. This reduced plasticising effect, when compared to green flax, also reduces the effect of moisture on the stiffness of Duralin flax at higher moisture content. Even though longer time is taken by the Duralin flax based composites, when compared to green fibre based composites, to attain a particular moisture content the effect of moisture on stiffness is lower than that of green flax composites.

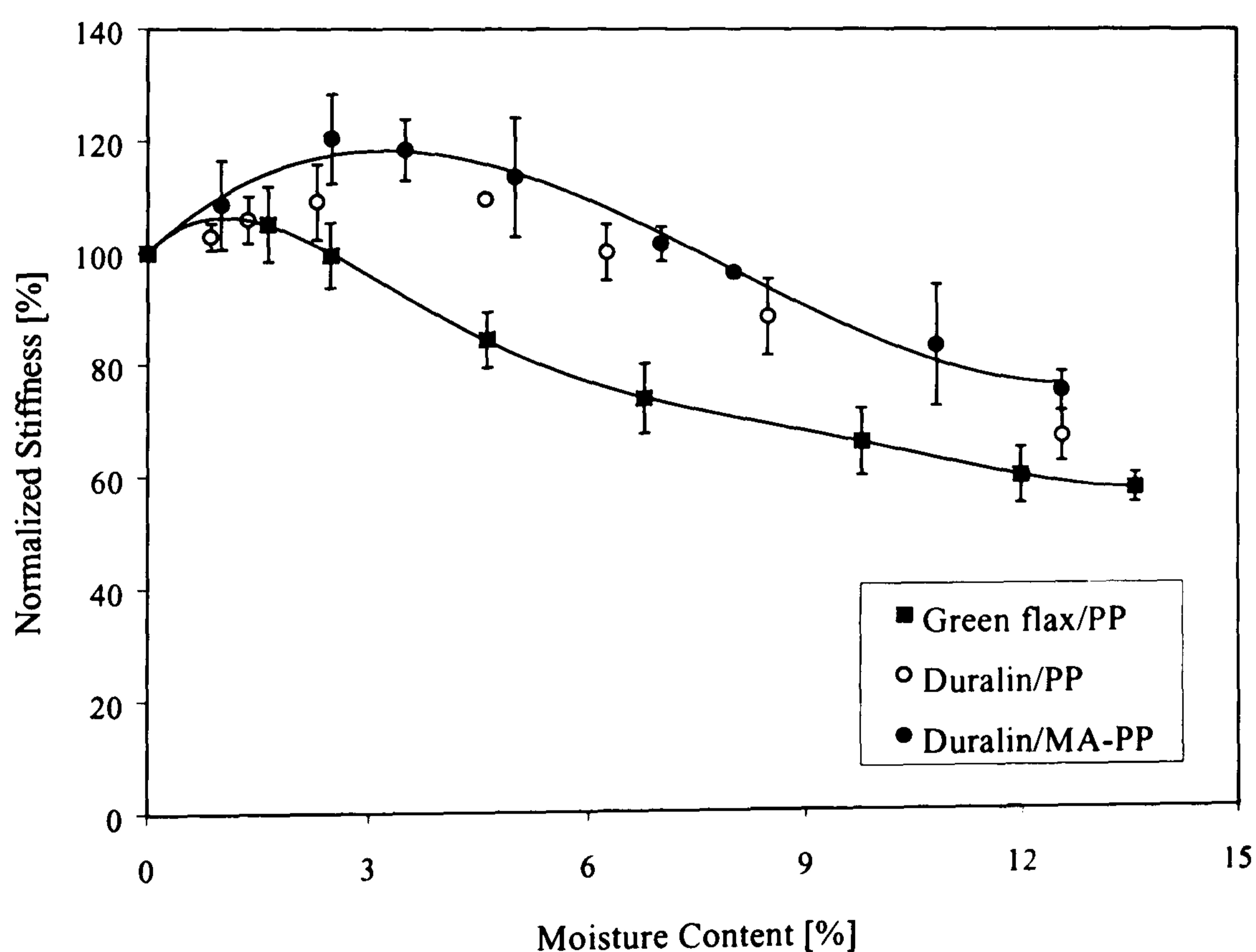


Figure 7.5 Effect of moisture content on the modulus of green flax/PP, Duralin/PP and Duralin/MA-PP composites. The data for Duralin/MA-PP are fitted using 3rd order polynomial equation ($y = 0.1016x^3 - 2.4119x^2 + 12.372x + 100.05$) with an R^2 value of 0.987 and data for green flax/PP are fitted using 6th order polynomial equation ($y = -0.0001x^6 + 0.0068x^5 - 0.1562x^4 + 1.7111x^3 - 8.8722x^2 +$

$13.567x + 100.02$) with an R^2 value of 0.99. The data were fitted using Excel program.

Figure 7.6 shows the normalised tensile strength as a function of moisture content. Compared to the drop in composite stiffness, the tensile strength of flax-fibre-reinforced composites is not so much affected by the water uptake. Similar effects of water absorption on composite mechanical properties were reported earlier for thermoplastic composite systems based on jute fibre (Karmaker and Hinrichsen, 1991). Although the overall drop in composite strength is not as significant as the drop in stiffness, it is clear that, again, the green fibre composites are more affected by the water uptake compared to the Duralin composites. At high moisture content, the strength of green flax/PP composite is about 25% lower than that of the dry reference sample. Similar to the trend in composite stiffness, also here an initial increase in composite performance with moisture content is observed for Duralin composites, whereas the green flax fibre composites show a more gradual decrease in composite strength with water uptake.

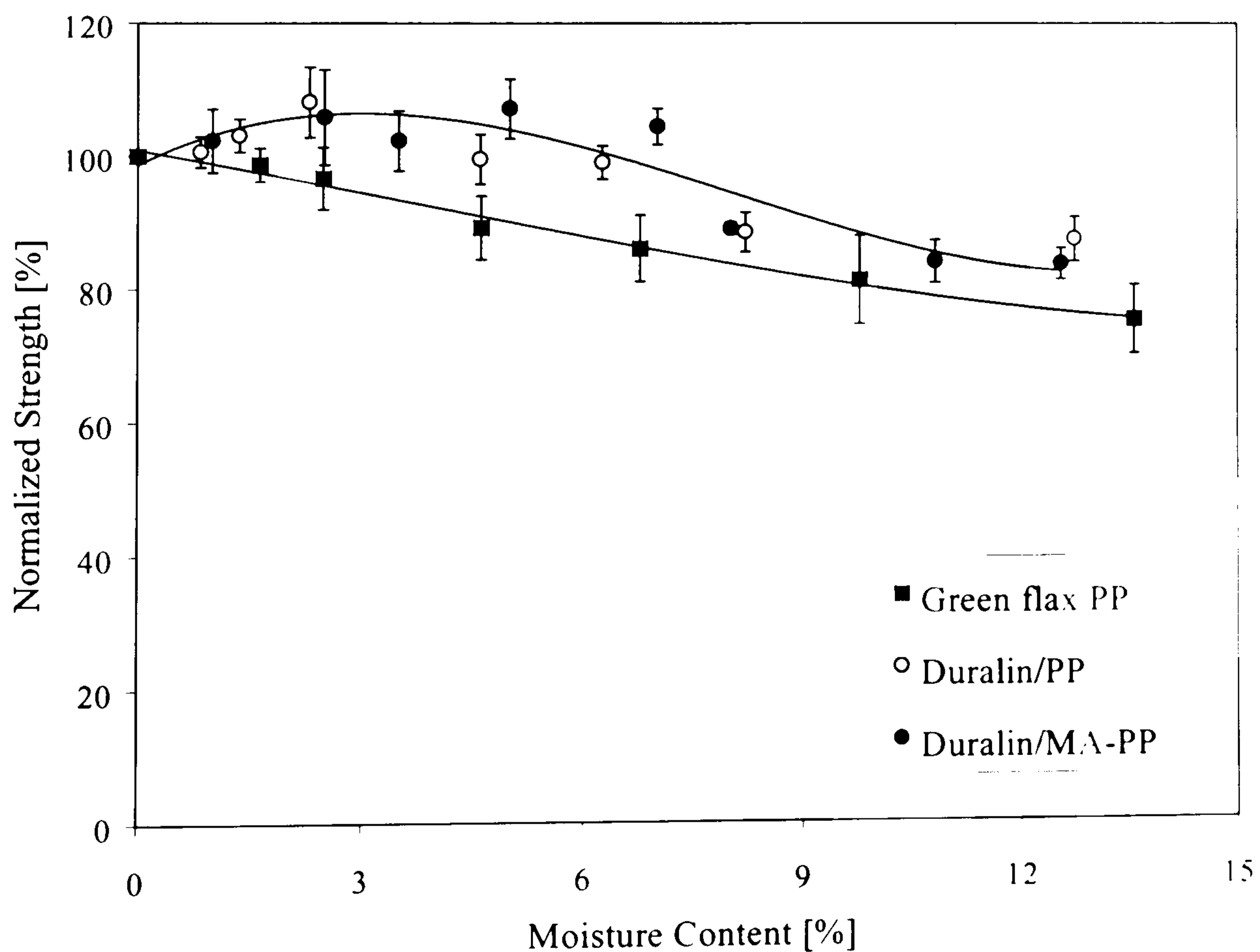


Figure 7.6 Effect of moisture content on the tensile strength of green flax/PP, Duralin/PP and Duralin/MA-PP composites. The data for Duralin/MA-PP are fitted using 3rd order polynomial equation ($y = 0.0475x^3 - 1.1439x^2 + 5.5888x + 98.651$) with an R^2 value of 0.85 and data for green flax/PP are fitted using 3rd order

polynomial equation ($y = 0.0046x^3 - 0.0518x^2 - 2.0247x + 100.88$) with an R^2 value of 0.98. The data were fitted using Excel program.

This behaviour seems to be in agreement with the environmental behaviour of the single Duralin fibres (Stamboulis et al., 2000) (Figure 7.7 and 7.8), where a maximum in fibre strength was observed at intermediate levels of relative humidity. As explained before the reason of increase in fibre strength on initial moisture uptake could be related to the densification of cellulose on initial moisture uptake. Initial absorption of moisture by amorphous regions leads to stress relaxation as well as molecular alignment which, probably, causes an initial increase in the tensile strength (Alinec, 1989). This also explains the differences between Duralin and green fibres as Duralin fibres were heat cured and therefore expected to react at a higher extent (as compared to green fibres) through the relaxation of the stresses built up during the curing process. Further absorption of moisture results into fibre swelling and water molecules act as a plasticising agent thus making the slippage of molecules easier and lowers the strength by reducing the forces holding the molecules together (Hearle, 1963).

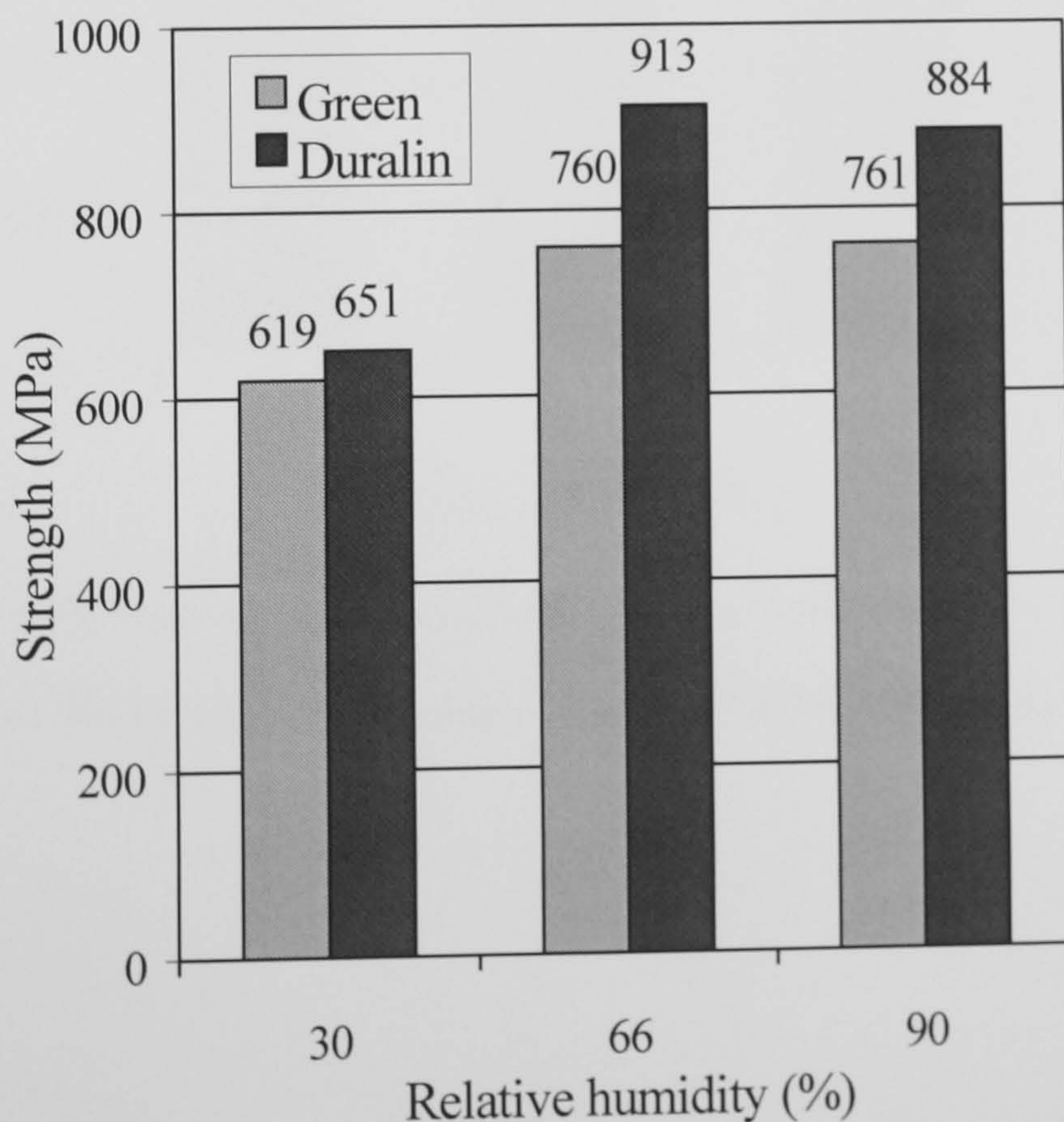


Figure 7.7 Effect of relative humidity on the average tensile strength of green- and Duralin flax fibres (8 mm gauge length) (Stamboulis et al., 2000).

However, the drop seen in composite strength at high moisture was not observed for single (green) fibres. It should be noted, however, that in contrast to the short environmental conditioning times in the case of fibres (Figure 7.9), the composites were immersed in water for several days or even weeks (Figure 7.2). During the environmental behaviour studies on flax fibres (Stamboulis et al., 2000) it has been observed that moisture causes fungus development on the fibre surface after a couple of days of exposure, resulting in degradation of the fibres and the decrease of their mechanical properties. This could also be the reason for the drop in strength for flax fibre composites at high moisture content levels. However, no presence of fungal growth was observed on the composite surface.

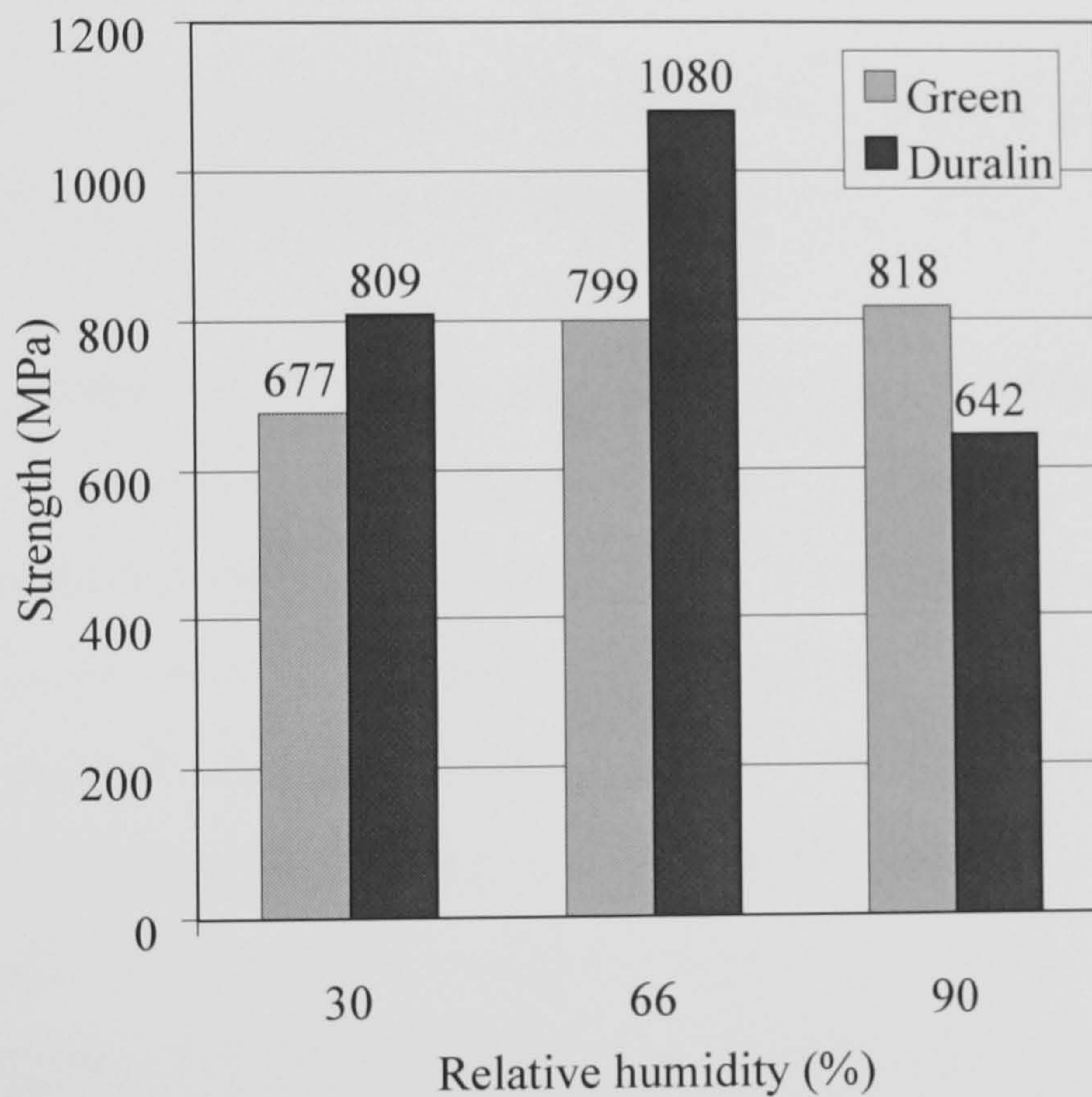


Figure 7.8 Effect of relative humidity on the average tensile strength of green- and Duralin flax fibres (3.5 mm gauge length) (Stamboulis et al., 2000).

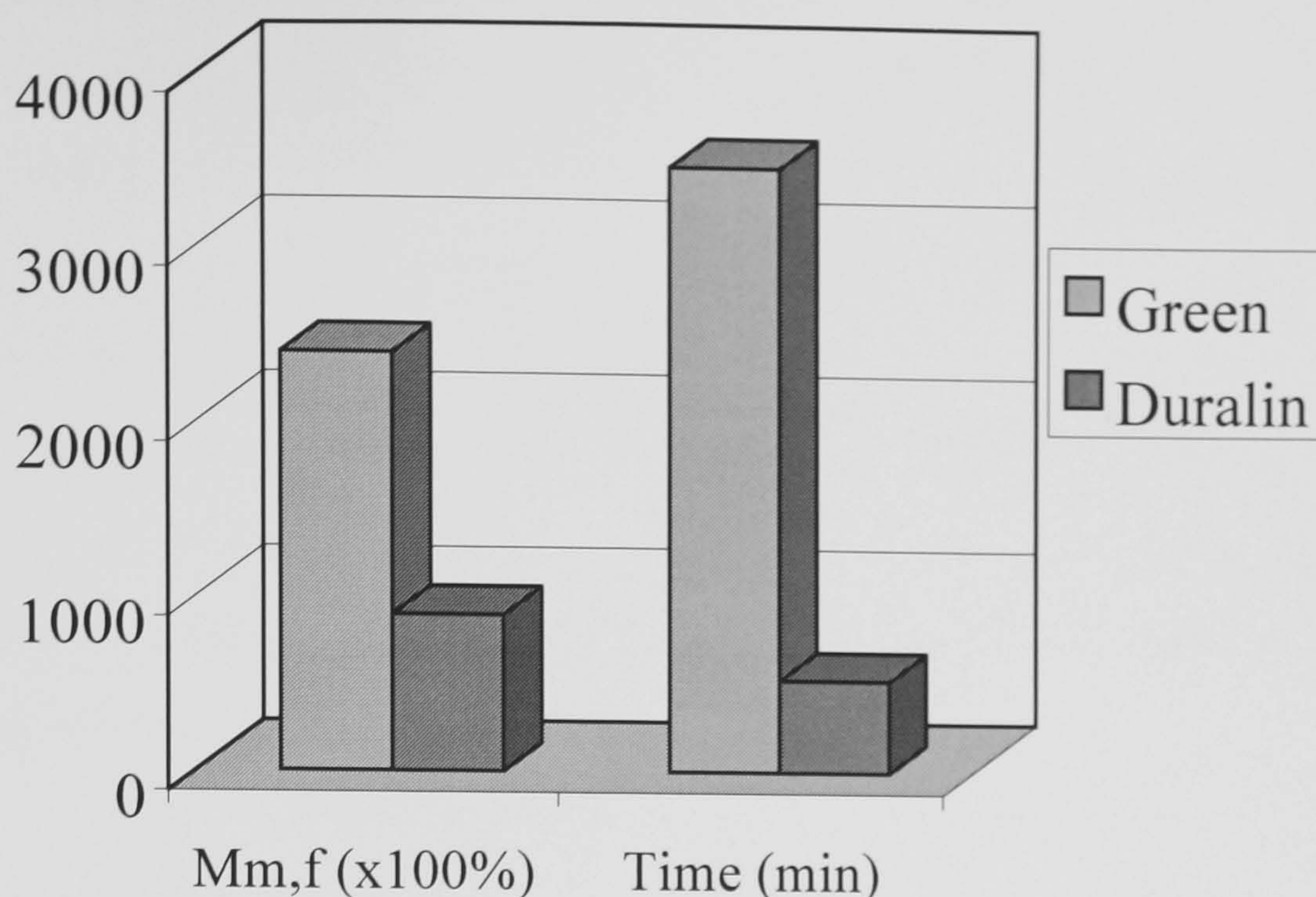


Figure 7.9 Time dependence of moisture absorption of green- and Duralin flax fibres at 93% of relative humidity (Stamboulis et al., 2000).

Since the diffusivity of Duralin-flax-fibre-reinforced composites is much lower than that of green flax/PP composites, these composites were immersed much longer in water than green flax fibre composites with similar moisture contents. For example, in the case of a Duralin flax/MA-PP composite a moisture content of 12% was reached after an immersion time of about two months, whereas in the green flax/PP composite this moisture content level was already reached after 8 days. Clearly, this may have an effect on the mechanical behaviour of the fibres and composites. Still, this relatively small drop in composite strength even after such a long exposure time is a clear indication for the good environmental durability of Duralin flax based composites. No effect of maleic-anhydride modified PP on residual stiffness and strength of Duralin composites was observed. Although the maleic-anhydride interface modification slowed down the water uptake (Figure 7.2), it does not seem to affect the (residual) mechanical properties of the interface and hence the composites. Studies by Karmaker et al. (Karmaker and Clemons, 1995; Karmaker, 1997) even suggest that the interfacial shear strength in natural fibre thermoplastic composite systems may increase with moisture absorption. They studied the effect of thickness swelling of fibres on the interfacial gap and on the mechanical and physical properties of ligno-cellulosic

fibre reinforced polypropylene. Through this study they showed that the gap between natural fiber and polypropylene can be filled by the dimensional increase of fibres when they are swollen by water, leading to higher interfacial shear strengths between fibre and polymer matrix. Unlike composite systems based on brittle thermosetting resins like unsaturated polyester, microcracking of the matrix as a result of fibre swelling is not likely to occur in the case of a ductile matrix like PP. Hence, rather than the result of interface failure or matrix cracking, the mechanical degradation of the composites at relatively long immersion times is most likely the result of fibre degradation.

7.4 Conclusions

The absorption of moisture by flax-fibre-reinforced polypropylene (PP) composites can adequately be described by Fick's law. The moisture content is linear to the square root of time until about two weeks of immersion in water. After that, the moisture content levels off to a maximum moisture content. The moisture resistance of natural-fibre-mat-reinforced thermoplastics (NMTs) based on flax fibres and a PP matrix can be improved by the use of upgraded Duralin flax fibres. The moisture absorption of upgraded flax/PP composites is about 30% lower than that of green flax composites and the dimensional stability (swelling) is also significantly improved. The use of maleic-anhydride modified PP as a compatibiliser for improved interfacial bonding lowers the diffusivity, being the water uptake rate, significantly. The maximum moisture content is however not affected by the interfacial properties. The stiffness of Duralin flax/PP composites shows an initial increase with moisture content, followed by a small drop in stiffness at high levels of moisture content. The stiffness reduction of green flax/PP composites is more pronounced and can be as high as 40% at moisture content levels of 12% and an immersion time of around 8 days. The tensile strength is not as much affected by the water uptake as the stiffness, which is in agreement with the fibre results (Stamboulis et al., 2000) where no drop in strength was observed with increasing relative humidity. Again also here the Duralin fibre composites show a better environmental durability compared to green flax/PP composites.

8. BIODEGRADABLE COMPOSITES BASED ON FLAX / POLY-HYDROXY-ALKANOATES

In this chapter, the literature about biopolymers and their composites is briefly included. The experimental results covering the effects of materials (i.e. fibre as well as matrix) and processing parameters on the mechanical properties of flax/PHB(HV) composites are reported and discussed.

8.1 Introduction

As mentioned in Chapter 1, nowadays ecological concern has resulted in a renewed interest in natural materials and issues such as recyclability and environmental safety are becoming increasingly important for the introduction of new materials and products. In Chapter 3-7 the results on PP/flax composites are reported and discussed. There are certain disadvantages in using PP as a matrix material for composite applications:

- a) The production of PP causes CO₂ imbalance in the environment,
- b) Since PP does not degrade via normal bio-degradation process therefore its disposal requires dumping, recycling or incineration methods. The addition of flax fibres limits the recyclability of these materials. The disposal of these materials through incineration would again result into environment pollution,
- c) Natural fibres tend to degrade near the processing temperature of most thermoplastics. Thermal degradation during processing not only limits the number of polymers that can serve as a matrix system but gives especially concern with respect to reprocessing.

Although one may get away with the narrow processing window for natural fibre composites in a single step process, it may give problems in the case of reprocessing and mechanical recycling. At this moment natural fibres are pushed because of their 'green image', mainly because they are renewable and can be incinerated at the end of the materials lifetime. However, the recycling issue is going to be key in answering the question: How green are natural fibres actually? In most cases, from an Eco-performance point-of-view, mechanical recycling is favoured over thermal recycling and landfill. Hence, problems related to thermal degradation during recycling and reprocessing may significantly lower the Eco-performance of the natural fibre composites. This is especially the case with a well recyclable polymer like PP, where the addition of natural fibres will strongly affect the recyclability and hence the Eco-performance of the resulting composite material. On the other hand, since car manufacturers are aiming to make every part either recyclable or biodegradable there still seems to be some scope for biocomposites based on biopolymers and natural fibres. Such biodegradable composites may, from a 'cradle-to-grave' point-of-view, have some advantages over traditional composites for certain applications.

Biopolymers like Polyhydroxybutyrate (PHB), Polylactic acid (PLA) and starch are some of the new candidates for the applications in composite areas as matrix materials (Gatenholm et al., 1992; Avella et al., 1993; Gatenholm and Mathiasson, 1994; Hermann et al., 1996). Generally, biopolymers are thermoplastic materials therefore offering advantages like low processing time, recyclability along with a feature of biodegradability. Apart from re-use or recycling, biocomposites offer additional recovery options, like composting, being fully integrated into natural cycles or carbon dioxide (CO₂) neutral combustion thus biocomposites also meet the steadily increasing environmental demands of legislative authorities.

The objective of the present research was to utilise the advantages offered by renewable resources (natural fibres) for the development of biocomposite materials.

8.1.1 Composites based on biopolymer matrices: a literature review

As seen in literature, some attempts have been made to develop composites based on bioplastics as matrix material. Gatenholm et al. (1992) studied the effect of introduction of cellulose fibres in PHB and found that addition of fibres (pulp) led to improvement in tensile strength and stiffness of these composites but the samples produced were very brittle. To enhance the toughness, PHB polymers with varying hydroxyvalerate (HV) contents were used. The defibrillation observed on extracted fibres suggested a possible hydrolysis of cellulose by crotonic acid formed in situ as a result of the thermal decomposition of PHB matrix. Gatenholm and Mathiasson (1994) analysed PHB samples, with and without cellulose fibres, for their molecular weight and found that processing of cellulose contributed to a greater amount of chain scission, plausibly caused by local overheating as a result of shear forces developed during processing.

Development of unidirectional composites based on PHB/HV matrix and regenerated cellulose continuous filaments as reinforcement has also been reported (Bourban et al., 1997). The results demonstrated promising mechanical properties of the PHB/HV – regenerated cellulosic fibres composites. Cellulosic fibres significantly increased the stiffness and strength of the PHB/HV matrix while maintaining the biodegradability of this material. Luo and Netravali (1999) studied the effect of pineapple fibre addition to PHB/HV matrix materials. In their study on unidirectional composites, though tensile properties increased longitudinally but it was significantly lower than the pure resin when measured in the transverse direction (i.e. perpendicular to fibre alignment). This significant reduction in tensile strength and stiffness in the direction perpendicular to fibre alignment was mainly attributed to poor interfacial adhesion between cellulosic fibre and PHB/V matrix, inter-fibrillar adhesion within pineapple fibre bundle and also presence of voids. Elongation-at-break reduced on fibre addition but was independent of fibre content when measured longitudinally and reduced gradually with fibre addition when measured in transverse direction. No significant effect of cellulose on PHB polymer crystallinity is reported (Avella et al., 1993; Luo and Netravali, 1999). In the case of steam exploded straw fibre /PHB composites, the fibres are reported to

interact with the amorphous phase of polymer leading to a slight increase of T_g (glass-transition temperature) and delay in the crystallisation process (Avella et al., 1993). However, Reinsch and Kelly (1997) reported that short wood fibres acted as nucleating sites for the crystallisation of PHB/HV and enhanced its crystallisation rate. The observed differences between the effect of wood fibre and pineapple leaf fibres, on PHB crystallinity is, attributed to the presence of lignin in the former (Luo and Netravali, 1999).

Other interesting biopolymers are polysaccharides like thermoplastic starch. Thermoplastic starch is extremely moisture sensitive. The moisture sensitivity of these biopolymers can be reduced by blending it with moisture resistant polyesters (Wollerdorfer and Bader, 1998). Addition of natural fibres improve the tensile properties of these biopolymers e.g. the addition of 15% (w/w) flax fibres to thermoplastic starch led to an increase in the tensile strength from around 9 MPa to around 37 MPa. Such composites can be attractive for applications like packaging, which have to be disposed off after certain usage.

Hermann et al. (1998) developed biocomposites by embedding natural fibres e.g. flax, hemp, ramie, etc. into biopolymeric matrices e.g. derivatives from cellulose, starch, lactic acid and polyhydroxybutyrate. According to authors the specific mechanical properties of some of biocomposites were comparable to glass fibre reinforced compounds and very well suited for anisotropic and specially tailored light-weight structural parts. The authors also reported about randomly oriented biocomposites based on shellac matrix reinforced by non-woven flax fibre (volume of 45%) with tensile strength in the range of 110 MPa. Since biopolymers are organic materials therefore they are combustible, which is an interesting option for a convenient refuse disposal. For structures intended to be flame resistant, however, it is a big disadvantage. Various flame resistant compounds have been identified and investigated, which also satisfy the standards and are harmless to humans (Hermann et al., 1998). The improved flame resistance can expand the usability of these composites, as it is one of the most important factors considered during selection of materials for applications like panelling elements in automotive, railways and aircraft.

Some of the matrices in biocomposites are based on polymers derived from biomaterials but they may not be biodegradable e.g. soya bean oil resin (Khot, 1998). Such composites can be disposed off by thermal recycling, which is CO₂ neutral and completely slag-free.

In the present chapter the results on the influence of addition of flax fibre (green flax) on the mechanical properties of biopolymers i.e. PHB and copolymer PHB/HV (Polyhydroxybutyrate-co-hydroxyvalerate) are reported and discussed.

PHB(/HV) was selected as a matrix material. Apart from the advantages mentioned above, PHB offers some other advantages like: -

- a) PHB is hydrophobic, therefore protects natural fibres from moisture,
- b) Mechanical properties of PHB are comparable to other polymers used for composite applications e.g. PP,
- c) PHB can be processed at low temperature (i.e. approx. 180° C) thus fibre degradation can be avoided.

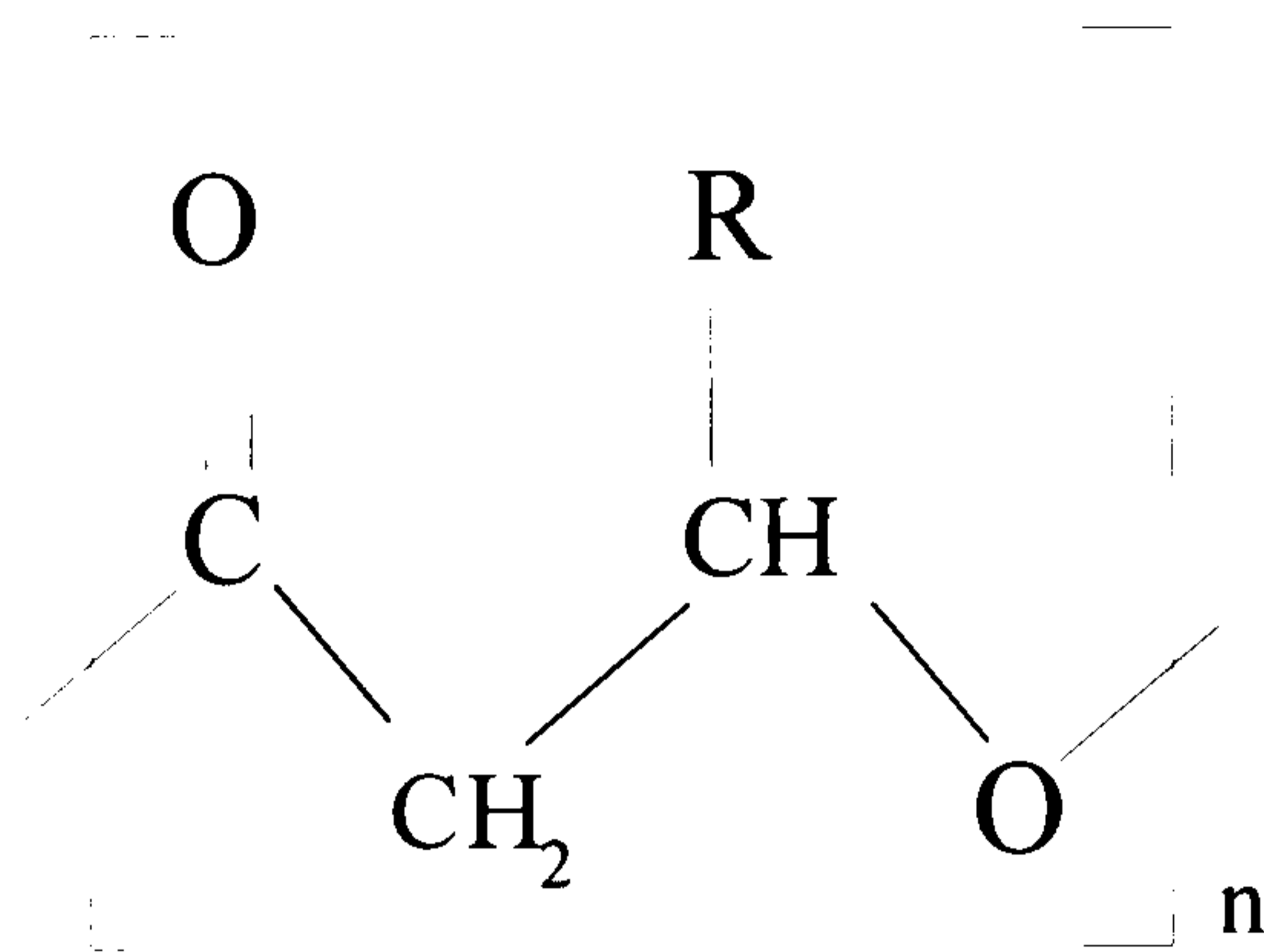
The various fibre, polymer and processing parameters studied, include:

- a) Fibre content,
- b) Copolymer content,
- c) Processing conditions (cooling temperature and annealing) and
- d) Processing methods (injection moulding and compression moulding).

8.1.2 Poly-hydroxy-alkanoates (PHAs)

Poly-hydroxy-alkanoates are biopolymers stored by a wide variety of bacteria as an energy reserve. Poly-hydroxy-butyrate (PHB), a naturally abundant PHA, was first isolated and characterised by Lemoigne in 1925 (De Koning, 1993). The chemical structure is shown in Figure 8.1. Apart from being a natural product, PHAs are also thermoplastic materials. In contrast to synthetic polymers PHAs have the fundamental advantage of being based on renewable resources and not dependent

on the supply of petroleum. Moreover, they are genuinely biodegradable, i.e. they can be completely digested by a wide variety of bacteria and fungi. Other notable features of PHAs are biocompatibility and hydrophobicity. The latter feature is unique among natural polymers.



R = -CH₃ for Hydroxybutyrate.
-C₂H₅ for Hydroxyvalerate.

Figure 8.1 Chemical structure of Polyhydroxyalkanoate.

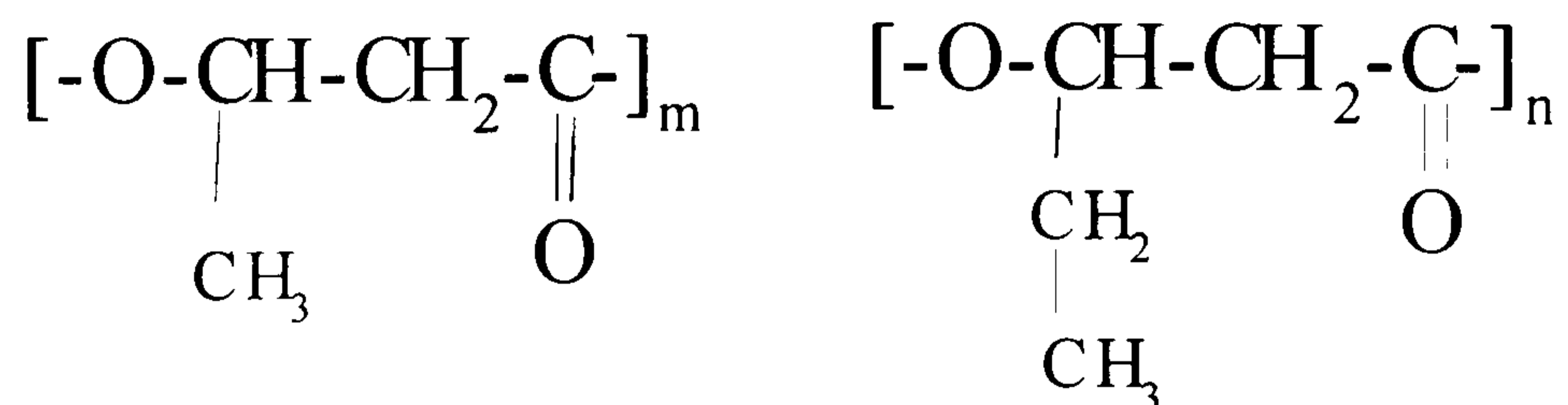
The homopolymer PHB has exceptional stereochemical regularity with hydroxybutyrate (HB) as a repeating unit. The chains are linear with R-stereochemical configurations, which implies that this polymer is 100% isotactic. This enables crystallisation. The spherulitic morphology depends on the crystallisation temperature. The overall rate of crystallisation of PHB shows a maximum in the range of 55-60°C.

The major disadvantage of PHB is the poor thermal stability. Traditional melt processing technologies lead to a rapid decrease of molecular weight, forming crotonic acid at temperatures slightly above the melting point. The tensile strength turns out to be strongly influenced by this. After a heat treatment for 10 min at 190 °C the tensile strength drops by 30% of its initial value (Hoffmann et al., 1994). Another disadvantage of PHB is its brittleness. Although as-moulded PHB shows ductile behaviour, upon storage at ambient temperature a detrimental ageing process seriously embrittles the materials (De Koning and Lemstra, 1993). To overcome the brittleness and instability during melt processing of PHB, copolymers with hydroxyvalerate (HV) have been developed. It has also been

shown that heat treatments (annealing) can be used to reduce the brittleness of PHB (De Koning and Lemstra, 1993).

8.1.3 Copolymers of poly-hydroxy-alkanoates

A limited range of bacteria is able to produce random copolymers based on the usual hydroxybutyrate monomer and hydroxyvalerate.



(a) Polyhydroxybutyrate

(b) Polyhydroxyvalerate

Crystallinities are similar for the whole range of PHB/HV copolymers and all copolymers show similar conformation characteristics as observed for PHB. The apparent ability of the two monomers units to co-crystallise might result from the fact that they possess and occupy approximately the same volume. Moreover, the crystalline structures of PHB and PHV possess similar chain conformations.

However, the considerable reduction of the heat of fusion upon HV inclusion clearly indicates that the HV units have to be regarded as unfavourable defects in the PHB crystal structure. The lower degree of crystallinity causes a lower melting point, which enables lower processing temperatures. However, this melting point reduction does not affect the thermal stability. Consequently, processing becomes less critical with increasing HV content, since the lower melting point widens the processability window.

8.2 Experimental

8.2.1 Materials

Investigations were made on native polymer PHB as well as PHB/HV copolymers (Biopol™). The biochemical pathway of PHB biosynthesis starts with the

conversion of an appropriate carbon substrate to acetate. For Biopol™ production, *A. eutrophus* bacteria were grown in a glucose-salts medium in a batch fermenter. Propionic acid was added to the culture to obtain the copolymers. The copolymers in granule form and pure PHB in powder form were all kindly supplied by Monsanto, Belgium. In Table 8.1, the melting temperature and molecular weight of biopolymers used, is listed. Figure 8.1 shows the schematic representation of the chemical structure of polyhydroxyalkanoates.

Table 8.1 Properties of Polyesters used.

Polymer	Grade	Melt Temperature (°C)	Molecular Weight (g/mole)
PHB	D000P	177	648,000
PHB/ 8% HV	D400GN	153	553,000
PHB/12% HV	D600GN	143	453,000

Ceres BV, Wageningen, the Netherlands kindly delivered the ‘green’ flax fibres, which were used as a reinforcement material. The fibres were in random mat form (650 g/m²) and short chopped fibres with a length of approx. 10mm.

8.2.2 Methods

8.2.2.1 Compression moulding:

Natural-fibre-mat-reinforced thermoplastics (NMT) composite plates, with different fibre contents, were manufactured using the compression moulding methods. In the case of native PHB/flax NMT composites, the calculated weight of PHB powder was spread on the layers of fibre mats followed by compression moulding. The copolymer (PHB/HV)/flax NMT composites were manufactured by film-stacking method. Films having thickness of approx. 1 mm were made in a temperature-controlled hydraulic press (Fontijne Holland, type TP400) by heating and compressing the granules for 5 minutes at 180°C and a maximum pressure of 1.5 MPa. In this film-stacking method, pre-dried randomly oriented, non-woven,

green flax fibre mats were stacked alternately with PHB/HV copolymer films to obtain a good fibre impregnation. All composite plates were heated for 12.5 minutes at a temperature of 180° C and pressure of approx. 8.0 MPa. The pressure was increased in steps to avoid the presence of bubbles and voids. To observe the effect of cooling temperatures the mould was cooled at two different temperatures i.e. 20°C and 60°C. To reduce the influence of moisture, all materials were dried in an oven at 80°C for at least 24 hours before moulding.

8.2.2.2 Injection moulding:

To study the effect of processing and changes in the fibre length, test specimen were also made using injection moulding method. For the same, copolymer granules (PHB / 8% HV) and short chopped green flax fibres having approx. 10 mm length, were used. The polymer granules and fibres were blended for 15 minutes at 170°C in a kneader (HBI System 90) run at 30 rpm. The mixed compound was granulated and injection moulded using an Arburg M270 injection-moulding machine. Processing specifications were:

Temperature Zone 1 to 5 (inclusive) : 160°C / 165°C / 170°C / 175°C / 180°C,

Injection pressure : 750 bar,

Mould temperature : 60°C,

Cooling time : 12 seconds.

8.2.2.3 Test methods:

Uniaxial tensile tests: on NMT composites (compression moulded) as well as randomly oriented short fibre composites (injection moulded) were performed on a Frank tensile testing machine (type 81565). All the composite plates were stored at ambient temperatures for 24 hours before testing. The tests were performed at a temperature of approx. 20°C and speed of 4.8 mm/min. In the case of NMT samples, the tensile tests were performed on test bars with rectangular cross-section and dimensions of 150 mm × 20 mm × 2 mm. For injection moulded samples the tensile tests were performed on dumbbell shaped specimen with dimensions of 150 mm × 10 mm × 3.5 mm according to the ASTM standard

D638M. For NMT composites as well as injection-moulded samples, an extensometer was used to monitor the elongation of the tested specimen. The initial modulus, tensile strength and strain-at-break were measured from the recorded stress-strain curves. For each condition ten different samples were tested. The samples were tested in the laboratory having controlled RH of about 60% and temperature of about 20°C.

Impact resistance: This was measured using Izod impact testing method. The tests were performed on the notched samples having dimensions of approx. 60 mm × 12.7 mm × 2 mm and notch dimensions according to the American standard ASTM D256. At least 5 test bars were tested for each composition and fibre content.

Dynamic mechanical thermal analysis (DMTA): The effect of cooling temperature, after compression moulding, on the glass transition temperatures of flax/PHB composites was determined using DMTA (Polymer Laboratories DMTA, MK III). The samples were analysed in the tensile mode (frequency: 1 Hz at a heating rate of 2°C/min and temperature range: -20°C to 100°C).

Differential scanning calorimetry (DSC): Studies on PHB/flax composites were done on Perkin Elmer DSC7 instrument. For the same the samples were heated from 130°C to 210°C at the heating rate of 20°C/min.

Fracture surface analysis: The fracture surface of flax/PHB composites was observed through Scanning electron microscope (SEM), Cambridge Stereoscan 200. For the same the samples were coated with gold/palladium.

Biodegradation: Injection moulded tensile bars of PHB / 8%HV reinforced with 20 volume % flax were buried in open soil at a depth of approximately 25 cm. Prior to burying the weight of each specimen was determined. At regular intervals of 4 weeks a tensile bar was dug up, cleaned, dried for 3 days at 80°C and stored at room temperature for another 3 days. After that the weight of the bar was determined. Finally a tensile test was performed on the sample using a Frank

81565 tensile tester at a strain rate of 10^{-3} s^{-1} at room temperature. The force was measured using a 10kN HBM load cell, whereas displacement was determined from crosshead displacement.

8.3 Results and discussion

8.3.1 NMT

Figure 8.2 shows the tensile strength of the flax/PHB NMT composites manufactured through compression moulding process, as a function of the fibre volume fraction. The tensile strength data of flax/PP (NMT) and glass-mat-reinforced thermoplastic (GMT) composites are also plotted.

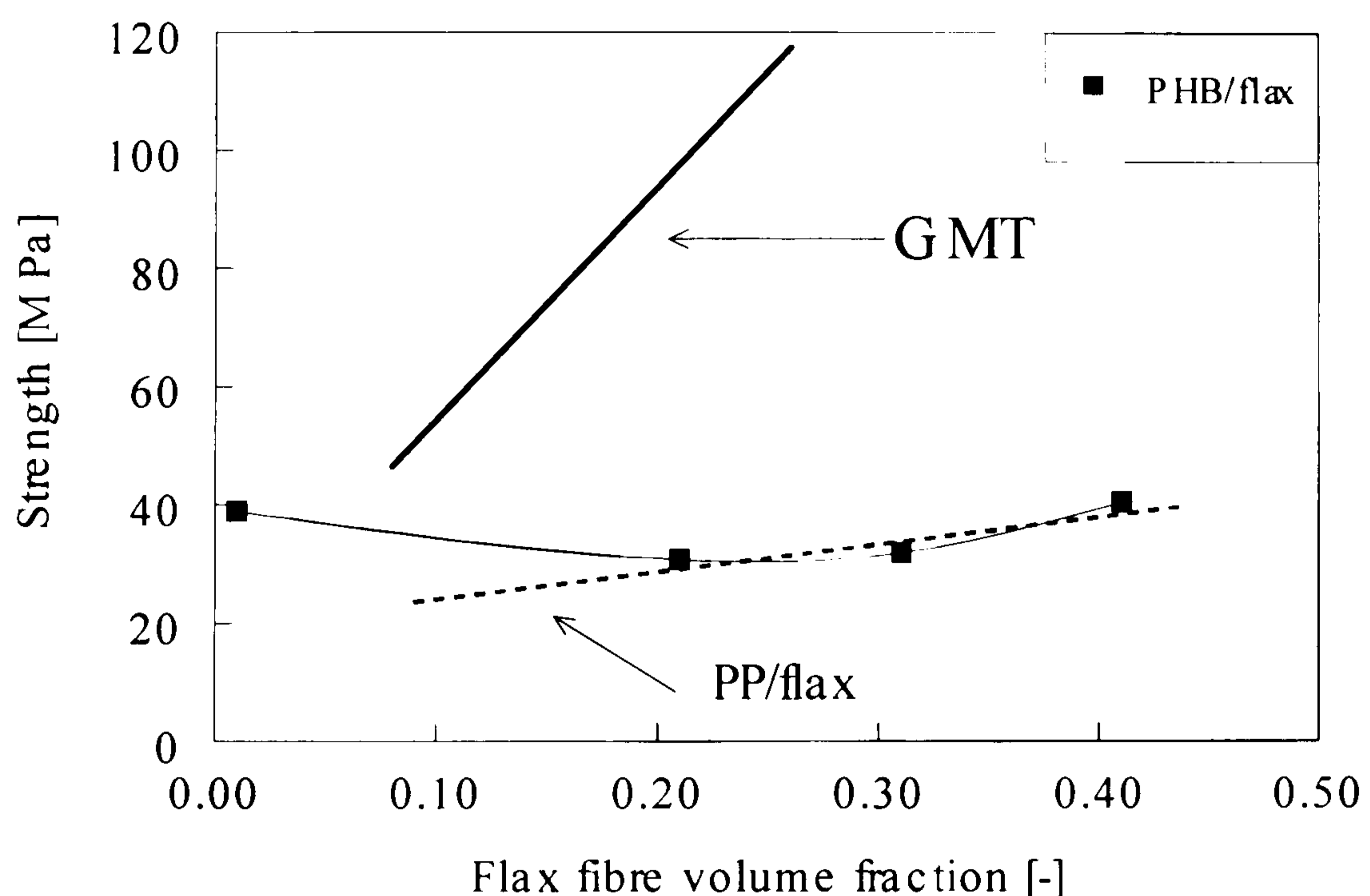


Figure 8.2 Tensile strength of PHB/flax NMT composites (■), PP/flax (NMT) and PP/glass fibre (GMT) composites as a function of fibre volume fraction. The PHB/flax data is fitted by Spline curve using Slide Write program.

On fibre addition, a small decrease in the flax/PHB composite strength followed by a small increase at higher volume fractions was observed. This could be because of the difference in quality of the different plates. Overall, it may be mentioned that no significant effect of fibre addition on the composite tensile strength was observed. This trend, of tensile strength with varying fibre volume fraction, was theoretically not expected as addition of fibre having lengths higher than critical

fibre length should increase the strength of the composite. One of the reasons for the observed trend could be imperfect bonding between fibre and matrix and therefore fibres act as crack initiators. Another reason might be the presence of woody parts in flax fibre mats or transverse fibre bundle splitting, which might act as crack initiator leading to a decrease in the strength which is probably compensated by an increase in reinforcement at higher volume fractions of fibres.

Figure 8.3 shows the initial modulus of the manufactured flax/PHB NMT composites as a function of the fibre volume fraction. The stiffness data of flax/PP NMT and GMT composites are also plotted. As expected, the stiffness of composites increased with fibre content. This shows that factors like weak bonding and presence of woody particles are not as critical for stiffness as they are for strength enhancement.

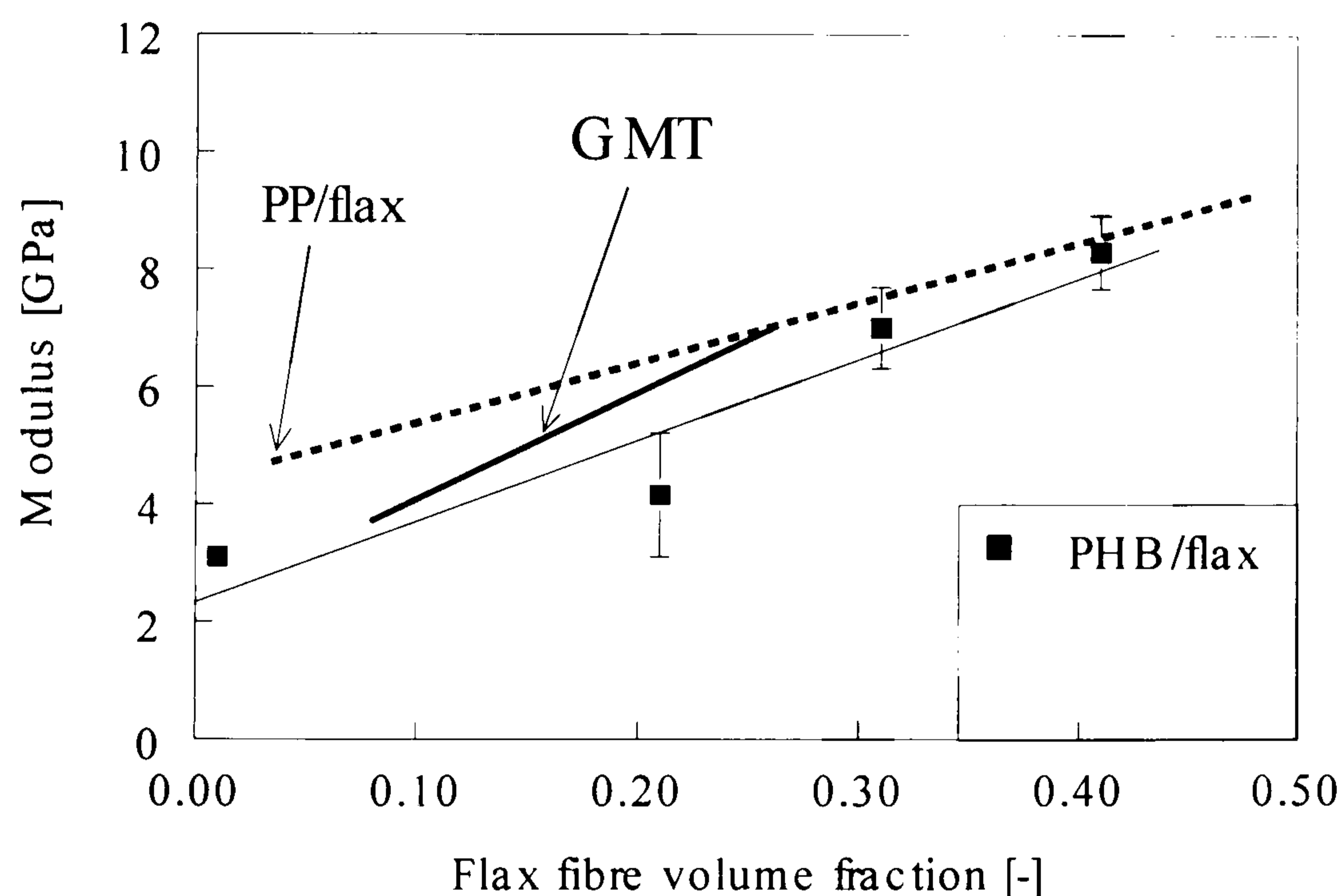


Figure 8.3 Initial modulus of PHB/flax NMT composites (■), PP/flax (NMT) and PP/glass fibre (GMT) composites as a function of fibre volume fraction. The PHB/flax data is fitted by linear curve, using slide write program, having an R^2 value of 0.88. The error bars show standard deviations.

Figure 8.4 shows the elongation-at-break of PHB/flax NMT composites as a function of fibre volume fraction. Addition of flax resulted in a lower elongation-at-break of composites i.e. approx. 1.5% for all fibre volume fractions. Flax fibres

have low elongation-at-break i.e. approx. 1.7% measured at a gauge length of 5 mm, therefore addition of these fibres constrains the elongation of the polymer matrix.

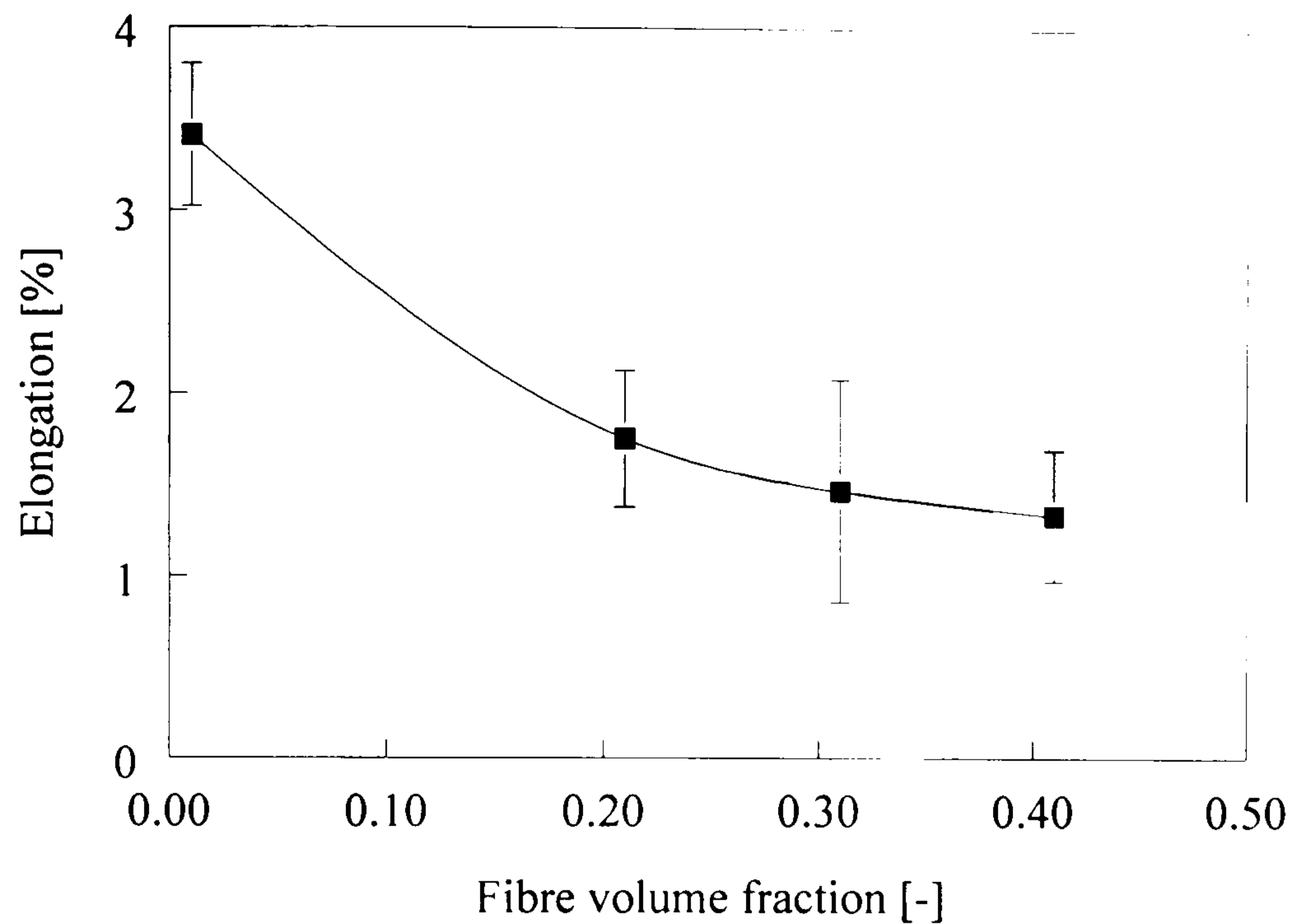


Figure 8.4 Elongation-at-break of PHB/flax NMT composites (■) as a function of fibre volume fraction. The data are fitted by Spline curve by Slide Write program and the error bars show standard deviations.

Figure 8.5 shows the influence of fibre content on the (notched Izod) impact resistance of PHB/flax NMT composites. The impact energy absorption increased with increasing flax fibre content and therefore leading to toughening of brittle PHB. The increase is probably due to fibre pull-out mechanism, which is prominent in the system with weak bonding between fibre and matrix. This was also observed through the SEM (Scanning electron microscope) pictures of the fracture surface of the tensile specimen, as shown in Figure 8.6. The phenomenon of PHB toughening through addition of flax fibres is quite interesting as far as cost-performance of this polymer is concerned. Addition of cheaper fibre not only reduces the cost of polymer but also improves the impact properties of PHB, which is quite important considering the brittle nature of the polymer.

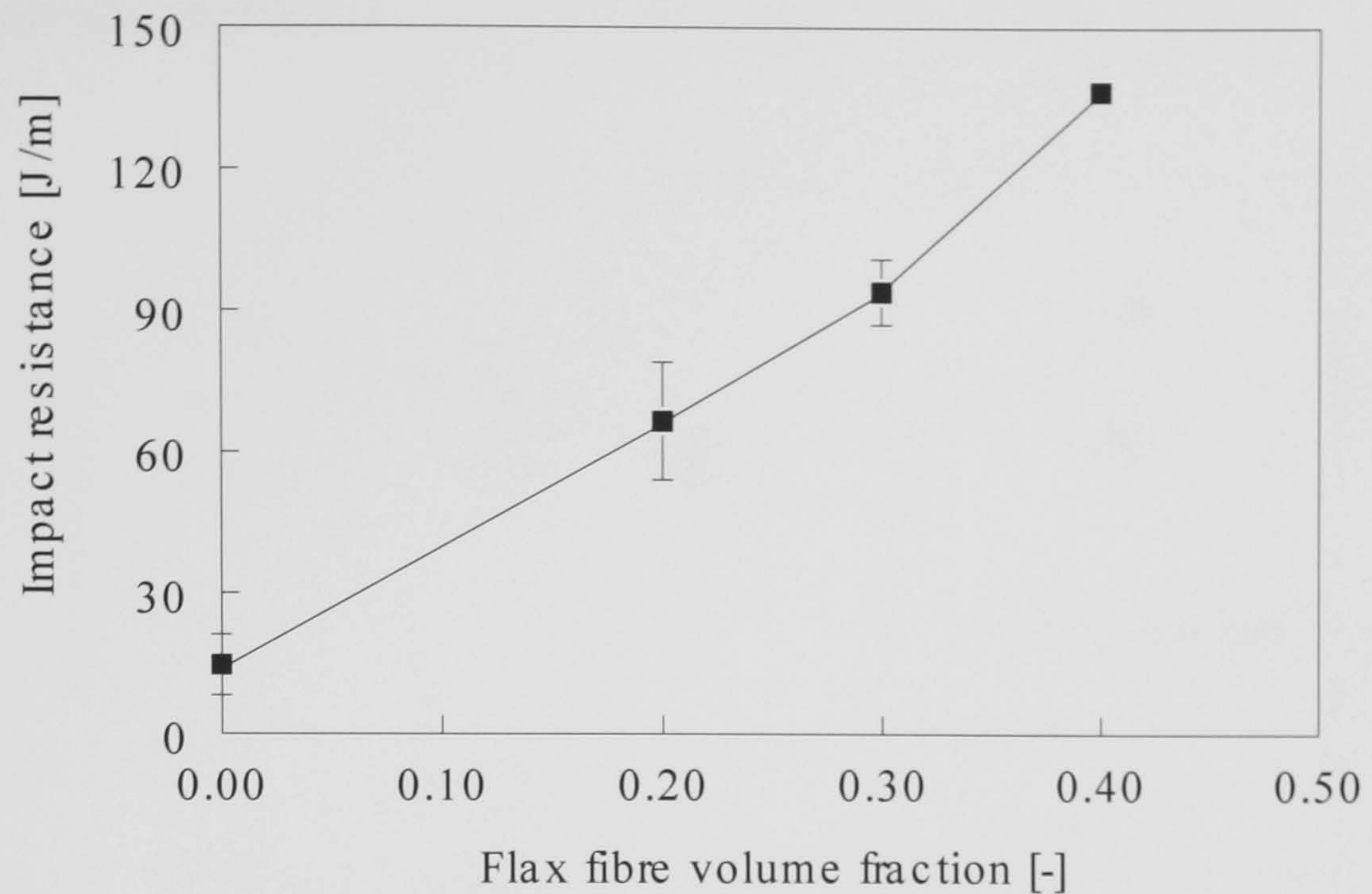


Figure 8.5 Notched Izod impact resistance of PHB/flax NMT composites (■) as a function of fibre volume fraction. The data are fitted by Spline curve using Slide Write program and the error bars show standard deviations.

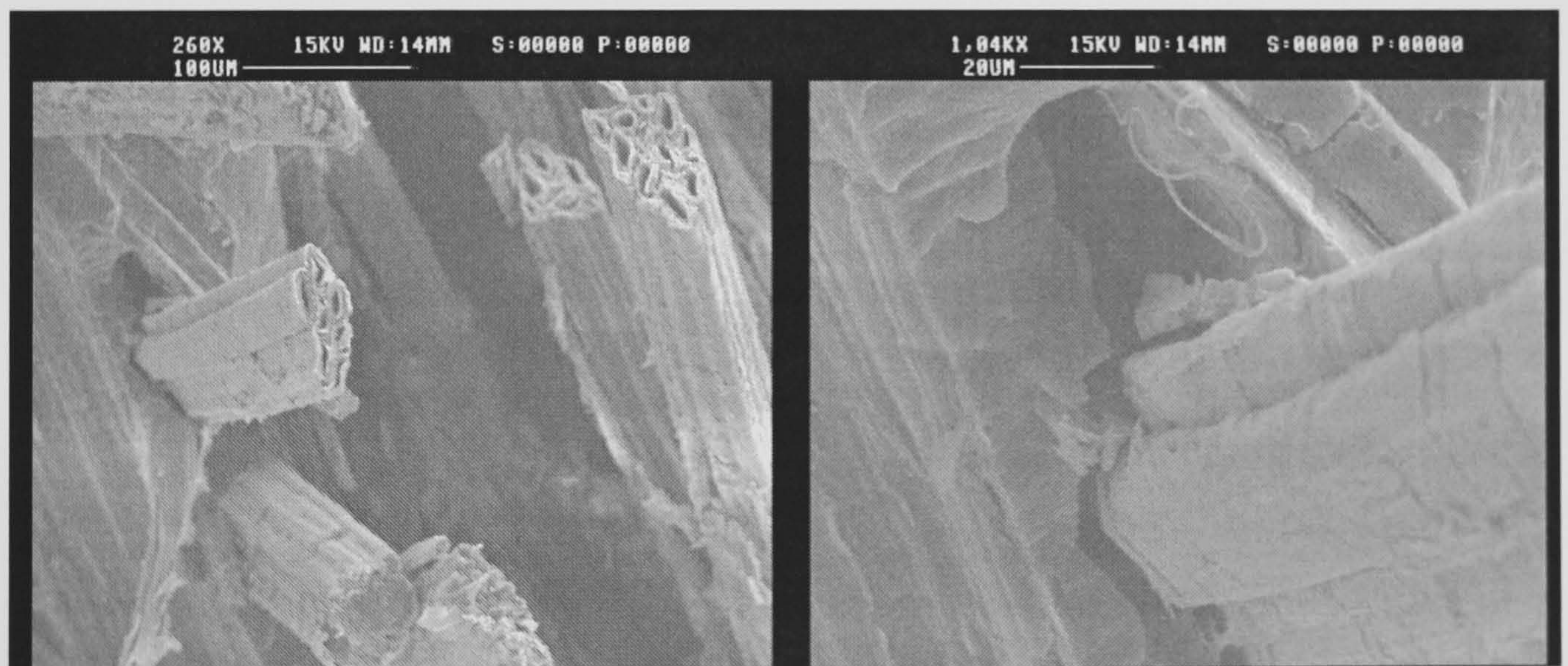


Figure 8.6 SEM pictures of impact fracture surface of PHB/flax NMT composites.

8.3.2 Influence of hydroxyvalerate content in the copolymer

Figure 8.7 shows the tensile strength of different grades of PHB/HV as a function of fibre volume fraction. In comparison with native PHB the copolymers had a somewhat lower strength, around 30 MPa, which was also reflected in composite

properties. Similar to the previous observations, the strength of the PHB HV/flax composites was almost constant with increasing fibre volume fraction.

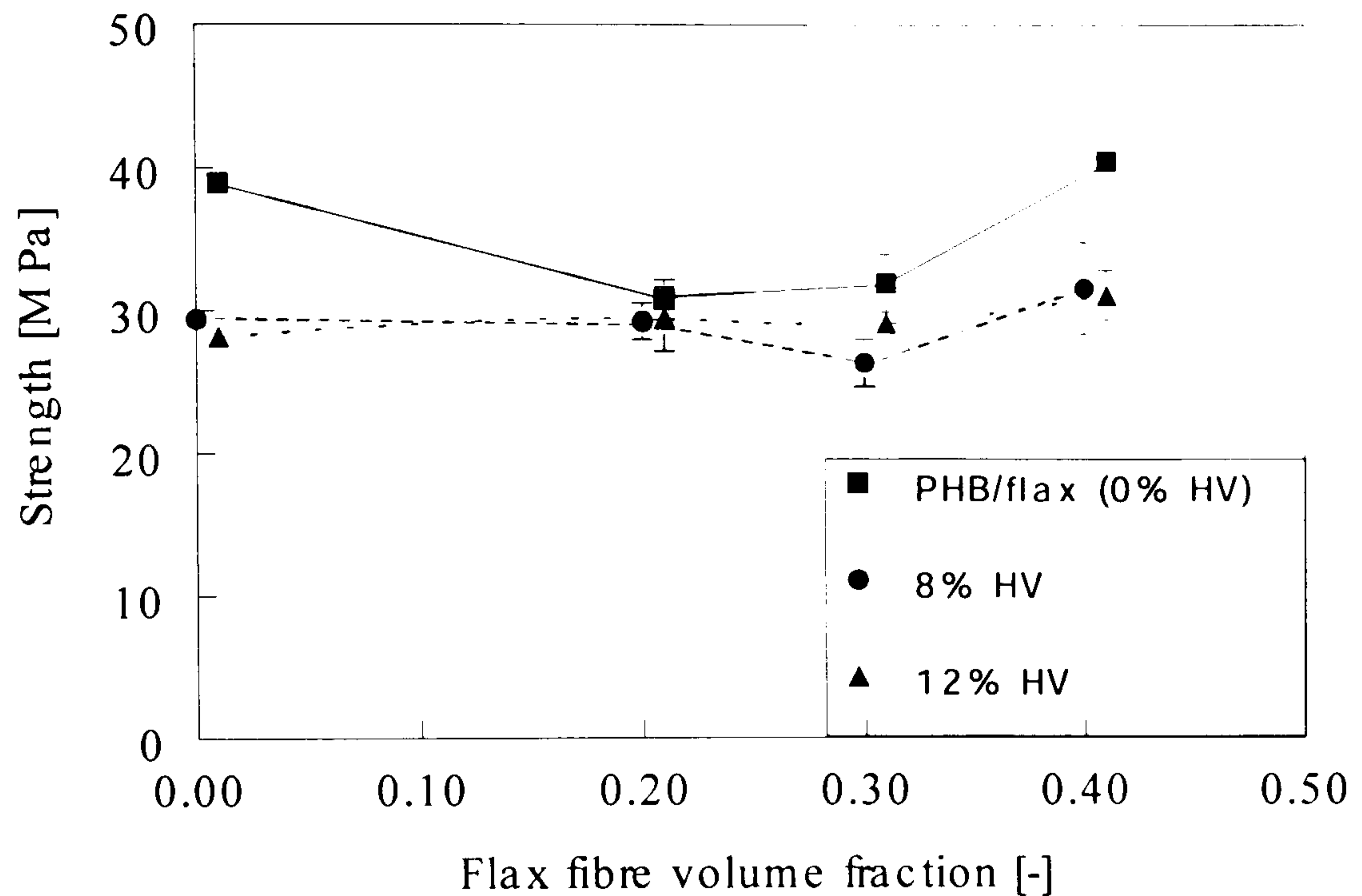


Figure 8.7 Tensile strength of flax/PHB(/HV) composites versus fibre volume fraction and HV content in the copolymer. The error bars show standard deviations (The data are simply connected by straight lines).

Figure 8.8 shows the influence of co-monomer content on the stiffness of PHB(/HV)/flax composites with varying amount of fibre volume fraction.

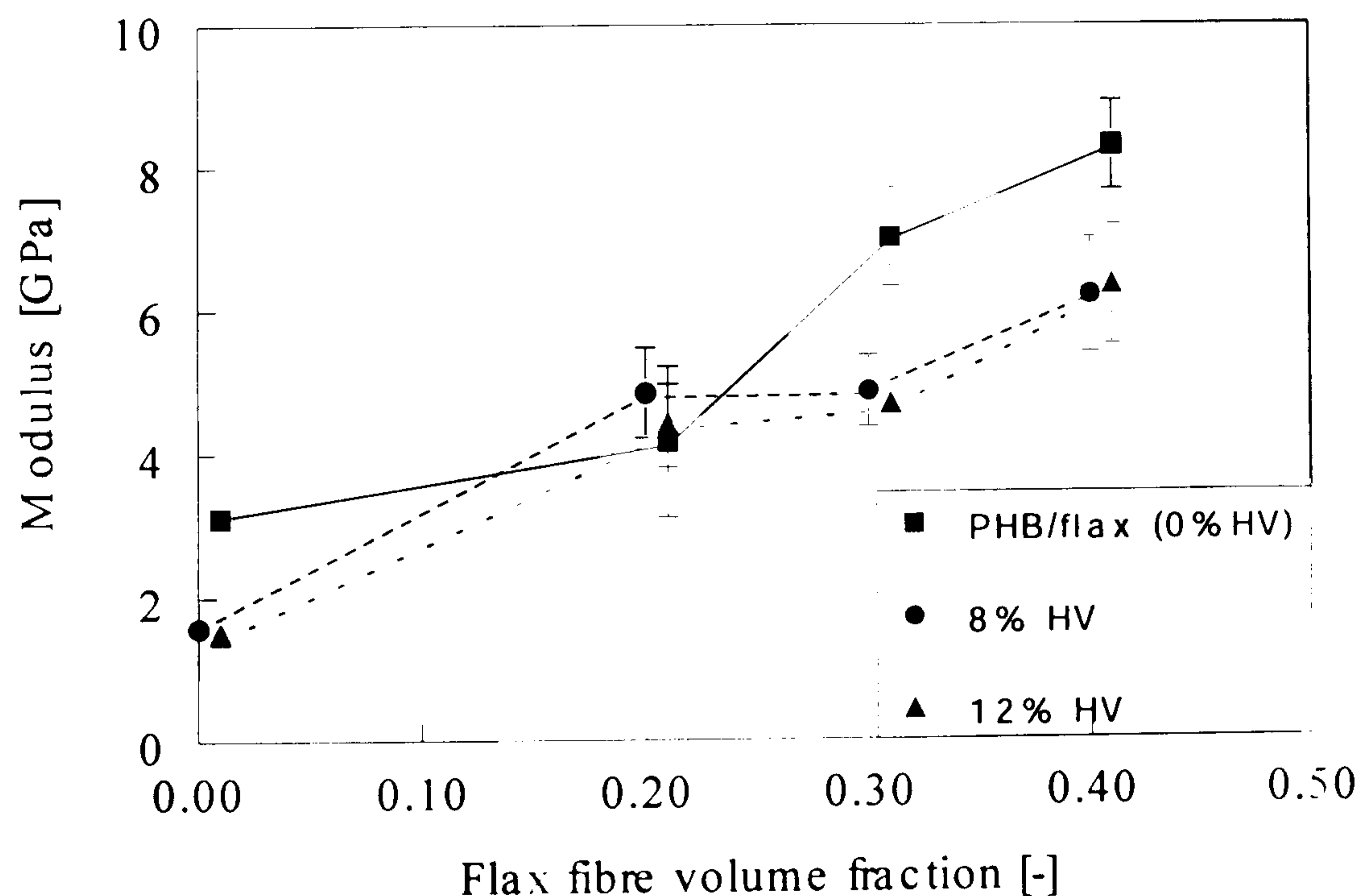


Figure 8.8 Tensile modulus of flax/PHB(/HV) composites versus fibre volume fraction and HV content in the copolymer. The error bars show standard deviations (The data are simply connected by straight lines).

The modulus of the copolymers was lower when compared to the modulus of PHB because of the reasons mentioned earlier i.e. inclusion of HV content leads to lower crystallinity and therefore more amorphous phase. On reinforcing the copolymers, the modulus increased rapidly. The effect of HV content on copolymer stiffness was also reflected in the composite properties as copolymer based composites exhibited lower stiffness when compared with the stiffness of the native PHB/flax composites.

Figure 8.9 shows the effect of HV content on the elongation-at-break of the PHB(/HV)/flax composites.

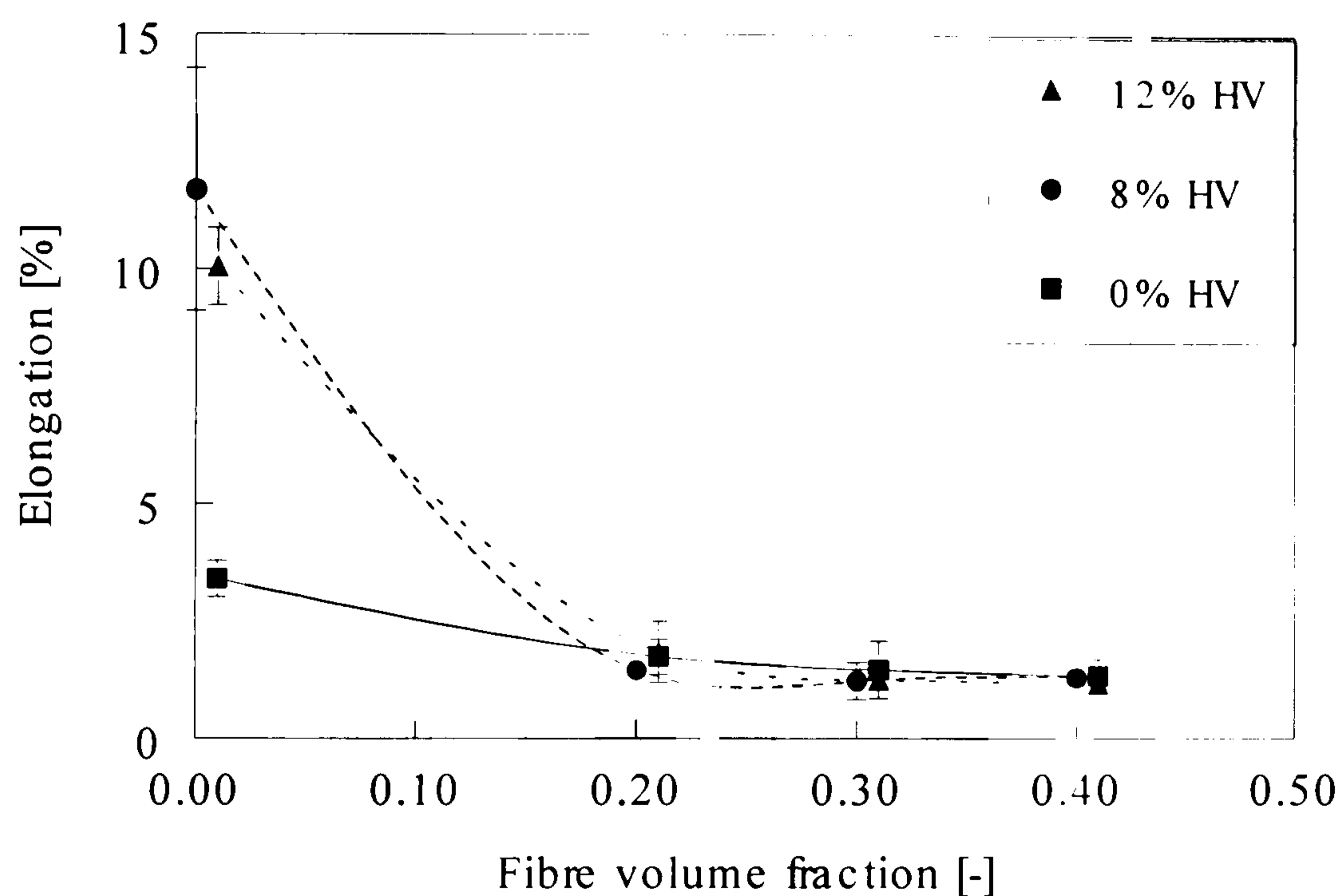


Figure 8.9 Elongation-at-break of flax/PHB(/HV) composites versus fibre volume fraction and HV content in the copolymer. The data are connected by Spline curve by Slide Write program and the error bars show standard deviations.

As expected, elongation-at-break of copolymer was higher than that of native PHB. The initial value of elongation-at-break of neat PHB was 3.4% whereas the copolymers (PHB/HV) had an elongation-at-break of around 10%. The higher elongation of the copolymers can be explained through the differences in morphology. Inclusion of the HV group led to lower amount of crystallinity and therefore more amorphous phase. Addition of flax reduced the elongation-at-break to approximately 1.5% for all flax volume fractions.

Figure 8.10 shows the (notched Izod) impact resistance of flax/PHB(/HV) NMT composites. The impact resistance of PHB/HV copolymers was observed to be higher than the PHB polymer. Since PHB is more crystalline than copolymers therefore it is more brittle than the latter but addition of fibre reversed the trend i.e. the composite based on pure PHB had higher impact strength than the composites based on copolymers. The difference in impact strength of composites based on PHB and copolymer is probably due to the differences in the wetting between fibre and the matrix. Since copolymers have lower melting point therefore at the processing temperature of PHB they might be having lower viscosity leading to improved wetting of the flax fibres. This improved wetting of copolymer might have led to lower impact strength when compared to PHB based composite. As the fibre volume fraction increased the effect of wetting also increased, which might have led to higher impact strength of PHB based composites as compared to copolymer based composites.

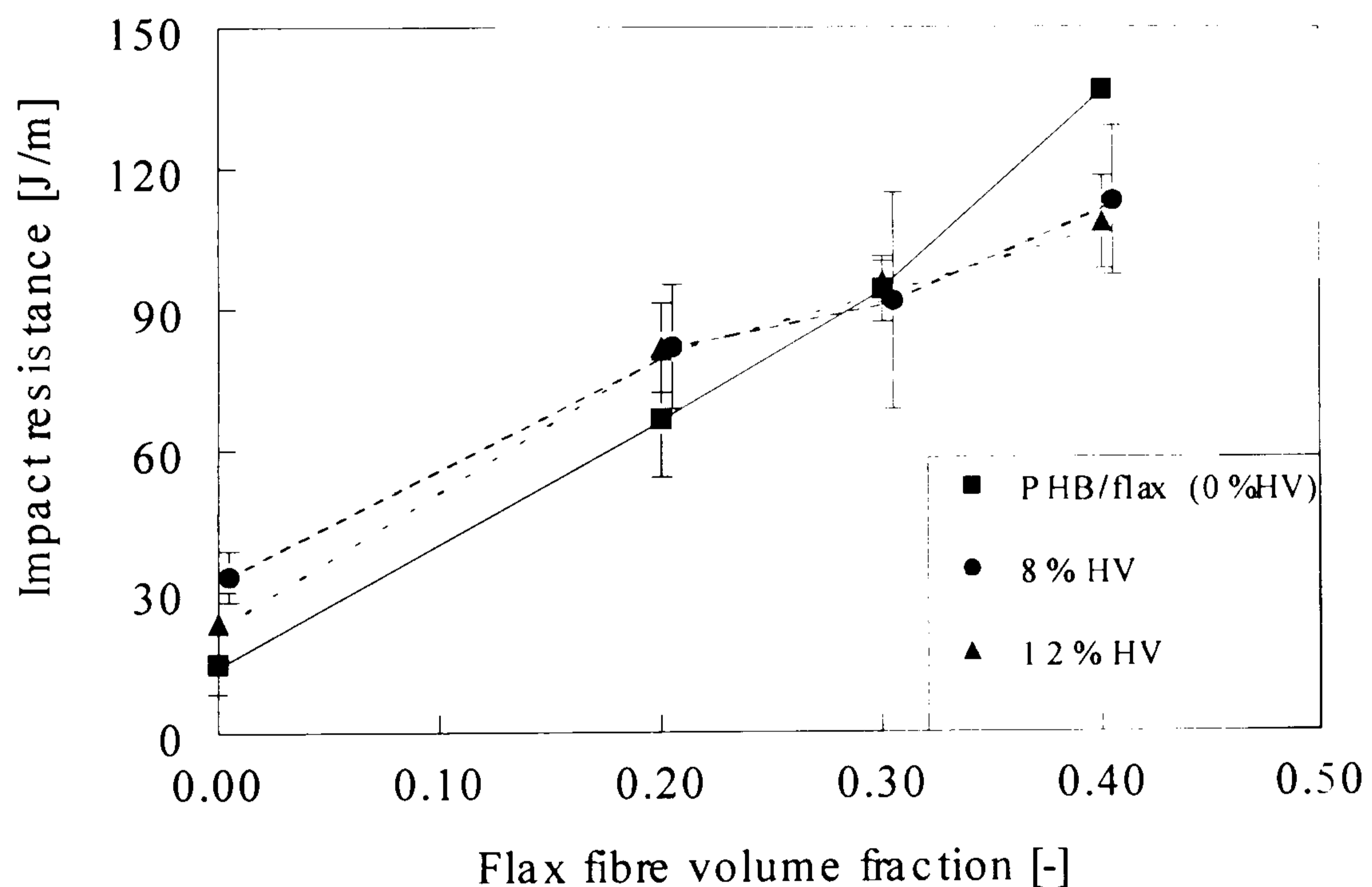


Figure 8.10 Notched Izod impact resistance of flax/PHB(/HV) NMT composites versus fibre volume fraction and HV content in the copolymer. The error bars show standard deviations and the average data are connected by straight lines.

However, both PHB based as well as PHB/HV based composites exhibited improved toughness on addition of flax fibres. As mentioned before, this improvement is an interesting result as far as cost-performance of the polymer is

concerned. Although PHB/HV copolymers are more expensive than PHB polymer but the mechanical performance of PHB based composites seems to be better than the former.

8.3.3 Influence of cooling temperature

Figure 8.11 shows the elongation-at-break (%) of PHB/flax NMT composites with different fibre content and compression moulded with different cooling temperatures.

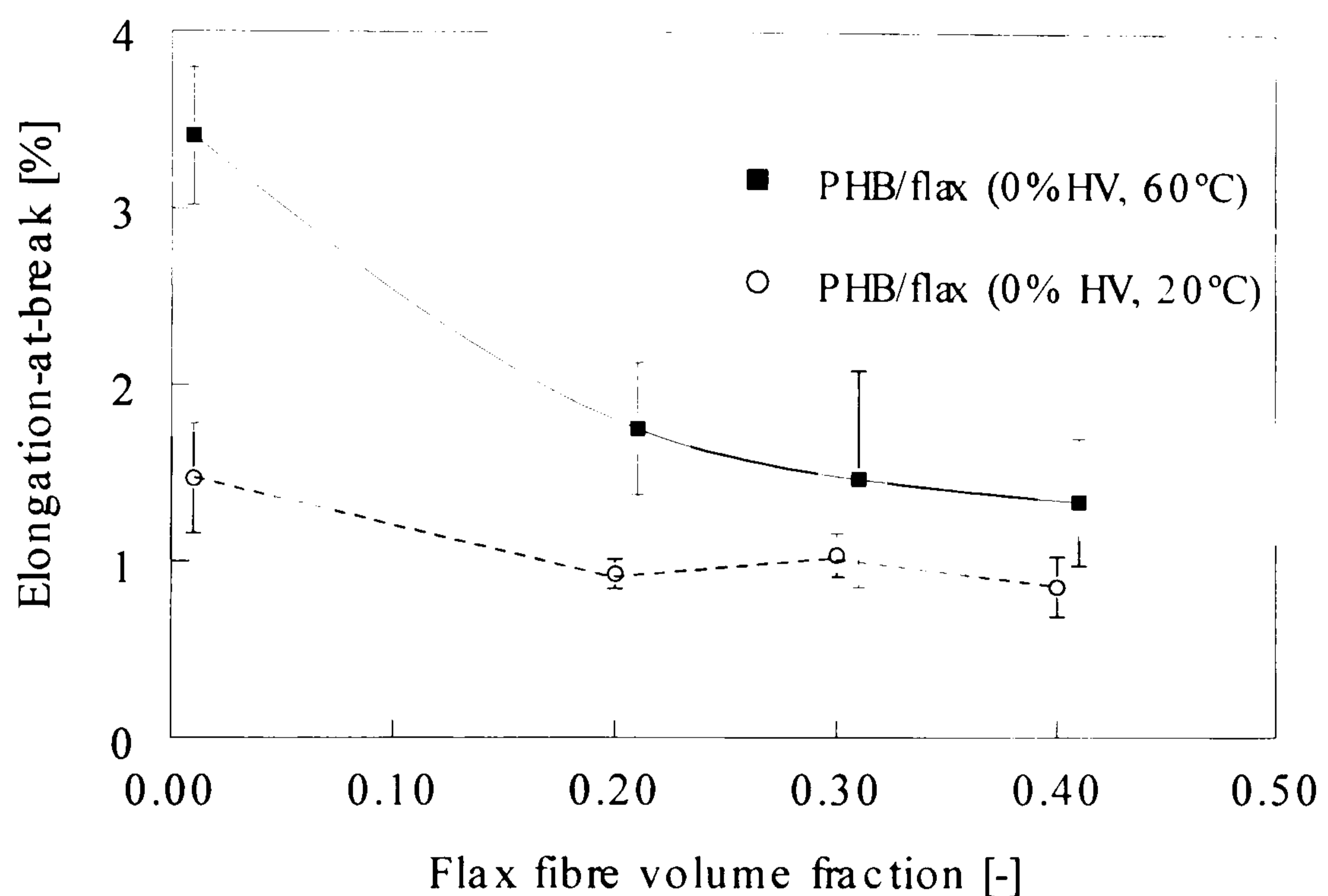


Figure 8.11 Elongation-at-break (%) of PHB/flax NMT composites as a function of fibre volume fraction and cooling temperature during compression moulding. The PHB/flax (60°C) data are fitted by Spline curve using Slide Write program and 20°C data are connected by straight lines. The error bars show standard deviations.

As seen in Figure 8.11, the elongation-at-break (%) of composites cooled at 20°C is lower than the samples cooled at 60°C. Additional experiments were done on PHB polymers, cooled at different temperatures, to observe the difference in morphology. Both dynamic mechanical thermal analysis (DMTA) and differential scanning calorimetry (DSC) were carried out to determine the differences in loss factor and crystallinity, respectively. Figure 8.12 shows the dynamic mechanical

characteristics of PHB samples cooled at 60°C and 20°C. The samples cooled at 60°C show higher loss factor ($\tan \delta$), which could be either because of higher amorphous content (lower crystallinity) or higher relaxation of the amorphous zone. DSC was performed to obtain more information on the crystallinity. DSC tests displayed higher heat of fusion/unit mass in case of samples cooled at 60°C than the samples cooled at 20°C during compression moulding. Therefore, the samples cooled at 60°C had higher crystallinity as well as higher relaxation of molecules in the amorphous zone. The former decreases the elongation and the latter has an increasing effect on the elongation. From the results (Figure 8.11 and 8.12) it can be mentioned that relaxation of amorphous zone due to cooling at 60°C plays a dominant role in enhancing the elongation of polymer as well as composites. Similar results were reported by De Koning (De Koning, 1993) where annealing of PHB not only enhanced the crystallinity but also improved the toughness through increased relaxation of the amorphous phase.

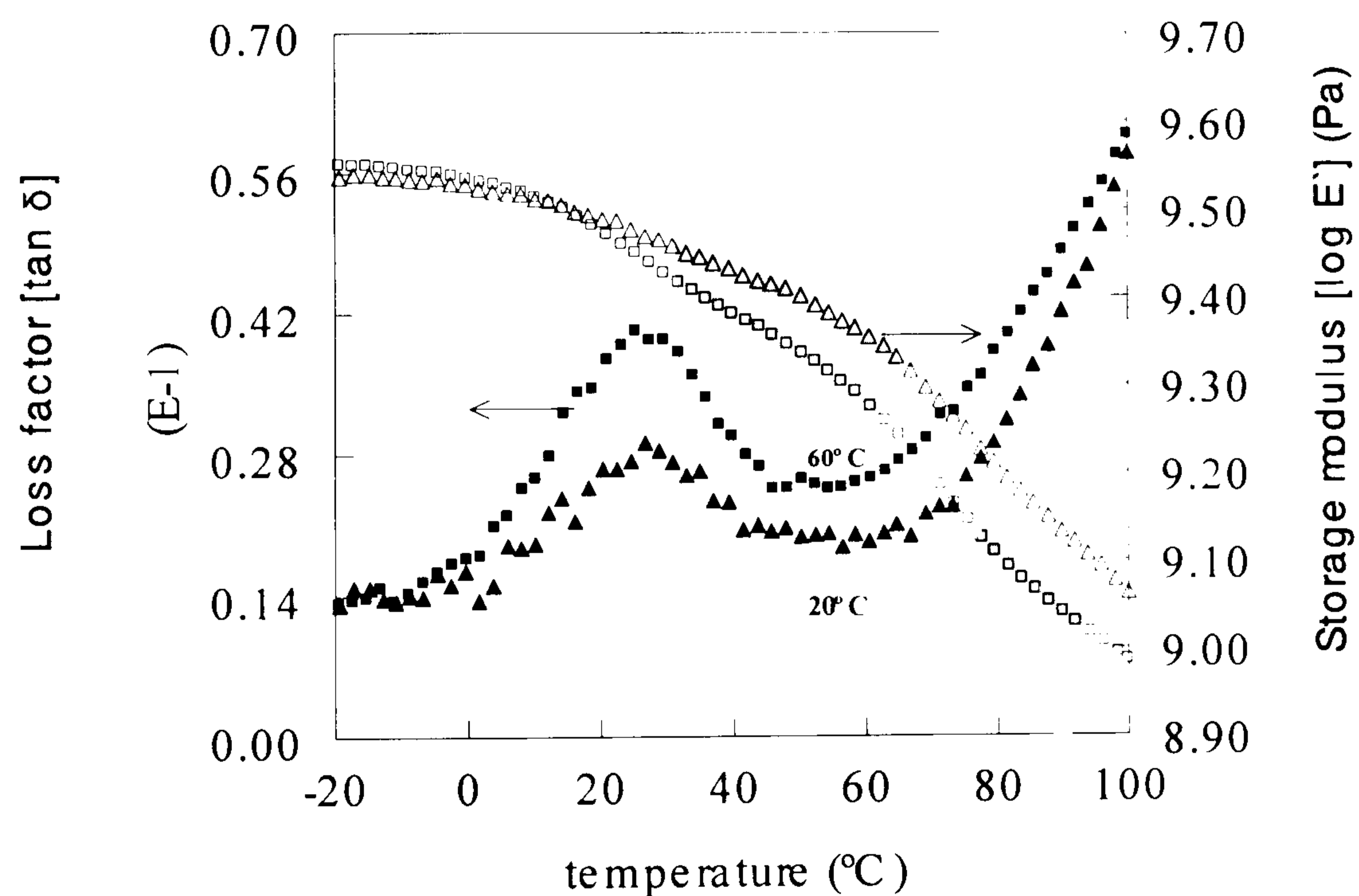


Figure 8.12 Dynamic mechanical characteristics versus temperature for compression moulded PHB samples, which were cooled at (■) 60°C and (▲) 20°C (mould temperature).

8.3.4 Injection moulded composites

As shown in Figure 8.13, 8.14 and 8.15, no significant effect of processing methods i.e. injection moulding and compression moulding, on the stiffness.

strength and elongation of the composites was observed. These results are similar to the ones shown in Chapter 6 where no effect of fibre length reduction, through injection moulding, on the strength and stiffness of flax/PP composite was observed. As shown in Chapter 6 (Figure 6.11 and 6.12) injection moulding reduced the average fibre length from ≈ 10 mm to ≈ 1 mm. In a separate study Van de Beld (2000) conducted micro-debond tests on flax/PHB microcomposites and reported data on interfacial shear strength equal to 8.9 MPa. From interfacial shear strength critical fibre length (L_c) was calculated, as shown in Chapter 5, which was 1.0mm. However, major portion of the fibre length after injection moulding was still higher than critical fibre length or had better orientation along the (tensile) testing direction of the composite as no effect of fibre length reduction on stiffness, strength and elongation of the composites was observed (Figure 8.13, 8.14 and 8.15). Injection moulding has some advantages like lower production time and higher reproducibility along with a disadvantage of reduced composite fracture toughness. As shown in Figure 8.16, samples made through injection moulding showed lower impact resistance (notched Izod), which was probably due to the reduced amount of fibre pull-out and energy absorption through fibre fracture. As the fibre length in injection moulded composites reduced to lengths in the range of critical fibre length therefore the energy absorption through fibre fracture was also reduced, as compared to compression moulded composites (Figure 8.16).

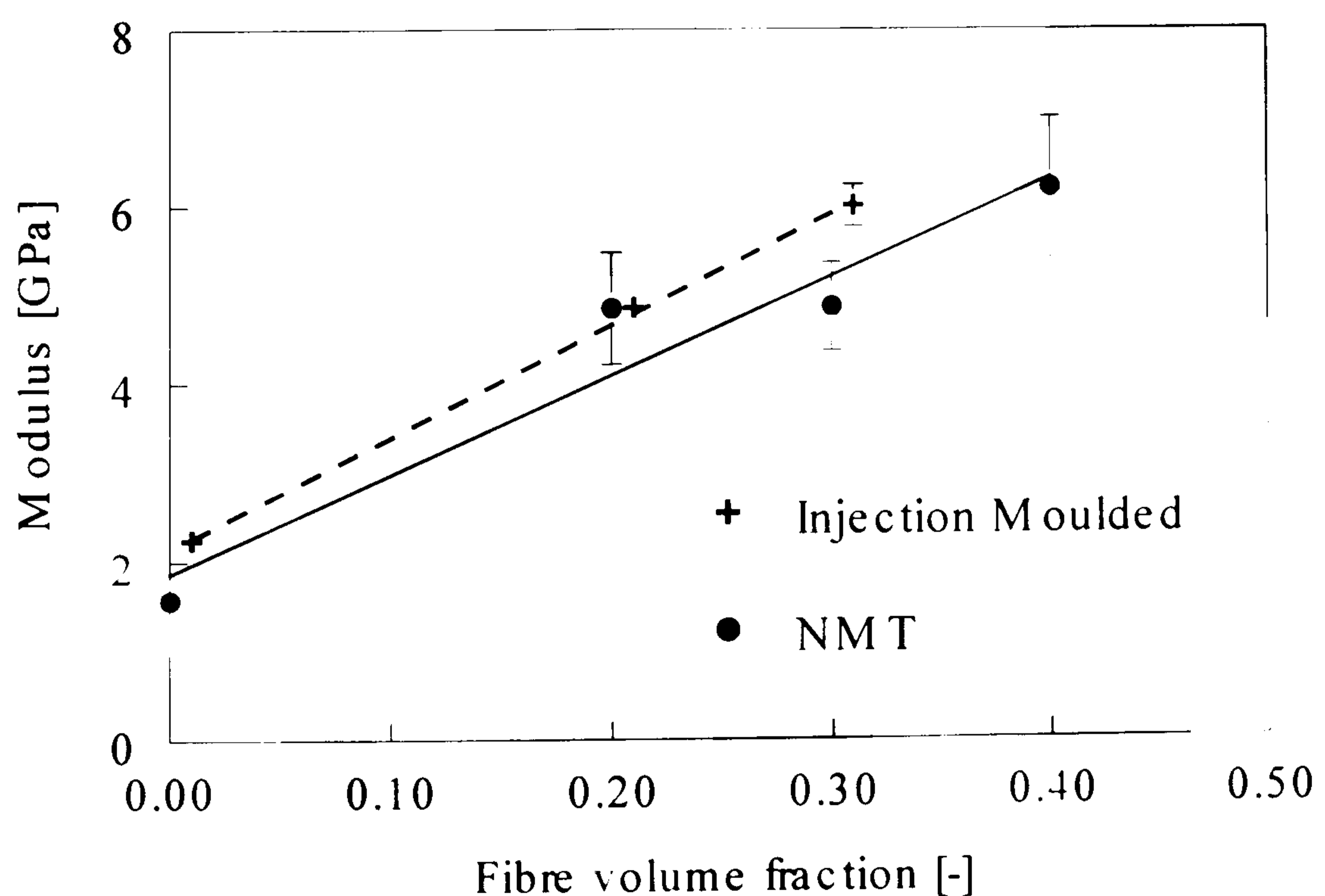


Figure 8.13 Initial modulus of PHB/flax composites as a function of fibre volume fraction and manufacturing method. The data are linearly fitted, using

Slide Write program, with R^2 values of 0.98 and 0.93 for injection moulded and NMT composites, respectively. The error bars show standard deviations.

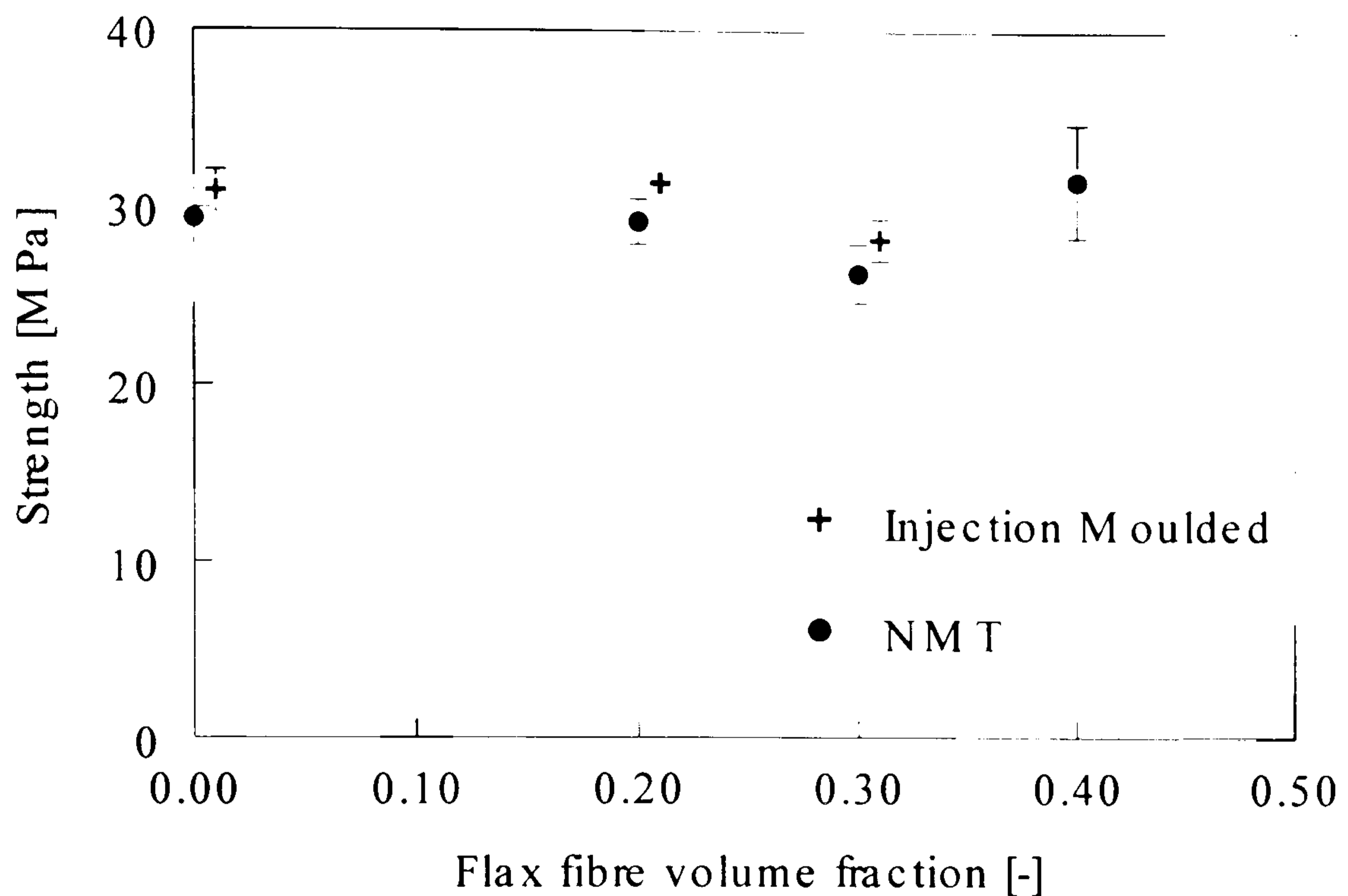


Figure 8.14 Tensile strength of PHB/flax composites as a function of fibre volume fraction and manufacturing method. The error bars show standard deviations.

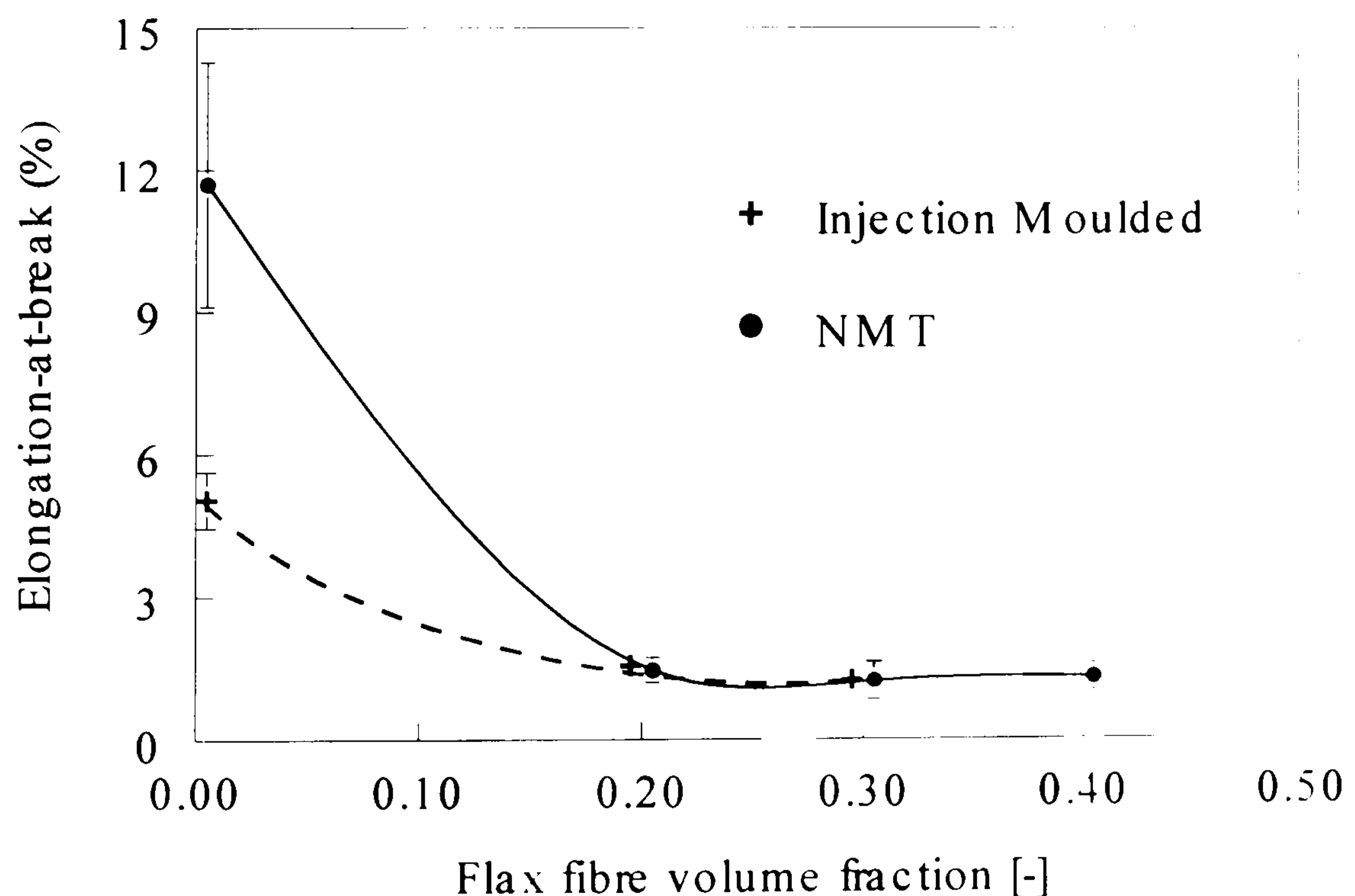


Figure 8.15 Elongation-at-break (%) of PHB/flax composites as a function of fibre volume fraction and manufacturing method. The data are fitted by Spline curve using Slide Write program and the error bars show standard deviations.

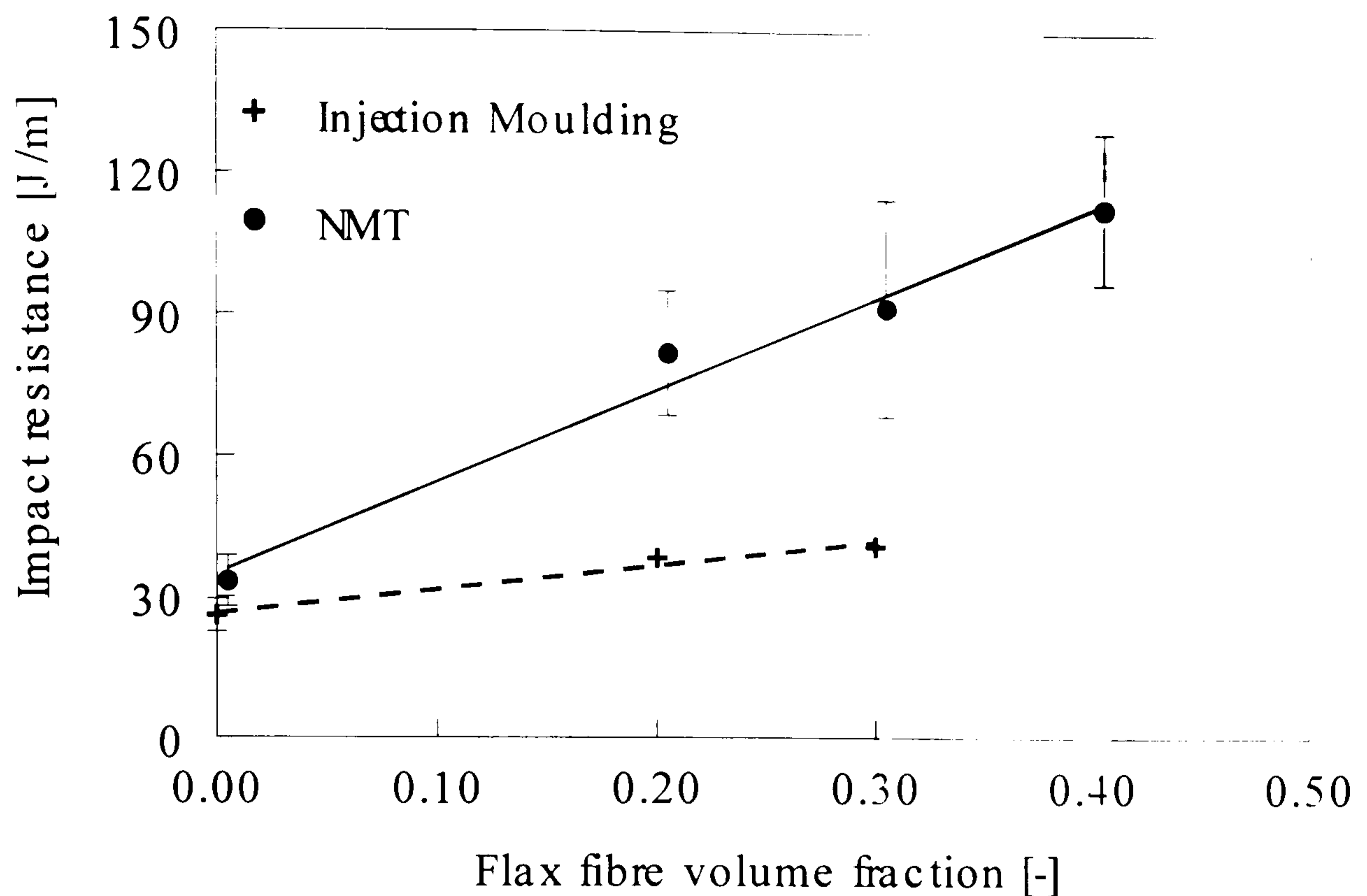


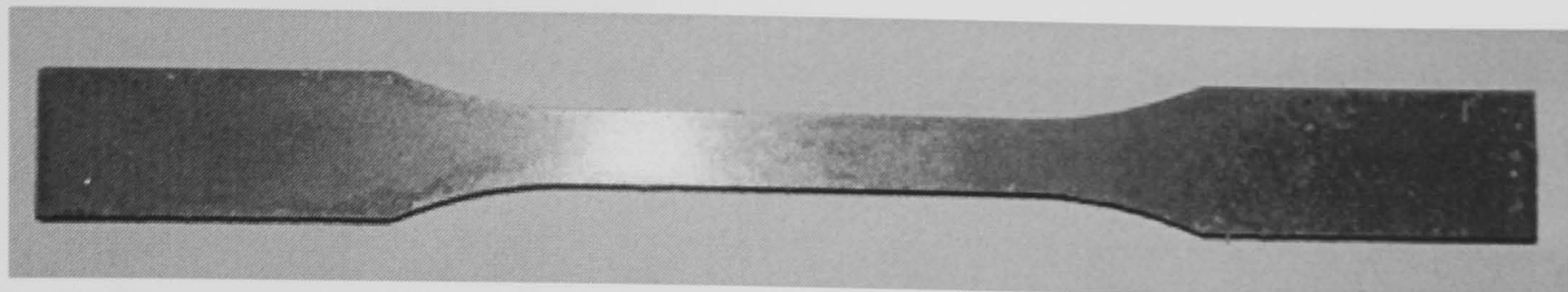
Figure 8.16 Notched Izod impact resistance of PHB/flax composites as a function of fibre volume fraction and manufacturing method. The data are linearly fitted, using Slide Write program, with R^2 values of 0.97 and 0.98 for injection moulded and NMT composites, respectively. The error bars show standard deviations.

8.3.5 Biodegradation

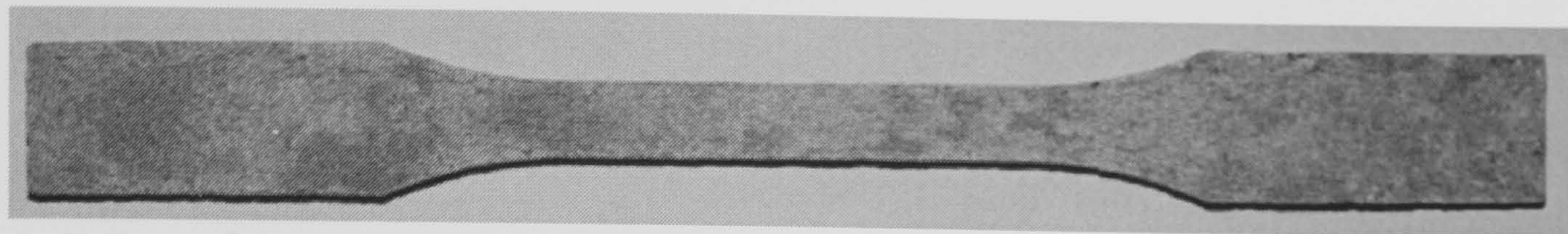
Biodegradability of a polymer can be a positive attribute as well as a disadvantage depending on the application. Applications, like packaging where material is required to degrade and become a part of life cycle after disposal, are suitable for bioplastics as well as biodegradable synthetic polymers. However, synthetic biopolymers may prove to be non-environment friendly in the sense that they are not CO_2 neutral. Bioplastics, which are manufactured through biomaterials, can be attractive for such applications, without harming the environment through harmful emissions.

Tensile bars of PHB/8%HV/flax composites, manufactured by injection moulding and having dog-bone shape, were buried in open soil to study the effect of biodegradation on composite properties. Figure 8.17 shows the pictures of tensile

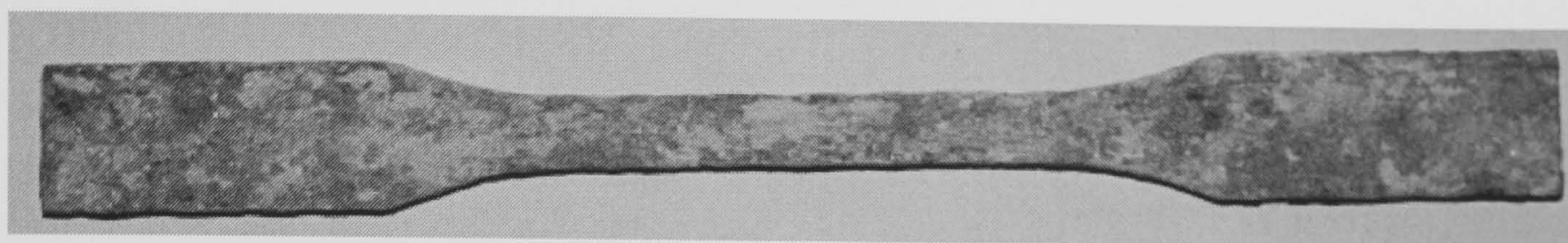
bars after several weeks of burying in the open soil. During the first two weeks after burial both tensile modulus and tensile strength decreased sharply. After the first two weeks the modulus and strength of the composite seemed to stabilise. The observed trend is shown in Figure 8.18. In contrast to this the mass decreased continuously during the first 20 weeks of burial, indicating biodegradation of the material. The effect of burial (degradation) on the normalised weight of PHB/8%HV/flax composites is shown in Figure 8.19. The observed differences in the effect of burial on tensile properties (Figure 8.18) and normalised weight (Figure 8.19) indicate that the initial drop, in modulus and strength of the composites, was not due to biodegradation or weight loss. The initial drop in modulus and strength may result from debonding due to moisture absorption in the first two weeks. After this initial drop in tensile properties the further effect on the tensile properties due to degradation was more gradual.



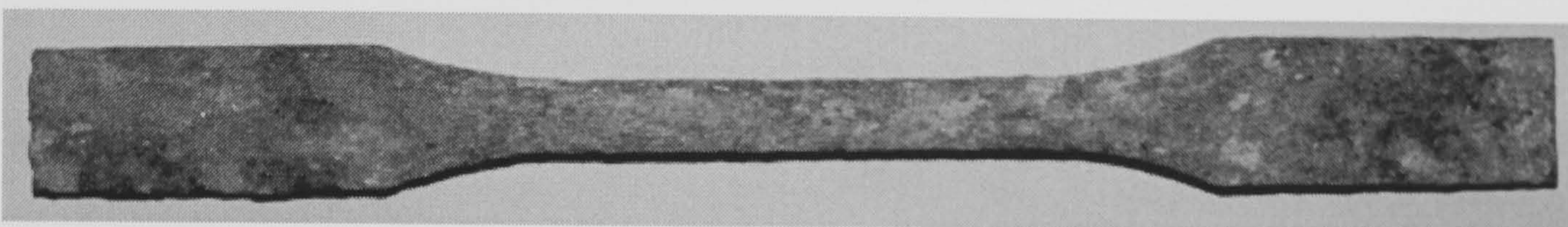
(a) PHB/green flax (0 weeks of burial)



(b) PHB/green flax (8 weeks of burial)



(c) PHB/green flax (16 weeks of burial)



(d) PHB/green flax (20 weeks of burial)



(e) PHB/green flax (24 weeks of burial)



(f) PHB/green flax (28 weeks of burial)

Figure 8.17 Pictures of different stages of biodegradation of PHB/8%HV/flax (20Volume %) composites.

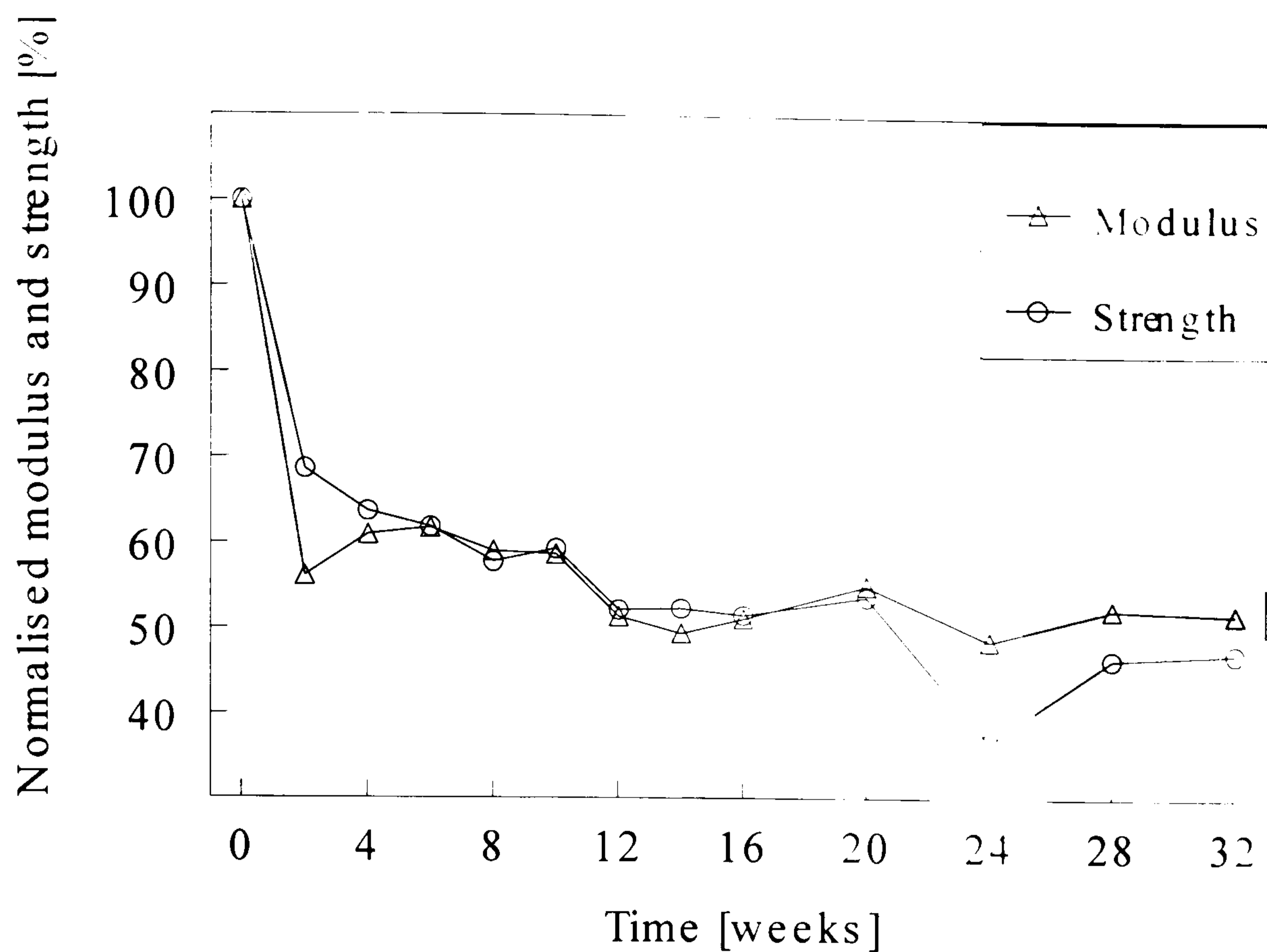


Figure 8.18 Normalised stiffness and strength of PHB/8%HV/flax composites after burial in soil. To make the figure clear, data points are connected by straight lines.

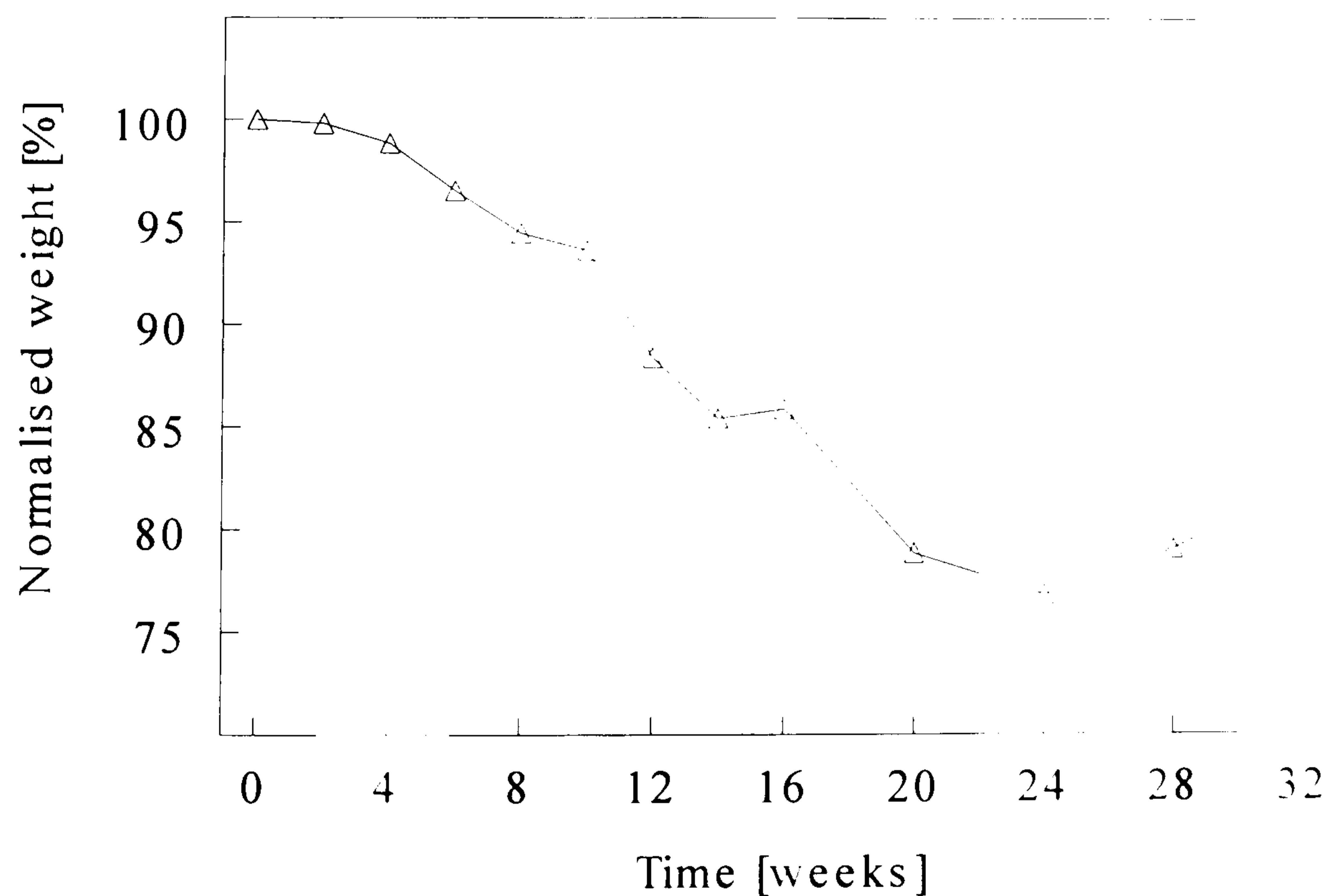


Figure 8.19 Normalised weight of tensile bars after burial in soil. To show the trend clearly, data points are connected by straight lines.

8.4 Conclusions

From the present study it can be concluded that:

- Addition of cheap flax fibres to an expensive and brittle PHB(HV) composite leads to enhanced toughness of the composites.
- Addition of (cheap) flax fibre to PHB can be advantageous as far as cost-performance of biopolymer composites is concerned.
- The strength of PHB based composites needs to be further optimised through modifications in fibre preparatory process (cleaning through carding and combing processes) and/or through modification of the fibre-matrix interface.
- Optimisation of processing conditions like cooling temperature can improve the properties of PHB/flax composites through increased relaxation of amorphous content. Koning (De Koning, 1993) had shown that ageing of PHB results into (embrittlement) reduction of impact strength, which can be toughened again through annealing. Addition of comonomers like HV has been considered as one of the ways to overcome the brittleness of PHB. These copolymers are more expensive than homopolymer PHB. Keeping in view the above mentioned shortcoming of PHB and its copolymer PHB/HV, addition of flax fibres along with controlled processing conditions seems to be a convenient way of toughening of PHB.
- Injection moulding may be advantageous over compression moulding because of lower production time and higher reproducibility. However, composites manufactured through injection moulding exhibited lower impact strength than those manufactured through compression moulding.
- Based on the biodegradation study of PHB/HV composites it can be concluded that the tensile properties drop significantly in the initial stage of degradation, which could be due to the fibre debonding. The drop in tensile properties is more gradual in the later stages of biodegradation.

9. LIFE CYCLE ANALYSIS (LCA) OF FLAX/POLYPROPYLENE COMPOSITES

This chapter includes theory about LCA and the LCA study of compression moulded flax fibre-mat-reinforced PP composite and glass fibre-mat-reinforced PP composite for an automotive and a non-automotive application.

9.1 Introduction

As mentioned earlier in Chapter 1, one of the major advantages of using natural fibre reinforced thermoplastic is based on the assumption that these composites would be environmentally friendly as far as processing and disposal of these materials is concerned. Natural fibres are CO₂ neutral, renewable, lightweight with good mechanical properties and produce less concern with safety and health. The glass fibre reinforced thermoplastics were taken as reference materials mainly because they have been successfully used in many applications like construction, automotive etc. Glass fibre reinforced thermoplastics have certain disadvantages such as:

- Glass fibres are very abrasive i.e. they increase wear of processing equipments such as moulds and extruders and machinery used to cut glass-fibre-reinforced products.
- Glass fibres can cause problems with respect to safety and health. They produce skin irritations and like asbestos fibres they can lodge in the lungs and can be absorbed in the body.
- Glass fibre reinforced plastics lead to problems with respect to their disposal at the end of their lifetime. Glass fibres cannot be thermally recycled by burning.
- Due to their brittleness glass fibres are also not easy to recycle mechanically.

They break easily during reprocessing thus lowering the mechanical properties of the recycled product significantly.

Goal and scope of the study

In Chapter 5 we found that the mechanical properties (strength and impact) of natural-fibre-mat-reinforced thermoplastic (NMTs) is much lower when compared with glass fibre-mat-reinforced thermoplastics (GMTs), but the effect of these materials on the environment was not studied. The environment impact is having increasing importance due to an increasing population and an increasing consumption. This makes clear that the environment cannot keep supporting this ever increasing burden. In this chapter the effect of NMT on the environment is studied through Life Cycle Analysis (LCA) computer program and compared with the existing material i.e. GMT.

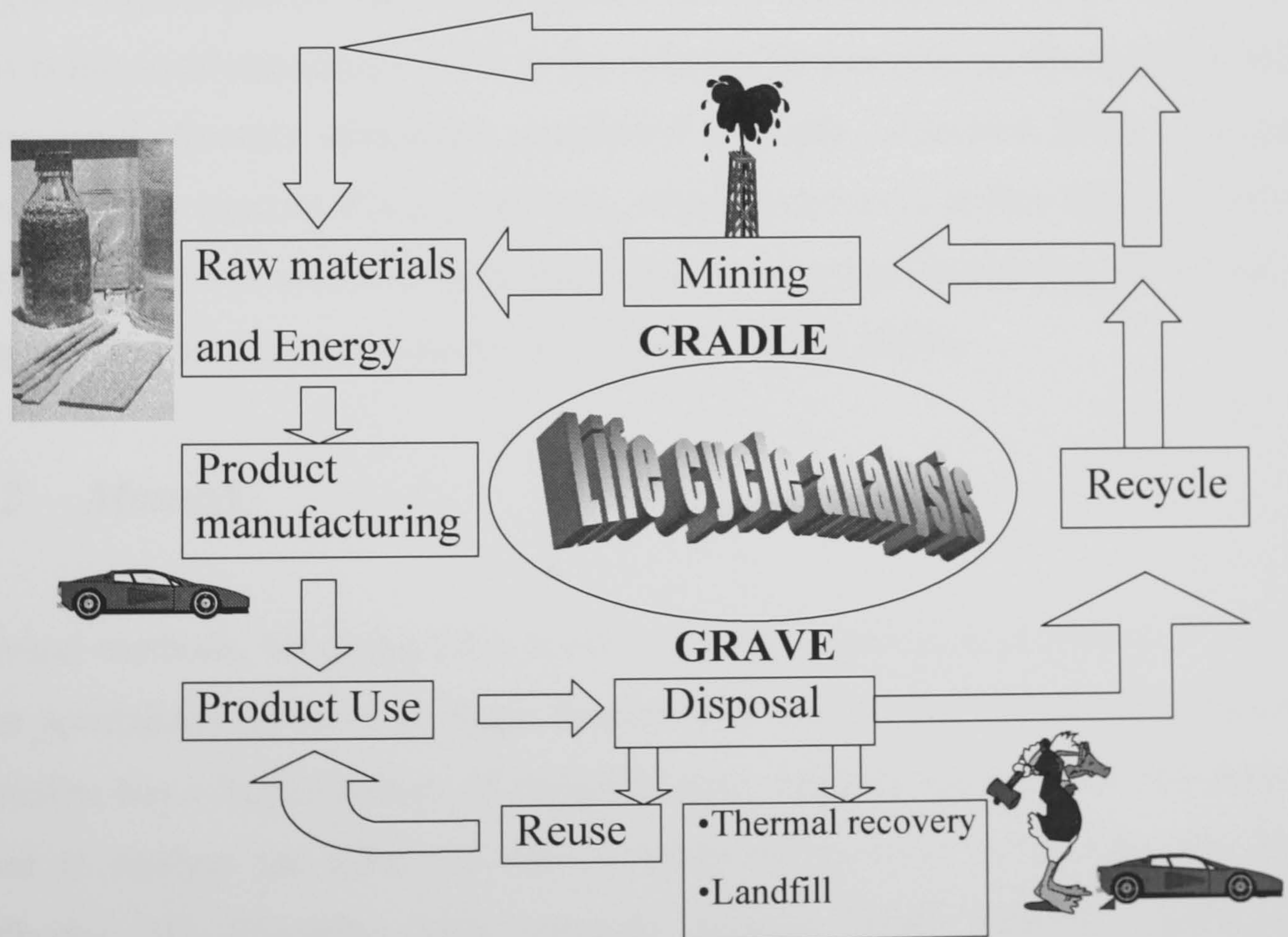


Figure 9.1 Flow diagram of life cycle of a product.

LCA is a method that considers all the inputs and outputs from or to the environment (involved in the production of a particular product or process) and quantifies these emissions in a number that indicates its 'damage to the

environment' (SimaPro User manual). This method has the large advantage that it not only considers the emissions during production of the investigated product, but also emissions during: production/mining of the needed raw materials, use and post-use i.e. disposal of the product. The disposal could include dumping or land filling, incineration to produce energy e.g. electricity, reuse of the product or recycling the material i.e. using the material as a raw material to produce same or another product. Figure 9.1 shows the various stages, which could be involved during a LCA study of a product or process.

Although natural fibres do not have clear advantages with respect to mechanical recycling issues, they do have ecological advantages over glass fibres, since they are renewable and can be incinerated. It is especially for the incineration aspect that natural fibres such as flax and hemp are considered as an interesting environmentally safe – alternative for the use of glass fibres as reinforcement in engineering polymeric materials (Vissers, 2000). Although, as will be shown later, this is not so advantageous as far as the effect of incineration on the environment is considered. Another advantage, mentioned regularly, of natural fibres over glass fibres is their (natural fibres') low cost, which however is in fact higher or almost same as the costs involved with glass fibre composites considering the processes required in flax fibre preparatory methods (De Bruijn, 1998).

9.2 *Material*

Several methods, for doing LCA study, are cited in literature (Rydberg, T., 1994). The specialised software package SimaPro 4.0 was chosen for this investigation. SimaPro has a large database of materials and processes and has been successfully used to analyse the effect of various products on the environment. The Eco-indicator '95 (SimaPro User manual; Vissers, 2000; SETAC, 1993) (the normalisation /evaluation method, *explained in the following section*) has been developed by Pré in collaboration with Philips, NedCar, Océ, Schuurink and several universities (Amsterdam, Leiden and Delft) as well as consultancies (TNO, Centrum voor Energiebesparing en Schone Energie). The Dutch government (Novem) sponsored the project.

9.3 *LCA theory*

There are many (biological) processes in our environment that are threatened with disruption by various emissions. These emissions are chemical or physical agents (substances, noise etc.) that are released into the environment as the result of human activities. Every emission plays a role in one or more environmental problems.

The most prominent of these problems are:

- **The greenhouse effect:** Caused by gases that block infra-red radiation; this effect disturbs the heat balance and could invoke serious climatic changes. The exact working of the greenhouse effect is still the subject of much research, but if present prognoses are confirmed the consequences could be far-reaching.
- **Depletion of the ozone layer:** The ozone layer is high above the earth. Most ozone is concentrated at the stratosphere, at about 25km in altitude, and is considered to be “good ozone”. Although ozone is actually very poisonous, it also has the useful property of absorbing ultra-violet radiation or UV from sunlight. UV is a form of radiation that is very harmful to both flora and fauna. For human beings, the main problems are increased danger of skin cancer, cataract and impaired immune systems. It is currently estimated that the ozone layer is already 5 to 10 percent thinner than when measurements began. A 1% decrease in total column ozone causes the amount of transmitted UV radiation, in the spectral region that damages deoxyribonucleic acid (DNA), to increase by about 2%. Although good ozone only represents a tiny fraction of the atmosphere, it is crucial for life on Earth. The damage is caused by chlorofluorocarbons (CFCs). These substances take an average of 20 years to find their way into the ozone layer. Thus even if we stop emissions of CFCs now, the damage will continue for a long time yet.

Depending on where ozone resides, it can protect or harm life on Earth. When it is close to the planet’s surface, in the air we breathe, ozone is a harmful pollutant that

causes damage to lung tissue and plants, and is considered to be “bad ozone”. It is a powerful photochemical oxidant that damages rubber, plastic and all plant and animal life. It also reacts with hydrocarbons from automobile exhaust and evaporated gasoline to form secondary organic pollutants.

- **Summer smog:** Summer smog is caused by the presence of nitrogen oxides and hydrocarbons in the air in combination with sunlight. These factors, which are chief “precursors” of ozone, react in the presence of sunlight to produce ozone and thus resulting in an excessive concentration of ozone in our own part of the atmosphere. The sources of these precursor pollutants include cars, trucks, power plants and factories, or wherever natural gas, gasoline, diesel fuel, kerosene and oil are combusted. These gaseous compounds mix like a thin soup, called as smog, in the atmosphere, and when they interact with sunlight, ozone is formed. Smog is harmful to people, and to flora and fauna. It is already causing economically serious damage to crops.
- **Winter smog:** In winter the concentrations of SPM (small particulate matter) and SO₂ can cause respiratory problems in people. This type of smog claimed 4000 victims in London in the winter of 1952. Nowadays this type of smog occurs mainly in Eastern and Central Europe.
- **Acidification:** Sulphur, nitrogen oxides and ammonia (from agriculture) cause a build-up of acidity in the soil. Plants, especially trees growing in sandy soils, suffer from this effect because certain poisonous substances pass into solution at raised acidity levels.
- **Eutrophication:** Phosphates and the same substances that cause acidification can result in a kind of 'over-fertilisation', an excessive accumulation of nutrients in the ground. It tends to promote monocultures, while plants that thrive on poorer soils disappear. In water, it can cause excessive algae growth.
- **Toxins in the air, water and soil:** There are many substances that are poisonous to human beings and to other ecosystems. These can be split into

different types, for example carcinogens and persistent toxins such as heavy metals. Some are more harmful to ecosystems, for instance pesticides.

- **Waste disposal:** Many countries are faced with an urgent shortage of facilities for solid waste disposal.
- **Other problems:** Stench, noise, landscape degradation, radioactivity etc.

Besides pollution, there is also the problem of raw materials becoming depleted. In particular, world stocks of fossil fuels and of certain metals give cause for much concern. Supplies could run out within a single generation. In this respect it is useful to distinguish between:

Energy supply: Stocks of fossil fuels and uranium are limited. The use of renewable energy sources like wind, water and solar power is hampered by many obstacles. Therefore the use of energy as such (disregarding the impacts from incineration etc.) is sometimes seen as an environmental impact.

Non-renewable resources: As is the case with fuels, the stocks of some metal ores are very limited. In a theoretical sense metal never disappears from the Earth and metal can always be recycled. In practice, exhaustion of ore reserves will have a significant economic impact.

Renewable resources: Renewable sources cannot be exhausted, but the production potential of renewable resources such as wood is limited.

Both pollution and extraction are forms of impact on the environment. In SimaPro, there are four main categories of impact: *airborne emissions, waterborne emissions, solid emissions and raw materials*. Within these categories, each kind of impact is identified as the exchange of a particular substance with the environment. This 'substance' could be a pollutant like dioxin, a waste product, or a raw material or energy source like iron ore or coal. Emissions involve the release

of a substance into the environment, while the use of raw materials involves the extraction of substances from the environment.

Determining the environmental soundness of a product is thus a far from simple matter. There are many criteria by which the product has to be judged. The result depends on the relative importance of these criteria.

Most products require a large variety of production, distribution, use and disposal processes. Each process can produce a large variety of emissions, and each emission has a very specific effect on the environment.

The complex interaction between a product and the environment is dealt with in an LCA method. There are two main steps in an LCA:

- Describe which emissions will occur and which raw materials are used during the life of a product. This is usually referred to as the *inventory* step.
- Assess what the impacts of these emissions and raw material depletions are. This is referred to as the *evaluation* step.

The principles, framework and methodological requirements for conducting and reporting LCA studies (environmental management) are described in the international standard ISO 14040, which also includes certain minimal requirements as well as limitations of LCA. Additional details regarding methods are provided in the complementary International standards ISO 14041, ISO 14042 and ISO 14043 concerning the various phases of LCA. According to ISO 14040, LCA shall have phases such as: definition of goal and scope, inventory analysis, impact assessment and interpretation of results, as shown in Figure 9.2. The standard includes methodology to be used for each phase of the study e.g. items to be included in the definition of scope of the study. The other standards in the ISO14040 series give additional details about LCA method such as:

ISO14041: Environmental management - Life Cycle Assessment – *Goal and Scope Definition and inventory analysis*

ISO14042: Environmental management - Life Cycle Assessment – *Life Cycle Impact Assessment*

ISO14043: Environmental management - Life Cycle Assessment – *Life Cycle Interpretation*

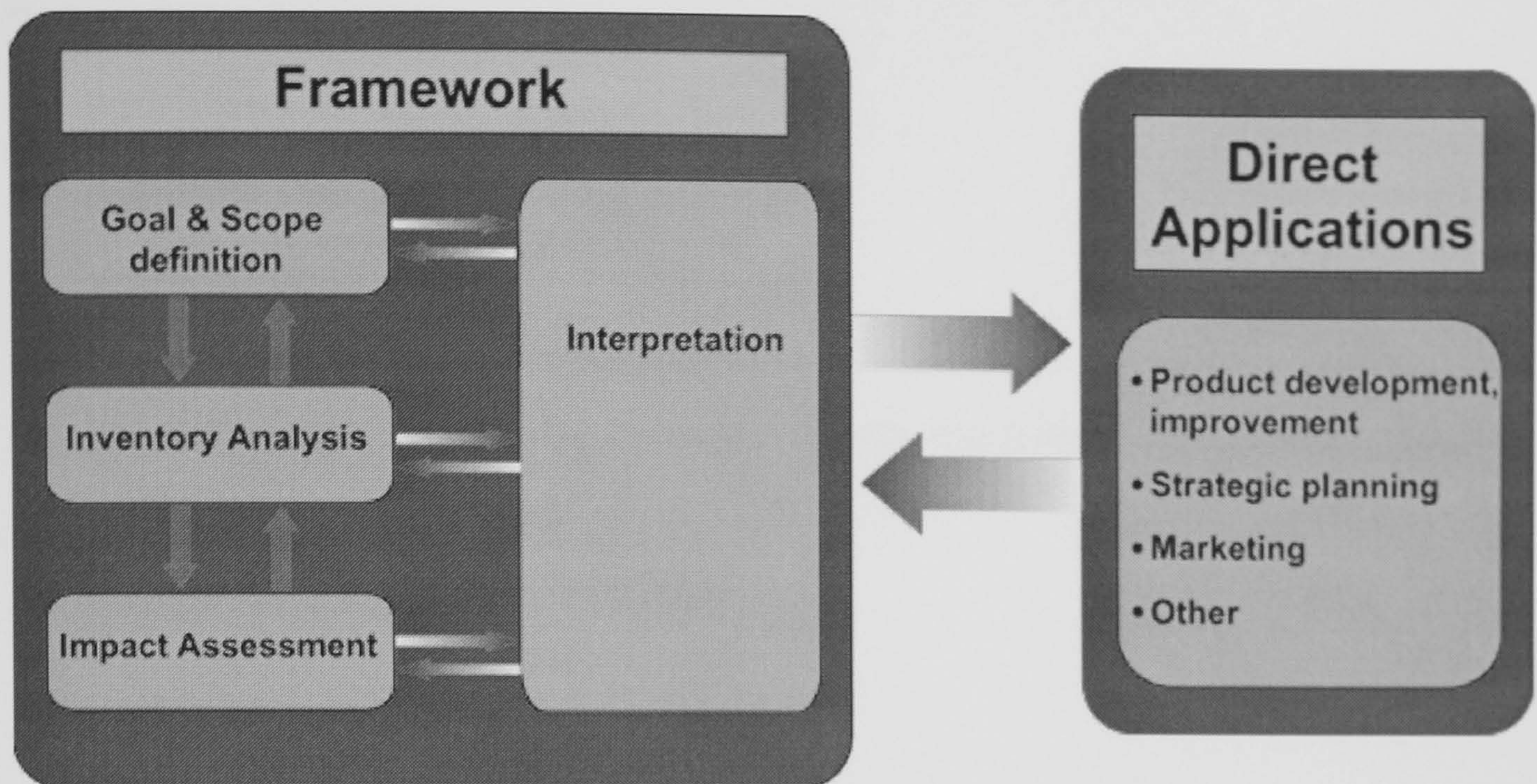


Figure 9.2 Phases of an LCA as described in ISO14040: 1997.

As shown above, LCA can assist in:

- identifying opportunities to improve the environmental aspects of products at various points in their life cycle;
- decision-making in industry, governmental or non-governmental organisations (e.g. strategic planning, priority setting, product or process design or redesign);
- marketing (e.g. an environmental claim, ecolabelling scheme or environmental product declaration).

LCA typically does not address the economic or social aspects of a product.

In the Code of Practice, it is recommended that the LCA be split into five stages (Source: SimaPro User manual):

1. Planning
 - Statement of objectives
 - Definition of the product and its alternatives
 - Choice of system boundaries
 - Choice of environmental parameters

- Choice of aggregation and evaluation method
 - Strategy for data collection
2. Screening
 - Preliminary execution of the LCA
 - Adjustment of plan
 3. Data collection and data treatment
 - Measurements, interviews, literature search, theoretical calculations, database search, qualified guessing.
 - Computation of the inventory table
 4. Evaluation
 - Classification of the inventory table into impact categories
 - Aggregation within the *category* (characterisation)
 - Normalisation
 - Weighting of different categories (valuation)
 5. Improvement assessment
 - Sensitivity analysis
 - Improvement priority and feasibility assessment

It is generally recognised that the first stage is extremely important. The result of the LCA is heavily dependent on the decisions taken in this phase. The screening LCA is a useful step to check the goal-definition phase. After screening it is much easier to plan the rest of the project.

The heart of the LCA method is an inventory of all the industrial processes that occur during the life cycle of a product. Besides the production phase, the life cycle processes include the distribution, use and final disposal of the product. The life cycle can be represented as a *process tree* structure (Figure 9.1 and 9.3).

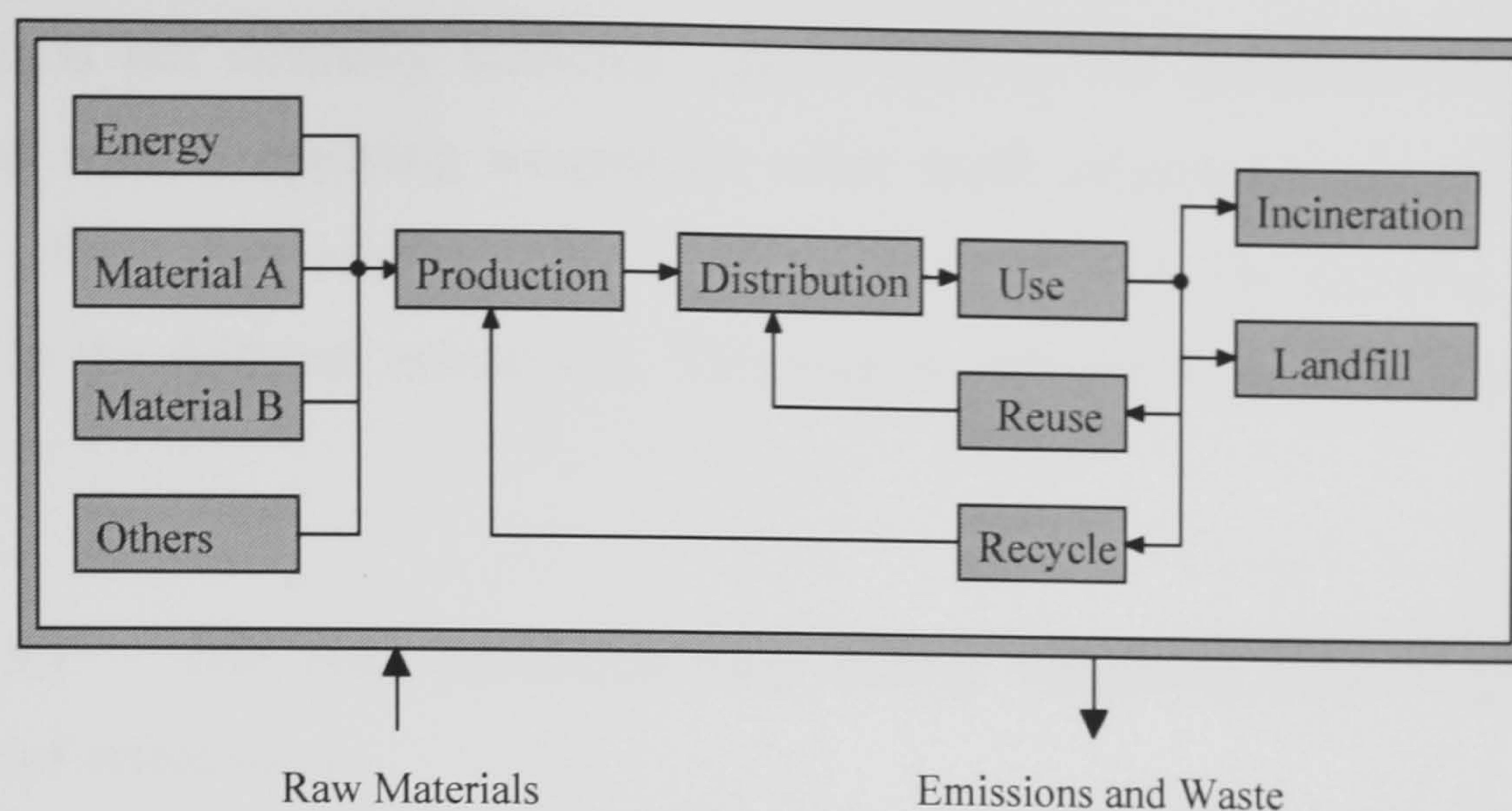


Figure 9.3 Example of a process tree (Source: SimaPro User manual).

Each box represents a process, which forms part of the life cycle. Every process has defined inputs and outputs.

There are three main steps during life cycle analysis:

1. ***Classification and characterisation***
2. ***Normalisation***
3. ***Evaluation***

The procedure is described here using fictional data (SimaPro User manual).

SimaPro 4 allows for these steps to be carried out, provided sufficient data are available.

Classification and characterisation

In the classification step, all impacts are sorted into classes according to the effect they have on the environment. For example, impacts that contribute to the greenhouse effect may be grouped together, as are impacts that contribute to ozone layer depletion. Certain impacts are included in more than one class. For example, NO_x emissions are toxic, acidifying and cause eutrophication.

The environmental impacts are aggregated within each class to produce an effect

score. It is not normally sufficient just to add up the quantities of substances involved without applying weightings, since some substances may have a more intense effect than others. This problem is dealt with by applying weighting factors to the different substances. This step is referred to as the characterisation step.

Table 9.1 The characterisation step (using weighting factors) produces a number of effect scores.

Emission	Quantity (kg)	Greenhouse	Ozone layer depletion	Human toxicity	Acidification
CO ₂	1.792	x 1			
CO	0.000670			X 0.012	
NO _x	0.001091			X 0.78	x 0.7
SO ₂	0.000987			X 1.2	X 1
Effect scores:		1.792	0	0.00204	0.0017

The table above gives an example of this calculation for a small part of the inventory table. It shows a number of impacts (airborne emissions) resulting from the manufacture of polyethylene. The grey area contains the weighting factors. The actual emissions are multiplied by this factor before they are added. The bottom line - the *effect scores* - gives the result of this operation.

In the comparison between glass and polyethylene the calculated effect scores can be displayed as a graph. The highest calculated effect score is scaled to 100%. This means the materials can only be compared per effect.

The interpretation of these scores may be less confusing than interpretation of separate impacts, but is by no means without problems. If all the scores for one product are higher than those for another, it is easy enough to conclude which is the more environmentally friendly. But if one has a higher score for acidification, while the other has a higher score for the greenhouse effect, for instance, it becomes difficult to justify such a conclusion. Interpretation depends on two factors:

1. The relative size of the effect compared to the size of the other effects. In this example it is important to see whether the ecotoxicity score of 100% refers to a

very high or an extremely low effect level.

- The relative importance of the effects cannot be seen here.

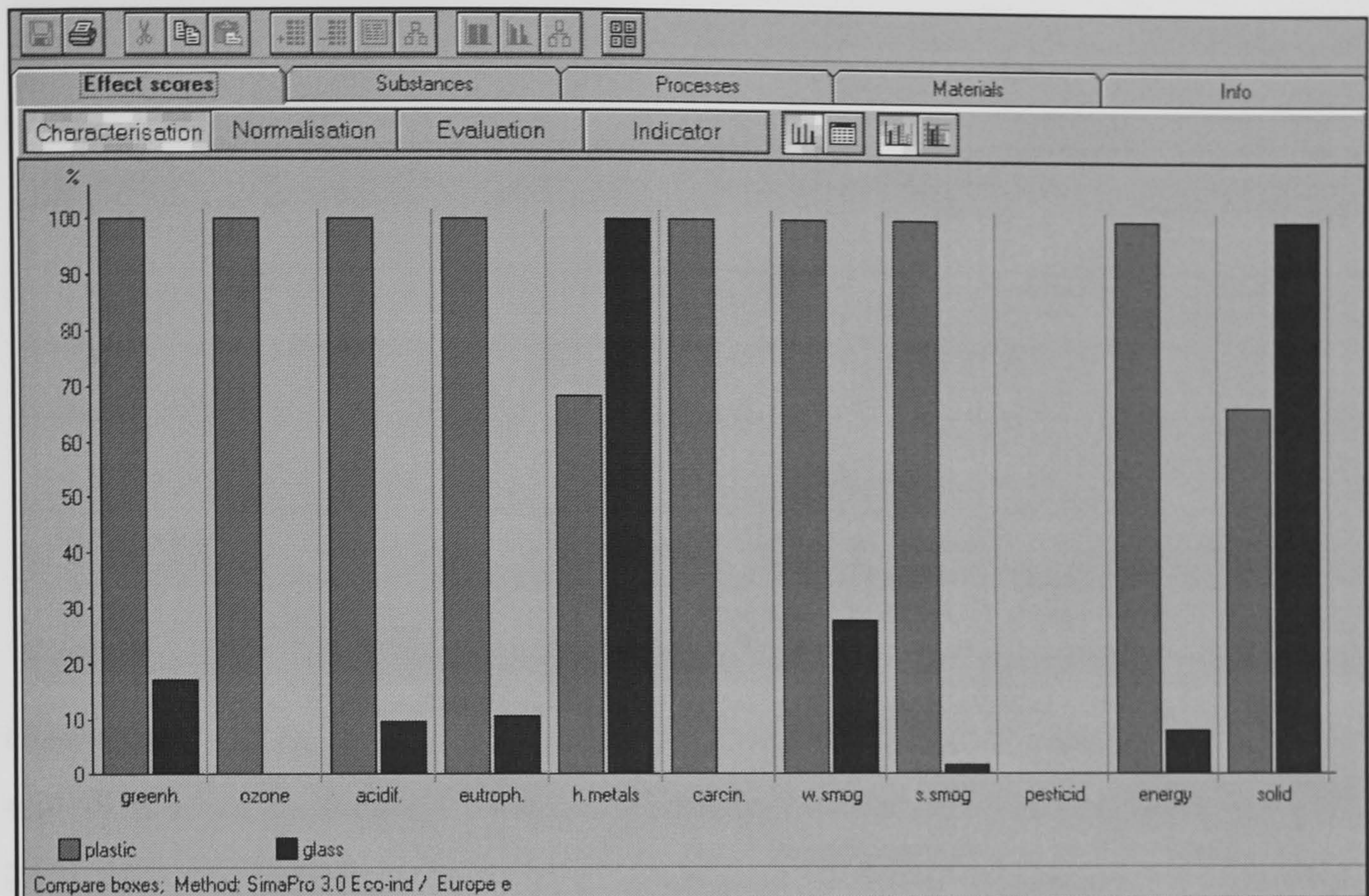


Figure 9.4 Example of a classification. The highest score is scaled to 100%. The classes are taken from the Eco-indicator 95 method: Greenhouse effect, Ozone layer depletion, Heavy metals, Carcinogen, Winter smog, Summer smog, Pesticides, Energy use Solid waste disposal.

Normalisation

In order to gain a better understanding of the relative size of an effect, a normalisation step is required. In this step the effects are divided by a "normal" effect, for instance the effects caused by an average person during a day or any other period. By doing this it is possible to see the relative contribution from the material production to each already existing effect. The graph below (Figure 9.5) shows such a normalisation step (fictional data). Normalisation is based on 1990 levels for Europe excluding the former USSR. Weighting is based on distance to target. Criteria for target levels are:

- One excess death per million per year
- 5% ecosystem degradation
- avoidance of smog periods

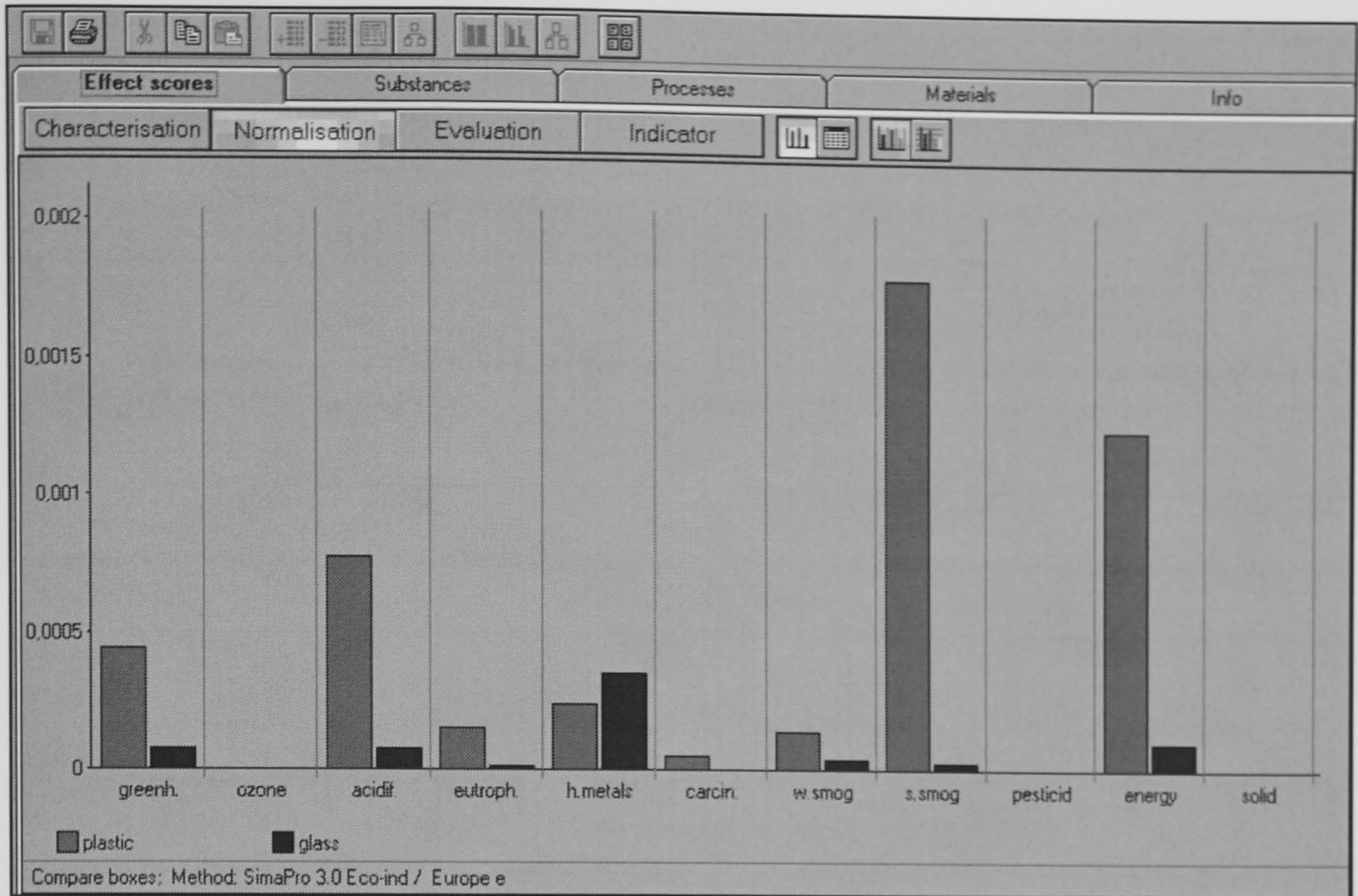


Figure 9.5 The normalised effect score. The length of the columns is now scaled to a normalised effect score. (Source: Manual of SimaPro LCA Computer Program)

After normalisation it becomes clear that the contributions to acidification, greenhouse effect, smog, and energy use are relatively high. The contributions to the other effects are almost negligible.

Evaluation of the normalised effect scores

Normalisation considerably improves our insight into the results. However, no final judgement can be made since not all effects will be considered to be of equal importance. In the evaluation phase the normalised effect scores are multiplied by a weighting factor representing the relative importance of the effect.

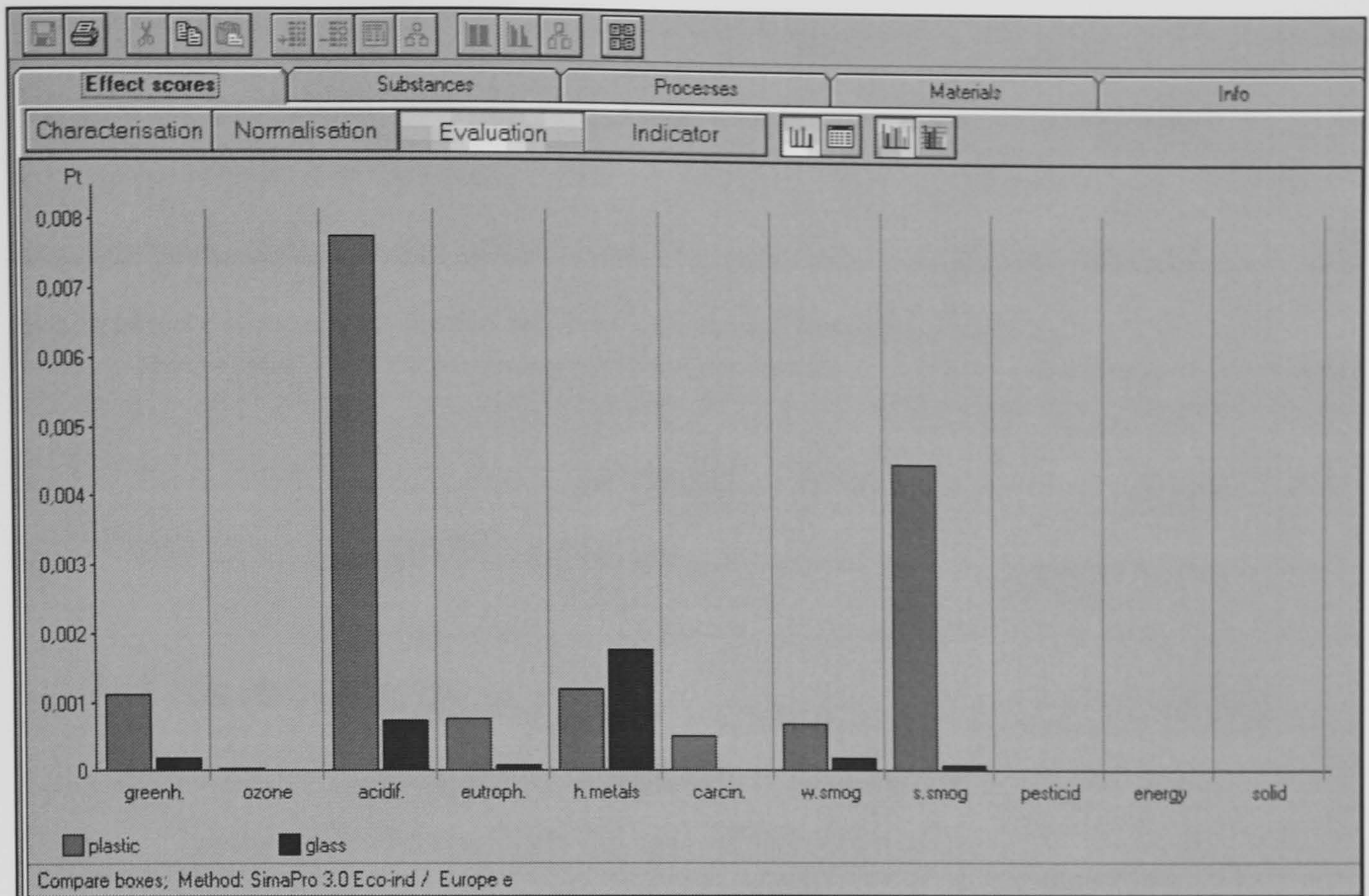


Figure 9.6 Evaluated effect scores. After weighting, the relative importance of the normalised effect scores are added (Source: Manual of SimaPro LCA Computer Program).

After weighting (Figure 9.6) the acidification has clearly gained in significance. The length of the columns actually represents the seriousness of the effects. This makes it possible to add the columns to calculate a final result.

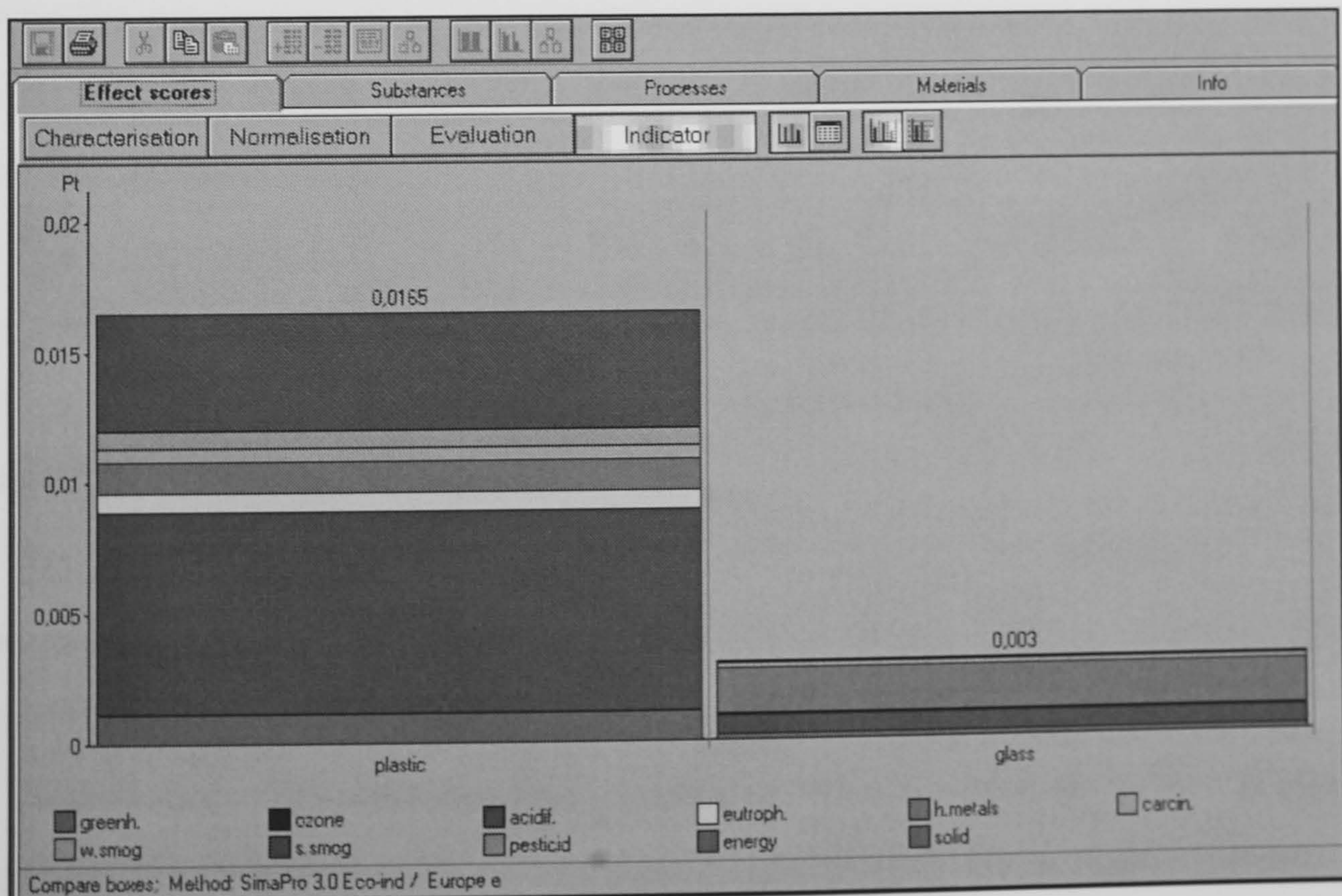


Figure 9.7 The weighted scores can be added for a final judgement. (Source: Manual of SimaPro LCA Computer Program)

The graph above (Figure 9.7) clearly shows a preference for glass. At this moment the system presented here is still very much under development and it is still debatable whether it is possible to obtain realistic weighting factors for the last stage in particular. On the other hand, the principle behind this method is accepted as a realistic procedure in the SETAC Code of Practice (SETAC, 1993).

However, it must be kept under notice that life cycle analysis is an interpretation i.e. it depends on the system boundaries.

9.3.1 LCA drawbacks

There are certain drawbacks with the use of SimaPro 4.0:

- Processing machines: Additional emissions to the environment caused by maintenance of machines are not incorporated in the analysis. This would lead to an interpretation that is slightly unfavourable for the NMT, because glass is harder and causes more wear.
- Growth: Additional herbicides, fungicides, insecticides and pesticides are needed to grow the plant from which flax fibres are produced. Emissions that occur during the production of oil or mineral ores are not considered and only emissions that take place during extraction and purification of oil and mineral-ore based materials are considered.
- Non-renewable sources: As is the case with fuels, the stocks of some metal ores are very limited. In a theoretical sense metal never disappears from the earth and metal can always be recycled. In practice, exhaustion of ore reserves will have a significant economic impact.
- Renewable sources: Renewable sources cannot be exhausted, but the production potential of renewable sources such as flax is limited, due to agricultural area and depletion of minerals.
- However, the methods like LCA cannot be used to weigh the effect of product, like GMT, on human health during their production as far as safety and health of the worker and users is considered. Such a method can only consider the effect of

material on the environment (excluding humans) from its cradle (mining of raw materials) to its grave (disposal).

9.4 Methods

As mentioned earlier, in the present chapter LCA study of the NMT is done and compared with the GMT composites. For the same SimaPro 4.0 computer program was used. Although in previous chapters, mechanical and environmental properties were compared and natural fibre composites seemed to be environment friendly but a clearer picture, as far as environment impact is concerned, can be obtained by carrying out an LCA study of both types of composites.

Definition of the product

For the present study we have considered two categories of products i.e. automotive application and non-automotive application. The parts, for example a car dashboard and office chair frame, were considered to be made by compression moulding. The data, for example energy required for producing a part via compression moulding, was collected from sources like Polynorm Plastics B.V. and through personal interviews with reliable sources such as GMT producer (Vissers, 2000).

Choice of system boundaries

For the present study the environmental emissions were considered in three phases of product life cycle i.e. raw-material production, product manufacturing and product disposal. The system did not include effects of processes like product and raw-material transportation, reuse (and durability) of the product, effect of materials on machinery life and maintenance. All the above mentioned processes would have effect on the life cycle of the products but, due to limitation of time, were not included in the study. The effect of materials on machinery maintenance was not included because of lack of comparative data from the manufacturer.

9.4.1 Inventory: materials in mining phase

Identification of the required materials is an important step in a life cycle analysis. The environmental emissions during the procurement of the raw materials are either included in the database or must be found in literature. The database should contain all relevant emissions that took place to obtain the raw materials (including mining, purification and production) e.g. effects of chemicals like pesticides, insecticides, fertilisers used during the production (farming) of flax fibres was included in the present LCA study. Some of the data such as energy consumption during manufacturing process was collected via interviews with the employees of companies involved such as IMAG-DLO, Crop Production Engineering Department (Production Technology and Chains, Wageningen, the Netherlands), Polynorm Plastics B.V., Research and Development (Roosendaal, the Netherlands) and Vantage Polymers Ltd. (175 Woodhouse Lane, Leeds LS2 3AR, United Kingdom).

It is assumed that the material is required for certain applications (e.g. automotive applications like car dash-board and non-automotive application like office chair) for which a particular property is specified. Only mechanical properties are considered and the environmental properties like durability, moisture pick-up etc. are ignored in the analysis. Although factors like durability are ignored in the present analysis it is worth mentioning that higher durability of GMT than NMTs would give a positive effect to GMT environmental impact (i.e. lower environmental impact) when compared to NMT. The mechanical properties considered are tensile strength, initial modulus (stiffness) and impact strength. The required tensile properties of a composite material for an automotive application are given in Table 9.2.

Table 9.2 Required properties for an automotive application (Vissers, 2000).

Composite	Tensile strength (MPa)	Stiffness (GPa)	Impact strength (kJm ⁻²)
Automotive application	45	3	20

Keeping in view the relation between properties and weight fraction of composites from Chapter 5 the estimate of the required volume fraction (and weight fraction) can be made. In Table 9.3 the estimated weight fractions of NMT and GMT for a required property are given.

Table 9.3 The estimated (approximate) fibre volume fraction (V_f) and weight fraction (W_f) of GMT and NMT required (Chapter 5) to obtain the required property for an automotive application.

Property	Value	NMT (V_f)	GMT (V_f)	NMT (W_f)	GMT (W_f)
Tensile strength	45 MPa	0.35	0.08	0.45	0.19
Stiffness	3.0 GPa	0.1	0.05	0.15	0.13
Impact strength (notched Charpy)	20 kJm^{-2}	0.25 (3.2 \times thickness)	0.13	0.34 (3.2 \times thickness)	0.29

As shown in Chapter 5 NMTs do not meet the impact criteria for an automotive application. However, the desired impact property of component may be obtained by increasing the thickness of the composite. Therefore for impact critical automotive application, in Table 9.3, the thickness of composite is mentioned as 3.2 times thickness of GMT (ratio of required impact strength to the experimentally obtained impact strength i.e. $20\text{kJm}^{-2} / 6.25\text{kJm}^{-2}$). To study the impact of life cycle of composite on the environment, 1 kg of GMT composite is taken as a reference material. To match the required property (Impact), since the thickness of NMT (with $0.34W_f$ or $0.25V_f$) has to be about three times to that of GMT, therefore NMT with a volume equivalent to 3.2 times volume of 1 kg GMT ($0.29W_f$, $\rho_{\text{GMT}} = 1.11 \text{ g/cc}$) would weigh ($0.34W_f$, $\rho_{\text{NMT}} = 1.03 \text{ g/cc}$) 2.96 kg. Such an increase in weight of the composite is practically not attractive, especially for an automotive application, because of the enhanced fuel consumption as well as increased costs. The effect of life cycle of NMT or GMT on the environment is calculated keeping in mind three mechanical properties i.e. strength, stiffness and impact. Similar to the example mentioned above, the equivalent weights of NMTs (equivalent to the volume of 1 kg of GMT) for different criterion are calculated and mentioned in Table 9.4.

Table 9.4 The weight of NMT having the same volume (3.2 times in the case of impact criterion) as 1 kg of GMT.

Property	Value	NMT (V_f)	GMT (V_f)	Weight of GMT (kg)	Weight of NMT (kg)
Tensile strength	45 MPa	0.35	0.08	1	1.04
Stiffness	3.0 GPa	0.1	0.05	1	0.97
Impact strength (notched Charpy)	20 kJm ⁻²	0.25 (3.2 × thickness)	0.13	1	2.96

9.4.2 Process tree: processing phase

Identification of the required processing steps and their corresponding energy and material consumption as well as emissions are often the most important steps in LCA.

Roughly two steps are identified in the production of GMT and NMT products out of glass fibres and polypropylene granulate:

1. Production of prepreg sheets out of the corresponding materials
2. Production of the product out of GMT or NMT sheets via compression moulding

Prepreg sheet production

The production of GMT sheets with 35% weight glass requires the following energy inputs (Table 9.5). The data covers the energy input for a yearly production including the reworking of the edge trimming and laminate scrap that is recycled in the plant.

Table 9.5 Energy consumption for the production of 1 kg GMT (prepreg) sheet.

Property	Value	Unit
Waste production*	1	%
Gas	0.6	KWh
Oil	0.002	KWh
Electricity	0.56	KWh

* A 1% waste production on a 1 kg product corresponds with 1.01 kg material.

It is assumed that the production of NMT and GMT sheets with different weight% (Table 9.3 and 9.4) of reinforcement (glass or flax) requires the same amount of energy (i.e. energy consumed in prepreg sheet production process).

Compression moulding

There are two large energy consumers in the compression moulding process and they are the (Infra-red) IR-heaters and the press. The total power demand of all 5 heating zones of the oven is estimated at 180 kW and the cycle time is 40 sec.

Table 9.6 Data concerning the compression moulding of a GMT product and a NMT product.

Property	GMT	NMT	Unit
Waste production	0.5	0.5	%
Cycle time	40	40	S
Power demand	360	360	KW
Energy consumption	14.4	14.4	MJ per product
	12	9.23	MJ per kg product

Since 1% wastage occurs at pre-preg manufacturing stage and 0.5% waste occurs at compression moulding stage therefore to manufacture the final products weighing 1kg GMT the initial material required would weigh 1.01 kg (glass mat + PP). Table 9.7 gives the initial weight of material required covered under different criterion.

Table 9.7 The extra weight of NMT required due to wastage during processing.

Property	Value	NMT (V_f)	Weight of NMT (kg)	Weight of NMT including waste (kg)
Tensile strength	45 MPa	0.35	1.04	1.06
Stiffness	3.0 GPa	0.1	0.97	0.98
Impact strength (notched Charpy)	20 kJm ⁻²	0.25 (3.2 × thickness)	2.96	3

9.4.3 Use phase: additional emissions and savings

An inventory of the emissions that take place during the use of the investigated product is also an important part of LCA. For the present study, as mentioned previously, the NMT composite, which could be used for an automotive application would satisfy all the (property) requirements. Such a composite part would be three times heavier than GMT part and hence the emissions involved would be higher in the case of NMT than the corresponding GMT part. For the present study three different criterion are used which would mean three different applications are considered i.e. application where design criterion is stiffness, strength or impact strength.

As mentioned earlier for an automotive application where, e.g. car bumper beam, the material should satisfy all design criterion i.e. strength, stiffness as well as impact strength (Table 9.7), the weight of the objects would contribute in the fuel consumption of an automobile. Thus a weight saving of the product is beneficial to the environment. For every kilogram that is saved in the weight of a car, approximately 6 kg of fuel is saved over the entire lifetime of the automobile. Higher savings are even possible if secondary weight savings are considered. A primary weight saving reduces the load in the other components leading to secondary savings. For an average European car these secondary weight effect can be as high as 150%, meaning that 1 kg primary weight reduction allows for 1.5 kg secondary weight savings. The weight of a product made from reference material

(GMT) is taken as 1 kg, while a product made from the NMT would weigh around 3 kg to satisfy the impact strength criteria.

Table 9.8 Calculation of additional fuel consumption because of added weight (for impact critical applications).

<i>Property</i>	<i>GMT</i>	<i>NMT</i>	<i>Units</i>
Weight	1	2.96	Kg
Density	1.11	1.10	g/cc
Additional fuel use	0	11.8	Kg
Diesel use*	0	500.42 ($\pm 10\%$)	MJ

* 0.0235 kg diesel has energy content of 1 MJ.

Similar to the above mentioned example (Table 9.8), for automotive applications where strength and stiffness are design criterion e.g. applications for car interior like door panelling or battery casing, the additional fuel consumption because of difference in weight between NMT and GMT are given in Table 9.9. As shown in Table 9.9, in the case of stiffness critical applications when compared to GMT, NMT is lighter in weight. The reduced weight of NMT, in the above-mentioned case, would lead to saving in fuel therefore negative sign is placed, for stiffness critical application, in Table 9.9.

Table 9.9 Calculation of additional fuel consumption because of added weight, for strength and stiffness criterion.

<i>Property</i>	<i>Value</i>	<i>Weight of GMT (kg)</i>	<i>Weight of NMT (kg)</i>	<i>Additional fuel use by NMT (kg)</i>	<i>Extra diesel use (MJ)</i>
Tensile strength	45 MPa	1	1.04	0.24	10.21
Stiffness	3.0 GPa	1	0.97	-0.18	-7.66

For applications not in automotive industry e.g. office furniture, the effect of life cycle, 'during usage', of the product on the environment is considered same in both the cases i.e. NMT as well as GMT.

9.4.4 Waste phase

The waste phase is the last step of LCA. The environmental impact of a product is influenced by the treatment (disposal scenario) after its use by the consumer. A product can be reused, recycled, incinerated or it may end up with the municipal waste. Recycling of post-consumer material depends on the application since the cleanliness of the material is very important. The material would be difficult to clean if it has come in contact with e.g. oil. If the material is clean with a thickness around 4 to 5 mm, a shredding step should be sufficient to recycle the material.

Different configurations varying in disposal scenario were examined by Sima Pro 4 with the Eco-Indicator'95. The various disposal scenarios considered include municipal waste, incineration and municipal waste with an additional impact of extra/reduced fuel required during the use of NMT product because of its extra/reduced weight, when compared to GMT, for automotive applications. In the incineration scenario all waste was considered to be treated in a modern waste incinerator.

The notations used for various combinations of NMT and GMT products, involving various use and disposal methods, are given in Table 9.10.

Normalisation was based on 1990 levels for Europe excluding the former USSR. Weighting was based on distance to target. Criteria for target levels were:

- One excess death per million per year
- 5% ecosystem degradation
- avoidance of smog periods

Table 9.10 Codes used for various combinations of composite criterion, use and disposal.

Description	Codes used
<i>Automotive applications (diesel savings during use included)</i>	
NMT- Strength criterion- Extra diesel use- disposal through municipal dumping	NSDM
NMT-Strength-Extra diesel use-Incineration	NSDI
NMT-Modulus-Diesel-Municipal	NMDM
NMT-Modulus-Diesel-Incineration	NMDI
NMT-Impact-Diesel-Municipal	NIDM
NMT-Impact-Diesel-Incineration	NIDI
<i>Non-automotive applications</i>	
GMT-Municipal	GM
GMT-Incineration	GI
NMT-Strength-Municipal	NSM
NMT-Strength-Incineration	NSI
NMT-Modulus-Municipal	NMM
NMT-Modulus-Incineration	NMI
NMT-Impact-Municipal	NIM
NMT-Impact-Incineration	NII

9.5 Results and discussions

The three applications fields, having to fulfil criterion of: tensile strength, stiffness and impact strength, for automotive and non-automotive applications were investigated for their environmental impact.

Non-automotive applications

The three steps discussed in Section 9.3, for non-automotive applications, resulted in the classification chart (Figure 9.8), normalised-effect score (Figure 9.9) and evaluated effects (Figure 9.10).

The evaluated impacts per category can be added together to give one indicator: the total interpretation of the environmental impact (Figure 9.11). From the indicator it can be seen that the environmental impact of NMT material is higher than the reference GMT alternative. The two main reasons that make NMT unfriendly are the need of pesticides and other chemicals to grow the flax fibre and extra weight of material required to fulfil the property criterion. Also, in our analysis we assumed that NMT material exhibited good flow properties during compression moulding, which is not the case as observed experimentally by Vissers (2000). Therefore, if included in LCA, the poor flow property of flax based NMT material would lead to a higher impact on the environment because of extra material required to make the same amount of product. Keeping in mind the reduced weight of NMT required, due to lower density of composite, for stiffness critical applications, the environmental impact of these composites is lower than composites fulfilling strength and impact criterion. Also, among stiffness criterion, disposal of composite through incineration is more harmful to environment when compared to municipal dumping.

Automotive applications

Similar to non-automotive applications, LCA study was also conducted on automotive applications. For automotive applications the effect of extra/reduced weight of composite on fuel consumption and hence its effect of environment is also considered. Figure 9.12, 9.13 and 9.14 show the classification chart, normalised effect score and an evaluation chart, respectively. Figure 9.15 shows the graphical representation of the indicator obtained by summarising the evaluated numbers, for automotive applications.

As seen from Figure 9.15, similar to non-automotive applications, the environmental impact of NMT composites, fulfilling stiffness criterion, is lower than NMT composites fulfilling strength and impact criterion. Due to reduced fuel consumption, which is because of lower weight of NMDM and NMDI composites, these composites seem to be attractive for automotive applications when compared to GMT composites, as far as environmental impact is considered. However, the

higher cost of NMT than GMT due to processing differences as well as higher amount of material required for proper flow of flax materials are drawbacks with NMT. Again, it is worth mentioning here that in the present LCA study the effect of GMT on human health during processing and use of composites and also the effect of glass fibre processing on machine wear is not considered because of lack of comparative data.

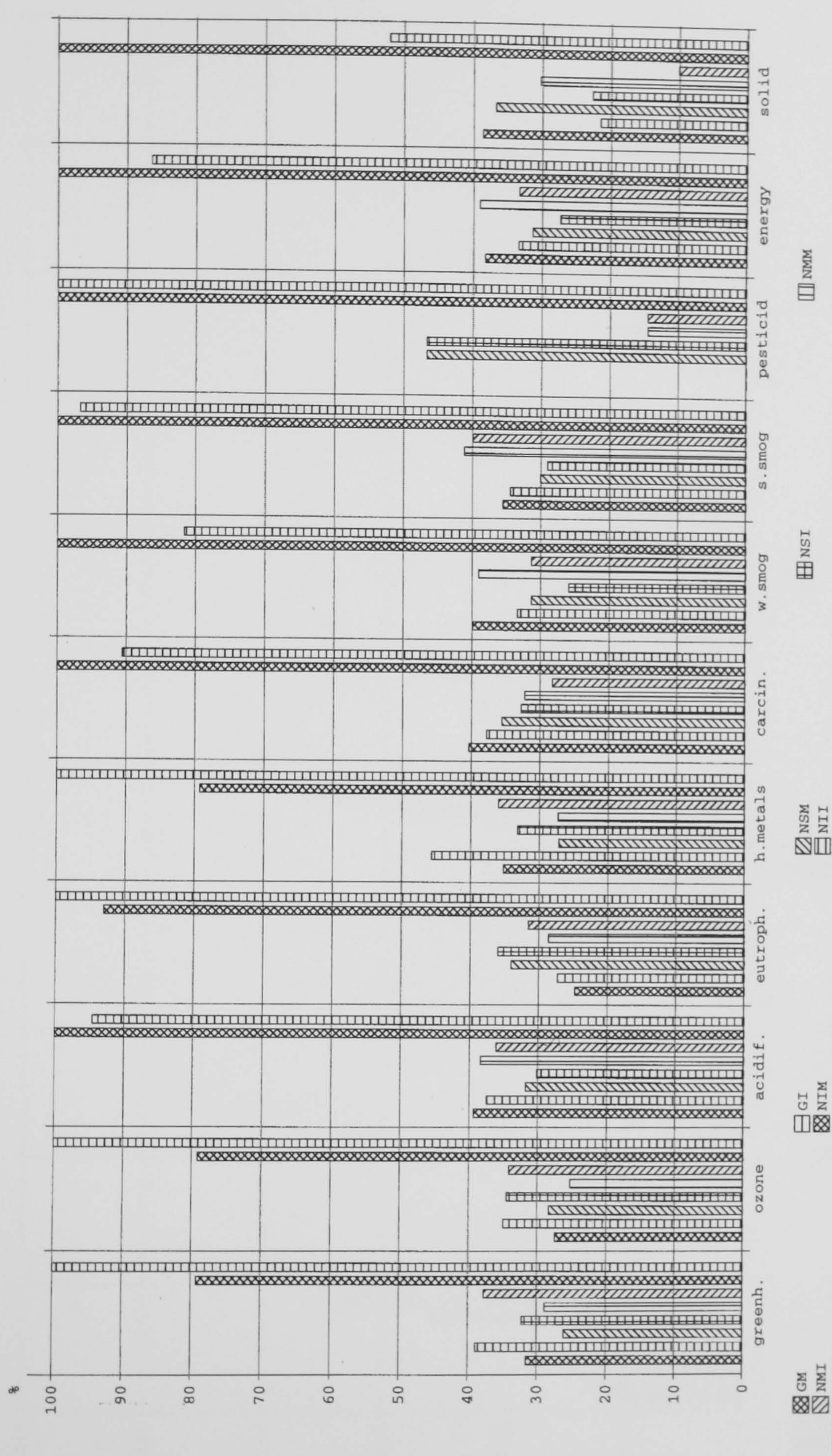
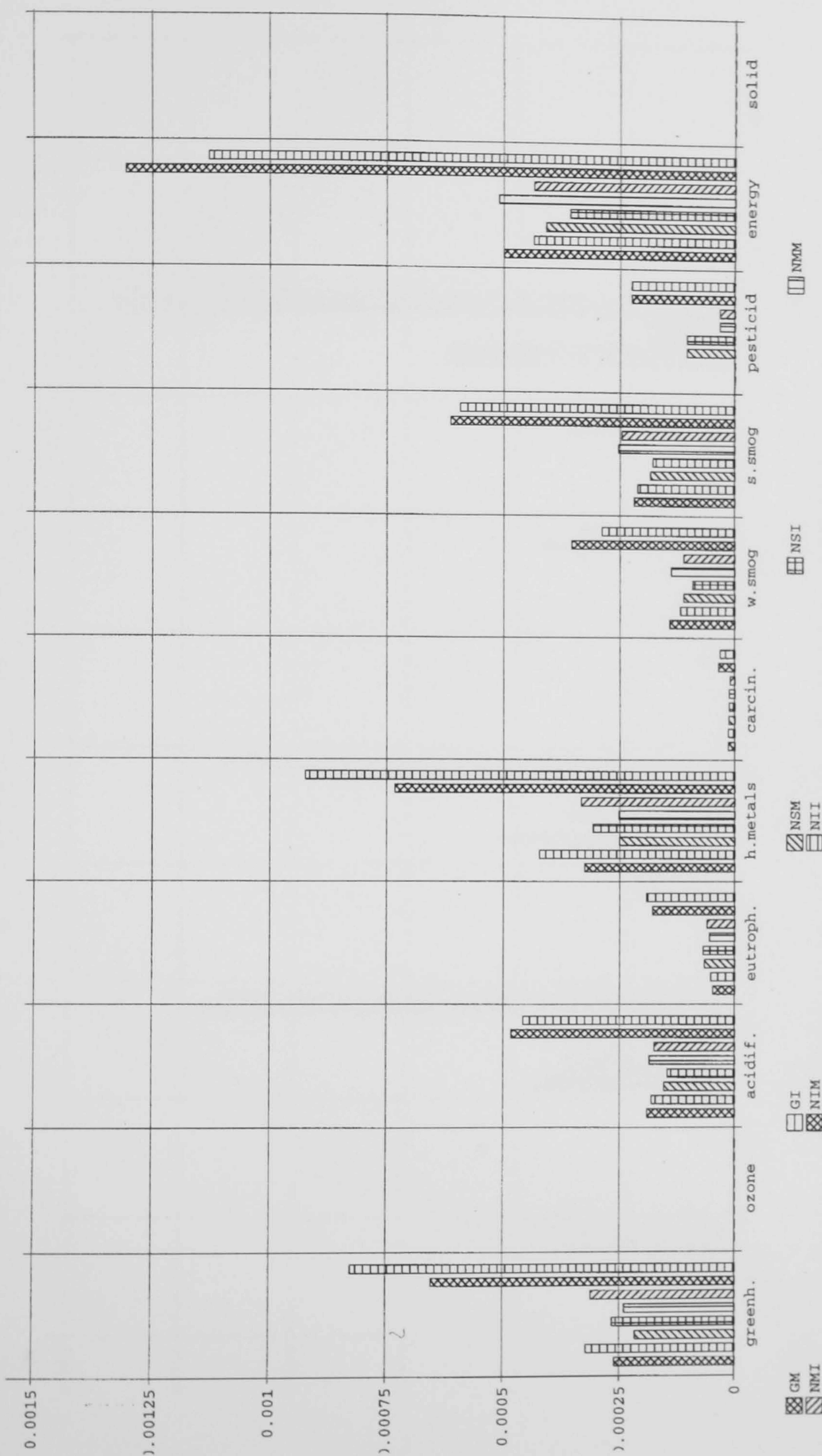
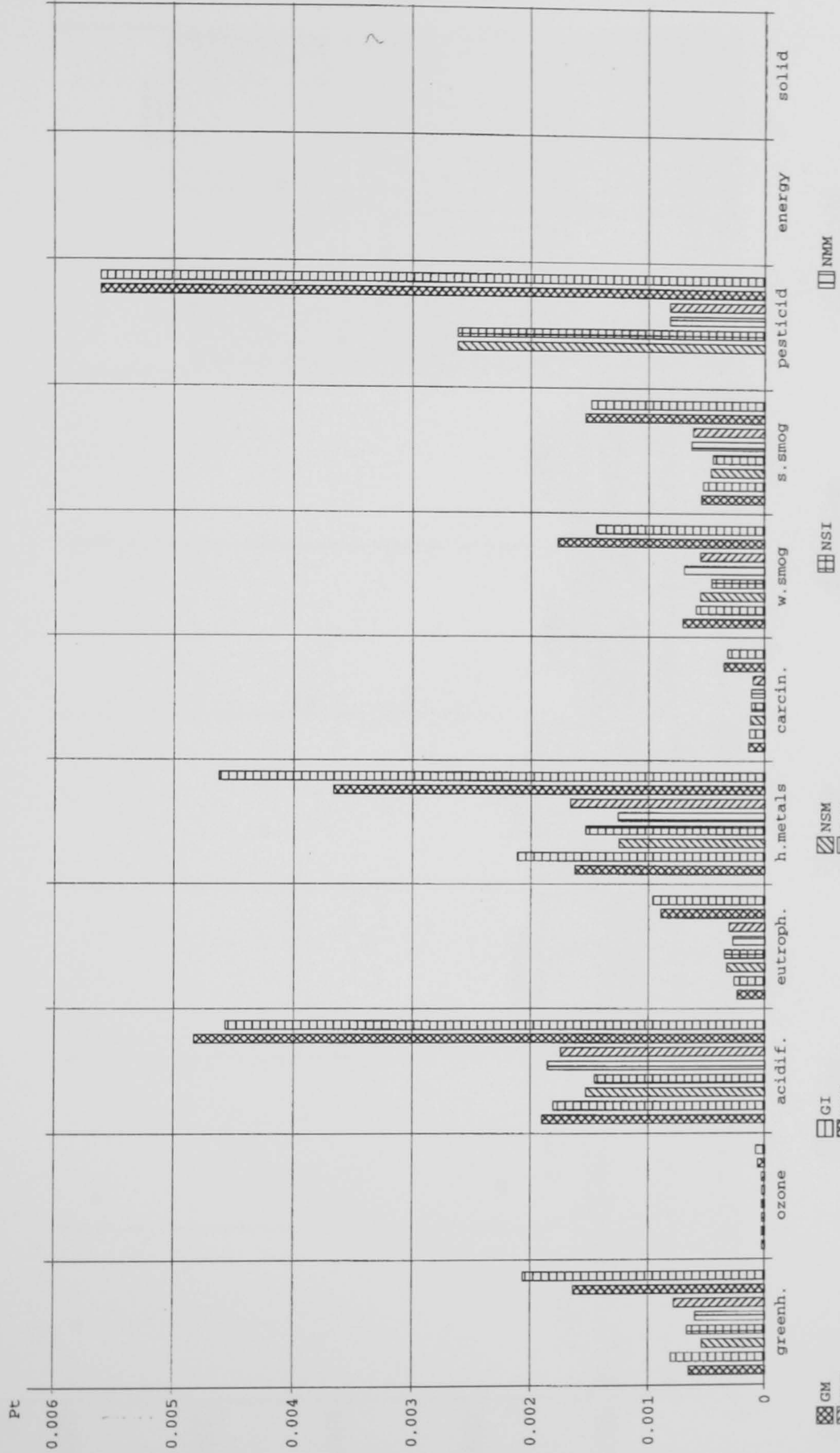


Figure 9.8 Graphical representation of the characterisation obtained by scaling the effects due to various combinations of composite use (for non-automotive applications) and disposal. The sequence of bars in each category is same as the sequence of codes, mentioned below the figure, starting from left top (GM) and ending at bottom right (NII).



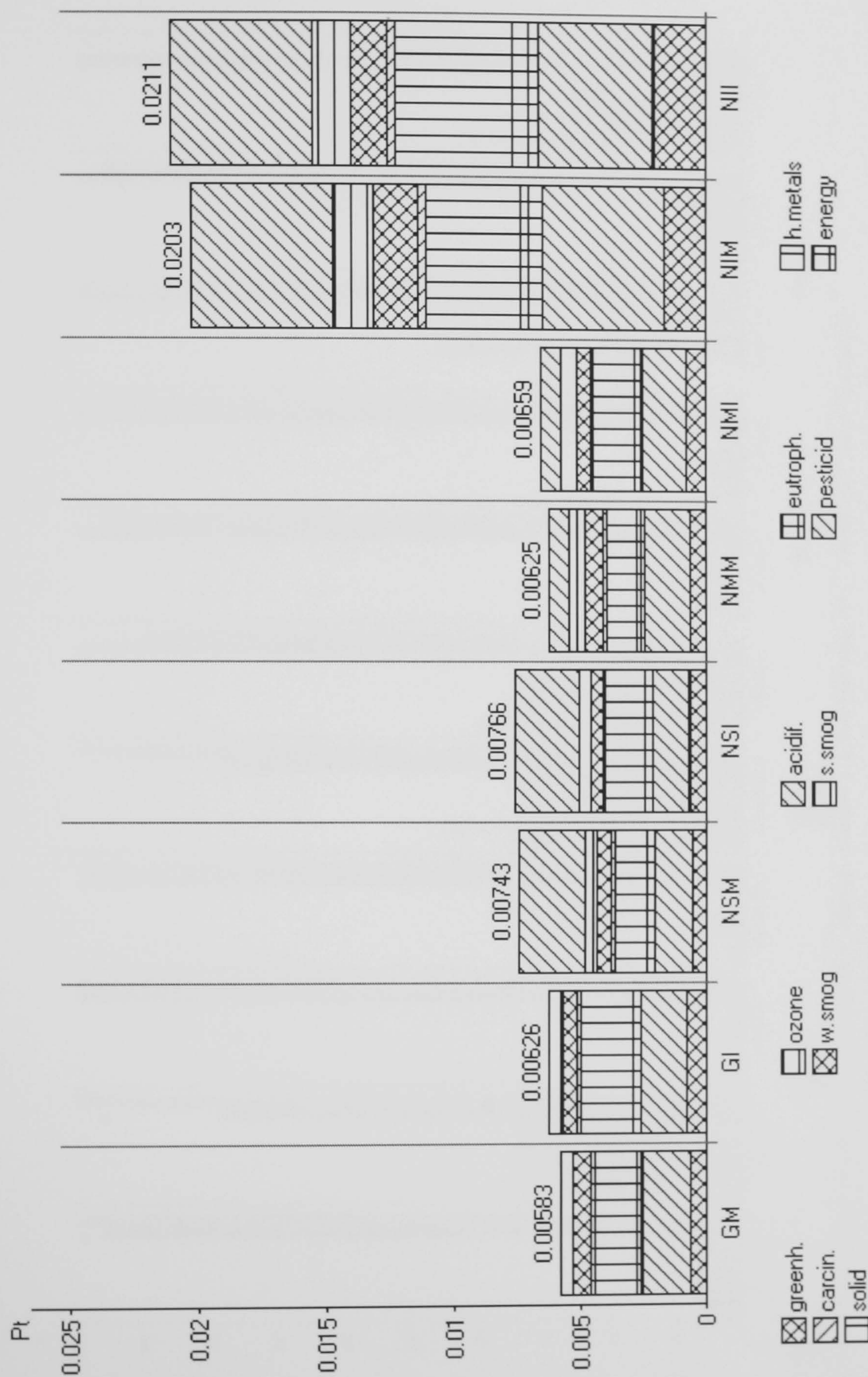
Compare report setup 'Non-automotive'; Method: SimaPro 3.0 Eco-indicator 95 / Europe e / normalisation

Figure 9.9 Graphical representation of the normalised effect score due to various combinations of composite use (for non-automotive applications) and disposal. The sequence of bars in each category is same as the sequence of codes, mentioned below the figure, starting from left top (GM) and ending at bottom right (NII).



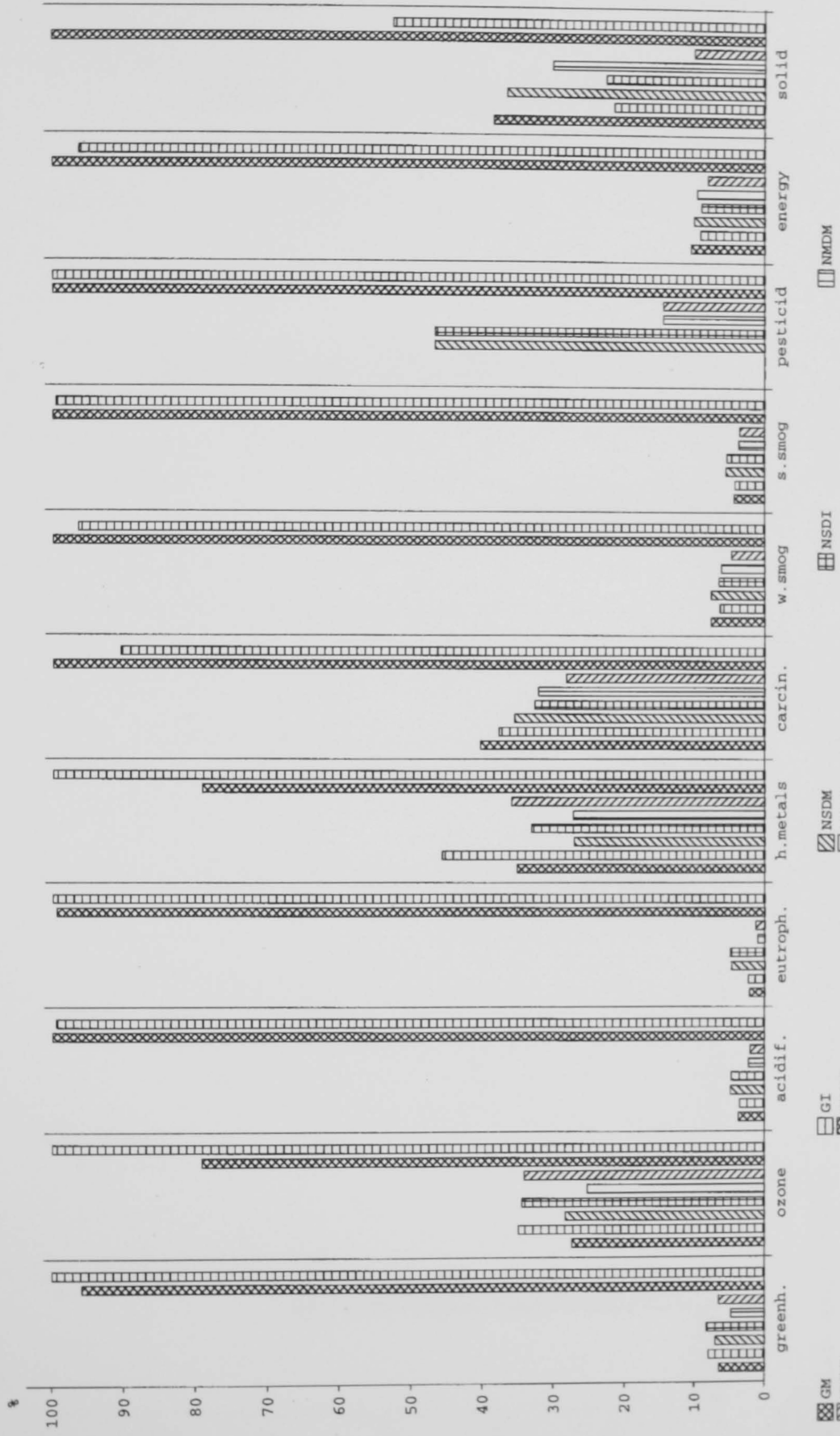
Compare report setup 'Non-automotive'; Method: SimaPro 3.0 Eco-indicator 95 / Europe e / evaluation

Figure 9.10 Graphical representation of the evaluated effect score due to various combinations of composite use (for non-automotive applications) and disposal. The sequence of bars in each category is same as the sequence of codes, mentioned below the figure, starting from left top (GM) and ending at bottom right (NII).



Compare report setup 'Non-automotive'; Method: SimaPro 3.0 Eco-indicator 95 / Europe e / indicator

Figure 9.11 Graphical representation of the indicator obtained by summarising the evaluated numbers for non-automotive applications.



Compare report setup 'Automotive applications'; Method: SimaPro 3.0 Eco-indicator 95 / Europe e / characterisation

Figure 9.12 Graphical representation of the characterisation obtained by scaling the effects due to various combinations of composite use (for automotive applications) and disposal. The sequence of bars in each category is same as the sequence of codes, mentioned below the figure, starting from left top (GM) and ending at bottom right (NIDI).

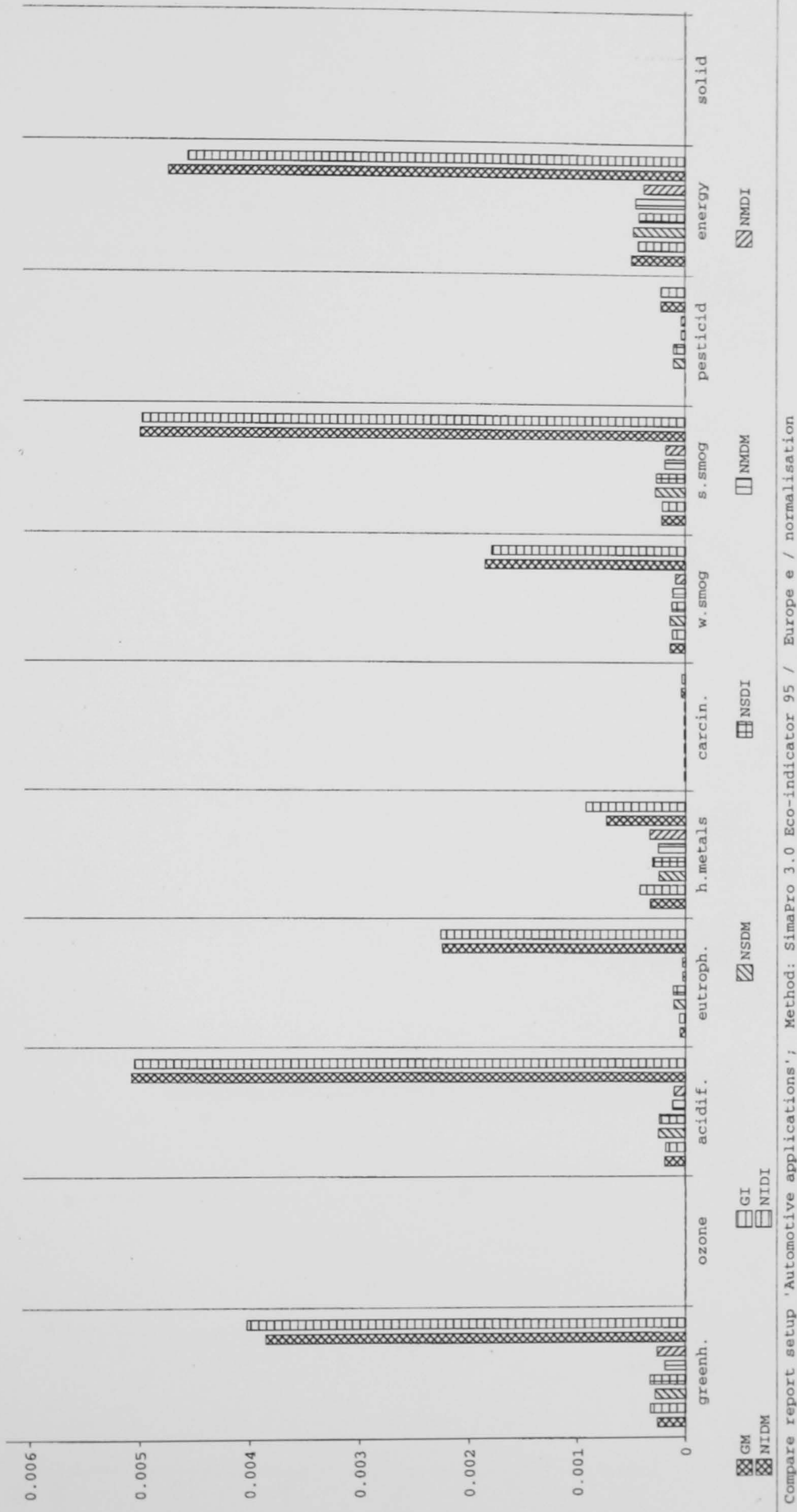


Figure 9.13 Graphical representation of the normalised effect score due to various combinations of composite use (for automotive applications) and disposal. The sequence of bars in each category is same as the sequence of codes, mentioned below the figure, starting from left top (GM) and ending at bottom right (NIDI).

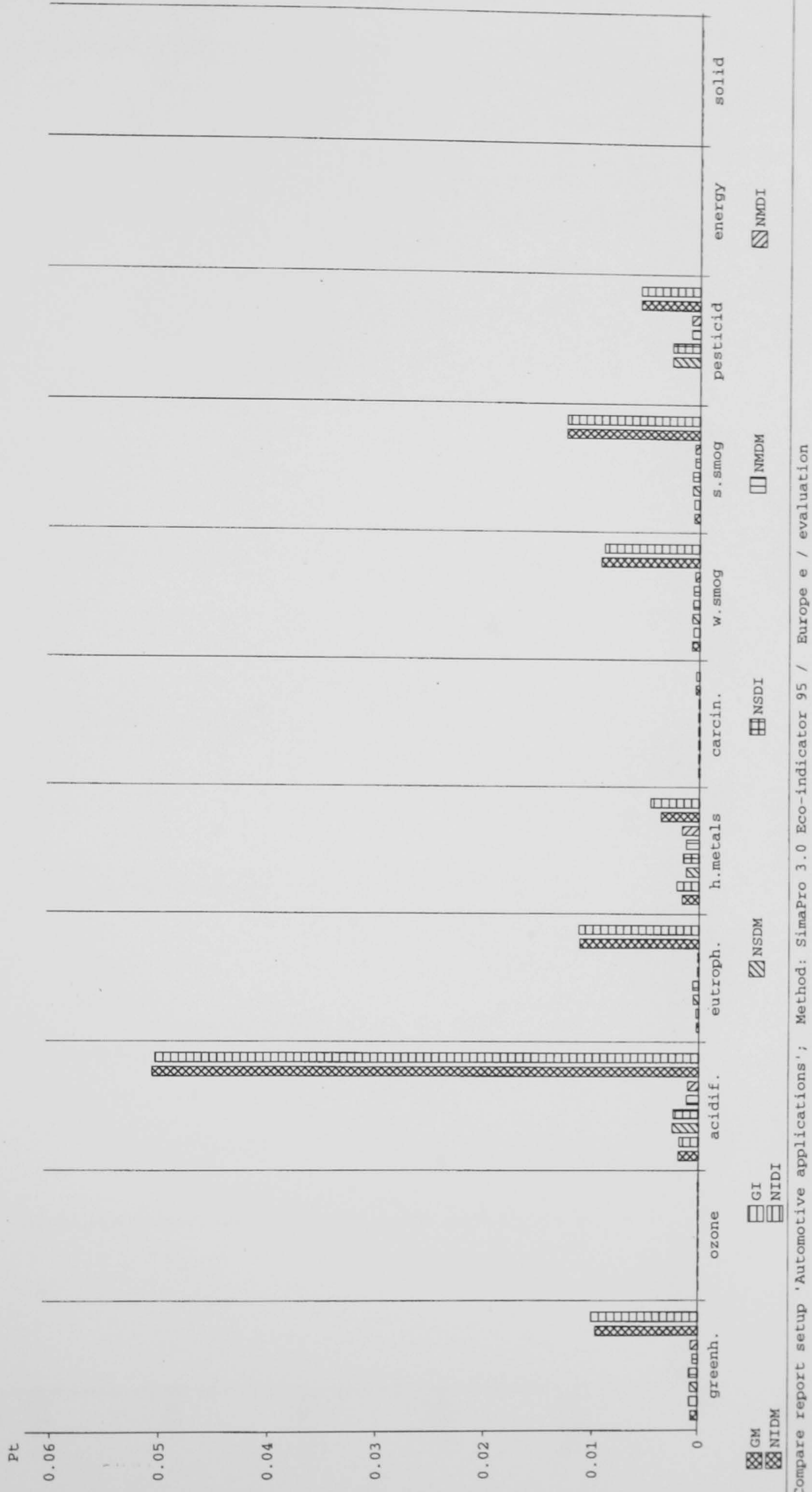
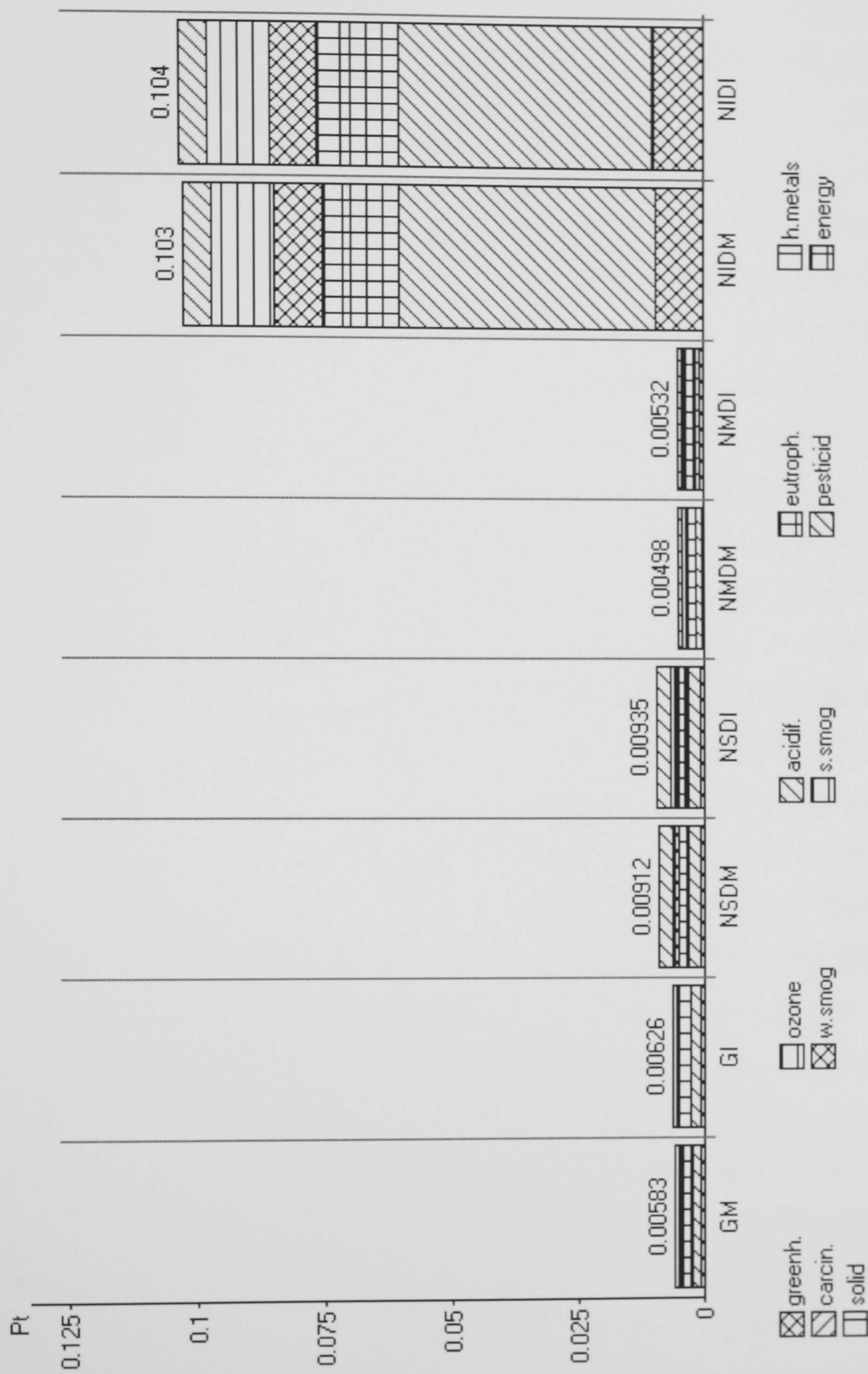


Figure 9.14 Graphical representation of the evaluated effect score due to various combinations of composite use (for automotive applications) and disposal. The sequence of bars in each category is same as the sequence of codes, mentioned below the figure, starting from left top (GM) and ending at bottom right (NIDI).



Compare report setup 'Automotive applications'; Method: SimaPro 3.0 Eco-indicator 95 / Europe e / indicator

Figure 9.15 Graphical representation of the indicator obtained by summarising the evaluated numbers for automotive applications.

9.5.1 Future improvement in environmental impact

As seen from the life cycle analysis the major drawbacks with natural fibres, as far as environmental impact is considered, include use of chemicals (insecticides, pesticides, fertiliser etc.) during its growth and higher fibre loading as well as weight of the composite part to enhance the strength and impact performance of the composite required for many composite applications. Usage of sustainable farming methods with low application of chemicals can certainly enhance the environment performance of these fibres. Another aspect is improvement in the property of these fibres and hence composites. Improvement in fibre processing methods (e.g. Duralin fibre) leading to enhanced properties of flax fibre can improve the environment performance, as lower fibre loading would be required which would reduce the environmental impact. According to LCA study though stiffness critical applications demand lower weight of flax fibres when compared to glass fibres even then the environmental impact (EI) is higher mainly due to chemicals used for farming, therefore (if the same farming methods are continued) further improvement of stiffness would be required to reduce the weight of fibres used and hence reduce the EI by around 7%. Since EI is proportional to the amount of chemicals or amount of flax used therefore an improvement of about 7% in the modulus of flax would be required. In other words the above mentioned reasoning shows that the average stiffness of flax fibre should improve from 40-45 GPa to around 50 GPa to reduce the EI. Similarly for strength the EI of flax fibre composite is 22% higher than glass fibre composite, which would mean an improvement in the strength of flax from around 710 MPa to 910 MPa is required to reduce EI. For impact critical application the EI of flax fibre composites is 71% higher than glass fibre composites, which is because of increased weight (fibre loading as well as composite thickness) of the composite part. The impact strength of glass fibre composites is around 3 times higher than flax fibre composites which strongly depends on fibre strength affecting fibre fracture energy as well as interfacial shear strength affecting fibre debond length. Such an improvement in impact strength is only possible by approaching the strength of fibre cells (roughly 1500 MPa) with sufficient length. In the case of automotive applications further improvement in EI can be obtained due to reduced weight of NMT through enhanced properties, as mentioned above. As shown earlier NMT composites due

to reduced weight and hence lower fuel consumption have lower EI for stiffness critical automotive applications.

9.6 Conclusions

A comparison between GMT and NMT manufactured by a current production method of prepreg followed by compression moulding into an automotive and non-automotive part was performed. The LCA analysis was performed for both the non-automotive and automotive part and three different types of performance requirements; i.e. stiffness, strength and impact resistance. The results of LCA showed that for most cases the environmental impact of NMT material is higher than the reference GMT. Despite their 'green' image natural fibre composites are therefore not necessarily an environmental friendly alternative to glass fibre composites in applications where especially strength and impact are the performance drivers. The reasons for the same include need for pesticides and other chemicals to grow the flax fibre and higher fibre loadings needed to fulfil the impact and strength criterion. Even in the case of stiffness based non-automotive applications, where NMT is lighter than GMT, the differences in environmental impact between GMT and NMT are very small and in the current analysis also here the poorest performance was shown for NMT due to the negative effect of pesticides. If we consider the experimentally observed problem of bad flow properties of NMT, higher weight of NMT would be required to make the same final product. The increased required weight of NMT would even lead to higher environment impact. However, in the case of automotive and stiffness critical applications NMT composites exhibited lower environmental impact when compared to GMT composites. This reduction in environment impact for NMT composites is mainly due to lower weight of natural fibre composite parts, which leads to lower fuel consumption during the use of composites and not so much the result of the use of 'green' fibres. In the case of automotive applications the main parameter that governs the LCA is the weight of the part. Hence, advantages of natural fibre composites are here only to be expected if weight savings are obtained over glass fibre composites. At this moment these weight savings can only be obtained in the case of stiffness critical applications.

10. CONCLUSIONS AND FUTURE RESEARCH

In this chapter some important conclusions from the present study are summarised. Also, suggestions for future research are mentioned.

10.1 Conclusions

From the present study it can be concluded that flax fibre is a good candidate for reinforcing thermoplastics because of its good mechanical properties. Because of its highly crystalline and oriented molecular morphology flax fibre exhibit isotropic mechanical properties and they are very sensitive to compressive loading. Flax fibre itself can be considered as an oriented short fibre composite containing micro-fibrils combined together by the matrix material of lignin, hemi-cellulose and pectin. The micro-fibrils are oriented in helical order along the fibre axis. The polar nature of flax fibre makes these fibres sensitive to moisture causing rotting and leading to low dimensional stability (swelling). The final properties of flax fibre depend on the processing and can be engineered through different processing methods. One of the examples of improved performance of flax fibre through processing is Duralin flax, which has lower moisture sensitivity along with improved mechanical properties. In addition, Duralin fibres have improved thermal stability. The use of Duralin fibres also resulted into a reduced amount of scatter in the composite mechanical properties when compared to composites based on e.g. dew-retted fibres. Flax fibres in general have low thermal stability and can be processed up to around 200-220°C, which limits the applicability of these fibres. Based on the thermal stability of flax fibres, polypropylene (PP) was selected as the principal matrix material for this study.

The tensile strength of flax fibre depends on the gauge length, which could be because of reduced number of weak points at smaller gauge lengths and different fracture modes i.e. rupture through a fibre cell at low gauge lengths and through pectin material when measured at longer gauge lengths.

One of the crucial factors affecting the property of a composite is the bonding between fibre and matrix. The fibre/matrix bond not only affects the mechanical properties but also environmental properties like moisture pick-up. Several methods are currently used and studied to improve fibre/matrix bonding. Both, chemical treatment of fibre and matrix, as well as physical modification i.e. developing specific matrix morphologies (transcrystallinity) through controlled processing conditions were used to enhance the interaction between flax fibre and PP matrix. Chemical modifications were done by two methods i.e. matrix modification and fibre coating.

An effort was made to enhance/optimize the mechanical properties of flax/polypropylene (PP) composites, mainly, through a micro-mechanical study. The effect on the interface was studied through micro-debond test. Fibre modification (coating the fibre with maleic-anhydride grafted polypropylene (MA-PP)) had no significant effect on the interfacial shear strength values. However, when the matrix was modified an optimal MA-PP concentration (in the matrix blend) was observed for the interfacial shear strength values. The observed trend can be attributed to the change in failure mode from adhesive to cohesive, which could be due to the reduced number of molecular entanglements in the case of modified PP and bulk matrix because of increased attachment with the polar flax fibres.

Cleaning of Duralin fibre in hot toluene improved the reactivity of flax fibre as observed through the increased amount of O/C ratio on the fibre surface (by Low Energy Ion Spectroscopy (LEIS) experiments). However, surprisingly it led to a reduction in the IFSS for all the concentrations of MA-PP in polymer bead in microdebonding tests showing the presence of an optimum O/C ratio on the fibre surface for enhanced bonding with a PP/MA-PP blend. The optimum concentration of 10wt% MA-PP, in the case of hot-cleaned Duralin fibre, was not affected which

showed that the optimum was independent of O/C ratio. No effect of MA-PP content on stiffness of the macrocomposite was observed. Study on the effect of MA-PP addition on the strength of (injection moulded) macrocomposites showed, similar to micro-composites, a presence of a critical concentration (20wt%) of MA-PP compatibiliser, which was however different to that for single fibre model composites (10wt% studied by micro-debond tests). This observed difference between critical concentration of MA-PP in micro- and macrocomposites could be due to the effect of fibre content and presence of impurities in macrocomposites. Environmental studies showed that the use of MA-PP as a compatibiliser for improved interfacial bonding lowered the moisture diffusivity, being the water uptake rate, significantly. The maximum moisture content was however not affected by the interfacial properties.

An attempt was also made to modify the fibre/matrix interphase through processing parameters like cooling rate, crystallinity temperature and cooling time. The influence of matrix modification on the crystallisation behaviour was also studied. These studies showed that flax fibres were good nucleating agents in polypropylene matrix leading to a uniform transcrystalline layer around the fibre surface. The crystallisation temperature, cooling rate and time influenced the thickness of a transcrystalline layer. Silane treatment of green flax led to enhancement in the transcrystalline layer thickness. In general a higher transcrystalline layer thickness was observed for higher crystallisation temperatures (T_c). A maximum T_c was observed in the case of Duralin flax/PP system when cooled to 130°C at 10°C/min, which can be explained by the effect of stress induced crystallisation. The effect of cooling rate was contradictory with different systems studied. A decrease in interfacial shear strength with increasing transcrystalline layer thickness, in the case of Duralin flax/PP micro-composites, was observed through fibre pull-out tests. However, the differences observed were very small and a large scatter in interfacial shear strength (IFSS) was observed. A typical value for the IFSS, with a transcrystalline layer as an interface, obtained in the present study through the fibre pull-out test was approximately 8 MPa.

The effect of slow cooling (read: transcrystallinity) on the tensile strength of macrocomposites, manufactured by compression moulding of flax/PP compound,

was also studied. Slow cooling of Duralin flax/PP compound resulted into a reduction in the tensile strength of the macrocomposites, which could be because of the drop in the tensile strength of flax fibre (Chapter 2). Also, the decrease in the tensile strength could be because of the reduction in the molecular entanglements as slow cooled samples exhibited higher levels of crystallinity and brittle fracture, which was observed through differential scanning calorimetric (DSC) studies and fracture surface morphology studies, respectively.

The effect of fibre characteristics on the mechanical properties of long fibre PP/flax composites was also studied. For the production of random PP/flax composites two production methods similar to the commercially known methods for glass/PP composites were used. First, the so-called film-stacking method based on flax non-woven fibre mats and secondly, a suspension impregnation or so-called paper-making process using short flax fibres. Material parameters that were studied for the optimisation of the mechanical performance of such composites were: fibre length, fibre volume fraction and fibre diameter. In order to get a better insight in the importance of these different parameters for the optimisation of composite performance, the experimental results were compared with model predictions using micromechanical models for random short-fibre-reinforced composites. As expected, there was a significant effect of fibre volume fraction on mechanical properties, whereas, no real experimental evidence for the anticipated increase in mechanical performance with increasing fibre length was found.

Based on the experimental results it can be concluded that the stiffness of the flax based natural fibre non-woven mat reinforced thermoplastics (NMTs) is comparable to E-glass based glass fibre non-woven mat reinforced thermoplastics (GMTs) composites. Especially, when focusing on the specific composite properties as a result of the low density of flax. In combination with the price-competitive character of flax fibres these materials might especially be of interest from a 'cost-performance' point of view. However, due to the relatively low tensile strength of the flax fibre bundles (technical fibres) compared to E-glass fibres, the tensile strength of flax based NMTs is significantly lower than that of their glass fibre counterparts. In short, it can be concluded that NMTs based on a PP matrix and flax fibres can compete with E-glass based GMT materials in stiffness critical

structures, whereas for strength and impact critical applications these materials still need to be optimised further. To close the gap with GMT these optimisations should mainly focus on fibre strength through new developments in the fibre opening process, rather than on the optimisation of the interfacial bond strength.

Based on the comparative study between compression moulded and injection moulded Duralin flax/PP composites, it can be concluded that the reduction in fibre length associated with injection moulding did not affect the tensile properties significantly. The reduction in the fibre length may be counterbalanced by the fibre orientation along the polymer flow and fibre efficiency through dimensional changes (fibre fibrillation).

Compounding of flax with PP was carried out by four different methods: kneader, Henschel kinetic mixer, production of long fibre thermoplastic (LFT) granules and twin-screw extrusion. The problem of fibre feeding, in the case of fluffy flax fibres, during mixing with polymer via extruder can be solved through the application of Amandus Kahl pelletising method. The pelletising method is cheaper than LFT method and also more uniform granules are obtained when compared with mixing by kneading. From the analysis of fibre length distribution in compressed fibre pills as well as compounded material, it was found that considerable fibre breakage occurs in the compounding stage itself in the case of kinetic mixing and extrusion. The addition of flax fibre led to a reduction in tensile strength when compared to pure PP. However the addition of compatibiliser (MA-PP) led to an improvement in the tensile properties. Due to the higher fibre lengths in LFT an increased composite toughness was observed. When different compounding methods are compared, the injection-moulded composites manufactured via kneader compounding showed the best strength and stiffness properties. However, kneader compounding was done at lab-scale, whereas the other compounding methods used (i.e. fibre pelletiser followed by twin-screw extrusion, Henschel kinetic mixer and LFT method) can be used for large-scale production.

Other polymers i.e. Nylon 6 and polyoxymethylene (POM) were also used to manufacture short fibre composites via injection moulding. The effect of fibre

addition on the tensile properties was more pronounced in the case of Nylon 6 when compared with non-polar polymers like PP and POM.

From the environmental durability study on flax fibre reinforced PP composites it can be stated that the absorption of moisture by the composites can adequately be described by Fick's law. The moisture content was linear to the square root of time until about two weeks of immersion in water. After that, the moisture content leveled off to a maximum moisture content. The moisture resistance of NMTs based on flax fibres and a PP matrix can be improved by the use of upgraded Duralin flax fibres. The moisture absorption of upgraded flax/PP composites was about 30% lower than that of green flax composites and the dimensional stability (swelling) is also significantly improved. The use of maleic-anhydride modified PP as a compatibiliser for improved interfacial bonding lowered the diffusivity, being the water uptake rate, significantly. The maximum moisture content was however not affected by the interfacial properties. The stiffness of Duralin flax/PP composites showed an initial increase with moisture content, followed by a small drop in stiffness at high levels of moisture content. The stiffness reduction of green flax/PP composites was more pronounced and can be as high as 40% at moisture content levels of 12% and an immersion time of around 8 days. The tensile strength was not as much affected by the water uptake as the stiffness, which was in agreement with the fibre results where no drop in strength was observed with increasing relative humidity. Again also here the Duralin fibre composites showed a better environmental durability compared to green flax/PP composites.

The advantage of biodegradability of natural fibres can be fully exploited by combining it with bioplastics to make biodegradable composites. For the same poly-hydroxyalkanoates (PHAs), along with flax fibre as reinforcement were studied. From the study it can be concluded that addition of (cheap) flax fibre to polyhydroxybutyrate (PHB) can be advantageous as far as cost-performance of biopolymer composites is concerned, especially for stiffness critical applications. The strength of PHB based composites needs to be further optimised through modifications in fibre preparatory process (cleaning through carding and combing processes) and/or through modification of the fibre-matrix interface. Based on the biodegradation study of PHB/HV composites it can be concluded that the tensile

properties drop significantly in the initial stage of degradation, which could be due to the fibre debonding. The drop in tensile properties is more gradual in the later stages of biodegradation.

One of the major advantages of using natural fibre reinforced thermoplastic is based on the assumption that these composites would be environment friendly as far as processing and disposal of the materials was concerned. A life cycle assessment (LCA) study was conducted on flax fibre reinforced PP composites and compared with GMT composites based on PP matrix. From the study it can be concluded that, for non-automotive applications as well as strength and impact critical automotive applications, PP and flax based NMTs are less environment friendly when compared with PP based GMT materials. Some of the factors contributing to the less environment friendly character of NMTs are the use of chemicals like fungicides, pesticides, herbicides and fertilisers during growth of flax fibres and higher weight of composite needed to satisfy tensile and impact properties criteria for automotive applications. Higher weight of NMTs when compared to GMTs would lead to higher fuel consumption. Due to weight saving, NMT composites for stiffness critical automotive applications showed better environmental performance when compared to GMT composites. However, there are certain disadvantages of LCA studies as some of the factors were not included such as the negative effect of using glass fibres on human health and maintenance of processing machines, which would be higher due to abrasive wear by glass fibres.

10.2 Directions for future research

Although natural fibres have some ecological advantages over glass fibres they also possess some disadvantages. Natural fibres can easily compete with glass fibres in terms of stiffness. However, the tensile strength, compressive strength and especially impact strength of natural fibre composites are relatively low compared to glass fibre composites. Especially NMT suffers from this because the material, which they have to replace, GMT, is often selected over for example sheet moulding compounds (SMC) because of their superior impact performance. At this

moment many research groups focus on the interfacial bond strength with the polymer matrix as a way to improve the properties of natural fibre composites. These interface modification schemes often follow schemes similar to the ones used in the past for glass fibre. However, unlike isotropic glass fibres natural fibres exhibit an anisotropic hierarchical composite-like structure (Chapter 2). Tailoring of interfaces within this hierarchical structure may turn out to be more important for bridging the (impact strength) gap with glass fibre systems than tailoring of the interface with the polymer matrix. Figure 10.1 shows the cross-sectional view of flax fibre bundle.



Figure 10.1 The cross-sectional view of flax fibre showing around 7 fibre cells together forming a technical flax fibre (fibre bundle) (Source: Dijon et al., 2001).

In Chapter 2 the strong length dependency of fibre strength was shown. The tensile strength shifts from around 250 MPa for technical fibres (bundle of cells) with lengths between 25 and 100mm to 1200 MPa for single fibre cells with a length of 3 mm. Therefore the fibre performance strongly depends on the fibre opening process and there is a clear need to develop processes which can extract these intrinsically strong cells from the bundles. The other route could be to bond the fibre cells within the bundle. The development of Duralin fibres is a step in the

latter direction. As shown in Chapter 5, the fibre efficiency improves by using improved fibre cleaning and separation.

Figure 10.2 shows the Kelly-Tyson model predictions for the tensile strength of NMT with varying interfacial shear strength and fibre efficiency. From the figure it can be observed that an increase in the IFSS (from 7 MPa to 18 MPa) at low fibre efficiency leads to negligible effect on the composite tensile strength. The effect is more pronounced at improved fibre efficiency (k). As explained in Chapter 5, the fibre efficiency parameter k , which is basically a fitting parameter, is included in Kelly-Tyson model to account for the fibre length, strength and orientation distribution in random short-fibre composites.

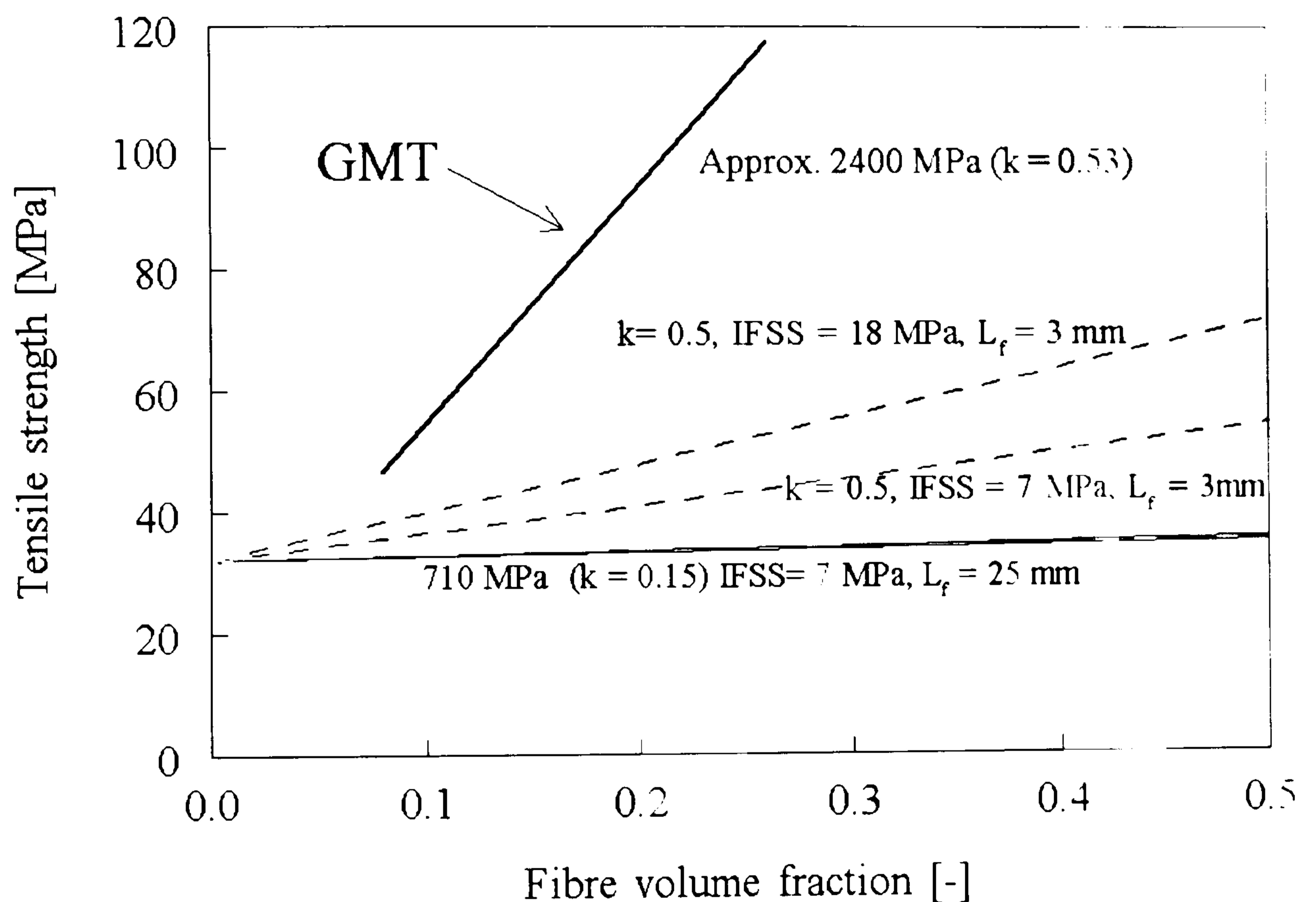


Figure 10.2 Kelly-Tyson model predictions of the tensile strength of NMT with varying interfacial shear strength and fibre efficiency.

Figure 10.3 shows the Kelly-Tyson model predictions for NMT composite strength with varying fibre strength. From the model predictions we can also learn that an increase of fibre strength at low fibre efficiency is not very effective for obtaining high composite strength and the effect is more prominent at high fibre efficiency. However, improvement of fibre efficiency through e.g. fibre cleaning and fibre separation would lead to reduced wettability of the natural fibre mats therefore

demanding different composite manufacturing routes like fibre blending with matrix fibres or paper-making methods. Also fibre separation through existing mechanical methods would lead to fibre damage therefore other methods to separate the fibre cells from the bundle should be explored e.g. chemically.

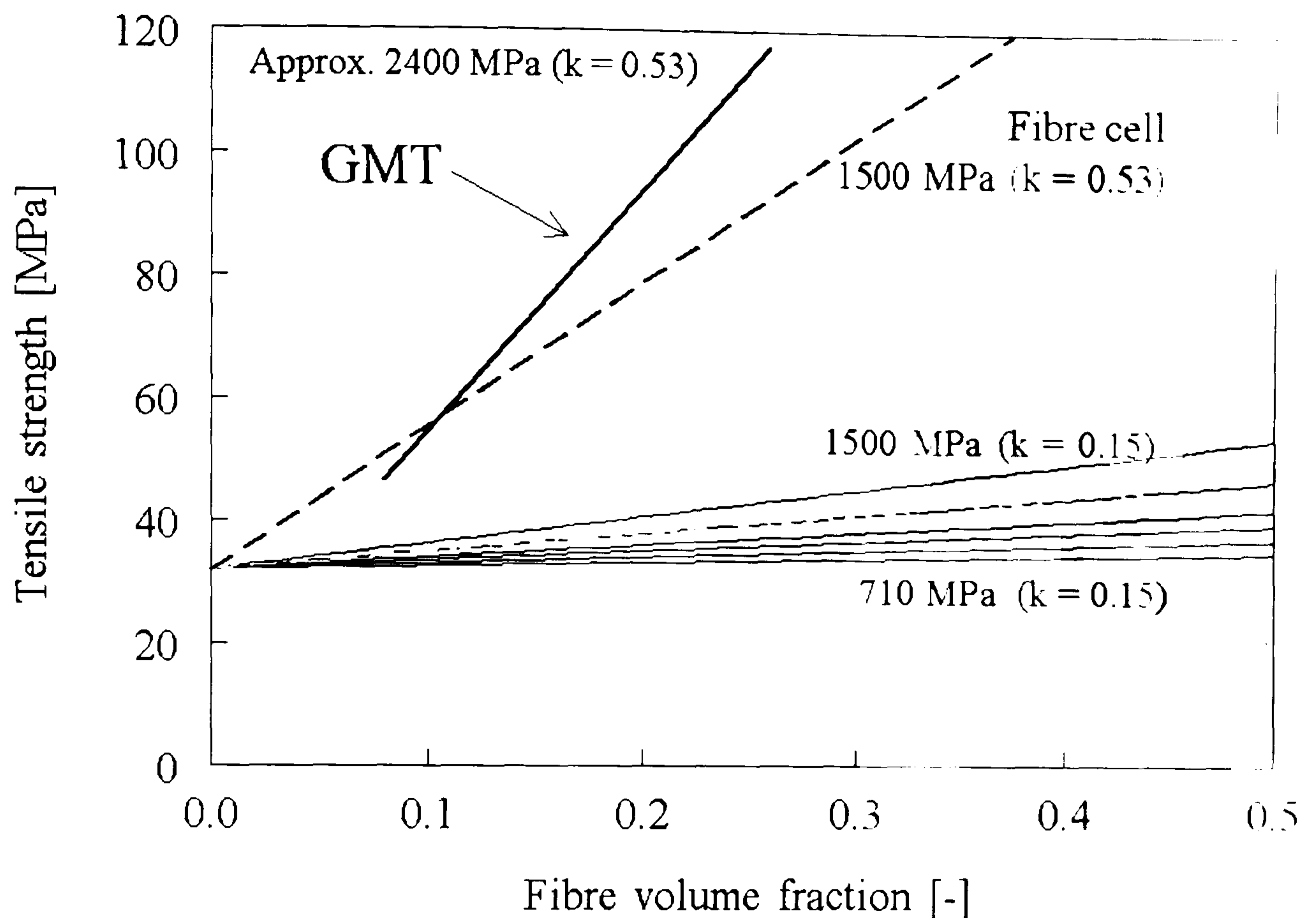


Figure 10.3 Kelly-Tyson predictions of the tensile strength of NMT with varying fibre strength and fibre efficiency.

In the above mentioned example a fibre efficiency (k) of 0.53 is used which is similar to the one used by Thomason et al. (1996) for GMT composites. However, glass fibres are isotropic and natural fibres are anisotropic with a hierarchical microstructure. Therefore the probability of transverse failure within a fibre bundle or even a fibre cell is very high. This will limit the ultimate fibre reinforcing efficiency. Hence, even flax fibre cells may not reach the efficiency parameter exhibited by isotropic glass fibres. Another attractive factor supporting natural fibre is the cost of natural fibres, which again will be higher as these fibres would be subjected to extensive cleaning and separation processes. One of the examples of work done in the above suggested direction was recently published by Matsumura et al. (2000) at Virginia Tech institute in USA where wood pulp microfibril reinforced nanocomposites were developed.

REFERENCES

- Aguilar-Vega, M. and Cruz-Ramos, C. (1995). "Properties of Henequen Cellulosic Fibres", *J. of Applied Poly. Sc.*, V56, 1245-1252.
- Alinec, B. (1989), "Volume Contraction of Cellulose-Water System". Symposium on the Cellulose-Water System, *Proceedings of the 10th Cellulose Conference (Cellulose and Wood, Chemistry and Tech.)*. Schuerch, C. (Ed.), Syracuse, New York, 1988, John Wiley and Sons, Inc., New York, 379.
- Avella, M., Martuscelli, E., Pascucci, B., Raimo, M., Focher, B. and Marzetti, A. (1993), "A New Class of Biodegradable Materials: Poly-3-hydroxy-butyrate / Steam Exploded Straw Fiber Composites. I. Thermal and Impact Behaviour", *Journal of Applied Poly. Sc.*, V49, 2091-2103.
- Bascom, W. D., and Lee, S. M. (1990), "Interphase in Fiber Reinforced Composites", *International Encyclopedia Of Composites, Volume 2*, VCH Publishers, Inc., New York, 411.
- Beck Tan, N.C., Peiffer, D.G. and Briber, R.M. (1996), "Reactive Reinforcement of Polystyrene/Poly(2-vinylpyridine) Interfaces", *Macromolecules*, 29, 4969.
- Berglund, L.A., and Ericson, M.L. (1995), "Glass Mat Reinforced Polypropylene", *Polypropylene: Structure, blends and composites, Vol.3*, Ed. Karger-Kocsis, Chapman & Hall, London, 202.
- Bijsterbosch, H. (1992), *Long Fiber Reinforced Polyamides*, Ph.D. Thesis, Twente University, Twente, The Netherlands.
- Bledzki, A.K. and Gassan, J. (1997), *Natural Fibre Reinforced Plastics*. N.P. Cheremisinof Ed. *Handbook of Engineering Polymeric Materials*, Marcel Dekker, Inc., New York, 787-809.
- Bledzki, A.K., Reihmane, S. and Gassan, J. (1996), "Properties and modification methods for vegetable fibers for natural fiber composites", *Journal of Applied Poly. Sc.*, V59, 8, 1329-1336.
- Bos, H.L., Oever, M.J.A. Van Den, and Peter, C.J.J. (1997), "Flax Fibre Strength and its Influence on Composite Properties". *Internationales Symposium*, Thüringisches Institut Für Textil Und Kunststoff – Forschung e.v., Rudolstadt, Thüringen, Germany, 3-4 September, (1997).

- Bos, H.L., Van den Oever, M.J.A. and Peters. O.C.J.J. (1998). "Structure-Property Relations of Annual Fibres and Their Influence on Composite Properties", *Proceedings of the VIII European Conference on Composite Materials (ECCM-8), Science, Technology and Applications, Vol. 2*, Crivelli Visconti, L. Ed., Naples, Italy, Woodhead Publishing Ltd., Cambridge, U.K., 105.
- Bourban, C., Karamuk, E., De Fondaumiere, M.J., Ruffieux, K., Mayer, J. and Wintermantel, E. (1997), "Processing and Characterization of a New Biodegradable Composite Made of a PHB/V Matrix and Regenerated Cellulosic Fibers", *J. of Environmental Poly. Degradation*, V5, N3, 159.
- Brooks, R. (2000), "Polymer Matrix Composites", *Comprehensive Composite Materials, Volume 2*, Kelly, A. and Zweben, C., Ed., Elsevier Science Ltd., Oxford, U.K., 999-1028.
- Broutman, L.J., Krock, R.H., Plueddemann, E.P., and Erickson, P.W. (1974), "Interfaces In Polymer Matrix Composites", *Composite Materials, Volume 6*, Academic Press, New York.
- Calipso LEIS Expertise Centre, (Business brochure), Eindhoven University of Technology.
- Chawla, K.K., and Bastos, A.C. (1979), "The Mechanical Properties of Jute Fibers and Polyester/Jute Composites", *Proc. 3rd Int. Conf. Mech. Behaviour of Materials, Vol. 3*, Pergamon Press, Toronto, 191.
- Chen, E.J.H. and Hsiao, B.S. (1992), "The Effects of Transcrystalline Interphase in Advanced Polymer Composites", *Poly. Eng. Sci.*, 32, 280-286.
- Chua, P.S. and Piggott, M.R. (1985), "Glass Fibre-Polymer Interface: I - Theoretical Consideration for Single Fibre Pull-out Tests", *Composites Sc. and Tech.*, V22, 33-42.
- Clark, R.L. and Kander, R.G. (1996), "Interphase Modification in Semicrystalline Polymer Matrix Composites and its Influence on Adhesion", *J. of Eng. and Appl. Science*, V2, 2568-2572.
- Clemons, C. M., Giacomini, A. J., and Koutsky, J. A. (1997). "Dynamic Fracture Toughness of Polypropylene Reinforced with Cellulose Fiber", *Poly. Eng. and Sci.*, 37 (6), 1012.
- Cockett, S.R. and Hilton, K.A. (1961). *Dyeing of Cellulosic Fibres and Related Processes*, Leonard Hill (Books) Ltd., London, U.K., 15.

- Cooper, G.A. (1970), "The Fracture Toughness of Composites Reinforced with Weakened Fibres", *J. Material Sc.*, 5, 645.
- Cottrell, A.H. (1964), "Strong Solids", *Proceedings Royal Society*, A282, 2.
- Cox, H.L. (1952), "The Elasticity and Strength of Paper and Other Fibrous Materials", *Brit. J. Applied Phys.*, 3, 72.
- Day, R.J. and Cauch Rodrigez, J.V. (1998), "Investigation of the Micromechanics of the Microbond Test", *Composites Sc. and Tech.*, 58, 907-914.
- De Bruijn, J.C.M. (1998), "Application of Renewable Fibre Reinforced Plastic Products", *Proceedings Of VIII European Conference On Composite Materials (ECCM-8)*, Ed. Visconti, I. C., Naples, Italy, June, 141.
- De Kok, J.M.M. (1995), "The Importance of Fibre-Matrix Adhesion", *Deformation, Yield and Fracture of Unidirectional Composites in Transverse Loading*, Ph.D. Thesis, Eindhoven University of Technology, Eindhoven, The Netherlands, ISBN 90-386-0076-3, 51. (www.mate.tue.nl/mate/pdfs/39.pdf)
- De Koning, G. and Lemstra, P.J. (1993), "Crystallisation Phenomena in Bacterial Poly[(R)-3-hydroxybutyrate]", *Polymer*, V34, 4089.
- De Koning, G.J.M. (1993), *Prospects Of Bacterial Poly((R)-3-Hydroxyalkanoates)*, Ph.D. Thesis, Eindhoven University Of Technology, Eindhoven, The Netherlands, ISBN 90-386-0322-3.
- Dellow, N. (2000), "Plastics Reinforced with Flax Straw for Automobiles", *Advanced Comp. Bulletin*, 1, 1.
- Dewilde, B. (1987), *Flax in Flanders Throughout The Centuries*, Lannoo, Tielt, Belgium.
- Dijon, G. (2002), *A Study of the Structure and the Mechanical Properties of Flax as a Reinforcing Fibre for Composites*, Ph.D. Thesis, Department of Materials and Department of Biology, Imperial College of Science, Technology and Medicine, University of London, UK.
- Dijon, G.(Guillaume), Baillie C. and Murphy, R. (2001), "A Study of the Structure and the Tensile Properties of Flax Fibers", *Proceedings of 6th International Conference on Woodfiber-Plastic Composites*, Madison, Wisconsin, USA, May 15-16, 2001, (www.forestprod.org).
- Drzal, L.T., Rich, M.J. and Lloyd, P.F. (1983), "Adhesion of Graphite Fibers to Epoxy Matrices. I. The Role of Fiber Surface Treatment", *J. Adhes.*, 16, 1.

- Ericson, M. and Berglund, L. (1992), "Deformation and Fracture of Glass-Mat-Reinforced Polypropylene", *Composite Sc. and Tech.*, 43, 269.
- Ericson, M. and Berglund, L. (1993), "Processing and Mechanical Properties of Oriented Preformed Glass-Mat-Reinforced Thermoplastics", *Composite Sc. and Tech.*, 49, 121.
- Felix, J. (1997), *Enhancing Interactions Between Cellulose Fibres And Synthetic Polymers*, Ph.D. Thesis, Chalmers University Of Technology, Göteborg, Sweeden.
- Felix, J.M., and Gatenholm, P. (1991), "The Nature of Adhesion in Composites of Modified Cellulose Fibers and Polypropylene", *J. of Applied Poly. Sci.*, V42, 609.
- Felix, J. M., and Gatenholm, P. (1994), "Effect of Transcrystalline Morphology on Interfacial Adhesion in Cellulose/Polypropylene Composites", *J. Material Sc.*, V29, 3043.
- Folkes, M.J. (1985), "Theoretical Background", *Short fibre reinforced thermoplastics*, Research Studies Press, Chichester, 16.
- Folkes, M.J. and Hardwick, S.T. (1987), "Direct Study of the Structure and Properties of Transcrystalline Layers", *J. Mater. Sci. Letters*, 6, 656-658.
- Folkes, M.J. and Hardwick, S.T. (1990), "Mechanical Properties of Glass/Polypropylene Multilayer Laminates", *J. Mater. Sci.*, 25, 2598-2606.
- Fu Shao-Yun and Lauke Bernd (1996), "Effects of Fiber Length and Fiber Orientation Distributions on the Tensile Strength of Short-Fiber-Reinforced Polymers", *Composite Sc. and Tech.*, 56, 1179.
- Fu, S.Y., Lauke, B., Mäder, E., Yue, C.Y. and Hu, X. (2000), "Tensile Properties of Short-Glass-Fiber- and Short-Carbon-Fiber-Reinforced Polypropylene Composites", *Composites: Part A*, V31, I10, 1117-1125.
- Garkhail, S.K., Heijenrath, R. and Peijs, T. (2000), "Mechanical Properties of Natural-Fibre-Mat-Reinforced Thermoplastics Based on Flax Fibres and Polypropylene", *Applied Composite Materials*, 7 (5 and 6), 351-372.
- Gassan, J. and Bledzki, A.K. (1997, April), "Effect of Moisture Content on the Properties of Silanized Jute-Epoxy Composites", *Poly. Composites*, V18, N2, 179.
- Gassan, J. and Bledzki, A.K. (1998), "Possibilities to Improve the Properties of Natural Fiber Reinforced Plastics by Fiber Modification", *Proceedings Of VIII*

- European Conference On Composite Materials (ECCM-8)*, Ed. Visconti, I. C., Naples, Italy, June, 111.
- Gassan, J. and Bledzki, A.K. (1999, August), "Effect of Cyclic Moisture Absorption Desorption on the Mechanical Properties of Silanized Jute-Epoxy Composites", *Polymer Composites*, V20, N4, 604.
- Gatenholm, P. and Mathiasson, A. (1994), "Biodegradable Natural Composites. II. Synergistic Effects of Processing Cellulose with PHB", *Journal of Applied Poly. Sc.*, 51, 1231-1237.
- Gatenholm, P., Bertilsson, H., and Mathiasson, A. (1993). "The Effect of Chemical Composition of Interphase on Dispersion of Cellulose Fibers in Polymers. I. PVC-Coated Cellulose in Polystyrene", *J. of Applied Poly. Sc.*, 49, 197.
- Gatenholm, P., Kubát, J., and Mathiasson, A. (1992), "Biodegradable Natural Composites. I. Processing and Properties", *J. of Applied Poly. Sc.*, 45, 1667.
- Gati, A. and Wagner, H.D. (1997), "Stress Transfer Efficiency in Semicrystalline-Based Composites Comprising Transcrystalline Interlayers", *Macromolecules*, V30, I13, 3933-3935.
- Gaur, U., Desio, G. and Miller, B. (1989), "Measuring Fiber/Matrix Adhesion in Thermoplastic Composites", *Plastics Engineering*, October, 43-45.
- Gibson, A.G. (1995), "Composites", *Polypropylene: Structure, blends and composites, Volume 3*, Ed. Karger-Kocsis, J., Chapman & Hall, University Press, Cambridge, U.K., 71.
- Giridhar, J., Kishore and Rao, R.M.V.G.K. (1986, April), "Moisture Absorption Characteristics of Natural Fibre Composites", *J. Reinforced Plastics and Composites*, V5, 141.
- Gong, L., Friend, A.D. and Wool, R.P. (1998), "Polymer-Solid Interfaces: Influence of Sticker Groups on Structure and Strength", *Macromolecules*, 31, 3706-3714.
- Gray, D.G. (1974), "Polypropylene Transcrystallization at the Surface of Cellulose Fibers", *J. Poly. Sci., Polym. Lett. Ed.*, V12, I9, 509-515.
- Gray, D.G. (1974b), "Transcrystallization Induced by Mechanical Stress on a Polypropylene Melt", *J. Polym. Sci., Polym. Lett. Ed.*, V12, I11 645-650.
- Gupta V.B., Mittal R.K. and Sharma P.K. (1989), "Some Studies on Glass Fiber-Reinforced Polypropylene. Part II: Mechanical Properties and Their

- Dependence on Fiber Length, Interfacial Adhesion and Fiber Dispersion". *Polymer Composites*, 10 (1), 16.
- Hearle, J.W.S., and Peters, R.H. (1963). *Fibre Structure*, Butterworth & Co. (Publishers) Ltd., London.
- Heijenrath, R.W.H. (1996), *Flax-Fibre-Reinforced Polypropylene Composites*, Masters Thesis, Centre for Polymers and Composites. Department of Chemical Engineering, Eindhoven University of Technology. Eindhoven, The Netherlands.
- Heijenrath, R. and Peijs, T. (1996), "Natural-Fibre-Mat-Reinforced Thermoplastic Composites Based on Flax Fibres and Polypropylene". *Advanced Composite Letters*, 5 (3), 81.
- Hermann, A.S., Nickel, J. and Riedel, U. (1998), "Construction Materials Based Upon Biologically Renewable Resources- From Components to Finished Parts", *Polymer Degradation and Stability*, 59, 251.
- Herrera-Franco, P.J., and Aguilar-Vega De, J. (1997), "Effect of Fiber Treatment on the Mechanical Properties of LDPE-Henequen Cellulosic Fiber Composites", *J. of Applied Poly. Sci.*, 65, 197.
- Heuvel, Van Den P.W.J. (1998), *An Experimental and Numerical Investigation Into Failure Phenomena In Multi-Fibre Microcomposites*, Ph. D. Thesis. Eindhoven University Of Technology, Eindhoven, The Netherlands, 1.
- Hoffmann, A., Kreuzberger, S. and Hinrichsen, G. (1994), "Influence of Thermal Degradation on Tensile Strength and Young's Modulus of Poly(hydroxybutyrate)", *Poly. Bulletin*, 33, 355.
- Hoogen, N. (1999), "Components from Flax-Reinforced Polypropylene in Mass Production", *Kunststoffe*, 89, 3, 103.
- Hornsby, P. R., Hinrichsen, E., and Tarvedi, K. (1997), "Preparation and Properties of Polypropylene Composites Reinforced with Wheat and Flax Straw Fibres", *J. Of Material Sc.*, 32, 1009.
- Huang, Y. and Petermann, J. (1995), "Transcrystalline Growth of Thermoplastics and LCPs During Isothermal Crystallization", *J. Appl. Poly. Sci.*, V55, 981-987.
- Hull, D. (1996), *Introduction to Composite Materials*, Cambridge University Press, New York.

- Jain, R.K., Lal, K., and Bhatnagar, H. L. (1986). "Thermal Studies on C-6 Substituted Cellulose and its Subsequent C-2 and C-3 Esterified Products in Air", *Eur. Polym. Journal*, V22, 112, 993.
- Jakopin, S. (1984) "Compounding Techniques for Fiber Reinforced Thermoplastics", *SPI / Composites Institute 39th Annual Conference*, Houston, Texas, 16-19 January, Society of the Plastics Industry Inc., 355 Lexington Avenue, New York, NY 10017, USA.
- Joly, C., Kofman, M. and Gauthier, R. (1996), "Polypropylene Cellulosic Fiber Composites: Chemical Treatment of the Cellulose Assuming Compatibilization between the Two Materials", *Journal of Materials Sc. – Pure Applied Chem.*, A33, 12, 1981-1996.
- Karmaker, A.C. (1997), "Effect of Water Absorption on Dimensional Stability and Impact Energy of Jute Fibre Reinforced Polypropylene", *J. Mat. Sci. Letters*, 16 (6), 462.
- Karmaker, A.C. and Clemons, C.M. (1995), "Water Absorption and Load Transferring Mechanisms in Polypropylene Reinforced with Lignocellulosic Fibers", *Annual Technical Conference - ANTEC, Conference Proceedings, Vol.2*, pp.2091.
- Karmaker, A.C. and Hinrichsen, G. (1991), "Processing and Characterization of Jute Fiber Reinforced Thermoplastic Polymers", *Polymer-Plastics Technology and Engineering*, 30 (5-6), 609.
- Karmaker, A. C. and Youngquist, J. A. (1996), "Injection Molding of Polypropylene Reinforced with Short Jute Fibers", *J. of Applied Poly. Sc.*, 62, 1147.
- Karmaker, A.C., Hoffmann, A. and Hinrichsen, G. (1994), "Influence of Water Uptake on the Mechanical Properties of Jute Fiber-Reinforced Polypropylene", *J. of Applied Poly. Sc.*, V54, 1803-1807.
- Karnani, R., Krishnan, M., and Narayan, R. (1997), "Biofiber-Reinforced Polypropylene Composites", *Poly. Engg. & Sc.*, 37 (2), 476.
- Kaur, B., Gur, I.S., and Bhatnagar, H. L. (1986), "Studies on Thermal Degradation of Cellulose and Cellulose Phosphoramides", *J. of Applied Poly. Sc.*, V31, 12, 667.
- Kelly, A. and Macmillan, N.H. (1986), *Strong Solids*, Clarendon Press, Oxford, 269.

- Kelly, A. and Tyson, W.R. (1965), "Tensile Properties of Fiber-Reinforced Metals. Copper/Tungsten and Copper/Molybdenum", *J. Mech. Phys. Solids*, V13, 16, 329.
- Khot, S. (1998), *Rigid Thermoset Polymers from Acrylated Epoxidized Triglycerides*, Ph.D. thesis, University of Delaware, Delaware, U.S.A.
- Krautz, F.G. (1971), "Glass Fiber Enhances High-Temperature Performance of Thermoplastics", *SPE Journal*, V27, N8, 74.
- Krenchel, H. (1964), *Fibre reinforcement*, Akademisk Forlag, Copenhagen.
- Kuruvila, J., Thomas, S. and Pavithran, C. (1995). "Effect of Ageing on the Physical and Mechanical Properties of Sisal-Fiber-Reinforced Polyethylene Composites", *Comp. Sc. & Tech.*, 53, 99.
- Kuruvila, J., Thomas, S., Pavithran, C., and Brahmakumar, M. (1993), "Tensile Properties of Short Sisal Fiber-Reinforced Polyethylene Composites", *J. Appl. Poly. Sci.*, V47, I10, 1731.
- Luo, S. and Natravali, A.N. (1999, June), "Mechanical and Thermal Properties of Environment-Friendly "Green" Composites Made From Pineapple Leaf Fibers and Poly(hydroxybutyrate-co-valerate) Resin", *Poly. Composites*, V20, N3, 367.
- Maldas, D., and Salamone, J. C. (1996), "Cellulose Filled Composites", *Polymeric Materials Encyclopedia, Volume 2*, CRC Press, Florida, U.S.A., 1079.
- Mallick, P.K. (1993), *Fiber - Reinforced Composites*, 2nd ed., Marcel Dekker, Inc., New York.
- Mandell, J.F., Chen, J.H. and McGarry, F.J. (1980), "A Microdebonding Test for In-situ Assessment of Fiber/Matrix Bond Strength in Composite Materials", *Int. J. Adhes.*, 1(1), 40.
- Marotzke, C. (1993), "Problems of the Determination of the Interface Strength with the Aid of the Single Fiber Pull-out Test", *Proceedings of the VI European Conference On Composite Materials (ECCM-6)*, 281-286.
- Matsumura, H., Sugiyama, J. and Glasser, W. (2000) "Cellulosic Nanocomposites. I. Thermally Deformable Cellulose Hexanoates from Heterogeneous Reaction" *Journal of Applied Poly. Sc.*, V78, I13, 2242-2253.
- Matthews, F. L., and Rawlings, R. D. (1994), "Reinforcement-Matrix Interface", *Composite Materials: Engineering and Science*, Chapman and Hall, London, 59.

- McGovern, J. N. (1984), "Fibers, Vegetable". *Encyclopedia Of Textiles, Fibers, and Nonwoven Fabrics*, ed. Grayson, M.. John Wiley & Sons, New York, 175.
- McGovern, J. N. (1987), "Fibers, Vegetable", *Encyclopedia of Poly. Sc. & Eng.*, II edition, V. 7, John Wiley & Sons Inc., New York, 16.
- Meurs, P. (1998), *Characterisation Of Microphenomena In Transversely Loaded Composite Materials*, Ph. D. Thesis (ISBN 90-386-0650-8). Eindhoven University Of Technology, Eindhoven, The Netherlands, 3.
- Meurs, P.F.M., Schreurs, P.J.G., Peijs, T., and Meijer, H.E.H. (1996). "Characterization of Interphase Conditions in Composite Materials", *Composites Part A*, 27A, 9, 781.
- Mieck, K. P., Lützkendorf, R. and Reussmann, T. (1996). "Needle Punched Hybrid Nonwovens of Flax and PP Fibers- Textile Semi-products for Manufacturing of Fiber Composites", *Poly. Composites*, 17 (6), 873.
- Mieck, K.P., Nechwatal, A., and Knobelsdorf, C. (1995a). "Faser-Matrix-Haftung in Kunststoffverbunden aus Thermoplastischer Matix und Flachs, 1. Die Ausrüstung mit Silanen", *Die Angewandte Makromolekulare Chemie*, V224, 73.
- Mieck, K.-P., Nechwatal, A. and Knobelsdorf, C. (1995b). "Faser-Matrix-Haftung in Kunststoffverbunden aus Thermoplastischer Matix und Flachs, 2. Die Anwendung von Funktionalisiertem Polypropylen", *Die Angewandte Makromolekulare Chemie*, 225, 37-49.
- Mieck, K.-P., Reussmann, T. and Knobelsdorf, C. (1997). "Textile Halbzeuge Für Biologisch Abbaubare Faserverbunde", *Kunststoffberater*, 5, 29.
- Miller, B., Muri, P. and Rebenfeld, L. (1987), "A Microbond Method for Determination of the Shear Strength of a Fiber/Resin Interface", *Composites Sc. and Tech.*, 28, 17-32.
- Misra, A., Deopura, B.L., Xavier, S.F., Hartley, F. D., and Peters, R. H. (1983). "Transcrystallinity in Injection Molded Polypropylene Glass Fiber Composites". *Die Angewandte Makromolekulare Chemie*, 113, 113.
- Moriwaki, T. (1996), "Mechanical Property Enhancement of Glass Fibre-Reinforced Polyamide Composite Made by Direct Injection Moulding Process", *Composites: Part A*, 27A, 15, 379-384.
- Morton, W.E., and Hearle, J.W.S. (1962). *Physical Properties Of Textile Fibres*. Butterworth & Co. (Publishers) Ltd. and the Textile Institute, London.

- Morton, W.E. and Hearle, J.W.S. (1975), *Physical Properties of Textile Fibres*, 2nd ed., John Wiley & Sons, Inc., New York.
- Mukherjee, R.R. and Radhakrishnan, T. (1972). "Long Vegetable Fibres", *Text. Progress*, 4, 4.
- Occhiello, E., Garbassi, F., Morra, M. and Nicolais, L. (1989). "Spectroscopic Characterization of Interfaces in Polymer Composites", *Comp. Sc. & Tech.*, V36, I2, 133.
- Oksman, K. (1997), *Improved Properties of Thermoplastic Wood Flour Composites*, Ph.D. Thesis, Luleå University of Technology, Skellefteå, Sweden.
- Oksman, K., and Nilsson, P. (1998), "Thermoplastic Composites Based on Natural Fibres", *Proceedings Of VIII European Conference On Composite Materials (ECCM-8)*, Ed. Visconti, I. C., Naples, Italy, June 1998, 133.
- Pan, N. (1993), "Theoretical Determination of the Optimal Fiber Volume Fraction and Fiber-Matrix Property Compatibility of Short Fiber Composites", *Polymer Composites*, 14, 85.
- Park Buyng-Dae, and Balatinecz, J.J. (1997), "Mechanical Properties of Wood-Fiber/Toughened Isotactic Polypropylene Composites", *Poly. Composites*, 18 (1), 79.
- Peijs, T., Garkhail, S., Hejenrath, R., Van den Oever, M. and Bos, H. (1998a), "Thermoplastic Composites Based on Flax Fibres and Polypropylene: Influence of Fibre Length and Fibre Volume Fraction on Mechanical Properties", *Macromol. Symp.*, 127, 193.
- Peijs, T., Van Melick, H., Garkhail, S. K., Pott, G., and Baillie, C. A. (1998b), "Natural-Fibre-Mat-Reinforced Thermoplastics Based on Upgraded Flax Fibres for Improved Moisture Resistance", *Proceedings Of VIII European Conference On Composite Materials (ECCM-8)*, Ed. Visconti, I. C., Naples, Italy, (June, 1998).
- Peters, R. H. (1963), "Flax", *Textile Chemistry. Volume I, The Chemistry Of Fibres*, Elsevier Publishing Company, New York, U.S.A.
- Peters, R. H. (1967), "Impurities in Fibres: Purification of Fibres", *Textile Chemistry. Volume II*, Elsevier Publishing Company, Amsterdam, The Netherlands.

- Piggott, M. R., and Dai, S. R. (1991), "Fiber Pull Out Experiments with Thermoplastics", *Poly. Engg. and Sc.*, 31, 17, 1246.
- Plati E. and Williams J.G. (1975), "The Determination of the Fracture Parameters for Polymers in Impact", *Poly. Engg. and Sc.*, V15, 6, 470-477.
- Pompe, G. and Maeder, E. (2000), "Experimental Detection of a Transcrystalline Interphase in Glass-Fibre/Polypropylene Composites", *Comp. Sci. and Tech.*, V60, 111, 2159-2167.
- Pott, G.T., Hueting, D. and Van Deursen, J. (2000), "Reduction of Moisture Sensitivity in Wood and Natural Fibres for Polymer Composites", *Proceedings Of 3rd International Wood and Natural Fibre Composites Symposium*, September 19-20, 2000, Kassel, Germany.
- Pott, G.T., Pilot, R.J. and van Hazendonk, J.M. (1997), "Upgraded Flax Fibres as Reinforcement in Polymer Composites", *Proc. of the 5th European Conference on Advanced Materials and Processes and Applications (EUROMAT 97), Vol.2 Polymers and Ceramics*, Maastricht, The Netherlands, 107, (21-23 April 1997).
- Prasad, N.S.K. (1992), *Hardy Composites*, C.S.I.R Golden Jubilee Series, New Delhi, 3.
- Prasad, S.V., Pavithran, C. and Rohtagi, P.K. (1983), "Alkali Treatment of Coir Fibers for Coir-Polyester Composites", *J. of Material Sc.*, V18, 15, 1443.
- Procotex Corporation NV (Business Brochure), Henleykaai 96, B-9000, Gent, Belgium.
- Rao, R.M.V.G.K., Chanda, Manas and Balasubramanian, N. (1983, October), "A Fickian Diffusion Model for Permeable Fibre Polymer composites", *J. Reinforced Plastics and Composites*, V2.
- Reinsch, V.E. and Kelley, S.S. (1997), "Crystallization of Poly(hydroxybutyrate-co-hydroxyvalerate) in Wood Fiber-Reinforced Composites", *J. of Applied Poly. Sc.*, V64, 19, 1785.
- Richardson, M.O.W. (1997), *Poly. Eng. Composites*. Applied Science Publishers Ltd., London.
- Rijsdijk, H.A., Contant, M., and Peijs, A.A.J.M. (1993), "Continuous-Glass-Fibre-Reinforced Polypropylene Composites: I. Influence of Maleic-Anhydride-Modified Polypropylene on Mechanical Properties", *Composites Sc. and Tech.*, 48, 161.

- Roelofsen, P.A. (1951), "Contradictory Data on Spiral Structures in the Secondary Cell Wall of Fibers of Flax, Hemp and Ramie". *Textile Research Journal*, V21, 412.
- Rosenthal, J. (1992), "A Model for Determining Fiber Reinforcement Efficiencies and Fiber Orientation in Polymer Composites". *Poly. Composites*, 13, 462.
- Ruyter, H.P., Hortulanus, A. and Dekker, J. (1993). "Cellulosic Fibrous Aggregate and a Process for its Preparation", *European Patent Application EP 373 726*.
- Rydberg, T., "Improved Environmental Performance of Products: Halocarbon Substitution, Packaging Development and Life Cycle Assessment", Post-graduation dissertation, School of Chemical Engineering, Department of Chemical Environmental Science, Chalmers University of Technology, Sweden.
- Sain, M. M. and Kokta, B. V. (1994), "Polyolefin-Wood Filler Composite. I. Performance of m-Phenylene Bismaleimide-Modified Wood Fiber in Polypropylene Composite", *J. of Applied Poly. Sc.*, 54, 1545.
- Sanadi, A.R., Caulfield, D.F., Jacobson, R.E., and Rowell, R.M. (1995). "Renewable Agricultural Fibers as Reinforcing Fillers in Plastics: Mechanical Properties of Kenaf Fiber-Polypropylene Composites", *Ind. Eng. Chem. Res.*, 34, 1889.
- Satyanarayana, K.G. et al. (1981), "On the Possibility of Using Natural Fibre Composites", *Composite Structures, Vol. 1*, Ed. Marshall, I.H., Elsevier Applied Sci., London, 618.
- Schultz, J., Lavielle, L., Carre, A. and Comien, P.J. (1989). "Surface Properties and Adhesion Mechanisms of Graft Polypropylenes", *J. of Materials Sc.*, V24, I12, 4639.
- Selzer, R. (1995), "Environmental Influences on the Bending Properties of Sisal Fiber Reinforced Polymer Composites", *Advanced Composite Letters*, 4 (3), 87.
- SETAC (1993), Society for Environmental Toxicology and Chemistry, Guidelines for Life-Cycle Assessment, a "Code of Practice", Brussels, Belgium.
- Sharma, H.S.S., Fraser, T.W., McCall, D., Shields, N. and Lyons, G. (1995). "Fine Structure of Chemically Modified Flax Fibre", *J. Text. Inst.*, V86, N4, 539.

- Sharpe, L. H., and Akovali, G. (1993), "The Interfacial Interactions in Polymeric Composites", *NATO Advanced Study Institute (ASI) Series, Series E : Applied Sciences Volume 230*, Kluwer Academic Publishers, and The Netherlands.
- SimaPro User manual by PRé Consultant B.V., The Netherlands.
- Springer, G.S. (1981), *Environmental effects on composite materials*, Westport.
- Stamboulis, A., Baillie, C.A., Garkhail, S.K., Van Melick, H.G.H. and Peijs, T. (2000), "Environmental Durability of Flax Fibres and their Composites Based on Polypropylene Matrix", *Applied Composite Materials*, V7, 15-6, 273-294.
- Strong, A. B. (1993), "Fiber Matrix Interactions", *High Performance and Engineering Thermoplastic Composites*, Technomic Publishing Company, Inc., Pennsylvania, p35.
- Thomason, J. L. and Van Rooyen, A. A. (1992), "Transcrystallized Interphase in Thermoplastic Composites: Part I: Influence of Fibre Type and Crystallization Temperature", *J. of Material Sc.*, 27, 889-896.
- Thomason, J.L. and Van Rooyen, A.A. (1992b), "Transcrystallized Interphase in Thermoplastic Composites: Part II: Influence of Interfacial Stress, Cooling Rate, Fibre Properties and Polymer Molecular Weight", *J. of Materials Sc.*, 27, 897-907.
- Thomason, J.L. and Vlug, M.A. (1996), "Influence of Fibre Length and Concentration on the Properties of Glass Fibre-Reinforced Polypropylene: 1. Tensile and Flexural Modulus", *Composites, Part A*, 27A, 477.
- Thomason, J.L. and Vlug, M.A. (1997), "Influence of Fibre Length and Concentration on the Properties of Glass Fibre-Reinforced Polypropylene: 4. Impact Properties", *Composites, Part A*, 28A, 277.
- Thomason, J.L., Vlug, M.A., Schipper, G. and Krikor, H.G.L.T. (1996), "Influence of Fibre Length and Concentration on the Properties of Glass Fibre-Reinforced Polypropylene: 3. Strength and Strain at Failure", *Composites, Part A*, 27, 1075.
- Van de Beld, T. (2000, May), *Green versus petro polymers*, Graduation project report, Eindhoven Polymer Laboratory, Eindhoven University of Technology, Eindhoven, The Netherlands.
- Van den Heuvel, P.W.J., Hogeweg, B. and Peijs, T. (1997), "Experimental and Numerical Investigation into the Single-Fibre Fragmentation Test: Stress Transfer by a Locally Yielding Matrix", *Composites- Part A*, 28A, 13, 237-249.

- Van den Oever, M. and Peijs, T. (1998), "Continuous-Glass-Fibre-Reinforced Polypropylene Composites, II. Influence of Maleic-Anhydride Modified Polypropylene on Fatigue Behaviour", *Composites- Part A*, 29A, 13, 227.
- Verpoest, I., and Jones, F. R. (1994), "Interfacial Bond Strength Determination-Critique", *Handbook Of Polymer - Fibre Composites, Polymer Sc. & Technology Series*, Longman Scientific & Technical, London, 230.
- Vissers, M.C. (2000), *Alternative Composites for the Automotive Industry, Can Glass Mat Reinforced Thermoplastics be replaced by Natural Mat Reinforced Thermoplastics or perhaps by All-Polypropylene Composites?*, Graduation project report, Stan Ackermans Institute, Centre for Technological Design, Eindhoven University of Technology, Eindhoven, The Netherlands, January, 2000.
- Voyutskii, S. S. (1963), *Autohesion and Adhesion of High Polymers*, Interscience, NewYork.
- Wagner, H.D., Gallis, H.E. and Wiesel, E. (1993), "Study of the Interface Kevlar 49-Epoxy Composites by means of Microbond and Fragmentation Tests: Effects of Materials and Testing Variables", *J. of Materials Sc.*, V28, 18, 2238-2244.
- Wang, G., and Harrison, I. R. (1994), "Study of the Preferential Crystallization of Polypropylene on the Surface of Wood Fibers", *ANTEC*, 1474.
- Wells J.K., and Beaumont, P.W.R. (1985), "Debonding and Pull-out Processes in Fibrous Composites", *J. Material Sc.*, 20, 1275.
- Wells, J.K. and Beaumont, P.W.R. (1985b), "Crack-tip Energy Absorption Processes in Fibre Composites", *J. Material Sc.*, 20, 2735.
- Wells, J.K. and Beaumont, P.W.R. (1988), "The Toughness of a Composite Containing Short Brittle Fibres", *J. Material Sc.*, 23, 1274.
- Wollerdorfer, M. and Bader, H. (1998), "Influence of natural fibres on the mechanical properties of biodegradable polymers", *Industrial Crops and Products*, V8, 105-112.
- Wood, J.R. and Marom, G. (1997), "Determining the Interfacial Shear Strength in the Presence of Transcrystallinity in Composites by the 'Single-Fibre Microcomposite Compressive Fragmentation Test'", *Appl. Comp. Mat.*, V4, 14, 197-207.

- Wool, R.P., Kusefoglu, S., Palmese, G., Khot, S. and Zhao, R. (2000), "High Modulus Polymers and Composites from Plant Oils". U.S. Patent 6.121.398.
- Wu, H.F. and Ferber, M.K. (1994), "Interfacial Mechanical Characterization of Nicalon SiC Fiber/Alumina-Based Composites", *J. Adhes.*, V45, 11-4, 89-102.
- Young, R.A., Denes, F., Nielsen, L. and Tu, X. (1995). "Improvement of Biobased Fiber-Plastic Composite Properties through Cold Plasma Treatments", *Proc. Woodfiber-Plastic Composites Conference*, Madison, Wisconsin, 227.
- Yue, C.Y. (1995), "Fibre-Matrix Interface", *Handbook Of Advanced Material Testing*, Ed. Cheremisinoff, N.P., Marcell Dekker, Inc., New York, 367.
- Zafeiropoulos, N., Baillie, C.A. and Matthews, F.L.. "A Study of the Effect of Surface Treatments on the Thermal Stability of Flax Fibres", *Submitted to Composites Part A*.
- Zafeiropoulos, N.E. (2001), *Engineering and Characterisation of the Interface in Flax/Polypropylene Composite Materials*, Ph. D. Thesis, Centre for Composite Materials and Department of Materials, Imperial College of Science, Technology and Medicine, University of London, London, U.K.
- Zafeiropoulos, N.E., Baillie, C.A. and Matthews, F.L. (2000), "Modification and Characterisation of the Interface in Flax/PP Composite Materials", *Proceedings Of The IX European Conference On Composite Materials (ECCM-9)*, Brighton, U.K., on CD, 4-7 June, 2000.

LIST OF PUBLICATIONS

1. Peijs, T., Garkhail, S., Heijenrath, R., Van Den Oever, M. and Bos, H. (1998), "Thermoplastic Composites Based on Flax Fibres and Polypropylene: Influence of Fibre Length and Fibre Volume Fraction on Mechanical Properties", *Macromolecular Symposia*, V127, 193-203.
2. Garkhail, S.K., Heijenrath, R.W.H. and Peijs, T. (2000), "Mechanical Properties of Natural-Fibre-Reinforced Thermoplastics Based on Flax Fibres and Polypropylene", *Applied Composite Materials*, V7, N5-6, 351-372.
3. Stamboulis, A., Baillie, C.A., Garkhail, S.K., Van Melick, H.G.H. and Peijs, T. (2000), "Environmental Durability of Flax Fibres and Their Composites Based on Polypropylene Matrix", *Applied Composite Materials*, V7, N5-6, 273-294.
4. Garkhail, S.K., Wieland, A.M.H., George, J. and Peijs, T., "Transcrystallisation in Flax / PP Composites – Effect of Crystallinity on the Mechanical Properties", *Polymer Composites*, accepted.

CONFERENCE PROCEEDINGS

1. Garkhail, S., Heijenrath, R., Van Den Oever, M., Bos, H. and Peijs, T., "Natural-Fibre-Mat-Reinforced Thermoplastic Composites Based on Flax Fibres and Polypropylene", *Proceedings of 11th International Conference on Composite Materials (ICCM-11), Vol. IV*, Scott, M.L., Ed., Gold Coast, Queensland, Australia, Australian Composite Structures Society, Woodhead Publishers Ltd., 1997, 794-803.
2. Peijs, T., Van Melick, H.G.H., Garkhail, S.K., Pott, G.T. and Baillie, C.A., "Natural-Fibre-Mat-Reinforced Thermoplastics Based on Upgraded Flax Fibres for Improved Moisture Resistance", *Proceedings of the 8th European Conference on Composite Materials (ECCM-8), Science, Technology and*

-
- Applications, Volume 2*, Crivelli Visconti, I., Ed., Naples, Italy, Woodhead Publishing Ltd., Cambridge, U.K., 1998, 119-126.
3. Garkhail, S.K., Meurs, E., Van de Beld, T. and Peijs, T., "Thermoplastic Composites Based on Biodegradable Matrices and Natural Fibres", *Proceedings of 12th International Conference on Composite Materials (ICCM-12), Volume V*, Paris, France, Woodhead Publishing, Cambridge, U.K., 1999.
 4. Garkhail, S.K., Bertens, P., George, J., Klompen, E.T.J. and Peijs, T., "Optimisation of Flax-Fibre-Reinforced-Polypropylene Composites Through Interfacial Adhesion", *Proceedings of 9th European Conference on Composite Materials (ECCM-9)*, Brighton, U.K., 4-7 June 2000, on CD ROM by IOM Communications.
 5. Peijs, T., George, J., Garkhail, S. and Klompen, E., "Processing, Properties and Applications of Flax Fibre Reinforced Composites", *Proceedings of 6th International Conference on Woodfiber-Plastic Composites*, Madison, Wisconsin, U.S.A., 15-16 May 2001.
 6. Garkhail, S.K. and Peijs, T., "Micromechanical Models as a Guide for Future Optimisations of Natural-Fibre-Reinforced Plastics", *EcoComp*, London, U.K., 3-4 September 2001.

Appendix 2A: Tensile strength plots for different flax fibre types.

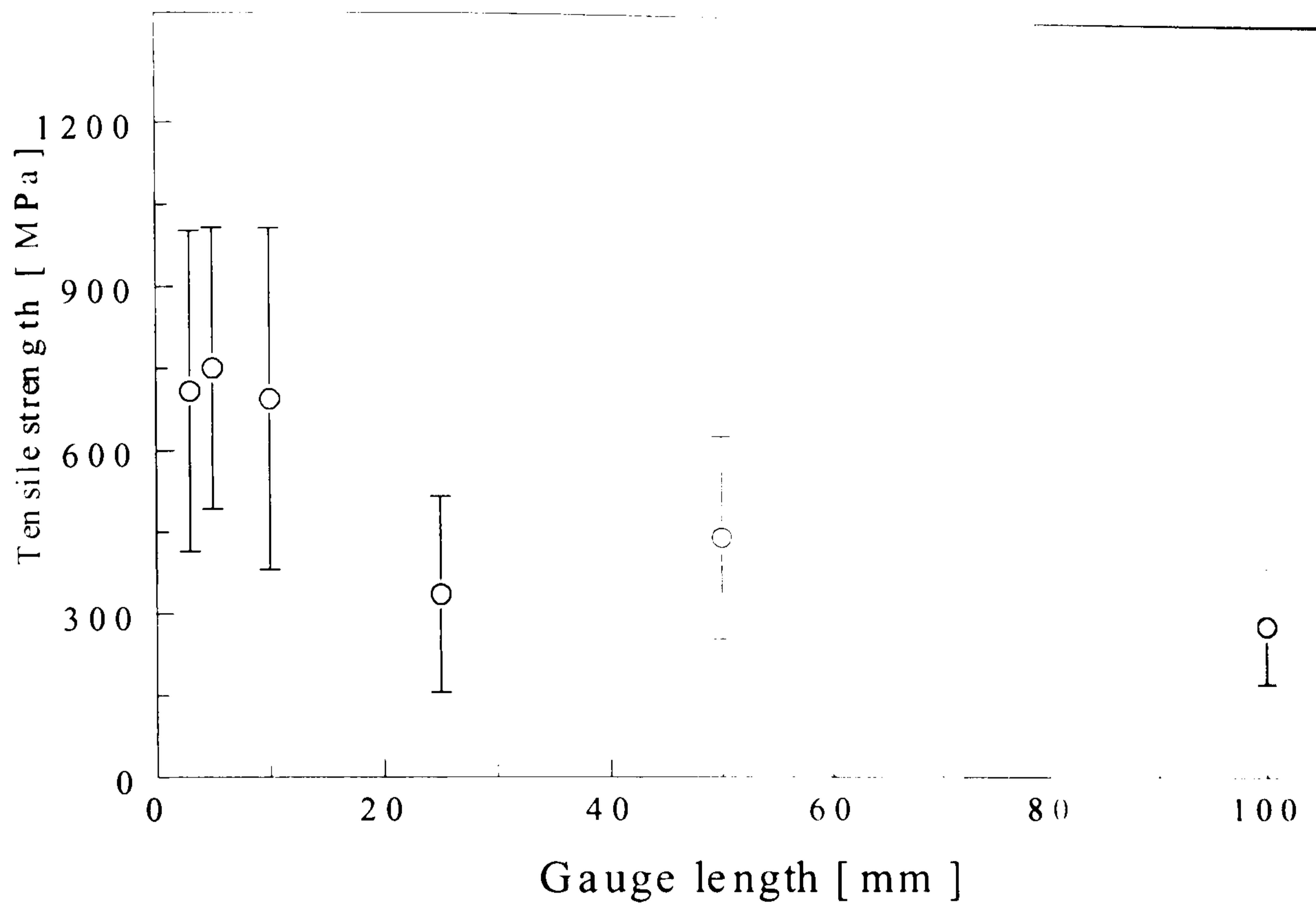


Figure 2A.1 Tensile strength of dew-retted flax vs. gauge length.

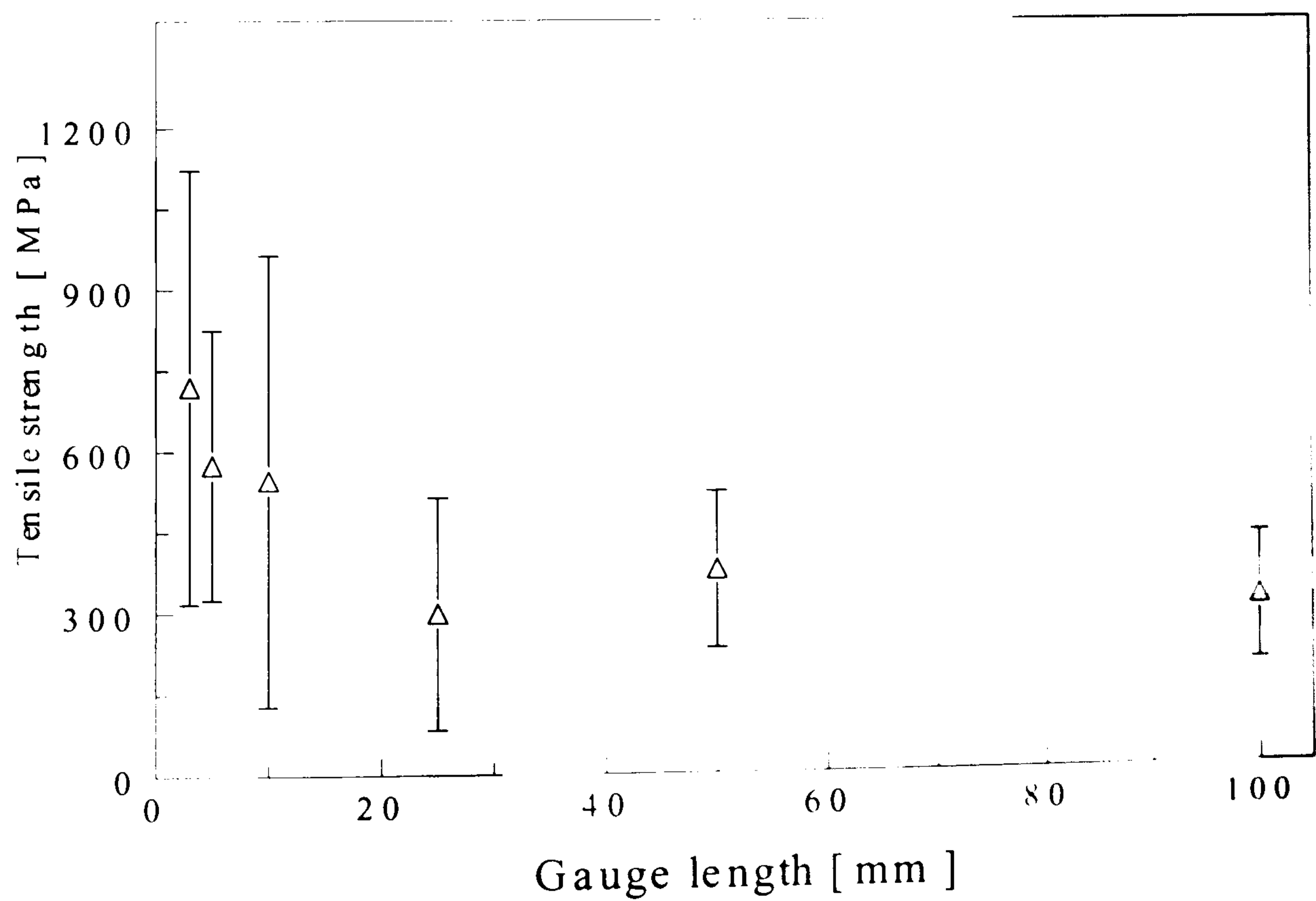


Figure 2A.2 Tensile strength of green flax vs. gauge length.

Appendix 2B: Tensile modulus plots for different flax fibre types.

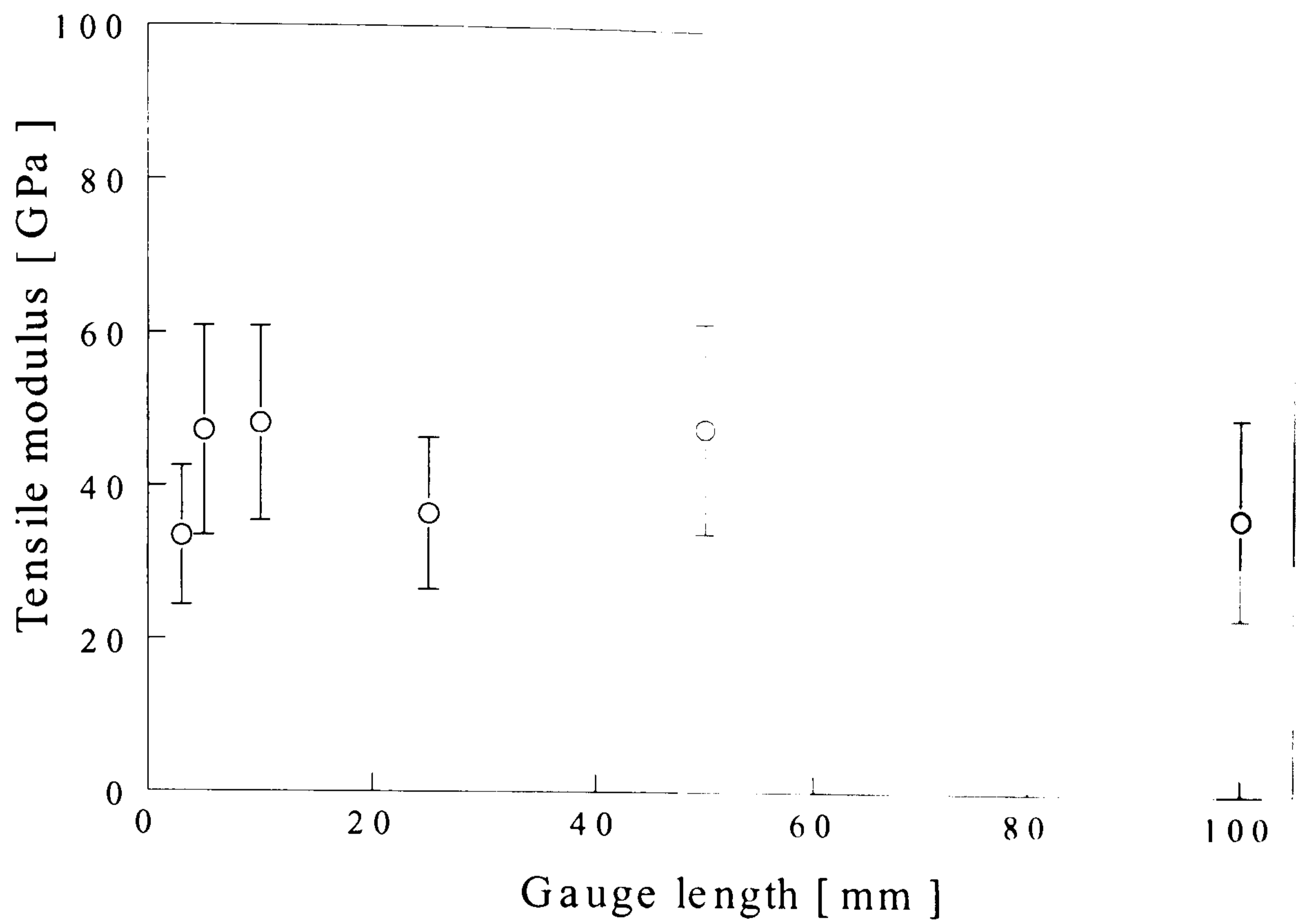


Figure 2B.1 Tensile modulus of dew-retted flax vs. gauge length.

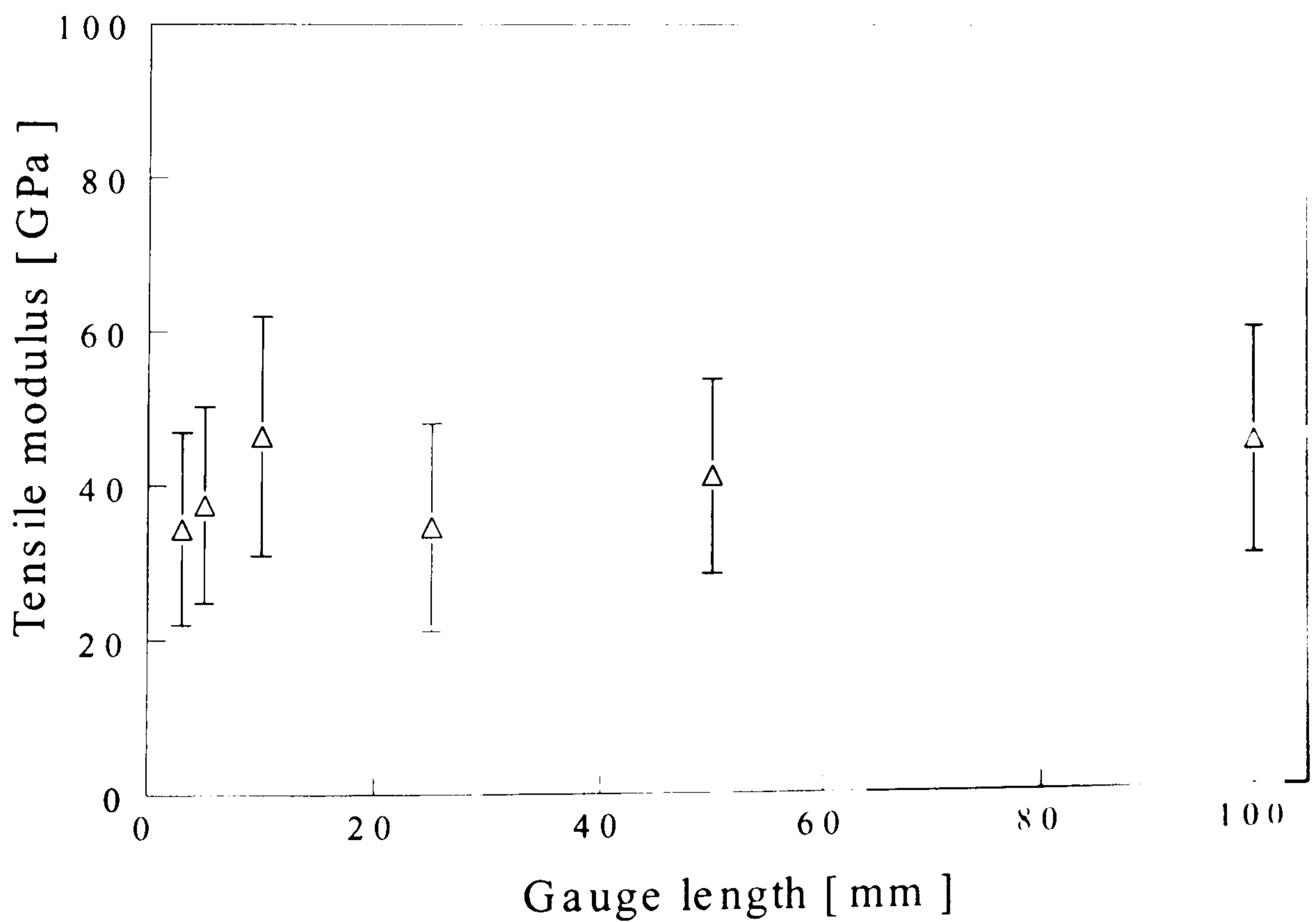


Figure 2B.2 Tensile modulus of green flax vs. gauge length.

Appendix 3A: Pull-out force vs. embedded length

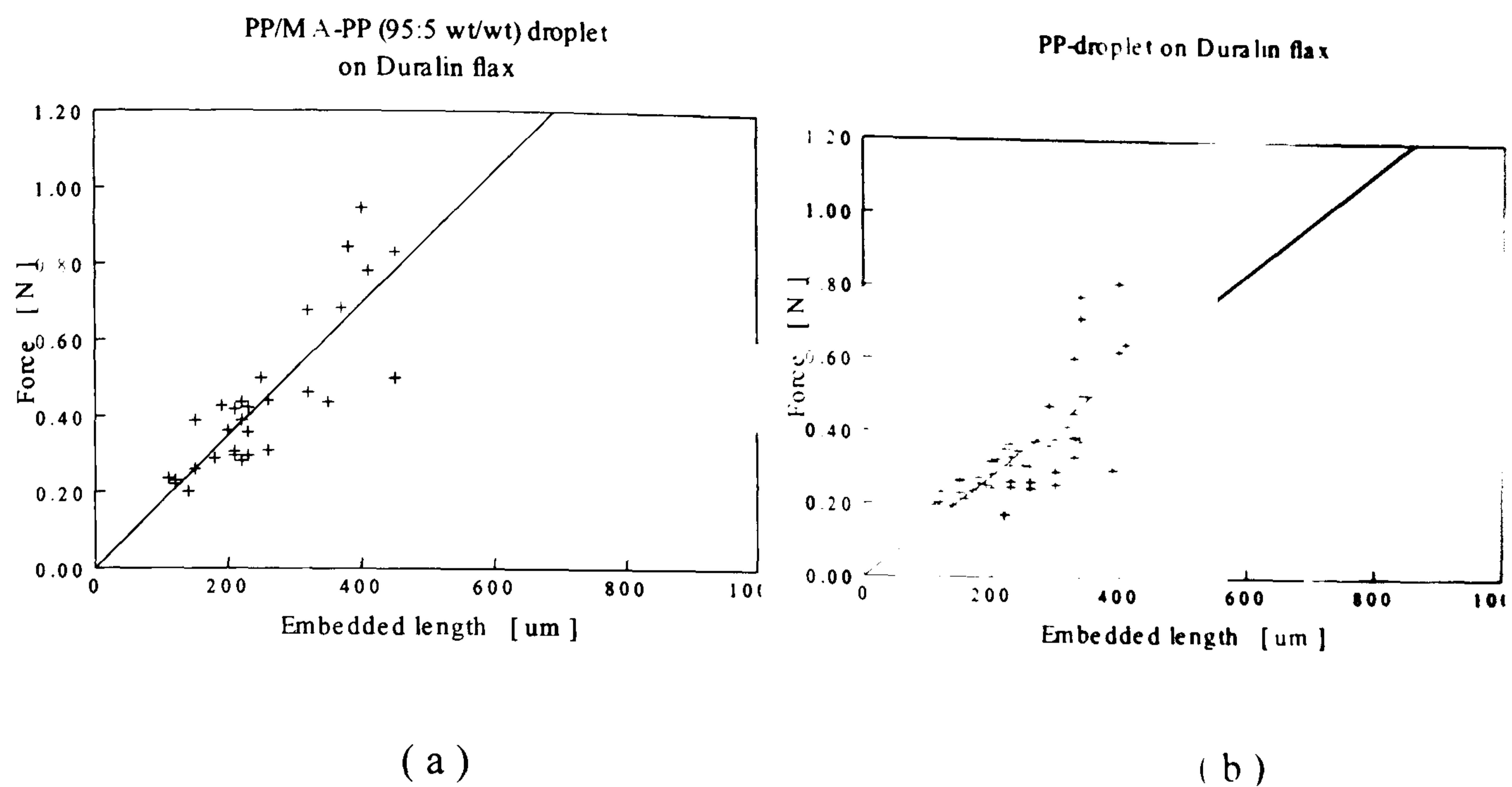


Figure 3A.1 Pull-out force vs. embedded length curve of Duralin flax with (a) pure PP matrix (b) blend of PP/MA-PP (95:5 wt/wt).

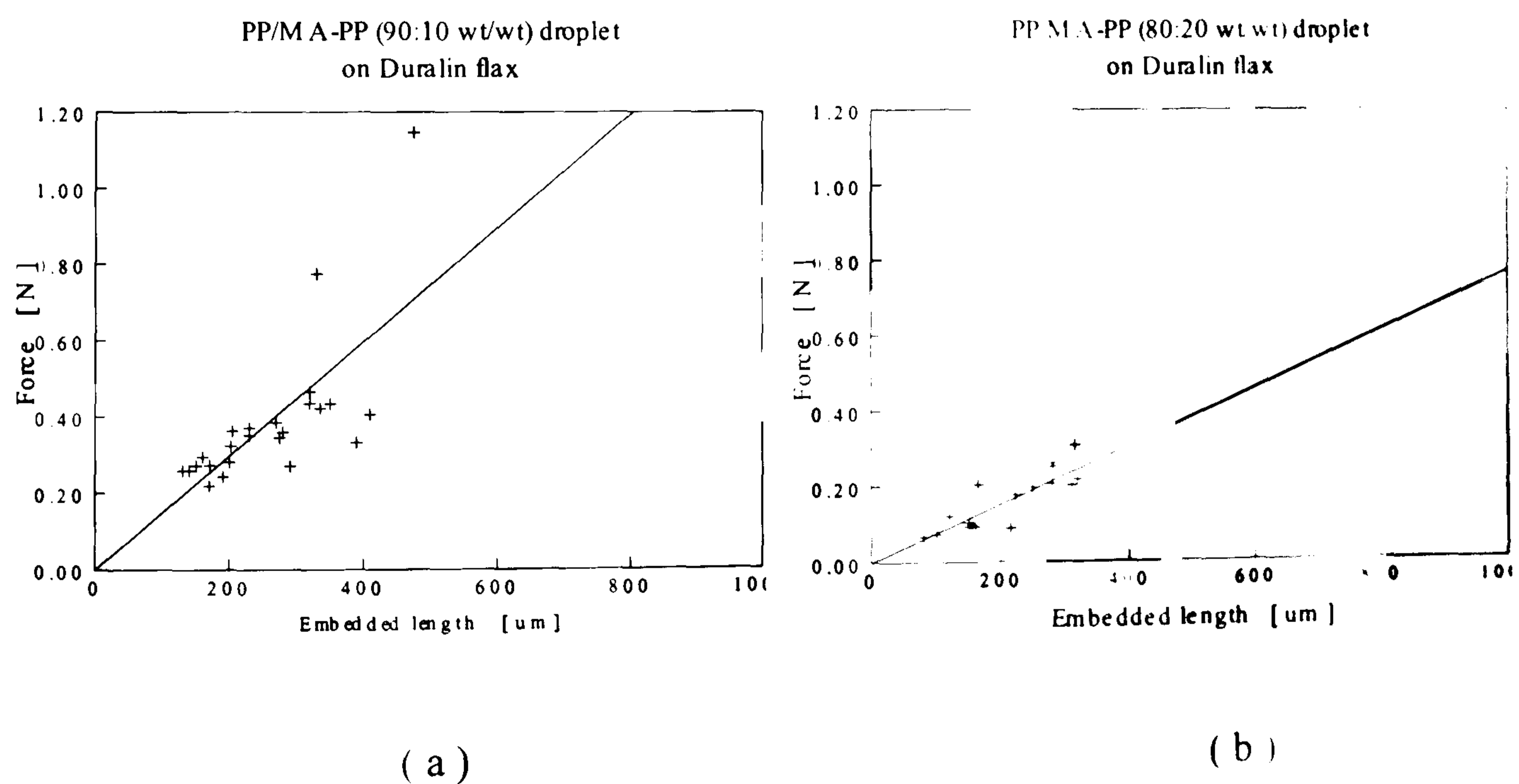


Figure 3A.2 Pull-out force vs. embedded length curve of Duralin flax with (a) blend of PP/MA-PP (90:10 wt/wt) and (b) blend of PP/MA-PP (80:20 wt/wt).

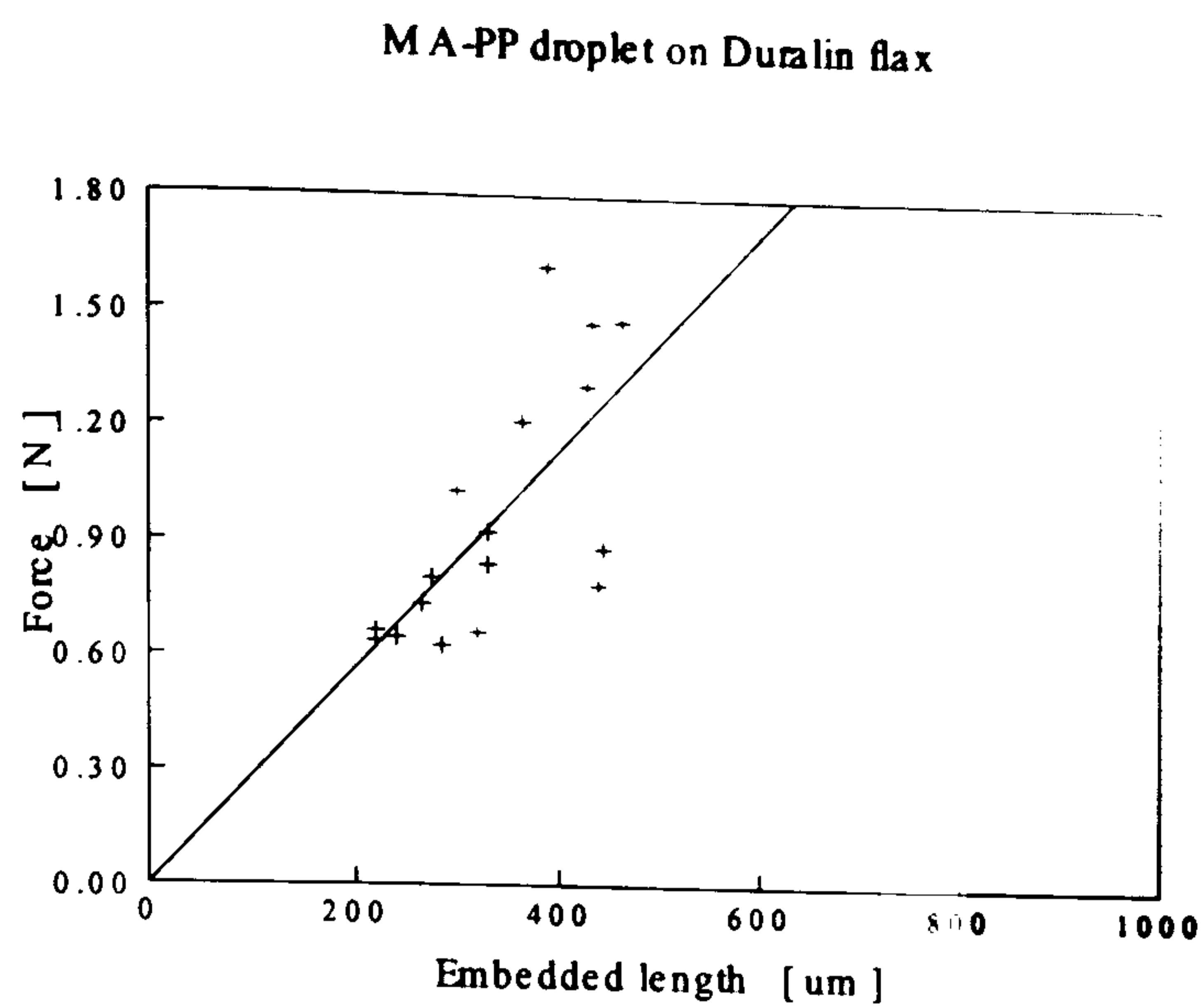


Figure 3A.3 Pull-out force vs. embedded length curve of Duralin flax with pure MA-PP matrix.

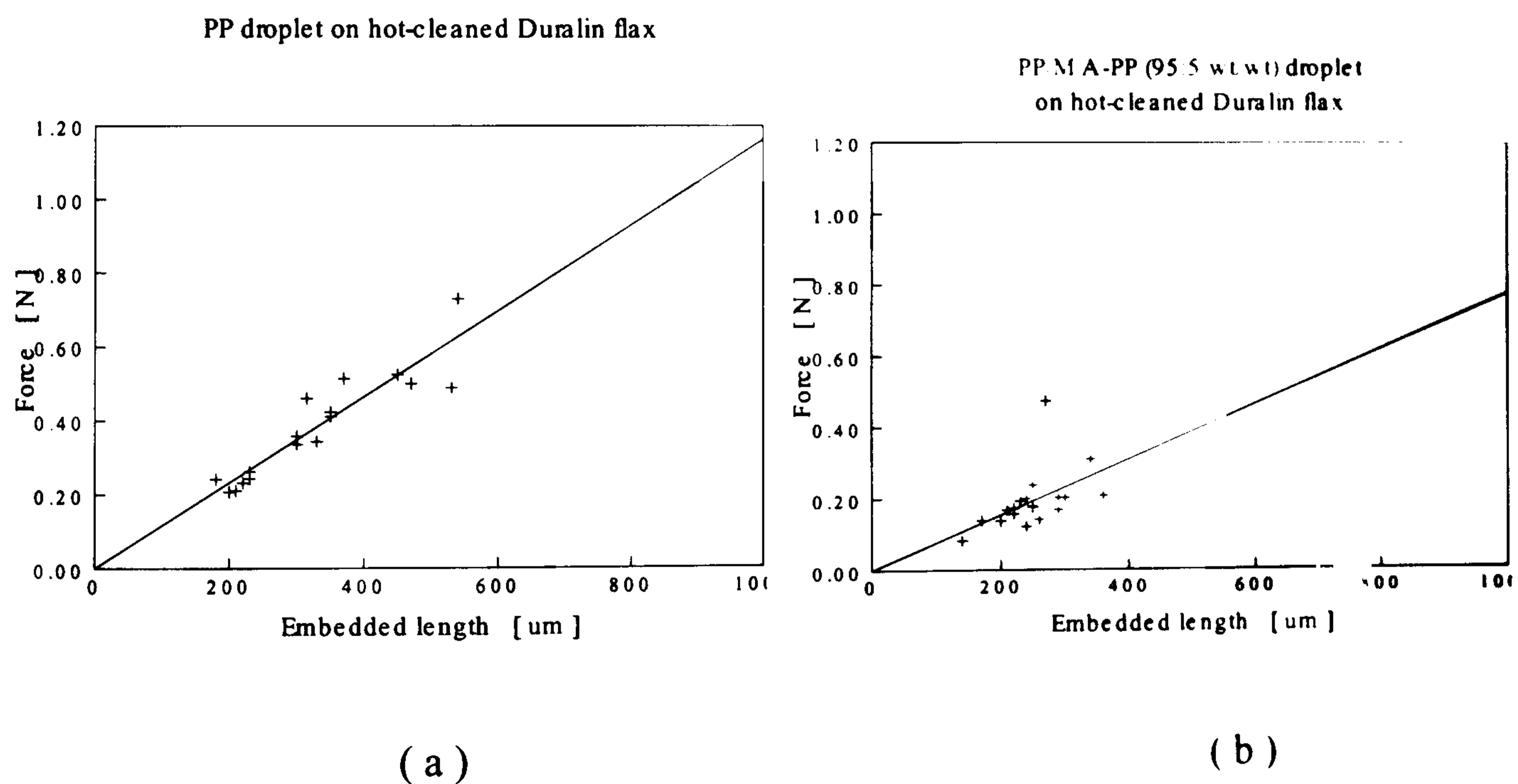


Figure 3A.4 Pull-out force vs. embedded length curve of hot-cleaned Duralin flax with (a) pure PP matrix (b) blend of PP/MA-PP (95:5 wt/wt).

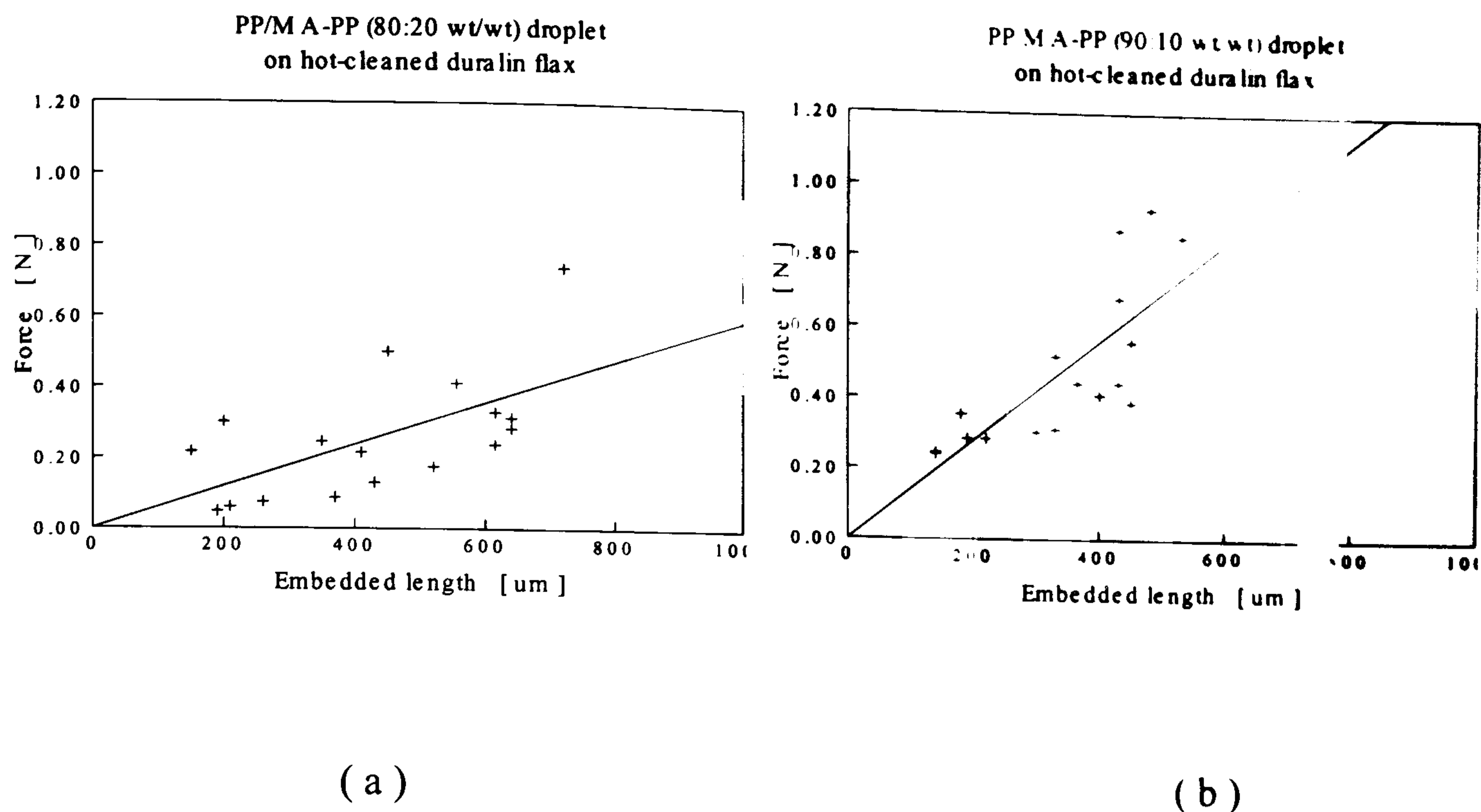


Figure 3A.5 Pull-out force vs. embedded length curve of hot-cleaned Duralin flax with (a) blend of PP/MA-PP (90:10 wt/wt) and (b) blend of PP/MA-PP (80:20 wt/wt).

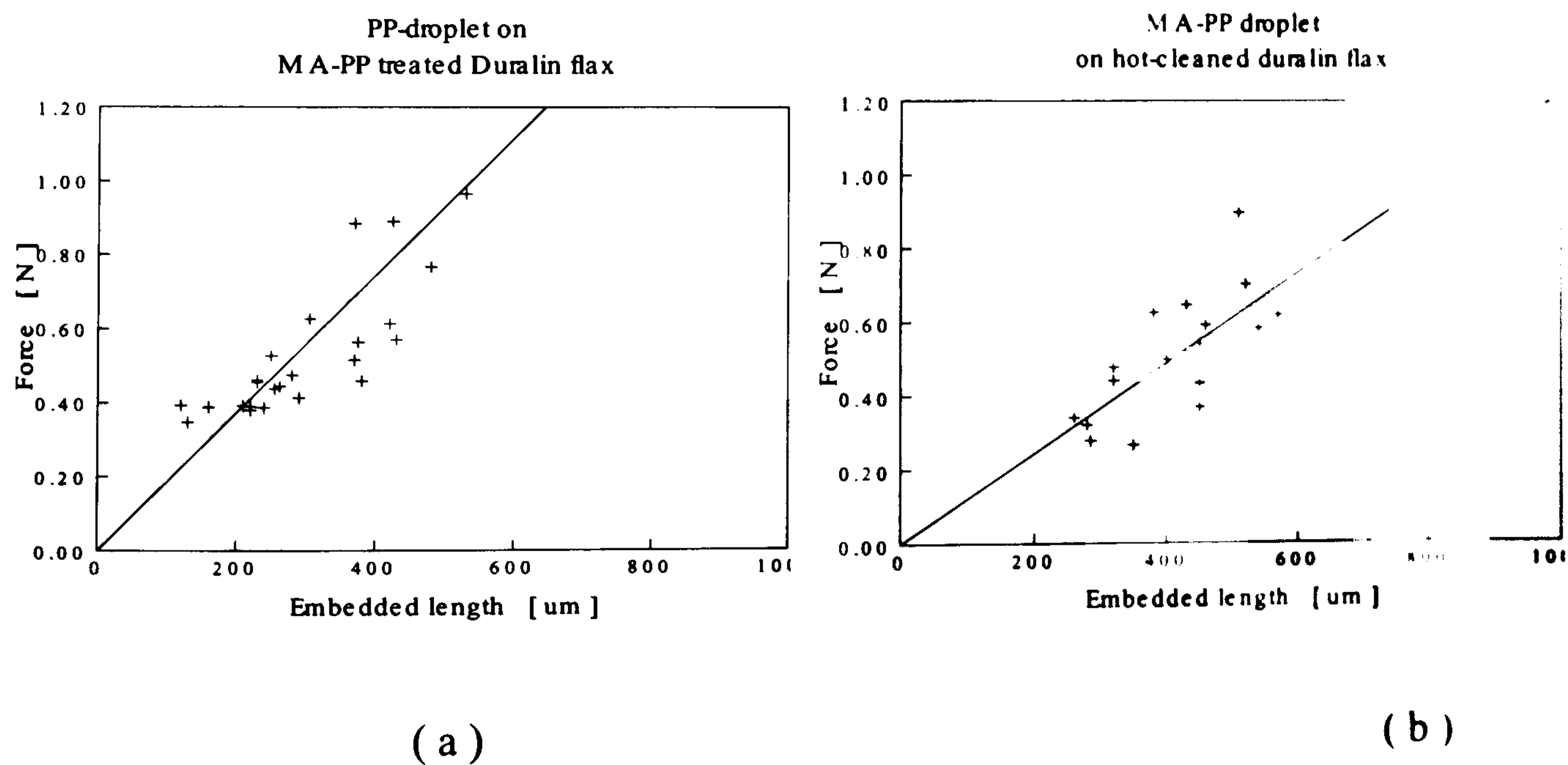


Figure 3A.6 Pull-out force vs. embedded length curve of (a) hot-cleaned Duralin flax with pure MA-PP matrix (b) MA-PP treated Duralin flax with pure PP matrix.

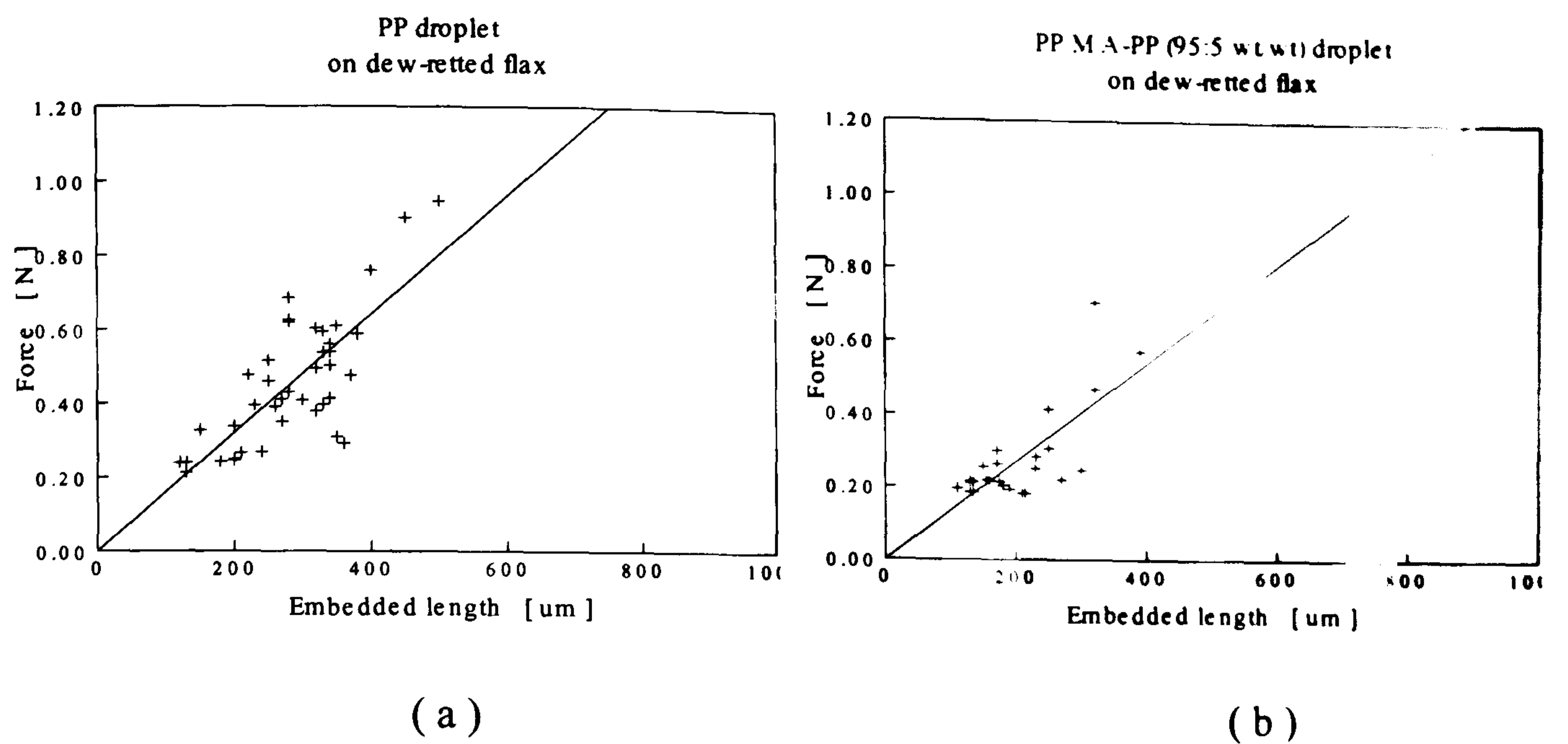


Figure 3A.7 Pull-out force vs. embedded length curve of dew retted flax with (a) pure PP matrix (b) blend of PP/MA-PP (95:5 wt/wt).

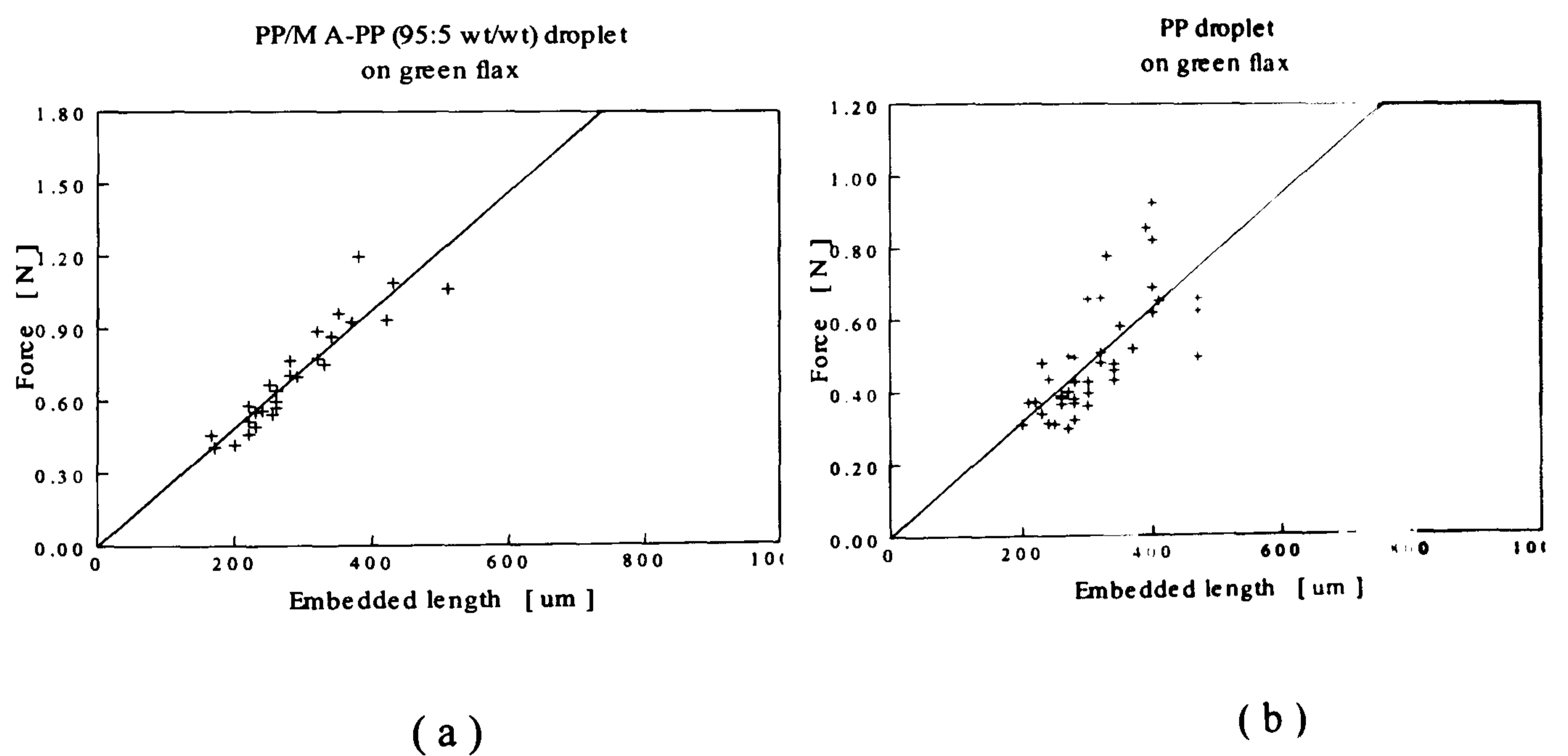


Figure 3A.8 Pull-out force vs. embedded length curve of green flax with a (a) pure PP matrix (b) blend of PP/MA-PP (95:5 wt/wt).

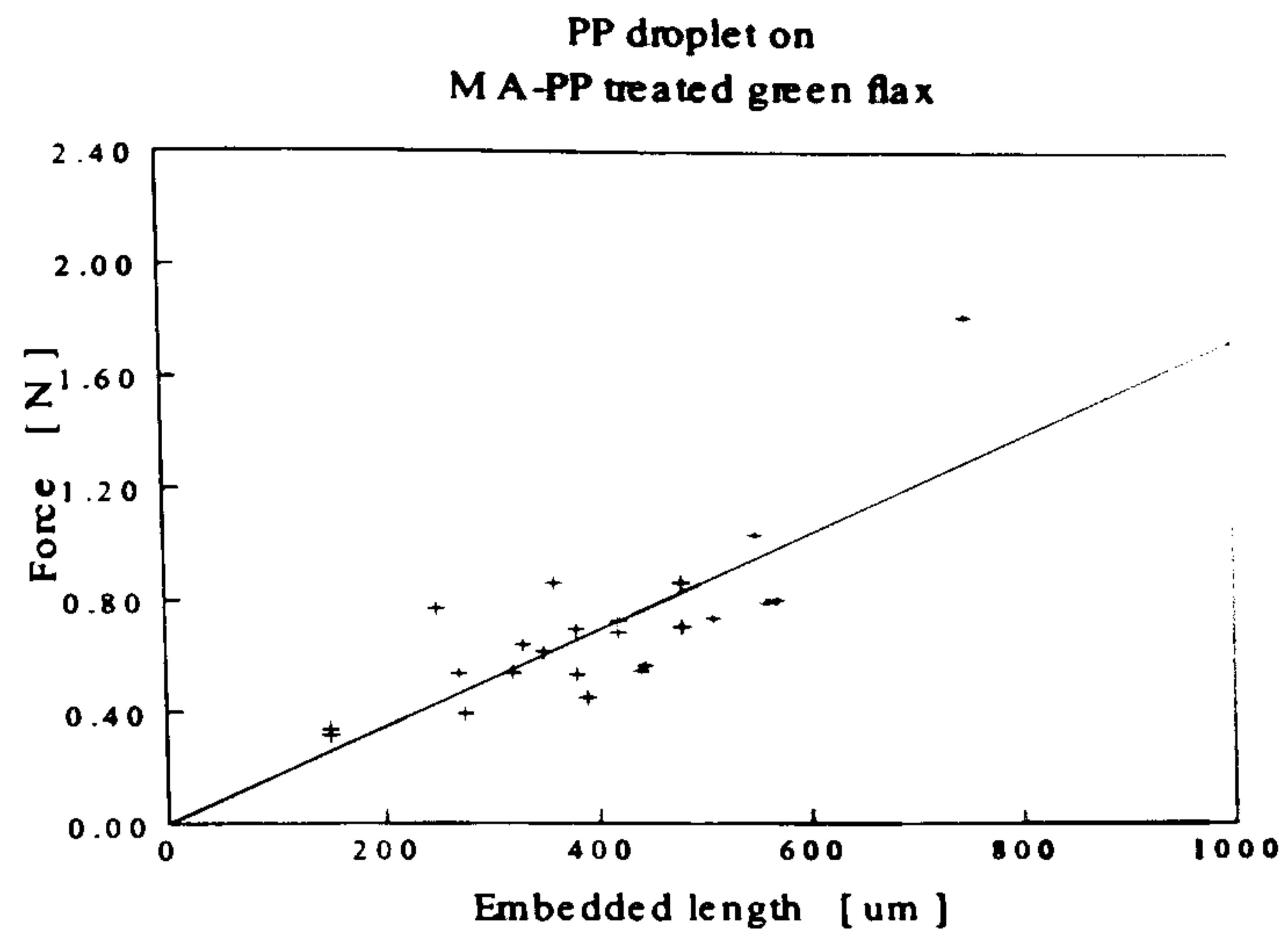


Figure 3A.9 Pull-out force vs. embedded length curve of MA-PP treated green flax with pure PP matrix.

Appendix 3B: ESEM pictures of different flax fibre types

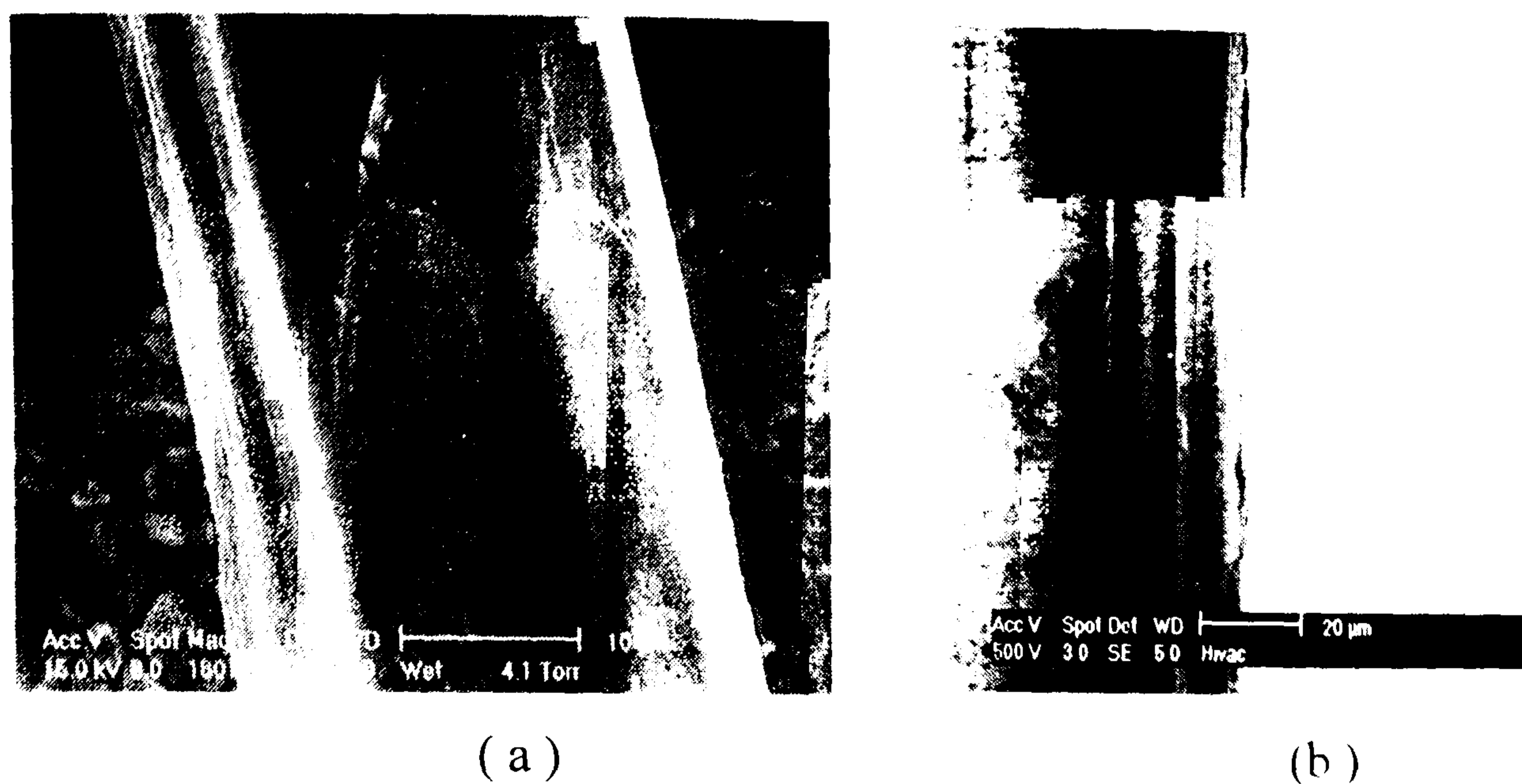


Figure 3B.1 ESEM picture of (a) MA-PP treated Duralin flax (b) normal Duralin flax.

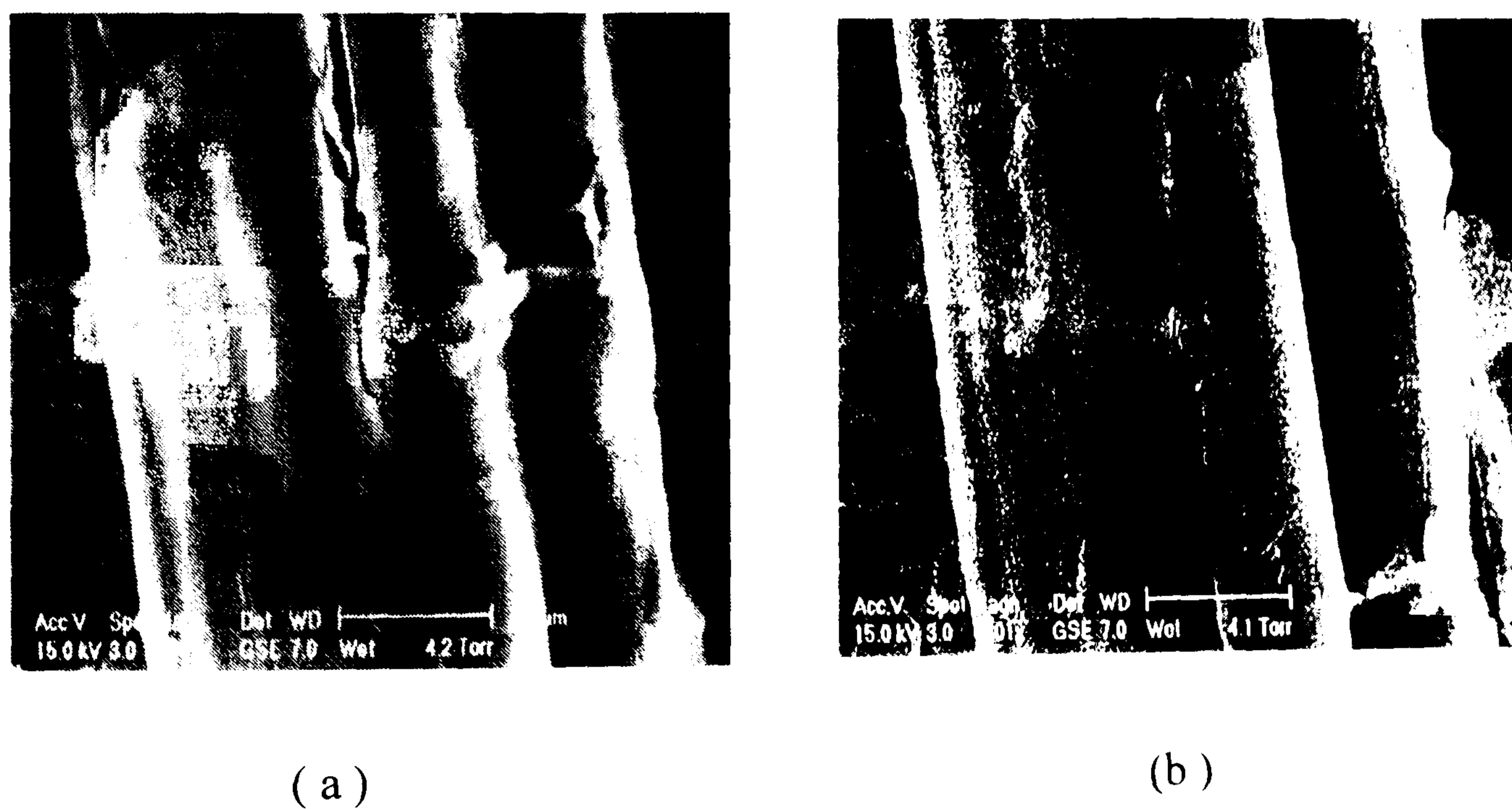


Figure 3B.2 ESEM picture of (a) MA-PP treated green flax (b) normal green flax.

UNIV.